

Feasibility of Gene Therapy for Late Neuronal Ceroid Lipofuscinosis

Dolan Sondhi, PhD; Neil R. Hackett, PhD; Robin L. Apblett, BA; Stephen M. Kaminsky, PhD; Robert G. Pergolizzi, PhD; Ronald G. Crystal, MD

Late infantile neuronal ceroid lipofuscinosis is a progressive childhood neurodegenerative disorder characterized by intracellular accumulation of autofluorescent material resembling lipofuscin in neuronal cells. This report summarizes the new therapies under consideration for late infantile neuronal ceroid lipofuscinosis, with a focus on strategies for in vivo gene therapy for the retinal and central nervous system manifestations of the disease.

Arch Neurol. 2001;58:1793-1798

Late infantile neuronal ceroid lipofuscinosis (LINCL; Batten disease) manifests between the ages of 2 and 4 years with seizures, ataxia, myoclonus, impaired vision, and delayed speech as the primary symptoms. The disease is characterized by cerebral and cerebellar atrophy, with progressive loss of neurons and retinal cells. The central nervous system (CNS) and retinal cells show characteristic autofluorescent curvilinear lysosomal storage bodies. The main component of this storage material is the mature form of subunit c of mitochondrial adenosine triphosphate synthetase, suggesting a defect in the turnover of this protein. Afflicted children develop blindness and become chair bound by the age of 4 to 6 years, with death by the age of 8 to 12 years.¹

Late infantile neuronal ceroid lipofuscinosis is caused by mutations in the *CLN2* (ceroid lipofuscinosis, neuronal 2) gene, a 6.7-kilo-base pair (kbp) gene with 13 exons and 12 introns mapped to 11p15 (**Figure, A**). The gene expresses 2.5- and 3.5-kbp messenger RNA transcripts.¹ Three mutations account for most cases of LINCL, including an intron G→C transversion in the invariant AG of the 3' splice junction of intron 5; an exon 6 C→T causing a premature stop; and an exon 10 G→C missense mutation.² The *CLN2* gene product is tripeptidyl peptidase I (TPP-I), a lyso-

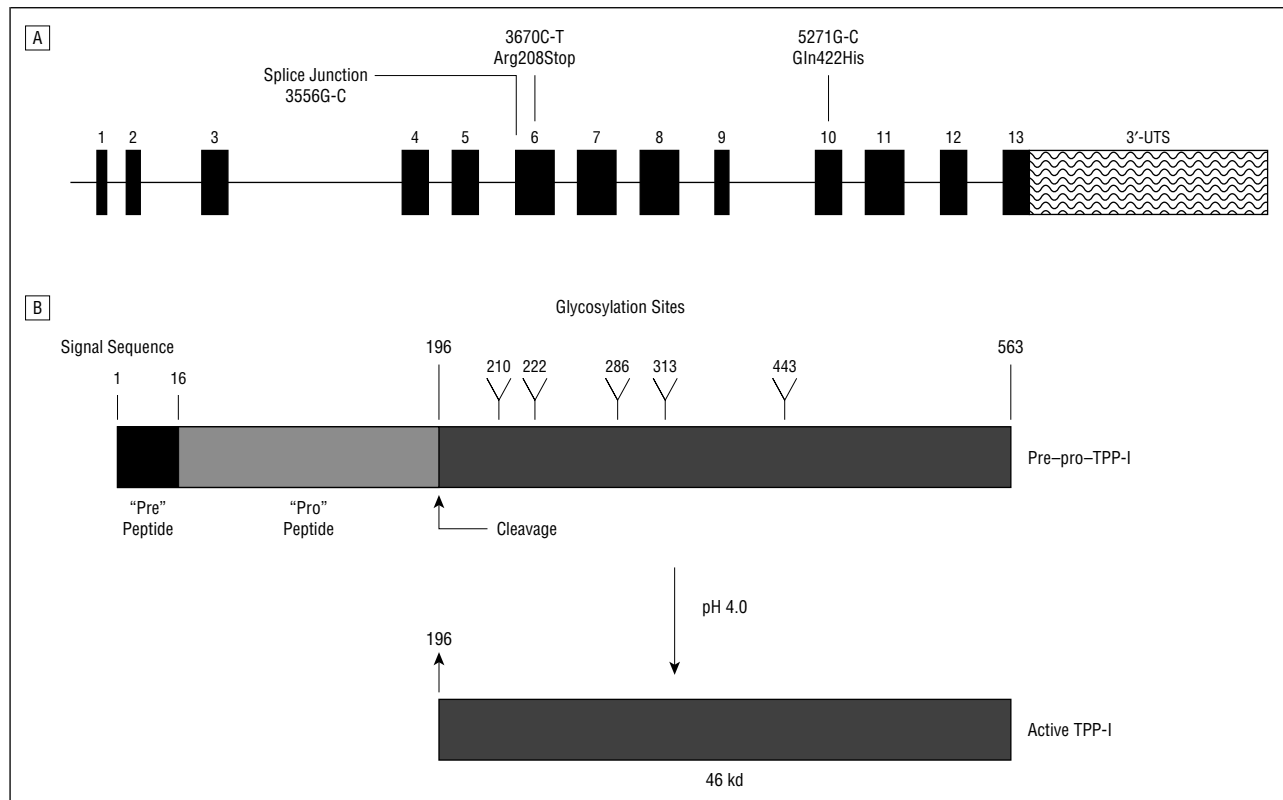
somal enzyme that progressively removes groups of 3 amino acids from the amino terminus of proteins (Figure, B). Tripeptidyl peptidase I is normally secreted into the extracellular milieu in a "pro-TPP-I" form that is then taken up via 2 mannose-6-phosphate high-affinity receptors, and shunted to lysosomes. The secreted pro-TPP-I protein is enzymatically inactive, but when acidified in the lysosomes it is autocatalytically converted to its active form.^{1,3}

NEW TREATMENT OPTIONS FOR LINCL

The goal of therapy for LINCL is to deliver active TPP-I to CNS and retinal cells in a sufficient amount and in time to prevent the cell loss. Theoretically, this goal could be achieved by enzyme augmentation therapy, allogeneic stem cell transplantation, and various forms of gene therapy. These strategies are all based on the concept that the pro-TPP-I protein is taken up via mannose-6-phosphate receptors on both the producer and the neighboring cells.^{4,5} The late emergence of an LINCL phenotype associated with mild mutations of the *CLN2* gene suggests that a therapy that would provide 5% to 10% of normal intracellular TPP-I activity would be sufficient to prevent progression of LINCL.²

It is uncertain what duration of therapy will be needed to impact the clinical phenotype. Because LINCL is a

From the Institute of Genetic Medicine and Belfer Gene Therapy Core Facility, Weill Medical College of Cornell University, New York, NY.



A, The *CLN2* (ceroid lipofuscinosis, neuronal 2) gene. The positions of the 3 most common mutations associated with late infantile neuronal ceroid lipofuscinosis are indicated: 3556G-C indicates an intron G→C transversion in the variant AG of a 3' splice junction; 3670C-T (Arg208Stop), an exon C→T transversion that prematurely terminates translation at amino acid 208 of 563; and 5271G-C (Gln422His), missense mutation. UTS indicates untranslated sequence. B, Tripeptidyl peptidase I (TPP-I) protein. The open reading frame of the *CLN2* gene encodes pre-pro-TPP-I (563 amino acids). The signal sequence (amino acids 1-16) directs the nascent protein to the secretory pathway with insertion into the endoplasmic reticulum and glycosylation at the sites indicated. The 547-residue pro-TPP-I protein is inactive until it is retaken up by the cell via the mannose-6-phosphate receptor system and until exposure to low pH in the lysosome, resulting in proteolytic cleavage at residue 196 to yield the 46-kd active mature product of 367 residues. Based on data from Sleat and colleagues.^{2,3}

hereditary disorder, it has been assumed that therapy must be continuous. However, because the clinical phenotype is not manifested until the age of 2 to 4 years, effective clearance of this material might “reset the clock” and delay progression of the disease, ie, transient augmentation of extracellular pro-TPP-I levels may provide protection of CNS and retinal cells for a few years. Contrary to this view is the hypothesis that TPP-I has critical functions other than the degradation of proteins accumulating in lysosomes, ie, the accumulation of metabolic by-products is not central to disease pathogenesis. This question will likely not be answered until clinical studies are carried out, but for now, it is prudent to have continuous augmentation of extracellular pro-TPP-I levels (and, hence, active intracellular TPP-I) in the target tissues as the highest priority.

Enzyme augmentation therapy is a strategy in which purified, recombinant pro-TPP-I would be infused into affected individuals. In addition to the challenge of producing and purifying the recombinant protein, the blood-brain barrier precludes effective TPP-I therapy for the CNS from being administered systemically. This could be circumvented by direct intracerebral administration of recombinant pro-TPP-I, but this is a difficult challenge given the diffuse nature of the CNS disease and the requirement for continuous augmentation.

Allogeneic stem cell therapy is based on the knowledge that bone marrow-derived stem cells can differentiate into blood monocytes that migrate to the brain to further differentiate into microglial cells.⁶ For LINCL, stem cell transplantation from a matched or partially matched donor would theoretically provide a cell source in the CNS for the normal TPP-I protein. It is unlikely, however, that this approach will work. In addition to the risk of long-term immunosuppression therapy, one attempt with stem cell therapy was unsuccessful in correcting the CNS pathology in a patient with LINCL, and the CNS abnormalities of mice with a related lysosomal storage disease are not corrected by stem cell therapy administered in the postnewborn period.^{7,8}

Gene therapy entails delivery of the *CLN2* complementary DNA (cDNA) to the target tissues as the source of TPP-I. Theoretically, if the transferred *CLN2* cDNA persists and continues to express TPP-I, there would be a continual local supply of the therapeutic protein. There are several approaches to consider for gene therapy for LINCL.

Systemic administration of autologous, genetically modified cells involves ex vivo modification of CD34⁺ stem cells (bone marrow or blood) to express the *CLN2* cDNA and intravenous administration of those modified cells to the patient. This strategy has the same logic as allogeneic therapy, but would not require long-term immunosup-

pression, and by using a strong constitutive promoter, the differentiated microglial cells would theoretically express large amounts of TPP-I. Unfortunately, gene transfer to CD34⁺ cells in humans has been successful only in conditions with positive selection pressure in vivo for the infused, transduced stem cells.⁹ This, together with the low rate of migration of monocytes into the CNS, diminishes the chances of success for this strategy.

Transplantation of genetically modified cells directly to the CNS has the advantage of ensuring high levels of local production of TPP-I. Most experimental systems have used autologous fibroblasts or allogeneic fetal neurons as the cells to be modified and transplanted.^{10,11} In addition to the social/political issues that may limit the use of fetal cells, this approach is not easily applicable to LINCL because of the diffuse nature of the CNS disease, requiring multiple sites of administration. This approach also has the risk of transplanting a large number of cells to a closed space. This safety issue, the challenge of obtaining large numbers of genetically modified autologous cells, and the necessity for *ex vivo* manipulation assign a low priority to this approach.

In vivo gene therapy is a strategy in which the *CLN2* cDNA would be directly delivered to cells throughout the CNS and retina, enabling the modified cells to produce TPP-I. This direct approach is the strategy most likely to succeed. The major challenge for *in vivo* gene therapy is whether the available gene transfer vectors can modify cells in the target tissues to produce sufficient amounts of TPP-I in the appropriate anatomic regions to stabilize and/or reverse the disease.

IN VIVO GENE THERAPY FOR LINCL: VECTORS AND EXPERIMENTAL STUDIES

Given the biological challenge and the available technology, we conclude that *in vivo* gene therapy is the most viable short-term option for treating the CNS and retinal manifestations of LINCL. Before discussing the practical aspects of initiating human gene therapy trials, it is useful to review the technology available to accomplish this and the experience of *in vivo* gene therapy in relevant models.

Gene Transfer Vectors

To efficiently transfer a gene to the nucleus of target cells of the CNS and retina, it is necessary to put the gene in a "vector," a carrier that helps to circumvent biological barriers to nucleic acid internalization to the nucleus, where it can use the normal cellular machinery to transcribe the exogenous gene. Viral gene transfer vectors capitalize on the property of viruses to efficiently transfer their genome to the nucleus of cells. These vectors are designed to be "replication deficient" by removal of critical genetic information. A viral gene vector used to treat LINCL would have the addition of an "expression" cassette containing the TPP-I cDNA controlled by an appropriate promoter. There are 3 types of gene transfer vectors, adeno-associated virus (AAV), lentivirus (LV), and adenovirus (Ad), that have the biological characteristics appropriate for effective *in vivo* gene transfer for

LINCL. Other vectors do not fit the needs of this clinical target (nonviral vectors have low efficiency and transient gene transfer/expression, murine retroviruses have low transduction efficiency *in vivo* and require target cells to be proliferating to transfer genes to the nucleus, and human herpes simplex virus has not been proved to be sufficiently safe for this application).

Adeno-associated viruses are small nonenveloped icosahedral parvoviruses with a 4.7-kbp single-stranded DNA genome.¹² All viral genes in AAV vectors are replaced by an expression cassette, leaving intact essential *cis* elements, including the inverted terminal repeats, the DNA packaging signal, and the replication origin.¹³ Adeno-associated vectors are effective in long-term gene transfer to¹⁴ the CNS and retina,¹⁵ and there is a good safety record in humans using AAV serotype 2.

Lentiviruses are a family of complex retroviruses that include the human immunodeficiency viruses. Lentivirus gene transfer vectors have the useful features of retroviral vectors (efficient integration in the chromosome, absence of viral genes from the genetic information transferred, and limited host responses to the vector), and the important added ability to infect nondividing cells such as those found in the CNS.¹⁶⁻¹⁸ However, there are concerns about the safety of LV vectors, given the serious nature of the human diseases attributable to members of this family.

Adenoviruses are nonenveloped icosahedral viruses with a double-stranded 36-kbp DNA genome that causes transient mild infections of the upper respiratory tract and intestine.¹⁹ Deletion of essential genes, typically E1, renders Ad replication deficient and leaves room for insertion of an expression cassette.²⁰ Most clinical experience with Ad vectors is with serotype 5. Because the Ad genome does not replicate or integrate into the genome, and these vectors initiate antivector host responses, Ad vectors mediate only transient expression. Because the brain is partially immunoprivileged, transgene expression from Ad vectors may persist for longer periods in the CNS than in other tissues. The critical questions for use of Ad for LINCL are as follows: (1) How long and at what levels is the protein expressed? (2) At a therapeutic dose, is readministration possible and at what intervals? (3) If expression of the *CLN2* gene can clear storage granules and prevent neuronal death, how long does the enzyme persist and how quickly do storage granules reaccumulate?

Following the death of a patient involved in a clinical trial using an Ad vector at the University of Pennsylvania, Philadelphia, in late 1999, there have been safety concerns about the intravascular use of high doses of Ad vectors.²¹ However, extensive assessment of the record by the Food and Drug Administration and the National Institutes of Health has shown that Ad is well tolerated at moderate doses, if administered directly to the target.^{22,23}

Lessons From Experimental Models

There is no animal model for LINCL. However, data from other experimental models support the use of AAV, LV, and Ad vectors to treat the CNS and retinal manifestations of LINCL. Most relevant are the data from mice with

mucopolysaccharidosis (MPS) VII (β -glucuronidase deficiency or Sly syndrome, a related lysosomal disorder). Mice with MPS VII are characterized by the accumulation of storage granules in CNS neurons and photoreceptor cell degeneration^{24,25} (untreated, these mice live 5 months). Like TPP-I, β -glucuronidase is normally secreted and taken up by neighboring cells using the mannose-6-phosphate receptor pathway. Studies of mice with MPS VII have established the following principles: (1) direct gene transfer to the CNS is required for correction of the storage defect in the adult brain^{8,26-28}; (2) there is cross correction, with transplantation of wild-type cells correcting mutant cells over an area much greater than the region of transplantation²⁹; and (3) AAV, LV, and Ad vectors can reverse storage and behavioral defects after direct CNS administration.³⁰⁻³⁴

Summary

Adeno-associated virus, LV, and Ad vectors appear to be suitable to treat the CNS and retinal manifestations of LINCL.

HUMAN GENE THERAPY FOR LINCL: PRACTICAL CONSIDERATIONS

The objective of clinical gene therapy trials for LINCL is to reverse the progress of the disease. Whether this can be achieved using current technology is not known, but if the preclinical efficacy and toxicology studies are sufficiently robust to support a clinical trial, the available scientific evidence, together with an overwhelming medical need for this rare, universally fatal disorder for which there is no therapy, strongly argues that resources should be devoted toward this end. The following are practical considerations to achieve this goal.

Vectors

Comparing the biological characteristics of the vectors, their known safety profiles, and theoretical risks with the biological features of LINCL, we conclude that the priorities for vector development for clinical use should be as follows: AAV is greater than LV, which is greater than Ad. Adeno-associated virus merits the highest priority because LINCL is a hereditary disorder, and there is good experimental evidence that AAV can mediate gene transfer with long-term expression in the CNS and retina. While LV has many of the same characteristics, it has to be given a lower priority because there is far less experience with LV compared with AAV in human trials, and because of the theoretical safety issue of using a vector partially derived from human immunodeficiency virus 1 genetic elements.

There are some drawbacks to AAV that should be considered. If there is overexpression of gene (or gene product), it could be toxic and cannot be switched off (unless a genetic "switch" is built into the vector). Some AAV genomes may integrate inappropriately, with the theoretical risk of inducing malignancy. Intravenous administration of an AAV vector expressing β -glucuronidase to neonatal mice with MPS VII resulted in long-

term survival, but many of the treated mice later developed hepatocellular carcinoma.³⁵ The origin of the hepatocellular carcinoma may be a consequence of the underlying pathology of the mice with MPS VII, rather than of the AAV vector therapy.

While Ad vectors may only provide transient expression, if the abnormal lysosomal storage is fundamental to the loss of neurons in patients with LINCL, then transient (1-2 weeks) expression of the *CLN2* cDNA in the CNS may provide sufficient TPP-I to clear the storage granules and "set the clock back," delaying the morbidity in children with LINCL by years. This concept, plus human safety data for Ad vector administration to the CNS for glioma,³⁶ suggests that Ad vectors should be developed for possible clinical use, albeit at a lower priority.

Expression Cassette

For gene therapy of LINCL, the expression cassette will be the *CLN2* human cDNA controlled by an active promoter. With the knowledge that gene transfer technology can only deliver genes to a limited percentage of cells in a target, the requirement to deliver the *CLN2* protein product in a diffuse fashion argues that high-level constitutive expression is necessary, ie, regardless of the vector used, the assumption of cross correction of neighboring cell types makes production of a high level of TPP-I protein of paramount consideration. Examples of such promoters include the Rous sarcoma virus long terminal repeat, the cytomegalovirus early/intermediate promoter/enhancer, and the chicken β -actin promoter with cytomegalovirus enhancer.³⁶⁻³⁸

Administration

There are 3 possible routes of delivery of vectors to the CNS: intravascular, intrathecal, or intracranial. For the retina, the vector can be administered directly to the subretinal or the vitreal space.

Theoretically, intravascular or intrathecal delivery could be used, but the substantial technology (intravascular) and doses (intrathecal) required for these strategies when balanced against the urgent clinical need for a therapy suggest this should be a low priority. The most direct approach to administration of vectors to the CNS is direct injection into the brain parenchyma. The requirement for diffuse administration necessitates injection into several sites, something achieved only with multiple burr holes. It is unknown how many of these will be required without knowing the diffusion characteristics of the vector and the TPP-I protein in the CNS of a large experimental animal. This variable is governed by the volume injected (a buffered sugar-salt solution is used as a vehicle for the vector) and by the diffusion characteristics of the vector in the target tissue. Because the CNS is a closed space, there is a limit to the volume that can be administered per unit time. A reservoir could be used to slowly administer the vector, but this will require studies of safety and vector stability, and their use may be associated with a risk of infection. Despite the diffuse nature of LINCL, there are some CNS regions (eg, the cortex and the cerebellum) that may play a dominant role in the

phenotype; these areas might be the primary targets for the initial studies. Alternatively, the vector could be administered repetitively. This has the advantage of being able to assess each single administration for adverse events before proceeding, but assumes that host defenses against the vector will not limit the safety and effectiveness of repeated administration.

For the retina, the most common effective procedure for vector administration is a single injection through a sclerotomy into the subretinal space.^{39,40} Alternatively, the vector can be administered with a single injection through the front of the eye, to the vitreous, or continuing through the vitreous into the superior subretinal space.⁴⁰

Dose Response

The administration of a gene transfer vector has the potential of inducing toxicity from the vector and/or transgene product. Because the CNS and retina may be sensitive to such adverse events, it would be prudent to limit the intensity and spatial distribution of any toxicity by initiating a gene transfer trial to these sites with low doses of the vector, and to administer the vector to a limited (local) region of the brain or to one eye. The development of gene therapy for LINCL must balance ethical issues (eg, using a low dose may not be efficacious for this fatal disorder) against safety issues (eg, persistent high-dose vector expression causing toxicity). If a conservative approach is taken using a low dose and/or administration to a limited region of the brain, the only solution is to consider readministration (if possible) after sufficient time passes to assess the toxicity from the first administration.

Repeat Administration

For most drugs, repeat administration is the norm. However, for LINCL, each administration to the CNS will require burr holes. Systemic immunity against a viral vector may preclude effective gene transfer on readministration, and host defenses against the vector may induce inflammation that may be unacceptable. Despite the fact that the CNS is a partially immunoprotected site, we predict that repeated administration of viral vectors to the CNS and retina may be safe but may not be progressively efficacious.⁴¹

Preclinical Data

Without the availability of a suitable model for LINCL, critical preclinical studies must address the following issues: (1) Will the TPP-I product diffuse throughout the brain in sufficient levels to provide efficacy? (2) What toxic effects are associated with administration of the vector at doses within and above the range likely to be used in the clinical studies? For each vector and each site, these studies need to be carried out with naive and antivector immune-positive animals, and with single and repeat administration. As another assessment of toxicity, the creation of transgenic mice with the *CLN2* cDNA will be useful to know if there is a phenotype associated with overexpression.

Regulatory and Ethical Issues

In the context that LINCL is a rare, fatal disease, it may be necessary to develop gene therapy for it by compressing the studies into a combined phase 1, 2, and 3 study that simultaneously assesses safety and efficacy parameters. The initial human studies will likely require a lower than therapeutic dose. While local delivery will be the safest way to start, it will likely not treat all aspects of the CNS disease. Furthermore, the parameters that measure clinical outcome in the CNS are relatively insensitive and may provide little information about the efficacy of gene transfer, ie, *CLN2* gene therapy studies in humans involving small numbers of patients may yield ambiguous data in posttherapy tests. Depending on the final inclusion/exclusion criteria, there will be a limited number of patients eligible for the therapeutic development pathway. There is an ethical dilemma regarding the recruitment of children with far advanced disease, but restrictive inclusion/exclusion criteria could radically reduce the number of available subjects for a trial. Because families are highly motivated to participate in a gene therapy trial for LINCL, clear consent materials will be necessary, as will provisions for extensive discussions before and during the study.

SUMMARY

There are many unanswered questions that will require assessment before proposing a clinical gene therapy trial for LINCL. Many decisions will require data generated from experimental animals. Objective, quantitative parameters will need to be developed before assessment of subjects with LINCL in a gene therapy protocol can be achieved. However, there is sufficient information available to conclude that if our assumptions regarding the biology are correct, the resources are available, and the regulatory climate is supportive, it is rational to initiate the preclinical safety and toxicity studies directed toward mounting clinical trials for the CNS and retinal manifestations of LINCL.

Accepted for publication April 23, 2001.

This study was funded in part by Nathan's Battle Foundation, Indianapolis, Ind.

We thank R. Boustany, MD, K. Wisniewski, MD, PhD, N. Zhong, MD, M. Sands, PhD, P. Lobel, PhD, P. Gutin, MD, M. Souweidane, MD, F. Marshall, MD, J. Bennet, MD, PhD, P. Leopold, PhD, and R. Zalaznick, BA, for helpful discussions and advice; and B. Charlot, T. Virgin-Bryan, and N. Mohamed, MPH, for preparation of the manuscript.

Corresponding author and reprints: Ronald G. Crystal, MD, Institute of Genetic Medicine, Weill Medical College of Cornell University, 515 E 71st St, Suite 1000, New York, NY 10021 (e-mail: geneticmedicine@med.cornell.edu).

REFERENCES

1. Williams RE, Gottlob I, Lake BD, Goebel HH, Winchester BG, Wheeler RB. *CLN2*: classic late infantile NCL. In: Goebel HH, Mole SE, Lake BD, eds. *The Neuronal Ceroid Lipofuscinoses (Batten Disease)*. Amsterdam, the Netherlands: IOS Press; 1999:37-54.

2. Sleat DE, Gin RM, Sohar I, et al. Mutational analysis of the defective protease in classic late-infantile neuronal ceroid lipofuscinosis, a neurodegenerative lysosomal storage disorder. *Am J Hum Genet.* 1999;64:1511-1523.
3. Sleat DE, Donnelly RJ, Lackland H, et al. Association of mutations in a lysosomal protein with classical late-infantile neuronal ceroid lipofuscinosis. *Science.* 1997;277:1802-1805.
4. Neufeld EF, Fratantoni JC. Inborn errors of mucopolysaccharide metabolism. *Science.* 1970;169:141-146.
5. Taylor RM, Wolfe JH. Cross correction of β -glucuronidase deficiency by retroviral vector-mediated gene transfer. *Exp Cell Res.* 1995;214:606-613.
6. Krivit W, Sung JH, Shapiro EG, Lockman LA. Microglia: the effector cell for reconstitution of the central nervous system following bone marrow transplantation for lysosomal and peroxisomal storage diseases. *Cell Transplant.* 1995;4:385-392.
7. Lake BD, Steward C, Oakhill A, Wilson J, Perham TG. Bone marrow transplantation in late infantile Batten disease and juvenile Batten disease. *Neuropediatrics.* 1997;28:80-81.
8. Sands MS, Barker JE, Vogler C, et al. Treatment of murine mucopolysaccharidosis type VII by syngeneic bone marrow transplantation in neonates. *Lab Invest.* 1993;68:676-686.
9. Cavazzana-Calvo M, Hacein-Bey S, de Saint BG, et al. Gene therapy of human severe combined immunodeficiency (SCID)-X1 disease. *Science.* 2000;288:669-672.
10. Kordower JH, Freeman TB, Snow BJ, et al. Neuropathological evidence of graft survival and striatal reinnervation after the transplantation of fetal mesencephalic tissue in a patient with Parkinson's disease. *N Engl J Med.* 1995;332:1118-1124.
11. Taylor RM, Wolfe JH. Decreased lysosomal storage in the adult MPS VII mouse brain in the vicinity of grafts of retroviral vector-corrected fibroblasts secreting high levels of β -glucuronidase. *Nat Med.* 1997;3:771-774.
12. Berns KI, Giraud C. Biology of adeno-associated virus. *Curr Top Microbiol Immunol.* 1996;218:1-23.
13. Carter B. Adeno-associated virus and adeno-associated virus vectors for gene delivery. In: Smyth Tempelton N, Lasic DD, eds. *Gene Therapy.* New York, NY: Marcel Dekker Inc; 2000:41-59.
14. McCown TJ, Xiao X, Li J, Breese GR, Samulski RJ. Differential and persistent expression patterns of CNS gene transfer by an adeno-associated virus (AAV) vector. *Brain Res.* 1996;713:99-107.
15. Bennett J, Maguire AM, Cideciyan AV, et al. Stable transgene expression in rod photoreceptors after recombinant adeno-associated virus-mediated gene transfer to monkey retina. *Proc Natl Acad Sci U S A.* 1999;96:9920-9925.
16. Akkina RK, Walton RM, Chen ML, Li QX, Planelles V, Chen IS. High-efficiency gene transfer into CD34⁺ cells with a human immunodeficiency virus type 1-based retroviral vector pseudotyped with vesicular stomatitis virus envelope glycoprotein G. *J Virol.* 1996;70:2581-2585.
17. Naldini L, Blomer U, Gallay P, et al. In vivo gene delivery and stable transduction of nondividing cells by a lentiviral vector. *Science.* 1996;272:263-267.
18. Reiser J, Harmison G, Kluepfel-Stahl S, Brady RO, Karlsson S, Schubert M. Transduction of nondividing cells using pseudotyped defective high-titer HIV type 1 particles. *Proc Natl Acad Sci U S A.* 1996;93:15266-15271.
19. Shenk T. Adenoviridae: the viruses and their replication. In: Fields B, Knipe D, Howley PM, eds. *Virology.* Philadelphia, Pa: Lippincott-Raven Publishers; 1996: 2111-2148.
20. Hackett NR, Crystal RG. Adenovirus vectors for gene therapy. In: Smyth Tempelton N, Lasic DD, eds. *Gene Therapy.* New York, NY: Marcel Dekker Inc; 2000: 17-40.
21. Sorelle R. Human gene therapy: science under fire. *Circulation.* 2000;101:e9023-e9024. Available at: <http://circ.ahajournals.org/cgi/content/full/101/12/e9023>. Accessed August 8, 2001.
22. Harvey B-G, Maroni J, O'Donoghue KA, et al. Safety of local delivery of low and intermediate dose adenovirus gene transfer vectors to individuals with a spectrum of comorbid conditions. *Hum Gene Ther.* In press.
23. Office of Recombinant DNA Activities. Safety Reports and Adverse Events for Human Gene Transfer Protocols Recombinant DNA Advisory Committee Meeting, December 8-10, 1999. NIH/ORDA. Available at: <http://www4.od.nih.gov/oba/rac/minutes/1299rac.pdf>. Accessed August 8, 2001.
24. Birkenmeier EH, Barker JE, Vogler CA, et al. Increased life span and correction of metabolic defects in murine mucopolysaccharidosis type VII after syngeneic bone marrow transplantation. *Blood.* 1991;78:3081-3092.
25. Lazarus HS, Sly WS, Kyle JW, Hageman GS. Photoreceptor degeneration and altered distribution of interphotoreceptor matrix proteoglycans in the mucopolysaccharidosis VII mouse. *Exp Eye Res.* 1993;56:531-541.
26. Gao C, Sands MS, Haskins ME, Ponder KP. Delivery of a retroviral vector expressing human β -glucuronidase to the liver and spleen decreases lysosomal storage in mucopolysaccharidosis VII mice. *Mol Ther.* 2000;2:233-244.
27. Ohashi T, Watabe K, Uehara K, Sly WS, Vogler C, Eto Y. Adenovirus-mediated gene transfer and expression of human β -glucuronidase gene in the liver, spleen, and central nervous system in mucopolysaccharidosis type VII mice. *Proc Natl Acad Sci U S A.* 1997;94:1287-1292.
28. Watson GL, Sayles JN, Chen C, et al. Treatment of lysosomal storage disease in MPS VII mice using a recombinant adeno-associated virus. *Gene Ther.* 1998;5: 1642-1649.
29. Skorupa AF, Fisher KJ, Wilson JM, Parente MK, Wolfe JH. Sustained production of β -glucuronidase from localized sites after AAV vector gene transfer results in widespread distribution of enzyme and reversal of lysosomal storage lesions in a large volume of brain in mucopolysaccharidosis VII mice. *Exp Neurol.* 1999; 160:17-27.
30. Bosch A, Perret E, Desmaris N, Heard JM. Long-term and significant correction of brain lesions in adult mucopolysaccharidosis type VII mice using recombinant AAV vectors. *Mol Ther.* 2000;1:63-70.
31. Bosch A, Perret E, Desmaris N, Trono D, Heard JM. Reversal of pathology in the entire brain of mucopolysaccharidosis type VII mice after lentivirus-mediated gene transfer. *Hum Gene Ther.* 2000;11:1139-1150.
32. Davidson BL, Brooks AI, Stein CS, et al. Correction of cellular pathology and behavioral deficits in adult β -glucuronidase-deficient mice after FIV vector-mediated gene transfer to brain [abstract]. *Mol Ther.* 2000;1:A688.
33. Stein CS, Ghodsi A, Derksen T, Davidson BL. Systemic and central nervous system correction of lysosomal storage in mucopolysaccharidosis type VII mice. *J Virol.* 1999;73:3424-3429.
34. Frisella WA, O'Connor LH, Vogler CA, et al. Intracranial injection of recombinant adeno-associated virus improves cognitive function in a murine model of mucopolysaccharidosis type VII. *Mol Ther.* 2001;3:351-358.
35. National Institutes of Health. Safety considerations in the use of AAV vectors in gene transfer clinical trials. Paper presented at: Fourth National Gene Transfer Safety Symposium; March 7, 2001; Rockville, Md.
36. Trask TW, Trask RP, Aguilar-Cordova E, et al. Phase I study of adenoviral delivery of the *HSV-tk* gene and ganciclovir administration in patients with current malignant brain tumors. *Mol Ther.* 2000;1:195-203.
37. Yoon SO, Lois C, Alvarez M, Alvarez-Buylla A, Falck-Pedersen E, Chao MV. Adenovirus-mediated gene delivery into neuronal precursors of the adult mouse brain. *Proc Natl Acad Sci U S A.* 1996;93:11974-11979.
38. Yukawa H, Takahashi JC, Miyatake SI, et al. Adenoviral gene transfer of basic fibroblast growth factor promotes angiogenesis in rat brain. *Gene Ther.* 2000; 7:942-949.
39. Ali RR, Sarra GM, Stephens C, et al. Restoration of photoreceptor ultrastructure and function in retinal degeneration slow mice by gene therapy. *Nat Genet.* 2000; 25:306-310.
40. Lau D, McGee LH, Zhou S, et al. Retinal degeneration is slowed in transgenic rats by AAV-mediated delivery of FGF-2. *Invest Ophthalmol Vis Sci.* 2000;41: 3622-3633.
41. Harvey BG, Leopold PL, Hackett NR, et al. Airway epithelial CFTR mRNA expression in cystic fibrosis patients after repetitive administration of a recombinant adenovirus. *J Clin Invest.* 1999;104:1245-1255.

Clinical Protocol

Administration of a Replication-Deficient Adeno-Associated Virus Gene Transfer Vector Expressing the Human *CLN2* cDNA to the Brain of Children with Late Infantile Neuronal Ceroid Lipofuscinosis

FDA-IND #11481
NIH (RAC) #0312-619

PRINCIPAL INVESTIGATOR: Ronald G. Crystal¹
SITE: New York Presbyterian Hospital-Cornell Medical Center
COINVESTIGATORS: Dolan Sondhi, Ph.D.,¹ Neil R. Hackett, Ph.D.,² Stephen M. Kaminsky, Ph.D.,² Stefan Worgall, M.D.,³ Philip Stieg, M.D., Ph.D.,⁴ Mark Souweidane, M.D.,⁴ Syed Hosain, M.D.,³ Linda Heier, M.D.,⁵ Douglas Ballon, Ph.D.,⁵ Miles Dinner, M.D.,⁶ Krystyna Wisniewski, M.D., Ph.D.,⁷ Michael Kaplitt, M.D., Ph.D.,⁴ Bruce M. Greenwald, M.D.,³ Joy D. Howell, M.D.,³ Kristin Strybing, N.P.,⁴ Jonathan Dyke, Ph.D.,⁵ and Henning Voss, Ph.D.⁵
AFFILIATIONS: ¹Department of Genetic Medicine, Weill Medical College of Cornell University, New York, NY 10021 (WMC), ²Department of Medicine, WMC, ³Department of Pediatrics, WMC, ⁴Department of Neurological Surgery, WMC, ⁵Department of Radiology, WMC, ⁶Department of Anesthesiology, WMC, ⁷Institute for Basic Research in Developmental Disabilities, Staten Island, NY 10314.

TABLE OF CONTENTS

- Overview of Late Infantile Neuronal Ceroid Lipofuscinosis
- Rationale for *In Vivo* Gene Therapy for the CNS Manifestations of LINCL
- Adeno-associated Serotype 2 Gene Transfer Vectors
- Overview of the Proposed Study
- Details of the Experimental Design
- End-Point Variables
 - Primary End Point
 - Secondary End Point
- Review and Monitoring
- Statistical Considerations
- Timeline
- Inclusion/Exclusion Criteria
 - Inclusion Criteria
 - Exclusion Criteria
- Risks of the Study
 - Delivery of the Vector and Surgical Procedures
 - AAV2_{CU}hCLN2 Vector
 - Tests and Procedures Designed to Evaluate Effectiveness and Safety
- Precautions to Minimize Risks
 - Management of Intercurrent Illness
 - Management of Adverse Events

Safety Issues for Healthcare Workers
 Environment
 Risk–Benefit Ratio
 Confidentiality of Data
 Details of the Drug to Be Used: AAV2_{CU}hCLN2, the Human *CLN2* Gene Transfer Vector
 AAV2_{CU}hCLN2 Construct
 Preclinical Efficacy Studies
 Efficacy Studies in Rats
 Efficacy Studies in Nonhuman Primates
 Preclinical Safety Data
 Safety Studies in Rats
 Safety Studies in Nonhuman Primates
 Clinical Preparation
 Risks Related to the Drug
 References
 Appendix I. Neurological Examination
 Appendix II. Graded Toxicity Scale to Define Adverse Reactions
 Appendix III. FDA-Mandated 15–Year Postvector Administration Annual Follow-up Questionnaire

ABSTRACT

Late infantile neuronal ceroid lipofuscinosis (LINCL) is a fatal childhood neurodegenerative lysosomal storage disease with no known therapy. There are estimated to be 200 to 300 children in the United States at any one time with the disease. LINCL is a genetic disease resulting from a deficiency of tripeptidyl peptidase I (TPP-I), a proteolytic enzyme encoded by *CLN2*, the gene that is mutated in individuals with LINCL. The subjects are chronically ill, with a progressive CNS disorder that invariably results in death, typically by age 8 to 12 years. The strategy of this clinical study is based on the concept that persistent expression in the CNS of the normal *CLN2* cDNA with production of sufficient amounts of TPP-I should prevent further loss of neurons, and hence limit disease progression. To assess this concept, an adeno-associated virus vector (AAV2_{CU}hCLN2) will be used to transfer to and express the human *CLN2* cDNA in the brain of children with LINCL. The vector consists of the AAV2 capsid enclosing the 4278-base single-stranded genome consisting of the two inverted terminal repeats of AAV serotype 2 and an expression cassette composed of the human cytomegalovirus (CMV) enhancer, the chicken β -actin promoter/splice donor and 5' end of the intron, the 3' end of the rabbit β -globin intron and splice acceptor, the human *CLN2* cDNA with an optimized Kozak translation initiation signal, and the polyadenylation/transcription stop codon from rabbit β -globin. The proposed study will include 10 individuals and will be divided into two parts. Group A, to be studied first, will include four individuals with the severe form of the disease. Group B of the trial will include six individuals with a moderate form of the disease. After direct intracranial administration of the vector, there will be neurological assessment based on the LINCL clinical rating scale and magnetic resonance imaging/magnetic resonance spectroscopy assessment of the brain in regions of vector administration. The data generated will help evaluate two hypotheses: (1) that it is safe to carry out direct intracranial administration of the AAV2_{CU}hCLN2 vector to the CNS of individuals with LINCL, and (2) that administration of the AAV2_{CU}hCLN2 vector will slow down or halt the progression of the disease in the central nervous system.

OVERVIEW OF LATE INFANTILE NEURONAL CEROID LIPOFUSCINOSIS

Late infantile neuronal ceroid lipofuscinosis (LINCL) is a form of Batten disease, the collective name for autosomal recessive disorders grouped together as the neuronal ceroid lipofuscinoses (NCLs). These are childhood neurodegenerative lysosomal storage diseases associated with intracellular accumulation of autofluorescent material resembling

lipofuscin in neuronal cells (Boustany, 1996; Williams *et al.*, 1999). Batten disease affects 1 in 12,500 to 100,000 births each year, making it the most common neurodegenerative disease of childhood. For all the NCLs, there is a progressive neurological decline characterized by cognitive impairment, visual failure, seizures, and deteriorating motor development. For LINCL, this invariably leads to a vegetative state and a shortened life span.

LINCL manifests itself at age 2 to 4 years (Williams *et*

al., 1999; Kurachi *et al.*, 2000). The major symptoms that bring children to medical attention are seizures, ataxia (loss of ability to coordinate voluntary movement), and myoclonus (sudden twitching of muscles or parts of muscles, without any rhythm or pattern). Ataxia, myoclonus, impaired speech, and developmental regression become apparent around this time or within a few months. The seizures are often the first manifestation, but there is variability among individuals with reference to the time of onset and the appearance of the collective symptoms. A gradual decline in visual ability follows with blindness by 4 to 6 years. Afflicted children generally become wheelchair bound between 4 and 6 years. Toward the late stages of the disease, feeding becomes very difficult, with resulting poor weight gain. Death occurs by age 8 to 12 years. There is currently no treatment for LINCL other than management of symptoms.

At a cellular level, LINCL is characterized by cerebral and cerebellar atrophy, with progressive loss of neurons and retinal cells (Boustany, 1996; Birch, 1999; Williams *et al.*, 1999). The CNS and retinal cells show characteristic autofluorescent, curvilinear lysosomal storage bodies (Boustany, 1996; Sleat *et al.*, 1997; Williams *et al.*, 1999). The main component of this storage material is the mature form of subunit c of mitochondrial ATP synthetase, suggesting a defect in the turnover of this protein (Ezaki *et al.*, 1995). Even though the storage bodies are present in cells throughout the body of individuals with LINCL, the primary pathology and the cause of morbidity are associated with the brain.

LINCL is caused by inheritance from both parents of chromosomes containing mutations in the *CLN2* gene. The gene is mapped to chromosomal locus 11p15, is 6.65 kb in length, and consists of 13 exons and 12 introns (Sharp *et al.*, 1997; Liu *et al.*, 1998). There are 24 known mutations of the tripeptidyl peptidase I (TPP-I) gene that are associated with LINCL (Sleat *et al.*, 1999) [Fig. 1 (shows the three most common mutations) and Table 1 (lists all known mutations)]. The primary translation product of the *CLN2* gene is a 563-residue “pre-pro” form of TPP-I that includes a 16-residue signal sequence, a 180-residue propeptide, and a 367-residue active mature form (Lin and Lobel, 2001) (Fig. 2). After cleavage of the signal peptide and glycosylation, a fraction of the 547-amino acid pro form is secreted from the cell. With a *pI* of 6.5, it diffuses into the local milieu, where it is picked up by cells via mannose 6-phosphate receptor-mediated endocytosis. After uptake, it is deliv-

ered to lysosomes, where the acidic pH induces cleavage of the propeptide at residues 195–196, resulting in a 367-residue, 46-kDa, active, mature form of the TPP-I protein.

The mature form of TPP-I functions as a tripeptidyl peptidase (Peltonen *et al.*, 2000). It also may have a role in the protection of cells from apoptosis (Puranam *et al.*, 1997). *In vitro* studies have demonstrated that addition of the pro form to cells derived from individuals with LINCL results in transport of the protein to lysosomes and significant amelioration of accumulation of the abnormal accumulated storage products (Lin and Lobel, 2001).

RATIONALE FOR *IN VIVO* GENE THERAPY FOR THE CNS MANIFESTATIONS OF LINCL

There are significant challenges for the development of a therapy for LINCL, including the inability of proteins to cross the blood–brain barrier (Bosch *et al.*, 2000); the pathology of the disease being throughout the brain (Mole, 1999), making it necessary to target the largest possible volume of the brain; potential toxicity due to overexpression of therapeutic protein; and immune responses to the delivery vehicle or TPP-I protein. The therapeutic strategies that have been considered for the treatment of this disorder, including enzyme augmentation therapy, allogeneic stem cell therapy, and gene therapy, have been reviewed in detail (Sondhi *et al.*, 2001). Importantly, because of the blood–brain barrier, neither the pro form nor the mature form of the protein can be effectively delivered to the brain via a vascular route, that is, the therapy (protein or gene) must be delivered directly to the CNS. Although extracellular delivery of the pro form will correct the abnormality, the half-life of the protein is 12 days (Lin and Lobel, 2001). Because it is impractical to repetitively deliver proteins to the CNS, a major advantage of gene therapy is that, once delivered to the CNS, it has the potential to be a constant source of the pro form of TPP-I within the brain.

Gene therapy can be viewed as a drug delivery system, in which the cDNA gene product is the drug of interest. In the present study, the coding regions of the *CLN2* gene will be delivered as a cDNA, and the gene product is the TPP-I protein. One clear advantage of the gene therapy approach is the sustained release nature of the transgene product without the need for repeat administration or indwelling catheters, as would likely be required if the strategy of direct protein administration were used. LINCL has several features that make it a good candidate for gene therapy. First, the disease is caused by mu-

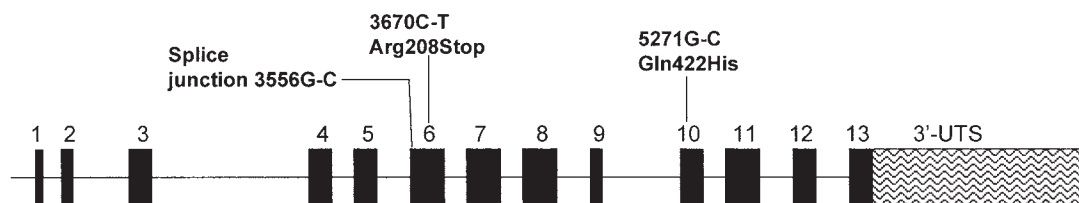


FIG. 1. Schematic diagram of the *CLN2* gene, showing the positions of the three most common mutations associated with LINCL. Adapted from Sondhi *et al.* (2001).

TABLE 1. KNOWN MUTATIONS OF THE *CLN2* GENE LINKED TO LINCL^a

Mutation ^b	Type	Location	Consequence	Frequency (%) ^c
1917C-T	Nonsense	Exon 3	Gln66Stop	2
1946A-G	Splice junction mutation	Exon 3	Generation of cryptic splice junction	1
1950G-A	Missense	Exon 3	Gly77Arg	1
3081-3091del	Deletion	Exon 4	Frameshift	2
3084C-T	Nonsense	Exon 4	Arg127Stop	1
3556G-A	Splice junction mutation	Intron 5	Aberrant splicing	3
3556G-C	Splice junction mutation	Intron 5	Aberrant splicing	38
3670C-T	Nonsense	Exon 6	Arg208Stop	32
4023T-A	Missense	Exon 7	Ile287Asn	1
4188A-G	Splice junction mutation	Intron 7	Generation of cryptic splice junction	1
4288-4295del	Deletion	Exon 8	Frameshift	3
4346G-A	Missense	Exon 8	Glu343Lys	3
4396T-G	Splice junction mutation	Intron 8	Aberrant splicing	1
4654T-C	Missense	Exon 9	Cys365Arg	1
4655G-A	Missense	Exon 9	Cys365Tyr	4
5159T-A	Missense	Exon 10	Val385Asp	1
5171G-A	Missense	Exon 10	Gly389Glu	4
5271G-C	Missense	Exon 10	Gln422His	8
5457G-A	Missense	Exon 11	Arg447His	2
5478C-A	Missense	Exon 11	Ala454Glu	1
5541C-T	Missense	Exon 11	Ser475Leu	1
6025G-C	Splice junction mutation	Intron 12	Aberrant splicing	1
6069InsA	Insertion	Exon 13	Frameshift	1
6151-6152delTC	Deletion	Exon 13	Frameshift	2

^aReproduced from Sondhi *et al.* (2001).

^bNucleotide number in gene followed by sequence change of wild type to mutant.

^cFrequency of occurrence among 57 individuals with LINCL; two mutations; 3556G-C and 3670C-T, together represent 60% of all mutations associated with the 114 alleles (both mutant alleles from each individual studied) (Sleat *et al.*, 1999).

tations in a single gene, it is a classic autosomal recessive disorder, and the missing/deficient protein has been characterized (Liu *et al.*, 1998). Comparisons of LINCL genotype and phenotype suggest that levels of TPP-I that are 5 to 10% of nor-

mal are associated with a less severe form of the disease with delayed age of onset and mortality (Sleat *et al.*, 1999) (K.E. Wisniewski and N. Zhong [Institute for Basic Research in Developmental Disabilities, Staten Island, NY], and R.M. Bous-

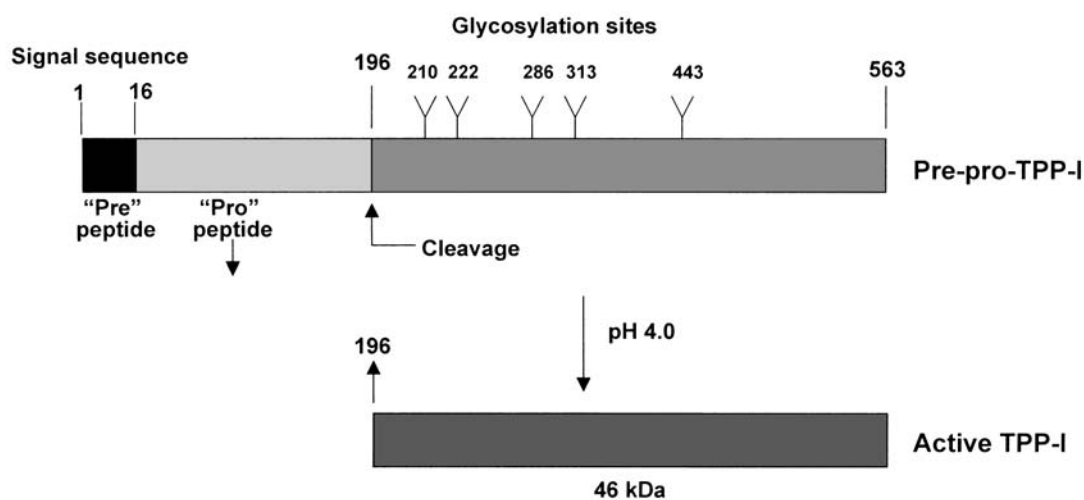


FIG. 2. Primary structure of the TPP-I protein. The *CLN2* open reading frame encodes a 563-amino acid product (pre-pro TPP-I). The signal sequence (amino acids 1–16) directs nascent protein to the secretory pathway with insertion into the endoplasmic reticulum and glycosylation at the sites indicated. The 563-residue pre-pro TPP-I is cleaved to form the 547-residue pro-TPP-I; this form is inactive until exposed to low pH in the lysosomes, which results in proteolytic cleavage at amino acids 195–196 to yield the active mature product of 367 residues (46 kDa). Adapted from Sondhi *et al.* (2001).

tany [Duke University Medical Center, Durham, NC], personal communication). In this regard, the severe phenotype of specific regions within the brain should be ameliorated if 5 to 10% of normal TPP-I levels can be achieved within those regions. Second, the protein is secreted and is capable of cross-correcting neighboring cells (Lin and Lobel, 2001). Thus, it is not necessary to transfer the normal *CLN2* cDNA to all of the cells in the CNS, because the transduced cells will secrete TPP-I protein that will be picked up by, and thus correct, cells in the local milieu. Cross-correction occurs by the uptake of the TPP-I protein precursor (the pro form secreted by the vector transduced cells; see below) mediated by mannose 6-phosphate (M6P) receptors (Lodish *et al.*, 2000; Lin and Lobel, 2001). The M6P recognition moiety, added to the TPP-I protein precursor during posttranslational processing, binds to intracellular receptors, which shuttles some TPP-I precursor to the lysosomal compartment and the rest is secreted for eventual M6P mediated endocytosis and trafficked to lysosomes. The TPP-I is released into the acidic compartment, where it is processed and the receptor is recycled. The implication of this biology for gene therapy is that the cells infected by the viral vector carrying the normal therapeutic gene act as the source of the corrective enzyme that will cross-correct the noninfected neighboring cells, thereby increasing the distribution of the protein, and thus enhancing the potential for success of the therapy. Third, LINCL is a fatal disorder with no known therapy. The LINCL phenotype is inevitably fatal in childhood after progressive degenerative neurologic deterioration. This is important, because there are risks to the proposed therapy and this justifies the risks outlined in this document.

Viral gene transfer vectors efficiently transfer their genome to the nucleus of cells. These vectors are designed to be "replication deficient" by removal of genetic information required for viral replication. AAV2_{CUh}CLN2, a viral gene transfer vector that we will use to treat LINCL in this study, includes an expression cassette containing the human *CLN2* cDNA controlled by an constitutive promoter that functions well in brain cells (Fig. 3). The AAV2 gene transfer vector has the biological characteristics appropriate for effective *in vivo* gene transfer for LINCL. The AAV2 vector mediates long-term gene expression in the CNS in experimental animal models (Elliger *et al.*, 1999; Sferra *et al.*, 2000; Frisella *et al.*, 2001) and it has a proven track record of safety in several clinical trials (Wagner *et al.*, 1998; Kay *et al.*, 2000; Leone and Simeone, 2000; Aitken *et al.*, 2001; High, 2001; Glader *et al.*, 2002; Janson *et al.*, 2002). Other gene transfer vectors do not meet requirements of this clinical target: nonviral vectors have low efficiency and transient gene transfer/expression; murine retroviruses have low transduction efficiency *in vivo* and require target cells to be proliferating to transfer genes to the nucleus; herpes simplex virus has minimal data regarding safety; lentivirus has a limited safety record in humans; and adenoviruses, although robust, lead to transient gene transfer that is not suitable for a human clinical study requiring persistent expression. Different serotypes of AAV may have different tropism for specific cells in brain (Chiorini *et al.*, 1999; Chen *et al.*, 2000; Davidson *et al.*, 2000). Studies in rodents suggests that the AAV5 serotype may provide better transgene distribution after CNS gene transfer than the AAV2 serotype (Davidson *et al.*, 2000; Haskell *et al.*, 2003). However, AAV5 vectors have not been used in humans and therefore potential toxicity of AAV5-based vectors is unknown,

and the methods to produce GMP-quality AAV5 vectors have not been developed. For these reasons, for the clinical development pathway, we have chosen AAV2-based vectors as the gene transfer vehicle of choice.

ADENO-ASSOCIATED SEROTYPE 2 GENE TRANSFER VECTORS

The AAV2_{CUh}CLN2 vector is based on the serotype 2 adeno-associated virus. AAV is a small nonenveloped icosahedral parvovirus with a 4.7-kb single-stranded DNA genome. AAV2 is a naturally replication-defective virus that depends on adenovirus (Ad) or herpes simplex virus gene products for replication (Berns and Giraud, 1996). The absence of any detectable pathology from wild-type AAV2 infections coupled with its ability to remain latent promoted its development as a gene transfer vector (Backlow, 1988; Muzyczka, 1992; Carter, 2000). Recombinant vectors based on AAV2 are effective in long-term gene transfer to skeletal and cardiac muscle, liver, brain, and retina (Kessler *et al.*, 1996; McCown *et al.*, 1996; Fisher *et al.*, 1997; Flannery *et al.*, 1997; Koeberl *et al.*, 1997; Maeda *et al.*, 1998; Bennett *et al.*, 1999; Chen *et al.*, 2000; Paterna *et al.*, 2000). AAV2 vectors are designed in a fashion such that all viral genes are replaced by an expression cassette for the transgene, leaving intact the essential *cis* elements of the genome, the inverted terminal repeats (ITRs), DNA packaging signal, and the replication origin (Backlow, 1988). Replication and packaging of AAV2 vectors requires all AAV2 and Ad helper functions to be provided *in trans*.

AAV2 vectors have been used in numerous models of neurological disorders (McCown *et al.*, 1996; During *et al.*, 1998; Mandel *et al.*, 1998; Lo *et al.*, 1999; Skorupa *et al.*, 1999) and are currently in clinical trials for cystic fibrosis (Aitken *et al.*, 2001) and hemophilia (Kay *et al.*, 2000; High, 2001; Glader *et al.*, 2002), and two CNS disorders, Canavan disease (During *et al.*, 1998) and Parkinson disease (During *et al.*, 2001). In the CNS, AAV2 vectors are able to deliver genes to neurons, with little to no toxicity or immunogenicity (McCown *et al.*, 1996; Mandel *et al.*, 1998; Lo *et al.*, 1999; Skorupa *et al.*, 1999; During *et al.*, 2001). Expression is usually delayed, peaking a few weeks after infection and is sustained for extended periods, presumably because of the ability of the vector to insert transgenes randomly into the host cell genome, or to form extrachromosomal concatamers (Chen *et al.*, 2001). Extensive preclinical data using AAV2 in the treatment of animal models of neuronopathic lysosomal storage diseases support the concept of using AAV2 gene transfer vectors to treat CNS disorders. For example, AAV2 vectors, expressing β -glucuronidase, have been injected into the brain of mucopolysaccharidosis type VII (MPS VII) mice and have been shown to lead to long-term expression of the β -glucuronidase gene (Frisella *et al.*, 2001). The spatial distribution of expressed protein was increased over time, and the lysosomal storage deficit was corrected over a wide area that exceeded the area over which the vector had spread and exceeded the obvious distribution of the enzyme detected histologically. The clearance of the storage defect led to behavioral improvements in the AAV2-treated mice. Importantly, there is also a track record of safety in the administration of AAV2 to humans including direct delivery to lung, sinus, skeletal muscle, liver, and the CNS (Wagner *et al.*, 1998;

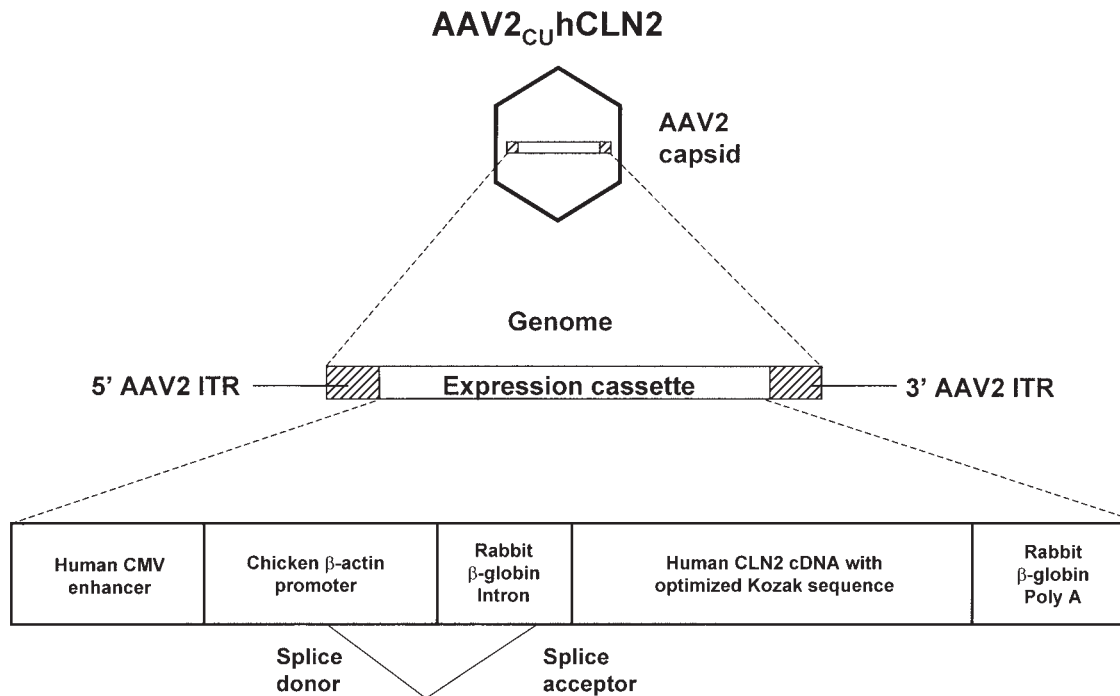


FIG. 3. Structure of the AAV2_{CU}hCLN2 vector. The vector consists of the AAV2 capsid enclosing the 4278 base single-stranded genome: there is expected to be an equimolar mixture of the two complementary strands. The genome consists of the two inverted terminal repeats of AAV serotype 2 (ITR, nucleotides 1–145 and 4531–4675 of GenBank J01901). The expression cassette comprises the human cytomegalovirus (CMV) enhancer [nucleotides 558–925 of GenBank x03922]; the chicken β -actin promoter/splice donor and 5' end of intron [nucleotides 268–1530 of GenBank x00182]; the 3' end of the rabbit β -globin intron and splice acceptor [nucleotides 1457–1551 of GenBank J00659]; the human cDNA for *CLN2* with an optimized Kozak translation initiation signal [nucleotides 13–1704 of GenBank BC014863]; and the polyadenylation/transcription stop from rabbit β -globin [nucleotides 1546–1827 of GenBank J00659].

Kay *et al.*, 2000; Leone and Simeone, 2000; Aitken *et al.*, 2001; High, 2001; Glader *et al.*, 2002; Janson *et al.*, 2002). There are two ongoing clinical CNS AAV2 studies: a phase I clinical trial using an AAV2 vector delivered intracranially to express aspartoacylase in the brain of children suffering from Canavan disease (Leone and Simeone, 2000; Janson *et al.*, 2002) and a phase I clinical trial using an AAV2 vector delivered intracranially to express two isoforms of the enzyme glutamic acid decarboxylase (GAD-65 and GAD-67) in the brain of adults with Parkinson disease (During *et al.*, 2001).

The strategy proposed in this protocol is for the intracranial delivery of an AAV2 vector encoding the human *CLN2* cDNA. The advantages of this direct injection strategy to treat LINCL include bypassing the blood–brain barrier and long-term expression of the transgene product (TPP-I) in the organ (brain) that is most affected.

OVERVIEW OF THE PROPOSED STUDY

The proposed clinical protocol of gene therapy for LINCL is designed to determine the safety/toxicity of direct administration of the AAV2_{CU}hCLN2 vector to the brain of children with LINCL, and to develop preliminary data regarding the ability of this therapy to prevent the progressive CNS deterioration inherent to this disorder. This strategy is based on the concept

that persistent expression of the normal *CLN2* cDNA in the CNS will result in the production of sufficient amounts of TPP-I to prevent further loss of neurons, and hence limit disease progression. The rationale for this approach is the knowledge that (1) genotype–phenotype correlations suggest 5 to 10% of normal TPP-I activity is sufficient to prevent clinical manifestations of LINCL (Sleat *et al.*, 1999); (2) TPP-I is secreted as a stable, precursor form and taken up by surrounding cells, and thus transfer and persistent expression of the normal *CLN2* cDNA in only a fraction of CNS cells should result in cross-correction of large numbers of cells (Lin and Lobel, 2001); (3) AAV2 vectors are capable of effectively transferring genes *in vivo* to the CNS neurons, where the gene is expressed on a persistent basis with negligible toxicity (McCown *et al.*, 1996; During *et al.*, 1998; Mandel *et al.*, 1998; Lo *et al.*, 1999; Skorupa *et al.*, 1999); (4) there is clinical experience using AAV2 vectors to safely transfer genes to human organs, including the CNS (Wagner *et al.*, 1998; Kay *et al.*, 2000; Leone and Simeone, 2000; Aitken *et al.*, 2001; During *et al.*, 2001; High, 2001; Glader *et al.*, 2002); and (5) preclinical data in rats and non-human primates demonstrate that it is feasible to use an AAV2 vector to deliver the normal *CLN2* cDNA to the CNS of experimental animals, with persistent expression of TPP-I.

The study will be carried out in two populations of children with LINCL. Group A will include $n = 4$ children with a total disability score of 0 to 4 (the severe forms of the disease; the

staging is based on a modification of the scale of Steinfeld *et al.* [2002], as detailed in the section End-Point Variables). Group B will include $n = 6$ children with a total disability score of 5 to 6, a moderate stage of the disease. All of the study population of 10 children (group A, $n = 4$ and group B, $n = 6$) will receive 3.6×10^{12} particle units of the AAV2_{CU}hCLN2 vector divided among 12 locations delivered through 6 burr holes (2 depths through each hole), 3 burr holes per hemisphere. The choice of the locations for the burr holes and catheter placement will be on a case-by-case basis because of the diffuse and variable nature of the disease presentation. The following criteria will guide selection of the sites of administration: (1) safety, (2) opportunity to achieve the broadest distribution throughout the CNS (other than the cerebellum and brainstem), and (3) protection of functional regions of the brain relevant to the disease. The choice of injection areas will be based on the neurological examination (see Appendix I for the standard format to be used) and CNS magnetic resonance imaging/magnetic resonance spectroscopy (MRI/MRS) assessment carried out the day before administration. Specifically, the criteria for site selection will include the following: (1) for safety reasons, no injections will be made into potentially risky areas (e.g., blood vessels, cysts, malformations, white matter tracts, Broca's area); (2) the broadest distribution possible will be achieved by administration to the frontal, parietal, and occipital cortices in both hemispheres; and (3) the effort to "protect functional regions of the brain" will be based on correlations between the neurological clinical observations and brain MRI findings, such that injections will be targeted toward parts of the brain that are judged to contain "salvageable" tissue (this criterion allows for a potential for correction that is likely to change the rate of decline in the LINCL rating scale). Each injection will involve vector deposition at two depths, neither of which is greater than 45 mm from the surface of the brain.

Regarding assessment of safety, routine clinical parameters will be used, as well as neurologic-specific parameters; these are detailed in the next section (Details of the Experimental Design). Regarding efficacy, the subject population will be assessed over time after treatment to obtain preliminary data regarding the efficacy of the therapy. The primary end-point variable will be the assessment of specific regions of the CNS to which the AAV2_{CU}hCLN2 vector is administered based on MRI and MRS (see below, End-Point Variables). All efficacy parameters will be assessed by comparing two baseline evaluations with evaluations 6 months and 18 months after vector administration.

DETAILS OF THE EXPERIMENTAL DESIGN

The clinical study is designed to assess the safety/toxicity and to develop preliminary efficacy data resulting from direct intracranial administration of the AAV2_{CU}hCLN2 vector to the brain of children with LINCL. Subjects for this study will be recruited from direct referrals to the principal investigator with the help of relevant foundations and support groups. The proposed protocol will include 10 individuals and will be divided into two parts. Group A, to be studied first, will include four individuals with the severe form of the disease. Group B of the trial will include six individuals with a moderate stage of the

disease. On the basis of recommendations of the Food and Drug Administration (FDA), subjects will be treated sequentially, with at least a 2-week follow-up period completed for all previously treated subjects. For both groups, two baseline evaluations will be performed to determine eligibility and establish baseline values for safety and efficacy parameters. Each individual will undergo two baseline evaluations that will include a general assessment (history, physical examination, vital signs, respiratory rate, temperature, and weight); general blood (chemistry, hematology, and coagulation) and type and screen; urine analysis; human immunodeficiency virus (HIV) test; vector-related tests (serum anti-AAV antibody levels), LINCL rating scale assessment, and MRI/MRS assessment. Genetic testing will be carried out as part of this research study. The DNA will be banked for verification of tests at the Arthur and Rochelle Belfer Gene Therapy Core Facility (515 East 71st Street, Room S1000, New York, NY 10021). DNA samples will be sent out for genomic analysis to the Institute for Basic Research in Developmental Disabilities (IBR), which is the research component of the New York State Office of Mental Retardation and Developmental Disabilities (1050 Forest Hill Road, Staten Island, NY 10314-6330). It will not be used for any other purpose.

Assessment of the children, decisions regarding eligibility and the order of participation, and decisions regarding regions of administration will be made by four coinvestigators in the study: Mark Souweidane, M.D., or Michael Kaplitt, M.D., the neurosurgeons who will be administering the vector; Syed Hossain, M.D., a pediatric neurologist; and Stefan Worgall, M.D., a general pediatrician. The principal investigator of the study, Ronald Crystal, M.D., will not participate in these decisions. Procedures involved in the protocol will be performed at New York Presbyterian Health Care System-Weill Medical College of Cornell University under the auspices of the Children's Clinical Research Center. After the acute hospitalization for surgery, follow-up visits will occur as outpatient visits at New York Presbyterian Hospital-Weill Cornell Medical Center (NYPH-WCMC). Day 14, Month 2, and Month 3 visits may be done at study individual's personal physician's office, but the findings will be recorded into the study database and the findings will be reviewed by the investigators. There will be no cost to the study individuals resulting from the research-related procedures in this protocol. The costs of travel and accommodations outside of the NYPH-WCMC for the family and the subjects will be the responsibility of the families of the study participants.

The study population that meets the entry criteria will be unblinded and separated into two groups (group A, $n = 4$ and group B, $n = 6$; Table 2). Each individual will receive a total

TABLE 2. STUDY GROUPS^a

Group	n	Vector	Total dose ^b (particle units)
A	4	AAV2 _{CU} hCLN2	3.6×10^{12}
B	6	AAV2 _{CU} hCLN2	3.6×10^{12}

^aAll subjects will receive the study drug at the same dose.

^bEach total dose will be divided among 12 locations delivered through 6 burr holes (2 depths through each hole), 3 burr holes per hemisphere.

dose of 3.6×10^{12} particle units of AAV2_{CUh}CLN2, divided among 12 locations delivered through 6 burr holes (2 depths through each hole), 3 burr holes per hemisphere.

The exact locations of the administration of the vector will be decided on a case-by-case basis as described above. Preoperative MRI will be used to guide the sites for the regions of administration and hence the burr holes. For standardization, the coronal sutures and bony landmarks of the cranium will be used to draw a line in the sagittal plane on the MRI. There will be 12 target sites per brain delivered through 6 burr holes (2 locations at varying depths through each hole) with 3 in each hemisphere.

Neurosurgical administration of AAV2_{CUh}CLN2 will involve drilling six small burr holes in the calvarium under general anesthesia in order to gain access to defined subcortical regions of the brain with a fine catheter. Individuals will be prepared for anesthesia and surgery in the standard fashion. They will fast from food and liquids after midnight, prior to the surgical procedure. Individuals will be transported to the operating room where monitors (three-lead modified EKG, pulse oximeter, capnography [a monitor that displays the level of exhaled carbon dioxide in the breathing tube]) will be applied; routine premedications will be administered as needed. Subjects will require a radial arterial line for continuous blood pressure monitoring and blood sampling.

The individual's head will then be prepped and draped, as anatomically indicated, in a standard sterile fashion using a betadine/alcohol solution. At the completion of successful burr holes (see above), catheters will be put in place. Intravenous mannitol (typically 1.0 g/kg, but at the anesthesiologist's discretion) may be given as needed to reduce brain edema throughout the period of vector administration.

A total of 3.6×10^{12} particle units of the AAV2_{CUh}CLN2 vector will be administered to the whole brain. The vector will be administered to each of the six sites in parallel. Each of the six sites will receive 0.6×10^{12} particle units, half at one site at the bottom of the needle track and half at a site approximately half-way up the needle track. The vector will be delivered by a microperfusion pump that accommodates six syringes simultaneously. The vector will have a concentration of approximately 2.0×10^9 particle units/ μ l, and will be delivered at 2.0 μ l/min at each site for a total of 300 μ l/site (6.0×10^{11} particle units/site). After the specified dose is administered to the six sites, the catheters will remain in place for 5 min to assure tissue penetration. The catheters will be withdrawn to approximate half-way from the bottom of the needle track to the brain surface, and the remaining 50% of the dose will be administered, in parallel, to each of the six sites exactly as described above. After the period of vector administration (estimated to be 2.5 to 3.0 hr), the surgical wounds will then be closed by standard techniques. A postoperative MRI will be performed within the first 48 hr after the surgical procedure. The exact time the MRI will be performed will be determined at the discretion of the neurological team. Each patient will be monitored postoperatively in a recovery room or intensive care unit until he/she is stable to be transferred to the Children's Clinical Research Center unit. Individuals will be discharged from the hospital at the discretion of the attending neurosurgeon. The total length of hospitalization is estimated at less than 7 days, assuming no postoperative complications occur (Janson *et al.*,

2002). The assessment will be carried out on the basis of the timeline in Table 3.

END-POINT VARIABLES

The primary end-point variable will include neurological assessment, using the LINCL clinical rating scale. The secondary end-point variable will be derived from MRI and MRS assessments of the CNS in regions of vector administration. All efficacy parameters will be assessed by comparing baseline evaluations with evaluations at time points after vector administration. There will be two pretherapy evaluations of all end points (the "screening" and "pretherapy" assessments) and two posttherapy evaluations, one at 6 months and one at 18 months.

Primary end point

The primary end point for the trial is neurological assessment, using the LINCL clinical rating scale. The neurological examination will be carried out according to a standard format (see Appendix I) with input from the parents/legal guardians as relevant. The clinical rating scale, referred to as a "CNS disability scale," is made up of individual sums of four-point scales for each of three activities; the ratings for each activity are summed, giving a CNS disability score. Each of the activities are rated 0 to 3, where 0 is the most severe form of the disease (see Table 4) (Steinfeld *et al.*, 2002). This scale, developed by Steinfeld *et al.* (2002), originally included the four major functional problems in LINCL (loss of motor performance, seizure activity, loss of vision, and loss of language). To adapt this scale to make it relevant for gene therapy for the CNS manifestations of LINCL, the vision part of the scale has been eliminated. In the modified clinical rating system, these are now three categories (Fig. 4 and Table 4). The seizure scores are included in the CNS disability score; because these children are conventionally treated with antiseizure medications, the seizure score may or may not have a significant impact, depending on the success of the antiseizure therapy. The score without the vision function is referred to as the "CNS disability score," and includes motor performance, seizure activity, and loss of language. To determine the CNS disability score for entry into the gene transfer protocol, the three individual categories (motor function, seizure activity, and language) are summed (Table 5).

The proposed gene transfer protocol includes 10 individuals, divided into 2 groups. Group A will include four individuals with the severe form of the disease (rated to have an average total disability score of 0 to 4). Group B of the trial will include six individuals who have been rated an average total disability score of 5 or 6 on the clinical rating scale (a moderate form of the disease).

Secondary end point

The secondary end-point variable will be the MRI/MRS assessment of the CNS in regions of vector administration. Anatomical measurements of brain parenchymal volume will be combined with proton spectroscopic imaging of the *N*-acetyl-

TABLE 3. TIMELINE OF THE STUDY^{a,b}

Category	Screening ^c	Pretherapy ^c	Day			Month						Years 3–15 ^d
			0	7	14	1	2	3	6	12	18	
AAV2 _{CU} hCLN2 administration ^c			■									
General assessment ^f	■											
Safety parameters												
General ^g	■	■		■	■	■	■	■	■	■	■	
Weight	■	■							■		■	
Blood												
CBC ^h	■	■		■		■			■	■	■	
ESR ⁱ	■	■										
Clotting ^j	■	■		■		■			■	■	■	
Chemistry ^k	■	■		■		■			■	■	■	
HIV	■											
Future (serum) ^l	■	■		■		■			■	■	■	
Type and screen ^m		■										
CLN2 genomic analysis ^f	■											
Urinalysis ⁿ	□	□		□		□			□	□	□	
Pregnancy test (urine) ^o	■											
EKG ^p	■	■										
Neurological assessment ^q	■	■		■	■	■			■		■	
Chest X-ray ^r	■	■				■			■		■	
MRI ^s			■									
Ophthalmology ^t	■											
Vector-related ^u												
Anti-AAV2 antibodies		■				■			■	■	■	
Future (WBC)		■		■							■	
FDA-mandated annual follow-up ^c												■
Efficacy parameters												
LINCL rating scale	■	■				■			■	■	■	
MRI/MRS ^v	■	■							■		■	

Symbols: ■, test required; □, test optional.

^aParameters listed are mandatory for the study; additional parameters will be assessed at the discretion of the physician caring for the individual, based on general medical practice for similar neurosurgical procedure in this age group; as there is no way to separate the acute postoperative effects on these parameters from those secondary to the vector per se, they are not included as mandatory for the protocol.

^bThe acceptable time windows for the assessment days are as follows: Screening parameters—6 months to 2 weeks before vector administration; baseline—2 weeks to –1 day before vector administration except for the MRI/MRS, which must be done within 24 hr of vector administration; for the assessments after vector administration:

Assessment	Number of days acceptable		
	±2	±5	±30
Day 7	■		
Day 14	■		
Month 1		■	
Month 2	■		
Month 3			■
Month 6			■
Month 12			■
Month 18			■
Years 3–15			■

^cThere will be two sets of baseline parameters obtained for the study: one will be referred to as the “screening” studies and the other as “pretherapy” studies. The screening studies can be carried out within 6 months to 2 weeks before administration of the vector. It is acceptable that the safety parameters for the screening studies be done outside of NYPH-WCMC, but the efficacy parameters must be done at NYPH-WCMC (it is acceptable if they are done for clinical purposes or another nontherapeutic protocol). The pretherapy studies must be carried out within 2 weeks of administration of the vector, with the exception of the MRI/MRS study, which must be done within 24 hr of administration of the vector; if greater than 2 weeks before administration of the vector, then all of the parameters must be reevaluated (listed as pretherapy).

TABLE 3. TIMELINE OF THE STUDY^{a,b} (CONT'D)

^dAs per the mandate of the FDA following the recommendations of the Biologic Response Modifiers Advisory Committee, all subjects in gene therapy trials must be monitored for a period of 15 years after vector administration.

^eTotal dose, 3.6×10^{12} particle units, in 12 equally divided doses; see text for details.

^fThe general assessment will be used to make the diagnosis of LINCL on clinical grounds plus *CLN2* genomic analysis; prior genomic analysis will be accepted.

^gGeneral—medical history, physical examination, vital signs (blood pressure, heart rate, respiratory rate, temperature).

^hCBC—hematocrit, hemoglobin, white blood count, differential, platelets.

ⁱESR—erythrocyte sedimentation rate.

^jClotting—prothrombin time, partial thromboplastin time.

^kChemistry—sodium, potassium, chloride, total CO₂, blood urea nitrogen (BUN), glucose, magnesium, uric acid, phosphate, creatinine, alanine amino transferase (SGPT), aspartate amino transferase (SGOT), calcium, serum total protein, albumin, alkaline phosphatase, bilirubin (total).

^lFuture (serum)—serum sample frozen for future use.

^mType and screen—blood type and screen to be performed as part of pretherapy tests before surgical procedure.

ⁿUrinalysis—appearance, specific gravity, pH, protein, glucose, ketones, bilirubin, hemoglobin, number and type of cells, characterization of sediment.

^oPregnancy test (urine): required for pubertal females.

^pEKG—electrocardiogram.

^qNeurological assessment—level of consciousness, speech, language, cranial nerves, motor strength, motor tone, abnormal movements, reflexes, upper extremity sensation, lower extremity sensations, gait, Romberg, nystagmus, coordination. Daily pediatric neurological assessments will be taken after day 0 vector administration and the data will be collected on days 1–7 and/or while the child is in-hospital in the ICU and Children's Clinical Research Center.

^rPosteroanterior and lateral.

^sMRI at 0 to 2 days for clinical postoperative care only (exact time will be determined at the discretion of the neurosurgeon); where the MRI/MRS efficacy assessments will all be carried out with the same MRI scanner, the MRI for postoperative clinical care will be carried out at the MRI scanner convenient for postoperative care.

^tEye test—routine ophthalmologic examination; this will be carried out as part of the screening study only, to help define the overall status of the LINCL.

^u"Vector-related" studies will include assessment of anti-AAV2 neutralizing antibodies and a sample of white blood cells (WBCs) to be reserved for future studies.

^vMagnetic resonance imaging (MRI)/magnetic resonance spectroscopy (MRS)—see text for details; all studies will be carried out on the same scanner located in New York Presbyterian Hospital. The scanner is a 3.0-T whole body system with an included head coil.

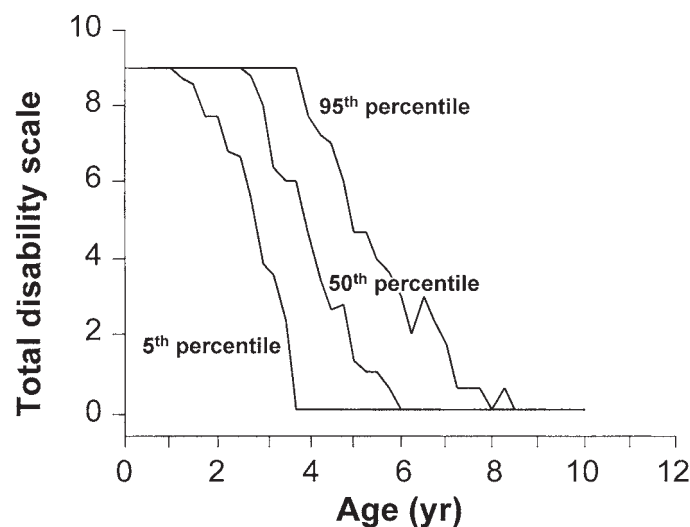


FIG. 4. CNS disability score obtained from 16 patients with *CLN2* mutations (modified from Steinfeld *et al.*, 2002), eliminating the vision score; shown with median, 5th, 50th, and 95th percentile of scores.

TABLE 4. CATEGORIES COMPRISING THE CNS DISABILITY SCORING SYSTEM FOR LATE INFANTILE NEURONAL CEROID LIPOFUSCINOSES

<i>Functional category</i>	<i>Rated as</i>	<i>Performance</i>	<i>Score</i>
Motor function	Normal	Walks normally	3
	Slight abnormality	Frequent falls, clumsiness obvious	2
	Moderate abnormality	No unaided walking or crawling only	1
	Severe abnormality	Immobile, mostly bedridden	0
Seizures ^a	Normal	No seizures per 3-month period	3
	Slight abnormality	1 or 2 seizures per 3-month period	2
	Moderate abnormality	1 seizure per month	1
	Severe abnormality	>1 seizure per month	0
Language	Normal	Normal	3
	Slight abnormality	Recognizably abnormal	2
	Moderate abnormality	Hardly understandable	1
	Severe abnormality	Unintelligible or no language	0

^aOn current medications as prescribed by their physician.

aspartate (NAA) resonance, a neuronal marker measurable by clinical magnetic resonance techniques (Birken and Olandorf, 1989). A 3.0-T magnetic resonance imaging system will be used for all measurements combined with the standard head resonator provided by the vendor. T₁- and T₂-weighted images will first be acquired over the whole brain during each scanning session. This will be followed by three-dimensional multivoxel proton spectroscopic imaging. Voxel sizes on the order of 8 mm³ will be used with a scan time of 15–20 min. Postprocessing will include calculation of parenchymal volumes in the regions of vector administration from the T₂-weighted series, and measurement of peak areas of NAA, using software developed in-house. The NAA peak area will be compared with neighboring resonances such as choline and creatine, and in addition calibrated against an external reference standard containing MR-visible brain metabolites including NAA at millimolar concentrations. The sensitivity profile of the head resonator will be mapped in advance to allow quantitative comparisons between the NAA peak area and the standard. While requiring a greater degree of subject cooperation than conventional MR scans, functional imaging end points, if attainable, could be directly compared with the clinical rating scale used as the primary end point. If possible, the total scan time for each subject will be designed to be completed within 90 min.

REVIEW AND MONITORING

The study will not commence without appropriate Institutional Review Board (IRB), Institutional Biosafety Committee (IBC), Children’s Clinical Research Center (CCRC), NIH DNA Recombinant Advisory Committee (RAC), and Food and Drug Administration (FDA) submissions and approvals as relevant. The clinical study will be carried out under the auspices of the Department of Genetic Medicine Clinical Operations and Regulatory Affairs (CORA) Core. Standard Operating Procedures (SOPs) are in place, describing the role and responsibilities of all participants. Case report forms will be prepared to collect all data described in the timelines. Eligibility forms will be prepared relevant to the inclusion/exclusion criteria and will be

signed by three physicians, who will verify that the individual meets the inclusion/exclusion criteria. Adverse events will be recorded on forms that will be prepared and graded on the basis of a toxicity scale (see Toxicity Scale, Appendix II). The principal investigator will review, sign, and date all adverse event forms. All adverse events (AEs) and serious adverse events (SAEs) will be reported to the Data Safety Monitoring Board of Weill Medical College (WMC), the local Institutional Review Board (IRB) and Institutional Biosafety Committee (IBC), the Children’s Clinical Research Center (CCRC), the NIH DNA Recombinant Advisory Committee (RAC), and the Food and Drug Administration (FDA) under regulations and guidelines relevant to each. A Research Coordinator on site, under the supervision of the CORA Core, will record the data and adverse events on the relevant forms. The CORA Core will have the responsibility of forwarding the adverse events reports to the RAC and FDA as relevant under their regulations and guidelines.

STATISTICAL CONSIDERATIONS

Individuals (other than the principal and coprincipal investigators) collect and tabulate the clinical parameters, using standard methods for clinical studies. The principal investigator and the CORA Core have extensive experience in clinical data management and verification, using standard methodology, including reporting requirements for regulatory groups. Consultation

TABLE 5. CNS DISABILITY SCORE CATEGORIES

<i>Rating</i>	<i>Sum of functional categories</i>
Normal	9
Mild	7–8
Moderate	5–6
Severe	0–4

^aThe “severe” range is broader than the mild and moderate range to reflect the fact that, for most, but not all, cases the seizure activity is controlled adequately by medications, and thus will usually contribute a seizure score of 3 (see Table 4).

on the statistical analysis will be done through the statistical consultant of the General Clinical Research Center (GCRC) of NYPH-WMC; the Weill Cornell group has used these resources for all other gene therapy studies. The end-point variables and the assessment of safety include a variety of parameters as discussed above. From the preliminary studies, we expect that the study will be safe and will show changes in end-point variables. However, should the results prove otherwise, depending on consultations with the appropriate regulatory groups, additional study individuals may be added to help answer specific questions.

To complete the trial via enrollment at a single study site in a reasonable amount of time (see the timeline in Table 3), and based on the available resources and subject population, a total of 10 subjects is a realistic recruitment goal for this trial. All efficacy parameters will be assessed by comparing baseline evaluations, to evaluations at time points after vector administration.

For this small trial, no formal statistical analysis will be carried out because the n value is too small. However, “response” will be defined as a subject maintaining his/her baseline disability score. As a guide to decision making: if all six subjects in group B with moderate disability fail to maintain their score, then it can be concluded that the response rate is less than 40% ($p < 0.05$). Confidence intervals for response rates will necessarily be wide with a sample size of six, but will be computed by exact methods.

TIMELINE

The project will take 17.5 to 18 years to complete. This is based on the following considerations. Accrual of the 10 subjects will occur over a period of 1 year. Each subject will be assessed for 1.5 years for safety and efficacy parameters (see the timeline in Table 3), for a total of 2.5 years. As per the mandate of the FDA, following the recommendations of the Biologic Response Modifiers Advisory Committee (Food and Drug Administration, 2004), all subjects in gene therapy trials must be monitored for a period of 15 years after vector administration, for a total of 17.5 to 18 years, depending on when the first and last subjects are dosed.

Yr 01. Produce, characterize, and test the AAV2_{CU}hCLN2 vector, gain approvals from the regulatory groups, develop the case report forms, and establish other monitoring parameters. Initiate the clinical study.

Yr 02–03. Complete recruitment of 10 individuals into the study.

Yr 04–05. Perform follow-up and analyze data.

Yr 03 to 17.5–18. Perform follow-up as mandated by the FDA (see Appendix III).

INCLUSION/EXCLUSION CRITERIA

The following is applicable to both groups A and B as indicated.

All individuals who meet the following criteria will be included without bias as to gender or race/ethnicity.

Inclusion criteria

1. A definitive diagnosis of late infantile neuronal ceroid lipofuscinosis, based on clinical phenotype and genotype, with *CLN2* gene mutations known to be associated with the disease.
2. The subjects must be between the age of 4 and 18 years.
3. All subjects will be naive, that is, they will not have previously participated in a gene therapy study for Batten disease.
4. Parents of study participants must agree to comply in good faith with the conditions of the study, including attending all of the required baseline and follow-up assessments.
5. Both parents or legal guardians must sign the child's informed consent form.
6. For group A, subjects will have an LINCL average total disability score of 0 to 4, the severe form of the disease.
7. For group B, subjects will have an LINCL average total disability score of 5 to 6, a moderate form of the disease.

Exclusion criteria

1. Patients with other significant medical or neurological conditions, particularly those that would create an unacceptable operative risk or risk to receiving the AAV2_{CU}hCLN2 vector. Examples include malignancy (other than skin cancer), congenital heart disease, liver or renal failure, or seropositivity for HIV. Each case will be individually reviewed and the final decision shall rest with the Eligibility Committee composed of three physicians other than the principal investigator, including a pediatric neurosurgeon, pediatric neurologist, and general pediatrician.
2. Individuals with heart disease that would be a risk for anesthesia.
3. History of hemorrhage or major risk factors for hemorrhage (e.g., abnormally low platelet counts).
4. Concurrent participation in any other FDA-approved Investigational New Drug clinical protocol is not allowed, although the principal investigator will work with other doctors to accommodate specific requests (e.g., a study of nutritional supplements probably would not be a disqualification).
5. Individuals who are at risk during MRI/MRS scans, including those with (a) a heart pacemaker and/or related implants, (b) a metal fragment/chip in the eye or other site(s), (c) an aneurysm clip in the brain, and (d) metallic inner ear implants.

RISKS OF THE STUDY

Delivery of the vector and surgical procedures

Regarding risks of delivery of the vector, the vector will be directly administered to the defined regions of the brain by injection under general anesthesia (for the surgery). The risks of vector administration are minimal compared with the surgery, including catheter placement. Risks of direct injection of the vector into the brain include the theoretical risk of bleeding, infection from the catheter, edema, and nerve damage. Risks of the actual administration of vector will be minimized by the slow infusion rate (2.0 μ l/min for each site) and small total volume infused (300 μ l for each site). Risks of the surgi-

cal procedure include pain or discomfort, nausea, vomiting, fever, edema, intracranial hemorrhage, seizures, infection, neurological deficit, stroke, anesthetic complications, electrolyte changes, paralysis, coma, or death (Janson *et al.*, 2002). After surgery, an intravenous line will be inserted into the subject's arm to administer fluids, nutrition, and/or medications. The risks linked with this procedure include pain, bruising, swelling, or blistering where the needle is put in the vein, damage to the vein, or rarely infection. For individuals selected on the basis of the inclusion/exclusion criteria listed above, long-term risks from the surgical procedures are minimal, but because of the invasive nature of surgery, including the placement of the catheter, unrelated to the delivery of the vector or the vector per se, it is expected that a variety of minor and major adverse events will occur.

AAV2_{CU}hCLN2 vector

Administration of the AAV2_{CU}hCLN2 vector has a number of risks. The first is an inflammatory response to vector administration. There is usually a mild local inflammatory response to administration of low doses of viral gene transfer vectors as proposed in this study, but this reaction is generally local and transient. Compared with controls, no significant inflammation was observed in experimental animals (rats, nonhuman primates) in the formal toxicology studies.

AAV vectors offer the possibility of insertional mutagenesis, in which the AAV genome inserts into the cellular genome at or close to a gene that regulates cell growth. This could result in loss of a level of control of cell division and increase the probability that the affected cell could progress toward cancer. The level of risk for AAV vectors is unknown although this mechanism has occurred in a clinical study using a retrovirus vector (an unrelated gene transfer vector) (Hacein-Bey-Abina *et al.*, 2003; McCormack and Rabbitts, 2004). To date, toxicology testing on the AAV2_{CU}hCLN2 vector and other AAV2-based vectors has not shown any evidence of such insertional mutagenesis.

In LINCL subjects who have no endogenous TPP-I activity, there is a possibility of an immune response against the TPP-I protein expressed by the vector. This reaction is not expected because the most common mutations in the *CLN2* gene result in the production of an inactive protein, nearly identical to the vector-derived protein and therefore unlikely to be immunogenic.

In the immediate area of AAV2_{CU}hCLN2 injection there may be local overexpression of TPP-I. The consequences of local TPP-I overexpression are unknown, but toxicology studies on rats and monkeys injected with the same vector have shown no toxicity resulting from long-term overexpression of TPP-I.

Adeno-associated virus may cause an immune response that may sensitize the study individual, resulting in an inability to participate in future studies of gene therapy using a similar adeno-associated virus vector.

Tests and procedures designed to evaluate effectiveness and safety

The following summarizes the risks involved in the tests and procedures described in this protocol. It should be noted that all the tests used are widely accepted tests in clinical medicine.

All tests are governed by regulatory bodies so that strict standards are upheld. These include limitations on the amount of blood that can be drawn and the amount of radiation the subjects can be exposed to in the protocol. All studies will be carried out by individuals with a great deal of expertise.

Blood. These involve drawing blood from a vein in the arm by usual venipuncture. The risks associated with the venipuncture procedure will include pain or bruising where the needle is put in the vein or, rarely, damage to the blood vessel. Rarely, people faint after blood drawing. The total amount of blood to be drawn per visit will be no more than 2.5% of the total blood volume, based on the child's age and weight. This amount is within the acceptable limits for human research according to the guidelines of the NYPH-WMC Children's Clinical Research Center (New York Presbyterian Hospital-Weill Medical College of Cornell University Children's Clinical Research Center, 2003).

MRI/MRS. Routine magnetic resonance testing itself involves no more than minimal risk. There is a strong (3.0 T) magnetic field, which exerts considerable force on paramagnetic or metal objects and disturbs electronic devices. Individuals who have (1) a heart pacemaker and/or related implants, (2) a metal fragment/chip in the eye or other site(s), (3) an aneurysm clip in the brain, or (4) metallic inner ear implants, cannot have an MRI scan as the magnetic field may dislodge the metal. All subjects or their parents/legal guardians will be required to complete a screening form before entry into the magnetic resonance scan room. To perform the MRI scan in the children, anesthesia is routinely used. It is crucial that the child lie still. A mixture of drugs might be given depending on the comfort level and cooperative nature of the subject. The standard regimen includes two sedative hypnotic drugs, midazolam and propofol, given through the vein. For many of the LINCL children, a general anesthetic will likely be required. In this case, a mixture of anesthetic vapors that are inhaled by the patient will be used. Anesthesia can have associated bad effects such as short-lived nausea, blurry vision, sore throat, feeling of fatigue, drowsiness, tiredness, and/or weakness. The side effects of the drugs are usually related to the breathing-related organs. These include hypoxia (decreased oxygen), laryngospasm (closure of the voice box that blocks the passage of air to the lungs), rhonchi (whistling or snoring sound heard with a stethoscope during breathing out as air passes through obstructed channels), coughing, respiratory depression (decreased rate and depth of breathing), airway obstruction, airway congestion (excessive accumulation of fluids in the airway), and/or shallow breathing. Decreased blood pressure, decreased heart rate and, in extreme cases, death may also occur. These are controlled through the use of monitors. The anesthesiologist will discuss the specifics of how the anesthesia will be given, depending on the child. In addition, placement of the intravenous line may cause mild discomfort or bruising at the intravenous site. Occasional light-headedness and, rarely, infection may occur at the site of infusion.

Chest X-ray. The total amount of radiation from the five chest X-rays has been judged safe according to institutional guidelines.

PRECAUTIONS TO MINIMIZE RISKS

The adeno-associated viral vector to be used has been genetically designed to be replication deficient. To minimize risks involved with the study, all prospective study subjects will undergo prestudy evaluation, including general assessment (medical history, physical examination, vital signs [blood pressure, heart rate, respiratory rate, temperature], weight); complete blood count and type and screen, urine analysis; and vector-related tests (serum anti-AAV antibody responses). These tests will uncover those candidates who are most likely to have complications related to these procedures and who will therefore not be considered for study. Should study participants suffer complications as a result of these procedures they will be treated in a standard fashion.

Management of intercurrent illness

All individuals will enter the study with the same therapy that is prescribed for them by their usual treating physician. Should intercurrent exacerbations of disease of any organ occur either during initial assessment or after therapy with the vector, the individual will be treated by conventional clinical therapy at the discretion of the physicians caring for the patient. During the period of intercurrent illness, assessment of safety and efficacy parameters will continue as defined by the protocol as long as such assessment does not interfere with the clinical care and welfare of the individual. If intercurrent illness occurs during the baseline period, efforts will be made to determine whether adeno-associated virus is involved. If the intercurrent illness during the baseline period is sufficiently severe to preclude continuation of the protocol, the individual will be removed from the protocol. If intercurrent illness occurs during the postvector administration period, efforts will be directed toward determining whether the adeno-associated vector genome is involved. If the intercurrent illness (independent of course) during this period is sufficiently severe to preclude further participation, the individual will be removed from the protocol for data collection purposes, but the follow-up will be continued until the illness is resolved and this will be reported to all the regulatory agencies.

Management of adverse events

Adverse reactions will be defined for each organ system on the basis of a four-point scale (see Toxicity Scale, Appendix II). All adverse reactions, whether attributable to administration of the vector or not, will be treated by conventional clinical therapy. Assessment of safety and efficacy parameters will continue as defined by the protocol as long as such assessment does not interfere with the clinical care and welfare of the patient. If a major (severity of 3 or 4 on a 4-point scale) adverse reaction occurs and is attributable to the vector, no additional patients will be treated until the data are discussed with the relevant regulatory groups. The occurrence of a major adverse reaction will be reported to the regulatory groups under the regulations and guidelines appropriate for each of these groups. If a major adverse event occurs in response to the obtaining of safety and efficacy parameters unrelated to the vector itself, the

assessment of safety and efficacy parameters will continue as defined by the protocol as long as such assessment does not interfere with the clinical care and welfare of the study individual. Should the study individual die while in this protocol, the family will be asked to give permission for a full autopsy to determine the precise cause of death. If possible, and if the death is within 60 days of vector administration, samples of tissues obtained at an autopsy will be evaluated for the presence of the adeno-associated vector genome. In the design of this protocol it is recognized that with the limited number of individuals to be studied and/or the doses used, no efficacy may be detected. If no efficacy is detected and there are no safety problems associated with the AAV vectors, the relevant regulatory groups may be asked to allow the number of study individuals to be increased.

Safety issues for healthcare workers

During the baseline period, there are no additional safety issues for the care workers beyond those for usual clinical procedures for the evaluation and care of individuals with Batten disease. During the period of vector administration in the operating suite, the healthcare workers will be exposed to no additional safety concerns beyond those for dealing with patients with a possible viral infection. The study individual will not be placed in isolation. All available prior experience with adeno-associated virus vectors administered has revealed no risk to healthcare workers. Recommendations of the institutional biosafety officers will be followed for handling patients, biologic material, bedding, towels, and so on. Appropriate training sessions developed by the investigators will be used to educate all healthcare workers as to the protocol and relevant hazards, precautions and procedures. Enteric precautions will be utilized during patient hospitalization.

Environment

There are several reasons to believe that the adeno-associated viral vectors do not pose a significant risk to the environment. First, wild-type AAV2 is nonpathogenic for humans. Second, there is no preexisting immunity. Third, AAV is dependent on other viruses (adenovirus, herpesvirus) to replicate. Fourth, because the adeno-associated vector is replication deficient, if released into the environment it will have a limited possibility to spread. Finally, if recombination were to occur, the most likely possibility is wild-type AAV, which is dependent on other viruses (adenovirus, herpesvirus) to replicate and therefore will not cause any problems.

RISK-BENEFIT RATIO

The disease LINCL is fatal with no known therapy. There are estimated to be 200 to 300 children in the United States at any one time with LINCL (K.E. Wisniewski, Institute for Basic Research in Developmental Disabilities, Staten Island, NY; personal communication). Because the disease phenotype is primarily associated with the CNS and the disease is genetic, the required gene transfer must be intracranial and the gene expression must be persistent, both of which increase the risk to

the participant. The disease is global throughout the CNS (other than the brainstem), thus requiring the treatment that is designed to cover as large a proportion of the brain as possible. Intracranial administration will require several burr holes in the skull and general anesthesia over several hours, and there is risk in the use of an AAV-based vector, a gene transfer vector associated with long-term expression. There are no blood tests, neurological assessments, electrophysiologic or imaging studies that can be used to definitively assess the consequences of the therapy. Together, these facts mandate that the investigators, families, and the FDA work together to develop a strategy that will minimize the risk, yet be of sufficient theoretical benefit to the participants such that it will be rational to initiate the study.

CONFIDENTIALITY OF DATA

Data will be abstracted from the subject's medical record by a research coordinator and recorded on case report forms that do not identify subjects by name. The data entered on the case report forms will be verified by the Clinical Operations and Regulatory Affairs Core study monitor against the subject medical records. Subject data will be entered into the database from these case report forms. Case report forms will be stored in a secure area of the Department of Genetic Medicine. The privacy of the study subjects and all confidentiality will be handled in accordance with NYPH-WMC, Health Insurance Portability and Accountability Act (HIPAA), and FDA guidelines. The relevant regulatory groups (IRB, IBC, GCRC, RAC, FDA, OHRP), including the Data Safety and Monitoring Board, the Belfer Gene Therapy Core Facility, and NYPH-WMC, will have access to subject case report forms and/or medical records that identify individual subjects. Any publication or presentation of data will not identify individual subjects by name.

DETAILS OF THE DRUG TO BE USED: AAV2_{CU}hCLN2, THE HUMAN CLN2 GENE TRANSFER VECTOR

The proposed protocol is for the intracranial delivery of an adeno-associated vector coding for the human *CLN2* cDNA to the central nervous system of the brain of children with late infantile neuronal ceroid lipofuscinosis.

AAV2_{CU}hCLN2 construct

The vector to be used in this protocol is AAV2_{CU}hCLN2, composed of an AAV2 gene transfer vector backbone (the inverted terminal repeats [ITRs] of AAV flanking the expression cassette) and an expression cassette with a human cytomegalovirus enhancer, the splice donor and left-hand intron sequence from chicken β -actin/right-hand intron sequence and splice acceptor from rabbit β -globin (this enhancer/promoter/intron sequence is referred to as "CAG"), the human *CLN2* cDNA (with an optimized Kozak translational initiation signal before the start codon), and a rabbit β -globin poly(A) sequence (see Fig. 3 for a schematic of the structure of AAV2_{CU}hCLN2). The clinical lots of AAV2_{CU}hCLN2, produced in the Weill Cornell

Belfer Gene Therapy Core Facility, will have a virus particle count of $2 C \pm D \times 10^{12}$ particle units/ml. All lots will fulfill all of the *in vitro* and *in vivo* safety criteria established by the FDA.

PRECLINICAL EFFICACY STUDIES

The rationale for proceeding with a clinical study to treat the CNS manifestations of LINCL is based on studies from our laboratory relating to the ability of an AAV2 vector encoding the normal *CLN2* gene to deliver TPP-I to the CNS of normal animals. Studies demonstrating the feasibility of the proposed human study were performed in both rats and nonhuman primates. The AAV2_{CU}hCLN2 vector (for rat studies, a similar vector expressing the rat *CLN2* gene, AAV2_{CU}rCLN2) was administered to the brain by direct intraparenchymal injection at 1 to 12 locations. Expression of TPP-I was assessed by immunohistological methods in thin sections at intervals from 2 weeks to 18 months after injection (rats) and at 5 to 13 weeks (nonhuman primates).

Efficacy studies in rats

Qualitative and quantitative histological analysis was undertaken to determine the level, duration, and volume of TPP-I expression that could be obtained by AAV-2-mediated gene transfer in rat brain. TPP-I expression was compared in different regions of the brain after AAV2_{CU}hCLN2 gene transfer. Examination of TPP-I expression by immunohistochemistry 4 weeks after a single striatal injection of 10^{10} particle units of AAV2_{CU}rCLN2 demonstrated robust TPP-I expression. Coimmunofluorescence studies with neuron-specific and glial-specific markers established that TPP-I was localized primarily in neurons, consistent with the reported tropism of the AAV2 vectors. There was no observed expression in astrocytes. To establish that expression of TPP-I could be observed after delivery to other CNS locations, injections of the same dose of AAV2_{CU}hCLN2 were made into several additional brain structures, including the frontal cortex, the parietal cortex, and the cerebellum. Examination of these regions 4 weeks after delivery confirmed TPP-I expression and neurotropism of AAV2 infection, with TPP-I expression seen in neuronal populations in all regions. TPP-I expression was widespread in the cortical injection regions, with neurons of both pyramidal and interneuron morphologies showing TPP-I expression.

Because successful gene therapy for LINCL requires long-term TPP-I expression, striatal TPP-I expression was evaluated at intervals from 2 weeks to 18 months after injection of 10^{10} particle units of AAV2_{CU}hCLN2. The data demonstrated a slow rise followed by long-term transgene expression after administration of an AAV vector to brain. At 2 weeks postinjection, there was no detectable TPP-I protein in the rat striatum, but by 1 month, TPP-I protein was observed. At 2 months a wider distribution of TPP-I protein was observed. The high-level, stable, AAV2-mediated expression of TPP-I in the CNS of rats persisted and comparable volume and intensity were observed at 4, 8, 12, and 18 months. As has been observed with AAV2 vectors expressing a marker gene (Kaspar *et al.*, 2002), cell

bodies staining positive for TPP-I expression were observed beyond the immediate region surrounding the site of injection, but whose axonal projections were located in the site of the injection. The data were consistent with retrograde transport of vector or transgene product along axons projecting into the striatum. As widespread delivery of the gene product throughout the brain is advantageous for treatment of LINCL, other brain regions that project to the striatum were examined to determine whether expression of TPP-I could be detected in projection neuronal populations after single intrastriatal administration of AAV2_{CUh}CLN2. Interestingly, neurons in the frontal cortex showed TPP-I expression as early as 2 months after delivery, and expression levels increased at 4 and 8 months relative to the earlier time points. TPP-I expression was also observed in neuronal populations in the thalamus and substantia nigra at the 8-month time point. Continued detection of TPP-I in neurons in these regions was observed at 12 months. In control rats, no TPP-I-positive cells were detected in these areas, using the human-specific monoclonal anti-TPP-I antibody.

In summary, the rat efficacy studies demonstrate that multiple regions of the brain can be successfully transduced by AAV2 vectors expressing the *CLN2* gene and that long-term TPP-I expression can be achieved. In addition, they showed that widespread distribution of TPP-I activity can be achieved by a single injection of the AAV2_{CUh}CLN2 vector.

Efficacy studies in nonhuman primates

The feasibility of successful transfer of the *CLN2* gene to the brains of African green monkeys has been demonstrated. Animals were injected in 12 locations, 6 each per hemisphere with 2 infusions at different depths through 3 burr holes per hemisphere. The dose per location was 3×10^{10} particle units for a total of 3.6×10^{11} particle units. Representative sections from the right hemisphere of brain 5 and 13 weeks after injection of AAV2_{CUh}CLN2 were assessed by immunohistochemical staining. Detectable levels of TPP-I expression were found, using human-specific monoclonal antibody with immunoperoxidase staining. The morphology of immunoperoxidase-stained sections in the cortex suggested that both interneurons and pyramidal neurons expressed TPP-I, whereas staining in the caudate nucleus showed expression in cells with the morphology of interneurons. Delivery to the hippocampus resulted in TPP-I expression in large multipolar hilar cells and, to a lesser extent, in dentate granule cells. Examination of TPP-I-expressing cells in the nonhuman primate brain by multiple immunofluorescence staining revealed that neuronal, but not glial, populations were infected at all injection sites. Successful expression of AAV2-delivered TPP-I in the nonhuman primate brain was not region specific as TPP-I could be detected in all injected regions. Consistent with delivery to the rat brain, these results validate that AAV2-mediated delivery of *CLN2* in the nonhuman primate brain results in persistent expression in multiple areas of the brain up to at least 13 weeks.

PRECLINICAL SAFETY DATA

Preclinical safety studies have been carried out in rats and nonhuman primates.

Safety studies in rats

The safety of administration of an AAV2_{CUh}CLN2 vector to the brain was evaluated in a total of 48 rats, with $n = 6$ per group (three males and three females per group). The rats were injected intracranially at two sites, one per hemisphere, at a single depth with a total of 2×10^{10} particle units of AAV2_{CUh}CLN2. An equal number of animals were injected with phosphate-buffered saline (PBS) as control. The study is focused on the long-term effects of AAV2_{CUh}CLN2 administration with data collection at 13, 26, 52, and 78 weeks (acute toxicology and shorter time points are not assessed as these have been assessed in the nonhuman primate safety studies). As agreed on with the FDA in a pre-IND meeting and follow-up discussions, the 13-week time point acts as a bridge to the nonhuman primate study. The outcome parameters of the study include animal and organ weight at necropsy, gross examination at necropsy, and histology of liver, kidney, lung, spleen, quadriceps, heart, gonads, and any abnormal organs observed at necropsy (two sections per organ). Histological analysis of brain was performed by taking 10 coronal sections at 0.3-mm intervals across the striatum (the injected region) and at 2-mm intervals through the rest of the brain. Blood analyses are carried out at the time of sacrifice.

This study is ongoing and it compares rats injected with AAV2_{CUh}CLN2 via the striatum with control rats injected with PBS. Studies at 13 weeks demonstrated no differences between control and vector groups for complete blood count, neutralizing antibody, and serum chemistry. Injection of AAV2_{CUh}CLN2 did not result in any pathological changes in brain attributable to the vector. The process of injection into brain produced the expected range of microscopic changes from needle trauma consisting of resolving hemorrhage and localized low-grade glial scarring along the track. Examination of brain, liver, kidney, lung, heart, skeletal muscle, spleen, testes, and ovaries showed no vector-related changes. The study is ongoing and the 26-, 52-, and 78-week data will be submitted to the FDA when it is available.

Safety studies in nonhuman primates

The study includes a total of 36 male African green monkeys who received intracranial administration of total doses of 3.6×10^{11} or 3.6×10^{10} particle units of the AAV2_{CUh}CLN2 vector, 3.6×10^{11} particle units of the control AAV2Null vector, or PBS at 1 μ l/min for a total volume (15 μ l at each of 12 locations) of 180 μ l. Each dose was divided (for each animal) among 12 locations delivered through 6 burr holes. The highest dose (3.6×10^{11} particle units) was chosen as being the scaled equivalent (for the total brain weight) of the planned human dose of 3.6×10^{12} particle units. In addition, three sham-operated animals were used as controls. The monkeys were observed for neurological/behavioral changes and routine general assessments (weight, temperature, pulse, blood pressure) and routine blood studies at specified intervals. At each of 1, 13, 26, and 52 weeks, a subset of animals is sacrificed and samples of brain, liver, kidney, lung, testes, heart, and skeletal muscle are collected for histological assessment.

Studies at 1, 12, and 26 weeks have been completed; the 52-week data will be submitted to the FDA when the data are available. This ongoing study compares control monkeys injected

with AAV2Null or PBS, or sham injected with monkeys injected with 3.6×10^{10} or 3.6×10^{11} particle units of AAV2_{CU}hCLN2. Serial blood samples collected at 3, 7, 14, 28, 56, 91, 180 days from surviving monkeys showed no differences in any parameter for complete blood count or serum chemistry among the groups. Behavioral assessment at similar time points also showed no vector-related differences among groups. Histopathological examination of the brain demonstrated that injection of AAV2_{CU}hCLN2 into the caudate nucleus, hippocampus, and cortex of some animals produced slight to mild and transient white matter edema (spongiosis) with reactive glial cells in the white matter of the corona radiating around the injection track; the change extended moderately rostrally and caudally. In the report of the pathologist from Pathology Associates (Charles River Laboratories, Frederick, MD), such changes are most likely attributable to the vehicle and are not typical of the cell-mediated immune reactions usually associated with vector injection. This change was reversible at 13 and 26 weeks and did not leave any microscopically discernable abnormalities. On the basis of the pathologist's experience with intracerebral injection, the magnitude of the reaction stands at the lowest of the possible range and in the opinion of the pathologist did not represent a significant safety concern.

CLINICAL PREPARATION

Clinical lots of AAV2_{CU}hCLN2, produced in the Belfer Gene Therapy Core Facility, Weill Medical College of Cornell University (New York, NY), will be placed in screw-capped cryovials that are purchased sterile. The cryovials are transparent polypropylene cryotubes (1.5 ml) with external threads and a self-standing bottom. The screw cap is virgin polyethylene and free from all heavy metals; the O-ring ensures a tight, secure seal. The vials are labeled with self-adhesive cryoresistant labels. The concentration of the final vector solution will be $2.0 (\pm 1) \times 10^{12}$ particle units/ml in PBS.

RISKS RELATED TO THE DRUG

AAV2_{CU}hCLN2 has not been used previously in humans, so the risks can only be theorized. Risks could be related to the delivery of the vector and surgical procedures or to the drug (AAV2_{CU}hCLN2 vector). These potential risks are presented in detail in the section Risks of the Study.

ACKNOWLEDGMENTS

We thank C. Hollmann, H. Suh, N. Mohamed, and T. Virgin-Bryan for help in preparing this manuscript. These studies were supported, in part, by Nathan's Battle Foundation, Indianapolis, IN; and the Will Rogers Memorial Fund, Los Angeles, CA.

REFERENCES

AITKEN, M.L., MOSS, R.B., WALTZ, D.A., DOVEY, M.E., TONELLI, M.R., McNAMARA, S.C., GIBSON, R.L., RAMSEY,

B.W., CARTER, B.J., and REYNOLDS, T.C. (2001). A phase I study of aerosolized administration of tgAAVCF to cystic fibrosis subjects with mild lung disease. *Hum. Gene Ther.* **12**, 1907–1916.

BACKLOW, N.R. (1988). Adeno-associated viruses of human. In: *Parvoviruses and Human Disease*. Patison, J.R., ed. (CRC Press, Boca Raton, FL) pp. 165–174.

BENNETT, J., MAGUIRE, A.M., CIDECIYAN, A.V., SCHNELL, M., GLOVER, E., ANAND, V., ALEMAN, T.S., CHIRMULE, N., GUPTA, A.R., HUANG, Y., GAO, G.P., NYBERG, W.C., TAZELAAR, J., HUGHES, J., WILSON, J.M., and JACOBSON, S.G. (1999). Stable transgene expression in rod photoreceptors after recombinant adeno-associated virus-mediated gene transfer to monkey retina. *Proc. Natl. Acad. Sci. U.S.A.* **96**, 9920–9925.

BERNS, K.I., and GIRAUD, C. (1996). Biology of adeno-associated virus. *Curr. Top. Microbiol. Immunol.* **218**, 1–23.

BIRCH, D.G. (1999). Retinal degeneration in retinitis pigmentosa and neuronal ceroid lipofuscinosis: An overview. *Mol. Genet. Metab.* **66**, 356–366.

BIRKEN, D.L., and OLENDORF, W.H. (1989). *N*-Acetyl-L-aspartic acid: A literature review of a compound prominent in ¹H-NMR spectroscopic studies of the brain. *Neurosci. Biobehav. Rev.* **13**, 1589–1591.

BOSCH, A., PERRET, E., DESMARIS, N., TRONO, D., and HEARD, J.M. (2000). Reversal of pathology in the entire brain of mucopolysaccharidosis type VII mice after lentivirus-mediated gene transfer. *Hum. Gene Ther.* **11**, 1139–1150.

BOUSTANY, R.M. (1996). Batten disease or neuronal ceroid lipofuscinosis. In: *Neurodystrophies and Neurolipidoses*. Moser, H.W., ed. (Elsevier Science, New York) pp. 671–700.

CARTER, B. (2000). Adeno-associated virus and adeno-associated virus vectors for gene delivery. In: *Gene Therapy*. Smyth Tempelton, N., and Lasic, D.D., eds. (Marcel Dekker, New York) pp. 41–59.

CHEN, S.J., TAZELAAR, J., MOSCIONI, A.D., and WILSON, J.M. (2000). *In vivo* selection of hepatocytes transduced with adeno-associated viral vectors. *Mol. Ther.* **1**, 414–422.

CHEN, Z.Y., YANT, S.R., HE, C.Y., MEUSE, L., SHEN, S., and KAY, M.A. (2001). Linear DNAs concatemerize *in vivo* and result in sustained transgene expression in mouse liver. *Mol. Ther.* **3**, 403–410.

CHIORINI, J.A., KIM, F., YANG, L., and KOTIN, R.M. (1999). Cloning and characterization of adeno-associated virus type 5. *J. Virol.* **73**, 1309–1319.

DAVIDSON, B.L., STEIN, C.S., HETH, J.A., MARTINS, I., KOTIN, R.M., DERKSEN, T.A., ZABNER, J., GHODSI, A., and CHIORINI, J.A. (2000). Recombinant adeno-associated virus type 2, 4, and 5 vectors: Transduction of variant cell types and regions in the mammalian central nervous system. *Proc. Natl. Acad. Sci. U.S.A.* **97**, 3428–3432.

DURING, M.J., SAMULSKI, R.J., ELSWORTH, J.D., KAPLITT, M.G., LEONE, P., XIAO, X., LI, J., FREESE, A., TAYLOR, J.R., ROTH, R.H., SLADEK, J.R., JR., O'MALLEY, K.L., and REDMOND, D.E., Jr. (1998). *In vivo* expression of therapeutic human genes for dopamine production in the caudates of MPTP-treated monkeys using an AAV vector. *Gene Ther.* **5**, 820–827.

DURING, M.J., KAPLITT, M.G., STERN, M.B., and EIDELBERG, D. (2001). Subthalamic GAD gene transfer in Parkinson disease patients who are candidates for deep brain stimulation. *Hum. Gene Ther.* **12**, 1589–1591.

ELLIGER, S.S., ELLIGER, C.A., AGUILAR, C.P., RAJU, N.R., and WATSON, G.L. (1999). Elimination of lysosomal storage in brains of MPS VII mice treated by intrathecal administration of an adeno-associated virus vector. *Gene Ther.* **6**, 1175–1178.

EZAKI, J., WOLFE, L.S., HIGUTI, T., ISHIDOH, K., and KOMINAMI, E. (1995). Specific delay of degradation of mitochondrial ATP synthase subunit c in late infantile neuronal ceroid lipofuscinosis (Batten disease). *J. Neurochem.* **64**, 733–741.

FISHER, K.J., JOOSS, K., ALSTON, J., YANG, Y., HAECKER, S.E., HIGH, K., PATHAK, R., RAPER, S.E., and WILSON, J.M. (1997).

- Recombinant adeno-associated virus for muscle directed gene therapy. *Nat. Med.* **3**, 306–312.
- FLANNERY, J.G., ZOLOTUKHIN, S., VAQUERO, M.I., LA VAIL, M.M., MUZYCZKA, N., and HAUSWIRTH, W.W. (1997). Efficient photoreceptor-targeted gene expression *in vivo* by recombinant adeno-associated virus. *Proc. Natl. Acad. Sci. U.S.A.* **94**, 6916–6921.
- FOOD AND DRUG ADMINISTRATION. 31st Biological Response Modifiers Advisory Committee Meeting, Gaithersburg, MD, October 24, 2003, briefing material and meeting transcripts. Available at URL: <http://www.fda.gov/ohrms/dockets/ac/01/briefing/3794b1.htm>.
- FRISELLA, W.A., O'CONNOR, L.H., VOGLER, C.A., ROBERTS, M., WALKLEY, S., LEVY, B., DALY, T.M., and SANDS, M.S. (2001). Intracranial injection of recombinant adeno-associated virus improves cognitive function in a murine model of mucopolysaccharidosis type VII. *Mol. Ther.* **3**, 351–358.
- GLADER, B., DAKE, M.D., RAZAVI, M., ZEHNDER, J.L., RUSTAGI, P., HUTCHISON, S., MANNO, C.S., KAYE, R., HERZOG, R.W., ARRUDA, V.R., LEONARD, D., GROSSBARD, E., CHEW, A., COUTO, L., MCCLELLAND, A., JOHNSON, F., HIGH, K.A., and MAY, M.A. A phase I safety study in patients with severe hemophilia B (factor IX deficiency) using adeno-associated viral vector to deliver the gene for human factor IX into the liver. Meeting of the 5th Gene Therapy Workshop, April 12, 2002, Children's Hospital of Philadelphia, Philadelphia, PA. Available at URL: www.hemophilia.org/research/geneabstracts_fri2.htm.
- HACEIN-BEY-ABINA, S., VON KALLE, C., SCHMIDT, M., MCCORMACK, M.P., WULFFRAAT, N., LEBOLCH, P., LIM, A., OSBORNE, C.S., PAWLIUK, R., MORILLON, E., SORENSEN, R., FORSTER, A., FRASER, P., COHEN, J.I., DE SAINT, B.G., ALEXANDER, I., WINTERGERST, U., FREBOURG, T., AURIAS, A., STOPPA-LYONNET, D., ROMANA, S., RADFORD-WEISS, I., GROSS, F., VALENSI, F., DELABESSE, E., MACINTYRE, E., SIGAUX, F., SOULIER, J., LEIVA, L.E., WISSLER, M., PRINZ, C., RABBITTS, T.H., LE DEIST, F., FISCHER, A., and CAVAZZANA-CALVO, M. (2003). LMO2-associated clonal T cell proliferation in two patients after gene therapy for SCID-X1. *Science* **302**, 415–419.
- HASKELL, R.E., HUGHES, S.M., CHIORINI, J.A., ALISKY, J.M., and DAVIDSON, B.L. (2003). Viral-mediated delivery of late-infantile neuronal ceroid lipofuscinosis gene, TPP-1 to the mouse central nervous system. *Gene Ther.* **10**, 34–42.
- HIGH, K.A. (2001). AAV-mediated gene transfer for hemophilia. *Ann. N.Y. Acad. Sci.* **953**, 64–74.
- JANSON, C., MCPHEE, S., BILANIUK, L., HASELGROVE, J., TESTAIUTI, M., FREESE, A., WANG, D.J., SHERA, D., HURH, P., RUPIN, J., SASLOW, E., GOLDFARB, O., GOLDBERG, M., LARIJANI, G., SHARRAR, W., LIOUTERMAN, L., CAMP, A., KOLODNY, E., SAMULSKI, J., and LEONE, P. (2002). Gene therapy of Canavan disease: AAV-2 vector for neurosurgical delivery of aspartoacylase gene (SPA) to the human brain [clinical protocol]. *Hum. Gene Ther.* **13**, 1391–1412.
- KASPAR, B.K., ERICKSON, D., SCHAFFER, D., HINH, L., GAGE, F.H., and PETERSON, D.A. (2002). Targeted retrograde gene delivery for neuronal protection. *Mol. Ther.* **5**, 50–56.
- KAY, M.A., MANNO, C.S., RAGNI, M.V., LARSON, P.J., COUTO, L.B., MCCLELLAND, A., GLADER, B., CHEW, A.J., TAI, S.J., HERZOG, R.W., ARRUDA, V., JOHNSON, F., SCALLAN, C., SKARSGARD, E., FLAKE, A.W., and HIGH, K.A. (2000). Evidence for gene transfer and expression of factor IX in haemophilia B patients treated with an AAV vector. *Nat. Genet.* **24**, 257–261.
- KESSLER, P.D., PODSAKOFF, G.M., CHEN, X., MCQUISTON, S.A., COLOSI, P.C., MATELIS, L.A., KURTZMAN, G.J., and BYRNE, B.J. (1996). Gene delivery to skeletal muscle results in sustained expression and systemic delivery of a therapeutic protein. *Proc. Natl. Acad. Sci. U.S.A.* **93**, 14082–14087.
- KOEBERL, D.D., ALEXANDER, I.E., HALBERT, C.L., RUSSELL, D.W., and MILLER, A.D. (1997). Persistent expression of human clotting factor IX from mouse liver after intravenous injection of adeno-associated virus vectors. *Proc. Natl. Acad. Sci. U.S.A.* **94**, 1426–1431.
- KURACHI, Y., OKA, A., MIZUGUCHI, M., OHKOSHI, Y., SASAKI, M., ITOH, M., HAYASHI, M., GOTO, Y., and TAKASHIMA, S. (2000). Rapid immunologic diagnosis of classic late infantile neuronal ceroid lipofuscinosis. *Neurology* **54**, 1676–1680.
- LEONE, P., and SIMEONE, F.A. (2000). Gene therapy of Canavan disease using AAV for brain gene transfer. *RAC* 381–(2000–01). Available at URL <http://www4.od.nih.gov/oba/rac/trialquery.asp?C2=3&piid=5509>.
- LIN, L., and LOBEL, P. (2001). Production and characterization of recombinant human CLN2 protein for enzyme-replacement therapy in late infantile neuronal ceroid lipofuscinosis. *Biochem. J.* **357**, 49–55.
- LIU, C.G., SLEAT, D.E., DONNELLY, R.J., and LOBEL, P. (1998). Structural organization and sequence of CLN2, the defective gene in classical late infantile neuronal ceroid lipofuscinosis. *Genomics* **50**, 206–212.
- LO, W.D., QU, G., SFERRA, T.J., CLARK, R., CHEN, R., and JOHNSON, P.R. (1999). Adeno-associated virus-mediated gene transfer to the brain: Duration and modulation of expression. *Hum. Gene Ther.* **10**, 201–213.
- LODISH, H., BERK, A., ZIPURSKY, S.L., MATSUDAIRA, P., BALTIMORE, D., and DARNELL, J. (2000). Protein sorting: Organelle biogenesis and protein secretion. In: *Molecular Cell Biology*. (W.H. Freeman and Company, New York) pp. 677–751.
- MAEDA, Y., IKEDA, U., SHIMPO, M., UENO, S., OGASAWARA, Y., URABE, M., KUME, A., TAKIZAWA, T., SAITO, T., COLOSI, P., KURTZMAN, G., SHIMADA, K., and OZAWA, K. (1998). Efficient gene transfer into cardiac myocytes using adeno-associated virus (AAV) vectors. *J. Mol. Cell. Cardiol.* **30**, 1341–1348.
- MANDEL, R.J., RENDAHL, K.G., SPRATT, S.K., SNYDER, R.O., COHEN, L.K., and LEFF, S.E. (1998). Characterization of intrastriatal recombinant adeno-associated virus-mediated gene transfer of human tyrosine hydroxylase and human GTP-cyclohydrolase I in a rat model of Parkinson's disease. *J. Neurosci.* **18**, 4271–4284.
- MCCORMACK, M.P., and RABBITTS, T.H. (2004). Activation of the T-cell oncogene LMO2 after gene therapy for X-linked severe combined immunodeficiency. *N. Engl. J. Med.* **350**, 913–922.
- MCCOWN, T.J., XIAO, X., LI, J., BREESE, G.R., and SAMULSKI, R.J. (1996). Differential and persistent expression patterns of CNS gene transfer by an adeno-associated virus (AAV) vector. *Brain Res.* **713**, 99–107.
- MOLE, S.E. (1999). Batten's disease: Eight genes and still counting? *Lancet* **354**, 443–445.
- MUZYCZKA, N. (1992). Use of adeno-associated virus as a general transduction vector for mammalian cells. *Curr. Top. Microbiol. Immunol.* **158**, 97–129.
- NEW YORK PRESBYTERIAN HOSPITAL-WEILL MEDICAL COLLEGE OF CORNELL UNIVERSITY CHILDREN'S CLINICAL RESEARCH CENTER. Clinical Testing Guidelines, Blood Drawing Sheet. August 26, 2003. URL: <http://ccrc.med.cornell.edu/patsafety/bloodvol/blooddrawingsheet.pdf>
- PATERNA, J.C., MOCSETTI, T., MURA, A., FELDON, J., and BUELER, H. (2000). Influence of promoter and WHV post-transcriptional regulatory element on AAV-mediated transgene expression in the rat brain. *Gene Ther.* **7**, 1304–1311.
- PELTONEN, L., SAVUKOSKI, M., and VESA, J. (2000). Genetics of the neuronal ceroid lipofuscinoses. *Curr. Opin. Genet. Dev.* **10**, 299–305.
- PURANAM, K., QIAN, W.H., NIKBAKHT, K., VENABLE, M., OBEID, L., HANNUN, Y., and BOUSTANY, R.M. (1997). Upregulation of Bcl-2 and elevation of ceramide in Batten disease. *Neuropediatrics* **28**, 37–41.
- SFERRA, T.J., QU, G., McNEELY, D., RENNARD, R., CLARK,

K.R., LO, W.D., and JOHNSON, P.R. (2000). Recombinant adeno-associated virus-mediated correction of lysosomal storage within the central nervous system of the adult mucopolysaccharidosis type VII mouse. *Hum. Gene Ther.* **11**, 507–519.

SHARP, J.D., WHEELER, R.B., LAKE, B.D., SAVUKOSKI, M., JARVELA, I.E., PELTONEN, L., GARDINER, R.M., and WILLIAMS, R.E. (1997). Loci for classical and a variant late infantile neuronal ceroid lipofuscinosis map to chromosomes 11p15 and 15q21-23. *Hum. Mol. Genet.* **6**, 591–595.

SKORUPA, A.F., FISHER, K.J., WILSON, J.M., PARENTE, M.K., and WOLFE, J.H. (1999). Sustained production of β -glucuronidase from localized sites after AAV vector gene transfer results in widespread distribution of enzyme and reversal of lysosomal storage lesions in a large volume of brain in mucopolysaccharidosis VII mice. *Exp. Neurol.* **160**, 17–27.

SLEAT, D.E., DONNELLY, R.J., LACKLAND, H., LIU, C.G., SOHAR, I., PULLARKAT, R.K., and LOBEL, P. (1997). Association of mutations in a lysosomal protein with classical late-infantile neuronal ceroid lipofuscinosis. *Science* **277**, 1802–1805.

SLEAT, D.E., GIN, R.M., SOHAR, I., WISNIEWSKI, K., SKLOWER-BROOKS, S., PULLARKAT, R.K., PALMER, D.N., LERNER, T.J., BOUSTANY, R.M., ULDALL, P., SIAKOTOS, A.N., DONNELLY, R.J., and LOBEL, P. (1999). Mutational analysis of the defective protease in classic late-infantile neuronal ceroid lipofuscinosis, a neurodegenerative lysosomal storage disorder. *Am. J. Hum. Genet.* **64**, 1511–1523.

SONDHI, D., HACKETT, N.R., APBLET, R.L., KAMINSKY, S.M., PERGOLIZZI, R.G., and CRYSTAL, R.G. (2001). Feasibility of gene therapy for late neuronal ceroid lipofuscinosis. *Arch. Neurol.* **58**, 1793–1798.


STEINFELD, R., HEIM, P., VON GREGORY, H., MEYER, K., ULLRICH, K., GOEBEL, H.H., and KOHLSCHUTTER, A. (2002). Late infantile neuronal ceroid lipofuscinosis: quantitative description of the clinical course in patients with CLN2 mutations. *Am. J. Med. Genet.* **112**, 347–354.

WAGNER, J.A., MORAN, M.L., MESSNER, A.H., DAIFUKU, R., CONRAD, C.K., REYNOLDS, T., GUGGINO, W.B., MOSS, R.B., CARTER, B.J., WINE, J.J., FLOTTE, T.R., and GARDNER, P. (1998). A phase I/II study of tgAAV-CF for the treatment of chronic sinusitis in patients with cystic fibrosis. *Hum. Gene Ther.* **9**, 889–909.

WILLIAMS, R.E., GOTTLÖB, I., LAKE, B.D., GOEBEL, H.H., WINCHESTER, B.G., and WHEELER, R.B. (1999). CLN 2. Classic late infantile NCL. In: *The Neuronal Ceroid Lipofuscinoses (Batten Disease)*. Goebel, H.H., Mole, S.E., and Lake, B.D., eds. (IOS Press, Amsterdam) pp. 37–54.

Appendix I

NEUROLOGICAL EXAMINATION

	<p>Subject Name _____</p> <p>Date _____</p> <p>Time _____</p>
--	---

2. Neurological assessment

Level of Consciousness	<input type="checkbox"/> Alert	<input type="checkbox"/> Drowsy	<input type="checkbox"/> Stuporous	<input type="checkbox"/> Comatose
Speech (articulation)	<input type="checkbox"/> Not evaluable		<input type="checkbox"/> Normal	<input type="checkbox"/> Dysarthria
Language	<input type="checkbox"/> Not evaluable		<input type="checkbox"/> Normal	<input type="checkbox"/> Aphasia
Cranial Nerves				
Visual fields (II)	<input type="checkbox"/> Not evaluable	<input type="checkbox"/> Normal	<input type="checkbox"/> Abnormal	
Eye movements (III, IV, VI)	<input type="checkbox"/> Not evaluable	<input type="checkbox"/> Normal	<input type="checkbox"/> Abnormal	
Jaw movement, facial sensations (V)	<input type="checkbox"/> Not evaluable	<input type="checkbox"/> Normal	<input type="checkbox"/> Abnormal	
Facial movements (VII)	<input type="checkbox"/> Not evaluable	<input type="checkbox"/> Normal	<input type="checkbox"/> Abnormal	
Hearing (VIII)	<input type="checkbox"/> Not evaluable	<input type="checkbox"/> Normal	<input type="checkbox"/> Abnormal	
Swallowing, pharynx, larynx (IX, X)	<input type="checkbox"/> Not evaluable	<input type="checkbox"/> Normal	<input type="checkbox"/> Abnormal	
Sternocleidomastoid (SCM), Trapezius (XI)	<input type="checkbox"/> Not evaluable	<input type="checkbox"/> Normal	<input type="checkbox"/> Abnormal	
Tongue (XII)	<input type="checkbox"/> Not evaluable	<input type="checkbox"/> Normal	<input type="checkbox"/> Abnormal	

(continued)

Appendix I

NEUROLOGICAL EXAMINATION (cont.)

Motor Strength

Trunk	<input type="checkbox"/> Not evaluable	<input type="checkbox"/> Normal	<input type="checkbox"/> Decreased
Upper extremities	<input type="checkbox"/> Not evaluable	<input type="checkbox"/> Normal	<input type="checkbox"/> Decreased
Lower extremities	<input type="checkbox"/> Not evaluable	<input type="checkbox"/> Normal	<input type="checkbox"/> Decreased

Motor Tone

Trunk	<input type="checkbox"/> Not evaluable	<input type="checkbox"/> Normal	<input type="checkbox"/> Decreased	<input type="checkbox"/> Increased
Upper extremities	<input type="checkbox"/> Not evaluable	<input type="checkbox"/> Normal	<input type="checkbox"/> Decreased	<input type="checkbox"/> Increased
Lower extremities	<input type="checkbox"/> Not evaluable	<input type="checkbox"/> Normal	<input type="checkbox"/> Decreased	<input type="checkbox"/> Increased

Abnormal Movements

Upper extremities	Left	<input type="checkbox"/> Yes	<input type="checkbox"/> No
	Right	<input type="checkbox"/> Yes	<input type="checkbox"/> No
Lower extremities	Left	<input type="checkbox"/> Yes	<input type="checkbox"/> No
	Right	<input type="checkbox"/> Yes	<input type="checkbox"/> No
Tongue		<input type="checkbox"/> Yes	<input type="checkbox"/> No

Reflexes

Biceps	Left	<input type="checkbox"/> Not evaluable	<input type="checkbox"/> Normal	<input type="checkbox"/> Decreased	<input type="checkbox"/> Increased
	Right	<input type="checkbox"/> Not evaluable	<input type="checkbox"/> Normal	<input type="checkbox"/> Decreased	<input type="checkbox"/> Increased
Triceps	Left	<input type="checkbox"/> Not evaluable	<input type="checkbox"/> Normal	<input type="checkbox"/> Decreased	<input type="checkbox"/> Increased
	Right	<input type="checkbox"/> Not evaluable	<input type="checkbox"/> Normal	<input type="checkbox"/> Decreased	<input type="checkbox"/> Increased
Knee	Left	<input type="checkbox"/> Not evaluable	<input type="checkbox"/> Normal	<input type="checkbox"/> Decreased	<input type="checkbox"/> Increased
	Right	<input type="checkbox"/> Not evaluable	<input type="checkbox"/> Normal	<input type="checkbox"/> Decreased	<input type="checkbox"/> Increased
Ankle	Left	<input type="checkbox"/> Not evaluable	<input type="checkbox"/> Normal	<input type="checkbox"/> Decreased	<input type="checkbox"/> Increased
	Right	<input type="checkbox"/> Not evaluable	<input type="checkbox"/> Normal	<input type="checkbox"/> Decreased	<input type="checkbox"/> Increased
Toes (Babinski)	Left	<input type="checkbox"/> Not evaluable	<input type="checkbox"/> Down	<input type="checkbox"/> Up	
	Right	<input type="checkbox"/> Not evaluable	<input type="checkbox"/> Down	<input type="checkbox"/> Up	

Upper Extremity Sensations

Pain/temp	Left	<input type="checkbox"/> Not evaluable	<input type="checkbox"/> Normal	<input type="checkbox"/> Decreased
	Right	<input type="checkbox"/> Not evaluable	<input type="checkbox"/> Normal	<input type="checkbox"/> Decreased
Light touch	Left	<input type="checkbox"/> Not evaluable	<input type="checkbox"/> Normal	<input type="checkbox"/> Decreased
	Right	<input type="checkbox"/> Not evaluable	<input type="checkbox"/> Normal	<input type="checkbox"/> Decreased

(continued)

Appendix I

NEUROLOGICAL EXAMINATION (cont.)

Position	Left	<input type="checkbox"/> Not evaluable	<input type="checkbox"/> Normal	<input type="checkbox"/> Decreased		
	Right	<input type="checkbox"/> Not evaluable	<input type="checkbox"/> Normal	<input type="checkbox"/> Decreased		
Vibration	Left	<input type="checkbox"/> Not evaluable	<input type="checkbox"/> Normal	<input type="checkbox"/> Decreased		
	Right	<input type="checkbox"/> Not evaluable	<input type="checkbox"/> Normal	<input type="checkbox"/> Decreased		
DSS	Left	<input type="checkbox"/> Not evaluable	<input type="checkbox"/> Normal	<input type="checkbox"/> Decreased		
	Right	<input type="checkbox"/> Not evaluable	<input type="checkbox"/> Normal	<input type="checkbox"/> Decreased		
Lower Extremity Sensations						
Pain/temp	Left	<input type="checkbox"/> Not evaluable	<input type="checkbox"/> Normal	<input type="checkbox"/> Decreased		
	Right	<input type="checkbox"/> Not evaluable	<input type="checkbox"/> Normal	<input type="checkbox"/> Decreased		
Light touch	Left	<input type="checkbox"/> Not evaluable	<input type="checkbox"/> Normal	<input type="checkbox"/> Decreased		
	Right	<input type="checkbox"/> Not evaluable	<input type="checkbox"/> Normal	<input type="checkbox"/> Decreased		
Position	Left	<input type="checkbox"/> Not evaluable	<input type="checkbox"/> Normal	<input type="checkbox"/> Decreased		
	Right	<input type="checkbox"/> Not evaluable	<input type="checkbox"/> Normal	<input type="checkbox"/> Decreased		
Vibration	Left	<input type="checkbox"/> Not evaluable	<input type="checkbox"/> Normal	<input type="checkbox"/> Present		
	Right	<input type="checkbox"/> Not evaluable	<input type="checkbox"/> Normal	<input type="checkbox"/> Present		
DSS	Left	<input type="checkbox"/> Not evaluable	<input type="checkbox"/> Absent	<input type="checkbox"/> Mild	<input type="checkbox"/> Moderate	<input type="checkbox"/> Severe
	Right	<input type="checkbox"/> Not evaluable	<input type="checkbox"/> Absent	<input type="checkbox"/> Mild	<input type="checkbox"/> Moderate	<input type="checkbox"/> Severe
Gait		<input type="checkbox"/> Not evaluable	<input type="checkbox"/> Normal	<input type="checkbox"/> Ataxic	<input type="checkbox"/> Spastic	<input type="checkbox"/> Brady
Romberg		<input type="checkbox"/> Not evaluable	<input type="checkbox"/> Negative	<input type="checkbox"/> Positive		
Nystagmus		<input type="checkbox"/> Not evaluable	<input type="checkbox"/> Absent	<input type="checkbox"/> Present		
Coordination						
Tremor	Left	<input type="checkbox"/> Not evaluable	<input type="checkbox"/> Normal	<input type="checkbox"/> Decreased		
	Right	<input type="checkbox"/> Not evaluable	<input type="checkbox"/> Normal	<input type="checkbox"/> Decreased		
Rapid alternating movements	Left	<input type="checkbox"/> Not evaluable	<input type="checkbox"/> Normal	<input type="checkbox"/> Present		
	Right	<input type="checkbox"/> Not evaluable	<input type="checkbox"/> Normal	<input type="checkbox"/> Present		
Finger to nose	Left	<input type="checkbox"/> Not evaluable	<input type="checkbox"/> Normal	<input type="checkbox"/> Present		
	Right	<input type="checkbox"/> Not evaluable	<input type="checkbox"/> Normal	<input type="checkbox"/> Present		
Knee	Left	<input type="checkbox"/> Not evaluable	<input type="checkbox"/> Normal	<input type="checkbox"/> Present		
	Right	<input type="checkbox"/> Not evaluable	<input type="checkbox"/> Normal	<input type="checkbox"/> Present		

Physician Name

Signature

Date

Appendix II


Graded Toxicity Scale to Define Adverse Reactions¹

PARAMETERS	Grade 1 (Minimal)	Grade II (Moderate)	Grade III (Severe)	Grade IV (Life Threatening)
A. HEMATOLOGIC				
Hemoglobin	10–10.9 gm/dL	7.0–9.9 gm/dL	<7.0 gm/dL	Cardiac failure secondary to anemia
WBC (leukocytosis)	>13,500–15,000 /mm ³	>15,000–20,000 /mm ³	20,000–30,000 /mm ³	>30,000
(leukopenia)	—	2,000–3,000 /mm ³	1,000–2,000 /mm ³	1,000 /mm ³
Platelets	—	50,000–75,000 /mm ³	25,000–49,999 /mm ³	<25,000 /mm ³
B. COAGULATION				
Prothrombin time (PT)	1.1–1.2 × ULN ²	1.3–1.5 × ULN	1.6–3.0 × ULN	>3.0 × ULN
Partial thromboplastin time (PTT)	1.1–1.6 × ULN	1.7–2.3 × ULN	2.4–3.0 × ULN	>3.0 × ULN
C. HEPATIC/GASTROINTESTINAL				
AST (SGOT)	1.1–4.9 × ULN	5.0–9.9 × ULN	10.0–15.0 × ULN	>15.0 × ULN
Bilirubin total	1.1–1.9 × ULN	2.0–2.9 × ULN	3.0–7.5 × ULN	>7.5 × ULN
Vomiting	2 episodes/day	3 episodes/day	4–6 episodes/day	Greater than 6 episodes per day or intractable vomiting
Diarrhea	Slight change in consistency and/or frequency in stools	Liquid stools	Liquid stools greater than 4× the amount or number normal for this child	Liquid stools greater than 8× the amount or number normal for this child
D. RENAL				
Creatinine	0.7–1.0 mg/dL (4–12 yrs)	1.1–1.6 mg/dL (4–12 yrs)	1.7–2.0 mg/dL (4–12 yrs)	>2.0 mg/dL (4–12 yrs)
	1.0–1.7 mg/dL (>12 yrs)	1.8–2.4 mg/dL (>12 yrs)	2.5–3.5 mg/dL (>12 yrs)	>3.5 mg/dL (>12 yrs)
E. NEUROLOGICAL				
LINCL disability scale	Since these children are already neurologically impaired, toxicity will be defined as: Grade I–1 point decrease from baseline; Grade II–2 point decrease from baseline; Grade III–3 point decrease from baseline; Grade IV–4 point decrease from baseline; since this is a progressive disease, even if there is no adverse effects, some deterioration is expected.			
F. OTHERS				
Fever ³	T 38.5–39.0° C	T 39.1–40° C	T 40.1–42° C	T >42° C
Skin	Scattered macular or papular eruption or erythema that is asymptomatic	Scattered macular or papular eruption or erythema with pruritis or other associated symptoms	Generalized symptomatic macular, papular or vesicular eruption	Exfoliative dermatitis or ulcerative dermatitis

¹During the vector and post-vector periods, all adverse reactions will be reported along with the clinical and laboratory assessment as to whether the adverse reaction is associated with the vector, the procedure used to assess safety or efficacy, or an intercurrent illness.

²ULN—upper limit normal.

³For greater than 6 hours despite antipyretic therapy.



Appendix III—FDA mandated annual follow-up

**Department of
Genetic Medicine**

**BATTEN DISEASE
PROTOCOL**

Site: NYPH-WMC
 Subject ID#: _____ Subject initials: _____

Protocol: # _____ “Administration of a Replication Deficient Adeno-associated Virus Gene Transfer Vector Expressing the Human CLN2 cDNA to the Brain of Children with Late Infantile Neuronal Ceroid Lipofuscinosis.”

Annual Follow-up Not Done

1. The year of follow-up (check one)
 3rd 4th 5th 6th 7th 8th 9th
 10th 11th 12th 13th 14th 15th

2. Date of initial telephone call: / /
 2.1 Contact successful: No Yes (skip to 6)
 ↓

3. Date of first follow-up telephone call: / /
 3.1 Contact successful: No Yes (skip to 6)
 ↓

4. Date of second follow-up telephone call: / /
 4.1 Contact successful: No Yes (skip to 6)
 ↓

5. Certified letter: Yes No
 ↓
 5.1 Patient responded: No Yes (skip to 7)
 ↓

Complete an Early Discontinuation and fax it to 212-746-8477

6. Spoke to patient: Yes Other(s)
 ↓
 6.1 Relationship to subject: _____

7. Subject status: Alive Deceased
 7.1 DOD: / /
 7.2 Autopsy: Yes No N/A

(continued)

Appendix III—FDA mandated annual follow-up (Cont.)

8. Current medications: N/A

Medication	Total Daily Dose	Date Began MMMDYY	Date Ended MMMDYY	Check if Ongoing	Primary Reason for Use
				<input type="checkbox"/>	
				<input type="checkbox"/>	
				<input type="checkbox"/>	
				<input type="checkbox"/>	
				<input type="checkbox"/>	
				<input type="checkbox"/>	
				<input type="checkbox"/>	
				<input type="checkbox"/>	
				<input type="checkbox"/>	
				<input type="checkbox"/>	
				<input type="checkbox"/>	

9. Date if last physical examination: //

9.1 Findings (i.e., evidence of cancer, neurological, autoimmune and hematological disorders):

10. Date last seen by private MD: //

11. Hospitalization since last contact: Yes No

11.1 Further information with regard to dates, diagnosis, hospital admitted, doctor/surgeons' name, address and telephone number.

12. Medical records requested: Yes No

I verify all details on this form represent a true record as stated via the telephone.

Name of person completing the form

Signature of person who completed form

Date

Investigator's signature

Date

Address reprint requests to:
Dr. Ronald G. Crystal
Department of Genetic Medicine
Weill Medical College of Cornell University
515 East 71ST Street, Suite 1000
New York, NY 10021

E-mail: geneticmedicine@med.cornell.edu

RESEARCH ARTICLE

AAV2-mediated CLN2 gene transfer to rodent and non-human primate brain results in long-term TPP-I expression compatible with therapy for LINCL

D Sondhi^{1,5}, DA Peterson^{2,5}, EL Giannaris¹, CT Sanders², BS Mendez¹, B De¹, AB Rostkowski², B Blanchard³, K Bjugstad³, JR Sladek Jr³, DE Redmond Jr⁴, PL Leopold¹, SM Kaminsky¹, NR Hackett¹ and RG Crystal¹

¹Department of Genetic Medicine, Weill Medical College of Cornell University, New York, NY, USA; ²Department of Neuroscience, Rosalind Franklin University of Medicine and Science, The Chicago Medical School, North Chicago, IL, USA; ³Department of Psychiatry, University of Colorado Health Science Center, Denver, CO, USA; and ⁴Neural Transplantation and Regeneration Program, School of Medicine, Yale University, New Haven, CT, USA

Late infantile neuronal ceroid lipofuscinosis (LINCL) is a fatal, autosomal recessive disease resulting from mutations in the CLN2 gene with consequent deficiency in its product tripeptidyl peptidase I (TPP-I). In the central nervous system (CNS), the deficiency of TPP-I results in the accumulation of proteins in lysosomes leading to a loss of neurons causing progressive neurological decline, and death by ages 10–12 years. To establish the feasibility of treating the CNS manifestations of LINCL by gene transfer, an adeno-associated virus 2 (AAV2) vector encoding the human CLN2 cDNA (AAV2_{cu}hCLN2) was assessed for its ability to establish therapeutic levels of TPP-I in the brain. *In vitro* studies demonstrated that AAV2_{cu}hCLN2 expressed CLN2 and produced biologically active TPP-I protein of which a fraction was secreted as the pro-TPP-I precursor and was taken up by nontransduced cells (ie, cross-correction). Following AAV2-mediated CLN2 delivery to the rat striatum, enzymatically active TPP-I protein was detected. By immunohistochemistry TPP-I protein was detected in striatal neurons (encompassing nearly half of the target structure) for

up to 18 months. At the longer time points following striatal administration, TPP-I-positive cell bodies were also observed in the substantia nigra, frontal cerebral cortex and thalamus of the injected hemisphere, and the frontal cerebral cortex of the noninjected hemisphere. These areas of the brain contain neurons that extend axons into the striatum, suggesting that CNS circuitry may aid the distribution of the gene product. To assess the feasibility of human CNS delivery, a total of 3.6×10^{11} particle units of AAV2_{cu}hCLN2 was administered to the CNS of African green monkeys in 12 distributed doses. Assessment at 5 and 13 weeks demonstrated widespread detection of TPP-I in neurons, but not glial cells, at all regions of injection. The distribution of TPP-I-positive cells was similar between the two time points at all injection sites. Together, these data support the development of direct CNS gene transfer using an AAV2 vector expressing the CLN2 cDNA for the CNS manifestations of LINCL.

Gene Therapy (2005) 12, 1618–1632. doi:10.1038/sj.gt.3302549; published online 28 July 2005

Keywords: AAV2; LINCL; Batten; CLN2; TPP-I; brain gene therapy

Introduction

Late infantile neuronal ceroid lipofuscinosis (LINCL) is an autosomal recessive, neurodegenerative lysosomal storage disease.^{1–3} Mutations in the CLN2 gene result in a deficiency in the lysosomal activity of tripeptidyl peptidase I (TPP-I), with consequent accumulation of autofluorescent material resembling lipofuscin in the lysosomes.^{4,5} This storage material consists of undegraded proteins, primarily subunit c of mitochondrial ATP synthase.^{6–8} Although all tissues of individuals with

LINCL are TPP-I deficient, retinal pigmented epithelial cells and central nervous system (CNS) neurons are the most sensitive to decreased activity of TPP-I, resulting in their progressive destruction.^{2,3,9,10} The consequences are progressive loss of vision and neurological decline beginning at about age 3 years with cognitive impairment, seizures, and deteriorating motor skills that lead to a vegetative state and death in middle to late childhood.^{1–3}

There are compelling data to suggest that direct CNS administration of an adeno-associated virus (AAV) vector expressing the CLN2 cDNA should be able to mediate expression of TPP-I in a sufficient number of neurons to slow down, and potentially halt, the progression of the CNS disease. First, AAV gene transfer vectors are capable of mediating transfer and persistence of expression of a variety of genes in the CNS.^{11–17} Second, mucopolysaccharidosis VII, a related lysosomal storage disease, has been successfully reversed in a knockout

Correspondence: Dr RG Crystal, Department of Genetic Medicine, Weill Medical College of Cornell University, 515 East 71st Street, Suite 1000, New York, NY 10021, USA

⁵These authors contributed equally to this paper

Received 22 July 2004; accepted 10 February 2005; published online 28 July 2005

mouse model by recombinant AAV2-mediated intracranial gene transfer.^{16,18–20} Third, a significant fraction of newly synthesized TPP-I protein is secreted as pro-TPP-I, a 563 amino-acid inactive form which can cross-correct nearby nontransduced cells through mannose 6-phosphate receptor-mediated uptake and subsequent activation in lysosomes to the 367 amino-acid mature form.^{21,22} This cross-correction between transduced cells and neighboring cells suggests that it will not be necessary to transfer the normal CLN2 cDNA to all the cells in the CNS, thus extending the effective range of gene transfer to broader regions of the brain.¹⁷ Finally, comparisons of genotype and phenotype of children with CLN2 mutations reveal that expression as low as 5% of normal TPP-I levels lead to a much milder form of the disease with a delayed age of onset, less severe symptoms, and a prolonged lifespan, suggesting that this level of enzyme activity is a reasonable target for therapy.²³ This target level of expression of the transferred cDNA is within levels that could be achieved with current AAV vector technology.

There are several challenges to the development of AAV-mediated CLN2 therapy for LINCL. The CNS manifestations of LINCL are diffuse, and thus successful gene therapy will need to provide TPP-I activity over as broad a volume of the brain as possible.^{1,2} Second, the absence of an experimental animal model for the disease until very recently²⁴ required that the detection of gene transfer-mediated TPP-I expression is above the background corresponding to normal expression in a naive animal. However, the target level for therapy is only 5% of the endogenous level and the various detection methods for TPP-I are not sensitive enough to detect this amount above the background. Finally, as with most genetic diseases, the optimal therapy would be to produce long-term expression of the therapeutic gene from a single administration of the vector.

Based on these considerations, this study is focused on assessment of CNS expression of TPP-I mediated by direct CNS administration of AAV2_{CU}hCLN2, an AAV serotype 2-based gene therapy vector applicable to treating LINCL. Direct CNS administration of AAV2_{CU}hCLN2 to rats and African green monkeys resulted in relatively stable and long-lasting expression of TPP-I within the CNS, which is promising for the development of gene therapy for LINCL.

Results

Function of AAV vectors in vitro

Cells infected with AAV2_{CU}hCLN2 were evaluated for TPP-I expression using both immunoperoxidase and immunofluorescence detection systems using a mouse monoclonal anti-human TPP-I antibody. Vector-mediated expression of TPP-I was evident using both immunoperoxidase and immunofluorescence detection (Figure 1a–d). The negative controls included cells infected with an AAV2_{CU}Null vector, which did not contain the CLN2 transgene (panels b, d) as well as naive cells (not shown). Treatment of CLN2-expressing cells with an irrelevant primary antibody (mouse anti-shiga toxin) did not show positive staining (not shown). High power images of immunofluorescence staining indicated that the antigen was distributed in a punctate pattern throughout the

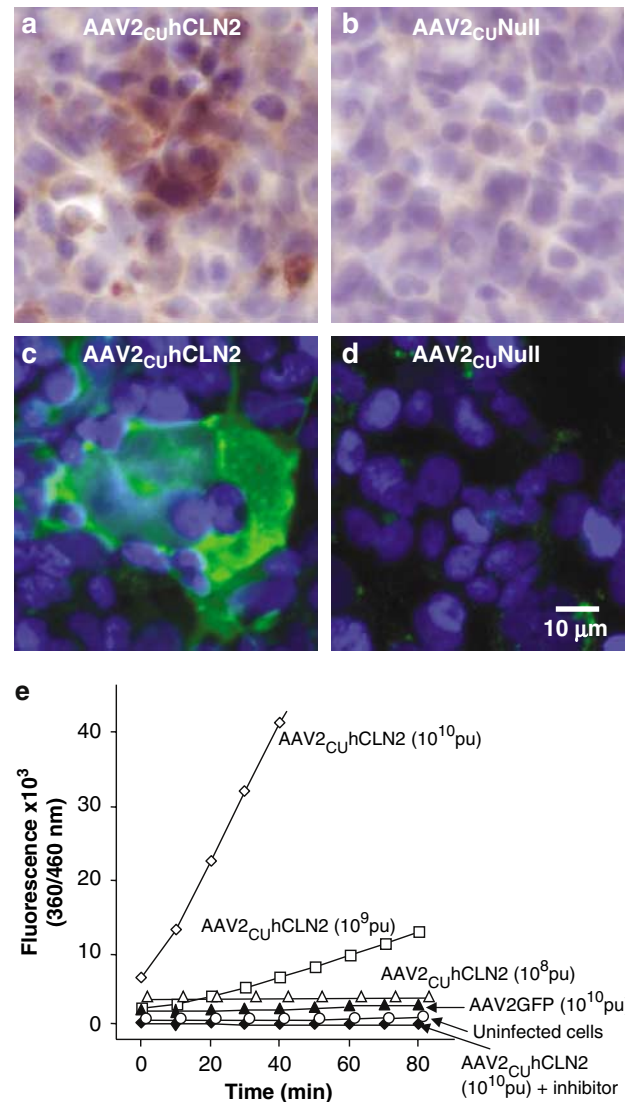


Figure 1 Function of the AAV2_{CU}hCLN2 vector in vitro. (a–d) Morphological detection of TPP-I following CLN2 gene transfer. 293ORF6 were infected with AAV2_{CU}hCLN2 or AAV2_{CU}Null at 10³ particles per cell and TPP-I expression was assessed after 2 days. Immunodetection of TPP-I was performed using a mouse anti-human TPP-I monoclonal antibody. For immunoperoxidase detection (a, b), primary antibody binding was detected by horseradish peroxidase-conjugated anti-mouse antibody followed by precipitation of diaminobenzidine. For immunofluorescence detection (c, d), the TPP-I primary antibody was detected with Alexa 488-conjugated anti-mouse antibody (green), the nuclei were stained with DAPI (blue) and the cells visualized by fluorescent microscopy. (e) Enzymatic activity of TPP-I secreted from transfected cells. 293ORF6 cells (10⁶ cells) were infected with AAV2_{CU}hCLN2 (10⁸–10¹⁰ pu) or AAV2GFP (10¹⁰ pu), a control AAV2 vector with a GFP transgene. After 48 h, the medium was collected, the pro-TPP-I was converted to active TPP-I at low pH and TPP-I activity was assessed. The time course of increase in fluorescence is shown for various conditions.

cytoplasm consistent with localization in intracellular organelles (not shown). High power images also revealed the presence of a low level of endogenous TPP-I expression in the human 293 cells, appearing as small groups of organelles restricted to an area of the cytoplasm close to the nucleus. Similar results of

vector-mediated TPP-I expression were obtained with cells infected with AAV2_{CU}rCLN2 (not shown).

Use of a TPP-I specific fluorogenic substrate showed that infection of cells by AAV expressing CLN2 resulted in TPP-I enzymatic activity in the cells with secretion into the media (Figure 1e). The background activity in the media from uninfected cells was <10 fluorescence units (FU)/min-ml with <10 FU/min-mg in the cell homogenate. As expected, TPP-I activity was dose-dependent with infection by 4×10^3 particle units (PU)/cell (4×10^9 pu total dose) of AAV_{CU}hCLN2 resulting in the secretion of $1.25 \pm 0.24 \times 10^5$ FU/min-ml, while infection by 4×10^4 pu/cell (4×10^{10} pu total dose) gave $9 \pm 0.6 \times 10^5$ FU/min-ml. The percentage of the total TPP-I activity in the media (as opposed to the cell-associated TPP-I activity) was $5.7 \pm 2\%$ at 4×10^3 pu/cell and $22.3 \pm 7\%$ at 4×10^4 pu/cell. Similar results of vector-mediated TPP-I activity were obtained with cells infected with AAV2_{CU}rCLN2 (not shown). Vector-derived TPP-I activity was demonstrated by lack of activity in controls including the assay of naive cells and cells transduced with comparable vectors with irrelevant transgene (AAV2GFP). The specificity of the assay for TPP-I activity was confirmed by inhibition using the TPP-I-specific enzyme inhibitor, Ala-Ala-Phe-chloro-methyl ketone.

In vitro cross-correction of LINCL-deficient fibroblasts mediated by AAV2_{CU}hCLN2

Like some other lysosomal storage disorders, LINCL is an attractive candidate for gene therapy due to cross-correction, where a portion of the newly synthesized pro-TPP-I made by transduced cells may be taken up by neighboring cells, thereby amplifying the number of cells with TPP-I activity. This pathway was demonstrated *in vitro* by showing transfer of TPP-I from the media of cells infected with AAV2_{CU}hCLN2 to fibroblasts derived from a LINCL patient. The specificity of the transfer was indicated by the inhibition observed on addition of 1 mM mannose-6-phosphate (an inhibitor of uptake mediated by mannose-6-phosphate-mediated endocytosis), which reduced uptake by the LINCL fibroblasts by 78% (Figure 2). To ensure that the TPP-I activity in fibroblasts was not due to carry over of vector, AAV2_{CU}hCLN2 levels were assessed in the media transferred to the LINCL fibroblasts. The level was <1% of the input level of vector. In a separate experiment, when this level of AAV2_{CU}hCLN2 was used to infect LINCL fibroblasts, it did not yield a level of TPP-I activity over the background TPP-I activity following exposure of LINCL fibroblasts to media from naive 293ORF6 cells.

TPP-I distribution following AAV2-mediated CLN2 delivery to the rat brain

Histological analyses and enzyme activity assays were used to determine the level, duration, and distribution of TPP-I expression that could be obtained by AAV2-mediated gene transfer in rat brain. Results obtained from transfer of the rat CLN2 gene (observed using the rabbit anti-TPP-I antibody) were indistinguishable from transfer of the human CLN2 gene (observed using the monoclonal anti-human TPP-I antibody). Results for both rat and human CLN2 gene delivered by AAV2-based vectors expression are described below.

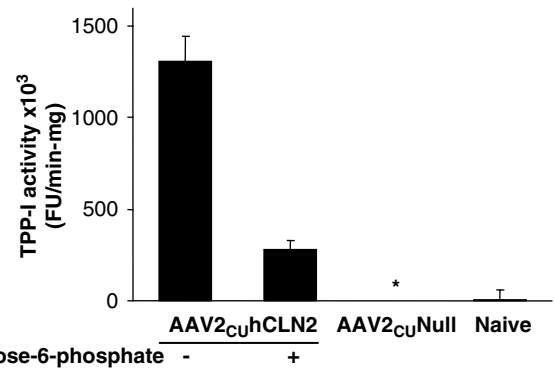


Figure 2 *In vitro* cross-correction of LINCL-deficient fibroblasts mediated by AAV2_{CU}hCLN2. Duplicate wells of 293ORF6 cells (10^6) were infected with AAV2_{CU}hCLN2 or AAV2_{CU}Null at 3×10^4 pu/cell or mock infected. After 24 h, the medium was removed, the cells washed twice with PBS and replaced with RPMI media which was collected after a further 72 h. This medium was collected diluted 1:3, and placed onto LINCL-deficient fibroblasts in the presence or absence of 1 mM mannose-6-phosphate. After 24 h, the fibroblasts were collected, lysed, and assayed for TPP-I activity using a fluorometric assay. The means and standard deviation of quadruplicates is shown. * = not detectable.

TPP-I enzymatic activity assays were carried out on tissue homogenates of coronal sections of the brain of naive, AAV2_{CU}Null and AAV2_{CU}rCLN2-injected rats (Figure 3). The TPP-I activity of the sections of the uninjected right striatum was similar across the brain with no significant difference between the AAV2_{CU}Null and AAV2_{CU}rCLN2 group ($P > 0.25$ all locations). However, in the injected hemisphere, in the slice corresponding to the injection site, there was a significantly higher TPP-I activity in the AAV2_{CU}rCLN2-injected mice ($P < 0.05$ compared to AAV2_{CU}Null group). The mean TPP-I activity ($n = 3$ animals/group) was 55% greater than the background for this region. No significant differences were observed among the groups at any other location of the injected hemisphere ($P > 0.05$).

The striatum was chosen as a delivery site for its relatively homogeneous cellular architecture and large volume relative to the rat brain as a whole. Immunohistochemical examination of TPP-I expression at 4 weeks following a single striatal injection of 10^{10} pu of AAV2_{CU}rCLN2 demonstrated robust TPP-I expression and the neuron-specific tropism of the AAV2-mediated gene delivery. The majority of striatal neurons in the injection region were found to express TPP-I, as determined by coexpression with NeuN, a marker for mature neurons (Figure 4). In contrast, adjacent GFAP-positive astrocytes did not contain detectable levels of TPP-I, nor were other TPP-I-positive/NeuN-negative cells observed by confocal microscopic analysis when registered focal plane series were evaluated for coexpression of cytoplasmic TPP-I and nuclear NeuN expression. Endogenous TPP-I gene expression was not observed at the dilution of the rabbit anti-TPP-I antibody used in this assay.

The TPP-I expression studies were not formal toxicology studies and did not use vector prepared within the requirements of Good Laboratory Practice. However, there was no observed behavioral difference between the AAV2_{CU}hCLN2-injected animals and the naive

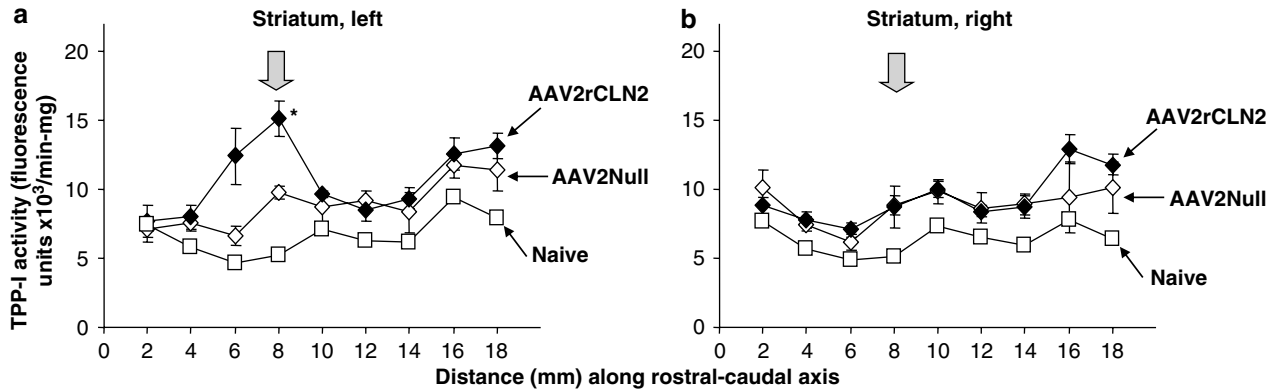


Figure 3 Spatial distribution of TPP-I enzymatic activity following stereotactic injection of AAV2_{cur}CLN2. Three rats were injected with 5 μ l of AAV2_{cur}CLN2 containing 5×10^9 pu into the left striatum, and as controls three rats were injected with 5 μ l of AAV2_{cur}Null containing 5×10^9 pu into the left striatum. After 4 weeks, the animals were killed and the fresh brain was excised from the six treated and from two age-matched naive (untreated) animals. Each brain was divided into nine sections of 2 mm width by coronal sectioning. Each section was then divided into left and right hemispheres and the cortex was discarded leaving the internal structures (including the striatum). Sections were separated and homogenized. The TPP-I activity was determined and normalized to protein concentration of homogenate. The plots show the spatial distribution along the rostral/caudal axis for the TPP-I activity. The vertical arrow shows the estimated location of vector administration. The section for which the TPP-I activity of three AAV2_{cur}CLN2-injected and three AAV2_{cur}Null-injected animals differ ($P < 0.05$) is shown with an asterisk. (a) Left (injected) hemisphere; (b) right (uninjected) hemisphere.

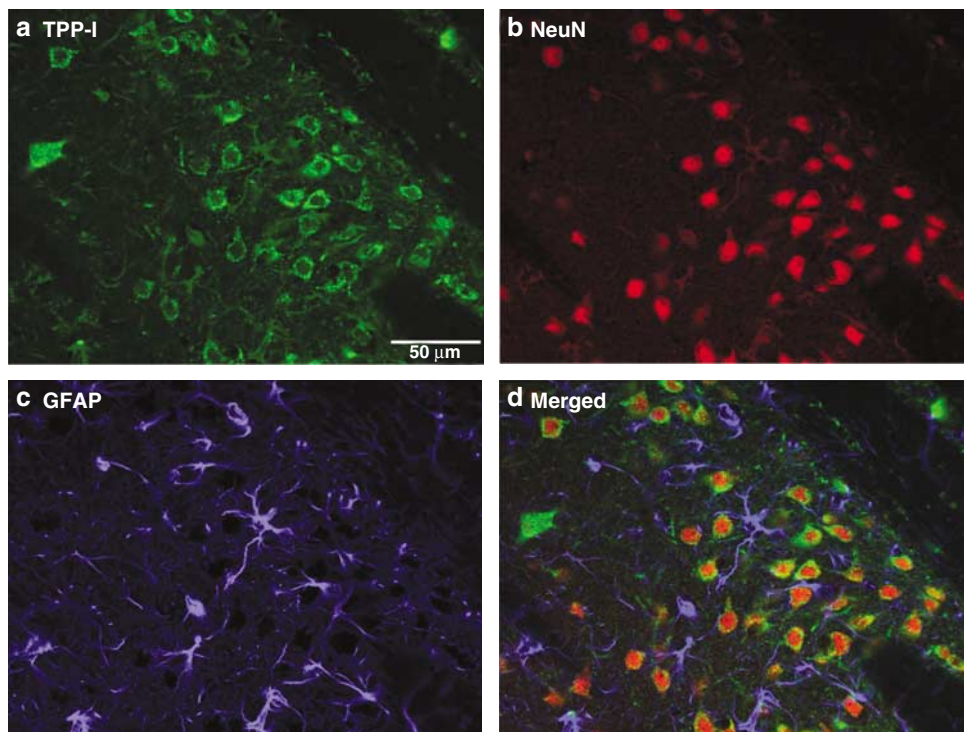


Figure 4 Preferential TPP-I accumulation in neurons following AAV2_{cur}CLN2 delivery to the rat striatum. Sections of rat brain were studied by immunofluorescence 4 week following striatal injection of 10^{10} pu of AAV2_{cur}CLN2. (a) Immunofluorescence detection of TPP-I (green) using the rabbit anti-TPP-I antibody and Cy2-conjugated secondary antibody; (b) immunofluorescence staining demonstrating neurons (red) in the same section as in panel (a) using anti-NeuN primary antibody and a Cy3-conjugated secondary antibody; (c) immunofluorescence detection of glia (blue) in the same section as in panel (a) using anti-glial fibrillary acidic protein (GFAP) primary antibody and a Cy5-conjugated secondary antibody; and (d) superimposition of the signals of TPP-I-expressing cells (green) with neuron-specific staining (red, NeuN) and glial-specific staining (blue, GFAP) demonstrating neuron-specific expression mediated by the AAV2_{cur}CLN2 vector. Smaller neurons show obvious colocalization of cytoplasmic TPP-I and the primarily nuclear NeuN expression. Two large neurons do not include the nucleus in the confocal optical plane of section and thus do not appear NeuN-positive in this image, but would demonstrate colocalization in subsequent focal planes. The magnification was identical in all panels; bar = 50 μ m.

controls nor was there a statistically significant difference in mortality ($P > 0.3$ by Kaplan–Meier analysis). Based on the triple immunofluorescence studies, there was

some degree of astrocytic hypertrophy observed around the injection site that is comparable with that normally seen following intracranial injection, but there was

no sign of inflammatory cell infiltration or vascular cuffing.

The pathology of LINCL is diffuse throughout the CNS. To establish that the cellular expression of TPP-I could be observed following delivery to CNS locations other than the striatum, injections of AAV2_{CU}rCLN2 were made into several brain structures including the frontal cortex, the parietal cortex (Figure 5), and the cerebellum (not shown). Examination of these regions 4 weeks following delivery confirmed TPP-I expression and neurotropism of AAV2 infection with TPP-I expression seen in neuronal populations in all regions. TPP-I expression was widespread in the cortical injection regions with neurons of both pyramidal and interneuron morphologies showing TPP-I expression. There was no observed TPP-I expression in astrocytes.

As a goal of the study was to obtain stable and long-term expression of the TPP-I transgene, the histology of striatal TPP-I expression was examined at intervals from 2 weeks to 18 months following injection of AAV2_{CU}hCLN2 (Figure 6). Transgene expression from AAV2 vectors is known to increase gradually over several weeks and to persist for months or years.^{25–27} Consistent with this, at 2 weeks postinjection, there was little detectable human TPP-I protein in the rat striatum, but by 1 month, abundant human TPP-I protein was observed. The high level, stable AAV2-mediated expression of human TPP-I in the rat striatum persisted at comparable volume and intensity at 4, 8, 12, and 18 months (Figure 5). Quantitative assessment of TPP-I expression is a challenge because of the difficulties in

standardizing the anti-TPP-I staining process, including the different reagent solutions used over time, and the differences in optimal immunostaining in the brains of rats from different ages. With this caveat, the Cavalieri estimator was used to quantify the TPP-I detected by immunostaining in the striatum over time (Table 1). The volume of cellular TPP-I expression expressed as a percentage of the striatum was variable ranging from 22 to 67% of the striatum at different time points. There was no correlation of average volume and time ($P > 0.7$ by linear regression).

As has been observed with AAV2 vectors expressing other transgenes,^{28,29} we observed a high level of TPP-I expression in cell populations not directly at the site of injection, but whose axonal projections were located in the site of the injection. As widespread delivery of the gene product throughout the brain is a goal of the current study, we examined other brain regions that project to the striatum to determine if expression of TPP-I could be detected in projection neuronal populations following single intrastriatal administration of AAV2_{CU}hCLN2. Interestingly, neurons in the cerebral cortex showed TPP-I expression as early as 2 months following delivery, and expression was more widespread at 4 and 8 months relative to the earlier time points (Figure 7). By 8 months, TPP-I expression was also observed outside of the striatal injection area in neuronal populations in the thalamus and substantia nigra. Continued detection of TPP-I in neurons in these regions was observed at 12 months (not shown) and 18 months. In addition, at 18 months, TPP-I-positive cells were also

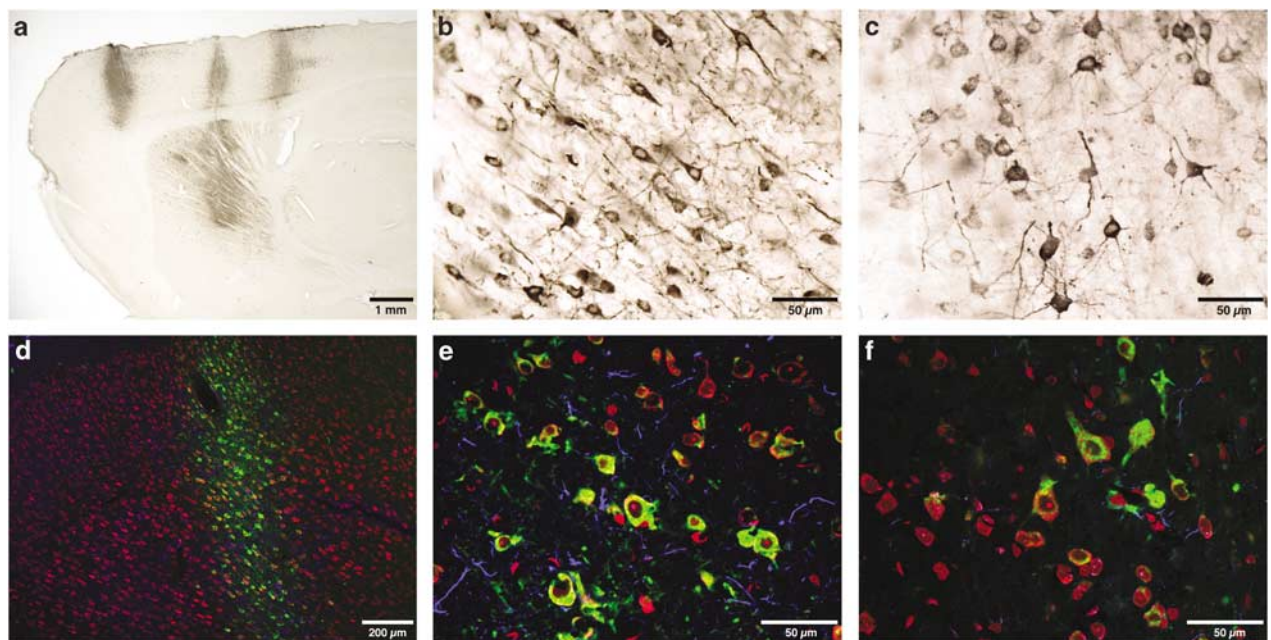


Figure 5 Comparison of AAV2_{CU}rCLN2-mediated expression of TPP-I in neurons in different delivery sites. (a) Delivery of AAV2_{CU}rCLN2 to the frontal cortex, striatum, and parietal cortex results in TPP-I expression as observed in a parasagittal section at 4 weeks. Immunoperoxidase-positive cells are observed in a wide region surrounding each injection site. (b) Higher magnification of the frontal cortex shows TPP-I positive cells with both the pyramidal morphology of projection neurons and the multipolar morphology of local circuit neurons. (c) A similar pattern of TPP-I staining is observed in cells of the parietal cortex. (d) Low magnification, multiple immunofluorescence appearance of a frontal cortex injection site showing the range of cell distribution and the morphology of TPP-I-expressing cells (green). (e) Colocalization of TPP-I expression (green) with a fluorescent nuclear marker (propidium iodide, red) and the astrocyte marker (GFAP, blue) shows that TPP-I is expressed by cells with a neuronal nuclear morphology, but not astrocytes in frontal cortex injection sites. (f) Localization of TPP-I in cells with a neuronal morphology, but not astrocytes is also observed in parietal injection sites. Bars in each panel indicate the size for the different magnifications.

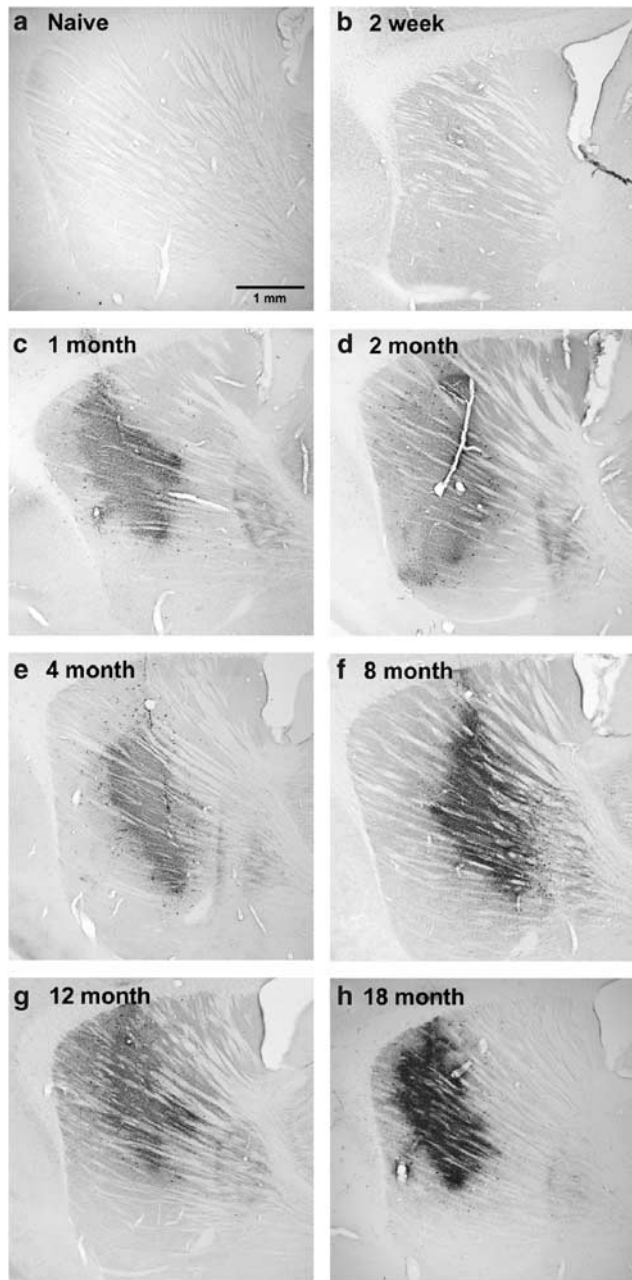


Figure 6 Time course of TPP-I protein accumulation following AAV2_{CU}-hCLN2 gene transfer. Rats ($n=3$ /group) were injected (10^{10} pu) into the striatum with $1 \mu\text{l}$ of AAV2_{CU}-hCLN2. After various time points, TPP-I distribution was assessed by anti-TPP-I immunoperoxidase staining on sagittal sections of the striatum of the injected hemisphere. Strong expression of TPP-I was detected at all time points from 1 to 18 months. (a) Naive; (b) 2 weeks; (c) 1 month; (d) 2 months; (e) 4 months; (f) 8 months; (g) 12 months; and (h) 18 months. Magnification bar = 1 mm for all panels.

observed in the contralateral (noninjected) hemisphere in the cortical regions that send commissural projections (projections crossing from the other hemisphere) to the striatum. In control rats, no TPP-I-positive cells were detected in these areas using the human-specific monoclonal anti-TPP-I antibody (not shown). Assessment of the extent of TPP-I-positive volume calculated as a percentage of the total hemisphere volume showed a

Table 1 Volumetric analysis of TPP-I expression in rat brain resulting from a single intrastriatal injection of AAV2_{CU}-hCLN2^{a,b}

Postdelivery interval (month)	TPP-I staining (% striatum)	TPP-I staining (% extrastriate hemisphere)	TPP-I staining (% total hemisphere)
1	42.9 ± 2.3	11.4 ± 1.0	15.8 ± 1.1
2	28.5 ± 10.2	10.6 ± 0.2	13.4 ± 1.2
4	39.4 ± 4.4	13.3 ± 1.9	17.0 ± 2.2
8	67.3 ± 1.2	11.8 ± 0.3	16.1 ± 0.3
12	46.0 ± 4.0	7.2 ± 0.5	10.2 ± 0.7
18	22.5 ± 2.5	0.6 ± 0.5^c	2.2 ± 0.5

^aTotal dose of 10^{10} particles units in $1 \mu\text{l}$.

^bShown are volumes of TPP-I-positive staining as a % of different reference volumes (striatum, extrastriate hemisphere, total hemisphere) \pm standard error of the mean at different time points following a single intrastriatal delivery of AAV2_{CU}-hCLN2; $n=3$ /rats were assessed for each time point.

^cOne animal in this group had no detectable extrastriate labeling and thus the mean is low and the variance is high.

range of values (2.2–17.0%; Table 1). There was no correlation of the TPP-I-positive volume calculated as a % of the total hemisphere with time ranging from 1 to 18 months ($P>0.8$).

TPP-I distribution after AAV2_{CU}-hCLN2 administration to the non-human primate brain

Expression of hCLN2 mediated by AAV2 delivery to the CNS was also observed in the brains of African green monkeys following injection of AAV2_{CU}-hCLN2 (Figures 8 and 9). Detectable levels of TPP-I expression were observed using human-specific monoclonal antibody via immunoperoxidase staining. The morphology of TPP-I-positive cells in the cortex suggested that by 5 weeks both interneurons and pyramidal neurons expressed TPP-I, while staining in the caudate nucleus showed expression in cells with the morphology of interneurons (Figure 8). Delivery to the hippocampus resulted in TPP-I expression in large multipolar hilar cells and, to a lesser extent, in dentate granule cells (Figure 9). Thus, successful expression of AAV2-mediated delivery of TPP-I in the non-human primate brain was not region dependent. The identity of TPP-I-expressing cells was revealed by multiple immunofluorescence staining using the TPP-I human-specific monoclonal antibody. To discriminate between true signal and the contribution of autofluorescence (predominantly seen at the shorter wavelengths in non-human primate brain tissue), detection of TPP-I was accomplished with secondary antibodies conjugated to the fluorophore Cy5, that, upon far red spectral excitation, emits at infrared wavelengths. Consistent with delivery to the rat brain, examination of TPP-I-expressing cells in the non-human primate brain by multiple immunofluorescence staining revealed that neuronal, but not glial, populations were infected at all injection sites (Figures 8 and 9). Persistence of expression is a key factor for developing therapies for disorders such as LINCL. To evaluate duration of TPP-I expression in the non-human primate brain, animals were assessed at 5 and 13 weeks and found to contain equivalent distribution of TPP-I-

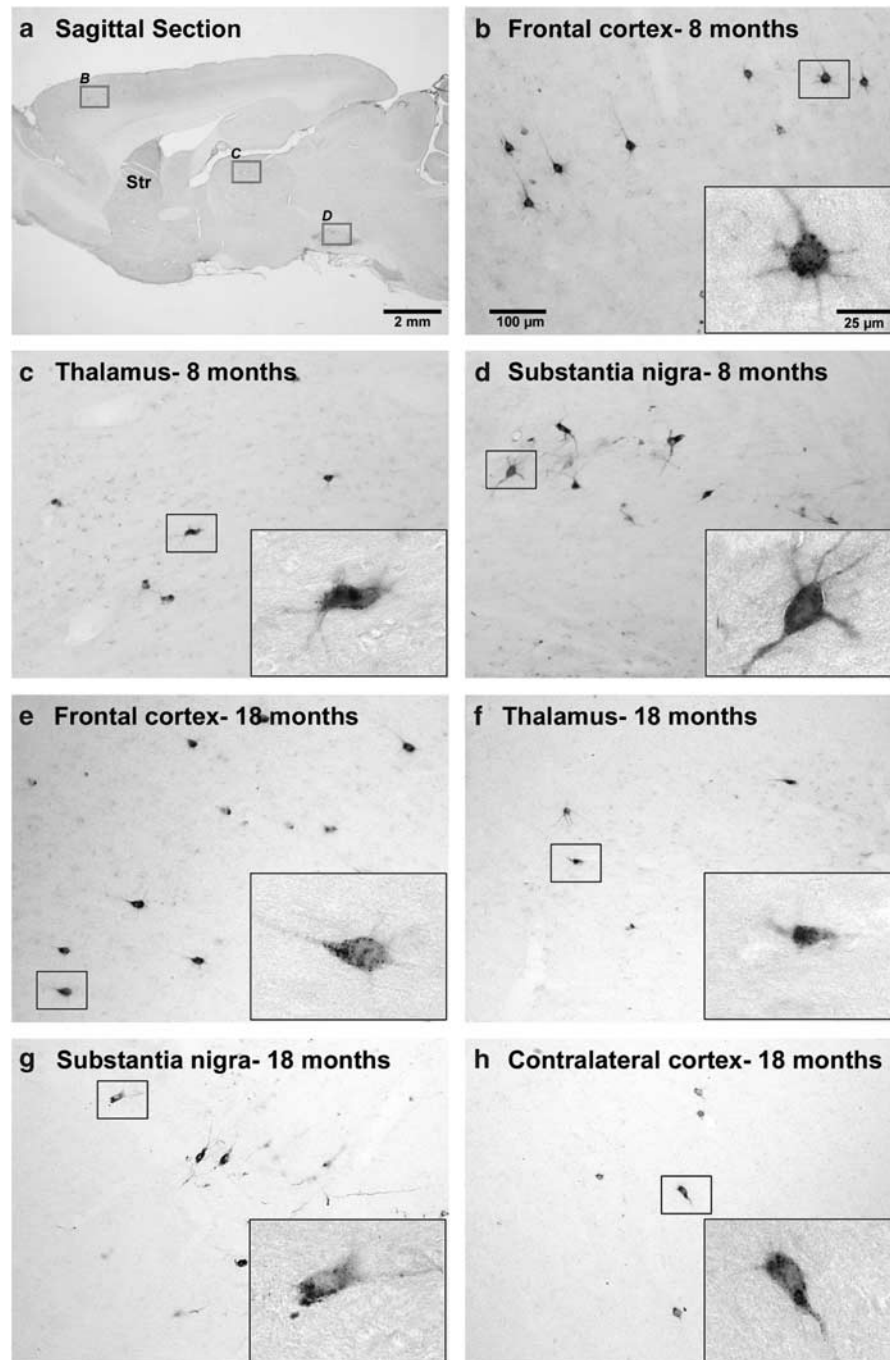


Figure 7 Expression of TPP-I in structures far from the injection site. Rats ($n=3$ /group) were injected into the striatum (Str) with 10^{10} pu in $1 \mu\text{l}$ of AAV2_{cu}hCLN2. TPP-I distribution was assessed by immunoperoxidase staining. Cell populations expressing robust levels of TPP-I were observed in a number of distant anatomical projection sites at all time points. Examples from 8 month (a–d) and 18 month (e–h) postinjection times are shown. (a) Representative sagittal section of brain showing location of structures analyzed in subsequent panels. This section is medial to the striatum so that only a tangential profile of the striatum is present here with sparse TPP-I expression. A section through the center of the striatum confirming TPP-I expression in this same animal is shown in Figure 6f; (b) high magnification of frontal cortex with TPP-I accumulation in pyramidal projection neurons; (c) thalamus, TPP-I stained multipolar neurons; (d) Substantia nigra, TPP-I stained large multipolar neurons; (e) frontal cerebral cortex, injected hemisphere TPP-I accumulation in pyramidal projection neurons at 18 months following gene delivery; (f) thalamus, injected hemisphere, TPP-I stained multipolar neurons; (g) Substantia nigra, injected hemisphere, TPP-I stained large multipolar neurons; (h) cerebral cortex, noninjected hemisphere with TPP-I accumulation in pyramidal projection neurons. Control rats had no TPP-I-positive cells in these areas (not shown). Magnification bar is indicated on panel a (for panel a alone) and b (for panels b–h). Cells indicated by the box are shown in higher magnification in the inset.

positive cells (Figure 9). As with the rats, other than minor physical damage along the area of injection, there were no signs of inflammatory cell infiltration or vascular cuffing.

Discussion

LINCL is a fatal childhood disease with no known therapy. Several features of LINCL make it a good

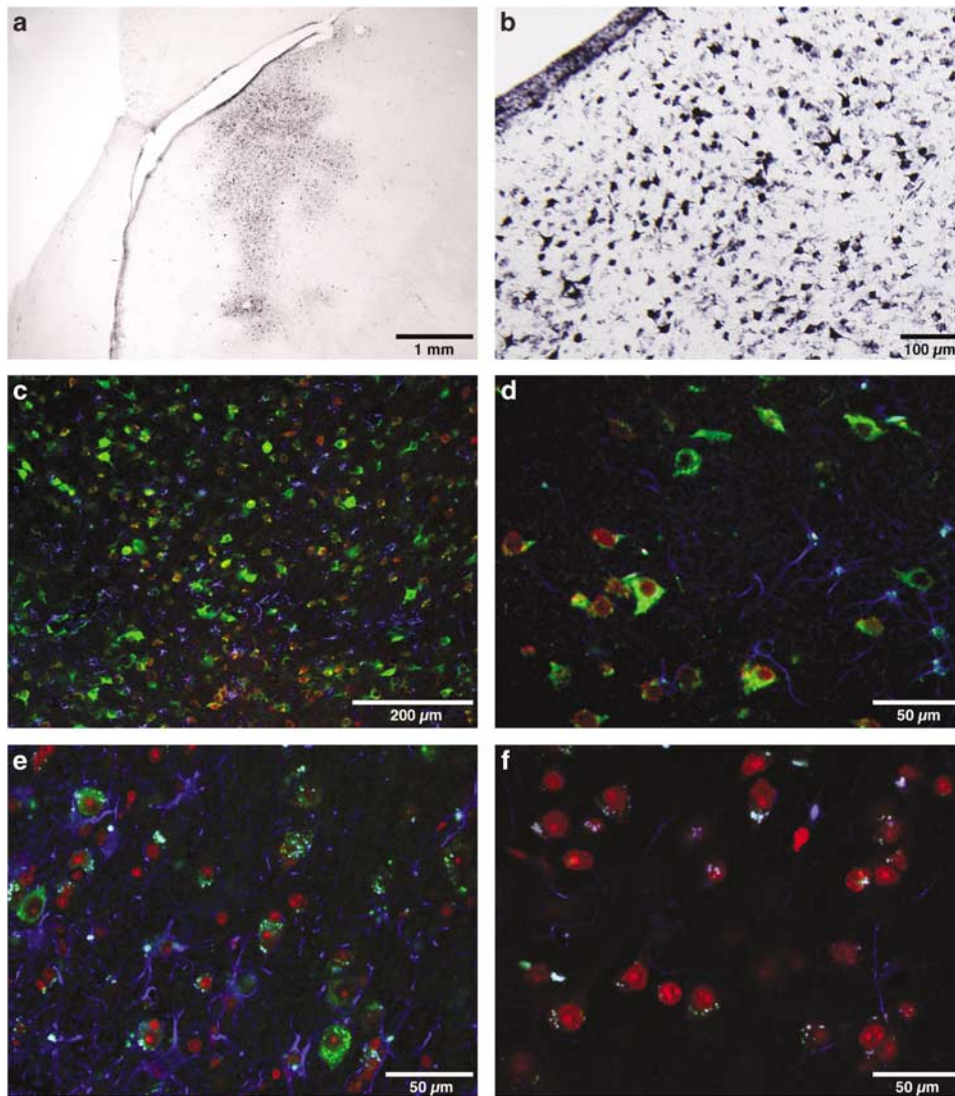


Figure 8 TPP-I expression by neurons in the cortex and caudate nucleus of the non-human primate brain 5 weeks following administration of AAV2_{CuH}CLN2. (a) Low magnification view of immunoperoxidase-stained TPP-I-positive cells in the head of the caudate nucleus. (b) The same region shown in (a) at higher magnification showing the widespread TPP-I expression in multipolar cells. (c) Similar view to (b) showing widespread expression of TPP-I in the caudate nucleus identified by immunofluorescence (green). (d) High magnification of TPP-I expression (green) in the head of the caudate nucleus in neurons stained with calbindin (red), but not astrocytes identified by their expression of GFAP (blue). (e) High magnification view of TPP-I-expressing cells (green) in the cortex, identified as neuronal by their morphological staining with propidium iodide (red) and absence of GFAP staining (blue). (f) Similar cortical region to that shown in (e) in a naïve control animal using the same labeling as described in (e), showing that the detection of TPP-I could be discriminated from background autofluorescence. Bars in each panel indicate the size for the different magnifications.

candidate for gene therapy, including the monogenetic nature of the disease, knowledge of the deficient TPP-I protein and the gene (CLN2) that encodes it, a need for only low target levels of the therapeutic protein, and the ability of this protein to be secreted and internalized into neighboring cells providing potential for cross-correction.^{4,21,23,30} In regard to technologies available today, gene therapy is the best option for this disorder to protect neural cells from death. The present study describes the successful delivery and long-term expression of CLN2 by an AAV2-based vector, and the assessment of its gene product, TPP-I, following delivery to rat and non-human primate brain. The data fulfills three critical requirements for the preclinical development of therapy for this disease: (1) long term duration of expression of the

therapeutic protein; (2) broad distribution of the therapeutic protein which may be a composite of infection and cross-correction; and (3) achieving sufficient levels of expression of the protein that should have therapeutic effect.

Duration

For the treatment of a chronic metabolic disorder such as LINCL, it is necessary to achieve long-term expression of TPP-I in the CNS. In this respect, the choice of vector is critical. In agreement with other reports,^{31–34} we have shown that an AAV2-based vector can maintain expression of the transgene and hence of the therapeutic protein for >1 year. In addition to the choice of vector, the choice of promoter is also critical for long-term high

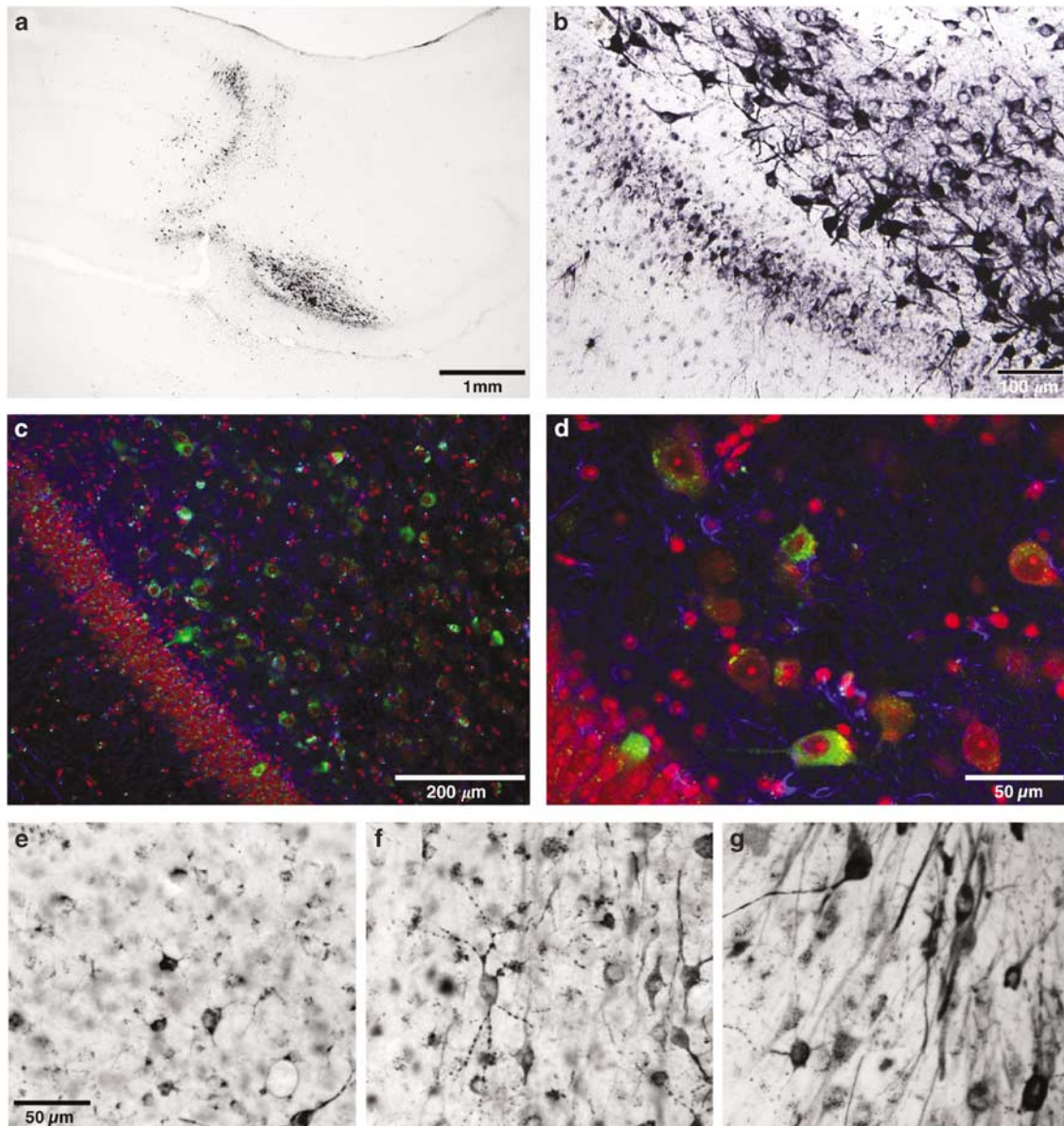


Figure 9 TPP-I expression in the non-human primate hippocampus at 5 and 13 weeks and in the cortex and caudate nucleus at 13 weeks following administration of AAV2_{CU}hCLN2. Panels (a–d), 5 weeks. (a) Low magnification view of immunoperoxidase staining for TPP-I at 5 weeks in the hippocampus. (b) Region of the hippocampal formation shown at higher magnification. TPP-I-positive staining is observed in cells of the dentate gyrus, the curving structure at the left and bottom of the panel. There is robust TPP-I staining of multipolar cells in the dentate hilus. (c) TPP-I-positive cells (green) in the hippocampus detected by multiple immunofluorescence staining (neuronal cells identified by morphological staining with propidium iodide, red and glial cells in blue with GFAP staining). (d) Higher magnification of the region in panel (c) shows punctate cytoplasmic accumulation of TPP-I (green) in cells of neuronal morphology of both the hilus and dentate granule cells as shown by their appearance with propidium iodide labeling (red). TPP-I staining is not seen in astrocytes (GFAP, blue, panels c and d). Panels (e–g). High magnification view of TPP-I expression in various regions following administration of AAV2_{CU}hCLN2 to the non-human primate CNS 13 weeks as assessed by immunoperoxidase staining. (e) Caudate nucleus; (f) cortex; and (g) hippocampus. Bars in each panel (a–d) indicate the size for different magnifications. The magnification for panels (e–g) is indicated in panel (e).

level expression, as some viral promoters have been linked to premature decline of transgene expression.^{35,36} In the present study, we utilized the CMV-enhanced chicken β -actin promoter with the β -actin/rabbit β -globin hybrid intron, a promoter/intron combination that has been shown to successfully drive the expression of an AAV vector-mediated transfer of a gene in the brain for >1 year.¹⁶ The combination of the long-term expressing vector AAV2 and a strong nonviral promoter led to robust TPP-I expression in the brain of rats for >18

months and for at least 3 months (the longest time period examined to date) in the brains of non-human primates in the present study. Owing to resources needed, there is limited data on long-term transgene expression in non-human primates beyond 90 days as described here, although one report shows persistent expression up to 134 days.¹³ In rats, after 1 month, although there was variability, there was no significant time-dependent change in the extent of transgene expression following AAV2_{CU}hCLN2 gene transfer as assessed by the TPP-I-

positive volume expressed as a percentage of the injected striatum or the injected hemisphere.

TPP-I distribution

Robust transduction of neurons was achieved following administration of the AAV2_{CU}hCLN2 vector to the rat and non-human primate brain. The neurotropic specificity of AAV2-based vectors has been previously observed with AAV2-mediated gene delivery.^{11,37,38} The neurotropism of AAV2 makes this vector suitable for use as a gene delivery vehicle for neurons, the target cell population for intervention in LINCL.^{2,9} In the rat, a single intrastriatal injection resulted in histological detection of TPP-I throughout both dorsal and ventral extents of the striatum. The extent of TPP-I expression encompassing, nearly half of the striatum, remained stable over time following gene delivery.

Of interest relevant to the goal of achieving widespread expression of TPP-I in the CNS was the observation in the rat that distant neurons expressed TPP-I after a lengthy interval following delivery. The distribution of these sites of extrastriatal TPP-I expression was highly variable over time but consistent with the known circuitry of striatal projections. Neurons in both the dorsal and ventral striatum receive input from cerebral cortex, thalamus, and the midbrain ventral tegmental area and substantia nigra.^{39–41} Thus, distant neurons, whose axons terminate in the region of vector delivery, were able over time to express TPP-I. There are two possible explanations for TPP-I expression in distant projection neurons. Previous reports have demonstrated that distant neurons can be transduced by retrograde transport of the viral vector following AAV2 delivery to the CNS.²⁸ Alternatively, the secreted TPP-I enzyme could be taken up by synaptic terminals and undergo retrograde transport to distant cell bodies. This mechanism would be consistent with the *in vitro* cross-correction data showing that TPP-I is secreted by cells transduced by AAV2_{CU}hCLN2 and subsequently taken up by nontransduced cells in a mannose-6-phosphate-dependent pathway. It would also be consistent with the extensive intracellular staining for TPP-I observed in transfected cells, where TPP-I was likely present in all compartments of the secretory and endocytic pathways. Whatever the mechanism of this retrograde expression, these results suggest that it may be possible to utilize the circuitry of neuronal connections to extend the effective expression of TPP-I to distant regions. This possibility greatly augments the therapeutic potential of each intracerebral injection and suggests that the circuitry of the brain should be taken into account when designing therapeutic delivery.

In a careful survey of sections of the brains of the AAV2_{CU}hCLN2 non-human primates, no TPP-I-positive cells far from the injection site suggestive of retrograde transport were seen. There may be two reasons for this. First, the retrograde transport observed in rats increased over time with a maximum at 8 months and monkeys were assessed at shorter time points due to resource limitations. Second, the sensitivity of the immunohistochemistry in the non-human primates was titrated down by use of lower levels of the monoclonal anti-TPP-I antibody than that used in the rats (1:15 000 as compared to 1:1000). This was done to suppress the endogenous

TPP-I background in the non-human primate tissue but this also reduces the sensitivity with which retrograde transport may be seen.

TPP-I protein levels

At present, there is no defined clinical benchmark for the minimum level of TPP-I expression required for successful therapeutic intervention for LINCL. Individuals who are heterozygous for LINCL have no disease phenotype suggesting that it will not be necessary to completely restore normal TPP-I levels.^{1–3} Furthermore, individuals with LINCL who have a mutation in CLN2 that results in 5–10% of normal TPP-I activity have delayed onset of the symptoms,²³ suggesting that as little as 5% of normal activity spread throughout the brain represents a reasonable target level for clinical benefit.

While a target of 5% of normal levels makes the goal of effective therapy for LINCL easier to achieve with gene therapy, the available analytical methods are not sufficiently sensitive to demonstrate an increase in only 5% over a background of normal TPP-I levels *in vivo*. For example, the variance in the TPP-I activity measurement on brain homogenates of naive rats was 24%, a value much greater than the target level. However, a TPP-I level was obtained that was 55% above background following AAV2_{CU}hCLN2 infection demonstrating that locally therapeutic levels are easily achieved. As no characterized TPP-I-deficient animal model is available, we are only able to evaluate TPP-I levels that are significantly increased over the background. There is a wide distribution of robust TPP-I-positive cells detected following AAV2-mediated gene delivery using immunohistochemistry under conditions that gave no signal for endogenous TPP-I. Although immunohistochemical staining does not allow for a linear quantitative estimation of protein levels, this technique is also not particularly sensitive to very low intracellular protein levels. Thus, immunohistochemical detection likely underestimates the true extent of CLN2 gene product expression, suggesting that at least the minimum target levels of TPP-I expression have been achieved in the identified regions.

Implications for future studies

This study supports the notion that AAV2-mediated CLN2 gene delivery to the CNS can meet the criteria of widespread, robust transgene expression of long duration required for the development of a therapeutic gene delivery strategy. The recent characterization of a CLN2-deficient mouse,²⁴ which displays a similar pathology as LINCL in humans will also allow the potential therapeutic benefit of intracranial gene transfer to be assessed more rigorously. There is currently favorable short-term safety data related to the intracranial transfer of AAV2_{CU}hCLN2 in human patients based upon the growing clinical experience of AAV2-mediated gene transfer to the brain for the treatment of Canavan and Parkinson's diseases.^{42,43} Therefore, it seems likely that there would be no significant safety issues related to intracranial transfer of AAV2_{CU}hCLN2 in human patients. In this context, LINCL is a candidate disease for further preclinical development of AAV2-mediated gene therapy.

Methods

Production of AAV2 vectors

The overall genome structure of all AAV vectors used in the study included (5'–3'): the 141 nt inverted terminal repeat (ITR) from AAV2; an expression cassette that included the CAG promoter (the human cytomegalovirus immediate/early enhancer; the promoter, the splice donor, and the left-hand intron sequence from chicken β -actin; the right-hand intron sequence and splice acceptor from rabbit β -globin);^{44–46} the cDNA of interest with an optimized Kozak consensus translation initiation signal prior to the start codon; the rabbit β -globin poly A/stop sequence; and the 141 nt ITR. The vectors were produced using two plasmids: (1) 'AAV2-ITR/expression' plasmid containing (5'–3'): the AAV2 ITR, CAG promoter, the cDNA of interest, the polyA/stop, and the AAV ITR; and (2) adenovirus/AAV helper gene plasmid (pPAK-MA2) containing (5'–3'): the mouse mammary tumor virus ITR promoter driving the AAV2 rep gene, followed by the AAV2 cap gene and the adenovirus serotype 5 VA, E2, and E4 genes, each driven by their own promoter.^{47,48}

The AAV2 vectors used in the study included: AAV2_{CU}hCLN2 (expression cassette includes the human CLN2 cDNA); AAV2_{CU}rCLN2 (identical to AAV2_{CU}-hCLN2 except that it has the rat CLN2 cDNA substituted for the human CLN2 cDNA); and AAV2_{CU}Null (used as a control, identical to AAV2_{CU}hCLN2 except that it has an untranslatable DNA sequence corresponding to intron 5 of the human vascular endothelial growth factor gene to match the size of the human CLN2 cDNA); and AAV2GFP used as a negative control (see Zolotukhin *et al*⁴⁹ for a description of AAV2GFP).

All of the AAV2 vectors were produced in the same manner using Polyfect™ (QIAGEN Sciences, Germantown, MD, USA) mediated cotransfection of 500 μ g of the expression cassette plasmid containing the transgene of interest and 1 mg of the AAV/adenovirus helper gene plasmid into a 10 Stack Cell Factory (NUNC™ Brand Products, VWR Scientific, West Chester, PA, USA) at 70% confluence of low passage 293 cells. Post transfection (72 h), the cells were harvested and a crude viral lysate made by three cycles of freeze/thaw, then clarified by centrifugation and purified by discontinuous iodixanol gradients and heparin agarose chromatography.⁵⁰

All vectors were assessed by quantitative PCR (TaqMan), capsid ELISA (Research Diagnostics, Flanders, NJ, USA), and by their ability to replicate in adenovirus-infected C12 cells (a cell line expressing the AAV2 rep and cap genes) with detection of the amplified genome by DNA hybridization.⁵¹ Evidence that the CLN2 vectors could direct the expression of the desired transgene product was established by assessing TPP-I enzyme activity (as described below). For the *in vitro* and *in vivo* experiments, all vectors were dosed on the basis of particle units as assessed by ELISA (Research Diagnostic Inc., Flanders, NJ, USA).

Morphological evaluation of TPP-I protein expression *in vitro*

The AAV2_{CU}hCLN2 vector was evaluated for its ability to produce TPP-I by indirect immunofluorescence and immunoperoxidase detection of CLN2 expression.

293ORF6 cells, from a human embryonic kidney cell line expressing adenovirus E1 and E4 genes⁵² were maintained in Dulbecco's modified Eagle's medium (DMEM, Invitrogen Life Technologies, Carlsbad, CA, USA) supplemented with 1 mM sodium pyruvate, 10% fetal bovine serum (FBS), 50 U/ml penicillin, 50 μ g/ml streptomycin, 2 mM L-glutamine, and 0.25 μ g/ml fungizone-amphotericin. For the AAV expression studies, the 293ORF6 cells (5×10^4 cells) were infected with AAV2_{CU}hCLN2 or AAV2_{CU}Null (10^3 particles/cell) in 30 μ l serum-free DMEM at 37°C. After 30 min, 2 ml of DMEM supplemented with 100 μ M ZnCl₂ were added to the cells to activate the E4 gene expression.⁵² After 2 days, the cells were washed twice with phosphate-buffered saline, pH 7.4 (PBS) and fixed with 4% paraformaldehyde (Electron Microscopy Sciences, Fort Washington, PA, USA) in PBS. For immunoperoxidase detection of TPP-I, the cells were then pretreated with 0.03% hydrogen peroxide (Sigma-Aldrich, St Louis, MO, USA) for 5 min, 22°C to quench endogenous peroxidase activity. The cells were then treated (20 min, 22°C) with blocking medium (5% goat serum, 1% bovine serum albumin (BSA), in PBS). Primary antibodies were diluted in blocking medium (1:100), including mouse anti-human CLN2 hybridoma supernatant (clone mAb 8C4, provided by Krystyna Wisniewski, Institute for Basic Research in Developmental Disabilities, Staten Island, NY, USA) and mouse anti-shiga toxin hybridoma supernatant as an irrelevant primary antibody control (clone 11F11, American Type Culture Collections, Manassas, VA, USA). The primary antibodies were applied for 60 min at 37°C, removed with three 5 min washes with 1% BSA in PBS. Horseradish peroxidase-based immunocytochemistry was performed using the Envision kit (Dako, Carpinteria, CA, USA) according to the manufacturer's instructions. Briefly, horseradish peroxidase-conjugated secondary antibody (anti-mouse) was applied to cells for 30 min at 37°C, washed three times in PBS, and treated with the diaminobenzidine-activator cocktail for 5 min at 22°C. Cells were counterstained using hematoxylin (Sigma-Aldrich) and imaged using a Leaf MicroLumina color charge coupled device (CCD) camera (ElectroImage, Great Neck, NY, USA).

For immunofluorescence detection of TPP-I, the cells were infected and fixed as described above, and then, after three washes in PBS, cells were postfixed in 100% methanol (–20°C, 20 min), and washed three times in PBS. The cells were then blocked and treated with primary antibodies as described above with the exception of hybridoma supernatants being diluted 1:10 instead of 1:100 and application at 22°C instead of 37°C. The primary antibodies were applied for 60 min and removed as described above and replaced with a secondary antibody for 45 min at 22°C (dilution of 1:100 in blocking medium, goat anti-mouse Alexa 488, Molecular Probes, Eugene, OR, USA). The secondary antibody was removed with three 5 min washes with 1% BSA in PBS followed by three rinses in PBS. Nuclei were stained with 4'-6-diamidino-2-phenylindole (DAPI, 2 μ g/ml in PBS, 5 min, 22°C, Molecular Probes). Cells were observed using widefield epifluorescence microscopy using an Olympus IX70 microscope. Images were captured using a Photometrics Quantix cooled CCD camera and analyzed using MetaMorph image analysis program (Universal Imaging, Downingtown, PA, USA).

Evaluation of TPP-I enzyme activity

The function of vector-derived TPP-I was demonstrated by assessing TPP-I enzyme activity using a fluorescently-activated specific substrate. In 24-well plates, 10^6 293ORF6 cells were incubated until 90% confluent and then infected (10^8 – 10^{10} pu) with AAV2_{CU}hCLN2, AAV2GFP (an irrelevant transgene control), or AAV2_{CU}-Null. Medium was collected 48 h postinfection and transferred to a 96-well plate. The cells were harvested separately and suspended in 100 μ l of 0.15 M NaCl, 0.1% Triton X-100 to make a lysate. Secreted enzyme in 10 μ l of medium was activated with 20 μ l of an activating solution (150 mM NaCl, 0.1 % Triton X-100, and 50 mM formic acid, pH 3.5) to mimic its natural activation in the lysosomes following reuptake.²¹ After incubation at 37°C for 30 min, 250 μ M Ala-Ala-Phe-7-amido-4-methylcoumarin (the TPP-I-specific substrate; Sigma-Aldrich) in 40 μ l of 150 mM NaCl, 0.1% Triton X-100, and 100 mM sodium acetate, pH 4.0 was added and a fluorescence (360/20 nm excitation, 460/25 emission) time course was then determined at 10 min intervals for 80 min at 37°C in a Cytofluor 4000 TC plate reader (PerSeptive Biosystems, Foster City, CA, USA).²¹ The activity of the vector-derived TPP-I was determined by calculating the change in FU per viral particle dose per min over a linear portion of the curve minus the corresponding activity in cells infected with a control vector encoding an irrelevant transgene. This assay provides an intrinsic specification for vector potency that can be applied independent of yield, a parameter that varies between different viral preparations. In this assay, vector preparations were accepted that gave $> 3 \times 10^{-6}$ FU/(min-ml media-pu). To demonstrate specificity of the assay, it was performed in the presence and absence of a TPP-I-specific inhibitor, Ala-Ala-Phe-chloro-methyl ketone (1 μ M, Sigma-Aldrich Co; see Lin and Lobel²¹ and Ezki et al⁵³).

In vitro cross-correction of LINCL-deficient fibroblasts mediated by AAV2_{CU}hCLN2

To assess the ability of AAV2_{CU}hCLN2 to direct the expression of a CLN2 product that will cross-correct neighboring cells, the medium of quadruplicate wells of 293ORF6 cells infected with 3×10^4 pu/cell AAV2_{CU}hCLN2 or AAV2_{CU}-Null was removed 24 h postinfection and the cells were washed twice with PBS. It was then replaced by fibroblast medium (RPMI 1640 media containing 1% glutamine, 10% FBS, 50 U/ml penicillin, 50 μ g/ml streptomycin, 2 mM L-glutamine and 0.25 μ g/ml fungizone-amphotericin) for 72 h. This medium was collected and assessed for pro-TPP-I content by enzymatic assay, and for AAV2_{CU}hCLN2 content by Taqman. LINCL fibroblasts (provided by P Lobel, Robert Wood Johnson Medical College) were cultured in fibroblast medium until 70% confluent at which time 30% of the medium was replaced by the media collected from the 293ORF6 cells with or without 1 mM mannose-6-phosphate as a competitive inhibitor of uptake. After 24 h, the cells were harvested and lysed in 150 mM NaCl, 0.1% Triton X-100 for assessment of TPP-I activity.

To insure that the TPP-I activity in the LINCL fibroblasts did not result from carry over of AAV2_{CU}hCLN2 in the media from the 293ORF6 cells initially infected by the vector, carry over was assessed in the media using TaqMan real-time quantitative PCR with

primers (forward: GTCAATGGGTGGAGTATTACGG and reverse: AGGTCATGTACTGGGCATAATGC) and probe (CAAGTGTATCATATGCCAAGTACGCCCCCT) specific to the CMV enhancer. The amount of AAV2_{CU}hCLN2 determined to be carried over by this method was used to directly infect the LINCL fibroblasts with assessment of the TPP-I activity in the media after 72 h.

CNS administration of AAV2 vectors in rats

To evaluate TPP-I expression and distribution following AAV2-mediated CLN2 delivery in a small animal model brain, Fischer 344 male rats (180–200 g; Taconic, Germantown, NY, USA) were used with Institutional Animal Care and Use Committee (IACUC) approval of all procedures. The rats were deeply anesthetized and positioned in a stereotaxic frame for unilateral injection into the left striatum (AP +0.6 mm, ML +2.8 mm, and DV –5.2 mm relative to Bregma), frontal cortex (AP +3.0, ML +2.8, DV –2.5), parietal cortex (AP –1.3, ML +2.5, DV –2.0), or cerebellum (AP –10.0, ML 2.5, DV –3.7). The AAV vectors, formulated in PBS (1.0–5.0 μ l per site), were injected at a rate of 0.2 μ l/min using a microprocessor-controlled infusion pump (Model 310, Stoelting, Wood Dale, IL, USA). The injection needle was left in position for 1 min prior to, and 2 min following delivery before being slowly withdrawn from the brain. Animals received either AAV2_{CU}hCLN2 (10^9 or 10^{10} pu) or AAV2_{CU}Null (10^9 or 10^{10} pu). Pilot experiments suggested that there was no effect of total injection volume (at constant vector dose) on the distribution or level of TPP-I under these conditions (not shown). Other animals received AAV2_{CU}Null (10^9 or 10^{10} pu) or PBS to control for the specificity of transgene expression.

Enzymatic assay of TPP-I activity in brain homogenate

To assess TPP-I enzymatic activity in the brain of AAV2_{CU}hCLN2-injected rats, vector injections were performed as described above, and at the relevant time, the animals were euthanized and the brains were harvested unfixed. The brains were rinsed in ice-cold PBS, placed in a rodent brain matrix, which was on ice (Electron Microscopy Sciences, Hatfield, PA, USA), and sliced into nine 2 mm coronal sections using matrix-specific razor blades. All sections were hemisected prior to analysis. Each half of the sections from the left hemisphere was further dissected into cortex and noncortex (striatum). Samples were stored at –80°C in microcentrifuge tubes until used. TPP-I activity was assayed by homogenization of the brain tissue in blank solution (150 mM NaCl, 1 mg/ml Triton X-100) using a disposable pellet pestle and 1.5 ml matching tube (Kimble-Kontes, Vineland, NJ USA). The homogenate was clarified by centrifugation and the supernatant was transferred onto a 96-well plate and assayed for TPP-I activity as described above. The activity of the transgene product was determined by calculating the change in fluorescence units per min per mg of protein (standardized by BCA protein assay, Pierce Biotechnology, Rockford, IL, USA).

Morphological evaluation of TPP-I protein expression in the rat brain

To assess TPP-I distribution and tropism at various time points after CNS administration of the vectors, rats were deeply anesthetized and perfused transcardially with

ice-cold PBS followed by ice-cold 4% paraformaldehyde in 0.1 M phosphate buffer (200 ml each). The brains were then harvested and immersed in the same fixative overnight, equilibrated in 30% sucrose at 4°C; serial 50 µm thick sagittal sections were later produced by freezing sliding microtomy.

Multiple immunofluorescence labeling was performed using antibodies specific for neurons (mouse anti-NeuN, 1:2500, Chemicon International, Temecula, CA, USA or mouse anti-calbindin, 1:5000, Swant, Bellinzona, Switzerland) or astrocytes (guinea pig anti-GFAP, 1:500, Advanced Immunochemical, Long Beach, CA, USA). Expression of the CLN2 transgene product was detected using antibodies against TPP-I. For specific detection of the human CLN2 transgene product, a mouse anti-human TPP-I antibody was used at a dilution of 1:1000. For detection of either human CLN2 or rat CLN2 transgene products, a rabbit anti-TPP-I antibody (provided by P Lobel, Robert Wood Johnson Medical College) was used at a dilution of 1:1000. When appropriate, sections were counterstained with the fluorescent nucleic acid dye, propidium iodide (1:5000 for 3 min; Molecular Probes). Propidium iodide labels all nuclei within the tissue section and acts as a 'fluorescent Nissl stain', permitting the phenotypic identity to cells to be established according to classic criteria used with Nissl staining.⁵⁴ Donkey secondary antibodies specific for relevant species were conjugated to biotin, Cy2, Cy3, or Cy5 or streptavidin-conjugated fluorophores (1:500; all from Jackson ImmunoResearch, West Grove, PA, USA) as appropriate for the specific discrimination of primary antibodies. Specificity of antibody detection was verified by staining uninfected tissue and by omission of primary antibodies in infected tissue. In separate sections, immunoperoxidase detection of the rat CLN2 transgene product was accomplished by quenching of endogenous peroxidase activity and incubation with rabbit anti-TPP-I polyclonal antibody (1:1000) or the human CLN2 transgene product by mouse anti-human TPP-I antibody (1:1000), followed by biotin-streptavidin amplification (Vectastain kit, Vector Laboratories, Burlingame, CA, USA) and visualization with a nickel chloride-enhanced diaminobenzidine reaction. Images were obtained by confocal microscopy (Olympus FluoView) for the immunofluorescence-stained material or brightfield images were obtained by digital image acquisition (Olympus BX50; Nikon D100) for the immunoperoxidase-stained material. Volume estimates of the extent of detectable TPP-I expression in the rat brain was carried out using the Cavalieri estimator on a one in six series of immunoperoxidase-stained sections through the entire hemisphere exclusive of the cerebellum, brainstem, and olfactory bulb.⁵⁵ Linear regression analysis was performed to assess volume changes over time.

CNS administration of AAV2 vectors in non-human primates

To evaluate TPP-I expression and distribution following AAV2-mediated CLN2 delivery in a large animal model brain, non-human primates were used. These studies were carried out at the St Kitts Biomedical Research Foundation, a facility that operates under Public Health Service regulations with IACUC oversight and with an assurance document filed at the National Institute of

Health. African green monkeys (*Chlorcebus aethiops sabaues*, male, 4.8–6.2 kg, feral, 5–10 years old) were deeply anesthetized and restrained in a stereotactic frame equipped with Hamilton microsyringes, which are controlled by a nano injector, stepper motorized injection pump (Stoelting Co., Wood Dale, IL, USA) for injection to 12 locations through six burr holes (two depths per burr hole), three per hemisphere of the AAV vector or diluent control. Injection coordinates for the prescribed brain structures in the African green monkey were determined from previously injected and sectioned brains and are translated to the stereotactic instrument frame of reference. Injections were made to the head of the caudate nucleus and overlying cerebral cortex (16.2 mm apart), body of the caudate nucleus and the overlying cerebral cortex (19.2 mm apart), and the hippocampal formation and overlying cerebral cortex (31.2 mm apart). Before and after each injection, the brain tissue was allowed to seal around the syringe needle. The vector or PBS was delivered at each site at 1 µl/min for a total volume of 180 µl (15 µl at each of 12 locations delivered over 15 min at each site). Each non-human primate received a total dose of 3.6×10^{11} pu of the AAV2_{CU}hCLN2 vector or 3.6×10^{11} pu of the control AAV2_{CU}Null vector or the diluent PBS.

Assessment of TPP-I expression in the non-human primate brain

To assess TPP-I distribution and tropism in the non-human primate CNS, at various time points after vector injection, the non-human primates were deeply anesthetized and transcardially perfused with cold PBS. The brains were immediately removed and kept on ice while uniform 4 mm coronal slabs were cut using a specially fabricated brain mold. The right hemisphere of each slab was placed in 4% paraformaldehyde for 3–7 days for immersion fixation prior to transfer to 30% sucrose. The left hemisphere of the slabs was saved for future analysis.

The 4 mm coronal slabs from the right hemisphere were further sectioned (50 µm slices) and used for immunoperoxidase detection and immunofluorescence in methods similar to that described for the rat tissue. However, to help to discriminate transgene product from endogenous protein, a 1:15 000 dilution of the primary monoclonal anti-TPP-I antibody was used for the non-human primate brain rather than the 1:1000 dilution used for sections of rat brain. To separate detection of TPP-I immunofluorescence from autofluorescence in non-human primate tissue, secondary antibodies were conjugated to Cy5, which fluoresces in the far red portion of the visible spectra. To maintain continuity to analysis of the rat tissue, signal detection of TPP-I was mapped to the green channel for image composition.

Acknowledgements

We thank P Lobel, Robert Wood Johnson Medical College, for providing the anti-TPP-I polyclonal antibody and the CLN2-deficient fibroblasts; K Wisniewski, Institute for Basic Research in Developmental Disabilities, for providing the anti-TPP-I monoclonal antibody; B Ferris, R McKinney, M Lam, B Bergman, J Qiu, E Salvin, E Vassallo, R Abplett, and the staff at the

St Kitts Biomedical Research Foundation for technical assistance; and N Mohamed and T Virgin-Bryan for help in preparing this manuscript. These studies were supported, in part, by Nathan's Battle Foundation, Indianapolis, IN; and the Will Rogers Memorial Fund, Los Angeles, CA.

References

- 1 Lysosomal enzymes. In: Scriver CR, Beaudet AL, Sly WS, Valle D, Stanbury JB, Wyngaarden JB, Fredrickson DS (eds). *The Metabolic and Molecular Basis of Inherited Disease*. McGraw-Hill, Inc.: New York, 1995, p 2427.
- 2 Williams RE et al. CLN 2. Classic Late Infantile NCL. In: Goebel HH, Mole SE, Lake BD (eds). *The Neuronal Ceroid Lipofuscinoses (Batten Disease)*. IOS Press: Amsterdam, 1999, p 37.
- 3 Haltia M. The neuronal ceroid-lipofuscinoses. *J Neuropathol Exp Neurol* 2003; **62**: 1–13.
- 4 Sleat DE et al. Association of mutations in a lysosomal protein with classical late-infantile neuronal ceroid lipofuscinosis. *Science* 1997; **277**: 1802–1805.
- 5 Vines DJ, Warburton MJ. Classical late infantile neuronal ceroid lipofuscinosis fibroblasts are deficient in lysosomal tripeptidyl peptidase I. *FEBS Lett* 1999; **443**: 131–135.
- 6 Palmer DN et al. Mitochondrial ATP synthase subunit c storage in the ceroid-lipofuscinoses (Batten disease). *Am J Med Genet* 1992; **42**: 561–567.
- 7 Umehara F et al. Accumulation of mitochondrial ATP synthase subunit c in muscle in a patient with neuronal ceroid lipofuscinosis (late infantile form). *Acta Neuropathol* 1997; **93**: 628–632.
- 8 Ezaki J, Tanida I, Kanehagi N, Kominami E. A lysosomal proteinase, the late infantile neuronal ceroid lipofuscinosis gene (CLN2) product, is essential for degradation of a hydrophobic protein, the subunit c of ATP synthase. *J Neurochem* 1999; **72**: 2573–2582.
- 9 Boustany RM. Batten disease or neuronal ceroid lipofuscinosis. In: Moser HW (ed). *Handbook of Clinical Neurology (Vol. 22, 66): Neurodystrophies and Neurolipidoses*. Elsevier Science B.V.: New York, 1996, p 671.
- 10 Birch DG. Retinal degeneration in retinitis pigmentosa and neuronal ceroid lipofuscinosis: an overview. *Mol Genet Metab* 1999; **66**: 356–366.
- 11 Kaplitt MG et al. Long-term gene expression and phenotypic correction using adeno-associated virus vectors in the mammalian brain. *Nat Genet* 1994; **8**: 148–154.
- 12 McCown TJ et al. Differential and persistent expression patterns of CNS gene transfer by an adeno-associated virus (AAV) vector. *Brain Res* 1996; **713**: 99–107.
- 13 During MJ et al. *In vivo* expression of therapeutic human genes for dopamine production in the caudates of MPTP-treated monkeys using an AAV vector. *Gene Therapy* 1998; **5**: 820–827.
- 14 Mandel RJ et al. Characterization of intrastriatal recombinant adeno-associated virus-mediated gene transfer of human tyrosine hydroxylase and human GTP-cyclohydrolase I in a rat model of Parkinson's disease. *J Neurosci* 1998; **18**: 4271–4284.
- 15 Davidson BL et al. Recombinant adeno-associated virus type 2, 4, and 5 vectors: transduction of variant cell types and regions in the mammalian central nervous system. *Proc Natl Acad Sci USA* 2000; **97**: 3428–3432.
- 16 Frisella WA et al. Intracranial injection of recombinant adeno-associated virus improves cognitive function in a murine model of mucopolysaccharidosis type VII. *Mol Ther* 2001; **3**: 351–358.
- 17 Haskell RE et al. Viral-mediated delivery of the late-infantile neuronal ceroid lipofuscinosis gene, TPP-I to the mouse central nervous system. *Gene Therapy* 2003; **10**: 34–42.
- 18 Skorupa AF et al. Sustained production of beta-glucuronidase from localized sites after AAV vector gene transfer results in widespread distribution of enzyme and reversal of lysosomal storage lesions in a large volume of brain in mucopolysaccharidosis VII mice. *Exp Neurol* 1999; **160**: 17–27.
- 19 Bosch A, Perret E, Desmaris N, Heard JM. Long-term and significant correction of brain lesions in adult mucopolysaccharidosis type VII mice using recombinant AAV vectors. *Mol Ther* 2000; **1**: 63–70.
- 20 Sferra TJ et al. Recombinant adeno-associated virus-mediated correction of lysosomal storage within the central nervous system of the adult mucopolysaccharidosis type VII mouse. *Hum Gene Ther* 2000; **11**: 507–519.
- 21 Lin L, Lobel P. Production and characterization of recombinant human CLN2 protein for enzyme-replacement therapy in late infantile neuronal ceroid lipofuscinosis. *Biochem J* 2001; **357**: 49–55.
- 22 Lin L, Sohar I, Lackland H, Lobel P. The human CLN2 protein/tripeptidyl-peptidase I is a serine protease that autoactivates at acidic pH. *J Biol Chem* 2001; **276**: 2249–2255.
- 23 Sleat DE et al. Mutational analysis of the defective protease in classic late-infantile neuronal ceroid lipofuscinosis, a neurodegenerative lysosomal storage disorder. *Am J Hum Genet* 1999; **64**: 1511–1523.
- 24 Sleat DE et al. A mouse model of classical late-infantile neuronal ceroid lipofuscinosis based on targeted disruption of the CLN2 gene results in a loss of tripeptidyl-peptidase I activity and progressive neurodegeneration. *J Neurosci* 2004; **24**: 9117–9126.
- 25 Xiao XF, Li JF, Samulski RJ. Efficient long-term gene transfer into muscle tissue of immunocompetent mice by adeno-associated virus vector. *J Virol* 1996; **70**: 8098–8108.
- 26 Lo WD et al. Adeno-associated virus-mediated gene transfer to the brain: duration and modulation of expression. *Hum Gene Ther* 1999; **10**: 201–213.
- 27 Thomas CE, Storm TA, Huang Z, Kay MA. Rapid uncoating of vector genomes is the key to efficient liver transduction with pseudotyped adeno-associated virus vectors. *J Virol* 2004; **78**: 3110–3122.
- 28 Kaspar BK et al. Targeted retrograde gene delivery for neuronal protection. *Mol Ther* 2002; **5**: 50–56.
- 29 Passini MA, Lee EB, Heuer GG, Wolfe JH. Distribution of a lysosomal enzyme in the adult brain by axonal transport and by cells of the rostral migratory stream. *J Neurosci* 2002; **22**: 6437–6446.
- 30 Sondhi D et al. Feasibility of gene therapy for late neuronal ceroid lipofuscinosis. *Arch Neurol* 2001; **58**: 1793–1798.
- 31 Daly TM et al. Prevention of systemic clinical disease in MPS VII mice following AAV-mediated neonatal gene transfer. *Gene Therapy* 2001; **8**: 1291–1298.
- 32 Passini MA, Wolfe JH. Widespread gene delivery and structure-specific patterns of expression in the brain after intraventricular injections of neonatal mice with an adeno-associated virus vector. *J Virol* 2001; **75**: 12382–12392.
- 33 Klein RL et al. Dose and promoter effects of adeno-associated viral vector for green fluorescent protein expression in the rat brain. *Exp Neurol* 2002; **176**: 66–74.
- 34 Klein RL, King MA, Hamby ME, Meyer EM. Dopaminergic cell loss induced by human A30P alpha-synuclein gene transfer to the rat substantia nigra. *Hum Gene Ther* 2002; **13**: 605–612.
- 35 Prosch S et al. Inactivation of the very strong HCMV immediate early promoter by DNA CpG methylation *in vitro*. *Biol Chem Hoppe Seyler* 1996; **377**: 195–201.
- 36 Fitzsimons HL, Bland RJ, During MJ. Promoters and regulatory elements that improve adeno-associated virus transgene expression in the brain. *Methods* 2002; **28**: 227–236.
- 37 Bartlett JS, Samulski RJ, McCown TJ. Selective and rapid uptake of adeno-associated virus type 2 in brain. *Hum Gene Ther* 1998; **9**: 1181–1186.

- 38 Chamberlin NL, Du B, de Lacalle S, Saper CB. Recombinant adeno-associated virus vector: use for transgene expression and anterograde tract tracing in the CNS. *Brain Res* 1998; **793**: 169–175.
- 39 Haber SN, Groenewegen HJ, Grove EA, Nauta WJ. Efferent connections of the ventral pallidum: evidence of a dual striato pallidofugal pathway. *J Comp Neurol* 1985; **235**: 322–335.
- 40 McGeorge AJ, Faull RL. The organization of the projection from the cerebral cortex to the striatum in the rat. *Neuroscience* 1989; **29**: 503–537.
- 41 Berendse HW, Groenewegen HJ. Organization of the thalamo-striatal projections in the rat, with special emphasis on the ventral striatum. *J Comp Neurol* 1990; **299**: 187–228.
- 42 Doring MJ, Kaplitt MG, Stern MB, Eidelberg D. Subthalamic GAD gene transfer in Parkinson disease patients who are candidates for deep brain stimulation. *Hum Gene Ther* 2001; **12**: 1589–1591.
- 43 Janson C et al. Clinical protocol. Gene therapy of Canavan disease: AAV-2 vector for neurosurgical delivery of aspartoacylase gene (ASPA) to the human brain. *Hum Gene Ther* 2002; **13**: 1391–1412.
- 44 Niwa H, Yamamura K, Miyazaki J. Efficient selection for high-expression transfectants with a novel eukaryotic vector. *Gene* 1991; **108**: 193–199.
- 45 Daly TM et al. Neonatal intramuscular injection with recombinant adeno-associated virus results in prolonged beta-glucuronidase expression *in situ* and correction of liver pathology in mucopolysaccharidosis type VII mice. *Hum Gene Ther* 1999; **10**: 85–94.
- 46 Daly TM et al. Neonatal gene transfer leads to widespread correction of pathology in a murine model of lysosomal storage disease. *Proc Natl Acad Sci USA* 1999; **96**: 2296–2300.
- 47 Grimm D, Kern A, Rittner K, Kleinschmidt JA. Novel tools for production and purification of recombinant adenoassociated virus vectors. *Hum Gene Ther* 1998; **9**: 2745–2760.
- 48 Qui JP, Mendez BS, Crystal RG, Hackett NR. Construction and verification of an Ad/AAV helper plasmid designed for manufacturing recombinant AAV vectors for human administration. *Mol Ther* 2002; **5**: S47–S48.
- 49 Zolotukhin S et al. A 'humanized' green fluorescent protein cDNA adapted for high-level expression in mammalian cells. *J Virol* 1996; **70**: 4646–4654.
- 50 Zolotukhin S et al. Recombinant adeno-associated virus purification using novel methods improves infectious titer and yield. *Gene Therapy* 1999; **6**: 973–985.
- 51 Clark KR, Voulgaropoulou F, Fraley DM, Johnson PR. Cell lines for the production of recombinant adeno-associated virus. *Hum Gene Ther* 1995; **6**: 1329–1341.
- 52 Brough DE et al. A gene transfer vector-cell line system for complete functional complementation of adenovirus early regions E1 and E4. *J Virol* 1996; **70**: 6497–6501.
- 53 Ezaki J, Takeda-Ezaki M, Kominami E. Tripeptidyl peptidase I, the late infantile neuronal ceroid lipofuscinosis gene product, initiates the lysosomal degradation of subunit c of ATP synthase. *J Biochem (Tokyo)* 2000; **128**: 509–516.
- 54 Peterson DA. The use of fluorescent probes in cell counting procedures. In: Evans SM, Janson AM, Nyengaard JR (eds). *Quantitative Methods in Neuroscience-A Stereological Approach*. Oxford University Press: Oxford, 2004, p 88.
- 55 Peterson DA et al. Central neuronal loss and behavioral impairment in mice lacking neurotrophin receptor p75. *J Comp Neurol* 1999; **404**: 1–20.

Review

Confronting the Issues of Therapeutic Misconception, Enrollment Decisions, and Personal Motives in Genetic Medicine-Based Clinical Research Studies for Fatal Disorders

LISA M. ARKIN,¹ DOLAN SONDHI,¹ STEFAN WORGALL,^{1,2} LILY HYON K. SUH,¹
NEIL R. HACKETT,³ STEPHEN M. KAMINSKY,³ SYED A. HOSAIN,² MARK M. SOUWEIDANE,⁴
MICHAEL G. KAPLITT,⁴ JONATHAN P. DYKE,⁵ LINDA A. HEIER,⁵ DOUGLAS J. BALLON,⁵
DIKOMA C. SHUNGU,⁵ KRYSZYNA E. WISNIEWSKI,⁶ BRUCE M. GREENWALD,²
CHARLEEN HOLLMANN,¹ and RONALD G. CRYSTAL^{1,3}

ABSTRACT

Genetic medicine-based therapies have unlocked the potential for ameliorating diseases previously considered inevitably fatal. Inherent in the clinical trials of genetic medicines are ethical issues of therapeutic misconception, enrollment decisions as they relate to the risks and benefits of research, and the complex relationships among funding sources, investigators, and the families of affected individuals. The purpose of this paper is to help define these complex issues relevant to the use of genetic medicines and to describe the strategy we have used to confront these issues in a phase I trial of adeno-associated virus-mediated gene transfer to the central nervous system of children with late infantile neuronal ceroid lipofuscinosis (LINCL), a fatal lysosomal storage disease associated with progressive neurodegeneration and death by mid-childhood. Our approach to these challenges should provide a useful paradigm for investigators initiating other genetic medicine-based studies to treat inevitably fatal diseases.

INTRODUCTION

GENETIC MEDICINES based on gene or stem cell transfer have created the possibility of treating fatal hereditary disorders heretofore considered untreatable (Aglietta *et al.*, 1998; Surbek *et al.*, 1999; Costantini *et al.*, 2000; Kohn, 2001; Balicki and Beutler, 2002; Hacein-Bey-Abina *et al.*, 2002; Cheng and Smith, 2003; Edelman *et al.*, 2004). As the technologies for these therapies are developed, basic and translational studies have led to initial trials in human subjects (<http://www4.od.nih.gov/oba/rac/protocol.pdf>; Aglietta *et al.*,

1998; Orlic, 2004; Svendsen and Langston, 2004; Lum, 2005; Smits *et al.*, 2005). Although the major focus in these trials has been on applying the gene/stem cell technology in a manner that is safe and will yield insights into efficacy, the concept of possible treatments for fatal disorders for which there are no alternative therapies raises several ethical issues, including the potential for therapeutic misconception, enrollment issues relevant to the inherent risks and benefits of phase I trials, and personal motives intertwined in the complex relationships among funding sources, investigators, and the families of affected individuals.

¹Department of Genetic Medicine, Weill Medical College of Cornell University, New York, NY 10021.

²Department of Pediatrics, Weill Medical College of Cornell University, New York, NY 10021.

³Belfer Gene Therapy Core Facility, Weill Medical College of Cornell University, New York, NY 10021.

⁴Department of Neurological Surgery, Weill Medical College of Cornell University, New York, NY 10021.

⁵Department of Radiology, Weill Medical College of Cornell University, New York, NY 10021.

⁶Institute for Basic Research in Developmental Disabilities, Staten Island, NY 10314.

There are major differences between the basic ethical requirements of carrying out clinical research studies and providing therapeutic treatment (Daugherty, 1999; Lidz *et al.*, 2004). The clinician owes primary allegiance to the patient's well-being, whereas the clinical investigator also has an obligation to ensure that the study generates valid data and therefore contributes to the scientific community (Shatz, 1990; Oberman and Frader, 2003). This balance is essential for meaningful clinical research; it is nowhere more complex than in phase I studies to evaluate the safety of novel genetic medicine treatments for fatal disorders, particularly in those affecting children.

The intent of this paper is to articulate these issues as they are relevant to clinical research with genetic medicines and to describe how we have responded to these challenges in planning and conducting a phase I trial of gene transfer to the central nervous system for late infantile neuronal lipofuscinosis (LINCL), a fatal, hereditary neurodegenerative disorder of children in which the subjects are completely vulnerable, not only because of their young age, but also because the disease progression renders them unable to communicate. Although each clinical application will have issues specific and unique to the disease and the genetic medicine being assessed, this paper should provide a useful paradigm for investigators planning gene and/or stem cell trials for fatal, untreatable disorders.

ISSUE 1: THERAPEUTIC MISCONCEPTION

Meaningful informed consent is a precondition for the ethical involvement of human subjects in clinical research (Lidz *et al.*, 2004). Therapeutic misconception is a failure on the part of subjects (or parents) to appreciate the risks and disadvantages associated with participation in a study (Applebaum, 2002; Miller and Brody, 2003; Oberman and Frader, 2003). This issue is made more complicated when research subjects have fatal, untreatable conditions and when the subjects are children.

U.S. federal regulations (45 CFR 46) require that consent documents disclose the nature and purpose of the study, foreseeable risks and benefits, appropriate alternatives, the confidentiality of the information collected, and include an explanation of compensation available, a discussion of how pertinent questions can be answered, and a statement that participation is voluntary (<http://www.hhs.gov/ohrp/humansubjects/guidance/45cfr46.htm#46.116>). In practice, there are significant challenges to adequate disclosure of the risks and benefits of genetic medicine-based studies and to the production of an informed consent that is intrinsically readable for the lay population.

Studies that evaluate the degree to which informed consent documents fully disclose the risks and benefits of human subject research present conflicting results. In a study of 272 consent forms for phase I therapy studies, Horng *et al.* (2002) found that 99% explicitly stated that the purpose was experimental research, and that 92% stated that the primary aim was to assess safety. In contrast, in a survey of 39 informed consent documents for phase I gene transfer trials, Henderson *et al.* (2004) found that 74% did not clearly convey to subjects that benefit was "unlikely" or "not expected," instead using language that was deemed "indeterminate."

Understanding and appreciation of the informed consent document

Even if the risks and benefits of a trial are appropriately disclosed in the consent document, participants/parents may still experience difficulty in appreciating these risks and benefits. In a study of adults in 40 different clinical trials, Lidz *et al.* (2004) found that 24% of subjects believed the study had no risks/disadvantages, despite having signed consent documents explicitly defining these risks/disadvantages. Overcoming this disjunction is a challenge in the consenting of severely ill patients/parents, who may selectively filter information because of their own sense of desperation. A study of 127 subjects in 4 clinical research protocols at the National Institutes of Health found that healthy volunteers could recall the greatest amount of information regarding a trial's risks after signing of the consent, whereas severely ill subjects retained the least (Schaeffer *et al.*, 1996).

Further compounding the problem, studies have shown that informed consent documents are often incomprehensible to the lay population of research subjects. Grossman *et al.* (1994) found that only 1–6% of consents for cancer trials met standards for an eighth grade level, and most measured at a college reading level. However, easy "readability" does not seem to be the sole answer. In a randomized, controlled trial of "standard" versus "easy to read" informed consents, Coyne *et al.* (2003) found that subjects receiving the "easy to read" documents did not demonstrate increased understanding of the study.

Disconnect between parental expectations and the reality of phase I trials

If the appreciation of risks and disadvantages associated with clinical trial participation inversely correlates with the severity of a patient's illness, then the parents of severely ill children may present inherently greater challenges to the informed consent process. A study of pediatric leukemia trials found that although 83% of physicians explained the nature of randomization during the informed consent process, 50% of parents could not subsequently explain what randomization meant, and were not aware that their child could receive placebo instead of study drug (Kodish *et al.*, 2004). A study of randomized, placebo-controlled pediatric oncology trials found that 40% of parents failed to understand the experimental design of the trial and believed they could choose the study drug administered to their child (Simon *et al.*, 2004). Among surveyed pediatric hematologists and oncologists, the most important stated reasons why parents enrolled their children in phase I trials were medical benefit (38%) and/or cure (28%) (Estlin *et al.*, 2000). Because pediatric phase I clinical trials tend to enroll children who are very ill, balancing parental hopes with the reality of risks and benefits for individual subjects remains a critical challenge to the process of obtaining informed consent. The reality is that few children with malignancies are "cured" by initial experimental treatments (Furman *et al.*, 1989; Ackerman, 1995).

In comparison with drug trials in the pregenetic medicine era, therapeutic misconception is an even greater challenge for clinical studies with genetic medicines. The diseases being studied are often fatal, with no alternative therapies. Often the subjects are children, and the disease process per se may render them unable to comprehend and/or communicate. When the un-

derlying disorder is a genetic disease, the parents often feel guilty for having been the “source” of the disease. Finally, “genetic medicines” have the connotation that they will provide a “magic cure” to correct the fundamental cause of the disease.

ISSUE 2: ENROLLMENT CRITERIA AND RISK VERSUS BENEFIT

Enrollment criteria as they pertain to a trial’s risks versus benefits represent an important ethical issue for genetic medicine-based trials. The death of a young adult participant in a dose-escalation gene transfer trial for individuals with ornithine transcarbamylase (OTC) deficiency brought attention to the risks associated with gene therapy trials and led to a shift in the paradigm for subject enrollment in genetic medicine studies. In the initial recommendations regarding enrollment and informed consent for the OTC deficiency trial, the ethicist consulted in the design of the trial recommended that investigators enroll adult volunteers with milder disease before enrolling younger, more severely affected individuals (Raper *et al.*, 1998; Marshall, 2000). This advice was based on the concept that it was more ethically sound to select subjects who could make the decision to enroll for themselves, rather than to depend on the consent of parents whose children had a fatal genetic disorder and were unable to assent for themselves.

The subsequent death in this trial of an individual with mild disease raised questions regarding the eligibility criteria in genetic medicine trials. Most genetic medicine studies subsequent to the OTC deficiency trial, including the LINCL trial described below, have inverted the paradigm for enrollment, enrolling more severely affected individuals before enrolling subjects with more moderate disease. This is premised on the risk–benefit ratio for subjects, which favors the earlier enrollment of severely affected individuals, largely because of the high level of risk and low expectation of benefit for gene transfer study participants. Although the paradigm seems to have shifted, criteria for enrollment decisions in genetic medicine-based trials should also be viewed with an understanding of the risks associated with invasive delivery procedures in the setting of advanced disease, which may alter the risk–benefit equation in favor of subjects with milder disease.

ISSUE 3: FUNDING AND PERSONAL MOTIVES

Issues of funding are central to the initiation of most studies in translational research. Most clinical trials are supported by industry. In 2002, more than 70% of the total U.S. investment in biomedical research and development came from the pharmaceutical industry, with only 12% from government funding (Hadley, 2004). A study of the translation of basic science to clinical trials found that industry ties were the strongest predictor for whether basic science studies moved to randomized, controlled clinical trials (Ioannidis, 2004).

Because diseases that affect a larger proportion of the population necessarily receive a greater apportionment of federal grant money, funding obstacles are increased for diseases given orphan status (affecting fewer than 200,000 people in the United States; <http://rarediseases.info.nih.gov/index.html>; [\[eases.org/\]\(http://www.fda.gov/orphan/\); <http://www.fda.gov/orphan/>; Haffner, 2004\). The issue of funding is even more complex for studies that aim to investigate novel therapies, such as genetic medicines, which are centered in the academic community and largely unsupported by the pharmaceutical industry. Because orphan diseases receive a smaller proportion of the “research funding pie,” money from private foundations can make a significant difference \(Hadley, 2004\). The families of affected individuals often establish private foundations to support research for their cause, providing funding opportunities that enable the initiation of translational studies that otherwise might not have been possible \(Dockser Marcus, 2002; Goldberg, 2004; Rowland, 2004; Weiner, 2004\). However, the use of private funding for these purposes also raises issues regarding enrollment in clinical trials. Whereas private funders are often personally motivated to have their support linked to the enrollment of affected family and friends in clinical trials, investigators owe primary allegiance to the scientific community, not to the source of funding \(Shatz, 1990; Oberman and Frader, 2003\).](http://www.raredis-</p>
</div>
<div data-bbox=)

Reactions to a child’s fatal diagnosis differ widely among parents. Some accept the diagnosis and commit themselves to providing comfort care for their child. At the opposite end of the spectrum, others gird themselves for battle, educating themselves to the level of experts, seeking out researchers from all over the world who are willing to devote themselves to their cause, and raising funds to implement clinical research (Lascari, 1978; Kornfeld and Siegel, 1979, 1980; Winerip, 1998; Kranish, 2001; Katz, 2002; Anand, 2003; Mitchell, 2005; Robinson, 2005). There are numerous examples in the popular media that document accounts of parents who have confronted their child’s fatal diagnosis with efforts to help implement novel, experimental treatments for their severely ill children, often subsuming their other responsibilities to the cause of this research (Winerip, 1998; Anand, 2003; Robinson, 2005). In addition, the popular literature suggests that those parents who undertake Herculean efforts for children diagnosed with fatal genetic diseases seem more likely to recognize and accept the inherent risks of experimental research. These accounts suggest that the parents of children with fatal genetic disorders may be more likely to view experimental research with greater objectivity than do the parents of severely ill pediatric oncology patients, because the outcome for parents whose children have been handed uniformly fatal diagnoses is predetermined. Conversely, it also could be argued that parents whose children are given fatal genetic diagnoses may be more likely to enroll in phase I clinical trials for this very reason, because no other treatment options exist, and the child’s outcome is otherwise guaranteed (Winerip, 1998; Grady, 2004, 2005).

CONFRONTING CONSENT, ENROLLMENT, AND PERSONAL MOTIVE ISSUES IN GENETIC MEDICINE TRIALS

We confronted these ethical issues in the development and execution of a phase I gene transfer trial for LINCL, a fatal lysosomal storage disease that results in progressive neurodegeneration and death between the ages of 8 and 12 years (Williams *et al.*, 1999; Crystal *et al.*, 2004). Affected children experience progressive neurological decline, followed by cog-

nitive impairment, visual failure, seizures, and deteriorating motor function invariably leading to a vegetative state and death (Williams *et al.*, 1999). The disorder lacks any treatment, aside from the management of symptoms. Our experimental gene therapy trial uses AAV2_{CU}hCLN2, an adeno-associated virus serotype 2 gene transfer vector to transfer the CLN2 cDNA to the brain of affected children (Crystal *et al.*, 2004). Like most phase I genetic medicine studies, the trial is primarily designed to determine safety. Secondly, the study design includes parameters to develop preliminary data regarding the ability of this therapy to prevent the progressive CNS deterioration that characterizes LINCL.

For this trial in particular, the phenotypic manifestations of LINCL presented particular challenges relevant to the ethical issues of therapeutic misconception, enrollment decisions, and personal motives. The rapid progression of the disease leaves patients cognitively impaired and noncommunicative, often within a few months of diagnosis (Wisniewski *et al.*, 2000; Steinfeld *et al.*, 2002). The disease is inevitably fatal and lacks any treatment. Consequently, parents may be more prone to view the research as a “cure” because of their own desperation, increasing the difficulty of avoiding therapeutic misconception. The correlation between genotype and the phenotypic manifestation of LINCL is not completely defined, and progression

varies among children with the disorder. The potential subject population includes a range from severe to moderately and mildly affected children (Williams *et al.*, 1999; Wisniewski *et al.*, 2000). The disease has been given orphan status, with approximately 200 individuals affected in the United States. Finally, private sources of funding were necessary to implement and carry out the clinical trial. Using established ethical considerations, the following will illustrate how the issues of therapeutic misconception, enrollment decisions, and personal motives reflect and reinforce one another and outline the strategy used to confront these issues in the LINCL trial.

General strategy

The LINCL trial is organized with a distinct division of labor (Fig. 1). The Principal Investigator, who is also the investigational new drug application (IND) holder/sponsor of the trial, maintains full oversight of the study but has circumscribed clinical responsibilities. The purposes of this clinical organization schema are (1) to guard against conflicts of interest by delimiting the patient care responsibilities of the Principal Investigator, who does not act in the role of physician in this trial; and (2) to ensure the independence of safety monitors and research subject advocates, whose primary responsibilities in-

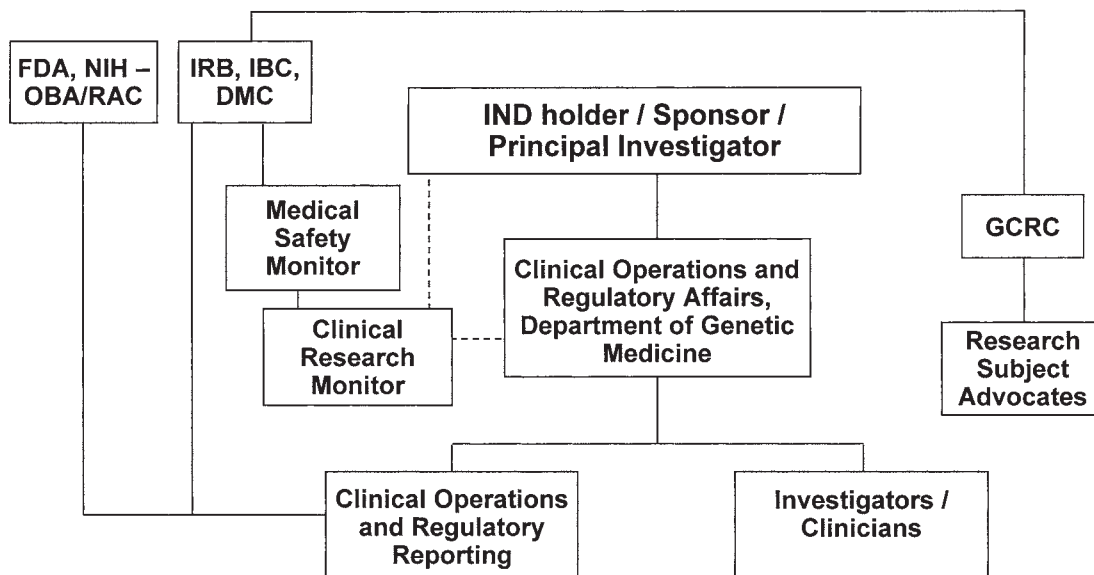


FIG. 1. Clinical organizational chart for the LINCL study (BB IND 11481). The Principal Investigator, who is also the IND holder/sponsor of the trial, maintains full oversight of the trial but has limited clinical responsibilities, which are allocated through the Clinical Operations and Regulatory Affairs (CORA) group in the Department of Genetic Medicine to its Clinical Operations and Regulatory Components and to the Co-Investigators/Clinicians. In addition, the safety monitors (the monitoring and quality assurance component of CORA) and the General Clinical Research Center (GCRC) research subject advocates, whose primary responsibilities involve the protection of human subjects, have lines of reporting independent from the Principal Investigator, in order to guard against conflicts of interest and to allow for autonomy in reporting. The Clinical Operations and Regulatory Affairs components of the CORA group report to the institutional Data Monitoring Committee (DMC), and three institutional oversight committees (Institutional Review Board [IRB], Institutional Biosafety Committee [IBC], and NIH General Clinical Research Center [GCRC]), as well as the federal regulatory/monitoring agencies, which include the Food and Drug Administration (FDA), National Institutes of Health—Office of Biotechnology Activities, Recombinant DNA Advisory Committee (NIH—OBA/RAC). This design is intended to separate reporting responsibilities and to clearly define the relationships between investigators, trial participants, and those involved with clinical operations, regulatory affairs, and safety monitoring.

volve the protection of research subjects and reporting to regulatory and oversight bodies. These individuals are disassociated from the Principal Investigator to allow for autonomy in reporting.

Issue 1 in the LINCL trial: therapeutic misconception

To avoid therapeutic misconception, our strategy begins with the use of two clinical protocols: one for the screening of subjects with the disease, and one for the LINCL gene transfer trial per se. The screening study aims to correlate LINCL genotypes with clinical parameters of disease manifestation and serves as a screening study for eligibility in the gene transfer protocol (Crystal *et al.*, 2004). All screening protocol subjects are informed that enrollment does not guarantee an invitation to participate in the gene transfer study.

Through the screening process, subjects undergo a series of tests that are used to assess possible eligibility in the gene transfer trial. If the decision to extend an invitation to participate in the gene transfer trial is made, parents are sent the study informed consent document (either electronically or via direct mail) several weeks before admission and instructed to discuss the protocol in detail with trusted advisors, including friends and family, physicians, and clergy, if relevant. The goal is full disclosure, so that parents may decide whether or not to enroll their child with the fullest extent of information, in the absence of time pressure, and in conjunction with others at home.

In spite of every best effort to fully guard against therapeutic misconception, the risk remains in any trial for fatal disorders, given the lack of treatment options available (Applebaum, 2002; Oberman and Frader, 2003; Lidz *et al.*, 2004). To deal with this issue, the informed consent is used as a forum for dialogue and discussion with the parents, so that they are informed in the most complete fashion and have the freedom to ask questions regarding the trial. Importantly, the informed consent document seeks to impress on parents two critical issues relevant to therapeutic misconception: the lack of potential benefit and the high degree of risk associated with the trial. The consent states: "We cannot and do not guarantee that your child will receive any benefits from this study. However, the knowledge gained in this research study will benefit others in the future. We hope AAV2_{CU}hCLN2 may prevent the disease from getting worse. However, this is an experimental research study, and there is no proof that this will occur." With regard to the level of risk associated with the trial, the first page of the consent document includes the following statement in boldface: "This research study involves a high level of risk to your child, including the risk of death."

The consent also details the specific risks associated with the trial, including details of all serious adverse events experienced by enrolled subjects to date. These events are sequentially incorporated into the document as they occur, producing a continuously evolving consent document that is meant to reflect all results of the study. Consequently, the document has been revised multiple times since the initiation of the trial. For example, one subject died 49 days after gene transfer, after presenting with status epilepticus 7 days after discharge, which was 14 days after vector administration. The consent form was revised to disclose this death and the possible reasons for it. After each revision of the document, all parents involved in the

trial, including those whose children have already received the gene transfer vector, are asked to resign the updated consent, indicating their awareness of any new risks and results of the trial.

On the day of admission for the gene transfer protocol, the consent is carried out by a pediatrician who is a co-investigator in the trial, in the presence of a Research Coordinator and an independent Research Subject Advocate from the NIH General Clinical Research Center at the New York Weill Cornell Medical Center (New York, NY) (Fig. 1). The Principal Investigator does not participate in the informed consent process. The Research Subject Advocate is present to ensure that subjects are protected in the informed consent process and that parents appear to appreciate the inherent risks and benefits of the trial. At the time of consent, the pediatrician explains the protocol and consent document in detail, with particular emphasis on the primary end point of the study—to assess the safety of the vector and its administration, not to prove efficacy. Importantly, the consent document describes the trial in terms of safety, not therapy. The words "gene transfer" are used instead of "gene therapy," which could carry the connotation of "cure" (King, 1999). To help the parents understand the early nature of this trial, the concept of the experimental design of the phase I trial is explained in the context of the classic phase I–IV pharmaceutical development process, in which safety is assessed first, before efficacy. It is emphasized that, even if the AAV2_{CU}hCLN2 vector were to sufficiently express the deficient gene in the central nervous system of these severely and moderately affected subjects, there would be limited therapeutic benefit secondary to the degree of cerebral atrophy associated with their disease state. The parents are explicitly told that they may withdraw their child from the study at any time, without prejudice. Whenever possible, we ask that both parents sign the document at the same time, indicating their mutual agreement to enroll a child in the trial.

Although it may be impossible to completely protect against therapeutic misconception, in this type of subject population the process of "decision monitoring" may provide an extra safeguard during the informed consent process. Decision monitoring requires the independent contact and questioning of research subjects and/or their parents after completion of the informed consent procedure (Schaeffer *et al.*, 1996; Kodish *et al.*, 2004). The aim is to determine the extent to which research subjects and/or parents have understood and appreciated the information presented during the informed consent process. The procedure allows for an unbiased, third-party check on the efficacy of the informed consent process by providing investigators with direct feedback from research subjects and/or parents. If confusion and/or misunderstanding persists after signing of the informed consent document, it is likely to be revealed during this third-party questioning, which would allow investigators to clarify and provide further explanation to research subjects before the initiation of study procedures.

Issue 2 in the LINCL trial: enrollment decisions and risk versus benefit

Decisions regarding enrollment in any clinical research study require a favorable risk–benefit ratio, in which the potential benefits to subjects and/or society outweigh the risks inherent in

the research (Emanuel *et al.*, 2000). With regard to enrollment decisions in our LINCL trial, this rationale favors the early enrollment of the most severely affected subjects first. The sequential enrollment of individuals on the basis of disease severity best fulfills these tenets by minimizing the risk–benefit ratio for individual subjects, while allowing time for data collection and analysis before the enrollment of healthier subjects (King, 2000; Kimmelman, 2005). This is based on the concept that, among subjects with a universally fatal diagnosis, those who are the most severely affected stand to lose the least and gain the most, because their prognosis is otherwise guaranteed. Further, because any trial may be associated with unexpected consequences, empiric data demonstrating the relative safety of the study drug further tilt the risk–benefit ratio toward the decision to enroll severe cases first.

Issue 3 in the LINCL trial: funding and personal motives

The ethical conduct of clinical research requires “fair subject selection” and “scientific validity” (Emanuel *et al.*, 2000). The former requires that wealthy and/or powerful individuals are not given favor in potentially beneficial research, and the latter requires the collection of reliable, reproducible data through scientific methods and principles. These concepts need to be considered in the context that sources of funding for orphan disease clinical trials often come from individuals with a personal investment in finding a treatment for the disorder. The central question concerns how to reconcile these competing interests and safeguard against conflicts of interest between investors and investigators. The presence of conflict does not limit the ability to manage it appropriately, and there are many examples of individuals who were personally dedicated to a particular cause, and whose commitment resulted in benefits for society as a whole (Anand, 2003; Weiner, 2004; Henig, 2005; Pollack, 2005).

Like many other studies to investigate experimental treatments for orphan diseases, the LINCL trial is partially funded (40% of total costs) by a private foundation (Nathan’s Battle Foundation) established by the father of two affected individuals (www.nathansbattle.com). In addition, the study is also funded by the NIH General Clinical Research Center at the New York Weill Cornell Medical Center (3%), and our Department of Genetic Medicine (Weill Medical College of Cornell University, New York, NY) (57%). More recently, some of the preclinical studies were funded by the National Institute of Neurological Diseases and Stroke (Bethesda, MD).

For private foundations and their supporters, issues of personal motivation, funding, and subject enrollment may be intricately intertwined (Merz *et al.*, 2002). In designing the trial, we were confronted with the question of how to separate the foundation, whose contributors are largely families of children with LINCL, from influence in the clinical study, particularly with regard to enrollment decisions. We developed a funding arrangement with protocol safeguards to ensure the fulfillment of ethical tenets and to protect against conflicts of interest within the study, as well as to ensure the scientific validity of the data. In designing these safeguards, our aim was to unlock the trial’s potential by allowing for the translation of the foundation’s personal interests into lasting benefits for society.

All funds from the foundation are made as a gift to the university. The foundation and its supporters have no control over

the way in which these funds are applied to the preclinical studies, the clinical trials per se, or in the enrollment of subjects. Subjects are selected from lists compiled from several sources. All correspondence with the families of subjects is made by our Clinical Operations and Regulatory Affairs group (Fig. 1). Once subjects have been screened, eligibility for the gene transfer trial is determined by four co-investigators in the trial—a general pediatrician, a pediatric neurologist, a molecular geneticist, and one of the two neurosurgeons who perform the vector administration procedure. None of these individuals are involved with the foundation. Enrollment decisions are made primarily on the basis of inclusion/exclusion criteria for the gene transfer trial, with attention to sequence of subject enrollment in the screening study and issues such as the ability to stay in proximity to our medical center before and for some time after the gene transfer and to return for scheduled assessments. In addition, clinical test results are extensively reviewed by the eligibility committee to ensure that the best candidate is selected for each available slot. The Principal Investigator does not play a role in enrollment decisions for the clinical trial.

ALTERNATIVE STRATEGIES

Several alternative strategies have been suggested to ease the difficulty of translating basic science findings into clinical trials for rare disease research. Some proponents, who point to the benefits of orphan disease legislation in the last 20 years, have argued for increased public funding and legislation to advance market-driven pharmaceutical research for orphan diseases (Iribarne, 2003; Haffner, 2004). The 1983 U.S. Orphan Drug Act has provided some relief since its implementation, expanding the number of drugs in development for the treatment of orphan diseases by providing incentives, including FDA market exclusivity, research tax credits for clinical trials of orphan diseases, and Orphan Product Development grants for pharmaceutical companies that develop drugs for the treatment of rare diseases (<http://www.fda.gov/orphan/>; Trouiller *et al.*, 2002). Aiding this process, the NIH Rare Diseases Clinical Research Network was established in 2003 to facilitate the collaboration of scientists from multiple disciplines with access to geographically distributed national research resources and patient populations (McDonald and Marciel, 2003). Others have argued for the creation of nonprofit pharmaceutical companies dedicated to the development of neglected compounds for use in the treatment of orphan diseases (Klausmeier, 2001; Hale, 2004). One strategy for nonprofit pharmaceutical companies is to track down compounds that have shown initial promise but are not being actively pursued by industry. The nonprofit could access development rights through a licensing agreement or a donation of the patent rights, and then develop the drug with philanthropic help. Another model is to expand academic–private partnerships through nonprofit companies, which would allow for rigorous drug development, a task for which the academic community is not well suited (Lehmann, 2001; Trouiller *et al.*, 2002; Iribarne, 2003).

RECOMMENDATIONS

Although each genetic medicine trial has specifics that will lead to differences in the means through which consent, en-

rollment, and issues of personal motives are handled, we suggest the adoption of the following universal guidelines in the design of phase I genetic medicine trials.

- Overall organization: It is useful to have two distinct protocols: one for screening and one for the genetic medicine study per se. This allows for gathering useful scientific data regarding the disease and a more focused assessment of eligibility criteria, without the pressure to initiate therapy for each subject. It is useful to separate the Principal Investigator from control of the clinical care of the subjects, the consent process and enrollment decisions. The clinical research monitor and physician medical study monitor should have a line of reporting to regulatory groups independent of the Principal Investigator, to allow for autonomy in reporting.
- Therapeutic misconception: As difficult as it may be, it is critical to deal as starkly as possible with issues of efficacy and risk in the consent forms and process. This includes explicitly stating that efficacy is “unlikely” and that the primary purpose of the study is to assess safety. If serious adverse events, including death, are possible, this should be explicitly stated. As new adverse events present in a trial, the consent form should be continuously altered to include them, and past as well as future participants should be informed of these risks. The consent form should be made as readable as possible without sacrificing relevant concepts and details. Anyone with possible conflicts should be divorced from the consent process, and an independent research subject advocate should participate in the consent process.

Finally, “decision monitoring” after the informed consent process may help to bridge the gap between investigators’ explanation of the informed consent and research subjects’ and/or parents’ understanding and appreciation of the document. Through this means, decision monitoring may help to illuminate the presence of therapeutic misconception before the initiation of study procedures, and thus help the investigators clarify and ultimately resolve any misunderstandings.
- Enrollment decisions: Decisions about enrollment should be made by experts on the relevant aspects of the disease and therapy to be tested, but only by those who are divorced from the funding sources or other potential conflicts of interest. In developing the inclusion/exclusion criteria for the trial, the investigators must be cognizant of risk-versus-benefit issues for the participants. Unless there are competing arguments to the contrary, if the proposed therapy carries significant potential risks, more severely affected subjects should be enrolled first.
- Funding and personal motives: All funding sources should be separated from any decisions regarding the study, including enrollment decisions.

ACKNOWLEDGMENTS

The authors thank N. Mohamed for help in preparing this manuscript. These studies were supported, in part, by NIH U01 NS047458 and WMC GCRC M01 RR00047, and by Nathan’s Battle Foundation (Greenwood, IN).

REFERENCES

- ACKERMAN, T.F. (1995). The ethics of phase I pediatric oncology trials. *IRB* **17**, 1–5.
- AGLIETTA, M., BERTOLINI, F., CARLO-STELLA, C., DE VINCENZI, A., LANATA, L., LEMOLI, R.M., OLIVIERI, A., SIENA, S., ZANON, P., and TURA, S. (1998). *Ex vivo* expansion of hematopoietic cells and their clinical use. *Haematologica* **83**, 824–848.
- ANAND, G. (2003). Clinical trials: For his sick kids, a father struggled to develop a cure. *Wall Street Journal*, August 26. <http://online.wsj.com/public/us> (accessed August 2005).
- APPLEBAUM, P.S. (2002). Clarifying the ethics of clinical research a path towards avoiding the therapeutic misconception. *Am. J. Bioethics* **2**, 22.
- BALICKI, D., and BEUTLER, E. (2002). Gene therapy of human disease. *Medicine (Baltimore)* **81**, 69–86.
- CHENG, S.H., and SMITH, A.E. (2003). Gene therapy progress and prospects: Gene therapy of lysosomal storage disorders. *Gene Ther.* **10**, 1275–1281.
- COSTANTINI, L.C., BAKOWSKA, J.C., BREAKFIELD, X.O., and ISACSON, O. (2000). Gene therapy in the CNS. *Gene Ther.* **7**, 93–109.
- COYNE, C.A., XU, R., RAICH, P., PLOMER, K., DIGNAN, M., WENZEL, L.B., FAIRCLOUGH, D., HABERMANN, T., SCHNELL, L., QUELLA, S., and CELLA, D. (2003). Randomized, controlled trial of an easy-to-read informed consent statement for clinical trial participation: A study of the Eastern Cooperative Oncology Group. *J. Clin. Oncol.* **21**, 836–842.
- CRYSTAL, R.G., SONDHI, D., HACKETT, N.R., KAMINSKY, S.M., WORGALL, S., STIEG, P., SOUWEIDANE, M., HOSAIN, S., HEIER, L., BALLON, D., DINNER, M., WISNIEWSKI, K., KAPLITT, M., GREENWALD, B.M., HOWELL, J.D., STRYBING, K., DYKE, J., and VOSS, H. (2004). Clinical protocol: Administration of a replication-deficient adeno-associated virus gene transfer vector expressing the human CLN2 cDNA to the brain of children with late infantile neuronal ceroid lipofuscinosis. *Hum. Gene Ther.* **15**, 1131–1154.
- DAUGHERTY, C.K. (1999). Impact of therapeutic research on informed consent and the ethics of clinical trials: A medical oncology perspective. *J. Clin. Oncol.* **17**, 1601–1617.
- DOCKSER MARCUS, A. (2002). Hiring your own scientist to find a cure: Families of terminally ill set up research foundations. *Wall Street Journal*, April 25. <http://online.wsj.com/public/us> (accessed August 2005).
- EDELSTEIN, M.L., ABEDI, M.R., WIXON, J., and EDELSTEIN, R.M. (2004). Gene therapy clinical trials worldwide 1989–2004: An overview. *J. Gene Med.* **6**, 597–602.
- EMANUEL, E.J., WENDLER, D., and GRADY, C. (2000). What makes clinical research ethical? *JAMA* **283**, 2701–2711.
- ESTLIN, E.J., COTTERILL, S., PRATT, C.B., PEARSON, A.D., and BERNSTEIN, M. (2000). Phase I trials in pediatric oncology: Perceptions of pediatricians from the United Kingdom Children’s Cancer Study Group and the Pediatric Oncology Group. *J. Clin. Oncol.* **18**, 1900–1905.
- FURMAN, W.L., PRATT, C.B., RIVERA, G.K., KRISCHER, J.P., KAMEN, B.A., and VIETTI, T.J. (1989). Mortality in pediatric phase I clinical trials. *J. Natl. Cancer Inst.* **81**, 1193–1194.
- GOLDBERG, C. (2004). Fragile promise: Parents push scientists to cure son’s disease. *Boston Globe*, July 20. <http://www.boston.com/tools/archives/> (accessed August 2005).
- GRADY, D. (2004). After baby’s grim diagnosis, parents try drastic treatment. *New York Times*, December 19. <http://query.nytimes.com/search/advanced> (accessed August 2005).
- GRADY, D. (2005). Despite desperate measures, baby with rare disease dies. *New York Times*, February 4. <http://query.nytimes.com/search/advanced> (accessed August 2005).

- GROSSMAN, S.A., PIANTADOSI, S., and COVAHEY, C. (1994). Are informed consent forms that describe clinical oncology research protocols readable by most patients and their families? *J. Clin. Oncol.* **12**, 2211–2215.
- HACEIN-BEY-ABINA, S., LE DEIST, F., CARLIER, F., BOUNEAUD, C., HUE, C., DE VILLARTAY, J.P., THRASHER, A.J., WULFFRAAT, N., SORENSSEN, R., DUPUIS-GIROD, S., FISCHER, A., DAVIES, E.G., KUIS, W., LEIVA, L., and CAVAZZANA-CALVO, M. (2002). Sustained correction of X-linked severe combined immunodeficiency by *ex vivo* gene therapy. *N. Engl. J. Med.* **346**, 1185–1193.
- HADLEY, C. (2004). The power of giving. *EMBO Rep.* **5**, 751–754.
- HAFNER, M.E. (2004). Developing treatments for inborn errors: Incentives available to the clinician. *Mol. Genet. Metab.* **81**(Suppl. 1), S63–S66.
- HALE, V. (2004). Creating more paths to hope. *Newsweek*, December 6. <http://www.msnbc.msn.com/id/3668484/site/newsweek/> (accessed August 2005).
- HENDERSON, G.E., DAVIS, A.M., KING, N.M., EASTER, M.M., ZIMMER, C.R., ROTHSCHILD, B.B., WILFOND, B.S., NELSON, D.K., and CHURCHILL, L.R. (2004). Uncertain benefit: Investigators' views and communications in early phase gene transfer trials. *Mol. Ther.* **10**, 225–231.
- HENIG, R.M. (2005). Racing with Sam. *New York Times*, January 30. <http://query.nytimes.com/search/advanced> (accessed August 2005).
- HORNG, S., EMANUEL, E.J., WILFOND, B., RACKOFF, J., MARTZ, K., and GRADY, C. (2002). Descriptions of benefits and risks in consent forms for phase I oncology trials. *N. Engl. J. Med.* **347**, 2134–2140.
- IOANNIDIS, J.P. (2004). Materializing research promises: Opportunities, priorities and conflicts in translational medicine. *J. Transl. Med.* **2**, 5.
- IRIBARNE, A. (2003). *MSJAMA*: Orphan diseases and adoptive initiatives. *JAMA* **290**, 116.
- KATZ, S. (2002). When the child's illness is life threatening: Impact on the parents. *Pediatr. Nurs.* **28**, 453–463.
- KIMMELMAN, J. (2005). Recent developments in gene transfer: Risk and ethics. *BMJ* **330**, 79–82.
- KING, N.M. (1999). Rewriting the "points to consider": The ethical impact of guidance document language. *Hum. Gene Ther.* **10**, 133–139.
- KING, N.M. (2000). Defining and describing benefit appropriately in clinical trials. *J. Law Med. Ethics* **28**, 332–343.
- KLAUSMEIER, W.H. (2001). A patient-supported strategy for therapy development in amyotrophic lateral sclerosis (ALS). *Am. J. Ther.* **8**, 329–332.
- KODISH, E., EDER, M., NOLL, R.B., RUCCIONE, K., LANGE, B., ANGIOLILLO, A., PENTZ, R., ZYZANSKI, S., SIMINOFF, L.A., and DROTAR, D. (2004). Communication of randomization in childhood leukemia trials. *JAMA* **291**, 470–475.
- KOHN, D.B. (2001). Gene therapy for genetic haematological disorders and immunodeficiencies. *J. Intern. Med.* **249**, 379–390.
- KORNFELD, M.S., and SIEGEL, I.M. (1979). Parental group therapy in the management of a fatal childhood disease. *Health Soc. Work* **4**, 99–118.
- KORNFELD, M.S., and SIEGEL, I.M. (1980). Parental group therapy in the management of two fatal childhood diseases: A comparison. *Health Soc. Work* **5**, 28–34.
- KRANISH, M. (2001). Against the odds cures for rare diseases could help us all, yet those who suffer from uncommon disorders are often left to fend for themselves. *Boston Globe*, August 5. <http://www.boston.com/tools/archives/> (accessed August 2005).
- LASCARI, A.D. (1978). The dying child and the family. *J. Fam. Pract.* **6**, 1279–1286.
- LEHMANN, V. (2001). New models for public-private partnerships in drug development. *Biotechnol. Dev. Monitor* **46**, 2–7.
- LIDZ, C.W., APPELBAUM, P.S., GRISSO, T., and RENAUD, M. (2004). Therapeutic misconception and the appreciation of risks in clinical trials. *Soc. Sci. Med.* **58**, 1689–1697.
- LUM, J. (2005). StemCells, Inc. issues FDA update on proposed clinical trial. Available at URL http://www.hypeandhope.com/wt/page/index/it_1112288500 (accessed August 2005).
- MARSHALL, E. (2000). Ethicist named in gene therapy suit. *ScienceNOW* **3**.
- MCDONALD, J., and MARCIEL, K. (2003). NIH establishes rare diseases clinical research network. *NIH News*, November 3. Available at URL <http://www.nih.gov/news/pr/nov2003/ncrr-03.htm> (accessed August 2005).
- MERZ, J.F., MAGNUS, D., CHO, M.K., and CAPLAN, A.L. (2002). Protecting subjects' interests in genetics research. *Am. J. Hum. Genet.* **70**, 965–971.
- MILLER, F.G., and BRODY, H. (2003). A critique of clinical equipoise: Therapeutic misconception in the ethics of clinical trials. *Hastings Center Rep.* **33**, 19–28.
- MITCHELL, E. (2005). One family challenge, for children with a rare disorder, medical answers don't come easily. *Newsday*, February 15. <http://pqasb.pqarchiver.com/newsday/search.html> (accessed August 2005).
- OBERMAN, M., and FRADER, J. (2003). Dying children and medical research: Access to clinical trials as benefit and burden. *Am. J. Law Med.* **29**, 301–317.
- ORLIC, D. (2004). The strength of plasticity: Stem cells for cardiac repair. *Int. J. Cardiol.* **95**(Suppl. 1), S16–S19.
- POLLACK, A. (2005). Investing for a profit and a daughter's health. *New York Times*, March 19. <http://query.nytimes.com/search/advanced> (accessed August 2005).
- RAPER, S.E., WILSON, J.M., YUDKOFF, M., ROBINSON, M.B., YE, X., and BATSHAW, M.L. (1998). Developing adenoviral-mediated *in vivo* gene therapy for ornithine transcarbamylase deficiency. *J. Inher. Metab. Dis.* **21**(Suppl. 1), 119–137.
- ROBINSON, P. (2005). Mum's cash bid to help sick son. *Yorkshire Evening Post*.
- ROWLAND, L.P. (2004). His brother's keeper: A story from the edge of medicine [Book Reviews]. *N. Engl. J. Med.* **350**, 2012–2013.
- SCHAEFFER, M.H., KRANTZ, D.S., WICHMAN, A., MASUR, H., REED, E., and VINICKY, J.K. (1996). The impact of disease severity on the informed consent process in clinical research. *Am. J. Med.* **100**, 261–268.
- SHATZ, D. (1990). Randomized clinical trials and the problem of sub-optimal care: An overview of the controversy. *Cancer Invest.* **8**, 191–205.
- SIMON, C.M., SIMINOFF, L.A., KODISH, E.D., and BURANT, C. (2004). Comparison of the informed consent process for randomized clinical trials in pediatric and adult oncology. *J. Clin. Oncol.* **22**, 2708–2717.
- SMITS, A.M., VAN VLIET, P., HASSINK, R.J., GOUMANS, M.J., and DOEVENDANS, P.A. (2005). The role of stem cells in cardiac regeneration. *J. Cell. Mol. Med.* **9**, 25–36.
- STEINFELD, R., HEIM, P., VON GREGORY, H., MEYER, K., ULLRICH, K., GOEBEL, H.H., and KOHLSCHUTTER, A. (2002). Late infantile neuronal ceroid lipofuscinosis: Quantitative description of the clinical course in patients with CLN2 mutations. *Am. J. Med. Genet.* **112**, 347–354.
- SURBEK, D.V., GRATWOHL, A., and HOLZGREVE, W. (1999). *In utero* hematopoietic stem cell transfer: Current status and future strategies. *Eur. J. Obstet. Gynecol. Reprod. Biol.* **85**, 109–115.
- SVENDSEN, C.N., and LANGSTON, J.W. (2004). Stem cells for Parkinson disease and ALS: Replacement or protection? *Nat. Med.* **10**, 224–225.
- TROUILLER, P., OLLIARO, P., TORREELE, E., ORBINSKI, J., LAING, R., and FORD, N. (2002). Drug development for neglected

- diseases: A deficient market and a public-health policy failure. *Lancet* **359**, 2188–2194.
- WEINER, J. (2004). *His Brother's Keeper: A Story from the Edge of Medicine*. (HarperCollins, New York).
- WILLIAMS, R.E., GOTTLOB, I., LAKE, B.D., GOEBEL, H.H., WINCHESTER, B.G., and WHEELER, R.B. (1999). CLN2: Classic late infantile NCL. In *The Neuronal Ceroid Lipofuscinoses*. H.H. Goebel, S.E. Mole, and B.D. Lake, eds. (IOS Press, Amsterdam), pp. 37–38.
- WINERIP, M. (1998). Fighting for Jacob. *New York Times Magazine*, December 6. <http://query.nytimes.com/search/advanced> (accessed August 2005).
- WISNIEWSKI, K.E., KIDA, E., CONNELL, F., and ZHONG, N. (2000). Neuronal ceroid lipofuscinoses: Research update. *Neurol. Sci.* **21**(Suppl. 3), S49–S56.

Address reprint requests to:
Dr. Ronald G. Crystal
Department of Genetic Medicine
Weill Medical College of Cornell University
515 East 71st Street, S-1000
New York, NY 10021

E-mail: geneticmedicine@med.cornell.edu

Received for publication May 26, 2005; accepted after revision July 19, 2005.

Published online: August 25, 2005.

Gene Therapy for the Late Infantile Form of Batten Disease

*Dolan Sondhi, Neil R. Hackett, Stephen M. Kaminsky, Mark M. Souweidane,
Michael G. Kaplitt, Ronald G. Crystal*

Abstract: This chapter describes a program to assess gene transfer as a therapeutic approach to delay the neurological decline in children with the late infantile form of neuronal ceroid lipofuscinosis (LINCL). The disease arises from autosomal recessive inheritance of rare mutations in the CLN2 gene leading to a deficiency in the lysosomal protease tripeptidyl peptidase I (TPP-I). The challenge for a potential treatment is to obtain a therapeutic level of the target protein throughout the brain over the long term. Direct injection into the brain of a gene transfer vector derived from AAV serotype 2, AAV2_{CU}hCLN2, was chosen as the most easily implemented approach to begin a human clinical study. Limited pre-clinical efficacy studies were performed in rats and monkeys to demonstrate feasibility. Upon proof of concept, a toxicology study and a manufacturing program were executed providing the supporting data for commencing a clinical study in June 2004. This ongoing study is providing an insight on the feasibility of this approach in slowing the neurodegeneration in children with LINCL as well as potentially using similar approaches to treat other neurodegenerative diseases of lysosomal storage.

Keywords: AAV2; intracranial gene therapy; clinical trial

I. INTRODUCTION

The neuronal ceroid lipofuscinoses are rare, autosomal recessive genetic lysosomal storage diseases with progressive neurological degeneration leading to death (Boustany, 1996; Goebel et al., 1999; Wisniewski and Zhong, 2001; Haltia, 2003). While originally classified on the basis of age of onset and histopathology, the neuronal ceroid lipofuscinoses can now be divided into at least eight separate diseases based on molecular genetic studies (Goebel et al., 1999; Wisniewski et al., 2001a, b). In 2001, we initiated a program to assess gene transfer as a therapeutic approach to delay the neurological decline in children with the late infantile form of neuronal ceroid lipofuscinosis (LINCL), commonly referred to as the late infantile form of Batten disease. This chapter describes the pre-clinical development pathway and the design of the clinical trial.

II. LINCL

There are approximately 200 children in the developed countries in various stages of LINCL. The disease manifests itself at age 2–4 (Kurachi et al., 2000). Although there is variability among individuals as to the time of onset, the major symptoms that bring children to medical attention are seizures, ataxia, myoclonus, impaired speech and developmental regression. Diagnosis is usually made by electron microscopy (EM) of lymphocytes, skin, conjunctiva or rectal tissue, which demonstrate the lysosomal storage bodies that are the hallmark of the disease. Characteristic electroencephalograms (EEG), visual evoked potentials (VEP) and electroretinograms (ERG) confirm the diagnosis (Boustany, 1996; Goebel et al., 1999; Mole, 1999). Genetic testing is available to determine the specific genes and mutations involved (Dawson and

Cho, 2000). There is evidence that more than one locus may be associated with LINCL (Sleat et al., 1997). Less definitive diagnostic methods include other neurophysiological studies, observation of a loss of cells within the retina, blood or urine tests (e.g., these patients show elevated levels of dolichol) and brain scans, such as computed tomography (CT) and magnetic resonance imaging (MRI), which reveal the loss of brain tissue. MRI studies show a marked diffuse parenchymal volume loss both infratentorially and supratentorially (Brockmann, 1996; Jarvela et al., 1997; Seitz et al., 1998; Vanhanen et al., 2004). The ventricles are

enlarged, likely because of dilation due to parenchymal volume loss and there is also mild white matter FLAIR hyperintensity (Brockmann et al., 1996; Jarvela et al., 1997; Seitz et al., 1998; Vanhanen et al., 2004; Fig. 1). A gradual decline follows and afflicted children generally become wheelchair bound and blind between 4 and 6 years, with death occurring by ages 8–12 (Williams et al., 1999). At a morphologic level, the disease is characterized by CNS atrophy, with progressive loss of neurons and retinal cells (Boustany, 1996; Birch, 1999; Williams et al., 1999; Haltia, 2003). Affected cells show characteristic autofluorescent, curvilinear

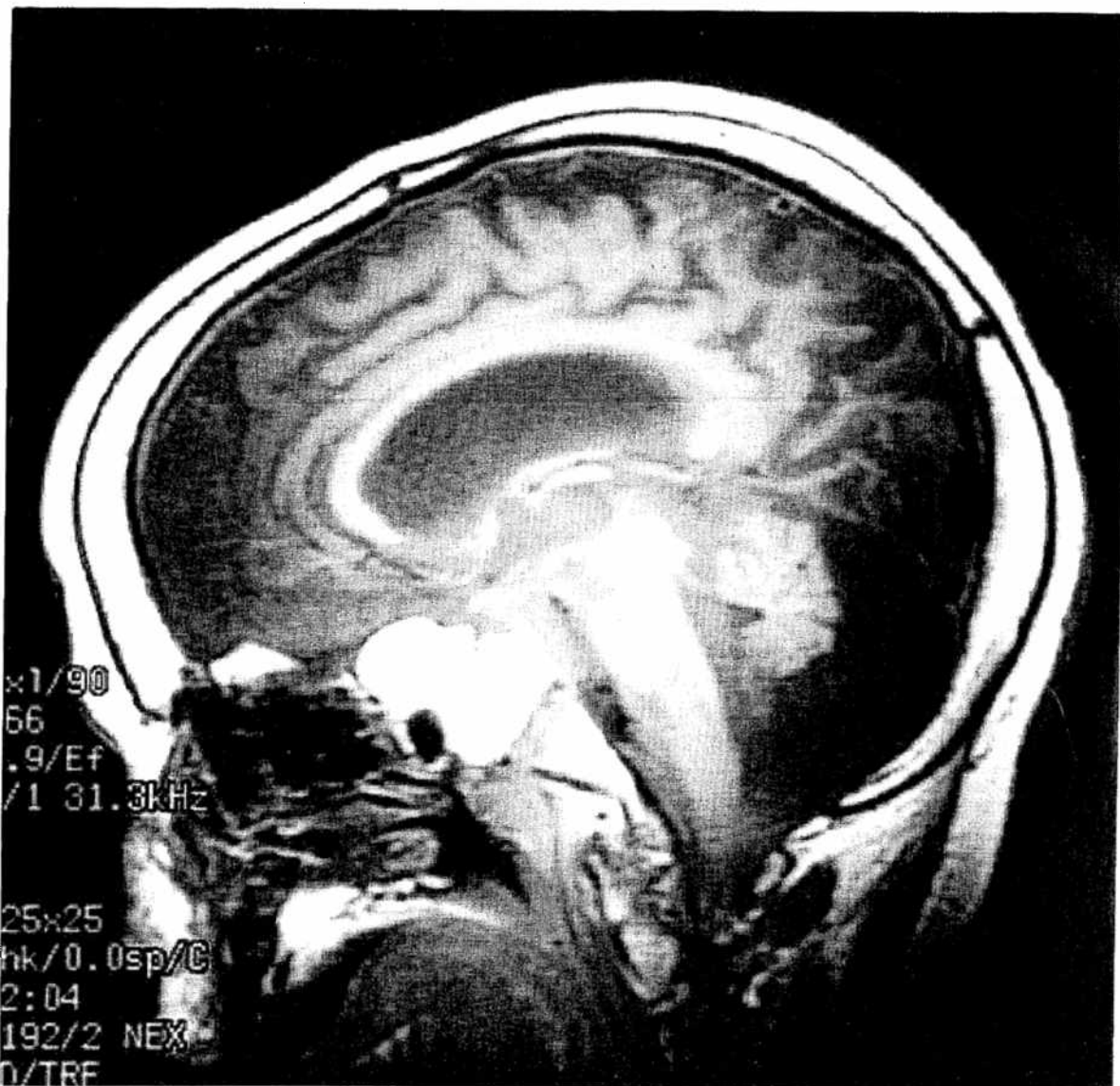


FIGURE 1 Magnetic resonance imaging of the brain of a 6-year-old child with LINCL.

lysosomal storage bodies. The main component of this storage material is the subunit c of mitochondrial ATP synthetase, suggesting a defect in the turnover of this protein (Palmer et al., 1992; Umehara et al., 1997; Ezaki et al., 1999). Even though the storage bodies are present in cells throughout the body, the primary pathology and the cause of morbidity is associated with the pathology in the brain. At present, the only treatments available for this devastating disease are palliative, such as anticonvulsants, physical and occupational therapy, adequate feeding and sleep and prevention of physical discomfort (Wisniewski and Zhong, 2001; Haltia, 2003). There are two early stage experimental therapies for Batten disease: the gene therapy clinical trial described in this chapter and a stem cells study that is in the early stages of obtaining clinical approval (<http://www.stemcellsinc.com/clinicaltrials/clinicaltrials.html>).

III. CLN2 GENE AND PROTEIN

LINCL is caused by the autosomal recessive inheritance of mutations in the CLN2 gene (Sleat et al., 1997).

The gene is mapped to chromosomal locus 11p15, is 6.65 kb in length and consists of 13 exons and 12 introns (Sleat et al., 1997). There are at least 24 identified mutations of the CLN2 gene that are associated with LINCL (Sleat et al., 1999). There is a large variability in the progress of the disease in different individuals and this is dependent on the specific mutation. For example, some mutations of the CLN2 gene result in a low but detectable level of enzyme activity, resulting in a delay of the onset of manifestations compared to other CLN2 mutations (Sleat et al., 1999). The primary translation product of the CLN2 gene is a 563 residue "pre-pro" form of TPP-I that includes a 16 residue signal sequence, a 180 residue propeptide and a 367 residue active mature form (Fig. 2; Lin et al., 2001). Following cleavage of the signal peptide, the 547 amino acid "pro" form is secreted into the endoplasmic reticulum with simultaneous addition of carbohydrates including mannose-6-phosphate (Lin and Lobel, 2001). From the endoplasmic reticulum it is trafficked primarily to the lysosome where the acidic pH induces autolytic cleavage of the propeptide at residues 196–197, resulting in a 367 residue, 46 kDa, active, mature form

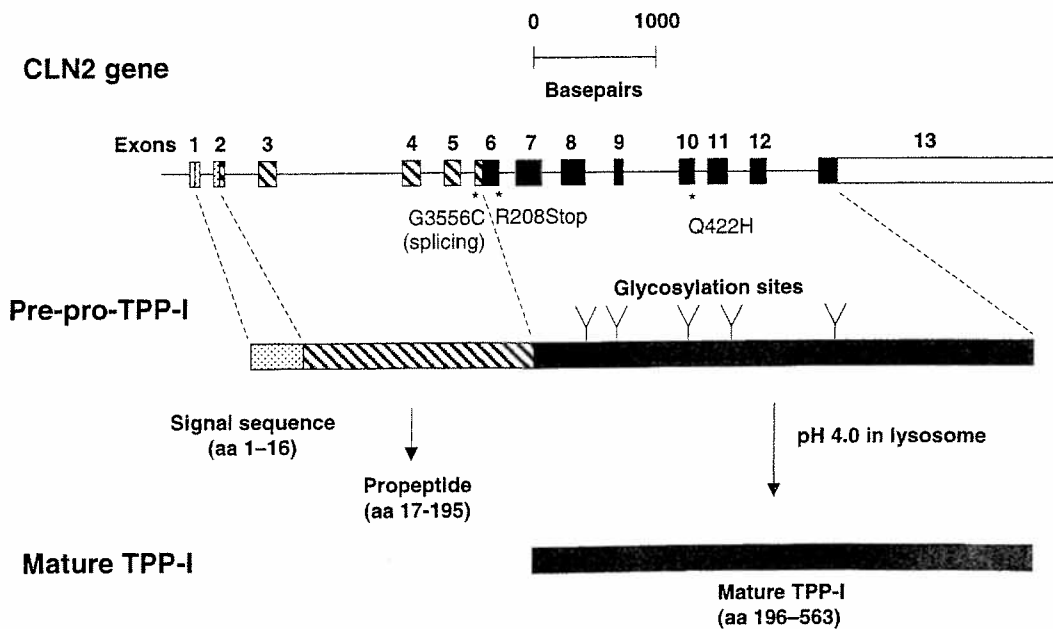


FIGURE 2 Schematic of the CLN2 gene, mutations and the TPP- I protein. The CLN2 gene consists of 13 exons (rectangles) and 12 introns. The locations of the three most common mutations in children with LINCL are shown. The gene is transcribed and spliced onto an mRNA that encodes a 563 amino acid (aa) product (pre-proTPP-I). The signal sequence (aa 1–16) directs the nascent protein to the secretory pathway with insertion into the endoplasmic reticulum and glycosylation at the sites indicated. Pre-pro TPP-I is cleaved to form the 547 residue proTPP-I; this form is inactive until exposed to low pH in the lysosomes which results in proteolytic cleavage at aa 196–197 to yield the active mature product of 367 residues (46 kDa).

of the TPP-I protein. But, a small fraction of the newly synthesized pro-TPP-I is trafficked out of the cell (Lin and Lobel, 2001). With a pI of 6.5, it diffuses in the local milieu until endocytosed via the mannose-6-phosphate receptor of nearby cells, delivered to their lysosomes and activated. The mature form of TPP-I functions as a tripeptidyl peptidase, which is presumed to have a role in protein turnover due to the accumulation of subunit c of mitochondrial ATP synthetase in the lysosome of subjects with no TPP-I activity (Palmer et al., 1992; Umehara et al., 1997; Ezaki et al., 1999). It may also have a role in the protection of cells from apoptosis (Lane et al., 1996; Dhar et al., 2002).

IV. THERAPEUTIC OPTIONS FOR TREATING THE CNS MANIFESTATIONS OF LINCL

In a previous review, we proposed that development of gene transfer with AAV2 vectors provided the best option for clinical advancement (Sondhi et al., 2001). This argument is summarized here.

Treatment of LINCL presents special challenges due to the fact that the primary pathology of the disease is centered in the brain (Boustany, 1996; Williams et al., 1999; Haltia, 2003). These challenges include: (1) it is assumed that the therapeutic protein, functional TPP-I, will need to be provided on a long-term and preferably permanent basis; (2) proteins are unable to cross the blood-brain barrier, which is formed in the vertebrate brain by tight junctions between capillary endothelial cells that isolate the CNS from most circulating macromolecules which may be administered via the bloodstream (Kniesel and Wolburg, 2000); (3) if the TPP-I protein (or CLN2 cDNA) were delivered directly to the CNS to circumvent the blood-brain barrier, it would require the same broad coverage throughout the CNS as the disease pathology; and (4) as with any drug, potential therapies for LINCL therapy will require a satisfactory toxicological profile at the effective dose and this will need to be determined in clinical studies.

There are three general therapeutic strategies that have been seriously considered for the treatment of this disorder: (1) allogeneic stem cell therapy; (2) enzyme replacement therapy; and (3) gene therapy. Each option presents unique challenges for delivery, distribution and duration with respect to the known pathology of LINCL and the potential risk/benefit ratio.

Within the limits of the current biological understanding, the technology available and the uncertain regulatory barriers, we have concluded that allogeneic

stem cell therapy is unlikely to be a viable therapeutic option in the short term. It is unknown if such cells can persist and migrate in the human brain and achieve the levels and spatial distribution of TPP-I required for therapy. Despite these concerns, there is an investigational new drug application currently submitted to the FDA for stem cell therapy for the late-infantile and infantile forms of Batten disease using primary neuronal precursors (<http://www.stemcellsinc.com/clinicaltrials/clinicaltrials.html>). The safety profile of stem cells is also unknown and clinical study will require cautious dose escalation and/or gradual expansion of the numbers of administration sites with assessment of long-term safety.

Enzyme replacement therapy has the significant, but theoretically solvable, challenge of producing the recombinant protein. The extensive resources required to produce the large amounts of recombinant protein required per patient would require the manpower and resources of the commercial biotechnology/pharmaceutical industry for this commercially unviable orphan disease target. Enzyme replacement therapy has been successfully used to treat systemic lysosomal storage diseases such as Fabry's disease (Ioannou et al., 2001), mucopolysaccharidosis type I (Turner et al., 2000) in animals and the non-neuropathic forms of Gaucher's disease in humans (www.genzyme.com/cerezyme/) with a therapeutic level being attained by weekly intravenous infusions of the recombinant enzyme. For neurological diseases such as LINCL, the blood-brain barrier precludes this approach unless a method could be devised to transiently permeabilize the blood-brain barrier to re-establish sufficient cellular TPP-I levels in the brain to reduce the aberrant lysosomal storage and halt progressive loss of neurons. While this would be a great breakthrough, to develop and validate a safe mechanism to penetrate the blood-brain barrier seems unlikely in the short term.

By contrast, gene therapy is a method that has a proven safety profile in humans (Crystal et al., 2002; Harvey et al., 2002) and can provide long-term production of the therapeutic protein in the brain of experimental animals (Frisella et al., 2001; Sondhi et al., 2005). The major challenge of gene therapy is to demonstrate that the currently available vectors are capable of producing sufficient amounts of TPP-I in the appropriate anatomic regions to achieve therapeutic levels to stabilize and/or reverse the progressive CNS deterioration associated with LINCL. The extensive animal data on gene transfer to the brain and a consideration of the biology of LINCL lead us to conclude that gene therapy is a viable option in

the short term. Because LINCL is a progressive, fatal disease of children, there is justification for experimental gene therapy for this disorder and a strong impetus to pursue the transition from basic research to clinical study as rapidly as possible.

Since the level and spatial requirements for TPP-I that would make an impact on disease in children with LINCL are largely unknown, a decision was made to proceed with the best candidate vector available at the time. These considerations eliminate gene-delivery strategies such as non-viral strategies (due to the low efficiency and transience of gene transfer), and lentivirus and herpes simplex virus (due to the safety concerns in humans). Although, these other approaches may provide effective and safe long-term gene transfer to the brain, there is insufficient safety and/or efficacy data for proceeding with the pre-clinical development of these vectors for LINCL without long development timelines. Since the vast majority of the target cells in the CNS do not proliferate, the gene transfer vector must be capable of effectively transferring a gene to quiescent cells. This constraint eliminates conventional retrovirus vectors based on the Maloney murine leukemia virus, which requires proliferating cells for efficient gene transfer. Retroviruses have been used in human trials with *ex vivo* transduction of hematologic stem cells, and there has been success with this approach when there is a selective advantage to the transduced cells (Cavazzana-Calvo et al., 2000). Because neither of these options are available to LINCL there is no basis for proceeding with a retroviral gene transfer study for LINCL in humans.

Once non-viral, retroviral, lentiviral and herpes viral vectors have been eliminated, there remain two possible gene transfer vectors for direct administration strategies: adenovirus (Ad) and adeno-associated virus (AAV).

V. CHALLENGES FOR EFFECTIVE GENE THERAPY OF LINCL

Constrained to the use of Ad or AAV as the candidate gene transfer vector, there are three challenges that were identified as critical to development for a treatment for LINCL: providing therapeutic levels of TPP-I protein, maintaining this level for sufficient duration and distributing therapeutically relevant levels throughout the brain.

The TPP-I protein concentration target is based on the delayed onset of the symptoms of LINCL in subjects, who have CLN2 mutations that reduce but do not eliminate TPP-I activity. There are rare examples

of people with 5–10% of normal TPP-I levels that have greatly delayed appearance of symptoms (Sleat et al., 1999). Therefore, we have posited that an effective therapy will achieve 5–10% or more of the normal endogenous TPP-I level. The caveat is that, while this level may be enough to prevent further damage in an initially healthy neuron, there is no evidence to gauge what TPP-I level is required to clear the pre-existing storage defect in a TPP-I-deficient neuron with inclusion bodies. In general, an Ad vector achieve higher expression levels than AAV vectors, especially in the first 2 weeks post-administration (Hackett et al., 2000; Haskell et al., 2003).

With respect to duration, since TPP-I activity is observed in animals of all ages it is intuitive that persistent expression of the CLN2 gene is required following gene transfer. Therefore, AAV, which provides long-term transgene expression in most tissues including brain, is a prime candidate vector. While Ad is a generally excluded therapeutic option for genetic diseases due to transient expression, it is not clear that it cannot play an important therapeutic role. In this context, we have developed the concept called “setting back the clock,” which will be tested in the future in LINCL knockout mice but is summarized here. This concept is based on the knowledge that, in LINCL, inclusion bodies are proposed to slowly accumulate in the neurons and at some threshold neuronal damage results. In this context, theoretically, gene transfer with Ad, which provides high-level TPP-I levels for a few weeks, may be sufficient to clear the inclusion bodies and thereby provide a period of protection from neurological damage. But the kinetics of inclusion body formation are unknown and there may be a burden of protein recycling in the developing brain with a slower rate thereafter. If gene transfer could reduce the amount of inclusion bodies early in development, even by transient expression of a therapeutic protein delivered by an Ad, vector the levels may be brought under the threshold for pathology and restore normal function to the brain in the long term.

Despite the appeal of the “setting back the clock” concept with Ad, the primary consideration in choice of vectors is safety and this finally dictated our choice of AAV2 for pre-clinical development. Ad is known to induce a strong anti-vector immune response and injection of adenoviral vectors into brain is known to be inflammatory (Smith et al., 1997; Bohn et al., 1999). By contrast, AAV vectors have consistently given rise to long-term transgene expression in experimental animals and have an excellent safety record in humans, including a few individuals who have received administration to the

brain (During et al., 2001; Janson et al., 2002). Although other AAV serotypes yield higher transgene expression level or more widespread transgene expression following administration to the brain, the pre-clinical development pathway, especially for a non-human-derived AAV would be much more complex and the danger of unanticipated side effects would be greater.

Another important consideration in developing gene therapy for LINCL is how to distribute the vector throughout the CNS. LINCL has a diverse set of symptoms that is not attributable to a focal neurological loss in the brain (Williams et al., 1999; Wisniewski et al., 2001b). Moreover, inspection of MRI images of children with LINCL suggest widespread neural atrophy (Fig. 1). It is known that AAV2 vectors do not spread widely after injection into the brain. A number of methods have been suggested to enhance vector distribution including the use of simultaneous heparin infusion or intra-ventricular vector injection with mannitol to permeabilize the blood-brain barrier (Nguyen et al., 2001; Mastakov et al., 2002a). While demonstration of success in experimental animals is important, the potential for a medical complication confounds pre-clinical development and clinical trails with two simultaneous experimental reagents. Further, the effective distribution of TPP-I in the brain following gene transfer does not require transduction of every cell because the expressed protein provides cross-correction to neighboring cells. As described above, addition of the pro-TPP-I to cells derived from individuals with LINCL results in a reduction in the accumulation of the abnormal storage products (Lin and Lobel, 2001). Therefore, cells that are not corrected through vector transduction can nevertheless acquire wild-type TPP-I protein from a neighboring transduced cell — a process referred to as cross-correction (Sondhi et al., 2005). Further, axonal transport of either vector or pro-TPP-I taken up at the distal end of axons can correct storage disorder at the cell body, which may be several millimeters away (Chamberlin et al., 1998; Sondhi et al., 2001; Kaspar et al., 2002; Passini et al., 2002). Therefore, injection of one region with vector results in TPP-I in distant cell bodies that have axonal projection to the injection site. With extensive knowledge of circuitry of the brain, sites of injection can be chosen to optimize distribution via axonal transport.

VI. PRE-CLINICAL EFFICACY STUDIES

Studies of AAV2-mediated gene transfer in the treatment of an animal model of mucopolysaccharidosis

VII (MPS VII (β -glucuronidase deficiency or Sly syndrome), a lysosomal storage disorder that bears many similarities to LINCL (Skorupa et al., 1999; Frisella et al., 2001), have established several principles relevant to the development of gene therapy for LINCL. MPS VII mice are characterized by the accumulation of storage granules in CNS neurons (untreated mice live up to 5 months) similar to LINCL. β -Glucuronidase, the deficient lysosomal enzyme, is normally secreted and cross-corrects neighboring cells via mannose-6-phosphate receptor-mediated uptake. Studies with MPSVII mice (Elliger et al., 1999; Skorupa et al., 1999; Stein et al., 1999; Bosch et al., 2000; Davidson et al., 2000; Sferra et al., 2000; Frisella et al., 2001) have established: (1) direct gene transfer to the CNS provides correction of storage defect in the adult brain; (2) transplantation of wild-type cells can correct mutant cells over an area much greater than the region of transplantation thus validating that cross-correction occurs; and (3) direct CNS administration of AAV delivered β -glucuronidase can reverse storage and behavioral defects and extend survival.

Incorporating the considerations for gene transfer for MPS VII, an AAV2 vector-based therapy was investigated for the delivery of therapeutic levels and distribution of TPP-I to the brain (Sondhi et al., 2005). Approval of a human clinical trial was based entirely on pre-clinical efficacy studies in wild-type (CLN2 +/+) animals (Crystal et al., 2004). A knockout mouse was reported late in the development process (see below), but was never considered critical to the clinical path by the regulatory groups (Sleat et al., 2004). Although scientifically interesting, there is no guarantee that the mouse model would provide an approximation of the human disease due to parallel or alternate pathways that exist in different species. Further, achieving therapeutic benefit in the mouse model would not necessarily predict the same outcome in humans due to the substantial differences in brain size and complex immunological differences between inbred mice and humans.

Studies in CLN2 +/+ animals required analytical methods that distinguished vector-derived TPP-I from the endogenous levels. To resolve this problem, a vector, AAV2_{CU}-hCLN2, with the human cDNA for CLN2 and an optimized Kozak sequence for translation initiation was used in conjunction with a monoclonal antibody specific to the human TPP-I protein. These reagents enabled the detection of vector-derived TPP-I in the context of normal endogenous TPP-I levels of the rat, but not of the monkey. Histology of rat brain using this monoclonal antibody provided evidence

that vector-derived TPP-I is present, however, quantitative measure of TPP-I was not possible nor was the evaluation of the limits of detection possible. In addition, a quantitative, enzymatic activity assay for TPP-I was used that was not species-specific, therefore, only TPP-I levels substantially above background could be reliably detected. These methods can distinguish those areas with TPP-I levels that are well above endogenous (which refers to the levels in normal individuals and is designated as 100%), but does not readily predict the volume around the injection site that will surpass the 5% target for therapeutic benefit. It is reasonable to assume that achieving the therapeutic levels is much broader than the tip of the iceberg seen with this assay of low sensitivity.

The AAV2 expression cassette included the CAG promoter on the basis of published data that it produced long-lasting gene expression in the brain via AAV2-mediated gene transfer (Niwa et al., 1991; Daly et al., 1999a,b). The CAG hybrid promoter consists of the enhancer of the cytomegalovirus IE1 gene, the chicken β -actin promoter, splice donor and intron and the splice acceptor of rabbit β -globin. The polyadenylation/transcription stop signals are also derived from rabbit β -globin. These signals controlled the expression of the human cDNA for CLN2 with an optimized Kozak context around the start codon. When packaged into the genome of AAV2, this vector is referred to as AAV2_{CU}hCLN2 (Crystal et al., 2004; Sondhi et al., 2005).

AAV2-mediated CLN2 gene transfer to the brain of rats was used to establish the general characteristics of TPP-I expression (Sondhi et al., 2005). With respect to time course, TPP-I was first detected by immunohistochemistry at ~4 weeks following gene transfer and extended up to the last time-point studied, which was 18 months (Fig. 3A, B). TPP-I was produced locally after injection of vector into a number of structures within the brain including cerebellum, frontal cortex, parietal cortex and the striatum. In each injected structure, triple immunofluorescence indicated that TPP-I-positive cells were also neuN positive (neurons) and not GFAP-positive cells (astrocytes). With respect to levels, injection of 2.5×10^9 particle units of AAV2_{CU}hCLN2 into striatum resulted in a TPP-I activity 1.5-fold the endogenous level at 4 weeks and remained stable in that range for at least 12 weeks. Therefore, AAV2_{CU}hCLN2 can achieve greater than the therapeutic target, at least locally at the site of injection.

TPP-I neurons positive for human TPP-I were detected a significant distance from the vector injection site indicating a mechanism of spread of the vector and/or TPP-I protein through the brain possibly by axonal

transport and/or cross correction of cells with extended processes (Fig. 3C, D). This even included neurons as far away as the hemisphere contralateral to the injection site (Fig. 3D). It was estimated that ~50% of the striatum and ~5% of the hemisphere contained TPP-I-positive neurons following a single injection of 10^{10} particle units into the striatum. Finally, while the literature indicates that immunity against a xenotropic gene delivered by AAV depends on the route of administration (Herzog et al., 2002; Song et al., 2002; Arruda et al., 2004; Chenuaud et al., 2004; Couto, 2004; Flotte, 2004; Gao et al., 2004), our studies in rats show that for intracranial injection of human TPP-I, this is not a problem, likely due to the immuno-privileged nature of the brain (Mastakov et al., 2002b).

The rat studies indicated that functional TPP-I could be delivered specifically to neurons, even at locations distant from the site of injection without stimulating immunity. However, it remained to be established if the extent of TPP-I activity spread seen in the rat brain, would translate to effective distribution in larger brains such as in non-human primates and ultimately in humans. It is possible that the spread is limited by distance per se or by anatomical barriers that are further apart in larger brains. Therefore, the brain of African green monkeys were injected with AAV2_{CU}hCLN2 and TPP-I expression was assessed by the enzymatic activity assay and immunohistochemistry. The dose was scaled with respect to brain size and, as with rats, TPP-I levels were significantly above the endogenous background at the site of injection suggesting that therapeutic levels could be obtained locally. By immunohistochemistry, TPP-I expression was detected in neurons around the injection site (Sondhi et al., 2005). Since the TPP-I protein in African green monkeys is 93% identical to the human protein, immunohistochemistry reagents required to distinguish vector-encoded human TPP-I from endogenous monkey TPP-I were not as sensitive. Thus, the possible spread of TPP-I from the injection site to neurons in distant brain structures could not be assessed.

While our data focused on the use of AAV serotype 2, which facilitated clinical development because of extensive safety data, other investigators have explored the use of adenoviral, AAV serotype 5 and lentiviral vectors for CLN2 gene transfer (Haskell et al., 2003). Similar to our experiments, a single injection of vector encoding the CLN2 gene into the cerebellum or striatum produced TPP-I expression detectable by immunofluorescence. TPP-I enzymatic activity was also detected at levels somewhat higher than those achieved with AAV2 vectors. Use of a β -galactosidase

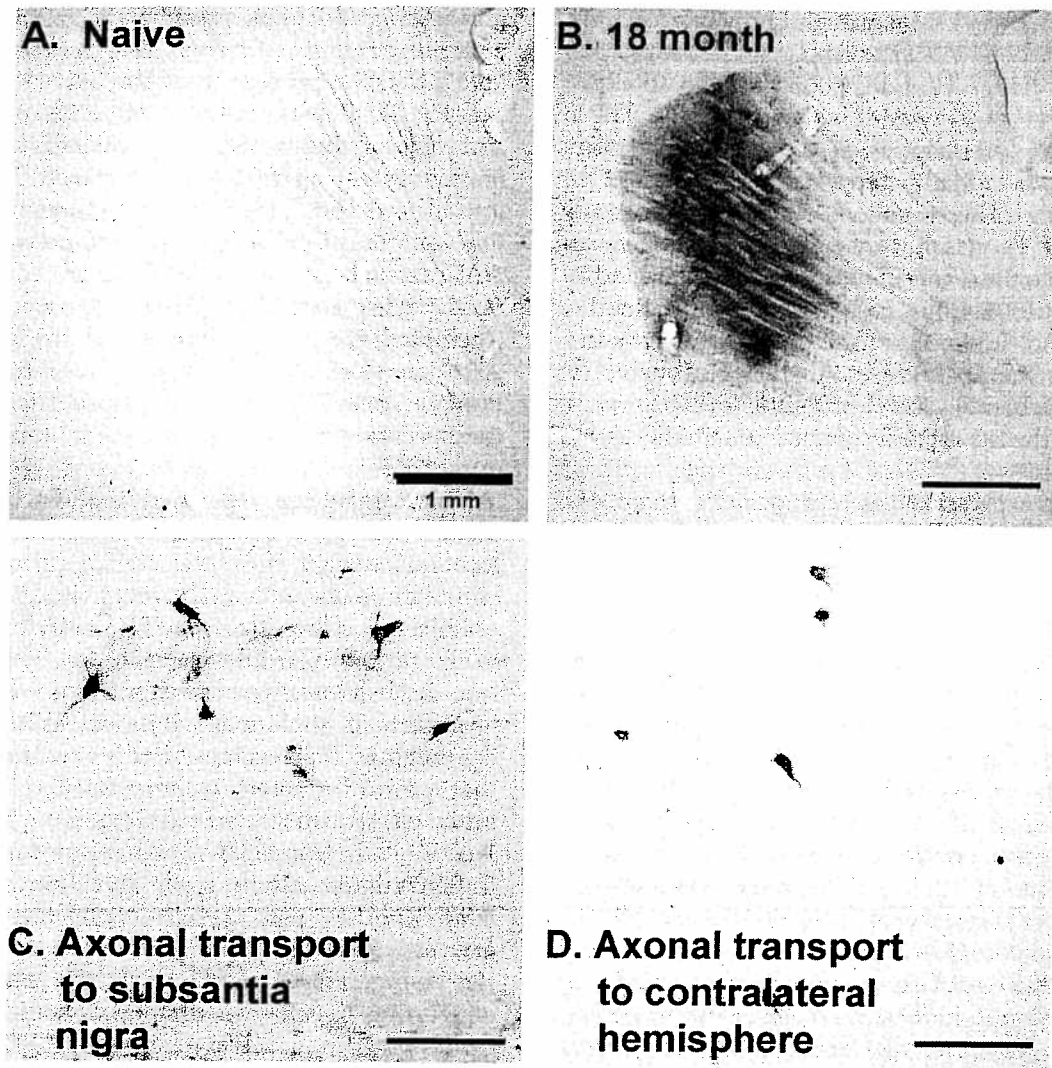


FIGURE 3 TPP-I protein accumulation following AAV2_{CU}hCLN2 gene transfer and expression of TPP-I in structures far from the injection site. Rats were injected into the striatum with 1 μ l (10^{10} particle units) of AAV2_{CU}hCLN2 and TPP-I distribution was assessed at 18 months by anti-TPP-I immunoperoxidase staining on sagittal sections of the striatum of the injected hemisphere. (A) naive; (B) AAV2_{CU}hCLN2 at 18 months TPP-I expression was observed in various regions far from the injection site; (C) TPP-I-positive cells in the substantia nigra at 18 months; and (D) TPP-I-positive cells in the contralateral hemisphere. Magnification bar = 1 mm for panels A and B and 50 μ M for panels C and D.

and TPP-I double expression vector provided evidence for cross-correction through the appearance of TPP-I-positive, β -galactosidase-negative cells.

VII. PRE-CLINICAL TOXICOLOGY STUDIES

With a complete set of data supporting efficacy, using an AAV2 vector our group proceeded to translate

this toward a clinical study. A decision to proceed with a pre-clinical program involves great cost and commitment of time. Therefore, development of a clinical candidate often occurs with a technology that is no longer state-of-the-art (in this case, AAV2 rather than newer serotypes that may offer better performance) as the various stages of development proceed. We decided to lock in the AAV2 platform with evidence of transgene expression, but not functional clearance of lysosomal storage in a knock out mouse (model available late in

our development process). This decision was made for the following reasons: (1) there is no evidence that the storage defect phenotype is the primary cause of disease therefore establishing a litmus test based on this attribute may be misleading; (2) although alternate serotypes of AAV have shown greater magnitude of transgene expression, the extent of this expression varies from species to species and may not be relevant to humans; (3) the use of AAV2 in clinical studies is well documented with a good safety profile thus improving the likelihood of "doing no harm" in a clinical trial; (4) therapeutic levels of TPP-I are significantly below the sensitivity of assays in our experimental animal studies, i.e., even if alternative serotypes yield higher levels of expression this may not be an advantage in the context of 5–10% of a normal level as target and the potential for adverse events due to overexpression may become an issue; and (5) the requirements for toxicology and development program for manufacturing and quality control for human use of a new serotype of AAV, for which there is no previous clinical precedence, is likely to be more stringent than that for AAV2.

The combination of evidence for long-term, moderate-level TPP-I production following AAV2_{CU}hCLN2 gene transfer along with the demonstration of axonal transport to widen the range of TPP-I distribution beyond the immediate injection site produced justification to proceed to the clinic (Sondhi et al., 2005). Moreover, the demonstration of efficacy in animal models in other lysosomal storage diseases such as MPSVII suggested at least a possibility of a successful outcome of a clinical study for LINCL (Stein et al., 1999; Frisella et al., 2001). Finally, clinical development is a process of iterative improvement and establishing the safety of an AAV2 platform for gene transfer would provide valuable data applicable to other gene transfer vectors for this and related diseases.

In light of the limitations of animal models to mimic all aspects of human biology and the urgent medical need for treatments for LINCL, we initiated a pre-clinical development program. This started with a consultation with the FDA for product design, proposals for a toxicology study and for the drug manufacturing process. The supportive response from the FDA arose at least in part from the severity of the disease in combination with an emerging picture of the expected toxicity profile of AAV2 vectors. For example, many groups have studied biodistribution of AAV vectors, the potential spread to gonads as well as the insertion of the vector DNA into the chromosome in testes (Kho et al., 2000; Arruda et al., 2001; Monahan et al., 2002; Couto et al., 2004; Pachori et al., 2004). These considerations are largely irrelevant

for a fatal childhood disease such as LINCL where death is inevitable in the absence of a successful therapy. Therefore, the stringency for toxicological parameters for a clinical study for a therapeutic for LINCL is reduced, which is analogous to developing a new drug for cancer where a degree of uncertainty on outcome and even the possibility of side effects are acceptable.

Pre-clinical studies to support an investigational new drug application included standard safety and toxicology assessment in rodents. No biodistribution study was required although samples of tissue were retained for future studies. The study involved comparing male and female Fisher 344 rats injected bilaterally into the striatum with AAV2_{CU}hCLN2 vs. phosphate-buffered saline-injected control rats over 18 months. The dose was 10^{10} particle units delivered directly to the rat brain and translates, on a weight basis to a dose of approximately 5×10^{12} in humans. The rats were observed three times a week and morbidity and mortality was noted. At specified times, a subset of rats were sacrificed with assessment of hematological and histopathological parameters. For all timepoints assessed there was no abnormality in the AAV2_{CU}hCLN2-treated group for any parameter of complete blood count or serum chemistry and the histopathological data for both groups were the same.

Behavioral assessment of rats is relatively unsophisticated and anomalies resulting from vector administration or transgene expression may be difficult to observe. Therefore, non-human primates were chosen as the second species for toxicology studies. Two groups received CNS administration of 3.6×10^{10} and 3.6×10^{11} particle units of AAV2_{CU}hCLN2 in parallel with various control (AAV2Null with no transgene, phosphate-buffered saline and sham-injected) groups. As planned for the human study, vector was administered to 12 locations through 6 burr holes. As with rats, a subset was sacrificed at intervals up to 1 year for assessment of hematological and histopathological parameters. In addition, the non-human primates in the study were videotaped with a prescribed list of challenges and the responding behaviors were recorded and analyzed via a standardized scoring algorithm. All remaining monkeys were also bled periodically to assess differential and serum chemistry.

As with the rat toxicology study, there were no abnormalities that were attributable to AAV2_{CU}hCLN2 gene transfer (for an example, see Fig. 4A demonstrating serum liver enzyme values over time). However, there was a minor evidence that the procedure of direct vector administration into 12 sites in the brain could cause local trauma. In this context, histopathological

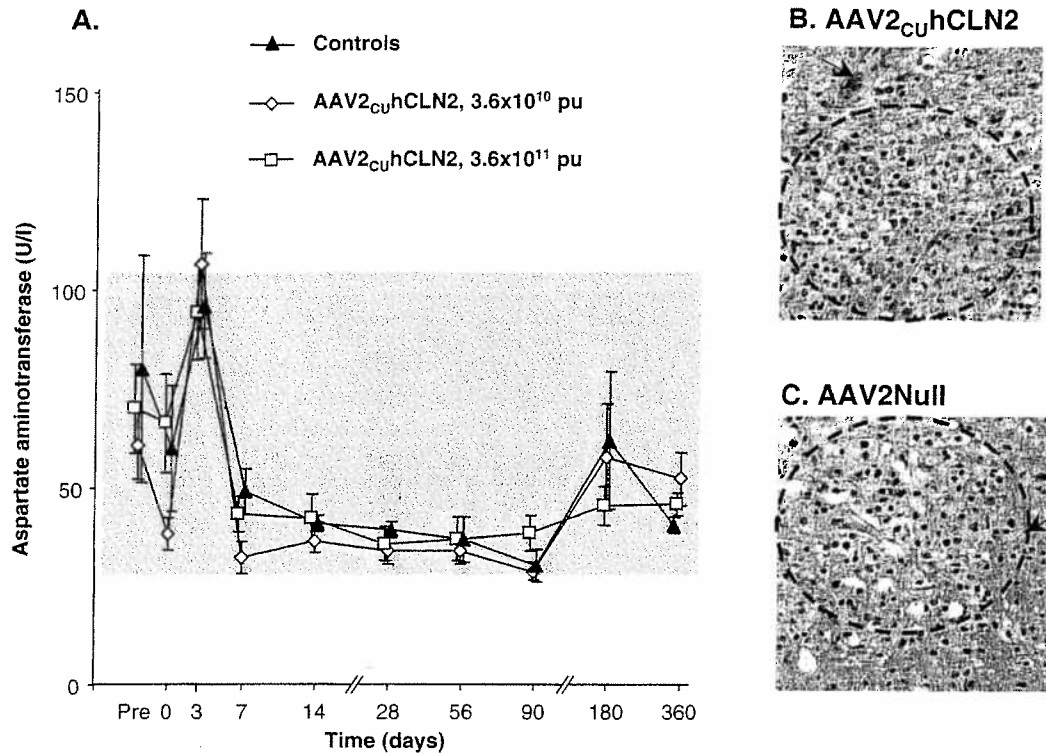


FIGURE 4 Acute effects of direct CNS administration of AAV₂_{CU}hCLN2 on serum liver enzyme levels and on histopathology in African green monkeys. African green monkeys ($n = 12$ per group) were injected with 3×10^{11} or 3×10^{10} particle units of AAV₂_{CU}hCLN2 and controls were injected with AAV2Null, PBS or sham injected. At various time points, all monkeys were sedated and blood was drawn for complete blood count and serum chemistry. (A) Aspartate aminotransferase for all surviving monkeys (mean \pm standard error) is shown with the shaded area representing the normal range. At weeks 1, 13, 26 and 52, a subset was sacrificed and histopathology analysis was performed. Examples of the injection site in the caudate are shown for monkeys sacrificed at 1 week with the area of gliosis shown by the dotted circle and the hemosiderin shown with an arrow. (B) AAV₂_{CU}hCLN2; (C) AAVNull.

examination showed mild gliosis and hemosiderin in the brain around the injection sites (Fig. 4B, C). This was injection related, was most pronounced at 1 week post-injection, and was resolved at the longer time-points. There was a similar level of severity in the control and AAV₂_{CU}hCLN2 groups.

VIII. MANUFACTURING THE CLINICAL GRADE AAV₂_{CU}HCLN2 VECTOR

The fact that LINCL is a fatal disease with a very small number of patients also impacts the requirements for manufacturing. In standard drug development, which anticipates large phase III trials and downstream development toward a marketed product, a scalable process and infrastructure development is critical. In the case of LINCL, these issues are moot because there

are only about 200 LINCL patients in the developed world. Therefore, the small-scale production process transferred from the research laboratory with transfection of adherent 293 cells in 10 stack Cell Factory was sufficient to make all of the vector necessary for the phase I/II trial and in the event of clinical benefit may be scaled up with minimal changes. The cells were transfected with two plasmids, the first containing the genome of the AAV₂_{CU}hCLN2 vector and the second plasmid pPAK-MA2 (similar to the pDG plasmid used in research laboratories containing the Ad E2, E4, VA) and AAV2 (rep and cap) helper functions (Grimm et al., 1998; Qui et al., 2002). The lysate was collected after 48 h and the vector purified by a iodixanol step gradient density centrifugation followed by heparin affinity chromatography (Zolotukhin et al., 1999).

Prior to manufacture of clinical lots, a development program was followed (Fig. 5) to ensure that

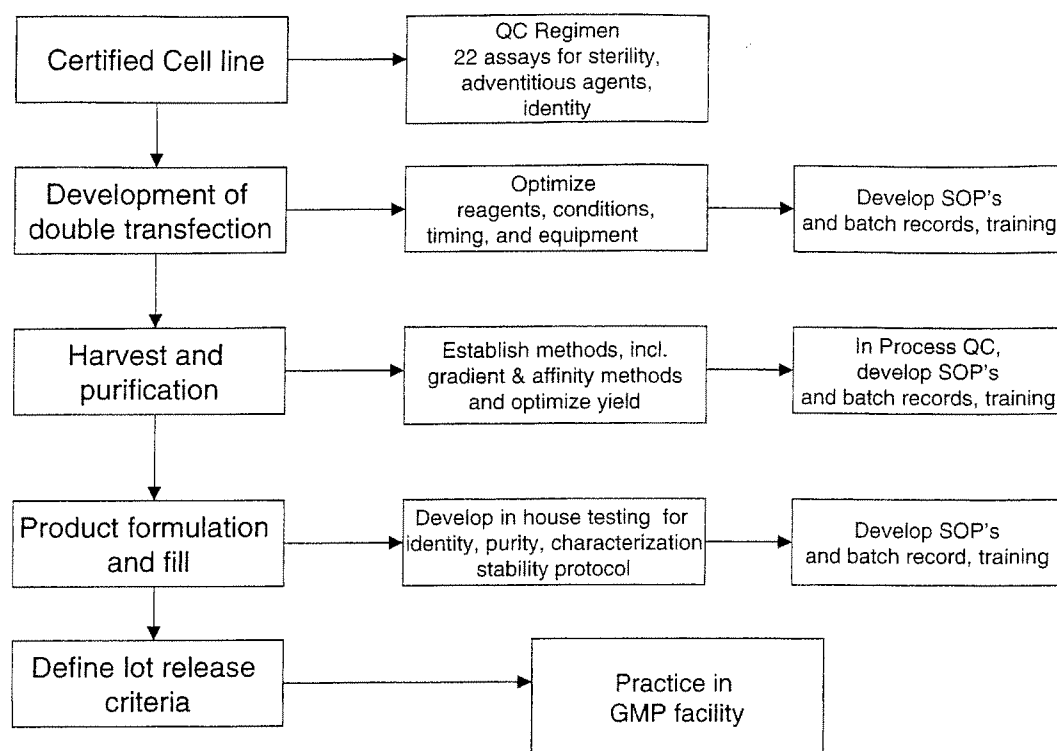


FIGURE 5 Development of a GMP production scheme for AAV₂_{CU}hCLN2. The left vertical path indicates steps in the manufacture of AAV. Boxes to the right of each step are the process development activities, assays and documentation requirements. QC = quality control; SOP = standard operating practice; GMP = good manufacturing practice.

a reproducible, well-controlled manufacturing process was available. The purpose of this program is to identify reagents compatible with the requirements of current good manufacturing practice (GMP), to develop standard operating procedures (SOPs), to train personnel and to understand critical aspects of the manufacturing process. Initially, the performance of a working cell bank from a certified human embryonic kidney 293 cell line was assessed to ensure yields were in line with those obtained in the research laboratory. The plasmids needed to make the AAV₂_{CU}hCLN2 vector were reengineered to confer kanamycin resistance on the host bacterium to eliminate the use of ampicillin, a potential allergen, which would require residual testing in the final product. The ability to transfect the 293 cells with different reagents and with different amounts of plasmid was assessed and a procedure using the Polyfect reagent (QIAGEN) and 1 mg of Ad/AAV helper plasmid and 0.5 mg of the vector plasmid was found optimal. Various aspects of the purification procedure were also optimized such as the final concentration and buffer exchange for

which a reverse dialysis procedure was devised. This process was sufficient to bring the 200 ml eluted from the heparin column in the last step of the purification to ~10 ml of the required concentration. In addition, quality control assays including *in vitro* gene transfer, replication-competent AAV titer and infectious titer were developed and validated. On the basis of this type of process development, a complete set of SOPs were drafted covering all steps of manufacturing and practice batches were performed under GMP conditions by GMP personnel for the purpose of training and in order to refine and fine tune these SOPs.

Following the development phase, seven clinical batches of vector have been purified (Table 1). In general, each batch was sufficient for only one or two patients, but yields have been improved following batch 5 by forced aeration of the cell factory following transfection. The gene transduction titers have been reproducible and stability of this parameter to storage has been demonstrated. In addition to in-house assessment of potency and purity, safety parameters have been assessed by contract laboratories. As for

TABLE 1 Properties of Clinical Batches of AAV2_{CU}hCLN2^a

Batch	Total yield (particle units)	Physical titer by ELISA (particle units/ml)	Genome titer (genome copies/ml)	Physical titer/genome copies	In vitro gene transfer ^b	Genomic DNA contamination (ng/dose) ^c
Lot 1	1.3 × 10 ¹²	1.0 × 10 ¹²	3.0 × 10 ¹⁰	35	85	160
Lot 2	5.0 × 10 ¹²	1.0 × 10 ¹²	7.4 × 10 ¹⁰	13.5	250	65
Lot 3	4.8 × 10 ¹²	1.2 × 10 ¹²	6.4 × 10 ¹⁰	18.7	297	83
Lot 4	7.5 × 10 ¹²	1.5 × 10 ¹²	7.1 × 10 ¹⁰	21.3	734	60
Lot 5	2.1 × 10 ¹²	3.0 × 10 ¹⁰	ND ^d	ND	ND	ND
Lot 6	1.6 × 10 ¹³	1.8 × 10 ¹²	1.1 × 10 ¹⁰	180	387	55
Lot 7	5.2 × 10 ¹²	1.1 × 10 ¹²	ND	ND	247	ND

^aThe characteristics of the seven candidate clinical batches of AAV2_{CU}hCLN2 are tabulated.

^bIn a standardized assay, vector (10¹⁰ pu) was used to infect 293 cells and the TPP-I activity of the media was assessed after 72 h.

^cGenomic DNA contamination was determined by Taqman realtime PCR using the rRNA gene as a target.

^dND = not determined.

toxicology, the fact that we are treating a fatal childhood disease and performing only a phase I study reduces the stringency of testing. For example, the lot release for the AAV2_{CU}hCLN2 vector contained testing for only a subset of adventitious agents compared to the lot release criteria used in applications relevant to a less severely diseased population. The critical drug control parameters that remain relevant are the identity, purity and potency of the active ingredient and the control and stability of this formulated reagent during delivery to the clinical trial subjects. The presence of adventitious agents and residuals of manufacture, likely to be relevant for long-term safety would come to the forefront when a therapeutic benefit was demonstrated.

As mentioned above, studies of vector stability under conditions for delivery to the patient remains a critical component of drug development. Under the proposed clinical study, a catheter composed of glass capillary is used for intracranial delivery. It was therefore essential to show that functional gene transfer by AAV2_{CU}hCLN2 vector was not diminished by the injection catheter. Under conditions mimicking the surgery, the vector was recovered from the catheter and the concentration and biological activity was assessed (Fig. 6). The concentrations of AAV2 in the first 50 µl was significantly diminished, possibly due to adherence to the walls of the catheter. The next 300 µl was recovered from the catheter with minimal loss in titer and potency. Therefore, during surgery the first 50 µl of vector is discarded prior to inserting the catheters into the brain, thereby assuring appropriate delivery of functional vector.

IX. CLINICAL PROTOCOL DESIGN

The design of clinical studies to assess safety and efficacy of AAV2_{CU}hCLN2 gene transfer as well as the anticipation of product development was complicated by the small number of patients available. According to the Batten disease registry, there are approximately 200 subjects in the USA with LINCL which is insufficient for traditional phases I, II, III studies consisting of initial safety, dose-escalation and a multi-center, randomized placebo-controlled double blind evaluation of efficacy. Instead, the current clinical study combines safety and efficacy with a single administration at a dose with the potential for therapeutic value (Crystal et al., 2004). The single dose used for the study is a total of 3.6 × 10¹² particle units divided among 12 locations. This is based on extrapolation of TPP-I activity in rats to the desired therapeutic levels and on practical surgical considerations. Injection of 10¹⁰ particle units into the brain of rat gave an excess TPP-I activity of 6000 units per gm of brain wet weight compared to the endogenous activity of 20000 units. Assuming linear scaling of expression with dose, the target of 10% endogenous TPP-I activity (i.e., 2000 units) over the whole human brain (1,000 g) would be derived from the injection of 3.3 × 10¹² particle units. An additional constraint is related to the risk of direct surgical injection into the brain. Greater than six burr holes were deemed inadvisable for safety reasons and a slow infusion rate of 2 µl/min through each of the six catheters was believed necessary to minimize local damage to the brain. Therefore, limiting time of administration to

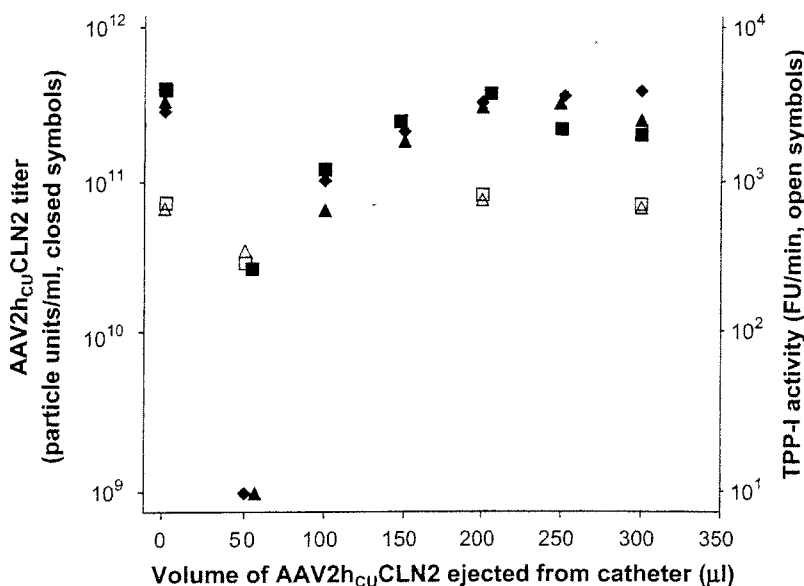


FIGURE 6 Stability of vector in the injection catheter. AAV2_{hCU}CLN2 (2×10^{11} pu/ml by ELISA) was loaded into a syringe and the needle/catheter assembly was attached. This was mounted on the delivery pump and vector was collected from the end of the catheter in 25 μ l aliquots were collected at a flow rate of 2 μ l per minute. Fractions were assayed in triplicate for physical titer by ELISA (closed symbols) and in duplicate by in vitro functional gene transfer assay (open symbols).

150 min (to limit time under anesthesia) we decided to deliver no more than 300 μ l per burr hole (150 μ l at each of two depths per burr hole). Since AAV2 vectors tend to aggregate at concentrations of $>2 \times 10^{12}$ pu/ml we were limited to a total dose of 3.6×10^{12} particle units.

All clinical trials have many challenging issues related to ethics and design. A particularly difficult decision for this clinical trial design was whether to treat LINCL patients with AAV2_{hCU}CLN2 at the mild or severe phase of the disease. For gene therapy, this issue is an ongoing dilemma. Due to the risk of direct surgical administration of vector into the brain, we decided to first treat patients with advanced LINCL for whom the impact of possible adverse events would have less impact on life expectancy. This decision is complicated by the fact that advanced LINCL patients have impairment in several organ systems and therefore there is a chance of serious adverse events possibly related to underlying disease but indistinguishable from effects the drug or surgery. In addition, it may be argued that the potential for benefit of gene transfer diminishes as the neurodegeneration in the brain increases. As a compromise, the trial was designed to start with five subjects with advanced disease (designated Group A) and, pending review by the regulatory

agencies, to proceed to six subjects with moderate disease (designated Group B; Crystal et al., 2004).

Administration of AAV2_{hCU}CLN2 to subjects with advanced LINCL also complicates the choice of safety endpoints. The toxicology studies in rats and non-human primates provided no evidence to anticipate likely adverse effects. Therefore, aside from the brain, there is no obvious anatomical site of interest for safety assessments. Moreover, the neurological tests and EEG normally used as sensitive tests of drug safety in normal children provide no insight in LINCL patients with severely degraded neurological function. Therefore, a set of standard medical and hematological assessment parameters were used to assess vector safety with the caveat that their significance is better understood in normal subjects than in children with LINCL.

Secondary to safety assessment are the efficacy endpoints, which provide additional challenges. The LINCL clinical rating scale in which the broad loss of brain function is the primary readout provided a useful starting point. This clinical rating scale, modified from an original model by Steinfeld et al. (2002), was constructed to provide an integrated sense of each patient's disease severity. The scale is comprised of three functional categories: motor function, seizures and language, each of which are rated

on a scale of 0–3 allowing for a total CNS disability score between 0 and 9. Patients receiving total disability ratings between 0 and 4 are categorized in the gene transfer protocol as “severe” or Group A, while those who receive total disability scores of 5–6 are classified as “moderate” or Group B. This scale was modified from an original design by Steinfeld et al. (2002), which included a categorization for vision. We eliminated this category for the following reasons: (1) most patients are blind by the time of enrollment in the trial, largely due to the rapid progression of the disease; and (2) the central nervous system vector delivery route selected for this trial proscribes the possibilities for visual improvement in subjects post vector administration, since retinal cells are not targeted for gene transfer. In addition, the Steinfeld scale categorized patients as “severe” if they received total CNS disability scores between 0 and 3. This was broadened in our modification to account for the fact that for most LINCL patients, seizure activity is adequately controlled by anti-convulsants, and subjects are therefore expected to receive seizure scores of “3” (indicating no grand mal seizures in the last 3 months).

Unfortunately, the modified LINCL clinical rating scale is relatively insensitive as an efficacy parameter. A favorable outcome for this trial might simply be a decrease in the rate of deterioration of this parameter but given variability among subjects and the relative insensitivity of the scale, it may take a long time and multiple subjects to see this impact. Although the rating scale is the most important tool, we also attempted to use magnetic resonance spectroscopy (MRS) to assess the status of the brain in LICNL patients. Previous studies have shown that there are decreases in *N*-acetylaspartate (NAA) concentration and increase in lactate concentration in the brains of LINCL patients (Brockmann et al., 1996; Jarvela et al., 1997; Seitz et al., 1998; Vanhanen et al., 2004). These assessments were made by the use of single voxel magnetic resonance spectrometers, but the advent of high magnetic field spectrometers has improved the resolution of these metabolites, thus local effects due to gene therapy may be evident from a lack of decrease in NAA concentration by the expected rate/amount. Therefore, the clinical protocol included both pre-surgical MRS spectroscopy as well as repeated assessments at 6 and 18 months post-therapy.

A full clinical protocol based on the considerations above was accepted by the local regulatory agencies (Institutional Review Board and Institutional Biosafety Committee). In conjunction with the efficacy data and toxicology data presented above, it was also reviewed

by the National Institutes of Health Recombinant DNA Advisory Committee, who opted for no detailed review and the Food and Drug Administration. Therefore, subject accrual and gene transfer in those enrolled in the trial is ongoing.

X. CONCLUSION

The program described above for commencing a clinical trial for LINCL by direct administration of AAV2 vector expressing CLN2 to the brain is a typical example of translational research in the academic setting. While missing some of the stringency that may be applied to a commercial entity in the development of a marketed drug, the program still consumed a substantial amount of resources and time. The overall cost is several million dollars and identification of support on the scale needed for such pre-clinical programs is difficult even in the context of the NIH roadmap for translational research. To maximize the return on the effort invested, other neurological lysosomal storage diseases may be subsequently identified that may benefit from a similar approach and the knowledge learned from the manufacturing program and toxicology studies for LINCL could be applied to these other diseases.

ACKNOWLEDGMENTS

We thank N. Mohamed for help in preparing this manuscript. These studies were supported, in part, by U01 NS04758, NIH M01RR00047 from The NIH and The Will Rogers Memorial Foundation, Los Angeles, CA, and Nathan's Battle Foundation, Greenwood, IN.

References

- Arruda, V.R., Fields, P.A., Milner, R., Wainwright, L., De Miguel, M.P., Donovan, P.J., Herzog, R.W., Nichols, T.C., Biegel, J.A., Razavi, M., Dake, M., Huff, D., Flake, A.W., Couto, L., Kay, M.A. and High, K.A. (2001) Lack of germline transmission of vector sequences following systemic administration of recombinant AAV-2 vector in males. *Mol. Ther.* 4: 586–592.
- Arruda, V.R., Schuettrumpf, J., Herzog, R.W., Nichols, T.C., Robinson, N., Lotfi, Y., Mingozzi, F., Xiao, W., Couto, L.B. and High, K.A. (2004) Safety and efficacy of factor IX gene transfer to skeletal muscle in murine and canine hemophilia B models by adeno-associated viral vector serotype 1. *Blood*, 103: 85–92.
- Birch, D.G. (1999) Retinal degeneration in retinitis pigmentosa and neuronal ceroid lipofuscinosis: an overview. *Mol. Genet. Metab.* 66: 356–366.
- Bohn, M.C., Choi-Lundberg, D.L., Davidson, B.L., Leranthe, C., Kozlowski, D.A., Smith, J.C., O'Banion, M.K. and Redmond, D.E.

- (1999) Adenovirus-mediated transgene expression in nonhuman primate brain. *Hum. Gene Ther.*, 10: 1175–1184.
- Bosch, A., Perret, E., Desmaris, N. and Heard, J.M. (2000) Long-term and significant correction of brain lesions in adult mucopolysaccharidosis type VII mice using recombinant AAV vectors. *Mol. Ther.*, 1: 63–70.
- Boustany, R.M. (1996) Batten disease or neuronal ceroid lipofuscinosis. In: Moser H.W., Ed., *Handbook of Clinical Neurology*, Vol. 22, No. 66. Neurodystrophies and Neurolipidoses. Elsevier Science B.V., New York, pp. 671–700.
- Brockmann, K., Pouwels, P.J., Christen, H.J., Frahm, J. and Hanefeld, F. (1996) Localized proton magnetic resonance spectroscopy of cerebral metabolic disturbances in children with neuronal ceroid lipofuscinosis. *Neuropediatrics*, 27: 242–248.
- Cavazzana-Calvo, M., Hacein-Bey, S., de Saint, B.G., Gross, F., Yvon, E., Nusbaum, P., Selz, F., Hue, C., Certain, S., Casanova, J.L., Bousso, P., Deist, F.L. and Fischer, A. (2000) Gene therapy of human severe combined immunodeficiency (SCID)-X1 disease. *Science*, 288: 669–672.
- Chamberlin, N.L., Du, B., de Lacalle, S. and Saper, C.B. (1998) Recombinant adeno-associated virus vector: use for transgene expression and anterograde tract tracing in the CNS. *Brain Res.*, 793: 169–175.
- Chenuaud, P., Larcher, T., Rabinowitz, J.E., Provost, N., Cherel, Y., Casadevall, N., Samulski, R.J. and Moullier, P. (2004) Autoimmune anemia in macaques following erythropoietin gene therapy. *Blood*, 103: 3303–3304.
- Crystal, R.G., Harvey, B.-G., Wisnivesky, J.P., O'Donoghue, K.A., Chu, K.W., Maroni, J., Muscat, J.C., Pippo, A.L., Wright, C.E., Kaner, R.K., Leopold, P.L., Kessler, P.D., Rasmussen, H.S., Rosengart, T.K. and Hollmann, C. (2002) Analysis of risk factors for local delivery of low and intermediate dose adenovirus gene transfer vectors to individuals with a spectrum of comorbid conditions. *Hum. Gene Ther.*, 13: 65–100.
- Crystal, R.G., Sondhi, D., Hackett, N.R., Kaminsky, S.M., Worgall, S., Stieg, P., Souweidane, M., Hosain, S., Heier, L., Ballon, D., Dinner, M., Wisniewski, K., Kaplitt, M.G., Greenwald, B.M., Howell, J.D., Strybing, K., Dyke, J. and Voos, H. (2004) Administration of a replication-deficient adeno-associated virus gene transfer vector expressing the human CLN2 cDNA to the brain of children with late infantile neuronal ceroid lipofuscinosis. *Hum. Gene Ther.*, 15: 1131–1154.
- Couto, L., Parker, A. and Gordon, J.W. (2004) Direct exposure of mouse spermatozoa to very high concentrations of a serotype-2 adeno-associated virus gene therapy vector fails to lead to germ cell transduction. *Hum. Gene Ther.*, 15: 287–291.
- Couto, L.B. (2004) Preclinical gene therapy studies for hemophilia using adeno-associated virus (AAV) vectors. *Semin. Thromb. Hemostat.*, 30: 161–171.
- Daly, T.M., Okuyama, T., Vogler, C., Haskins, M.E., Muzyczka, N. and Sands, M.S. (1999a) Neonatal intramuscular injection with recombinant adeno-associated virus results in prolonged beta-glucuronidase expression in situ and correction of liver pathology in mucopolysaccharidosis type VII mice. *Hum. Gene Ther.*, 10: 85–94.
- Daly, T.M., Vogler, C., Levy, B., Haskins, M.E. and Sands, M.S. (1999b) Neonatal gene transfer leads to widespread correction of pathology in a murine model of lysosomal storage disease. *Proc. Natl. Acad. Sci. USA*, 96: 2296–2300.
- Davidson, B.L., Brooks, A.I., Stein, C.S., Heth, J.A., Dubernsky, T.W., Sauter, S.L., Cory-Slechta, D.A. and Federoff, H.J. (2000) Correction of cellular pathology and behavioral deficits in adult b-glucuronidase-deficient mice after FIV vector-mediated gene transfer to brain. *Mol. Ther.*, 1: A688.
- Dawson, G. and Cho, S. (2000) Batten's disease: clues to neuronal protein catabolism in lysosomes. *J. Neurosci. Res.*, 60: 133–140.
- Dhar, S., Bitting, R.L., Rylova, S.N., Jansen, P.J., Lockhart, E., Koeberl, D.D., Amalfitano, A. and Boustany, R.M. (2002) Flupirtine blocks apoptosis in batten patient lymphoblasts and in human postmitotic CLN3- and CLN2-deficient neurons. *Ann. Neurol.*, 51: 448–466.
- During, M.J., Kaplitt, M.G., Stern, M.B. and Eidelberg, D. (2001) Subthalamic GAD gene transfer in Parkinson disease patients who are candidates for deep brain stimulation. *Hum. Gene Ther.*, 12: 1589–1591.
- Elliger, S.S., Elliger, C.A., Aguilar, C.P., Raju, N.R. and Watson, G.L. (1999) Elimination of lysosomal storage in brains of MPS VII mice treated by intrathecal administration of an adeno-associated virus vector. *Gene Ther.*, 6: 1175–1178.
- Ezaki, J., Tanida, I., Kanehagi, N. and Kominami, E. (1999) A lysosomal proteinase, the late infantile neuronal ceroid lipofuscinosis gene (CLN2) product, is essential for degradation of a hydrophobic protein, the subunit c of ATP synthase. *J. Neurochem.*, 72: 2573–2582.
- Flotte, T.R. (2004) Immune responses to recombinant adeno-associated virus vectors: putting preclinical findings into perspective. *Hum. Gene Ther.*, 15: 716–717.
- Frisella, W.A., O'Connor, L.H., Vogler, C.A., Roberts, M., Walkley, S., Levy, B., Daly, T.M. and Sands, M.S. (2001) Intracranial injection of recombinant adeno-associated virus improves cognitive function in a murine model of mucopolysaccharidosis type VII. *Mol. Ther.*, 3: 351–358.
- Gao, G., Leberer, C., Weiner, D.J., Grant, R., Calcedo, R., McCullough, B., Bagg, A., Zhang, Y. and Wilson, J.M. (2004) Erythropoietin gene therapy leads to autoimmune anemia in macaques. *Blood*, 103: 3300–3302.
- Grimm, D., Kern, A., Rittner, K. and Kleinschmidt, J.A. (1998) Novel tools for production and purification of recombinant adeno-associated virus vectors. *Hum. Gene Ther.*, 9: 2745–2760.
- Goebel, H.H., Mole, S.E. and Lake, B.D. (1999) *The Neuronal Ceroid Lipofuscinoses (Batten Disease)*. IOS Press, Amsterdam.
- Hackett, N.R. and Crystal, R.G. (2000) Adenovirus vectors for gene therapy. In: Smyth Timpelton N. and Lasic D.D., (Eds.), *Gene Therapy*. Marcel Dekker, New York, pp. 17–40.
- Haltia, M. (2003) The neuronal ceroid-lipofuscinoses. *J. Neuro-pathol. Exp. Neurol.*, 62: 1–13.
- Harvey, B.-G., Maroni, J., O'Donoghue, K.A., Chu, K.W., Muscat, J.C., Pippo, A.L., Wright, C.E., Hollmann, C., Wisnivesky, J.P., Kessler, P., Rasmussen, H., Rosengart, T.K. and Crystal, R.G. (2002) Safety of local delivery of low and intermediate dose adenovirus gene transfer vectors to individuals with a spectrum of comorbid conditions. *Hum. Gene Ther.*, 13: 15–63.
- Haskell, R.E., Hughes, S.M., Chiorini, J.A., Alisky, J.M. and Davidson, B.L. (2003) Viral-mediated delivery of the late-infantile neuronal ceroid lipofuscinosis gene, TPP-I to the mouse central nervous system. *Gene Ther.* 10: 34–42.
- Herzog, R.W., Fields, P.A., Arruda, V.R., Brubaker, J.O., Armstrong, E., McClintock, D., Bellinger, D.A., Couto, L.B., Nichols, T.C. and High, K.A. (2002) Influence of vector dose on factor IX-specific T and B cell responses in muscle-directed gene therapy. *Hum. Gene Ther.*, 13: 1281–1291.
- Ioannou, Y.A., Zeidner, K.M., Gordon, R.E. and Desnick, R.J. (2001) Fabry disease: preclinical studies demonstrate the effectiveness of alpha-galactosidase. A replacement in enzyme-deficient mice. *Am. J. Hum. Genet.*, 68: 14–25.

- Janson, C., McPhee, S., Bilaniuk, L., Haselgrove, J., Testaiuti, M., Freese, A., Wang, D.J., Shera, D., Hurh, P., Rupin, J., Saslow, E., Goldfarb, O., Goldberg, M., Larijani, G., Sharrar, W., Liouterman, L., Camp, A., Kolodny, E., Samulski, J. and Leone, P. (2002) Clinical protocol. Gene therapy of Canavan disease: AAV-2 vector for neurosurgical delivery of aspartoacylase gene (ASPA) to the human brain. *Hum. Gene Ther.*, 13: 1391-1412.
- Jarvela, I., Autti, T., Lamminranta, S., Aberg, L., Raininko, R. and Santavuori, P. (1997) Clinical and magnetic resonance imaging findings in Batten disease: analysis of the major mutation (1.02-kb deletion). *Ann. Neurol.*, 42: 799-802.
- Kaspar, B.K., Erickson, D., Schaffer, D., Hinh, L., Gage, F.H. and Peterson, D.A. (2002) Targeted retrograde gene delivery for neuronal protection. *Mol. Ther.*, 5: 50-56.
- Kho, S.T., Pettis, R.M., Mhatre, A.N. and Lalwani, A.K. (2000) Safety of adeno-associated virus as cochlear gene transfer vector: analysis of distant spread beyond injected cochlea. *Mol. Ther.*, 2: 368-373.
- Kniessel, U. and Wolburg, H. (2000) Tight junctions of the blood-brain barrier. *Cell. Mol. Neurobiol.*, 20: 57-76.
- Kurachi, Y., Oka, A., Mizuguchi, M., Ohkoshi, Y., Sasaki, M., Itoh, M., Hayashi, M., Goto, Y. and Takashima, S. (2000) Rapid immunologic diagnosis of classic late infantile neuronal ceroid lipofuscinosis. *Neurology*, 54: 1676-1680.
- Lane, S.C., Jolly, R.D., Schmechel, D.E., Alroy, J. and Boustany, R.M. (1996) Apoptosis as the mechanism of neurodegeneration in Batten's disease. *J. Neurochem.*, 67: 677-683.
- Lin, L. and Lobel, P. (2001) Production and characterization of recombinant human CLN2 protein for enzyme-replacement therapy in late infantile neuronal ceroid lipofuscinosis. *Biochem. J.*, 357: 49-55.
- Lin, L., Sohar, I., Lackland, H. and Lobel, P. (2001) The human CLN2 protein/tripeptidyl-peptidase I is a serine protease that autoactivates at acidic pH. *J. Biol. Chem.*, 276: 2249-2255.
- Mastakov, M.Y., Baer, K., Kotin, R.M. and During, M.J. (2002a) Recombinant adeno-associated virus serotypes 2- and 5-mediated gene transfer in the mammalian brain: quantitative analysis of heparin co-infusion. *Mol. Ther.*, 5: 371-380.
- Mastakov, M.Y., Baer, K., Symes, C.W., Leichtlein, C.B., Kotin, R.M. and During, M.J. (2002b) Immunological aspects of recombinant adeno-associated virus delivery to the mammalian brain. *J. Virol.*, 76: 8446-8454.
- Mole, S.E. (1999) Batten's disease: eight genes and still counting? *Lancet*, 354: 443-445.
- Monahan, P.E., Jooss, K. and Sands, M.S. (2002) Safety of adeno-associated virus gene therapy vectors: a current evaluation. *Expert Opin. Drug Safety*, 1: 79-91.
- Nguyen, J.B., Sanchez-Pernaute, R., Cunningham, J. and Bankiewicz, K.S. (2001) Convection-enhanced delivery of AAV-2 combined with heparin increases TK gene transfer in the rat brain. *Neuroreport*, 12: 1961-1964.
- Niwa, H., Yamamura, K. and Miyazaki, J. (1991) Efficient selection for high-expression transfectants with a novel eukaryotic vector. *Gene*, 108: 193-199.
- Pachori, A.S., Melo, L.G., Zhang, L., Loda, M., Pratt, R.E. and Dzau, V.J. (2004) Potential for germ line transmission after intramyocardial gene delivery by adeno-associated virus. *Biochem. Biophys. Res. Commun.*, 313: 528-533.
- Palmer, D.N., Fearnley, I.M., Walker, J.E., Hall, N.A., Lake, B.D., Wolfe, L.S., Haltia, M., Martinus, R.D. and Jolly, R.D. (1992) Mitochondrial ATP synthase subunit c storage in the ceroid-lipofuscinoses (Batten disease). *Am. J. Med. Genet.*, 42: 561-567.
- Passini, M.A., Lee, E.B., Heuer, G.G. and Wolfe, J.H. (2002) Distribution of a lysosomal enzyme in the adult brain by axonal transport and by cells of the rostral migratory stream. *J. Neurosci.*, 22: 6437-6446.
- Qui, J.P., Mendez, B.S., Crystal, R.G. and Hackett, N.R. (2002) Construction and verification of an Ad/AAV helper plasmid designed for manufacturing recombinant AAV vectors for human administration. *Mol. Ther.*, 5: S47-S48.
- Seitz, D., Grodd, W., Schwab, A., Seeger, U., Klose, U. and Nagele, T. (1998) MR imaging and localized proton MR spectroscopy in late infantile neuronal ceroid lipofuscinosis. *Am. J. Neuroradiol.*, 19: 1373-1377.
- Sferra, T.J., Qu, G., McNeely, D., Rennard, R., Clark, K.R., Lo, W.D. and Johnson, P.R. (2000) Recombinant adeno-associated virus-mediated correction of lysosomal storage within the central nervous system of the adult mucopolysaccharidosis type VII mouse. *Hum. Gene Ther.*, 11: 507-519.
- Skorupa, A.F., Fisher, K.J., Wilson, J.M., Parente, M.K. and Wolfe, J.H. (1999) Sustained production of beta-glucuronidase from localized sites after AAV vector gene transfer results in widespread distribution of enzyme and reversal of lysosomal storage lesions in a large volume of brain in mucopolysaccharidosis VII mice. *Exp. Neurol.*, 160: 17-27.
- Sleat, D.E., Donnelly, R.J., Lackland, H., Liu, C.G., Sohar, I., Pullarkat, R.K. and Lobel, P. (1997) Association of mutations in a lysosomal protein with classical late-infantile neuronal ceroid lipofuscinosis. *Science*, 277: 1802-1805.
- Sleat, D.E., Gin, R.M., Sohar, I., Wisniewski, K., Sklower-Brooks, S., Pullarkat, R.K., Palmer, D.N., Lerner, T.J., Boustany, R.M., Uldall, P., Siakotos, A.N., Donnelly, R.J. and Lobel, P. (1999) Mutational analysis of the defective protease in classic late-infantile neuronal ceroid lipofuscinosis, a neurodegenerative lysosomal storage disorder. *Am. J. Hum. Genet.*, 64: 1511-1523.
- Sleat, D.E., Wiseman, J.A., El Banna, M., Kim, K.H., Mao, Q., Price, S., Macauley, S.L., Sidman, R.L., Shen, M.M., Zhao, Q., Passini, M.A., Davidson, B.L., Stewart, G.R. and Lobel, P. (2004) A mouse model of classical late-infantile neuronal ceroid lipofuscinosis based on targeted disruption of the CLN2 gene results in a loss of tripeptidyl-peptidase I activity and progressive neurodegeneration. *J. Neurosci.*, 24: 9117-9126.
- Smith, J.G., Raper, S.E., Wheeldon, E.B., Hackney, D., Judy, K., Wilson, J.M. and Eck, S.L. (1997) Intracranial administration of adenovirus expressing HSV-TK in combination with ganciclovir produces a dose-dependent, self-limiting inflammatory response. *Hum. Gene Ther.*, 8: 943-954.
- Sondhi, D., Hackett, N.R., Apblett, R.L., Kaminsky, S.M., Pergolizzi, R.G. and Crystal, R.G. (2001) Feasibility of gene therapy for late neuronal ceroid lipofuscinosis. *Arch. Neurol.*, 58: 1793-1798.
- Sondhi, D., Peterson, D.A., Giannaris, E.L., Sanders, C.T., Mendez, B.S., Bishnu, D., Rostkowski, A., Blanchard, B., Bjugstad, K., Sladek, J.R.J., Redmond, D.E., Leopold, P.L., Kaminsky, S.M., Hackett, N.R. and Crystal, R.G. (2005) AAV2-mediated CLN2 gene transfer to rodent and non-human primate brain results in long-term TPP-I expression compatible with therapy for LINCL. *Gene Ther.*, 12: doi: 10.1038/sj.gt.3302549.
- Song, S., Scott-Jorgensen, M., Wang, J., Poirier, A., Crawford, J., Campbell-Thompson, M. and Flotte, T.R. (2002) Intramuscular administration of recombinant adeno-associated virus 2 alpha-1 antitrypsin (rAAV-SERPINA1) vectors in a nonhuman primate model: safety and immunologic aspects. *Mol. Ther.*, 6: 329-335.
- Stein, C.S., Ghodsi, A., Derksen, T. and Davidson, B.L. (1999) Systemic and central nervous system correction of lysosomal storage in mucopolysaccharidosis type VII mice. *J. Virol.*, 73: 3424-3429.

- Steinfeld, R., Heim, P., von Gregory, H., Meyer, K., Ullrich, K., Goebel, H.H. and Kohlschutter, A. (2002) Late infantile neuronal ceroid lipofuscinosis: quantitative description of the clinical course in patients with CLN2 mutations. *Am. J. Med. Genet.*, 112: 347–354.
- Turner, C.T., Hopwood, J.J. and Brooks, D.A. (2000) Enzyme replacement therapy in mucopolysaccharidosis I: altered distribution and targeting of alpha-L-iduronidase in immunized rats. *Mol. Genet. Metab.*, 69: 277–285.
- Umehara, F., Higuchi, I., Tanaka, K., Niiyama, T., Ezaki, J., Kominami, E. and Osame, M. (1997) Accumulation of mitochondrial ATP synthase subunit c in muscle in a patient with neuronal ceroid lipofuscinosis (late infantile form). *Acta Neuropathol.*, 93: 628–632.
- Vanhänen, S.L., Puranen, J., Autti, T., Raininko, R., Liewendahl, K., Nikkinen, P., Santavuori, P., Suominen, P., Vuori, K. and Hakkinen, A.M. (2004) Neuroradiological findings (MRS, MRI, SPECT) in infantile neuronal ceroid-lipofuscinosis (infantile CLN1) at different stages of the disease. *Neuropediatrics*, 35: 27–35.
- Williams, R.E., Gottlob, I., Lake, B.D., Goebel, H.H., Winchester, B.G. and Wheeler, R.B., CLN 2. (1999) Classic late infantile NCL. In: Goebel H.H., Mole S.E. and Lake B.D., (Eds.), *The Neuronal Ceroid Lipofuscinoses (Batten Disease)*. IOS Press, Amsterdam, pp. 37–55.
- Wisniewski, K.E., Kida, E., Golabek, A.A., Kaczmarek, W., Connell, F. and Zhong, N. (2001a) Neuronal ceroid lipofuscinoses: classification and diagnosis. *Adv. Genet.*, 45: 1–34.
- Wisniewski K. and Zhong N. (Eds.) (2001) *Batten Disease: Diagnosis, Treatment and Research*. Academic Press, New York.
- Wisniewski, K.E., Zhong, N. and Philippart, M. (2001b) Pheno/genotypic correlations of neuronal ceroid lipofuscinoses. *Neurology*, 57: 576–581.
- Zolotukhin, S., Byrne, B.J., Mason, E., Zolotukhin, I., Potter, M., Chesnut, K., Summerford, C., Samulski, R.J. and Muzyczka, N. (1999) Recombinant adeno-associated virus purification using novel methods improves infectious titer and yield. *Gene Ther.*, 6: 973–985.

Safety of Direct Administration of AAV2_{CU}hCLN2, a Candidate Treatment for the Central Nervous System Manifestations of Late Infantile Neuronal Ceroid Lipofuscinosis, to the Brain of Rats and Nonhuman Primates

NEIL R. HACKETT,^{1,2,*} D. EUGENE REDMOND,^{3,4,*} DOLAN SONDHI,² E. LELA GIANNARIS,¹ ELIZABETH VASSALLO,¹ JAMIE STRATTON,¹ JIANPING QIU,¹ STEPHEN M. KAMINSKY,¹ MARTIN L. LESSER,⁵ GENE S. FISCH,⁵ SERGE D. ROUELLE,⁶ and RONALD G. CRYSTAL^{1,2}

ABSTRACT

Late infantile neuronal ceroid lipofuscinosis (LINCL), a pediatric autosomal recessive neurodegenerative lysosomal storage disorder, results from mutations in the CLN2 gene and consequent deficiency in tripeptidyl-peptidase I (TPP-I) and progressive destruction of neurons. We have previously demonstrated that CNS gene transfer of AAV2_{CU}hCLN2 (an AAV2-based vector expressing the human CLN2 cDNA) in rats and nonhuman primates mediates long-term TPP-I expression in the CNS neurons [Sondhi, D., Peterson, D.A., Giannaris, E.L., Sanders, C.T., Mendez, B.S., De, B., Rostkowski, A., Blancard, B., Bjugstad, K., Sladek, J.R., Redmond, D.E., Leopold, P.L., Kaminsky, S.M., Hackett, N.R., and Crystal, R.G. (2005). *Gene Ther.* 12, 1618–1632]. The present study tests the hypothesis that direct CNS administration of a clinical-grade AAV2_{CU}hCLN2 vector to the CNS of rats and nonhuman primates at doses scalable to humans has a long-term safety profile acceptable for initiating clinical trials. Fischer 344 rats were injected bilaterally via the striatum with 2×10^{10} particle units (PU) of AAV2_{CU}hCLN2, using saline as a control. At 13, 26, and 52 weeks, vector and phosphate-buffered saline-injected rats were killed ($n = 6$ per time point), and blood, brain, and distant organs were assessed. There were no biologically significant differences between control and vector groups for complete blood count, serum chemistry, and neutralizing anti-AAV2 antibody levels. CNS administration of AAV2_{CU}hCLN2 did not result in any pathological changes in the brain that were attributable to the vector, although microscopic changes were observed along the track consistent with needle trauma. A total dose of 3.6×10^{10} or 3.6×10^{11} PU of AAV2_{CU}hCLN2 was administered to the CNS of African Green monkeys at 12 locations, targeting the caudate nucleus, hippocampus, and overlying cortices. Monkeys ($n = 3$ at each dose) were killed 1, 13, 26, or 52 weeks after injection. Controls included sham-injected, saline-injected, and AAV2_{CU}Null-injected (3.6×10^{11} PU) monkeys. There were no biologically significant differences among vector-injected and control groups in any parameter of the general assessment, complete blood count, or serum chemistry assessed at multiple time points after vector administration. Importantly, no abnormal behavior was observed in any group in videotaped neurological assessment, where behaviors were quantified before administration and at multiple time points afterward. Histopathological examination of the CNS demonstrated that 1 week after administration, AAV2_{CU}hCLN2 produced transient minor white matter edema with reactive glial cells in the corona radiata of the cerebrum along the injection track and in the surrounding white matter. This abnormality was not observed at 13, 26, or 52 weeks. Together with the long-term gene expression after gene transfer, these findings supported the initiation of clinical trials to assess the safety of AAV2_{CU}hCLN2 administration to individuals with LINCL.

¹Belfer Gene Therapy Core Facility, Weill Medical College of Cornell University, New York, NY 10021.

²Department of Genetic Medicine, Weill Medical College of Cornell University, New York, NY 10021.

³Department of Psychiatry and Surgery, Yale University, New Haven, CT 06520.

⁴Axion Research Foundation, Hamden, CT 06517.

⁵Biostatistics Unit, North Shore/Long Island Jewish Institute for Medical Research, Manhasset, NY 11030.

⁶Pathology Associates Division, Charles River Laboratories, Frederick, MD 21701.

*N.R.H. and D.E.R. contributed equally to this paper.

INTRODUCTION

LATE INFANTILE NEURONAL CEROID LIPOFUSCINOSIS (LINCL) is a fatal autosomal recessive disorder resulting from mutations in the CLN2 gene and consequent deficiency in its product tripeptidyl-peptidase I (TPP-I) (Sleat *et al.*, 1997; Williams *et al.*, 1999; Haltia, 2003). In the central nervous system (CNS), TPP-I deficiency results in accumulation of membrane proteins in lysosomes, leading to a loss of neurons and causing progressive neurological decline (Palmer *et al.*, 1992; Umehara *et al.*, 1997; Ezaki *et al.*, 1999; Vines and Warburton, 1999). The prevalence of the disease is low, with approximately 200 known cases in the United States. The symptoms begin at approximately 3 years of age with seizures, ataxia, impaired vision, and speech and developmental regression. A gradual decline follows and afflicted children generally become wheelchair bound by 4 to 6 years, with death occurring by ages 8 to 12 years (Sleat *et al.*, 1997; Haltia, 2003). At a morphologic level, the disease is characterized by CNS atrophy, with progressive loss of neurons and retinal cells (Boustany, 1996; Sleat *et al.*, 1997; Birch, 1999; Haltia, 2003). There is no treatment for LINCL other than symptom management.

In the absence of any available treatment for LINCL, we have developed a program using adeno-associated virus (AAV) gene transfer vectors to deliver the normal human CLN2 cDNA to neurons to provide persistent expression of TPP-I to halt the neurodegeneration that characterizes the disease. LINCL has several features that make it a good candidate for gene therapy (Sondhi *et al.*, 2001). In addition to being a classic autosomal recessive disorder caused by mutations in a single gene, comparisons of genotype and phenotype suggest that TPP-I levels that are 5 to 10% of normal should be sufficient to significantly delay mortality (Sleat *et al.*, 1999). Importantly, like other lysosomal proteins, a fraction of the newly synthesized precursor to TPP-I is secreted and is taken up by neighboring cells by cross-correction via the mannose 6-phosphate receptor pathway (Lin *et al.*, 2001; Haskell *et al.*, 2003). This is an advantage for gene therapy, in that it is not necessary to transfer the normal CLN2 cDNA to all of the cells in the brain, effectively leveraging gene transfer to improve TPP-I distribution beyond the range of vector diffusion.

In prior studies, we have demonstrated that CNS administration to the rat brain of 10^{10} particle units (PU) of a gene transfer vector based on AAV2 expressing the human cDNA for CLN2 (AAV2_{CU}hCLN2) results in local TPP-I activity that is 55% over the endogenous background (Sondhi *et al.*, 2005). If spread over the whole brain, this would correspond to levels of ~5% of the endogenous level, a level that should be therapeutic on the basis of genotype/phenotype correlations (Sleat *et al.*, 1999). TPP-I-positive neurons were seen in regions of the brain distant from the injection site, at locations consistent with axonal transport of vector or TPP-I enzyme. Finally, TPP-I was observed to persist in the rat and nonhuman primate brain after gene transfer. Together, these observations established the feasibility of effective gene transfer to the human brain, using an AAV2 vector with prospects for a therapeutic level of TPP-I.

The objective of the present study was to assess the hypothesis that administration of therapeutic doses of a clinical-grade AAV2_{CU}hCLN2 vector to the CNS of rodents and non-human primates will have minimal vector-related toxicity,

acceptable for moving to human trials. The toxicology studies were designed with input from the Center for Biologics Evaluation and Research, Food and Drug Administration (Rockville, MD), to assess short- and long-term effects of AAV2_{CU}hCLN2 administration using a clinical-grade AAV2_{CU}hCLN2 vector produced under Good Manufacturing Practice (GMP) conditions. The data show that clinical-grade AAV2_{CU}hCLN2 can be administered to rats and nonhuman primates with no significant side effects attributable to the vector.

MATERIALS AND METHODS

Gene transfer vectors

The genome of AAV2_{CU}hCLN2 includes the inverted terminal repeats (ITR) from AAV2 surrounding the expression cassette (Crystal *et al.*, 2004; Sondhi *et al.*, 2005). The expression cassette includes the CAG promoter (consisting of the human cytomegalovirus immediate-early enhancer, the splice donor and the left-hand intron sequence from chicken β -actin, the splice acceptor from rabbit β -globin) (Niwa *et al.*, 1991; Daly *et al.*, 1999a,b), the human CLN2 cDNA with an optimized Kozak translational initiation signal before the start codon, and a rabbit β -globin poly(A) sequence. The AAV2_{CU} Null control vector is identical to AAV2_{CU}hCLN2 except that the CAG promoter drives transcription of an untranslatable DNA sequence corresponding to intron 5 of the human vascular endothelial growth factor gene to match the size of human CLN2 cDNA (Sondhi *et al.*, 2005).

Both of the recombinant AAV2 vectors were produced under GMP conditions by cotransfection of 293 cells in a 10-stack Nunclon Δ Cell Factory (Nalge Nunc International, Rochester, NY) with 500 μ g of an expression cassette plasmid (pAAV2-CAG-hCLN2) carrying the human CLN2 cDNA or an expression plasmid carrying irrelevant sequence to be used as control (p-AAV2-CAG-Null) and 1 mg of an adenovirus/AAV2 helper plasmid (pPAK-MA2), using PolyFect reagent (Qiagen Sciences, Germantown, MD) (Fig. 1). At 72 hr posttransfection, the cells were harvested ($1150 \times g$, 15 min) and a crude viral lysate (CVL) was made by three cycles of freeze-thawing. Cellular DNA was digested with Benzoase (50 U/ml; Sigma-Aldrich, St. Louis, MO) and the CVL was cleared by centrifugation at $3300 \times g$ for 20 min and applied to a discontinuous iodixanol gradient followed by affinity chromatography on heparin-agarose.

Vector concentration in particle units was determined by anti-capsid ELISA (RDI Division of Fitzgerald Industries, Concord, MA). To validate the function of the AAV2_{CU}hCLN2 preparations, *in vitro* gene transfer was assessed by measurement of tripeptidyl-peptidase I enzymatic activity after infection of 293-ORF6 cells with AAV2_{CU}hCLN2 (Brough *et al.*, 1996; Lin and Lobel, 2001). All vectors used in the toxicology studies were shown to be sterile by growth for 14 days on medium supporting the growth of aerobic bacteria, anaerobic bacteria, or fungi; endotoxin free to a level of <20 U of endotoxin per milliliter by the Endosafe method (Charles River, Charleston, SC); and uncontaminated by mycoplasma to a level of <1000/ml, using a quantitative polymerase chain reaction assay (AppTec Laboratory Services, Camden, NJ).

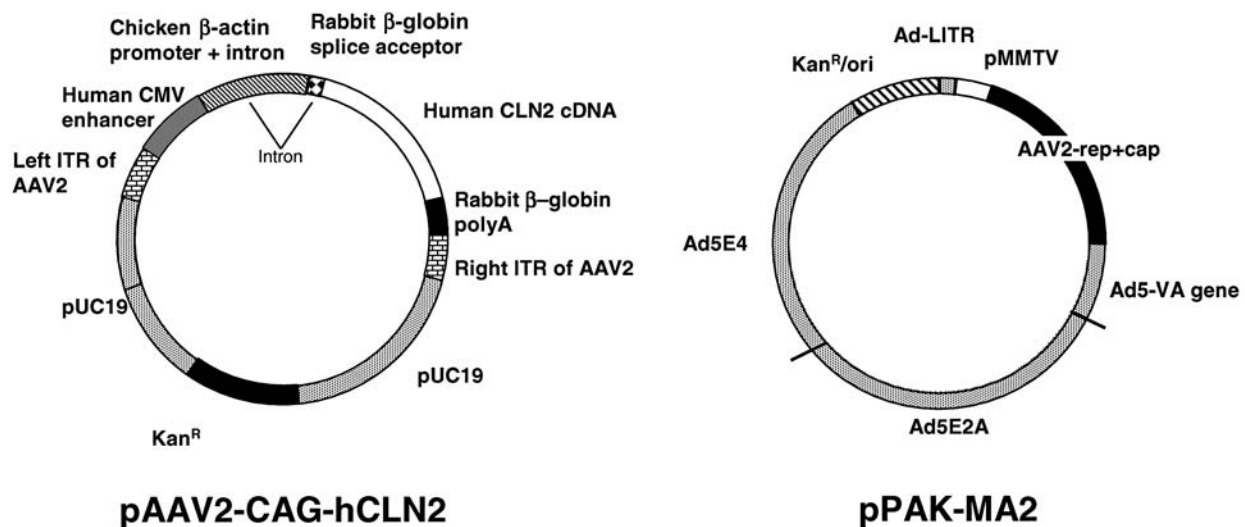


FIG. 1. Structure of the plasmids used for GMP AAV2_{CU}hCLN2 vector production. The AAV2_{CU}hCLN2 vector is made by cotransfection of 293 cells with the two plasmids, shown schematically. The expression plasmid pAAV2-CAG-hCLN2 is a pUC19 derivative with the ampicillin resistance gene deleted and replaced by a kanamycin resistance gene. Within that backbone is the genome of AAV2_{CU}hCLN2, consisting of the two inverted terminal repeats of AAV2 (ITRs, nucleotides 1–145 and 4531–4675 of GenBank J01901) surrounding an expression cassette composed of the human cytomegalovirus (CMV) enhancer (nucleotides 558–925 of GenBank x03922), the chicken β -actin promoter/splice donor and intron (nucleotides 268–1530 of GenBank x00182), the splice acceptor of the rabbit β -globin intron (nucleotides 1457–1551 of GenBank J00659), the human cDNA for CLN2 with an optimized Kozak translation initiation signal (nucleotides 13–1704 of GenBank BC014863), and the polyadenylation/transcription stop from rabbit β -globin (nucleotides 1546–1827 of GenBank J00659). The helper plasmid pPAK-MA2 is also based on a kanamycin resistance replicon and contains the VA gene (nucleotides 9856 to 11548 of GenBank M73260) and E2A and E4 genes (nucleotides 21438–35935) of Ad serotype 5. Expression of the AAV2 *rep* gene is driven by a mouse mammary tumor virus (MMTV) promoter (nucleotides 583–1325 of GenBank AF228552) and expression of the AAV2 *cap* gene is driven by the endogenous p40 promoter of AAV2.

Rat toxicology studies

Administration and monitoring. Fischer 344 rats (160 to 200 g; Taconic, Germantown, NY) were deeply anesthetized and positioned in a stereotaxic frame (model 310; Stoelting, Wood Dale, IL). The skull was exposed through a cranial midline incision, the location of bregma was recorded, and the desired coordinates for the left (A/P, +0.06 cm; M/L, +0.28 cm) and right (A/P, +0.06 cm; M/L, –0.28 cm) striata were calculated. The needle of the injection syringe, preloaded with vector or vehicle, was sequentially adjusted to the desired location on each side and the skull was marked. A hole was then drilled in the skull at each of the marked positions, using a MultiPro drill (model 395 T6; Dremel, Mount Prospect, IL) with a 0.8-mm carbide burr (AH62-0030; Harvard Apparatus, Holliston, MA). The stereotaxic frame arm was then returned to the position of the left striatum and locked in place, and the needle was slowly lowered into the burr hole until the opening of the beveled needle was aligned with the skull. This coordinate was marked as the dorsal/ventral (D/V) reference location, and from this the desired D/V coordinates for the left and right striata were calculated (D/V, –0.52 cm from dura). Next, the needle was lowered extremely slowly to the adjusted D/V coordinate for the left striatum. After 1 min, the injection pump was started for the injection of vector (AAV2_{CU}hCLN2 at 2×10^{12} PU/ml) or phosphate-buffered saline (PBS) into the left striatum at 0.2 μ l/min for 25 min. The needle was left in place for 2 min after the in-

jection and then retracted slowly; the process was repeated for the right striatum. The incision site was sutured in one layer, using 4.0 Polysorb sutures, and the rat was removed from the stereotaxic frame. The animals were monitored while recovering from anesthesia and checked twice daily for the first 2 days. Subsequently, the health status of all rats was checked three times weekly and recorded on health monitoring forms. Any abnormalities were monitored with the assistance of the veterinary staff of the Research Animal Resource Center of Weill-Cornell (New York, NY).

Necropsy. Thirteen, 26, and 52 weeks after vector administration, three male and three female rats each from vehicle and vector groups were killed (Table 1). The rats were deeply anesthetized via an intraperitoneal injection of sodium pentobarbital, and the body surface and all orifices were inspected and any external abnormalities were noted. The abdomen and thorax were exposed and 2.5–3.0 ml of blood was collected via cardiac puncture for complete blood count, complete chemistry profile (both performed by Antech Diagnostics, Southaven, MS), and anti-AAV neutralizing antibodies (see below). The pulmonary arteries and descending aorta were clamped. An incision was made in the left ventricle and a blunted catheter was guided through the incision and into the aorta, permitting perfusion with 200 ml of PBS at a flow rate of 6 ml/min. During the perfusion, the abdomen and thorax were inspected for the presence of tumors and the testes or ovaries, spleen, liver, kid-

TABLE 1. EVALUATION OF TOXICOLOGY OF DIRECT CNS ADMINISTRATION OF AAV2_{CU}hCLN2 TO THE RAT^a

Parameter	Time of assessment (weeks after vector administration)			
	0	13	26	52
Vector/vehicle administration ^b	✓			
Postmortem ^c				
Complete blood count ^d		✓	✓	✓
Chemistry ^e		✓	✓	✓
Anti-AAV antibodies ^f		✓	✓	✓
Weight and organ weight		✓	✓	✓
Histopathology ^g		✓	✓	✓

^aThe schedule for injection of study drug and subsequent assessment is shown.

^bVector (or PBS vehicle) was administered on day 0 at a total dose of 2×10^{10} particle units, 5 μ l each into the left and right striatum.

^cAll assessments were performed at time of sacrifice on 12 rats at each time point, 6 treated with vector and 6 treated with PBS, $n = 3$ male and $n = 3$ female in each group. Blood was collected by heart puncture.

^dCBC (hematocrit, hemoglobin, WBC, RBC, differential, platelets).

^eComprehensive chemistry (albumin, alkaline phosphatase, alanine aminotransferase, aspartate aminotransferase, blood urea nitrogen, calcium, chloride, cholesterol, creatine phosphokinase, creatinine, globulin, glucose, phosphorus, potassium, sodium, total bilirubin, total protein).

^fSerum was collected at sacrifice for anti-AAV2 neutralizing antibody assay.

^gRats were perfused with cold PBS and internal organs were examined. The brain, liver, lung, kidney, heart, spleen, gonads, and quadriceps were excised and weighed and one piece was submerged in paraformaldehyde for routine histopathology.

ney, quadriceps, and any abnormal organs were examined, removed, and weighed and portions of each organ were placed in chilled 4% paraformaldehyde. The rats were then further perfused with 200 ml of chilled 4% paraformaldehyde. After the perfusion was completed, the heart, lung, and brain were removed, weighed, and preserved in 4% paraformaldehyde. Organ samples for histology were stored at 4°C for 72 hr, at which time they were transferred to 30% sucrose in 0.1 M phosphate buffer, pH 7.4.

Histopathology. The brains and organs were shipped to Pathology Associates (Division of Charles River Laboratories, Frederick, MD) for histopathology. The brains were trimmed in a rat brain matrix every 4 mm, generating eight coronal sections regularly distributed throughout the brain and embedded in paraffin. All blocks were sectioned once at 5 μ m except for the block containing the injection site in the striatum, which was sectioned 10 times at 5 μ m in a stepwise fashion. All other organs were trimmed once and embedded in paraffin and 5- μ m sections were cut. All slides were stained with hematoxylin and eosin for microscopic evaluation in a blinded fashion by a

board-certified veterinary pathologist. The results were unblinded after the evaluation was complete and the key was provided.

Anti-AAV2 neutralizing antibody. Anti-AAV2 neutralizing antibody titers were assessed by mixing serial 2-fold dilutions of serum, starting at a 1:10 dilution, with 2×10^8 PU of AAV2LacZ for 30 min at 37°C. The mixture was then used to infect 293-ORF6 cells in a 96-well plate (Brough *et al.*, 1996). After growth for 48 hr, a cell lysate was made and the β -galactosidase activity was determined. The reciprocal dilution required for 50% inhibition of infection was interpolated. In all assays, positive control serum from a normal human was included and the assay was accepted only if the reciprocal titer for that serum was 200 ± 50 .

African green monkey toxicology studies

Administration and monitoring. African green monkeys (*Cercopithecus aethiops sabaeus*, male, 4.0 to 6.5 kg, feral, estimated age of 5 to 10 years) were used for these experiments. Each nonhuman primate received intracranial administration of a total dose of 3.6×10^{10} PU (low dose) or 3.6×10^{11} PU (high dose) of the AAV2_{CU}hCLN2 vector or 3.6×10^{11} PU of the AAV2_{CU}Null control vector or PBS at 1 μ l/min for a total volume of 180 μ l (15 μ l at each of 12 locations; Table 2). An additional control was sham-injected animals, which involved insertion of the injection needle into all locations but no administration. Six burr holes (three symmetrical holes per hemisphere) were drilled through the skull of anesthetized monkeys, followed by the lowering of the syringe sequentially to two defined depths per burr hole for injection of vector or vehicle. Injections were made to the head of the caudate nucleus and overlying the cerebral cortex (16.2 mm apart), the body of the caudate nucleus and the overlying cerebral cortex (19.2 mm apart), and the hippocampal formation and overlying cerebral cortex (31.2 mm apart).

Monkeys were anesthetized with pentobarbital (25 mg/kg, intravenous) and the heads were shaved. Preoperatively, each monkey received (intramuscularly) atropine (0.5 mg), long-acting penicillin (600,000 units), and iron dextran (150 mg). An intravenous line was inserted with 0.9% saline infusion. An endotracheal tube was inserted and monkeys were monitored continually and received assisted ventilation if required. The animal was first set up in the stereotaxic head holder and midline incisions were made and the muscles retracted to each side. Precise holes were drilled at the six stereotaxic points of entry, using a Foreman high-speed drill with a diamond ball bit. A stereotaxic carrier containing a Stoelting microsyringe injector with a Hamilton 710 series 100- μ l syringe and a replaceable 2-in., 22-gauge beveled needle was attached to the stereotaxic frame. Ninety microliters of the appropriate vector or PBS was then drawn up into the chamber. Cortical injections were made first and then the cannula was lowered to the site of the caudate or hippocampus. After each injection was made at a rate of 1 μ l/min, 2 min was allowed to elapse before the cannula was withdrawn slowly and repositioned for the next injection. The syringe was refilled once with 90 μ l to inject all 12 sites sequentially. After the final injections, the wound was closed by approximating the muscle layers with chromic suture, clo-

TABLE 2. PARAMETERS AND TIME OF ASSESSMENT FOR NONHUMAN PRIMATE TOXICOLOGY EVALUATION OF DIRECT ADMINISTRATION OF AAV2_{CU}hCLN2^a

Parameter	Time of assessment (days after vector administration) ^b									
	Pre	0	3	7	14	28	56	91	180	360
General safety										
Body temperature	✓	✓	✓	✓	✓	✓	✓	✓	✓	✓
Vital signs ^c	✓	✓	✓	✓	✓	✓	✓	✓	✓	✓
Weight	✓	✓	✓	✓	✓	✓	✓	✓	✓	✓
Hematology										
CBC ^d	✓	✓	✓	✓	✓	✓	✓	✓	✓	✓
Chemistry ^e	✓	✓	✓	✓	✓	✓	✓	✓	✓	✓
Anti-AAV antibodies	✓	✓	✓	✓	✓	✓	✓	✓	✓	✓
Neurological assessment ^f	✓			✓	✓	✓	✓	✓	✓	✓
Postmortem ^g				✓ ^h				✓ ⁱ	✓ ^j	✓ ^k

^aThe major groups of tests and components are listed with the times of assessment. ✓, procedure required.

^bPre, <14 days before vector administration. Day 0, analysis was performed on sample obtained after anesthesia but before vector or PBS administration. Tests were performed on the designated day \pm 1 day for day 3, 7, and 14 time points; \pm 3 days for day 28, 56, and 90 time points; and \pm 7 days for day 180 and 360 time points. On day 0, $n = 12$ monkeys were injected with 3.6×10^{11} PU of AAV2_{CU}hCLN2 (high dose), $n = 12$ were injected with 3.6×10^{10} PU of AAV2_{CU}hCLN2, $n = 3$ were injected with 3.6×10^{11} PU AAV2_{CU}Null, $n = 3$ were sham injected, and $n = 4$ were injected with PBS.

^cVital signs (pulse, respiratory rate).

^dCBC (hematocrit, hemoglobin, RBC, WBC, differential, platelets).

^eComprehensive mammalian chemistry (albumin, alkaline phosphatase, alanine aminotransferase, aspartate aminotransferase, blood urea nitrogen, calcium, chloride, cholesterol, creatine phosphokinase, creatinine, globulin, glucose, phosphorus, potassium, sodium, total bilirubin, total protein).

^fFor neurological assessment, the nonhuman primates were videotaped with a standard series of challenges and quantitative parameters were extracted from the videotapes.

^gThe whole brain and samples of liver, lung, kidney, heart, testes, spleen, and biceps were obtained at sacrifice for routine histology.

^hAt the 7-day time point, $n = 3$ of the high-dose AAV2_{CU}hCLN2, $n = 3$ of the low-dose AAV2_{CU}hCLN2, and $n = 1$ of the AAV2_{CU}Null monkeys were killed.

ⁱAt the 91-day time point, $n = 3$ of the high-dose AAV2_{CU}hCLN2, $n = 3$ of the low-dose AAV2_{CU}hCLN2, $n = 3$ of the sham-injected, and $n = 1$ of the AAV2_{CU}Null monkeys were killed.

^jAt the 180-day time point, $n = 3$ of the high-dose AAV2_{CU}hCLN2, $n = 3$ of the low-dose AAV2_{CU}hCLN2, and $n = 1$ of the AAV2_{CU}Null monkeys were killed.

^kAt the 360-day time point, $n = 3$ of the high-dose AAV2_{CU}hCLN2, $n = 3$ of the low-dose AAV2_{CU}hCLN2, and $n = 4$ of the PBS-injected monkeys were killed.

sure of the subcutaneous tissue also with chromic suture, and a skin closure using Vicryl. The wound was then sealed with collodion and the monkey was removed from the stereotaxic holder and observed in the recovery area until it was awake, at which time it was returned to its cage. Monkeys were assessed three times a day during recovery from surgery and daily thereafter.

Less than 2 weeks before surgery, on the day of administration, and on days 3, 7, 14, 28, 56, 91, 180, and 360 postinjection, animals were sedated for general assessment and for blood draw for complete blood count (CBC) and serum chemistry (both by Antech Diagnostics) and anti-AAV neutralizing antibodies. Because there was sequential sacrifice of monkeys, the number of observations decreased as the experiments proceeded.

Less than 2 weeks before surgery and at 7, 14, 28, 56, 91, 180, and 365 days postsurgery, monkeys were assessed for behavior. Again, because of sequential sacrifice of subsets of the nonhuman primates, there were more observations closer to the time of vector administration. These animals were videotaped

in the absence of stimuli and with specific food and threat scenarios. Specific behaviors were quantitated by blinded observers from the video tape. Two types of behaviors were quantitated: normal behaviors and identifiable abnormal behaviors. The normal behaviors were grouped into 5 summary scores, based on a previous data set of more than 50,000 observations (Taylor *et al.*, 1994, 1997).

Necropsy and sample collection. At intervals, a subset of the injected monkeys was killed for necropsy. The monkeys were first anesthetized with ketamine, vital signs were recorded, and blood was collected from the femoral vein. The monkey was then killed with a lethal dose of pentobarbital. The animal was then perfused with cold PBS and pieces of the testes, spleen, liver, kidney, lung, quadriceps, and heart were examined, removed, and placed in chilled 4% paraformaldehyde. During perfusion, the abdomen and thorax were explored for the presence of tumors. After the perfusion was completed, the brain was removed. Organ samples for histology were stored in paraformaldehyde at 4°C for 72 hr, at which time they were transferred

to 30% sucrose in 0.1 M phosphate buffer. The whole brain was divided into 4-mm coronal slabs (approximately 15 per animal), which were bisected with the right sections being immersed in 4% paraformaldehyde with transfer to sucrose after 72 hr.

Histopathology. All histologic assessments were carried out by Pathology Associates (Frederick, MD). The collection of a single section from each slab required paraffin embedding, and rough cutting of the block until a complete section was obtained. The four most frontal and four most occipital slabs were processed in paraffin *in toto*, and a single section was cut from the cranial face of each block (total of eight slides). For each of the seven middle slabs containing the injection sites, one section was obtained from each side of the block (caudal and rostral), giving a total of 14 sections. All 22 slides of brain (numbered 1 to 22 from the frontal to the occipital level) were stained with hematoxylin and eosin, for microscopic evaluation by a board-certified veterinary pathologist. The stained sections were carefully examined for evidence of neuronal death, axonal degeneration, or abnormal glial cell reactions. The pathologist was blinded as to the study groups on evaluation of the slides. The results were unblinded after the evaluation was complete and the key was provided.

Statistical analysis

In the rat study, statistical assessment of all parameters (organ weights, CBC, and serum chemistry) used analysis of variance (ANOVA) with treatment group (AAV2_{CU}hCLN2 vector versus PBS vehicle control) and sex as factors and time as a covariate. Because there was a total of 39 dependent variables, a cutoff of $p < 0.01$ was taken as a potentially significant difference between the vector and vehicle groups to reduce the chance of incorrectly rejecting the null hypothesis.

For statistical analysis of the nonhuman primate data (general assessment, CBC, blood) a mixed models analysis was used with time as a repeated measure. This method was required because of the study design, which had decreasing numbers of animals over time, leading to reduced numbers of values. Preliminary analysis with PBS, sham, and AAV2_{CU}Null as separate control groups gave high intragroup variance and was also complicated by the fact that the PBS animals were all killed at 52 weeks whereas the sham group was killed at 13 weeks. Therefore the three control groups were pooled to reduce the variance. In a preliminary assessment of the dependent measures, three variables (creatinine phosphokinase [CPK], aspartate aminotransferase [AST], and white blood cell count [WBC]) were noted to show unusual skewness; several tests of normality indicated these data were probably not normally distributed. On the basis of this analysis, those variables were transformed using \log_{10} transformations and assessed with the mixed models analysis on \log CPK, \log AST, and \log WBC. All other dependent variables were assessed without transformation. For all dependent variables, the main effects of group (control, low-dose AAV2_{CU}hCLN2, or high-dose AAV2_{CU}hCLN2) and time, and the interaction of group and time, were assessed. A main effect of group with $p < 0.01$ was taken as rejection of the null hypothesis that there was no difference between the groups. As with the rat analyses, a low p value was used because of the presence of multiple dependent variables.

To assess the effects of treatment on brain histopathology, χ^2 tests were used to compare the number of animals per group with and without the histopathological characteristic of interest. Because there were three control groups (sham, PBS, and AAV2_{CU}Null), we first assessed whether there were differences among the three control groups before combining them for comparison with the AAV2_{CU}hCLN2 low- and high-dose groups. To assess the impact of treatment on behaviors of the nonhuman primates, a separate analysis of the short-term and long-term effects was performed to increase the possibility of observing an effect of treatment group. Both analyses used the general linear models procedure with the type III mean squares analysis with animal within group as an error term, as implemented by SAS software (SAS Institute, Cary, NC).

RESULTS

Vector production

A preclinical toxicology study necessitates using AAV2_{CU}hCLN2 that is manufactured under the same conditions as the vector to be used in the human clinical study. On the basis of the proposed human dose of 3.6×10^{12} PU/subject and the small number of LINCL patients to be treated, scalability of the manufacturing process was not a major consideration. Therefore a two plasmid cotransfection system was chosen with product purification by iodixanol gradients and heparin affinity chromatography (Zolotukhin *et al.*, 1999; Sondhi *et al.*, 2005). Human embryonic kidney 293 cells from a certified working cell bank were grown in 10-stack cell factories and cotransfected with PolyFect by two plasmids, pAAV2-CAG-hCLN2 and pPAK-MA2 (Fig. 1). Both plasmids use the kanamycin resistance gene for propagation in *Escherichia coli*, thereby obviating the use of ampicillin, a potential allergen. The first plasmid contains the genome of the AAV2_{CU}hCLN2 vector. The second plasmid contains all of the AAV2 and Ad helper functions required for AAV2 vector replication and packaging. On the basis of yield of infectious AAV2 particles and total yield by capsid and ELISA and genome copies, the pPAK-MA2 helper plasmid was demonstrated to give comparable yields of AAV2 vectors in side-by-side comparisons with pDG, a widely used AAV2 helper plasmid that contains the ampicillin resistance gene (Grimm *et al.*, 1998; Crystal *et al.*, 2004).

Rat toxicology

Mortality. For each of the PBS and AAV2_{CU}hCLN2 groups, on the day after surgery, one rat was found dead or moribund, necessitating sacrifice. Examination of both rats suggested the cause of death to be head trauma associated with the surgical procedure. On day 152 after vector administration, one AAV2_{CU}hCLN2-injected rat was found dead. On the basis of histopathological examination, the cause of death in this animal was hemorrhage in the thalamus due to large granular cell leukemia observed in the thalamus, liver, and spleen. On day 329 after vector administration a second rat of the AAV2_{CU}hCLN2 group was found moribund. It was rehydrated but did not improve and therefore was killed the next day. The histopathology examination on this animal suggested the cause

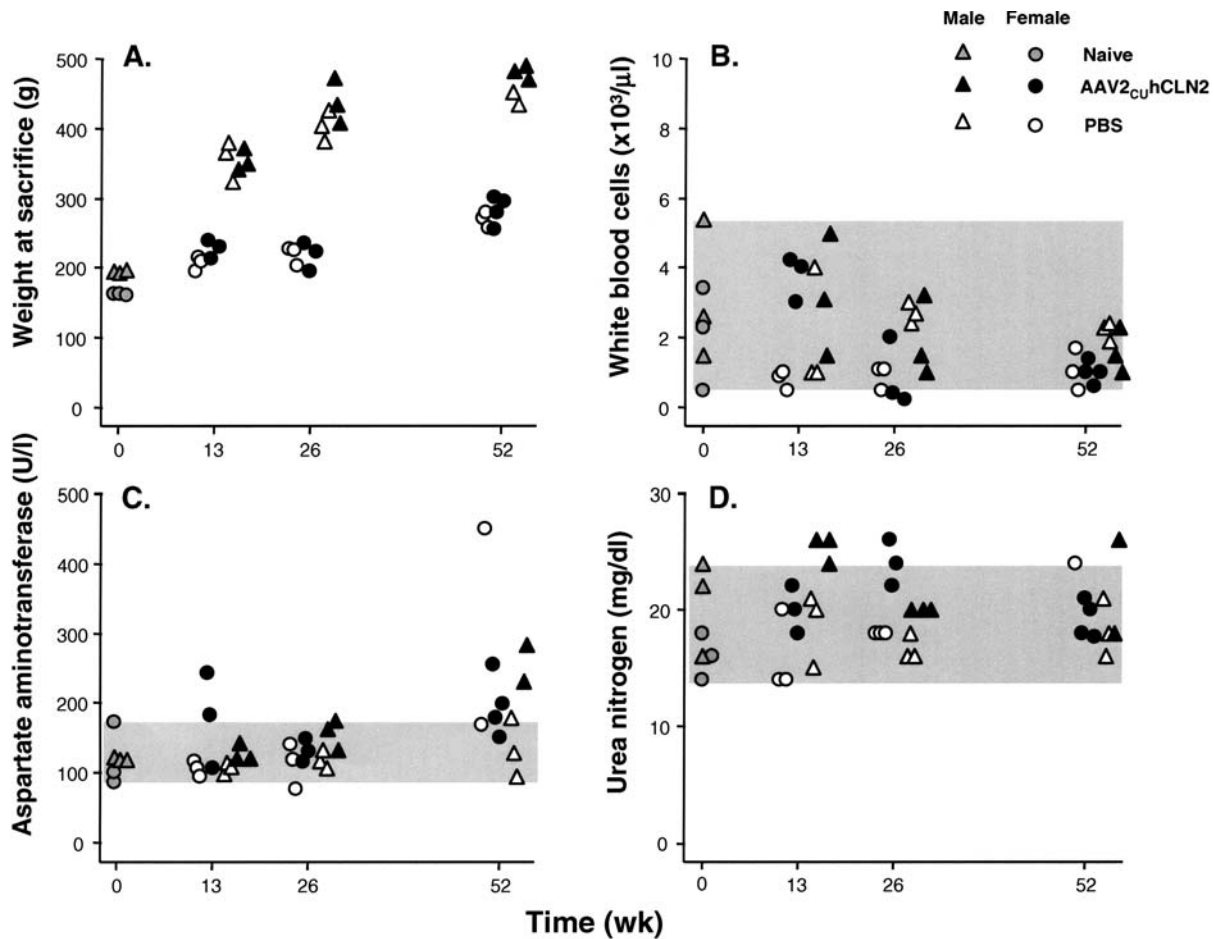


FIG. 2. Effect of CNS administration of AAV2_{CU}hCLN2 on selected general safety and hematological parameters in rats. Male (triangles) and female (circles) rats (age, 7 to 10 weeks) were injected bilaterally via the striatum with 2×10^{10} PU of AAV2_{CU}hCLN2 (solid symbols) or PBS (open symbols). Thirteen, 26, or 52 weeks after vector administration, subsets of rats were killed and assessed by general safety and hematological tests. As a basis for comparison, rats of similar age and sex (three naive females and three naive males) were also assessed. Data for all available rats are plotted for four selected parameters: (A) Weight of animal at sacrifice; (B) white blood cell count; (C) aspartate aminotransferase; and (D) urea nitrogen. For (B–D), the shaded areas represent the normal range based on analysis of six naive rats (7 to 10 weeks of age).

of death to be chronic progressive nephropathy with secondary mineralization of the kidney and myocardium.

General safety parameters. For the subset of rats killed 13, 26, or 52 weeks postadministration ($n = 3$ males and $n = 3$ females per treatment group), the internal organs were inspected for overt abnormalities or tumors. None were found. There was no difference in time-dependent weight gain between the AAV2_{CU}hCLN2 and PBS groups (Fig. 2 and Table 3). For all organs, as expressed as a percentage of total weight, there was no difference between AAV2_{CU}hCLN2 and PBS groups (Fig. 2 and Table 3).

Hematological parameters. Blood was collected at sacrifice and assessed by complete blood count consisting of 13 variables. For 12 of these variables (hemoglobin, hematocrit, red blood cell count, mean corpuscular hemoglobin, mean corpuscular volume, mean corpuscular hemoglobin content, platelets, neutrophils, lymphocytes, monocytes, eosinophils, and ba-

sophils), there was no significant difference ($p > 0.01$) between AAV2_{CU}hCLN2 and PBS groups (Fig. 2 and Table 3). For the white blood cell count, there was a significant difference between vehicle and vector group ($p = 0.006$). The mean and standard deviation of the white blood cell count for the AAV2_{CU}hCLN2-treated group (all sexes and time points) was $(2.0 \pm 1.3) \times 10^3/\mu\text{l}$ whereas the mean for the PBS-treated rats was $(1.6 \pm 1.0) \times 10^3/\mu\text{l}$. Both values fall within the normal range [$(2.6 \pm 1.7) \times 10^3/\mu\text{l}$] based on our analysis of six naive rats (7 to 10 weeks of age).

Serum collected at sacrifice was assessed by a mammalian chemistry panel consisting of 17 variables. For 15 of these variables (glucose, creatinine, total protein, albumin, total bilirubin, alkaline phosphatase, alanine aminotransferase, aspartate aminotransferase, cholesterol, phosphorus, sodium, potassium, chloride, globulin, and creatine phosphokinase) there was no significant difference ($p > 0.01$) between AAV2_{CU}hCLN2 and PBS groups (Table 3). For two parameters (calcium [$p = 0.0014$] and urea nitrogen [$p = 0.0005$]), there was a signifi-

TABLE 3. TOXICOLOGY PARAMETERS AFTER AAV2_{CU}hCLN2 ADMINISTRATION TO THE RAT BRAIN^a

General safety		Complete blood count		Serum chemistry	
Organ weight	p Value ^b	Parameter	p Value	Parameter	p Value
Total body weight	0.63	Hemoglobin	0.32	Glucose	0.49
Brain	0.62	Hematocrit	0.21	Urea nitrogen	<0.001
Lung	0.02	RBC	0.94	Creatinine	0.80
Quadriceps	0.48	WBC	<0.01	Bilirubin	0.18
Liver	0.26	MCV	0.35	Alkaline phosphatase	0.01
Gonads	0.77	MCH	0.40	ALT	0.25
Spleen	0.48	MCHC	0.35	AST	0.13
Heart	0.46	Platelets	0.27	Cholesterol	0.80
Kidney	0.75	Neutrophils	0.86	CPK	0.97
		Lymphocytes	0.48	Calcium	<0.01
		Monocytes	0.08	Potassium	0.52
		Eosiniphils	0.23	Sodium	0.64
		Basophils	0.77	Phosphorus	0.21
				Chloride	0.06
				Total protein	0.83
				Albumin	0.77
				Globulin	0.91

^aThe outcome parameters are divided into groups and *p* values for an effect of drug on that parameter are presented. *Abbreviations*: RBC, red blood cell count; WBC, white blood cell count; MCV, mean corpuscular volume; MCH, mean corpuscular hemoglobin; MCHC, mean corpuscular hemoglobin content; ALT, alanine aminotransferase; AST, aspartate aminotransferase; CPK, creatine phosphokinase.

^b*p* Values were assessed by ANOVA, using sex and treatment group as factors and time (13, 26, and 52 weeks) as an independent variable. The reported *p* value is a test of the null hypothesis that there is no difference between the AAV2_{CU}hCLN2 and PBS groups for that parameter.

cant difference between the AAV2_{CU}hCLN2 and PBS groups. The mean and standard deviation of serum calcium for the AAV2_{CU}hCLN2-treated group (all sexes and time points) was 11.3 ± 0.5 mg/dl whereas that for the PBS-treated rats was 10.8 ± 0.7 mg/dl. Both values fall within the normal range (11.1 ± 0.3 mg/dl based on analysis of six naive rats, 7 to 10 weeks of age). The mean and standard deviation of urea nitrogen for the AAV2_{CU}hCLN2-treated group (all sexes and time points) was 21.6 ± 3.0 mg/dl whereas that for the PBS-treated rats was 17.9 ± 2.8 mg/dl. Both values fall within the normal range (18.3 ± 3.9 mg/dl based on analysis of six naive rats, 7 to 10 weeks of age).

Anti-AAV2 neutralizing titers. The anti-AAV2 neutralizing titers were <10 for all serum samples at all time points whether derived from PBS- or AAV2_{CU}hCLN2-injected rats.

Brain histopathology. Multiple full coronal sections of brain were examined, representing an extensive survey of all areas of the brain, including frontal, temporal, and occipital cortex, deep cortex, corona radiata including the hippocampus, the diencephalon, and midbrain including the thalamus, midbrain, cerebellum, and medulla oblongata. Hematoxylin and eosin-stained sections were carefully examined for evidence of neuronal death, axonal degeneration, or abnormal glial cell reactions.

Microscopic changes in brain histology were observed at 13, 26, and 52 weeks at the level of the striatum (injection site) in one or several of the step sections taken throughout that area (Fig. 3). These changes consisted of circumscribed dorsoventral linear foci of gliosis (mononuclear microglial cells and as-

trocytes), sometimes accompanied by pigment-laden macrophages (hemosiderin). The severity of these changes was generally classified as minimal with occasional sections showing mild pathology. Extension was confined to the path of needle puncture. These microscopic changes were not seen in either group in any other part of the brain and extended only minimally from the injection site. The frequency of injection track capture, and severity of these pathological changes, were similar between the AAV2_{CU}hCLN2 and vehicle groups (Table 4). For example, the overall frequency of injection track hemosiderin in the PBS group when all time points were combined was 7 of 22 compared with 6 of 21 in the AAV2_{CU}hCLN2 group, an insignificant difference (*p* = 0.11 by χ^2 test). In only one of the 26-week PBS rats was the hemosiderin classified as mild, and all other examples were classified as minimal. With respect to injection track gliosis, there was actually a higher frequency in the PBS group than in the AAV2_{CU}hCLN2 group after all time points were combined (*p* < 0.01).

There was a small focus of fibrosis in the leptomeninges of the frontal cortex in a single week 13 PBS animal, and an occasional focus of superficial cortical loss with scarring in week 26 and week 52 animals at the intracerebral injection access site (subdural cortex). These changes were considered to be due to the localized trauma of injection and their incidence and severity did not reflect a relationship to the test article. There were no microscopic changes that were considered to be related to the presence of the viral vector construct at week 13, 26, or 52. Inflammatory changes sometimes associated with intracerebral injection of a viral vector, such as perivascular lymphocyte infiltrates, were not seen.

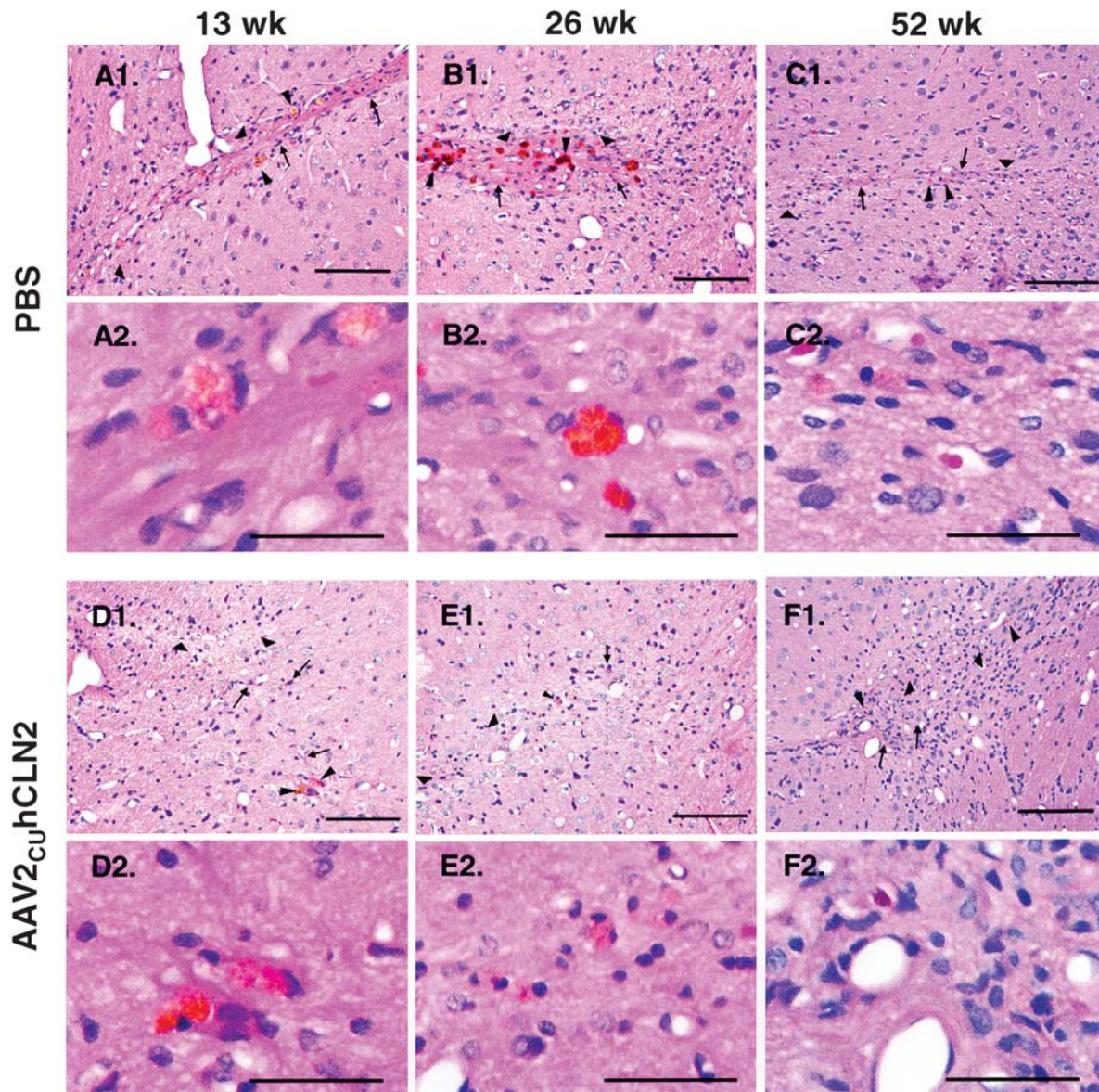


FIG. 3. Histopathology of brain of AAV2_{CU}hCLN2-treated rats. For each treatment and time point, one example of a coronal section of the striatum in the region of injection is shown. These examples are selected to show the range of pathologies observed and are not necessarily typical of any one group. The hematoxylin and eosin-stained sections are 5 μ m thick. Scale bar: 100 μ m. (A1–C1) PBS-injected rats; (D1–F1) AAV2_{CU}hCLN2-injected rats. (A1 and D1) Thirteen weeks after vector administration; (B1 and E1) 26 weeks after vector administration; (C1 and F1) 52 weeks after vector administration. Examples of reactive microglial cells (wide arrowheads), reactive astrocytes and filamentous astrocyte processes (long arrows), and hemosiderin within microglial cells (narrow arrowheads) are indicated. Panels A2–F2 (corresponding to panels A1–F1, respectively) show higher magnification views of the abnormal histopathology. Scale bar: 50 μ m.

Histopathology of other organs. On gross examination of rats at sacrifice, no abnormal structures or tumors were found with the exception of those rats that died prematurely. Histopathological examination of other organs at weeks 13, 26, and 52 showed abnormalities of the type commonly observed in rats, and there were no trends suggesting treatment relationship. Abnormalities such as cardiomyopathy in the heart, clear cell focus in the liver, chronic progressive nephropathy in the kidney, and hemosiderin and extramedullary hematopoiesis in the

spleen were observed at comparable incidence in PBS controls and treated rats at weeks 13, 26, and 52.

Nonhuman primate toxicology

Anti-AAV2 neutralizing titers. The anti-AAV2 neutralizing titers were assessed for a subset of the nonhuman primates before and after vector administration. At the time of administration the mean reciprocal anti-AAV2 neutralizing titer was $28 \pm$

TABLE 4. QUANTITATION OF INJECTION TRACK PATHOLOGY IN AAV2_{CU}hCLN2-INJECTED AND PBS-INJECTED CONTROL RATS^a

	Time point (weeks)	PBS	AAV2 _{CU} hCLN2	p Value ^b
Injection track hemosiderin	13	2/9	1/9	0.52
	26	3/6	1/6	0.22
	52	2/7	4/6	0.17
	All time points	7/22	6/21	0.81
Injection track gliosis	13	4/9	1/9	0.11
	26	6/6	3/6	0.04 ^c
	52	4/7	3/6	0.79
	All time points	14/22	7/21	0.006 ^d

^aAt the time points indicated, rats were killed and perfused and the brains were sent for sectioning, Hematoxylin and eosin staining, and reading by a board-certified pathologist. Listed are the number of rats in which the indicated pathology was found/total killed at that time point. At the 13- and 52-week time points, additional rats were examined beyond the planned number of three males and three females to fill in missing laboratory values.

^b*p* Values were calculated by χ^2 test comparing the PBS and AAV2_{CU}hCLN2 groups.

^cAt the 26-week time point there is a marginally significantly higher detection of injection track hemosiderin in the PBS group.

^dOverall there was a higher frequency of detection of injection track gliosis in the PBS group than in the AAV2_{CU}hCLN2 group.

10 and at 56 days after vector administration this was unchanged (42 ± 26 , $p > 0.6$).

General safety parameters. There was no mortality for any monkey in any group over the 52 weeks of the study. The periodic assessments included pulse, respiratory rate, temperature, and weight. Statistical analysis (Table 5) showed no effect of treatment group for any of the general safety parameters ($p > 0.01$ all variables).

Complete blood count. Statistical analysis (Table 5) showed no effect of group (controls, low dose, and high dose) for any of

the complete blood count parameters: hemoglobin, hematocrit, platelet count, white blood cell count, red blood cell count, lymphocyte count, neutrophil count, and monocyte count, all of which were expressed as a function of the white blood cell count ($p > 0.01$ all variables). For several CBC parameters, there was a significant impact of time. For example, in the individual monkeys, there was a transient drop in hematocrit in all groups, which recovered into the normal range in about 30 days (Fig. 4). Similarly, among the group means, there was a postsurgical increase in platelet count that slowly dropped to presurgery levels (Fig. 5). However, the statistical analyses showed that these transient changes were not dependent on treatment group.

TABLE 5. TOXICOLOGY PARAMETERS AFTER AAV2_{CU}hCLN2 ADMINISTRATION TO NONHUMAN PRIMATE BRAIN^a

General safety		Complete blood count		Serum chemistry	
Parameter	p Value ^b	Parameter	p Value	Parameter	p Value
Weight	0.93	Hemoglobin	0.73	Glucose	0.01
Pulse	0.86	Hematocrit	0.65	Urea nitrogen	0.17
Respiratory rate	0.28	RBC	0.70	Creatinine	0.10
Temperature	0.77	WBC	0.57	Bilirubin	0.72
		Platelets	0.47	Alkaline phosphatase	0.76
		Neutrophils	0.71	ALT	0.30
		Lymphocytes	0.63	AST	0.50
		Monocytes	0.51	Cholesterol	0.01
				CPK	0.93
				Calcium	0.81
				Potassium	0.76
				Sodium	0.87
				Phosphorus	0.18
				Chloride	0.67
				Total protein	0.93
				Albumin	0.25
				Globulin	0.40

^aThe outcome parameters are divided into groups and *p* values for an effect of drug on that parameter are presented. *Abbreviations:* RBC, red blood cell count; WBC, white blood cell count; ALT, alanine aminotransferase; AST, aspartate aminotransferase; CPK, creatine phosphokinase.

^b*p* Values were assessed by a mixed models analysis with time (pre, 7, 14, 28, 56, 91, 180, and 365 days) as a repeated measure. The reported *p* value is a test of the null hypothesis that there is no difference between the high-dose AAV2_{CU}hCLN2 animals, the low-dose AAV2_{CU}hCLN2 animals and control animals (PBC, AAV2_{CU}Null, and sham combined) for that parameter.

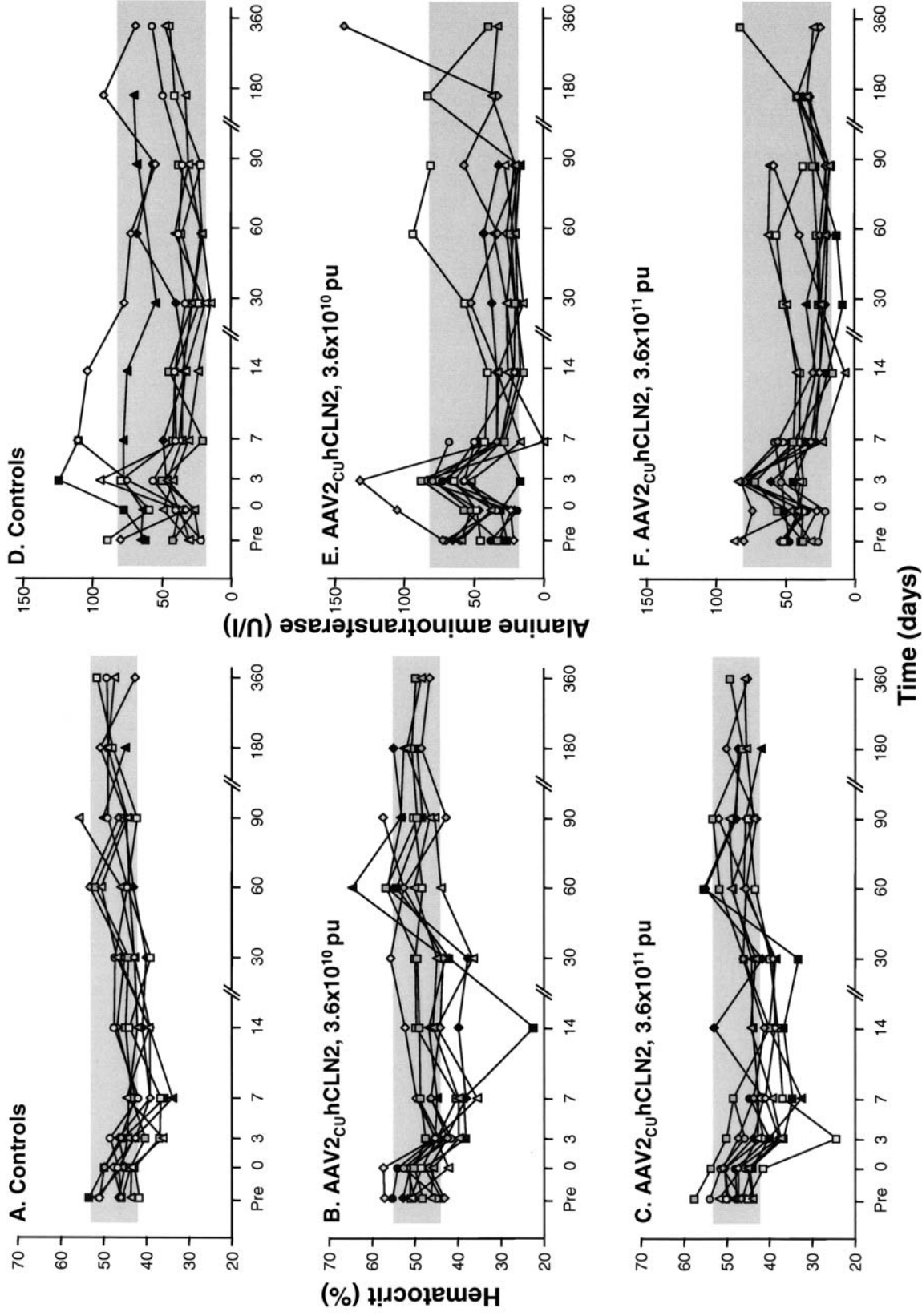


FIG. 4. Effect of CNS administration of AAV2_{CU}hCLN2 on selected hematological parameters in African green monkeys. Shown are data from individual monkeys. Thirty-four African green monkeys were assessed for general health and hematological parameters. A subset ($n = 10$ total) was designated controls (**A** and **D**) and injected in 12 sites intracranially with PBS ($n = 4$), sham injected ($n = 3$), or injected with AAV2_{CU}Null ($n = 3$). Two groups ($n = 12$ each) received AAV2_{CU}hCLN2 at a dose of 3.6×10^{10} PU (**B** and **E**) or 3.6×10^{11} PU (**C** and **F**). Monkeys were assessed and bled before surgery (pre), on the day of administration (day 0), and on days 3, 7, 14, 30, 60, 90, 180, and 360. The values for two selected parameters, hematocrit (left, **A–C**) and alanine aminotransferase (right, **D–F**), are plotted for individual animals. Note that a subset of each group was killed for histopathology at intervals and therefore the number of measurements decreases with time. The normal range for each parameter, calculated as the 5th to 95th percentile of measurement on all monkeys presurgery, is shown as the shaded area.

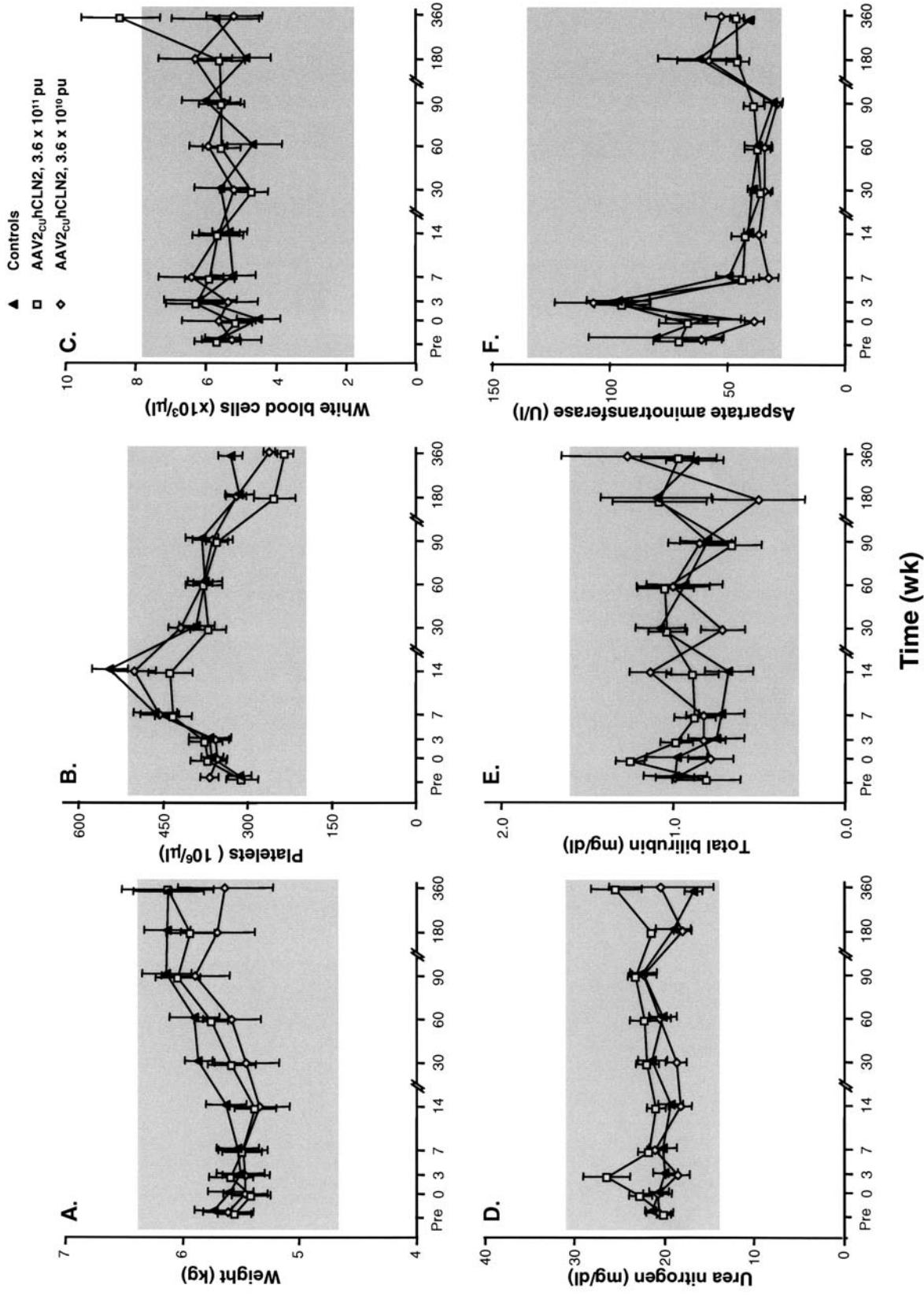


FIG. 5. Effect of direct CNS administration of AAV2_{Cu}hCLN2 on selected safety and hematological parameters in African green monkeys. Shown are means of treatment groups. The animals studied are described in the legend to Fig. 4. The mean values for six selected parameters are shown as a function of time: (A) weight; (B) platelets; (C) white blood cell count; (D) urea nitrogen; (E) total bilirubin; and (F) aspartate aminotransferase. Error bars represent the standard error for the measured parameters based on up to $n = 12$ animals per group at the early time points and as few as $n = 3$ at the last time point. The normal range for each parameter was calculated as the 5th to 95th percentile of measurement on all monkeys presurgery and is shown as a shaded area.

Serum chemistry. Statistical analysis showed no effect of treatment group (controls, low dose, and high dose) for 15 of 17 serum chemistry parameters (urea nitrogen, creatinine, total protein, albumin, globulin, total bilirubin, alkaline phosphatase, alanine aminotransferase, aspartate aminotransferase, calcium, phosphorus, sodium, potassium, chloride, and creatinine phosphokinase; Table 5). There was a significant effect of treatment group on serum cholesterol ($p = 0.007$). The mean value (all time points) for the control group was 115 ± 2.0 mg/dl (standard error) versus 121 ± 3.0 mg/dl for the low-dose group and 102 ± 1.5 for the high-dose group. However, these differences are within the normal range of 91 to 160 mg/dl, based on a survey of 40 normal African green monkeys presurgery. In addition, there was a significant effect of treatment group on glucose ($p = 0.005$). The mean value (all time points) for the control group was 80 ± 2.3 mg/dl (standard error) versus 91.9 ± 3.14 mg/dl for the low-dose group and 85 ± 2.7 for the high-dose group. These differences are within the normal range of 51 to 155 mg/dl, based on a survey of 40 normal African green monkeys presurgery. As seen for some of the CBC parameters, some of the serum chemistry parameters, such as alanine aminotransferase (plotted for individual monkeys; see Fig. 4) and aspartate aminotransferase (plotted as means for each group; see Fig. 5), showed transient changes in all groups postsurgery, but these were not different among different treatment groups.

Brain histopathology. For each brain, 22 slides (numbered 1 [frontal] to 22 [occipital]) containing coronal sections of one hemisphere were examined. These slides represented an extensive survey of all areas of the brain, including frontal, temporal, and occipital cortex, deep cortex, corona radiata including the hippocampus, the diencephalon, and midbrain including the thalamus, midbrain, cerebellum, and medulla oblongata, including the olivary nucleus. The sections were carefully examined for evidence of neuronal death, axonal degeneration, or

abnormal glial cell reactions. In some week 52 brains (one PBS, two low-dose CLN2, and one high-dose CLN2) there were large clear spaces around vessels and within the brain parenchyma consistent with perfusion and/or freeze artifact.

Histopathological changes were observed in the vicinity of injection, consisting of circumscribed dorsoventral linear foci of gliosis (mononuclear microglial cells and astrocytes). The gliosis was of minimal to moderate severity in multiple sections of all monkeys (AAV2_{CU}Null and both doses of AAV2_{CU}-hCLN2) at the 1-week time point (Table 6). At later time points, injection site gliosis was observed in a subset of both the control and AAV2_{CU}-hCLN2 monkeys (Table 6). To assess the correlation with the AAV2_{CU}-hCLN2 vector, it was necessary to combine the control monkeys, which is justified by the fact that there is no difference in the rate of detection of injection site gliosis ($p = 0.2$ by χ^2 test) between the PBS, sham, and AAV2_{CU}Null control groups. When the control groups are combined, there was no difference in the rate of detection of injection site gliosis between the AAV2_{CU}-hCLN2 groups and the controls (χ^2 test, $p = 0.6$ comparing all control with the low-dose and high-dose groups combining all time points). Multifocally, there were hemosiderin-laden macrophages in the leptomeninges consistent with slight hemorrhage related to the mechanical trauma of needle puncture. These changes were observed in both the control and treated groups at all time points greater than 1 week. They were located in the rostral and temporal cerebrum in an area consistent with the injection site, including the cerebral cortex, corona radiata, and caudate nucleus, sometimes reaching the hippocampus and the lateral ventricle (Fig. 6). The frequency was the same in all three control groups ($p = 0.35$) and there was no difference between the controls and the low and high-dose AAV2_{CU}-hCLN2 groups ($p = 0.1$). In addition, there was slight injection track axonal degeneration or necrosis (spheroids) in 5 of 24 AAV2_{CU}-hCLN2 monkeys and 3 of 10 control monkeys independent of time point.

The dorsal aspect of the cortex, where the injection catheter entered the brain, showed discrete foci of proteinaceous ma-

TABLE 6. QUANTITATION OF ABNORMAL BRAIN PATHOLOGY IN AAV2_{CU}-hCLN2-INJECTED NONHUMAN PRIMATES^a

Treatment	n	Time points (weeks)	Injection track gliosis	Injection track hemosiderin	Subdural necrosis
AAV2 _{CU} -hCLN2 (3.6×10^{10} PU)	3	1	1 minimal 2 mild	None	3 mild
AAV2 _{CU} -hCLN2 (3.6×10^{11} PU)	3	1	2 mild 1 moderate	None	1 moderate 2 mild
AAV2 _{CU} Null (3.6×10^{11} PU)	3	1,13,26	1 moderate 1 mild 1 minimal	1 minimal	1 moderate 1 mild
PBS	4	52	3 minimal	2 minimal	3 minimal
Sham	3	13	1 mild	None	3 minimal
AAV2 _{CU} -hCLN2 (3.6×10^{10} PU)	9	13, 26, 52	3 mild 4 minimal	3 minimal 2 mild	4 minimal 1 mild
AAV2 _{CU} -hCLN2 (3.6×10^{11} PU)	9	13, 26, 52	5 minimal 2 mild	1 minimal	6 minimal 1 mild

^aHistopathological findings as graded by the veterinary pathologist are tabulated for the various injection groups and time points. The PBS, null, and sham control groups are separated. Abnormal pathology was classified as minimal, mild, or moderate and the number of animals of each group with at least one section of that level is recorded. All other animals of the group showed no abnormalities of this type.

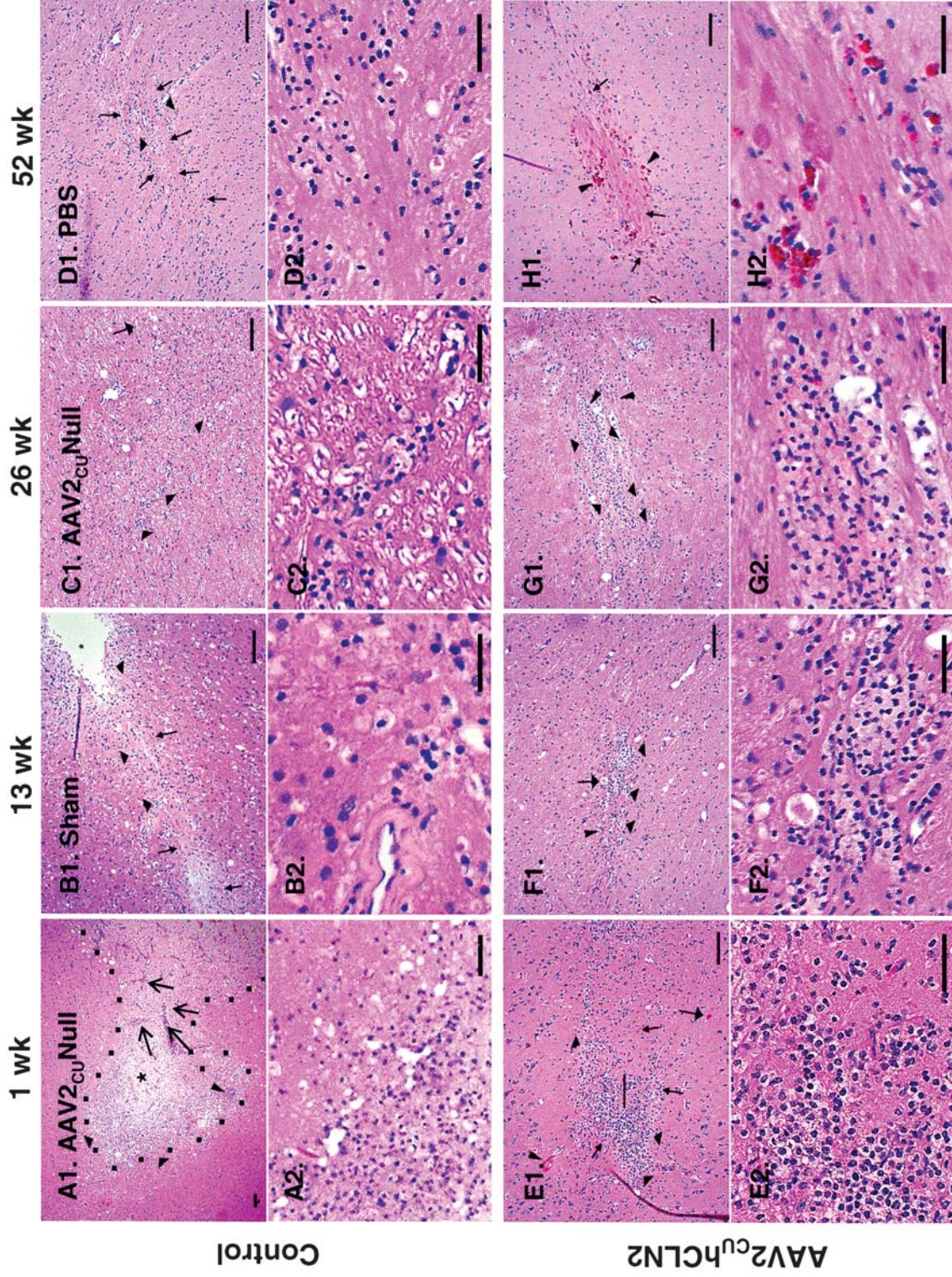


FIG. 6. Histopathology of brain of AAV2_{Cu}hCLN2-treated African green monkeys. For each treatment and time point, one example of a coronal section from one of the regions of injection is shown. These examples are selected to show the range of pathologies observed and are not necessarily typical of any one group. The hematoxylin and eosin-stained sections are 5 μ m thick. Scale bars: (A1–H1) 200 μ m; (B1–H1) 500 μ m; (A1) Cortex 1 week after AAV2_{Cu}Null injection; (B1) cortex 13 weeks after sham injection; (C1) cortex 26 weeks after AAV2_{Cu}Null injection; (D1) cortex 52 weeks after PBS injection; (E1) cortex 1 week after AAV2_{Cu}hCLN2 injection; (F1) cortex 13 weeks after AAV2_{Cu}hCLN2 injection; (G1) cortex 26 weeks after AAV2_{Cu}hCLN2 injection; (H1) cortex 52 weeks after AAV2_{Cu}hCLN2 injection. Examples of reactive microglial cells (wide arrowheads), reactive astrocytes and filamentous astrocyte processes (long closed-head arrows), hemosiderin within microglial cells (narrow arrowheads), track necrosis and/or cavitation (asterisks, *), reactive blood vessels (long open-head arrows), and outline of injection track changes (dotted line) are indicated. Panels A2–H2 (corresponding to panels A1–H1, respectively) show higher magnification views of the abnormal histopathology. Scale bars: (A2) 150 μ m; (B2) 50 μ m; (C2–H2) 100 μ m.

terial accumulation in the leptomeninges. These foci had produced slight compression of the superficial cortex resulting in subjacent cortical gliosis with a localized wedge of pressure necrosis in the superficial cortex (subdural cortical necrosis). These changes were also observed at equal frequency when comparing the control groups (sham controls [3 of 3], PBS controls [3 of 4], AAV2_{CU}Null control [2 of 3], $p = 0.70$) and when comparing the combined control groups with the low-dose (8 of 12) and high-dose (10 of 12) AAV2_{CU}hCLN2-treated nonhuman primates ($p = 0.6$). Although there was mild hemorrhage observed in six of seven brains observed 1 week after injection, independent of treatment group, there was no obvious hemorrhage at subsequent time points. Minimal mononuclear cell infiltration was observed in the injection track in one of three low-dose AAV_{CU}hCLN2 week 26 animals and in one PBS control at week 52. There was a small nonorganized fibrin embolus in a leptomeningeal vessel of the occipital cortex in a single low-dose AAV2_{CU}hCLN2 week 13 animal.

The only change potentially related to treatment was observed at week 1 and consisted of minimal to mild spongiosis. Spongiosis was observed in the corona radiata of the cerebrum along the injection track, and in the surrounding white matter, extending moderately in the corona radiata rostrally and caudally. Spongiosis was characterized by slight edema that slightly increased the extracellular space, and was accompanied by reactive glial cells. This change was observed in two of three low-dose AAV2_{CU}hCLN2 monkeys (grade 1) and in two of three high-dose AAV2_{CU}hCLN2 monkeys (grade 2) but not in the single AAV2_{CU}Null monkey. Reactive glial cells consisted primarily of astrocytes with prominent cell processes and open-faced nuclei. Identical reactive glial cells were observed at, and immediately adjacent to, the injection track in the absence of edema in the AAV2_{CU}Null controls.

Histopathology of other organs. No tumors or visible abnormalities of any organ were found in any nonhuman primate from any treatment group at sacrifice. In histopathological examination of other organs, there were some microscopic changes including a multifocal ischemic fibrosis in the heart of a high-dose week 26 animal and diffuse marked atrophy of the testis in a low-dose AAV2_{CU}hCLN2 week 13 animal.

Behavioral analysis. Over the period of the study, all surviving monkeys were observed for neurological behavior by videotaping in the absence of stimuli and with specific food and threat scenarios. Five specific types of behavior (anxiety, arousal, sedation, quiet, and healthy) were quantitated by blinded observers from that video tape. Statistical analysis showed that there was no systematic effect of observer on the quantitative outcome parameters (p values between 0.65 and 0.13, testing the hypothesis that there was no difference between observers for five different quantitative measures of behavior).

There was no abnormal behavior observed in any of the treated or untreated monkeys in the formal toxicology study. The monkeys were specifically observed for food-eating problems, appearance, delayed movement, poverty of movement, and tremor; none of these were observed for any AAV2_{CU}hCLN2-treated or control animals.

The normal behaviors were also compared among groups. Because of the decreasing numbers of monkeys over time, short-term and long-term effects of treatment group were assessed independently. There was no effect of treatments group on any of the five specific types of normal behavior, nor on the sum of all healthy behaviors (Table 7). This was true both for the monkeys that were observed over 52 weeks ("long term") as well as for the larger group of monkeys observed for up to 26 weeks ("short term").

TABLE 7. DEPENDENCE OF BEHAVIORAL SUMMARY SCORES ON TREATMENT GROUP

<i>Behavior</i>	<i>Short-term effects^a</i>	<i>Long-term effects^b</i>
Anxiety sum ^c	0.74	0.99
Arousal sum ^d	0.36	0.25
Sedation sum ^e	0.98	0.37
Quiet behavior ^f	0.96	0.83
Healthy sum ^g	0.76	0.7
Any neurological abnormality	NA ^h	NA

^aThis column gives the p values for testing the hypothesis that the variable is unaffected by treatment group considering the time points (pre, 7, 14, 28, 56, 91, and 180 days). The analysis uses general linear models procedure with the type III mean squares analysis with animal within group as an error term, as recommended by Winer (1971).

^b p Values for testing the hypothesis that the variable is unaffected by treatment group, using only the pre, 26-week, and 52-week data for the 10 animals that were observed for 52 weeks. The analysis uses the type III mean squares analysis with animal within group as an error term, as recommended by Winer (1971).

^cSum of five behaviors associated with anxiety (chewing, penile erection, scratching, self-grooming, and yawn).

^dSum of six behaviors associated with arousal (bipedal lookout, shift, tail flagging, threaten outside, vertical climb, and vocalization).

^eSum of two behaviors associated with sedation (eyes closed, and freeze).

^fSum of four quiet behaviors (cage pick, self-groom, drinking, and eating).

^gSum of anxiety, arousal, sedation, and quiet behaviors.

^hNA, not applicable as none of those behaviors were observed in any monkey in any group.

DISCUSSION

These data describe the pivotal toxicology studies performed to prepare for a human clinical trial of CNS administration of AAV2_{CU}hCLN2 in subjects with LINCL. The experience with AAV vectors in humans is limited and few subjects have received direct administration of AAV vectors into the CNS, as is required for LINCL (During *et al.*, 2001; Janson *et al.*, 2002). Using a clinical-grade vector produced under GMP conditions, an extensive series of toxicology studies was carried out in rats and nonhuman primates with assessment of general safety, histopathology, and behavioral assessment after direct CNS administration of vector. In rats, there were no biologically significant changes seen for any safety parameter and the histopathological changes were similar in the AAV2_{CU}hCLN2 and control animals, limited to minor changes attributable to the injection per se. In nonhuman primates, there were no significant changes in blood count, serum chemistry, or general safety parameters between high- or low-dose AAV2_{CU}hCLN2 groups and control animals. Histopathological examination of the brain showed mild dose-independent changes along the injection track at the 1-week time point but not thereafter. Importantly, periodic, blinded, semiquantitative assessment of videotapes of the nonhuman primates showed no difference in multiple parameters of behavior of the nonhuman primates observed over the course of the 1-year study in both AAV2_{CU}hCLN2 groups and control animals. Together, these observations support the concept that CNS administration of the AAV2_{CU}hCLN2 vector has a safety profile acceptable for initiating human trials to treat LINCL.

Safety of AAV2 vectors: preclinical studies

Various experimental animal studies have demonstrated a favorable safety profile with gene transfer by adeno-associated virus serotype 2 vectors to a variety of organs. Favre *et al.* (2001) reported normal organ histopathology and the absence of significant hematological abnormalities after intramuscular administration of an AAV2 vector encoding erythropoietin into rhesus and cynomolgus macaques. Similarly, Flotte *et al.* (2004) performed an extensive series of toxicology studies in rabbits and nonhuman primates and reported no pathology associated with AAV2 vectors encoding α_1 -antitrypsin or the cystic fibrosis transmembrane regulator delivered to the epithelial surface of the lung and by the intravenous route. Relevant to the CNS route in the present study, Janson *et al.* (2002) demonstrated the absence of behavioral changes up to 1 week after intracranial administration of an AAV2 vector expressing aspartoacylase to the CNS of nonhuman primates.

Safety of AAV2 vectors: clinical studies

AAV2-derived vectors have been administered to various human organs including the nasal, airway, and sinus epithelium and by the intramuscular route with minimal safety issues (Kay *et al.*, 2000; Aitken *et al.*, 2001; Wagner *et al.*, 2002; Flotte *et al.*, 2003; Manno *et al.*, 2003; Moss *et al.*, 2004). Of significance to the study reported here, the human aspartoacylase cDNA has been administered to the CNS of children with Canavan disease both in the context of an AAV2-derived plasmid

and an AAV2 vector, and the data to date suggest that this is well tolerated (P. Leone, personal communication). A trial delivering glutamic acid decarboxylase via AAV2 to the CNS subthalamic nucleus of individuals with Parkinson's disease is also proceeding without significant safety concerns (M. Kaplitt, personal communication).

Trauma associated with administration to the CNS

As LINCL is a neurodegenerative disorder that affects the entire brain, an effective therapy should target as large a portion of the brain as possible. Although there are several innovative strategies to deliver genes to the brain that have been developed in experimental animals (Nguyen *et al.*, 2001; Mastakov *et al.*, 2002a), our study design takes the most direct administration strategy with insertion of fine catheters into several regions of the CNS and slow infusion of the vector. There are significant challenges to this strategy. First, to attain a larger distribution of the transgene product, it is essential to target multiple locations, thereby requiring multiple burr holes. In our LINCL gene transfer strategy, this issue was addressed by maximizing the delivery of the vector through each burr hole by delivering vector to two sites along the same needle track. Second, there can be no significant increases in intracranial pressure. As delivery of the vector requires introduction of fluid into a closed space, it is essential to do so at a flow rate that will minimize the risk of increased intracranial pressure or hemorrhage. To address this concern, the vector was delivered at a rate of 1 μ l/min, a rate known to be safe for intracranial delivery in nonhuman primates (Bohn *et al.*, 1999; Smith *et al.*, 1999; Kozlowski *et al.*, 2001; Muramatsu *et al.*, 2002).

The slow flow rate for delivery of vector means a long procedure, and thus an increased risk of time under anesthesia. Although the surgical procedure for the delivery of the AAV2_{CU}hCLN2 vector to the CNS was optimized to prevent trauma, the surgical administration of the vector (rather than the vector itself) did pose some minor risks. This has also been seen in other studies. For example, in the preclinical studies in preparation for human gene therapy with Canavan disease, the only deaths in toxicology studies were attributed to surgical complications (Janson *et al.*, 2002). In addition, intracerebral hemorrhage is a common complication of stereotactic surgery (Field *et al.*, 2001). The histopathological changes in the nonhuman primates seen in this study were the same in the sham group (with needle insertion only and no fluid infusion) as in the PBS-, AAV2_{CU}Null-, and AAV2_{CU}hCLN2-injected groups and resembled those previously described as occurring after puncture wounds. This suggests that all of the abnormal histopathology that arises is a result of the needle insertion and that the infusion rate and test object cause no additional histopathology. This is corroborated in multiple studies in which extensive gliosis has been observed at the site of needle insertion into the brain (Ma *et al.*, 1991; Lo *et al.*, 1999; Xue and Del Bigio, 2001). In addition, there is rapid infiltration of macrophages after needle trauma that may not be seen in this study because by 1 week microglial cells are more prevalent (Kaur *et al.*, 1987; Fujita *et al.*, 1998). Consistent with these observations, we observed local hemorrhage and local gliosis in histopathological examination of nonhuman primate brains 1 week postsurgery. In nonhuman primates, in which administration of vector was performed serially at 12 different positions,

the slow infusion rate necessitated anesthesia for up to 5 hr. A number of parameters of serum chemistry including liver enzymes were transiently increased after surgery in all groups independent of AAV2_{CU}hCLN2 treatment. Finally, the multiple blood samples collected around the time of surgery mitigated by the surgery itself resulted in a transient anemia that resolved over time (Atabek *et al.*, 1995). Taken together, although there is trauma associated with surgical delivery of the vector, it is mild and reversible, and did not result in any mortalities.

Vector-related host responses

The recombinant AAV2_{CU}hCLN2 vector does not contain any viral genes that express viral proteins; thus, any vector-related host responses can be directed only to the viral capsid. Anti-vector neutralizing antibodies have been shown to be evoked in response to intravenous and intramuscular administration of AAV2 vectors (Chirmule *et al.*, 2000; Xiao *et al.*, 2000). When the vectors are administered systemically, these antibodies are sufficient to block or significantly reduce the effect of readministration of another vector of the same serotype (Moskalenko *et al.*, 2000; Xiao *et al.*, 2000; Gao *et al.*, 2002). Even though the brain is thought to be immunoprivileged, when there are high systemic levels of anti-AAV2 immunity, this can act as a barrier to effective gene transfer to the brain by AAV2 vectors. For example, injection of wild-type AAV2 into rats was sufficient to evoke neutralizing titers of >51,200 and this was effective in blocking AAV2-mediated gene transfer of the glial-derived neurotrophic factor (GDNF) gene (Penden *et al.*, 2004). But at lower anti-AAV2 neutralizing titers, there was only a weak negative correlation of the efficacy of gene transfer with neutralizing titer (Sanftner *et al.*, 2004). In the present study, there were no increases in anti-AAV2 neutralizing titer after direct CNS gene transfer to rats or nonhuman primates. These data are consistent with a previous study using CNS administration of AAV2-based vectors in nonhuman primates, which resulted in no change in anti-AAV neutralizing titers (Janson *et al.*, 2002). In rats, CNS administration may induce limited antivector immunity that results in a partial barrier against reuse of the same serotype, especially a short time after the first administration (Mastakov *et al.*, 2002b), and may limit the domain over which transgene expression is observed (Sanftner *et al.*, 2004). This response to AAV vectors is mild compared with the strong inflammatory response after CNS administration of adenoviral gene transfer vectors (Smith *et al.*, 1997).

Transgene-related host response

Systemic administration of AAV vectors may evoke an anti-transgene immune response and there are attempts to harness this response by using AAV as a vaccine carrier (Manning *et al.*, 1997; Xin *et al.*, 2002). But the major determinant of the antitransgene immune response is whether the expressed transgene protein is recognized as foreign by the host. In animal studies of factor IX gene transfer, using AAV2-based vectors delivered by the intramuscular and intravenous route, anti-factor IX antibodies are observed (Herzog *et al.*, 2002; Arruda *et al.*, 2004; Couto, 2004). Baboons administered an AAV2 vector expressing the human α_1 -antitrypsin gene by the intramuscular route developed antibodies against human α_1 -antitrypsin

(Song *et al.*, 2002). Macaques administered various serotypes of AAV vectors expressing erythropoietin (EPO) via the intramuscular route developed autoimmune anemia due to a strong humoral response to monkey EPO (Chenuaud *et al.*, 2004; Flotte, 2004; Gao *et al.*, 2004).

In contrast to these reports, there are several studies that describe long-term transgene expression mediated by AAV2, although immunological responses to the transgene product were not studied (Xiao *et al.*, 1996; Herzog *et al.*, 1997; Hernandez *et al.*, 1999; Monahan *et al.*, 2002). In the present study, the human cDNA for CLN2 was administered to animals that were wild type for the endogenous CLN2 genes that encode proteins 87% (rat; GenBank AH81775) and 97% (African green monkey; our unpublished data) identical to the human protein. Transgene expression was not explicitly assessed in this toxicology study, but it is expected on the basis of the proven potency of the vector *in vitro* and the results of our previous efficacy study (Sondhi *et al.*, 2005). In addition, although antitransgene immunity was not examined, whatever antitransgene response may have occurred after CNS administration of AAV2_{CU}hCLN2 is not sufficient to block long-term transgene expression in the CNS (Sondhi *et al.*, 2005).

Tumorigenesis

There has been some concern that AAV may cause cancer by insertional mutagenesis, following the observation that 10% of newborn mucopolysaccharide type VII knockout mice whose life had been prolonged by AAV2 gene transfer developed hepatocellular carcinoma or angiosarcoma over an 18-month time period (Donsante *et al.*, 2001; Monahan *et al.*, 2002). In the present study in rats, two mortalities were observed in the AAV2_{CU}hCLN2 group 152 and 329 days after vector injection. The cause of death of one was granular cell leukemia, whereas the other was due to a common disease in this strain of rats, chronic progressive nephropathy, unrelated to cancer. Granular cell leukemia is a common neoplasia in Fischer 344 rats (Boorman *et al.*, 1990), and therefore unlikely to be associated with the AAV vector. No tumors were observed in the nonhuman primates over a 1-year period after administration of the vector. In conjunction with other long-term toxicology studies, the absence of vector-related tumors in both rats and nonhuman primates in this study helps mitigate the concern about tumorigenesis related to AAV serotype 2 vectors.

Germ line transmission

A theoretical concern for AAV gene transfer is heritable genetic change due to insertion of AAV-derived DNA into the germ line. There are multiple studies on biodistribution and germ line transmission of the genome of AAV2 vectors that demonstrate that, although vector is disseminated from the administration site to many organs, including testes, there is no heritable insertion of AAV-derived DNA into the sperm genome (Kho *et al.*, 2000; Arruda *et al.*, 2001; Monahan *et al.*, 2002; Pachori *et al.*, 2004). Direct exposure of mouse sperm to AAV2 vectors failed to yield germ line transmission (Couto *et al.*, 2004). On the basis of those prior studies, in consultation with the U.S. Food and Drug Administration, biodistribution studies were not explicitly assessed in this study. Direct CNS

administration is unlikely to provide large amounts of vector systemically. For example, direct intracochlear administration of an AAV vector resulted in no detectable vector in liver, lung, heart, spleen, or kidney (Kho *et al.*, 2000). Because LINCL is a fatal childhood disease, germ line transmission is extremely unlikely to be an issue in human recipients of the AAV2_{CU}-hCLN2 vector.

ACKNOWLEDGMENTS

The authors thank the staff at the St. Kitts Biomedical Research Foundation, the staff at the Axion Research Foundation, and C. Harris and C. Bradley Bowman, Pathology Associates, for technical assistance; and N. Mohamed for help in preparing this manuscript. These studies were supported, in part, by U01 NS047458; the Nathan's Battle Foundation (Greenwood, IN); and the Will Rogers Memorial Fund (Los Angeles, CA).

REFERENCES

- AITKEN, M.L., MOSS, R.B., WALTZ, D.A., DOVEY, M.E., TONELLI, M.R., MCNAMARA, S.C., GIBSON, R.L., RAMSEY, B.W., CARTER, B.J., and REYNOLDS, T.C. (2001). A phase I study of aerosolized administration of tgAAVCF to cystic fibrosis subjects with mild lung disease. *Hum. Gene Ther.* **12**, 1907–1916.
- ARRUDA, V.R., FIELDS, P.A., MILNER, R., WAINWRIGHT, L., DE MIGUEL, M.P., DONOVAN, P.J., HERZOG, R.W., NICHOLS, T.C., BIEGEL, J.A., RAZAVI, M., DAKE, M., HUFF, D., FLAKE, A.W., COUTO, L., KAY, M.A., and HIGH, K.A. (2001). Lack of germline transmission of vector sequences following systemic administration of recombinant AAV-2 vector in males. *Mol. Ther.* **4**, 586–592.
- ARRUDA, V.R., SCHUETTRUMPF, J., HERZOG, R.W., NICHOLS, T.C., ROBINSON, N., LOTFI, Y., MINGOZZI, F., XIAO, W., COUTO, L.B., and HIGH, K.A. (2004). Safety and efficacy of factor IX gene transfer to skeletal muscle in murine and canine hemophilia B models by adeno-associated viral vector serotype 1. *Blood* **103**, 85–92.
- ATABEK, U., ALVAREZ, R., PELLO, M.J., ALEXANDER, J.B., CAMISHION, R.C., CURRY, C., and SPENCE, R.K. (1995). Erythropoietin accelerates hematocrit recovery in post-surgical anemia. *Am. Surg.* **61**, 74–77.
- BIRCH, D.G. (1999). Retinal degeneration in retinitis pigmentosa and neuronal ceroid lipofuscinosis: An overview. *Mol. Genet. Metab.* **66**, 356–366.
- BOHN, M.C., CHOI-LUNDBERG, D.L., DAVIDSON, B.L., LERANTH, C., KOZLOWSKI, D.A., SMITH, J.C., O'BANION, M.K., and REDMOND, D.E. (1999). Adenovirus-mediated transgene expression in nonhuman primate brain. *Hum. Gene Ther.* **10**, 1175–1184.
- BOORMAN, G.A., EUSTIS, S.L., ELWELL, M.R., and MONTGOMERY, C. (1990). *Pathology of the Fischer Rat: Reference and Atlas*. (Academic Press, San Diego, CA).
- BOUSTANY, R.M. (1996). Batten disease or neuronal ceroid lipofuscinosis. In: Moser, H.W., ed. *Handbook of Clinical Neurology* (Vol. 22): *Neurodystrophies and Neurolipidoses* (Elsevier Science, New York), pp. 671–700.
- BROUGH, D.E., LIZONOVA, A., HSU, C., KULESA, V.A., and KOVESDI, I. (1996). A gene transfer vector–cell line system for complete functional complementation of adenovirus early regions E1 and E4. *J. Virol.* **70**, 6497–6501.
- CHENUAUD, P., LARCHER, T., RABINOWITZ, J.E., PROVOST, N., CHEREL, Y., CASADEVALL, N., SAMULSKI, R.J., and MOULLIER, P. (2004). Autoimmune anemia in macaques following erythropoietin gene therapy. *Blood* **103**, 3303–3304.
- CHIRMULE, N., XIAO, W., TRUNEH, A., SCHNELL, M.A., HUGHES, J.V., ZOLTICK, P., and WILSON, J.M. (2000). Humoral immunity to adeno-associated virus type 2 vectors following administration to murine and nonhuman primate muscle. *J. Virol.* **74**, 2420–2425.
- COUTO, L.B. (2004). Preclinical gene therapy studies for hemophilia using adeno-associated virus (AAV) vectors. *Semin. Thromb. Hemost.* **30**, 161–171.
- COUTO, L., PARKER, A., and GORDON, J.W. (2004). Direct exposure of mouse spermatozoa to very high concentrations of a serotype-2 adeno-associated virus gene therapy vector fails to lead to germ cell transduction. *Hum. Gene Ther.* **15**, 287–291.
- CRYSTAL, R.G., SONDHI, D., HACKETT, N.R., KAMINSKY, S.M., WORGALL, S., STIEG, P., SOUWEIDANE, M., HOSAIN, S., HEIER, L., BALLON, D., DINNER, M., WISNIEWSKI, K., KAPLITT, M.G., GREENWALD, B.M., HOWELL, J.D., STRYBING, K., DYKE, J., and VOOS, H. (2004). Administration of a replication-deficient adeno-associated virus gene transfer vector expressing the human CLN2 cDNA to the brain of children with late infantile neuronal ceroid lipofuscinosis. *Hum. Gene Ther.* **15**, 1131–1154.
- DALY, T.M., OKUYAMA, T., VOGLER, C., HASKINS, M.E., MUZYCZKA, N., and SANDS, M.S. (1999a). Neonatal intramuscular injection with recombinant adeno-associated virus results in prolonged β -glucuronidase expression *in situ* and correction of liver pathology in mucopolysaccharidosis type VII mice. *Hum. Gene Ther.* **10**, 85–94.
- DALY, T.M., VOGLER, C., LEVY, B., HASKINS, M.E., and SANDS, M.S. (1999b). Neonatal gene transfer leads to widespread correction of pathology in a murine model of lysosomal storage disease. *Proc. Natl. Acad. Sci. U.S.A.* **96**, 2296–2300.
- DONSANTE, A., VOGLER, C., MUZYCZKA, N., CRAWFORD, J.M., BARKER, J., FLOTTE, T., CAMPBELL-THOMPSON, M., DALY, T., and SANDS, M.S. (2001). Observed incidence of tumorigenesis in long-term rodent studies of rAAV vectors. *Gene Ther.* **8**, 1343–1346.
- DURING, M.J., KAPLITT, M.G., STERN, M.B., and EIDELBERG, D. (2001). Subthalamic GAD gene transfer in Parkinson disease patients who are candidates for deep brain stimulation. *Hum. Gene Ther.* **12**, 1589–1591.
- EZAKI, J., TANIDA, I., KANEHAGI, N., and KOMINAMI, E. (1999). A lysosomal proteinase, the late infantile neuronal ceroid lipofuscinosis gene (CLN2) product, is essential for degradation of a hydrophobic protein, the subunit c of ATP synthase. *J. Neurochem.* **72**, 2573–2582.
- FAVRE, D., PROVOST, N., BLOUIN, V., BLANCHO, G., CHEREL, Y., SALVETTI, A., and MOULLIER, P. (2001). Immediate and long-term safety of recombinant adeno-associated virus injection into the nonhuman primate muscle. *Mol. Ther.* **4**, 559–566.
- FIELD, M., WITHAM, T.F., FLICKINGER, J.C., KONDZIOLKA, D., and LUNSFORD, L.D. (2001). Comprehensive assessment of hemorrhage risks and outcomes after stereotactic brain biopsy. *J. Neurosurg.* **94**, 545–551.
- FLOTTE, T.R. (2004). Immune responses to recombinant adeno-associated virus vectors: Putting preclinical findings into perspective. *Hum. Gene Ther.* **15**, 716–717.
- FLOTTE, T.R., ZEITLIN, P.L., REYNOLDS, T.C., HEALD, A.E., PEDERSEN, P., BECK, S., CONRAD, C.K., BRASS-ERNST, L., HUMPHRIES, M., SULLIVAN, K., WETZEL, R., TAYLOR, G., CARTER, B.J., and GUGGINO, W.B. (2003). Phase I trial of intranasal and endobronchial administration of a recombinant adeno-associated virus serotype 2 (rAAV2)-CFTR vector in adult cystic fibrosis patients: A two-part clinical study. *Hum. Gene Ther.* **14**, 1079–1088.

- FLOTTE, T.R., BRANTLY, M.L., SPENCER, L.T., BYRNE, B.J., SPENCER, C.T., BAKER, D.J., and HUMPHRIES, M. (2004). Phase I trial of intramuscular injection of a recombinant adeno-associated virus α_1 -antitrypsin (rAAV2-CB-hAAT) gene vector to AAT-deficient adults. *Hum. Gene Ther.* **15**, 93–128.
- FUJITA, T., YOSHIMINE, T., MARUNO, M., and HAYAKAWA, T. (1998). Cellular dynamics of macrophages and microglial cells in reaction to stab wounds in rat cerebral cortex. *Acta Neurochir.* **140**, 275–279.
- GAO, G., LEBHERZ, C., WEINER, D.J., GRANT, R., CALCEDO, R., MCCULLOUGH, B., BAGG, A., ZHANG, Y., and WILSON, J.M. (2004). Erythropoietin gene therapy leads to autoimmune anemia in macaques. *Blood* **103**, 3300–3302.
- GAO, G.P., ALVIRA, M.R., WANG, L., CALCEDO, R., JOHNSTON, J., and WILSON, J.M. (2002). Novel adeno-associated viruses from rhesus monkeys as vectors for human gene therapy. *Proc. Natl. Acad. Sci. U.S.A.* **99**, 11854–11859.
- GRIMM, D., KERN, A., RITTNER, K., and KLEINSCHMIDT, J.A. (1998). Novel tools for production and purification of recombinant adeno-associated virus vectors. *Hum. Gene Ther.* **9**, 2745–2760.
- HALTIA, M. (2003). The neuronal ceroid-lipofuscinoses. *J. Neuropathol. Exp. Neurol.* **62**, 1–13.
- HASKELL, R.E., HUGHES, S.M., CHIORINI, J.A., ALISKY, J.M., and DAVIDSON, B.L. (2003). Viral-mediated delivery of the late-infantile neuronal ceroid lipofuscinosis gene, TPP-I to the mouse central nervous system. *Gene Ther.* **10**, 34–42.
- HERNANDEZ, Y.J., WANG, J., KEARNS, W.G., LOILER, S., POIRIER, A., and FLOTTE, T.R. (1999). Latent adeno-associated virus infection elicits humoral but not cell-mediated immune responses in a nonhuman primate model. *J. Virol.* **73**, 8549–8558.
- HERZOG, R.W., HAGSTROM, J.N., KUNG, S.H., TAI, S.J., WILSON, J.M., FISHER, K.J., and HIGH, K.A. (1997). Stable gene transfer and expression of human blood coagulation factor IX after intramuscular injection of recombinant adeno-associated virus. *Proc. Natl. Acad. Sci. U.S.A.* **94**, 5804–5809.
- HERZOG, R.W., FIELDS, P.A., ARRUDA, V.R., BRUBAKER, J.O., ARMSTRONG, E., MCLINTOCK, D., BELLINGER, D.A., COUTO, L.B., NICHOLS, T.C., and HIGH, K.A. (2002). Influence of vector dose on factor IX-specific T and B cell responses in muscle-directed gene therapy. *Hum. Gene Ther.* **13**, 1281–1291.
- JANSON, C., MCPHEE, S., BILANIUK, L., HASELGROVE, J., TESTAIUTI, M., FREESE, A., WANG, D.J., SHERA, D., HURH, P., RUPIN, J., SASLOW, E., GOLDFARB, O., GOLDBERG, M., LARIJANI, G., SHARRAR, W., LIOUTERMAN, L., CAMP, A., KOLODNY, E., SAMULSKI, J., and LEONE, P. (2002). Gene therapy of Canavan disease: AAV-2 vector for neurosurgical delivery of aspartoacylase gene (ASPA) to the human brain [clinical protocol]. *Hum. Gene Ther.* **13**, 1391–1412.
- KAUR, C., LING, E.A., and WONG, W.C. (1987). Origin and fate of neural macrophages in a stab wound of the brain of the young rat. *J. Anat.* **154**, 215–227.
- KAY, M.A., MANNO, C.S., RAGNI, M.V., LARSON, P.J., COUTO, L.B., MCCLELLAND, A., GLADER, B., CHEW, A.J., TAI, S.J., HERZOG, R.W., ARRUDA, V., JOHNSON, F., SCALLAN, C., SKARSGARD, E., FLAKE, A.W., and HIGH, K.A. (2000). Evidence for gene transfer and expression of factor IX in haemophilia B patients treated with an AAV vector. *Nat. Genet.* **24**, 257–261.
- KHO, S.T., PETTIS, R.M., MHATRE, A.N., and LALWANI, A.K. (2000). Safety of adeno-associated virus as cochlear gene transfer vector: Analysis of distant spread beyond injected cochleae. *Mol. Ther.* **2**, 368–373.
- KOZLOWSKI, D.A., BREMER, E., REDMOND, D.E., GEORGE, D., LARSON, B., and BOHN, M.C. (2001). Quantitative analysis of transgene protein, mRNA, and vector DNA following injection of an adenoviral vector harboring glial cell line-derived neurotrophic factor into the primate caudate nucleus. *Mol. Ther.* **3**, 256–261.
- LIN, L., and LOBEL, P. (2001). Production and characterization of recombinant human CLN2 protein for enzyme-replacement therapy in late infantile neuronal ceroid lipofuscinosis. *Biochem. J.* **357**, 49–55.
- LIN, L., SOHAR, I., LACKLAND, H., and LOBEL, P. (2001). The human CLN2 protein/tripeptidyl-peptidase I is a serine protease that autoactivates at acidic pH. *J. Biol. Chem.* **276**, 2249–2255.
- LO, W.D., QU, G., SFERRA, T.J., CLARK, R., CHEN, R., and JOHNSON, P.R. (1999). Adeno-associated virus-mediated gene transfer to the brain: duration and modulation of expression. *Hum. Gene Ther.* **10**, 201–213.
- MA, K.C., CHANG, Z.H., SHIH, H., ZHU, J.H., and WU, J.Y. (1991). The compensatory ‘rebound’ of reactive astrogliosis: Glial fibrillary acidic protein immunohistochemical analysis of reactive astrogliosis after a puncture wound to the brain of rats with portocaval anastomosis. *Acta Neuropathol.* **82**, 72–77.
- MANNING, W.C., PALIARD, X., ZHOU, S., PAT, B.M., LEE, A.Y., HONG, K., WALKER, C.M., ESCOBEDO, J.A., and DWARKI, V. (1997). Genetic immunization with adeno-associated virus vectors expressing herpes simplex virus type 2 glycoproteins B and D. *J. Virol.* **71**, 7960–7962.
- MANNO, C.S., CHEW, A.J., HUTCHISON, S., LARSON, P.J., HERZOG, R.W., ARRUDA, V.R., TAI, S.J., RAGNI, M.V., THOMPSON, A., OZELO, M., COUTO, L.B., LEONARD, D.G., JOHNSON, F.A., MCCLELLAND, A., SCALLAN, C., SKARSGARD, E., FLAKE, A.W., KAY, M.A., HIGH, K.A., and GLADER, B. (2003). AAV-mediated factor IX gene transfer to skeletal muscle in patients with severe hemophilia B. *Blood* **101**, 2963–2972.
- MASTAKOV, M.Y., BAER, K., KOTIN, R.M., and DURING, M.J. (2002a). Recombinant adeno-associated virus serotypes 2- and 5-mediated gene transfer in the mammalian brain: Quantitative analysis of heparin co-infusion. *Mol. Ther.* **5**, 371–380.
- MASTAKOV, M.Y., BAER, K., SYMES, C.W., LEICHTLEIN, C.B., KOTIN, R.M., and DURING, M.J. (2002b). Immunological aspects of recombinant adeno-associated virus delivery to the mammalian brain. *J. Virol.* **76**, 8446–8454.
- MONAHAN, P.E., JOOSS, K., and SANDS, M.S. (2002). Safety of adeno-associated virus gene therapy vectors: A current evaluation. *Expert Opin. Drug Saf.* **1**, 79–91.
- MOSKALENKO, M., CHEN, L., VAN ROEY, M., DONAHUE, B.A., SNYDER, R.O., MCARTHUR, J.G., and PATEL, S.D. (2000). Epitope mapping of human anti-adeno-associated virus type 2 neutralizing antibodies: Implications for gene therapy and virus structure. *J. Virol.* **74**, 1761–1766.
- MOSS, R.B., RODMAN, D., SPENCER, L.T., AITKEN, M.L., ZEITLIN, P.L., WALTZ, D., MILLA, C., BRODY, A.S., CLANCY, J.P., RAMSEY, B., HAMBLETT, N., and HEALD, A.E. (2004). Repeated adeno-associated virus serotype 2 aerosol-mediated cystic fibrosis transmembrane regulator gene transfer to the lungs of patients with cystic fibrosis: A multicenter, double-blind, placebo-controlled trial. *Chest* **125**, 509–521.
- MURAMATSU, S., FUJIMOTO, K., IKEGUCHI, K., SHIZUMA, N., KAWASAKI, K., ONO, F., SHEN, Y., WANG, L., MIZUKAMI, H., KUME, A., MATSUMURA, M., NAGATSU, I., URANO, F., ICHINOSE, H., NAGATSU, T., TERAOKA, K., NAKANO, I., and OZAWA, K. (2002). Behavioral recovery in a primate model of Parkinson’s disease by triple transduction of striatal cells with adeno-associated viral vectors expressing dopamine-synthesizing enzymes. *Hum. Gene Ther.* **13**, 345–354.
- NGUYEN, J.B., SANCHEZ-PERNAUTE, R., CUNNINGHAM, J., and BANKIEWICZ, K.S. (2001). Convection-enhanced delivery of AAV-2 combined with heparin increases TK gene transfer in the rat brain. *Neuroreport* **12**, 1961–1964.
- NIWA, H., YAMAMURA, K., and MIYAZAKI, J. (1991). Efficient selection for high-expression transfectants with a novel eukaryotic vector. *Gene* **108**, 193–199.
- PACHORI, A.S., MELO, L.G., ZHANG, L., LODA, M., PRATT, R.E.,

- and DZAU, V.J. (2004). Potential for germ line transmission after intramyocardial gene delivery by adeno-associated virus. *Biochem. Biophys. Res. Commun.* **313**, 528–533.
- PALMER, D.N., FEARNLEY, I.M., WALKER, J.E., HALL, N.A., LAKE, B.D., WOLFE, L.S., HALTIA, M., MARTINUS, R.D., and JOLLY, R.D. (1992). Mitochondrial ATP synthase subunit c storage in the ceroid-lipofuscinoses (Batten disease). *Am. J. Med. Genet.* **42**, 561–567.
- PENDEN, C.S., BURGER, C., MUZYCZKA, N., and MANDEL, R.J. (2004). Circulating anti-wild-type adeno-associated virus type 2 (AAV2) antibodies inhibit recombinant AAV2 (rAAV2)-mediated, but not rAAV5-mediated, gene transfer in the brain. *J. Virol.* **78**, 6344–6359.
- SANFTNER, L.M., SUZUKI, B.M., DOROUDCHI, M.M., FENG, L., McCLELLAND, A., FORSAYETH, J.R., and CUNNINGHAM, J. (2004). Striatal delivery of rAAV-hAADC to rats with preexisting immunity to AAV. *Mol. Ther.* **9**, 403–409.
- SLEAT, D.E., DONNELLY, R.J., LACKLAND, H., LIU, C.G., SOHAR, I., PULLARKAT, R.K., and LOBEL, P. (1997). Association of mutations in a lysosomal protein with classical late-infantile neuronal ceroid lipofuscinosis. *Science* **277**, 1802–1805.
- SLEAT, D.E., GIN, R.M., SOHAR, I., WISNIEWSKI, K., SKLOWER-BROOKS, S., PULLARKAT, R.K., PALMER, D.N., LERNER, T.J., BOUSTANY, R.M., ULDALL, P., SIAKOTOS, A.N., DONNELLY, R.J., and LOBEL, P. (1999). Mutational analysis of the defective protease in classic late-infantile neuronal ceroid lipofuscinosis, a neurodegenerative lysosomal storage disorder. *Am. J. Hum. Genet.* **64**, 1511–1523.
- SMITH, D.E., ROBERTS, J., GAGE, F.H., and TUSZYNSKI, M.H. (1999). Age-associated neuronal atrophy occurs in the primate brain and is reversible by growth factor gene therapy. *Proc. Natl. Acad. Sci. U.S.A.* **96**, 10893–10898.
- SMITH, J.G., RAPER, S.E., WHEELDON, E.B., HACKNEY, D., JUDY, K., WILSON, J.M., and ECK, S.L. (1997). Intracranial administration of adenovirus expressing HSV-TK in combination with ganciclovir produces a dose-dependent, self-limiting inflammatory response. *Hum. Gene Ther.* **8**, 943–954.
- SONDHI, D., HACKETT, N.R., APBLET, R.L., KAMINSKY, S.M., PERGOLIZZI, R.G., and CRYSTAL, R.G. (2001). Feasibility of gene therapy for late neuronal ceroid lipofuscinosis. *Arch. Neurol.* **58**, 1793–1798.
- SONDHI, D., PETERSON, D.A., GIANNARIS, E.L., SANDERS, C.T., MENDEZ, B.S., DE, B., ROSTKOWSKI, A., BLANCARD, B., BJUGSTAD, K., SLADEK, J.R., REDMOND, D.E., LEOPOLD, P.L., KAMINSKY, S.M., HACKETT, N.R., and CRYSTAL, R.G. (2005). AAV2-mediated CLN2 gene transfer to rodent and non-human primate brain results in long term TPP-1 expression compatible with therapy for LINCL. *Gene Ther.* **12**, 1618–1632.
- SONG, S., SCOTT-JORGENSEN, M., WANG, J., POIRIER, A., CRAWFORD, J., CAMPBELL-THOMPSON, M., and FLOTTE, T.R. (2002). Intramuscular administration of recombinant adeno-associated virus 2 α -1 antitrypsin (rAAV-SERPINA1) vectors in a non-human primate model: Safety and immunologic aspects. *Mol. Ther.* **6**, 329–335.
- TAYLOR, J.R., ELSWORTH, J.D., ROTH, R.H., SLADEK, J.R., and REDMOND, D.E. (1994). Behavioral effects of MPTP administration in the vervet monkey: A primate model of Parkinson's disease. In: Woodruff, M.L., and Nonneman, A.J., eds. *Toxin-Induced Models of Neurological Disorders*. (Plenum Press, New York), pp. 139–173.
- TAYLOR, J.R., ELSWORTH, J.D., ROTH, R.H., SLADEK, J.R., and REDMOND, D.E. (1997). Severe long-term 1-methyl-4-phenyl-1,2,3,6-tetrahydropyridine-induced parkinsonism in the vervet monkey (*Cercopithecus aethiops sabaeus*). *Neuroscience* **81**, 745–755.
- UMEHARA, F., HIGUCHI, I., TANAKA, K., NIIYAMA, T., EZAKI, J., KOMINAMI, E., and OSAME, M. (1997). Accumulation of mitochondrial ATP synthase subunit c in muscle in a patient with neuronal ceroid lipofuscinosis (late infantile form). *Acta Neuropathol.* **93**, 628–632.
- VINES, D.J., and WARBURTON, M.J. (1999). Classical late infantile neuronal ceroid lipofuscinosis fibroblasts are deficient in lysosomal tripeptidyl peptidase I. *FEBS Lett.* **443**, 131–135.
- WAGNER, J.A., NEPOMUCENO, I.B., MESSNER, A.H., MORAN, M.L., BATSON, E.P., DIMICELI, S., BROWN, B.W., DESCH, J.K., NORBASH, A.M., CONRAD, C.K., GUGGINO, W.B., FLOTTE, T.R., WINE, J.J., CARTER, B.J., REYNOLDS, T.C., MOSS, R.B., and GARDNER, P. (2002). A phase II, double-blind, randomized, placebo-controlled clinical trial of tgAAVCF using maxillary sinus delivery in patients with cystic fibrosis with antrostomies. *Hum. Gene Ther.* **13**, 1349–1359.
- WILLIAMS, R.E., GOTTLÖB, I., LAKE, B.D., GOEBEL, H.H., WINCHESTER, B.G., and WHEELER, R.B. (1999). CLN2: Classic late infantile NCL. In: Goebel, H.H., Mole, S.E., and Lake, B.D., eds. *The Neuronal Ceroid Lipofuscinoses (Batten Disease)*. (IOS Press, Amsterdam), pp. 37–54.
- WINER, B.J. (1971). *Statistical Principles in Experimental Design*. (McGraw-Hill, New York).
- XIAO, W., CHIRMULE, N., SCHNELL, M.A., TAZELAAR, J., HUGHES, J.V., and WILSON, J.M. (2000). Route of administration determines induction of T-cell-independent humoral responses to adeno-associated virus vectors. *Mol. Ther.* **1**, 323–329.
- XIAO, X., LI, J., and SAMULSKI, R.J. (1996). Efficient long-term gene transfer into muscle tissue of immunocompetent mice by adeno-associated virus vector. *J. Virol.* **70**, 8098–8108.
- XIN, K.Q., OOKI, T., MIZUKAMI, H., HAMAJIMA, K., OKUDELA, K., HASHIMOTO, K., KOJIMA, Y., JOUNAI, N., KUMAMOTO, Y., SASAKI, S., KLINMAN, D., OZAWA, K., and OKUDA, K. (2002). Oral administration of recombinant adeno-associated virus elicits human immunodeficiency virus-specific immune responses. *Hum. Gene Ther.* **13**, 1571–1581.
- XUE, M., and DEL BIGIO, M.R. (2001). Acute tissue damage after injections of thrombin and plasmin into rat striatum. *Stroke* **32**, 2164–2169.
- ZOLOTUKHIN, S., BYRNE, B.J., MASON, E., ZOLOTUKHIN, I., POTTER, M., CHESNUT, K., SUMMERFORD, C., SAMULSKI, R.J., and MUZYCZKA, N. (1999). Recombinant adeno-associated virus purification using novel methods improves infectious titer and yield. *Gene Ther.* **6**, 973–985.

Address reprint requests to:

Dr. Ronald G. Crystal
Department of Genetic Medicine
Weill Medical College of Cornell University
515 East 71st Street, S-1000
New York, NY 10021

E-mail: geneticmedicine@med.cornell.edu

Received for publication April 22, 2005; accepted after revision September 14, 2005.

Published online: November 30, 2005.

Intracranial Delivery of CLN2 Reduces Brain Pathology in a Mouse Model of Classical Late Infantile Neuronal Ceroid Lipofuscinosis

Marco A. Passini,¹ James C. Dodge,¹ Jie Bu,¹ Wendy Yang,¹ Qi Zhao,¹ Dolan Sondhi,² Neil R. Hackett,² Stephen M. Kaminsky,² Qinwen Mao,³ Lamya S. Shihabuddin,¹ Seng H. Cheng,¹ David E. Sleat,⁴ Gregory R. Stewart,¹ Beverly L. Davidson,³ Peter Lobel,⁴ and Ronald G. Crystal²

¹Neuroscience, Genzyme Corporation, Framingham, Massachusetts 01701, ²Genetic Medicine, Weill Medical College of Cornell University, New York, New York 10021, ³Internal Medicine, University of Iowa College of Medicine, Iowa City, Iowa 52242, and ⁴Center for Advanced Biotechnology and Medicine, Robert Wood Johnson Medical College, Piscataway, New Jersey 08854

Classical late infantile neuronal ceroid lipofuscinosis (cLINCL) is a lysosomal storage disorder caused by mutations in *CLN2*, which encodes lysosomal tripeptidyl peptidase I (TPP1). Lack of TPP1 results in accumulation of autofluorescent storage material and curvilinear bodies in cells throughout the CNS, leading to progressive neurodegeneration and death typically in childhood. In this study, we injected adeno-associated virus (AAV) vectors containing the human *CLN2* cDNA into the brains of *CLN2*^{-/-} mice to determine therapeutic efficacy. AAV2_{CU}hCLN2 or AAV5_{CU}hCLN2 were stereotactically injected into the motor cortex, thalamus, and cerebellum of both hemispheres at 6 weeks of age, and mice were then killed at 13 weeks after injection. Mice treated with AAV2_{CU}hCLN2 and AAV5_{CU}hCLN2 contained TPP1 activity at each injection tract that was equivalent to 0.5- and 2-fold that of *CLN2*^{+/+} control mice, respectively. Lysosome-associated membrane protein 1 immunostaining and confocal microscopy showed intracellular targeting of TPP1 to the lysosomal compartment. Compared with control animals, there was a marked reduction of autofluorescent storage in the AAV2_{CU}hCLN2 and AAV5_{CU}hCLN2 injected brain regions, as well as adjacent regions, including the striatum and hippocampus. Analysis by electron microscopy confirmed a significant decrease in pathological curvilinear bodies in cells. This study demonstrates that AAV-mediated TPP1 enzyme replacement corrects the hallmark cellular pathologies of cLINCL in the mouse model and raises the possibility of using AAV gene therapy to treat cLINCL patients.

Key words: AAV; LINCL; neurodegeneration; TPP1; Batten; lysosomal storage disease

Introduction

The neuronal ceroid lipofuscinoses (NCLs) are a group of at least seven inherited lysosomal storage disorders (LSDs) characterized by the intracellular accumulation of autofluorescent storage material, which is the hallmark cellular phenotype for this disease family (Hofmann and Peltonen, 2001). In addition, many of the NCLs contain ultrastructural pathology that can be visualized by electron microscopy. These include granular osmiophilic deposits, curvilinear bodies, and fingerprint profiles for infantile NCL (INCL), classical late infantile NCL (cLINCL), and juvenile NCL, respectively (Elleder et al., 1999; Haltia, 2003; Beaudoin et al., 2004). Lysosomal pathology predominately occurs in the CNS, but some storage defect can also be found in visceral tissue (Car-

penter et al., 1972; Hofmann and Peltonen, 2001). cLINCL, also known as Jansky-Bielschowsky disease, is caused by mutations in *CLN2* (Sleat et al., 1997) that encodes the lysosomal enzyme tripeptidyl peptidase I (TPP1) (Rawlings and Barrett, 1999; Vines and Warburton, 1999). cLINCL patients typically exhibit neurological impairment beginning at 2–4 years of age that can be verified by electroencephalography and magnetic resonance imaging (Autti et al., 1997; Williams et al., 1999). Disease progression is unyielding and leads to ataxia, mental retardation, blindness, dementia, seizures, and death between the ages of 7 and 15 years (Hofmann and Peltonen, 2001). There is currently no effective treatment for cLINCL.

Patients with cLINCL may benefit from gene therapy because it is a monogenic disease. Introducing a functional version of *CLN2* to the brain by intracranial injection of a viral vector may remove storage material and rescue cells from dysfunction. This strategy was shown to be effective in other mouse and cat models of LSDs treated with adeno-associated virus (AAV) vectors (Skorupa et al., 1999; Bosch et al., 2000; Sferra et al., 2000; Frisella et al., 2001; Matalon et al., 2003; Passini et al., 2003, 2005; Cressant et al., 2004; Desmaris et al., 2004; Griffey et al., 2004; Klugmann et al., 2005; Rafi et al., 2005; Vite et al., 2005). However,

Received June 29, 2005; revised Dec. 2, 2005; accepted Dec. 5, 2005.

This work was supported by National Institutes of Health Grants U01 NS047458 (R.G.C.) and R01 NS037918 (P.L.), Batten Disease Support and Research Association, Roy J. Carver Trust, and Nathan's Battle Foundation. We thank T. Taksir, D. Griffiths, D. Matthews, P. Piepenhagen, H. Collins, M. El-Banna, E. Giannaris, E. Vassallo, L. Curtin, and Department of Comparative Medicine for assistance.

Correspondence should be addressed to Marco A. Passini, Genzyme Corporation, One Mountain Road, Framingham, MA 01701-9322. E-mail: marco.passini@genzyme.com.

DOI:10.1523/JNEUROSCI.2676-05.2006

Copyright © 2006 Society for Neuroscience 0270-6474/06/261334-09\$15.00/0

until only recently, an appropriate mouse model was not available to test this therapeutic approach for cLINCL. Previous studies in normal rodents and nonhuman primates showed that human TPP1 protein could be expressed in the brain after intracranial injection of recombinant AAV vectors that contained the human CLN2 cDNA (Haskell et al., 2003; Sondhi et al., 2005). Those studies also demonstrate that human TPP1 protein is secreted by transduced cells and taken up by neighboring cells via receptor-mediated endocytosis, similar to that observed for other lysosomal enzymes (Neufeld, 1991).

A CLN2 knock-out mouse model of cLINCL was recently generated and characterized (Sleat et al., 2004). *CLN2*^{-/-} mice contain undetectable levels of TPP1 activity, which results in lysosomal pathology and progressive neurodegeneration that recapitulate the human disease (Sleat et al., 2004). In this study, we investigated the ability of AAV gene therapy to correct lysosomal storage pathology in *CLN2*^{-/-} mice. Our results demonstrate that the mutant brain responds to AAV-mediated TPP1 enzyme replacement by showing a substantial reduction in brain pathology. The information in this study provides proof-of-principle that delivery of human CLN2 cDNA to the diseased brain is a promising strategy for treating cLINCL.

Materials and Methods

AAV vector production. The genomic structures of AAV2_{CU}hCLN2 and AAV5_{CU}hCLN2 were identical to each other and contained serotype-2 inverted terminal repeats and the human CLN2 cDNA under the control of the cytomegalovirus enhancer chicken β -actin promoter. The AAV2_{CU}NULL control vector was also similar except that the human CLN2 cDNA was substituted with a noncoding DNA sequence of equal size. The detailed description of the recombinant genomes used in this study and the production and characterization of AAV2_{CU}hCLN2 and AAV2_{CU}NULL were reported previously by Sondhi et al. (2005). AAV5_{CU}hCLN2 was produced by cotransfection of helper plasmid pPAK-MA5 and CLN2 plasmid pAAV2-CAG-hCLN2 in a 10-Stack Cell-Factor (VWR Scientific, West Chester, PA) containing human 293 cells. Seventy-two hours after transfection, cells were harvested, and viral lysate was collected, treated with benzonase, clarified by centrifugation, and purified by discontinuous iodixanol gradients. Pooled fractions containing AAV5 were treated with 0.5% octyl glucopyranoside, loaded onto a Q-HP anion exchange column, eluted using a linear 0–1 M NaCl gradient, and concentrated by dialysis against 120 g/L dextran-40. *In vitro* enzyme assays verified that AAV2_{CU}hCLN2 and AAV5_{CU}hCLN2 expressed TPP1. Viral vectors were made under good manufacturing practice, and the titers of AAV2_{CU}hCLN2, AAV2_{CU}NULL, and AAV5_{CU}hCLN2 were 2.0×10^{11} genome copies (gc)/ml.

Injection of AAV vectors into the *CLN2*^{-/-} brain. All procedures were performed under a protocol approved by the Institutional Animal Care and Use Committee. Mice were housed under 12 h light/dark cycle and were provided with food and water *ad libitum*. The genotypes of *CLN2*^{-/-}, *CLN2*^{+/-}, and *CLN2*^{+/+} littermates were confirmed by PCR as described previously (Sleat et al., 2004). In the pilot study, 25 *CLN2*^{-/-} mice at 6 or 10 weeks of age underwent stereotaxic brain surgery and were injected into two sites along a single needle tract with AAV2_{CU}hCLN2 ($n = 14$), AAV2_{CU}NULL ($n = 7$), or saline ($n = 4$). Injections were performed in the thalamus (2.00 mm caudal to bregma, 1.75 mm right of midline, 3.50 mm ventral to pial surface) and hippocampus (2.00 mm caudal to bregma, 1.75 mm right of midline, 1.75 mm ventral to pial surface) of the right hemisphere. Three microliters (6.0×10^8 gc) of either vector were dispensed with a Hamilton syringe (Hamilton, Reno, NV) into each structure for a total of $6 \mu\text{l}$ (1.2×10^9 gc) per brain. In the serotype comparison study, 17 *CLN2*^{-/-} mice at 6 weeks of age underwent stereotaxic brain surgery and received six injections (three per hemisphere) in six different needle tracts with AAV2_{CU}hCLN2 ($n = 8$) or AAV5_{CU}hCLN2 ($n = 9$). Injections were done bilaterally in the motor cortex (1.00 mm rostral to bregma, 1.25 mm from midline, 1.25 mm ventral to pial surface), thalamus (2.00 mm caudal to bregma, 1.75 mm

from midline, 3.50 mm ventral to pial surface), and cerebellum (6.00 mm caudal to bregma, 1.50 mm from midline, 1.50 mm ventral to pial surface). Three microliters (6.0×10^8 gc) of either vector were injected with a Hamilton syringe for a total of $9 \mu\text{l}$ (1.8×10^9 gc) per hemisphere and $18 \mu\text{l}$ (3.6×10^9 gc) per brain. The injections in both the pilot and serotype comparison studies were performed at a rate of 0.5 $\mu\text{l}/\text{min}$, and the needle was left in place for 2 min after each injection to minimize upward flow of viral solution after raising the needle.

Evaluation of TPP1 enzyme activity in vivo. For measurement of TPP1 activity, mice were perfused with PBS, and brains were removed and cut into 2 mm coronal slabs using a brain matrix (Harvard Apparatus, Holliston, MA). Tissue extracts were prepared by homogenization in 150 mM NaCl and 1 g/L Triton X-100 using a disposable pellet pestle and 1.5 ml matching tube (Kimble-Kontes, Vineland, NJ) and clarified by centrifugation. Supernatants were analyzed for TPP1 activity as described previously (Sohar et al., 2000) after incubation at pH 3.5 to activate TPP1 precursor (Lin et al., 2001). The final activity of TPP1 was calculated by measuring the change in fluorescence units (FU) per minute per milligram of protein (standardized by BCA protein assay; Pierce, Rockford, IL).

Immunohistochemistry. Brains designated for histological analysis were drop fixed in 4% paraformaldehyde, pH 7.4, for 48 h, cut with a vibratome into 50 μm sections, and stored free floating in KPB (0.1 M potassium phosphate, pH 7.4) at 4°C. Brain sections were blocked in 5% normal donkey serum, 0.2% Triton X-100, and 0.1 M potassium phosphate saline, pH 7.2, for 1 h at room temperature (RT). A human-specific CLN2 polyclonal antibody (Haskell et al., 2003) was diluted 1:1000 in blocking solution and added to brain sections for 1 h at RT, followed by overnight incubation at 4°C. An anti-rabbit biotinylated secondary antibody (Jackson ImmunoResearch, West Grove, PA) was diluted 1:250 in PBS and incubated on brain sections for 1 h at RT. TPP1 immunopositive cells were visualized with a streptavidin–fluorescein conjugate (Jackson ImmunoResearch). Purkinje cells were labeled with calbindin D monoclonal antibody (Sigma, St. Louis, MO) at 1:2500 dilution, neurons were labeled with neuron-specific nuclear protein (NeuN) monoclonal antibody (Chemicon, Temecula, CA) at 1:100 dilution, astrocytes were labeled with glial fibrillary acidic protein (GFAP) monoclonal antibody (Sigma) at 1:1000 dilution, and lysosomes were labeled with lysosome-associated membrane protein (LAMP1) monoclonal antibody (BD Biosciences, San Jose, CA) at 1:1000 dilution. Calbindin D- and GFAP-positive cells were detected with donkey anti-mouse secondary antibody conjugated to cyanine 3 (Jackson ImmunoResearch). NeuN- and LAMP1-positive cells were detected with biotinylated anti-mouse or anti-rat secondary antibody, respectively, and visualized with streptavidin–Alexa Fluor 546 conjugate (Invitrogen, Carlsbad, CA). All sections were mounted on glass slides, coverslipped with Vectashield (Vector Laboratories, Burlingame, CA), and viewed under epifluorescence and confocal microscopy.

Brain autofluorescence. Autofluorescent storage material was assessed by mounting 50 μm free-floating vibratome sections from KPB storage onto glass slides, coverslipping with Vectashield, and viewing under 4',6'-diamidino-2-phenylindole epifluorescence (Sleat et al., 2004). Exposure-matched digital images were taken from comparable regions of treated and untreated brains, and the amount of autofluorescent storage was quantified using the MetaMorph Image Analysis System (Universal Imaging Corporation, Downingtown, PA). The percentage of autofluorescence in AAV-treated *CLN2*^{-/-} brains relative to untreated *CLN2*^{-/-} brains was calculated as follows: (1) storage of a given brain structure was determined in untreated *CLN2*^{-/-} mice, and an overall average (mean) for each structure was calculated; (2) storage of the corresponding brain structures for each AAV-treated animal was determined and compared with the average autofluorescence in untreated *CLN2*^{-/-} mice to generate a relative percentage; and (3) the relative percentages of all mice for each structure were tabulated to give an overall mean and SE.

Electron microscopy. Fifty micrometer sagittal brain sections from AAV-treated and untreated groups were dehydrated and infiltrated in 100% Spurr's resin for 24 h, embedded between two plastic sheets, and baked at 60°C for 16 h. The thalamus was dissected from the embedded

sample, and ultrathin 50 nm sections were cut with a diamond knife, placed on grids, and then stained with uranyl acetate and lead citrate. Stained sections were examined with a Hitachi (Tokyo, Japan) H700 transmission electron microscope, and photos of cells with similar cross-sectional area were taken. The size of inclusions was determined using the Bioquant Software (Bioquant Image Analysis Corporation, Nashville, TN), and the total combined area of the inclusions in each cell were grouped as small ($1 \mu\text{m}^2$ or less), medium ($2\text{--}8 \mu\text{m}^2$), and large ($9 \mu\text{m}^2$ or greater). Three brains were processed from each group, and 40 random cells were examined in each brain for a total of 120 cells per group. The number of cells containing inclusions of different sizes were counted and compiled for statistical analysis.

Statistics. The amount of autofluorescent storage material and the number of curvilinear bodies in cells were analyzed with one-way ANOVA and Dunnett's *post hoc* test using GraphPad Prism version 4.0 (GraphPad Software, San Diego, CA). All values with $p < 0.05$ were considered significant.

Results

Human TPP1 expression and reduction of storage pathology

Storage pathology in $CLN2^{-/-}$ mice is present by 5 weeks of age, and the progressive nature of the disease results in ataxia, seizures, and a median lifespan of 19–20 weeks (Sleat et al., 2004). An initial pilot study was conducted to determine whether AAV_{2CU}hCLN2 could transduce the $CLN2^{-/-}$ brain and reduce autofluorescent storage. $CLN2^{-/-}$ mice were either 10 weeks (cohort 1) or 6 weeks (cohort 2) of age at time of surgery. A total of 1.2×10^9 gc of AAV_{2CU}hCLN2 or AAV_{2CU}NULL were injected along a single needle tract into the thalamus and hippocampus of the right hemisphere. Mice from cohort 1 were killed at 6 weeks after injection and processed for TPP1 activity and expression. Mice from cohort 2 were killed at 13 weeks after injection and analyzed for TPP1 expression and reduction of autofluorescent storage material.

For biochemical analysis at 6 weeks after injection, brains treated with AAV_{2CU}hCLN2 ($n = 6$), AAV_{2CU}NULL ($n = 3$), or saline ($n = 2$) were separated into two hemispheres. Each hemisphere was further dissected into 2 mm coronal slabs, homogenized, and analyzed for TPP1 activity (Fig. 1). The background TPP1 activity as defined by multiple assays of untreated $CLN2^{-/-}$ mouse brain homogenate was $150 \pm 120 \text{ FU} \cdot \text{min}^{-1} \cdot \text{mg}^{-1}$ protein, in contrast to the average activity of $32,800 \pm 6800 \text{ FU} \cdot \text{min}^{-1} \cdot \text{mg}^{-1}$ in wild-type mouse brain. The region corresponding to the injection tract (slab 3) in AAV_{2CU}hCLN2-treated brains exhibited enzyme activity that approached $CLN2^{+/+}$ controls, and the two adjacent regions (slabs 2 and 4) had TPP1 activity less than that found in $CLN2^{+/+}$ control mice. In contrast, the rostralmost and caudalmost regions of the ipsilateral hemisphere (slabs 1 and 5) and the entire contralateral hemisphere had negligible TPP1 activity, comparable with AAV_{2CU}NULL- and saline-injected $CLN2^{-/-}$ mice.

For histological analysis at 6 weeks after injection, brains treated with AAV_{2CU}hCLN2 ($n = 4$), AAV_{2CU}NULL ($n = 2$), and saline ($n = 1$) were cut into 50 μm vibratome sections and analyzed by immunohistochemistry to determine the TPP1 expression pattern *in situ*. AAV_{2CU}hCLN2-treated brains had many TPP1 immunopositive cells concentrated around the injection sites in the ipsilateral hippocampus and thalamus (Fig. 2). Confocal microscopy showed TPP1 in a punctate cytoplasmic staining pattern that colocalized with LAMP1, indicating that TPP1 was targeted to the lysosomes (Fig. 2D–F). Although the majority of expression was localized to the cytoplasm, a portion of TPP1 was also observed in dendrites (Fig. 2G). Ectopic distribution of TPP1 to dendritic structures may be attributable to over-

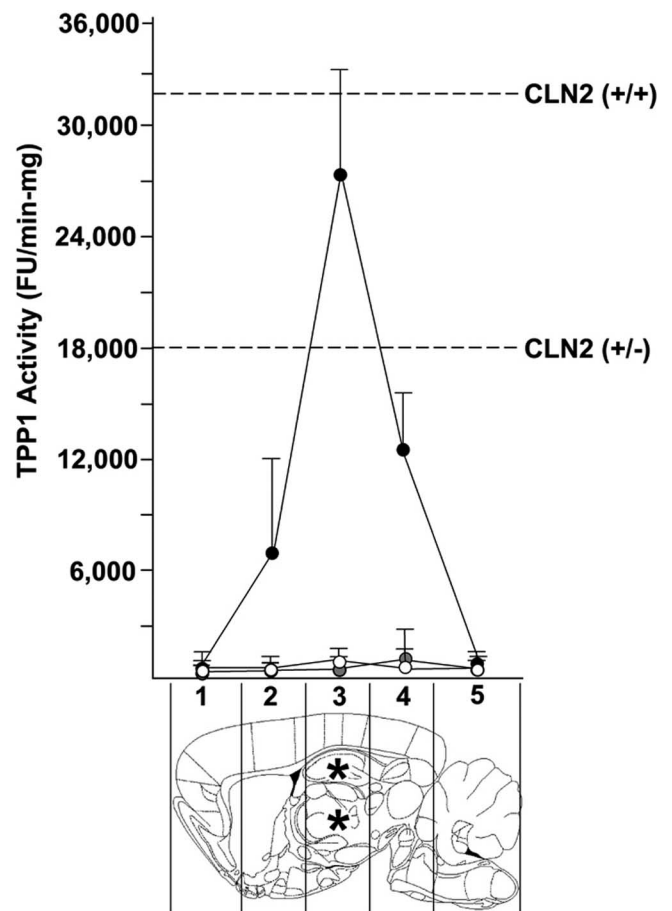


Figure 1. TPP1 activity in the $CLN2^{-/-}$ brain at 6 weeks after injection. Brains were cut into 2 mm coronal slabs as shown at the bottom, with corresponding amount of enzyme activity plotted above for the following samples: AAV_{2CU}hCLN2 ipsilateral hemisphere (black circles), AAV_{2CU}hCLN2 contralateral hemisphere (gray circles), and control AAV_{2CU}NULL or saline ipsilateral hemisphere (white circles). TPP1 activity approached wild-type levels in the brain slab (3) that contained the hippocampus and thalamus injection sites. The two adjacent slabs (2 and 4) contained some elevated levels of TPP1 activity. The rostral brain (slab 1), cerebellum (slab 5), and the entire contralateral (uninjected) hemisphere of AAV_{2CU}hCLN2-treated brains had levels of enzyme activity indistinguishable from AAV_{2CU}NULL-treated and saline brains. The dashed lines correspond to the relative levels of TPP1 activity in untreated $CLN2^{+/+}$ and $CLN2^{+/-}$ control brains. The total number of animals was $n = 6$ for AAV_{2CU}hCLN2 injected and $n = 5$ for control injected (AAV_{2CU}NULL and saline). Asterisks in the brain image show location of the injection sites. Data are means \pm SEM.

abundance of expressed protein in transduced cells. Similarly, viral vector-mediated expression of other lysosomal enzymes resulted in labeling of dendrites and, in some cases, labeling of axonal tracts (Passini et al., 2002; Haskell et al., 2003; Hennig et al., 2003; Griffey et al., 2005; Luca et al., 2005). Consistent with the enzyme activity data (Fig. 1), there was negligible TPP1 expression in regions distal to the injection site, including the motor cortex, cerebellum, the contralateral hemisphere, and in brains injected with AAV_{2CU}NULL or saline (data not shown).

The efficacy of AAV2 gene therapy for treating autofluorescent storage was determined. Mice from cohort 2 were allowed to survive to 19 weeks (13 weeks after injection) so that a direct comparison could be made with end-stage $CLN2^{-/-}$ control mice that normally accumulate a substantial (maximum) amount of storage at this age and die (Sleat et al., 2004). Immunohistochemistry verified the presence of TPP1 in the brain (Fig. 3A, B), with an expression pattern similar to mice at 6 weeks after injection. There was a substantial decrease in autofluorescent

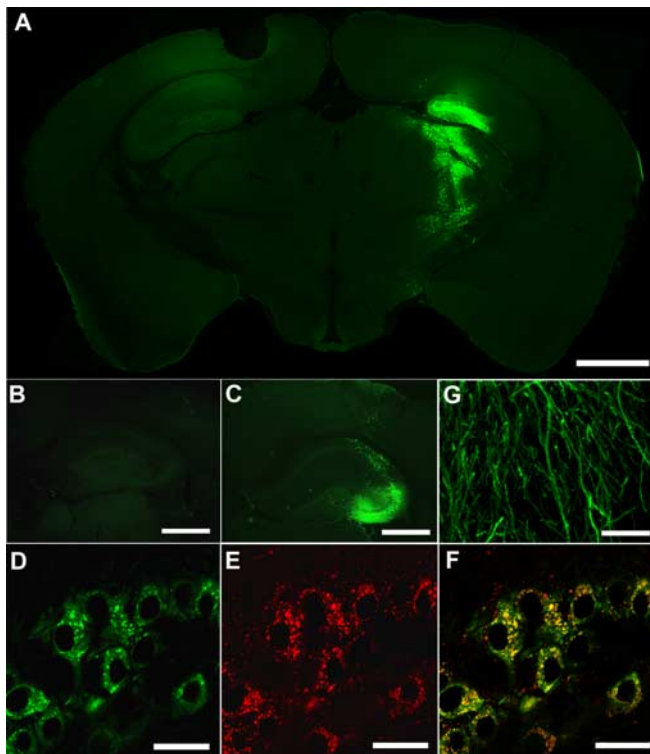


Figure 2. TPP1 expression in the $CLN2^{-/-}$ brain at 6 weeks after injection with AAV₂_{CU}hCLN2. TPP1 immunopositive cells were detected in the hippocampus and thalamus of the ipsilateral hemisphere but not in the contralateral hemisphere (**A**). Close-up of the ipsilateral hippocampus showed that there was no detectable TPP1 immunostaining in untreated brains (**B**) compared with robust TPP1 immunostaining in AAV₂_{CU}hCLN2-treated brains (**C**). High-magnification confocal images of cell bodies in the hippocampus demonstrated that TPP1 (**D**) and LAMP1 (**E**) were present in an overlapping punctate pattern (**F**, yellow signal). High-magnification confocal images of CA3 pyramidal dendrites showed positive immunostaining for TPP1 (**G**). Scale bars: **A**, 1 mm; **B**, **C**, 100 μ m; **D–G**, 20 μ m.

storage material in the ipsilateral hippocampus and thalamus with AAV₂_{CU}hCLN2 (Fig. 3*C,D*) but not with AAV₂_{CU}NULL (Fig. 3*E,F*). The amount of storage reduction was quantified using the MetaMorph System Analysis software (see Materials and Methods). The hippocampus and thalamus of AAV₂_{CU}hCLN2-treated $CLN2^{-/-}$ brains ($n = 4$) contained an average of 39.3 ± 11.8 and $30.8 \pm 7.1\%$ autofluorescence storage material relative to AAV₂_{CU}NULL- and saline-injected $CLN2^{-/-}$ mice ($n = 3$), respectively ($p < 0.05$). However, distal structures in the ipsilateral hemisphere and the entire contralateral hemisphere of AAV₂_{CU}hCLN2-treated mice contained autofluorescent storage that was equivalent to that found in age-matched AAV₂_{CU}NULL and saline $CLN2^{-/-}$ control mice (data not shown). Untreated $CLN2^{+/+}$ mice had virtually no detectable autofluorescence in the brain (Fig. 3*G,H*).

Comparison of AAV2 and AAV5 vectors in $CLN2^{-/-}$ mice

The pilot study showed that AAV2 gene therapy could reduce autofluorescent storage in the $CLN2^{-/-}$ mouse brain. However, other AAV serotype vectors may provide more effective therapy. AAV5 is a good candidate to deliver the human CLN2 cDNA because this serotype showed improved transduction of mammalian brain compared with AAV2 (Davidson et al., 2000; Burger et al., 2004; Cressant et al., 2004; Desmaris et al., 2004; Paterna et al., 2004). We thus compared the overall efficacy of titer-matched AAV₂_{CU}hCLN2 ($n = 8$) and AAV₅_{CU}hCLN2 ($n = 9$) after bilateral injection into the motor cortex, thalamus, and cerebellum of

6-week-old $CLN2^{-/-}$ mice. These structures contain high levels of cellular pathology and represent challenging regions to determine the efficacy of gene therapy vectors. A total of 6.0×10^8 gc of either serotype was injected into each structure.

At 13 weeks after injection, mice were killed and brain hemispheres were separated from each other. The left hemisphere was analyzed for TPP1 activity, and the right hemisphere was analyzed for TPP1 expression and for the reduction of autofluorescent storage material and curvilinear bodies. AAV₂_{CU}hCLN2-treated mice produced TPP1 activity similar to $CLN2^{+/+}$ controls in corresponding tissue slabs containing the motor cortex (slab 2), thalamus (slab 3), and cerebellum (slab 5) (Fig. 4). In contrast, AAV₅_{CU}hCLN2-treated mice produced TPP1 activity approximately twofold higher than $CLN2^{+/+}$ control mice in these same three regions (Fig. 4). There were essentially null levels of TPP1 activity in slab 4 of AAV₂_{CU}hCLN2- and AAV₅_{CU}hCLN2-treated brains, indicating that there was no significant diffusion of virus or TPP1 protein.

Immunohistochemical analysis of the right hemisphere confirmed the presence of TPP1 in brain. A sagittal view at the level of the thalamic injection site showed many TPP1 immunopositive cells with AAV₂_{CU}hCLN2 and AAV₅_{CU}hCLN2 (Fig. 5*A,B*). TPP1 cells were also detected in the injected motor cortex and cerebellum (Fig. 5*C–E*). TPP1 was targeted to the lysosomes as verified by LAMP1 immunostaining (data not shown). Colocalization of TPP1 with NeuN showed that the majority of transduced cells were neurons (Fig. 5*F,G*). Neither serotype vector transduced astrocytes, as demonstrated by the lack of colocalization with GFAP (Fig. 5*H,I*). Double immunostaining with calbindin (red) and TPP1 (green) showed colocalization of signal (yellow) in Purkinje cells of the cerebellum (Fig. 5*J–M*). Although not all Purkinje cells contained exogenous protein, there were substantially more Purkinje cells positive for TPP1 with AAV₅_{CU}hCLN2 compared with AAV₂_{CU}hCLN2. This observation is consistent with the natural tropism of AAV5 for this cell layer after cerebellar injection (Alisky et al., 2000). However, there were regions in both the AAV5- and AAV2-treated cerebellum that were negative for calbindin, indicating that there was some Purkinje cell loss (Fig. 5*I*). Outside the injection sites, scattered TPP1 immunopositive cells were detected in nearby striatum and hippocampus with both vectors. TPP1 was also routinely detected in the ependyma with AAV₅_{CU}hCLN2 but not with AAV₂_{CU}hCLN2, which is consistent with the strong infectivity of AAV5 for the ventricular lining (Davidson et al., 2000; Watson et al., 2005).

Similar to our pilot study, untreated $CLN2^{-/-}$ mice contained abundant levels of autofluorescence at 19 weeks of age (Fig. 6*A–C*). The robust TPP1 immunostaining observed in the brain (Fig. 5) resulted in a substantial decrease of autofluorescent storage in the corresponding brain structures (Fig. 6*D–I*). As determined using the MetaMorph Image Analysis System, AAV-treated mice contained ~ 30 – 70% ($p < 0.05$) autofluorescent storage in the motor cortex, thalamus, cerebellum, striatum, and hippocampus compared with untreated $CLN2^{-/-}$ mice (Fig. 6*J*). There was no significant difference between the two vectors in the amount of autofluorescence that was cleared. However, regions distal to the injection tracts, such as the caudal neocortex and brainstem, had little-to-no reduction of autofluorescent storage, consistent with the negligible levels of TPP1 activity in these regions (slab 4) (Fig. 4).

The ultrastructural hallmark phenotype in cLINCL patients is curvilinear bodies. A random sampling of 120 cells along the anteroposterior and mediolateral axes of the thalamus (40 cells

per brain, three brains per group) by electron microscopy showed that this pathological marker was found in many cells of *CLN2*^{-/-} mice (Fig. 7A) but never in *CLN2*^{+/-} mice (Fig. 7B). *CLN2*^{-/-} mice treated with AAV2_{CU}hCLN2 (Fig. 7C) or AAV5_{CU}hCLN2 (Fig. 7D) had significantly ($p < 0.01$) less number of cells positive for curvilinear bodies in the thalamus compared with untreated *CLN2*^{-/-} mice (Fig. 7E). Furthermore, the curvilinear bodies in cells that did contain them were smaller in size than those found in untreated *CLN2*^{-/-} mice (Fig. 7E). For example, only 0.8 and 2.5% of cells in AAV2_{CU}hCLN2- and AAV5_{CU}hCLN2-treated brains contained inclusions 9 μm^2 or greater, respectively ($p < 0.01$). This was in contrast to untreated *CLN2*^{-/-} mice in which 26% of cells contained curvilinear bodies of this size.

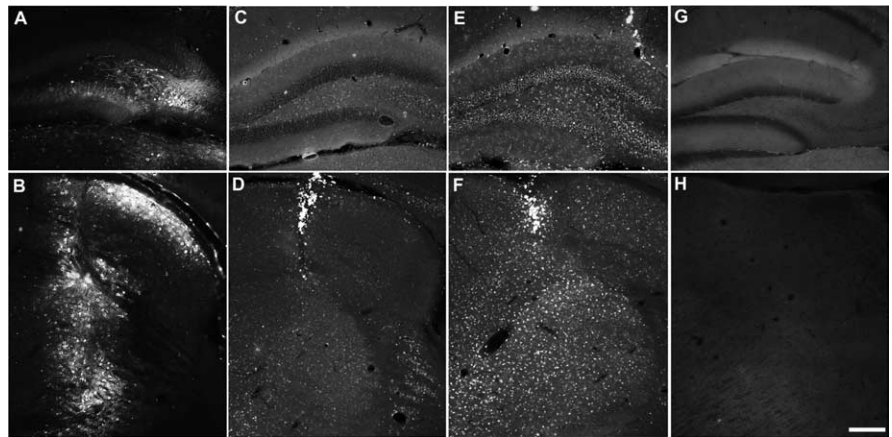


Figure 3. Overlapping regions of TPP1 expression and reduction of autofluorescent storage material at 13 weeks after injection. AAV2_{CU}hCLN2 (**A–D**) or AAV2_{CU}NULL (**E, F**) was injected into the hippocampus (**A, C, E**) and thalamus (**B, D, F**). TPP1 was present in the injected structures (**A, B**). This resulted in a substantial reduction of autofluorescent storage material in both structures (**C, D**). In contrast, injection of AAV2_{CU}NULL did not reduce autofluorescent storage in the hippocampus or thalamus (**E, F**). Untreated *CLN2*^{+/+} control mice contained undetectable levels of autofluorescence in the hippocampus (**G**) and thalamus (**H**). Scale bar, 250 μm .

Discussion

Collectively, the NCL (“Batten”) family are the most prevalent neurological genetic disorders affecting children (Hofmann and Peltonen, 2001). cLINCL is a type of NCL that is caused by mutations in the *CLN2* locus on chromosome 11 (Sleat et al., 1997). A mouse model was recently generated by targeted disruption of the *CLN2* gene (Sleat et al., 2004). *CLN2*^{-/-} mice contain many of the neurological deficits found in cLINCL patients, such as ataxia, loss of motor function, brain atrophy, axonal degeneration, and the intracellular accumulation of autofluorescent storage and curvilinear bodies throughout the brain (Sleat et al., 2004). Storage pathology in *CLN2*^{-/-} mice is present by 5 weeks of age, the earliest time examined (Sleat et al., 2004). The progressive nature of the disease and the global neuropathology in *CLN2*^{-/-} mice result in a median lifespan of 19–20 weeks.

The present study shows that *CLN2*^{-/-} mouse brains injected with AAV2_{CU}hCLN2 or AAV5_{CU}hCLN2 contain substantially less autofluorescent storage and curvilinear bodies than untreated mutants. Colocalization with LAMP1 and subsequent decrease in cellular pathology indicates that human TPP1 was targeted to lysosomes. The amount of lysosomal pathology reduced in treated animals were comparable between the two serotype vectors despite the higher levels of TPP1 activity resulting from AAV5_{CU}hCLN2. This suggests that enzyme activity above a certain threshold amount may not provide additional therapeutic relief. Typically, restoration of activity to 10–15% of normal levels is sufficient to correct storage pathology in the majority of LSDs, and this is often accepted as a target for gene therapy (Neufeld, 1991; Kaye and Sena-Esteves, 2002).

AAV-mediated enzyme replacement therapy is effective in preventing new storage from accumulating and/or degrading existing storage. Brains treated with AAV2_{CU}hCLN2 or AAV5_{CU}hCLN2 had an average of 30–70% autofluorescent storage in structures targeted by the viral vectors compared with untreated *CLN2*^{-/-} mice. There were a few AAV-treated animals that contained ~10% autofluorescent storage in the injected structures, which is an almost complete reduction of pathology. Electron microscope analysis also shows that only 16–26% of cells in AAV-treated brains had discernable curvilinear bodies compared with 59% in untreated *CLN2*^{-/-} mice. Furthermore, the cells in AAV-treated brains that did contain these ultrastruc-

tural inclusions were smaller and rarely approached the 9 μm^2 size that was frequently observed in untreated *CLN2*^{-/-} mice. These data are encouraging because lysosomal storage in cLINCL patients and in *CLN2*^{-/-} mice form highly insoluble aggregates that could be refractory to therapy (Hofmann and Peltonen, 2001). AAV gene therapy is thus an effective strategy to treat LSDs that contain aberrant storage material.

TPP1 was restricted to the injected sites and nearby structures, indicating that there was little viral and/or protein spread, which explains the lack of global correction in the brain. Although transduced cells that overexpress and secrete TPP1 can supply nontransduced cells with enzyme by mannose-6-phosphate receptor-mediated endocytosis (Lin and Lobel, 2001), this process likely occurred in the vicinity of the injection sites. A more widespread TPP1 distribution may be achieved with longer treatment or by administering AAV vector preparations (preps) with higher titers. An extended postinjection time point could provide transduced cells the time needed to “ramp-up” enzyme production, which was shown to be the case for AAV2_{CU}hCLN2 in the normal rodent brain (Sondhi et al., 2005). Time points that exceeded 8 months resulted in higher enzyme activity and detection of TPP1 in areas of the brain with synaptic connections to the injection site (Sondhi et al., 2005). Similarly, widespread distribution of palmitoyl protein thioesterase (PPT) in a mouse model of INCL occurred at 7 months after injection (Griffey et al., 2005). These data suggest that distribution of TPP1 (and other NCL enzymes) may be achieved at longer time points but cannot be measured directly in the *CLN2*^{-/-} mouse model because of the shorter lifespan. Alternatively, injecting high-titer AAV preps may convert transduced cells into highly efficient enzyme factories for TPP1 secretion and transport in a shorter period of time. Injections into the normal rat striatum using an AAV5-hCLN2 vector that was half-log higher in titer than the one used in the current study resulted in widespread enzyme activity and evidence of cross-correction by 10 weeks after injection (Haskell et al., 2003). This was also shown for another lysosomal enzyme, in which axonal transport of β -glucuronidase was detected as early as 5–8 weeks after injection with high titer AAV in a mouse model of Mucopolysaccharidosis VII disease (Sly syndrome) (Passini et al., 2002; Hennig et al., 2003).

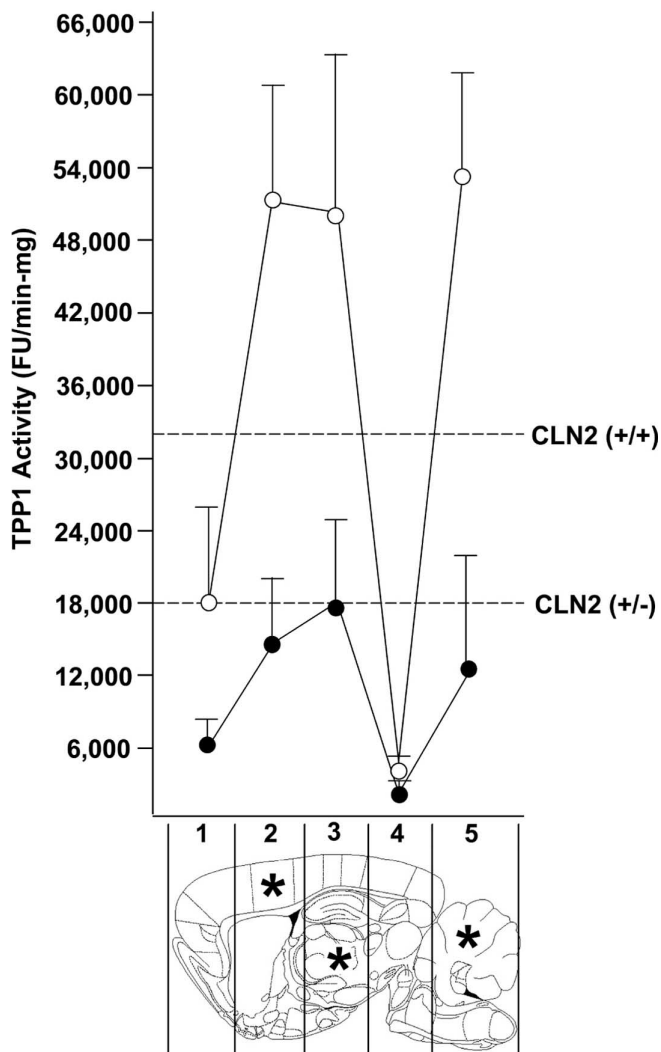


Figure 4. Comparison of TPP1 activity in AAV2_{CU}hCLN2- or AAV5_{CU}hCLN2-treated brains at 13 weeks after injection. AAV2-injected brains (black circles) contained heterozygote levels of TPP1 activity in brain slabs containing the injection sites (slabs 2, 3, 5). Despite matching titers, AAV5-injected brains (white circles) had substantially higher levels of TPP1 activity in the same corresponding brain slabs. Disparate enzyme activity was also detected in the frontal brain (slab 1) with the two serotype vectors. AAV-treated brains had essentially null levels of TPP1 activity in slab 4. The dashed lines correspond to the relative levels of TPP1 activity in untreated CLN2^{+/-} and CLN2^{+/+} brains. Asterisks in the brain image show location of the injection sites. Data are means \pm SEM.

The reasons underlying the inefficient spread of AAV are not clear. One possibility may also be attributable to the low titers of AAV used in this study because the primary attachment receptors for AAV2 and AAV5 are abundantly found in the brain (Bartlett et al., 1998; Summerford and Samulski, 1998; Walters et al., 2001). Low-titer AAV preps may become sequestered at the injection site because there would presumably be enough cell-surface receptors available to bind the majority of virions. In contrast, high-titer AAV preps may saturate cell-surface receptors at the injection site, thereby producing a gradient of virions that extend the sphere of transduction to more distal locations. High-titer AAV preps are also capable of undergoing retrograde axonal transport to distal sites, establishing secondary areas of protein production (Kaspar et al., 2002, 2003; Burger et al., 2004; Passini et al., 2005). This is also supported by a dose–response study that showed loss of axonal transport with decreasing titers

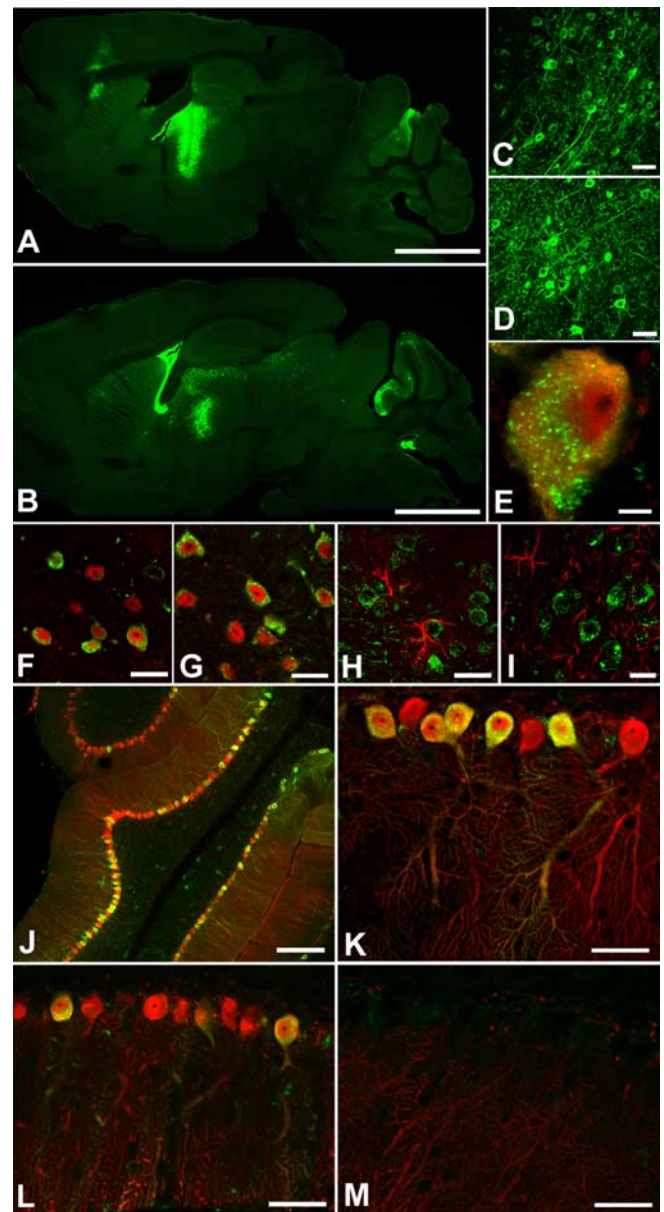


Figure 5. Comparison of TPP1 expression between AAV2_{CU}hCLN2 (A, C, F, H, L) and AAV5_{CU}hCLN2 (B, D, E, G, I–K, M) at 13 weeks after injection. Robust TPP1 immunopositive cells were detected in the thalamus with AAV2 (A) and AAV5 (B). Adjacent sagittal sections contained many cells positive for TPP1 in the motor cortex (C, D). A 100 \times confocal image of a Purkinje cell with TPP1 (green) in cytoplasmic vesicles consistent with endosomal-lysosomal targeting (E). Double immunohistochemistry showed that the TPP1 (green) surrounded NeuN-positive nuclei (red), confirming that both serotype vectors were neurotrophic (F, G). In contrast, very few cells contained for TPP1 (green) and GFAP (red), demonstrating that astrocytes were inefficiently transduced by AAV2 or AAV5 (H, I). Low (J) and high (K) magnification confocal images of AAV5_{CU}hCLN2-treated cerebellum showed that many Purkinje cells contained TPP1. There were substantially less Purkinje cells positive for TPP1 in AAV2_{CU}hCLN2-treated brains (L). Purkinje cell loss in the cerebellum of an AAV5-treated brain (M). Scale bars: A, B, 2 mm; C, D, 50 μ m; E, 5 μ m; F–I, 20 μ m; J, 200 μ m; K–M, 40 μ m.

of AAV vectors (Kaspar et al., 2003). Alternatively, widespread AAV distribution may be achieved with pressure-mediated, convection-enhanced delivery (Bankiewicz et al., 2000; Nguyen et al., 2001). Coinjection of AAV with hyperosmotic agents or molecules that bind to their receptors may also provide broader distribution (Mastakov et al., 2001; Burger et al., 2005; Hadaczek et al., 2004), although it is unclear whether toxicity associated with coinjection strategies make it useful in the clinic.

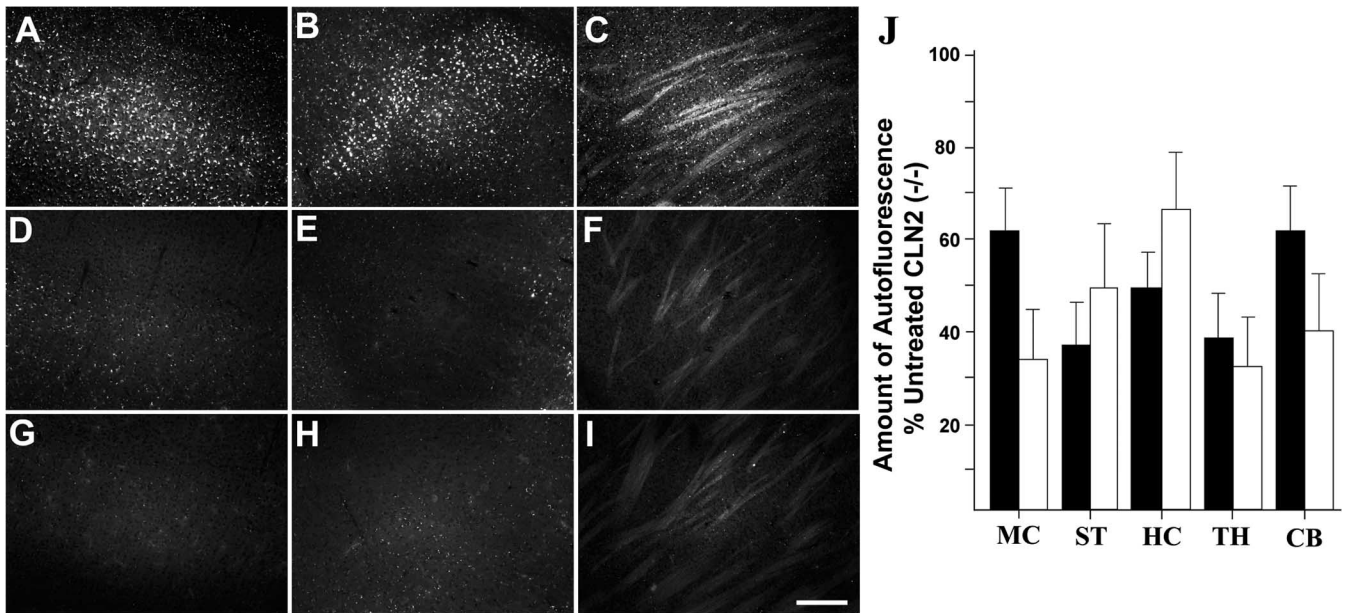


Figure 6. Reduction of brain autofluorescence with AAV_{2C}hCLN2 or AAV_{5C}hCLN2 at 13 weeks after injection. Shown are the motor cortex (**A, D, G**), thalamus (**B, E, H**), and striatum (**C, F, I**). Untreated *CLN2*^{-/-} mice have high levels of autofluorescent storage material at 19 weeks of age (**A–C**). Injection of AAV_{2C}hCLN2 (**D–F**) or AAV_{5C}hCLN2 (**G–I**) substantially reduced autofluorescent storage. The intensity of autofluorescence was quantified from exposure-matched digital images, and the results were plotted as the percentage of autofluorescent storage to untreated *CLN2*^{-/-} control mice (**J**). The background level of autofluorescence in untreated *CLN2*^{+/+} mice was <5%. A total of four animals were analyzed from each group. Black bars, AAV_{2C}hCLN2-treated *CLN2*^{-/-} mice; white bars, AAV_{5C}hCLN2-treated *CLN2*^{-/-} mice. Data are means ± SEM. Scale bar: 250 μm. MC, Motor cortex; ST, striatum; HC, hippocampus; TH, thalamus; CB, cerebellum.

The issue of spread of expressed protein is critical in large brains and in humans. Exploiting brain circuits to distribute TPP1 by axonal transport would be beneficial for widespread distribution of enzyme in cLINCL patients. Several mouse models of LSD show potential disruption of vesicular transport through axons (Walkley, 1998). However, despite these disruptions, many lysosomal enzymes undergo axonal transport to distal locations in disease brain, such as β-glucuronidase (Passini et al., 2002; Hennig et al., 2003), arylsulfatase A (Luca et al., 2005), and acid sphingomyelinase (Dodge et al., 2005; Passini et al., 2005). PPT1 is also widely distributed in the INCL mouse, demonstrating that disease-compromised neurons of the Batten brain support axonal transport (Griffey et al., 2005). Although these data provide optimism that axonal transport may be a general property of lysosomal enzymes in affected brain, it still remains to be verified that TPP1 can become distributed through axons of the cLINCL brain.

In summary, we show that AAV-mediated TPP1 enzyme replacement is effective in reducing the hallmark cellular pathologies in a newly described *CLN2* knock-out mouse model of cLINCL. The progressive nature of the disease suggests that TPP1 played a definitive role in preventing the development of storage in *CLN2*^{-/-} brains. This would, at the minimum, provide therapeutic benefits by halting any additional progression of the dis-

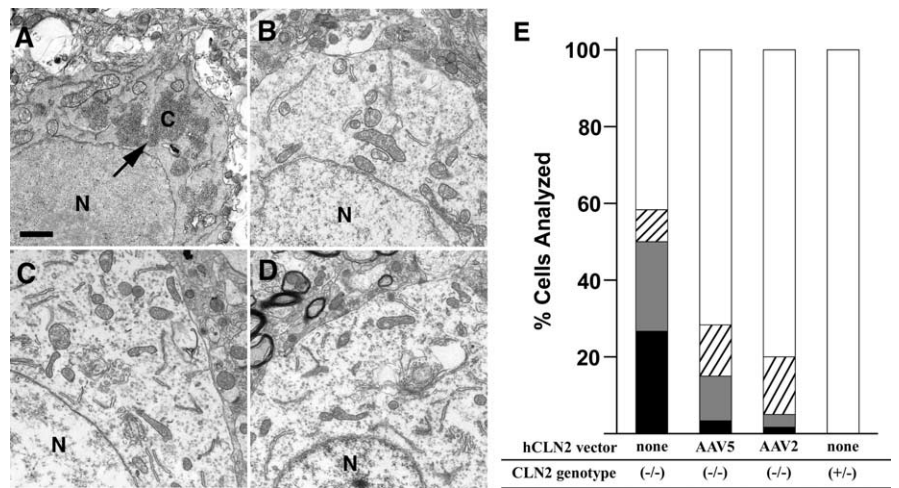


Figure 7. Electron microscope analysis of curvilinear bodies in AAV-treated and untreated thalamus. Untreated *CLN2*^{-/-} brains contain ultrastructural inclusions (arrow) classified as curvilinear bodies (**A**). In contrast, every cell from *CLN2*^{+/-} mice (**B**) and the majority of cells in *CLN2*^{-/-} mice treated with AAV_{2C}hCLN2 (**C**) or AAV_{5C}hCLN2 (**D**) did not contain these inclusions. A random sampling of 120 cells per group were analyzed, and the percentage of cells without or with curvilinear bodies of various sizes were plotted as stacked bar graphs (**E**). Black bars, The percentage of cells that contain inclusions with a combined area of 9 μm² or greater; gray bars, the percentage of cells that contain inclusions with a combined area of 2–8 μm²; hatched bars, the percentage of cells that contain inclusions with a combined area of 1 μm² or less; white bars, the percentage of cells that contain no inclusions. Scale bar, 1 μm. C, Curvilinear body; N, nucleus.

ease in cLINCL patients. TPP1 may have also degraded existing storage material because injections were done at a time when lysosomal pathology was present in the *CLN2*^{-/-} brain. This would be particularly relevant for treating late-stage patients with severe forms of the disease. In conclusion, the information in this study provides supporting evidence that AAV gene therapy may be a potential strategy for treating cLINCL.

References

- Alisky JM, Hughes SM, Sauter SL, Jolly D, Dubensky TW, Staber PD, Chiorini JA, Davidson BL (2000) Transduction of murine cerebellar neurons with recombinant FIV and AAV5 vectors. *NeuroReport* 11:2669–2673.
- Autti T, Raininko R, Vanhanen SL, Santavuori P (1997) Magnetic resonance techniques in neuronal ceroid lipofuscinoses and some other lysosomal diseases affecting the brain. *Curr Opin Neurol* 10:519–524.
- Bankiewicz KS, Eberling JL, Kohutnicka M, Jagust W, Pivrotto P, Bringas J, Cunningham J, Budinger TF, Harvey-White J (2000) Convection-enhanced delivery of AAV vector in parkinsonian monkeys; in vivo detection of gene expression and restoration of dopaminergic function using pro-drug approach. *Exp Neurol* 164:2–14.
- Bartlett JS, Samulski RJ, McCown TJ (1998) Selective and rapid uptake of adeno-associated virus type 2 in brain. *Hum Gene Ther* 9:1181–1186.
- Beaudoin D, Hagenzieker J, Jack R (2004) Neuronal ceroid lipofuscinosis: what are the roles of electron microscopy, DNA, and enzyme analysis in diagnosis? *J Histotechnol* 27:237–243.
- Bosch A, Perret E, Desmaris N, Heard JM (2000) Long-term and significant correction of brain lesions in adult mucopolysaccharidosis type VII mice using recombinant AAV vectors. *Mol Ther* 1:63–70.
- Burger C, Gorbatyuk OS, Velardo MJ, Peden CS, Williams P, Zolotukhin S, Reier PJ, Mandel RJ, Muzyczka N (2004) Recombinant AAV viral vectors pseudotyped with viral capsids from serotypes 1, 2, and 5 display differential efficiency and cell tropism after delivery to different regions of the central nervous system. *Mol Ther* 10:302–317.
- Burger C, Nguyen FN, Deng J, Mandel RJ (2005) Systemic mannitol-induced hyperosmolality amplifies rAAV2-mediated striatal transduction to a greater extent than local co-infusion. *Mol Ther* 11:327–331.
- Carpenter S, Karpati G, Andermann F (1972) Specific involvement of muscle, nerve, and skin in late infantile and juvenile amaurotic idiocy. *Neurology* 22:170–186.
- Cressant A, Desmaris N, Verot L, Breyot T, Froissart R, Vanier MT, Maire I, Heard JM (2004) Improved behavior and neuropathology in the mouse model of Sanfilippo type IIIB disease after adeno-associated virus-mediated gene transfer in the striatum. *J Neurosci* 24:10229–10239.
- Davidson BL, Stein CS, Heth JA, Martins I, Kotin RM, Derksen TA, Zabner J, Ghodsi A, Chiorini JA (2000) Recombinant adeno-associated virus type 2, 4, and 5 vectors: transduction of variant cell types and regions in the mammalian central nervous system. *Proc Natl Acad Sci USA* 97:3428–3432.
- Desmaris N, Verot L, Puech JP, Caillaud C, Vanier MT, Heard JM (2004) Prevention of neuropathology in the mouse model of Hurler syndrome. *Ann Neurol* 56:68–76.
- Dodge JC, Clarke J, Song A, Bu J, Yang W, Taksir TV, Griffiths D, Zhao Q, Schuchman EH, Cheng SH, O'Riordan CR, Shihabuddin LS, Passini MA, Stewart GR (2005) Intracerebellar injection of different AAV serotype vectors encoding human ASM corrects neuropathology and motor deficits in a mouse model of Niemann-Pick A disease. *Proc Natl Acad Sci USA* 102:17822–17827.
- Elleder M, Lake BD, Goebel HH, Rapola J, Haltia M, Carpenter S (1999) Definitions of the ultrastructural patterns found in NCL. In: *The neuronal ceroid lipofuscinoses*, Ed 1 (Goebel HH, Mole SE, Lake BD, eds), pp 5–15. Amsterdam: IOS.
- Frisella WA, O'Connor LH, Vogler CA, Roberts M, Walkley S, Levy B, Daly TM, Sands MS (2001) Intracranial injection of recombinant adeno-associated virus improves cognitive function in a murine model of mucopolysaccharidosis type VII. *Mol Ther* 3:351–358.
- Griffey M, Bible E, Vogler C, Levy B, Gupta P, Cooper J, Sands MS (2004) Adeno-associated virus 2-mediated gene therapy decreases autofluorescent storage material and increases brain mass in a murine model of infantile neuronal ceroid lipofuscinosis. *Neurobiol Dis* 16:360–369.
- Griffey M, Macauley SL, Ogilvie JM, Sands MS (2005) AAV2-mediated ocular gene therapy for infantile neuronal ceroid lipofuscinosis. *Mol Ther* 12:413–421.
- Hadaczek P, Mirek H, Bringas J, Cunningham J, Bankiewicz K (2004) Basic fibroblast growth factor enhances transduction, distribution, and axonal transport of adeno-associated virus type 2 vector in rat brain. *Hum Gene Ther* 15:469–479.
- Haltia M (2003) The neuronal ceroid lipofuscinoses. *J Neuropathol Exp Neurol* 62:1–13.
- Haskell RE, Hughes SM, Chiorini JA, Alisky JM, Davidson BL (2003) Viral-mediated delivery of the late-infantile neuronal ceroid lipofuscinosis gene, TPP-1 to the mouse central nervous system. *Gene Ther* 10:34–42.
- Hennig AK, Levy B, Ogilvie JM, Vogler CA, Galvin N, Bassnett S, Sands MS (2003) Intravitreal gene therapy reduces lysosomal storage in specific areas of the CNS in mucopolysaccharidosis VII mice. *J Neurosci* 23:3302–3307.
- Hofmann SL, Peltonen L (2001) The neuronal ceroid lipofuscinoses. In: *The metabolic and molecular basis of inherited disease*, Ed 8 (Scriver CR, Beaudet AL, Sly WS, Valle D, eds), pp 3877–3894. New York: McGraw-Hill.
- Kaspar BK, Erickson D, Schaffer D, Hinh L, Gage FH, Peterson DA (2002) Targeted retrograde gene delivery for neuronal protection. *Mol Ther* 5:50–56.
- Kaspar BK, Llado J, Sherkat N, Rothstein JD, Gage FH (2003) Retrograde viral delivery of IGF-1 prolongs survival in a mouse ALS model. *Science* 301:839–842.
- Kaye EM, Sena-Esteves M (2002) Gene therapy for the central nervous system in the lysosomal storage disorders. *Neurol Clin N Am* 20:879–901.
- Klugmann M, Leightlein CB, Symes CW, Serikawa T, Young D, Doring MJ (2005) Restoration of aspartoacylase activity in CNS neurons does not ameliorate motor deficits and demyelination in a model of Canavan disease. *Mol Ther* 11:745–753.
- Lin L, Lobel P (2001) Production and characterization of recombinant human CLN2 protein for enzyme-replacement therapy in late infantile neuronal ceroid lipofuscinosis. *Biochem J* 357:49–55.
- Lin L, Sohar I, Lackland H, Lobel P (2001) The human CLN2 protein/tripeptidyl-peptidase I is a serine protease that autoactivates at acidic pH. *J Biol Chem* 276:2249–2255.
- Luca T, Givogri MI, Perani L, Galbati F, Follenzi A, Naldini L, Bongarzone ER (2005) Axons mediate the distribution of arylsulfatase a within the mouse hippocampus upon gene delivery. *Mol Ther* 12:669–679.
- Mastakov MY, Baer K, Xu R, Fitzsimons H, Doring MJ (2001) Combined injection of rAAV with mannitol enhances gene expression in the rat brain. *Mol Ther* 3:225–232.
- Matalon R, Surendran S, Rady PL, Quast MJ, Campbell GA, Matalon KM, Tyring SK, Wei J, Peden CS, Ezell EL, Muzyczka N, Mandel RJ (2003) Adeno-associated virus-mediated aspartoacylase gene transfer to the brain of knockout mouse for canavan disease. *Mol Ther* 7:580–587.
- Neufeld EF (1991) Lysosomal storage diseases. *Annu Rev Biochem* 60:257–280.
- Nguyen JB, Sanchez-Pernaute R, Cunningham J, Bankiewicz KS (2001) Convection-enhanced delivery of AAV2 combined with heparin increases TK gene transfer in the rat brain. *NeuroReport* 12:1961–1964.
- Passini MA, Lee EB, Heuer GG, Wolfe JH (2002) Distribution of a lysosomal enzyme in the adult brain by axonal transport and by cells of the rostral migratory stream. *J Neurosci* 22:6437–6446.
- Passini MA, Watson DJ, Vite CH, Landsburg DJ, Feigenbaum AL, Wolfe JH (2003) Intraventricular brain injection of AAV1 in neonatal mice results in complementary patterns of neuronal transduction to AAV2 and total long-term correction of storage lesions in the brains of β -glucuronidase-deficient mice. *J Virol* 77:7034–7040.
- Passini MA, Macauley SL, Huff MR, Taksir TV, Bu J, Wu I-H, Piepenhagen PA, Dodge JC, Shihabuddin LS, O'Riordan CR, Schuchman EH, Stewart GR (2005) AAV vector-mediated correction of brain pathology in a mouse model of Niemann-Pick A disease. *Mol Ther* 11:754–762.
- Paterna JC, Feldon J, Bueler H (2004) Transduction profiles of recombinant adeno-associated virus vectors derived from serotypes 2 and 5 in the nigrostriatal system of rats. *J Virol* 78:6808–6817.
- Rafi MA, Rao HZ, Passini MA, Curtis M, Vanier MT, Zaka M, Luzi P, Wolfe JH, Wenger DA (2005) AAV-mediated expression of galactocerebrosidase in brain results in attenuated symptoms and extended life span in murine models of globoid cell leukodystrophy. *Mol Ther* 11:734–744.
- Rawlings ND, Barrett AJ (1999) Tripeptidyl-peptidase I is apparently the CLN2 protein absent in classical late-infantile neuronal ceroid lipofuscinosis. *Biochim Biophys Acta* 1429:496–500.
- Sferra TJ, Qu G, McNeely D, Rennard R, Clark KR, Lo WD, Johnson PR (2000) Recombinant adeno-associated virus-mediated correction of lysosomal storage within the central nervous system of the adult mucopolysaccharidosis type VII mouse. *Hum Gene Ther* 11:507–519.
- Skorupa AF, Fisher KJ, Wilson JM, Parente MK, Wolfe JH (1999) Sustained production of β -glucuronidase from localized sites after AAV vector gene transfer results in widespread distribution of enzyme and reversal of ly-

- sosomal storage lesions in a large volume of brain in mucopolysaccharidosis VII mice. *Exp Neurol* 160:17–27.
- Sleat DE, Donnelly RJ, Lackland H, Liu CG, Sohar I, Pullarkat RK, Lobel P (1997) Association of mutations in a lysosomal protein with classical late-infantile neuronal ceroid lipofuscinosis. *Science* 277:1802–1805.
- Sleat DE, Wiseman JA, El-Banna M, Kim KH, Mao Q, Price S, Macauley SL, Sidman RL, Shen MM, Zhao Q, Passini MA, Davidson BL, Stewart GR, Lobel P (2004) A mouse model of classical late-infantile neuronal ceroid lipofuscinosis based on targeted disruption of the CLN2 gene results in a loss of tripeptidyl-peptidase I activity and progressive neurodegeneration. *J Neurosci* 24:9117–9126.
- Sohar I, Lin L, Lobel P (2000) Enzyme-based diagnosis of classical late infantile neuronal ceroid lipofuscinosis: comparison of tripeptidyl peptidase I and pepstatin-insensitive protease assays. *Clin Chem* 46:1005–1008.
- Sondhi D, Peterson DA, Giannaris EL, Sanders CT, Mendez BS, De B, Rostkowski A, Blanchard B, Bjugstad K, Sladek JR, Redmond DE, Leopold PL, Kaminsky SM, Hackett NR, Crystal RG (2005) AAV2-mediated CLN2 gene transfer to rodent and non-human primate brain results in long-term TPP1 expression compatible with therapy for LINCL. *Gene Ther* 12:1618–1632.
- Summerford C, Samulski RJ (1998) Membrane-associated heparan sulfate proteoglycan is a receptor for adeno-associated virus type 2 virions. *J Virol* 72:1438–1445.
- Vines DJ, Warburton MJ (1999) Classical late infantile neuronal ceroid lipofuscinosis fibroblasts are deficient in lysosomal tripeptidyl peptidase I. *FEBS Lett* 443:131–135.
- Vite CH, McGowan JC, Niogi SN, Passini MA, Drobatz KJ, Haskins ME, Wolfe JH (2005) Effective gene therapy for an inherited diffuse CNS disease in a large animal model. *Ann Neurol* 57:355–364.
- Walkley SU (1998) Cellular pathology of lysosomal storage disorders. *Brain Pathol* 8:175–193.
- Walters RW, Yi SM, Keshavjee S, Brown KE, Welsh MJ, Chiorini JA, Zabner J (2001) Binding of adeno-associated virus type 5 to 2,3-linked sialic acid is required for gene transfer. *J Biol Chem* 276:20610–20616.
- Watson DJ, Passini MA, Wolfe JH (2005) Transduction of the choroid plexus and ependyma in neonatal mouse brain by VSV-G pseudotyped lentivirus and adeno-associated virus type 5 vectors. *Hum Gene Ther* 16:49–56.
- Williams RE, Gottlob I, Lake BD, Goebel HH, Winchester BG, Wheeler RB (1999) CLN2 classic late infantile NCL. In: *The neuronal ceroid lipofuscinoses*, Ed 1 (Goebel HH, Mole SE, Lake BD, eds), pp 37–54. Amsterdam: IOS.

Enhanced Survival of the LINCL Mouse Following CLN2 Gene Transfer Using the rh.10 Rhesus Macaque-derived Adeno-associated Virus Vector

Dolan Sondhi¹, Neil R Hackett^{1,2}, Daniel A Peterson³, Jamie Stratton², Michael Baad², Kelly M Travis³, James M Wilson⁴ and Ronald G Crystal^{1,2}

¹Department of Genetic Medicine, Weill Medical College of Cornell University, New York, New York, USA; ²Belfer Gene Therapy Core Facility, Weill Medical College of Cornell University, New York, New York, USA; ³Department of Neuroscience, Rosalind Franklin University of Medicine and Science, The Chicago Medical School, North Chicago, Illinois, USA; ⁴Division of Transfusion Medicine, Department of Pathology and Laboratory Medicine, University of Pennsylvania School of Medicine, Philadelphia, Pennsylvania, USA

Late infantile neuronal ceroid lipofuscinosis (LINCL) is a lysosomal storage disorder caused by mutations in the *CLN2* gene and a deficiency of tripeptidyl peptidase I (TPP-I). Prior studies with adeno-associated virus (AAV) serotype 2 or 5 mediated transfer of the *CLN2* complementary DNA to the central nervous system (CNS) of *CLN2*^{-/-} mice cleared CNS storage granules, but provided no improvement in the phenotype or survival of this model of LINCL. In this study, AAV serotypes (AAV2, AAV5, AAV8, and AAVrh.10) were compared for the delivery of the same *CLN2* expression cassette. AAVrh.10, derived from rhesus macaque, provided the highest TPP-I level and maximum spread beyond the site of injection. The AAVrh.10-based vector functioned equally well in naive rats and in rats previously immunized against human serotypes of AAV. When administered to the CNS of *CLN2*^{-/-} mice, the AAVrh.10*CLN2* vector provided widespread TPP-I activity comparable to that in the wild-type mice. Importantly, the AAVrh.10*CLN2*-treated *CLN2*^{-/-} mice had significant reduction in CNS storage granules and demonstrated improvement in gait, nest-making abilities, seizures, balance beam function, and grip strength, as well as having a survival advantage.

Received 5 July 2006; accepted 2 October 2006; published online 19 December 2006. doi:10.1038/sj.mt.6300049

INTRODUCTION

Late infantile neuronal ceroid lipofuscinosis (LINCL, a form of Batten Disease) is an autosomal recessive lysosomal storage disorder that results in progressive neurological degeneration.^{1,2} LINCL is caused by mutations in the *CLN2* gene that result in the deficiency of tripeptidyl peptidase I (TPP-I), a lysosomal enzyme that is responsible for degrading membrane proteins.^{3,4} Neurons are particularly sensitive to the lysosomal accumulation

of storage material, and individuals with LINCL have extensive, progressive neurodegeneration in all parts of the brain, resulting in a vegetative state and death by the age of 8–12 years.^{1,2}

Direct transfer of the normal *CLN2* coding sequence to the central nervous system (CNS) is one strategy for achieving sustained TPP-I expression levels in brain.^{5–7} Adeno-associated viral vectors (AAV) are ideally suited for this purpose, as they infect neurons and provide persistent expression.^{5,6,8–15} We have previously demonstrated that human-derived AAV serotypes 2 and 5 vectors encoding *CLN2* provide long-term expression of TPP-I in the CNS of *CLN2*^{-/-} mice, and reduce the numbers of lysosomal storage granules in the CNS. However, a sustained improvement in function or survival of the knockout mice was not observed suggesting that insufficient amounts of TPP-I were present.⁷

In developing a strategy to enhance the ability of AAV vectors to treat CNS-related neurodegenerative disorders, we hypothesized that maintaining the same genome but changing the capsid of the vector may provide higher expression levels and wider distribution of TPP-I in the CNS. In a comparison of 25 different AAV serotypes for levels of expression following intrapleural administration,¹⁶ we observed the highest levels of expression of a secreted marker protein with AAVrh.10, a clade E, non-human primate (rhesus macaque)-derived AAV gene transfer vector. Based on this experience, and with preliminary studies showing that AAVrh.10-mediated remarkable levels of TPP-I in the CNS of normal rats, we assessed the ability of AAVrh.10 vectors to effectively deliver the *CLN2* complementary DNA (cDNA) to the CNS of *CLN2*^{-/-} mice and to produce TPP-I in sustained levels sufficient to provide significant improvement in function and survival of this murine model of LINCL. Using the same genome with AAV2-inverted terminal repeats packaged in different AAV capsids, the data shows that, on an equal dose basis, the AAVrh.10 vector gave the highest levels of TPP-I expression and provided the best spread of TPP-I beyond the immediate administration site compared to the commonly used AAV 2, 5,

Correspondence: Ronald G Crystal, Department of Genetic Medicine, Weill Medical College of Cornell University, 515 East 71st Street, S-1000, New York, New York 10021, USA. E-mail: geneticmedicine@med.cornell.edu

and 8 capsids. As AAVrh.10 is derived from a rhesus macaque, we reasoned that it might be more applicable to use in humans owing to the absence of pre-existing anti-vector immunity. Not only was AAVrh.10 able to mediate better levels and spread of the TPP-I protein in the CNS, but it also functioned equally well in naïve animals and in animals previously immunized against the human serotypes of AAV. When the AAVrh.10 vector expressing *CLN2* was administered to the CNS of *CLN2*^{-/-} mice, the AAVrh.10CLN2-treated mice showed widespread TPP-I activity that reached the levels observed in wild-type mice. Importantly, the mice receiving the AAVrh.10 vector had improvement in gait, nest-making abilities, frequency of seizures, balance beam performance, and grip strength as well as having a survival advantage.

RESULTS

Distribution and activity of TPP-I gene product by different AAV serotypes

Rats were administered with the same dose (2.5×10^9 gc (genome copy)) of a *CLN2* expression construct packaged into the capsids of AAV2, AAV5, AAV8, or AAVrh.10. Four weeks after administration of AAV2hCLN2, TPP-I-positive staining was observed with little spread from the site of injection (Figure 1a-c). In agreement with our previous report,⁶ the morphology of TPP-I-positive cells was consistent with the transduction of neurons, whereas the white matter tracts passing through the striatum were devoid of TPP-I staining (Figure 1d). Administration of AAV5hCLN2 resulted in a much wider distribution, spreading throughout the extent of the striatum in the rostrocaudal axis, and with some spread in the mediolateral axis (Figure 1e-g). As with AAV2, cells of neuronal morphology were found to express TPP-I (Figure 1h). The distribution of TPP-I staining following delivery of AAV8hCLN2 was similar to that observed with AAV5, but the density of TPP-I-positive cells was greater (Figure 1i-l). In contrast to AAV2, 5, and 8, administration of AAVrh.10CLN2 produced a very intense signal with substantial spread that filled most of the striatum except for the white matter tracts (Figure 1m-o). TPP-I-positive cells were intensely stained in cell bodies and in their proximal processes (Figure 1p).

The morphological data was complemented by TPP-I enzymatic activity assays of brain homogenate using the same dose of the four different AAV vectors. The AAV2 vector gave peak TPP-I levels that were 1.3 ± 0.4 times the endogenous level (Figure 1q). The AAV5hCLN2 vector mediated peak TPP-I activity of 1.5 ± 0.2 times and AAV8hCLN2 produced a peak activity that was 2.4 ± 0.6 times the endogenous level. By contrast, AAVrh.10CLN2 produced an activity that was 6.4–1.6 times the endogenous level. This level was significantly higher than for the AAV2 and AAV5 vectors ($P < 0.05$), but not different from that for the AAV8 vector ($P = 0.06$). As AAVrh.10 provided both a high level and a wide distribution of TPP-I, follow-up studies were focused on AAVrh.10.

AAVrh.10 is neurotropic

As neurons are primarily at risk with LINCL, it was important to show that transduction with AAVrh.10 vectors resulted in TPP-I

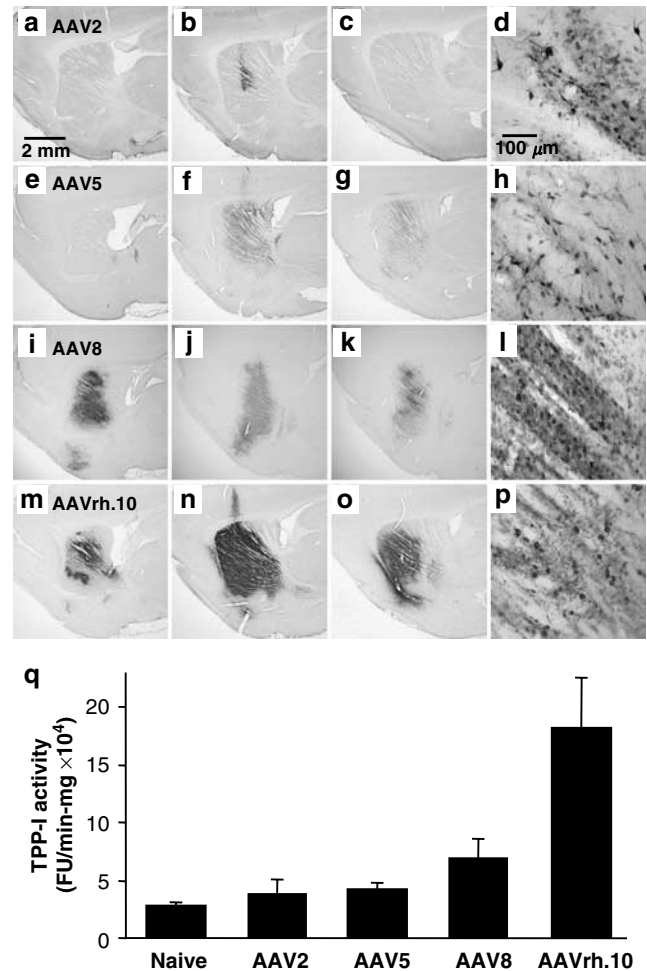


Figure 1 Comparison of TPP-I protein expression following injection of different AAV vectors expressing *CLN2* into striatum of rats. Rats ($n = 6$ /group) were injected into the striatum with 2.5×10^9 gc (in $5 \mu\text{l}$) of AAV2hCLN2, AAV5hCLN2, AAV8hCLN2, or AAVrh.10CLN2. The experiment included age-matched naïve controls ($n = 6$; not shown; all were negative). After 4 weeks, animals ($n = 3$ /group) were killed, and TPP-I distribution was assessed by immunohistochemical staining. (a-c) Series of $50 \mu\text{m}$ sagittal sections, $250 \mu\text{m}$ apart from medial to lateral, of the injected striatum for AAV2-mediated gene transfer of the *CLN2* cDNA. (d) Higher magnification showing the density of staining in the striatum resulting from gene transfer with AAV2. (e-h) AAV5, panels similar to a-d for AAV2. (i-l) AAV8. (m-p) AAVrh.10. Scale bar in a indicative of scale in a-c, e-g, i-k, m-o and scale bar in d indicative of scale in d, h, l, and p. (q) The remaining animals in each experimental group ($n = 3$ /group) were also killed at 4 weeks, the brain cut into 2 mm sagittal sections, bisected and the inner (non-cortical) material was separated and homogenized, and TPP-I activity was measured and adjusted for protein concentration. Data are mean \pm SE for the peak section corresponding to the location of vector administration.

activity in neurons. Adjacent sections were stained by multiple immunofluorescence to reveal the cell types expressing TPP-I using the mature neuronal marker, NeuN, and the astrocytic marker, glial fibrillary acidic protein (GFAP). As with the immunoperoxidase staining, TPP-I expression was observed throughout the striatum of rats except in white matter tracts (Figure 2a). Detection of coexpression by confocal microscopy revealed that TPP-I expression colocalized with neurons in the

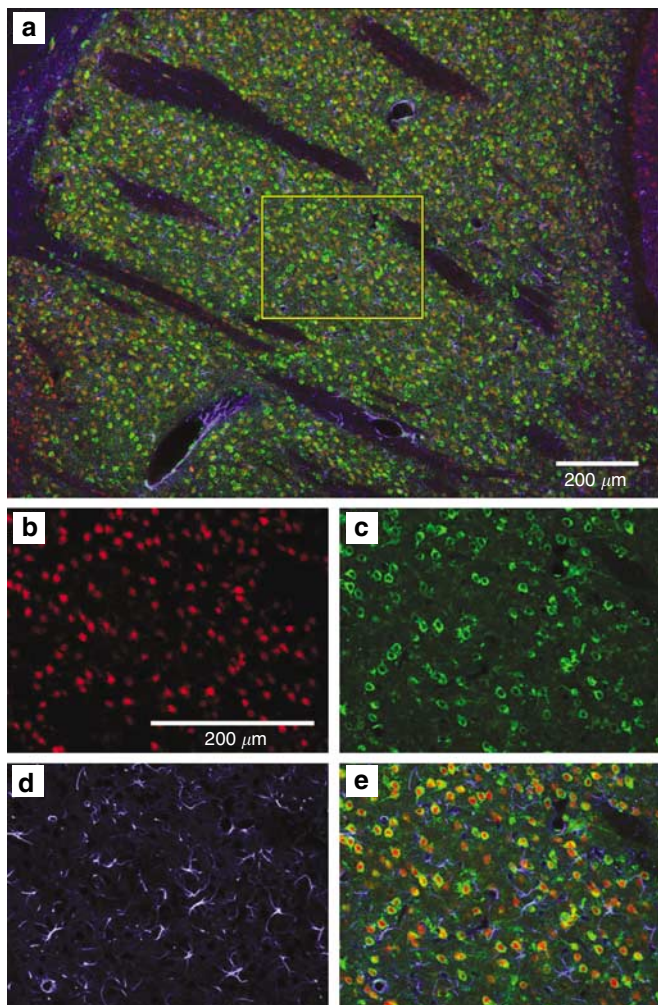


Figure 2 Preferential accumulation of TPP-I in neurons following AAVrh.10-mediated gene transfer to rat striatum. Sections of rat brain were studied by immunofluorescence 4 weeks following striatal injection of 2.5×10^9 gc of AAVrh.10CLN2. **(a)** Superimposition of the signals of TPP-I expressing cells (green) with neuron-specific staining (red, NeuN) and glial-specific staining (blue, GFAP) demonstrating neuron-specific expression mediated by the AAVrh.10 vector in the striatal region. **(b-e)** Higher power views of section outlined in **a**. **(b)** Immunofluorescent staining demonstrating neurons (red) using anti-NeuN; **(c)** immunofluorescent detection of TPP-I (green) in the same section as in **b**; **d** immunofluorescent detection of glia (blue) in the same section as in **b** using anti-GFAP antibody; and **e** superimposition of the signals of TPP-I expressing cells (green) with neuron-specific staining (red, NeuN) and glial-specific staining (blue, GFAP) demonstrating neuron-specific expression. Bar = 200 μ m (**a** and **b-e**).

parenchyma of the striatum (**Figure 2b-e**). Some expression was also noted in the endothelial cells, the choroid plexus, and the meningeal cells (not shown). Triple immunofluorescence studies using neuronal (NeuN) and glial (GFAP) markers in addition to TPP-I showed a strong colocalization of TPP-I with NeuN and no colocalization with GFAP (**Figure 2**). TPP-I cells that did not show apparent colocalization with the primarily nuclear neuronal marker, NeuN, were confirmed to be neuronal by examining adjacent focal planes. Thus, gene transfer with AAVrh.10 provides the required neuronal tropism to treat LINCL.

Projection neurons express TPP-I following striatal injection

Axonal transport may represent a powerful mechanism making use of the connections of the CNS to distribute therapeutic protein beyond the injection site. In our previous study using AAV2 vectors, retrograde transport was observed only at >2 months following gene transfer.⁶ In contrast, in serial sagittal sections examined in rats that received a single injection of AAVrh.10CLN2 into the striatum, axonal transport was readily visible at 4 weeks with strongly TPP-I-positive staining cells found in several structures with projections to the striatum including the frontal cortex, thalamus, and substantia nigra (**Figure 3a**). The intensity of TPP-I staining observed in the substantia nigra approached that seen in the injected area of the striatum. In all three of these regions, the TPP-I-positive cells were multipolar cells with the morphology of neurons (**Figure 3b-d**). To confirm the identity of these cells, adjacent sections were stained using multiple immunofluorescence. As in the striatal target region, TPP-I-positive cells in these projection regions were confirmed to be neuronal based upon their coexpression with the mature neuronal marker, NeuN, and an absence of colocalization with the astrocytic marker, GFAP (**Figure 3e-g**). This data is consistent with extensive axonal transport of vector or TPP-I protein from the site of injection.

AAVrh.10 gene delivery produces widespread expression of TPP-I

To quantitatively assess the extent of TPP-I spread following CLN2 gene transfer, volume estimates were performed comparing all serotypes of AAV (**Figure 3h**). AAV2 produced an overall TPP-I-positive tissue volume of 1.0 mm³, all of which was localized to the striatum at this vector concentration and time point. AAV5hCLN2 gene transfer produced a total TPP-I tissue volume of 10.3 mm³, of which 7.3 mm³ was within the striatum and 3 mm³ was outside. Although AAV8 staining intensity was greater than AAV5, the TPP-positive tissue volume was equivalent to AAV5. The volume of TPP-I-positive tissue for both AAV5 and AAV8 was significantly greater than for AAV2 ($P < 0.001$, both comparisons). However, AAVrh.10CLN2 gene transfer produced a total TPP-I-positive tissue volume of 19.6 mm³, of which 9 mm³ was within the striatum and 10.6 mm³ was outside. Thus, while AAV5, AAV8, and AAVrh.10 gene transfer were all able to provide TPP-I to over 75% of the rat striatum (no difference between vectors, $P > 0.05$), the AAVrh.10 vector provided a significantly larger domain of detectable TPP-I beyond the boundaries of the injected structure than either AAV5 or AAV8 ($P < 0.01$, both comparisons).

Use of non-human primate AAVrh.10 avoids problems of pre-immunity

The use of an AAV vector derived from a non-human primate may provide a therapeutic advantage by removing a barrier to gene transfer owing to pre-existing anti-vector immunity in human recipients. To assess this concept, rats were immunized against AAVrh.10 and against the three common human

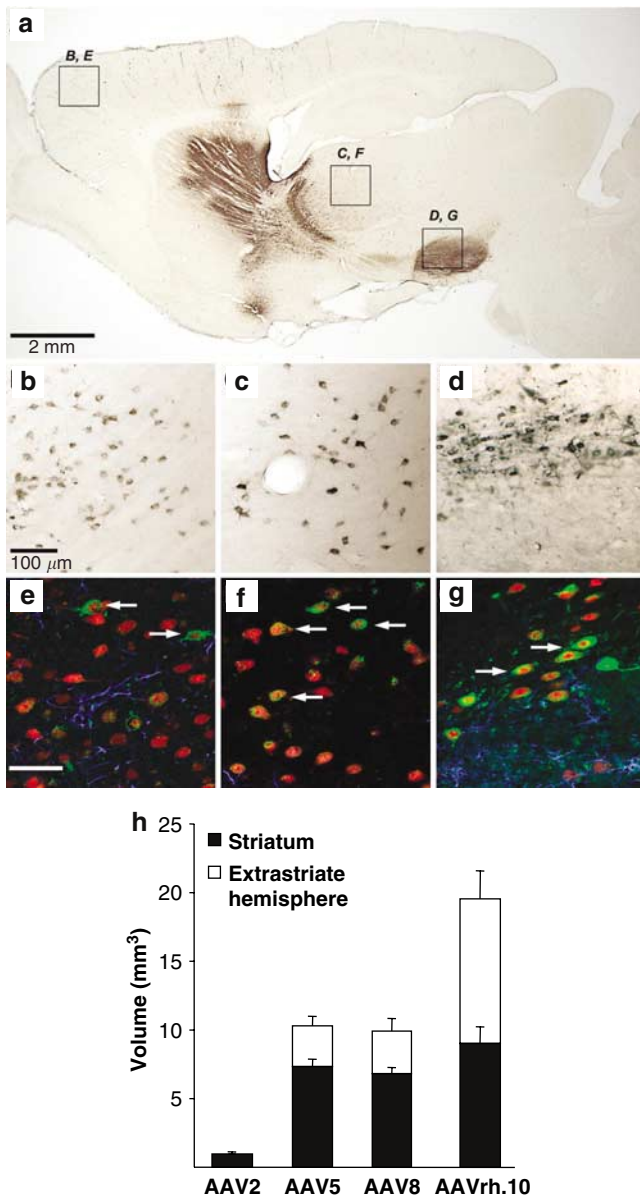


Figure 3 Distribution of TPP-I outside the striatal region of injection following AAVrh.10-mediated gene transfer to the rat CNS. Sections of rat brain were studied by immunohistochemical staining 4 weeks following striatal injection of 2.5×10^9 gc of AAVrh.10CLN2. (a) Sagittal section of the brain showing various TPP-I-positive regions outside the TPP-I-positive striatum. The TPP-I-positive regions indicated by the boxed region are magnified in the panels below; (b) frontal cortex; (c) thalamus; (d) substantia nigra. Superimposition of the signals of TPP-I expressing cells (green) with neuron-specific staining (red, NeuN) and glial-specific staining (blue, GFAP) in the (e) frontal cortex; (f) thalamus; and (g) substantia nigra. Bar = 2 mm for a, 100 μ m for b-d, and 50 μ m for e-g. (h) Volumetric analysis. Serial sections of immunohistochemically stained brains were analyzed using the Cavalieri estimator to determine the TPP-I-positive volume both within (shaded) and outside (open) the striatum. The data are the mean for $n = 3$ rats per vector.

serotypes, AAV1, 2, and 5 (Figure 4a). When the rats immunized against the human serotypes received injection of AAVrh.10 vector into the striatum, there was no difference between the vector-immunized and naïve groups ($P > 0.5$, Figure 4b). By

contrast, pre-immunization against AAVrh.10 was sufficient to reduce significantly TPP-I activity following injection of AAVrh.10 into the striatum ($P < 0.05$ compared with level in previously naïve recipients, Figure 4b).

Assessment of the impact of AAVrh.10CLN2 injection on TPP-I levels in $CLN2^{-/-}$ mice

As AAVrh.10 appeared to give better spread and higher levels of TPP-I activity after injection into the rat brain, we assessed its impact on $CLN2^{-/-}$ mice. Seven week-old mice were injected with AAVrh.10CLN2 at four locations per hemisphere. Following killing, TPP-I activity was undetected in coronal sections of the brain (Figure 5a). TPP-I activity was undetected in brain homogenates from naïve and phosphate-buffered saline (PBS)-injected $CLN2^{-/-}$ mice. Wild-type mice had a TPP-I activity of approximately 3.9×10^4 FU/min-mg, which was spatially uniform from the most rostral section to the most caudal. Injection of the $CLN2^{-/-}$ mice at four locations in each hemisphere resulted in TPP-I activities that varied from $4.7 \pm 2.2 \times 10^4$ FU/min-mg in the most rostral section to levels of $> 36 \times 10^4$ FU/min-mg in the more caudal sections. The TPP-I levels achieved in AAVrh.10CLN2-injected $CLN2^{-/-}$ mice varied from 1 to 27 times the wild-type level, depending on the location.

To further assess distribution of TPP-I activity following intracranial injection, serum and various organs of the $CLN2^{-/-}$ mice were assessed for TPP-I activity. Injection of AAVrh.10CLN2 into the brain parenchyma resulted in TPP-I activities that were greater than or equal to wild-type levels and greater than the background levels in untreated or PBS-treated $CLN2^{-/-}$ mice ($P > 0.05$, all comparisons; Figure 5b) in serum and all organs tested. The organs with the highest levels were liver > spleen > heart, kidney, lung, muscle, and serum. TaqMan realtime polymerase chain reaction established the presence of small amounts of vector in lung, spleen, and liver of some AAVrh.10CLN2-treated mice above the detection limit of < 0.05 copies/cellular genome.

Delivery of AAVrh.10hCLN2 to $CLN2^{-/-}$ mice reduces autofluorescence

To evaluate any therapeutic outcome of AAVrh.10CLN2 treatment, the extent of autofluorescence in AAVrh.10CLN2-injected and control mice was determined. Distinct cellular inclusion of lipofuscin-associated autofluorescence was observed in the striatum (Figure 6a), the thalamus (Figure 6d), and the cerebellum (Figure 6g) of $CLN2^{-/-}$ mice. In $CLN2^{-/-}$ mice receiving injections of AAVrh.10CLN2 to these regions, there was a reduction of autofluorescence in most of the field (Figure 6b, e and h, respectively). Expression of TPP-I in these regions was confirmed by immunofluorescence staining of the tissue with detection of TPP-I at a longer wavelength (not shown). Quantification of lipofuscin-associated autofluorescing particles revealed that there was a 44% reduction in the striatum (Figure 6c), 42% reduction in the thalamus (Figure 6f), and a 41% reduction in the cerebellum as a result of regional TPP-I expression (Figure 6i). These differences were significant ($P < 0.05$ compared with the untreated $CLN2^{-/-}$ mice).

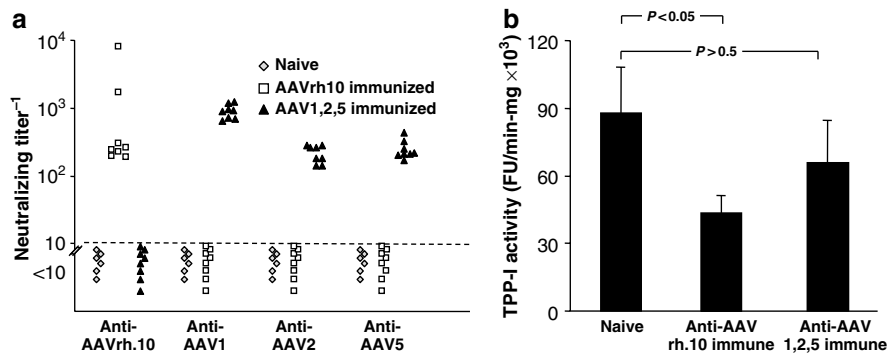


Figure 4 Impact of pre-immunization against common human AAV serotypes on gene transfer by AAVrh.10. **(a)** Neutralizing antibody titers. Six-week-old rats were injected subcutaneously at 3-week intervals with AAV1, 2, and 5, or rh.10 vectors containing irrelevant transgenes (2×10^{10} gc of AAV1lacZ, AAV2lacZ and AAV5GFP, or AAVrh.10 GFP). At 6 weeks following initial subcutaneous injection, serum anti-vector neutralizing immunity was assessed. The anti-AAV1, 2, and 5-immunized mice and the AAVrh.10 immunized mice were then administered 2.5×10^9 gc of AAVrh.10CLN2 to the CNS. **(b)** TPP-I activity. After a further 4 weeks, the brains were cut into 2 mm sagittal sections and homogenized and the TPP-I activity was determined and normalized to protein concentration. The mean and SE TPP-I activity for the peak section, at the site of injection for $n = 8$ pre-immunized and $n = 6$ naive rats is shown.

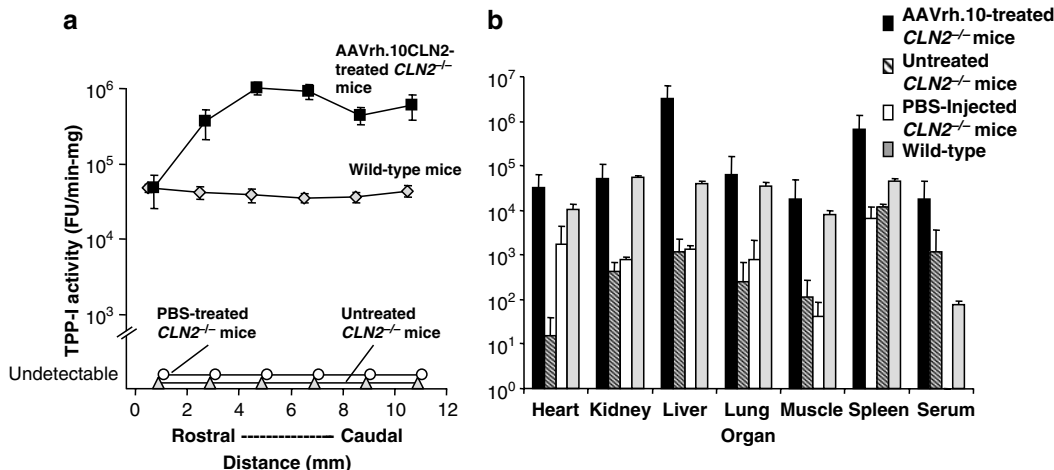


Figure 5 TPP-I activity resulting from intracranial administration of AAVrh.10CLN2 in the brain and other visceral organs of $CLN2^{-/-}$ mice. Mice were injected at eight locations (bilaterally into the upper striatum, lower striatum, thalamus, and cerebellum) with either PBS or AAVrh.10CLN2 (2×10^{10} gc in 3μ l per location). When moribund, the vector- ($n = 14$) or PBS-injected mice ($n = 7$), the control uninjected mice ($CLN2^{-/-}$, $n = 14$) and the uninjected wild-type ($CLN2^{+/+}$, $n = 15$) mice were killed. **(a)** TPP-I activity in the CNS. The brain was cut into 2 mm coronal sections. Each section was homogenized, and TPP-I activity was measured and adjusted for protein concentration. **(b)** TPP-I activity in other organs. Various visceral organs were collected from the same mice, homogenized and TPP-I activity was measured and adjusted for protein concentration.

Impact of AAVrh.10CLN2 on the gait of $CLN2^{-/-}$ mice

Gait analysis of mice was conducted at 18 weeks of age when the untreated $CLN2^{-/-}$ mice are at their worst. In wild-type mice, the footprints for the hind paws are largely superimposed on those for the front paws and there is no dragging of the limbs (Figure 7a). In untreated $CLN2^{-/-}$ mice, there was disordered gait with dragging of feet and poor coordination between the forepaw and the ipsilateral hindpaw. However, in the $CLN2^{-/-}$ mice injected with AAVrh.10CLN2, there was a noticeable improvement in the coordination of the paws and reduced limb dragging.

Impact of AAVrh.10CLN2 on home cage activity of $CLN2^{-/-}$ mice

In pilot experiments, the AAVrh.10CLN2-treated $CLN2^{-/-}$ mice were observed to be in a better physical condition and showed

more normal activities than untreated $CLN2^{-/-}$ controls which exhibited increased nest-making activity and a decrease in tremors. For nest-making activity, the wild-type mice showed consistent activity with increasing age, whereas untreated and PBS-treated $CLN2^{-/-}$ mice showed decreasing activity until death (Figure 7b). AAVrh.10GFP-injected mice showed similar age-dependent reduction of nest making (not shown). By contrast, the AAVrh.10CLN2-treated mice showed a consistent pattern of nest making, with activity less than in the wild-type mice ($P < 0.001$ by analysis of variance with group as factor and time as covariate), but significantly greater than in the untreated or PBS-treated $CLN2^{-/-}$ mice ($P < 0.001$). With regard to tremors, the wild-type mice showed no tremors at any age, whereas PBS-treated, untreated (Figure 7c) or AAVrh.10GFP-treated $CLN2^{-/-}$ mice (not shown) showed more tremors with

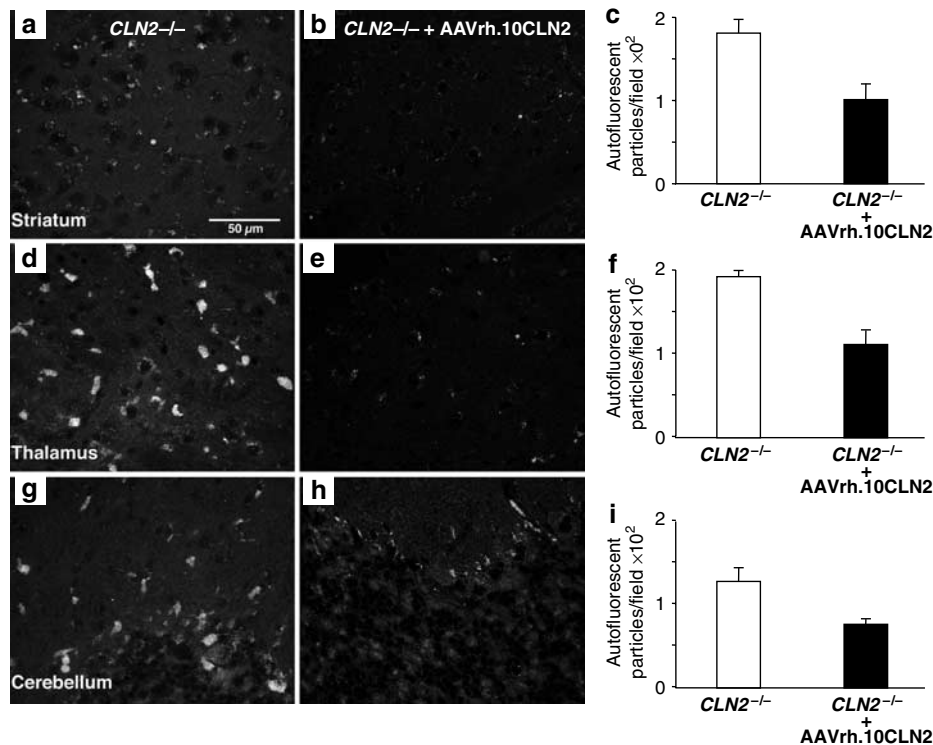


Figure 6 Lipofuscin-associated autofluorescence assessed in the CNS of $CLN2^{-/-}$ mice following CNS administration of AAVrh.10CLN2. Lipofuscin-associated autofluorescence observed in the various regions of the brain of mice that were killed owing to morbidity (~16–18 weeks for untreated $CLN2^{-/-}$ mice; 18–22 weeks for AAVrh.10CLN2-treated mice) including: (a) striatum, untreated $CLN2^{-/-}$ mice; (b) striatum, $CLN2^{-/-}$ mice treated with AAVrh.10CLN2; (c) quantitative data from striatum for naive $CLN2^{-/-}$ and AAVrh.10CLN2-treated mice; (d) thalamus, untreated $CLN2^{-/-}$ mice; (e) thalamus, $CLN2^{-/-}$ mice treated with AAVrh.10CLN2; (f) quantitative data from thalamus for naive $CLN2^{-/-}$ and AAVrh.10CLN2-treated mice; (g) cerebellum, untreated $CLN2^{-/-}$ mice; (h) cerebellum, $CLN2^{-/-}$ mice treated with AAVrh.10CLN2; and (i) quantitative data from cerebellum for naive $CLN2^{-/-}$ and AAVrh.10CLN2-treated mice. For c, f and i, quantification of lipofuscin-associated autofluorescent particles (\pm SEM) in a $1,856 \times 1,450 \mu\text{m}$ field in the various regions of the brain in the $CLN2^{-/-}$ -uninjected mice and $CLN2^{-/-}$ mice treated with AAVrh.10CLN2, and expression of TPP-1 was confirmed by immunofluorescence staining of the tissue with detection of TPP-1 at a longer wavelength (not shown).

increasing age. The AAVrh.10-treated $CLN2^{-/-}$ mice showed intermediate values with a worse tremor rating than wild-type mice ($P < 0.001$), but better tremor rating than untreated or PBS-treated $CLN2^{-/-}$ mice ($P < 0.05$).

AAVrh.10CLN2 delivery leads to improved performance in behavioral tasks

AAVrh.10CLN2-injected mice and controls were also assessed weekly for performance in tests that combine motor and sensory skills. Assessment of $CLN2^{-/-}$ mice by the balance beam test showed an age-dependent decrease in the time that the mouse could stay on the beam, from > 3 min at ages up to 12 week with a rapid decline thereafter (Figure 7d). By contrast, wild-type mice retained the ability to stay on the beam up to age > 20 week. Intracranial delivery of AAVrh.10CLN2 produced a delay in the decline of performance with age. Injection of neither PBS (Figure 7d) nor AAVrh.10GFP (not shown) impacted age-dependent deterioration. AAVrh.10CLN2-treated mice is performed better than untreated or PBS-treated $CLN2^{-/-}$ mice ($P < 0.01$, analysis of variance with age as covariate starting at week 16), although the performance of AAVrh.10CLN2-treated $CLN2^{-/-}$ mice was poorer than the performance of wild-type mice ($P < 0.01$).

Assessment of $CLN2^{-/-}$ mice by the grip strength test showed an age-dependent deterioration (Figure 7e). Wild-type mice showed strong performance on the test, which did not change with age. Injection of neither PBS nor AAVrh.10GFP (not shown) altered age-dependent deterioration. In $CLN2^{-/-}$ mice injected with AAVrh.10CLN2, there was a delay in the deterioration of performance with age ($P < 0.01$, compared to untreated or PBS-treated $CLN2^{-/-}$ mice, analysis of variance with age as covariate, commencing at week 8). The performance of AAVrh.10CLN2-treated $CLN2^{-/-}$ mice did not match that of wild-type mice ($P < 0.01$).

AAV10rh.10CLN2 delivery leads to enhanced survival in $CLN2^{-/-}$ mice

The median age of survival of the AAVrh.10CLN2-injected $CLN2^{-/-}$ mice was 162 days compared with 128 days for the uninjected $CLN2^{-/-}$ mice, 117 days for PBS-injected $CLN2^{-/-}$ mice (Figure 8), and 119 days for the AAVrh.10GFP-injected $CLN2^{-/-}$ mice (not shown). Kaplan–Meier analysis suggested that injection with PBS marginally decreased survival (the PBS-treated $CLN2^{-/-}$ mice had a significantly shorter lifespan than the untreated $CLN2^{-/-}$ mice, $P < 0.05$). In contrast, the AAVrh.10CLN2-injected $CLN2^{-/-}$ mice exhibited a significant

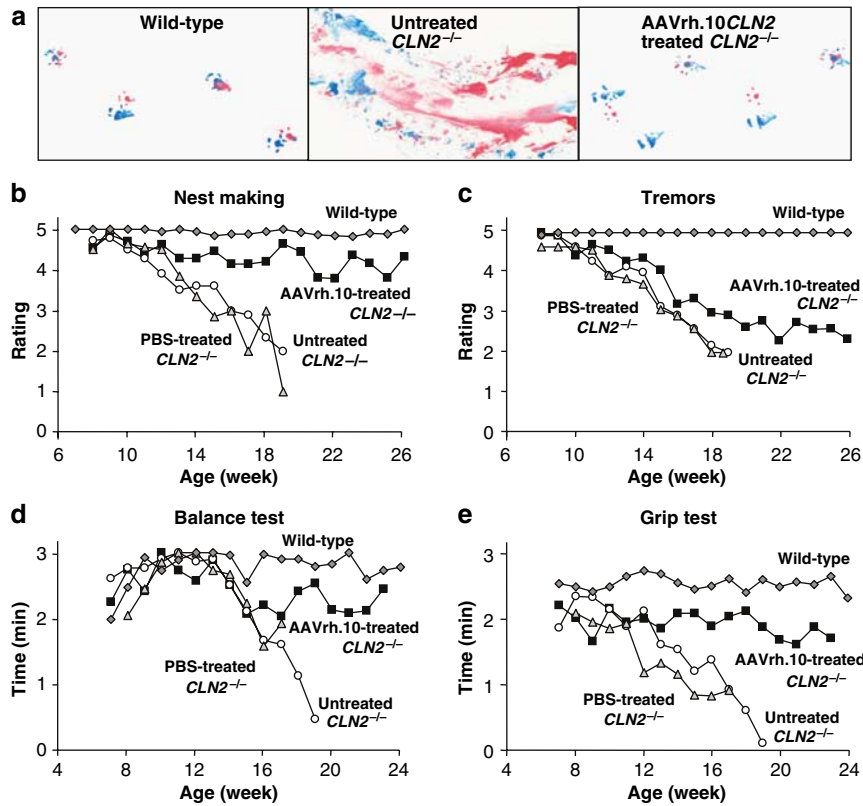


Figure 7 Impact of AAVrh.10CLN2 administration on phenotype of *CLN2*^{-/-} mice. Mice were assessed weekly after administration of vector or PBS at 7 weeks of age. **(a)** Gait analysis. The front feet of each mouse were dipped in red ink and the rear feet were dipped in blue ink. The mouse was placed at the light end of a tunnel over a sheet of white paper. As the mouse runs to the dark end of the tunnel, the footprints are recorded. Representative examples are shown for mice of 18 weeks of age. Left: wild-type *CLN2*^{+/+} mouse; middle: untreated *CLN2*^{-/-} mouse; and right: AAVrh.10CLN2 treated *CLN2*^{-/-} mouse. **(b)** Nest making. Effect of administration of AAVrh.10CLN2 on the ability of *CLN2*^{-/-} mice to create and upkeep nests (scale 0–5, see Materials and Methods). **(c)** Tremors. Effect of administration of AAVrh.10CLN2 on tremors in *CLN2*^{-/-} mice (scale 0–5, see Materials and Methods). **(d)** Balance. Effect of administration of AAVrh.10CLN2 on performance of *CLN2*^{-/-} mice on the balance beam. **(e)** Grip strength. Effect of administration of AAVrh.10CLN2 on performance of *CLN2*^{-/-} mice on grip strength. The number of mice per group for **b** and **c** included: untreated *CLN2*^{-/-}, *n* = 14; AAVrh.10CLN2-injected *CLN2*^{-/-}, *n* = 14; PBS-injected *CLN2*^{-/-}, *n* = 14; *CLN2*^{+/+}, *n* = 16. The number of mice for **d** and **e** included: untreated *CLN2*^{-/-}, *n* = 21; AAVrh.10CLN2-injected *CLN2*^{-/-}, *n* = 20; PBS-injected *CLN2*^{-/-}, *n* = 14, and *CLN2*^{+/+}, *n* = 22.

survival advantage over the untreated *CLN2*^{-/-} and PBS-treated *CLN2*^{-/-} mice (*P* < 0.001 both comparisons).

DISCUSSION

Successful gene therapy for LINCL and other lysosomal storage disorders that affect the CNS requires neurotropic gene delivery, expression of therapeutic levels of protein for a long duration with extensive spread through the brain. Previously, we have shown that an AAV2 vector containing *CLN2* can achieve locally high levels of TPP-I for at least 18 months⁶ and can clear storage granules in the CNS of *CLN2*^{-/-} mice, but with no reported improvement in performance or mortality.⁷ In this study, we compared several AAV serotypes for TPP-I expression following CNS administration. Overall, the non-human primate-derived serotype, AAVrh.10, expressing the *CLN2* cDNA produced the highest levels and broadest distribution of TPP-I expression. Immunity to human AAV serotypes did not affect *CLN2* gene transfer by AAVrh.10CLN2, an important consideration for gene delivery in human subjects who may have been exposed to AAV. CNS delivery of AAVrh.10CLN2 to *CLN2*^{-/-} mice restored

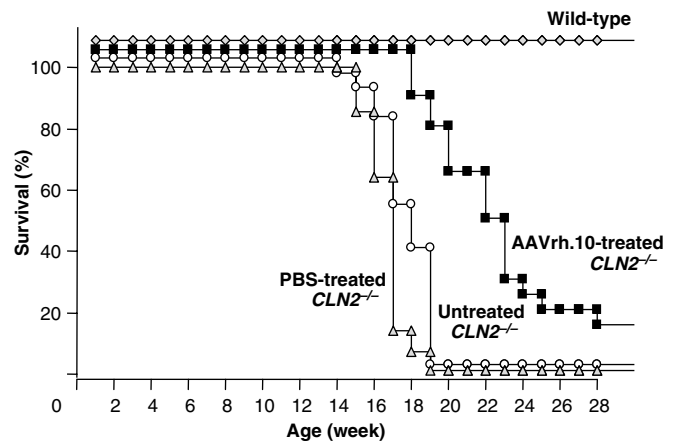


Figure 8 Impact of administration of AAVrh.10CLN2 on survival of *CLN2*^{-/-} mice. *CLN2*^{-/-} mice were administered AAVrh.10CLN2 into eight locations in the brain for a total of 1.6 × 10¹¹ gc. Survival was assessed three times per week. Any mouse that appeared moribund was killed and the age of death was recorded. The number of animals per group assessed: *CLN2*^{-/-}, *n* = 21; *CLN2*^{-/-} + AAVrh.10CLN2, *n* = 20; *CLN2*^{-/-} + PBS, *n* = 14; and *CLN2*^{+/+}, *n* = 22.

normal levels of TPP-I and reduced the accumulated autofluorescent particles in the brain. Assessment of treated *CLN2*^{-/-} mice found that delivery of AAVrh.10CLN2 significantly improved behavioral activity and performance compared to controls and, most importantly, extended survival.

Suitability of AAVrh.10 for widespread CNS delivery

Widespread expression is an important therapeutic goal for AAV-mediated gene transfer of *CLN2* cDNA. The limited extent of transduction by AAV2 vectors may result from sequestration of viral particles by adherence to their extracellular heparin-binding sites. Methods have been proposed to increase distribution by vector formulation with heparin or the simultaneous injection of mannitol to modify diffusion in the brain.¹⁷⁻¹⁹ Other serotypes of AAV offer an alternative route to wider distribution of transgene product. For example, AAV5 achieves wider distribution than does AAV2,²⁰⁻²² and improved distribution of gene transfer at the injection site has also been reported for the non-human-derived AAV serotypes AAV8,^{23,24} and recently for AAVrh.10 with a reporter gene.²⁵ The contribution of receptor binding to the enhanced distribution with the AAVrh.10 vector is unclear as the receptors are unknown.

In addition to local distribution at the delivery site, additional spread of gene product or vector by retrograde transport has been reported in the CNS following the delivery of AAV2^{6,26,27} and AAV9.²⁵ Using a single intrastriatal injection of AAV2 vector expressing *hCLN2*, we previously observed TPP-I expression in the frontal cortex 2 months post-injection, and in the thalamus and the substantia nigra, 8 months post-injection.⁶ In this study, more evidence of early retrograde transport was seen. This may reflect the overall higher expression level achieved with AAVrh.10, which is desirable provided that there is no local toxicity.

Suitability of AAVrh.10 for therapeutic use

From prior toxicology studies with an AAV2 vector and the identical expression cassette as in this study,²⁸ we know that the transgene *per se* is not toxic. One consideration for the use of AAVrh.10 vector in a clinical setting is that pre-existing antibodies to the capsid resulting from prior viral exposure could negatively impact transgene expression and/or be a risk to the patient.²⁹ The AAV2 capsid-derived peptide PADVFMVP-QYGYLTL has been identified as the dominant AAV2-induced cellular immunity-related epitope in humans who received AAV gene transfer to the hepatic artery.³⁰ This epitope is present in the capsids of multiple AAV serotypes and cellular immunity to this determinant in gene therapy subjects immune to human AAVs could theoretically result in the elimination of transduced cells. The high level of expression in AAVrh.10CLN2-treated mice previously immunized to AAV serotypes 1, 2, and 5 suggests that the cellular immunity to epitopes shared among the capsids of multiple serotypes of AAV does not lead to the elimination of transduced cells. Non-human primate-derived serotypes may be advantageous for clinical use owing to their efficiency and distribution and also by reducing the probability of attenuated gene transfer owing to pre-existing immunity. Further, considering the possibility that expression of

a therapeutic gene may not be maintained throughout the patient's lifetime, the use of non-human primate-derived AAVs may provide the option for repeat administration without immune barriers.

Intracranial delivery of AAVrh.10CLN2 to different regions of the *CLN2*^{-/-} mice resulted in elevated levels of TPP-I activity that were greater than wild-type levels, but also resulted in restoration of TPP-I levels in peripheral tissue of *CLN2*^{-/-} mice to at least the level found in wild-type mice. As the blood-brain barrier prevents TPP-I from exiting the CNS, it seems unlikely that the source of this peripheral TPP-I is from the transduced neurons. The most likely source for the peripheral TPP-I expression is the leakage of the AAVrh.10CLN2 vector into the peripheral circulation at the time of intracranial injection, and TaqMan polymerase chain reaction established the presence of small amounts of vector genome in some tissues 4 week following vector injection. This possibility is substantiated by the observation of TPP-I-positive endothelial cells, choroid plexus, and meningeal cells in brain sections. Distribution of viral particles into the vascular system could account for the detection of TPP-I activity in such diverse peripheral tissue. Theoretically, this could be an advantage, as more broad-spaced distribution of TPP-I activity is an advantage for the treatment of LINCL, which is not confined to the CNS.¹ Conversely, transvascular spread of this AAV serotype may allow some level of delivery to the brain after intravenous injection, but the doses of vector required to achieve efficiency would likely be prohibitive in regard to systemic toxicity.

The accumulation of autofluorescing particles in the perinuclear cytoplasm is an indicator of the severity of cellular toxicity in *CLN2*^{-/-} mice.^{7,31} Clearance of cellular debris is a criterion to evaluate therapeutic strategies.^{7,32} We observed a significant decline in the extent of autofluorescing particles in targeted brain regions following delivery of AAVrh.10CLN2. Whether the clearance of the storage granules represents prevention or reversal is unknown.

Effect of AAVrh.10CLN2 delivery on behavior and survival

The most important measures of therapeutic success are the improvement in overall behavioral function and survival. In our prior study, there was no improvement in performance or survival in spite of reduced cellular pathology following AAV2-mediated *CLN2* delivery to *CLN2*^{-/-} mice.⁷ Another study using AAV2-mediated delivery of the palmitoyl protein thioesterase-1 cDNA into the *CLN1*^{-/-} mice (to assess the closely related disease, infantile neuronal ceroid lipofuscinosis) found improvement in cellular pathology and a variety of activity and sensorimotor tasks, but no improvement in survival.³³ In this study, we found that delivery of the *CLN2* gene by AAVrh.10 resulted in improvements in gait, nest-building activity, tests of sensorimotor performance, and in reduced tremor compared with those of controls. The increased performance and longevity mediated by AAVrh.10 vector was afforded by treatment with AAVrh.10CLN2 at 7 weeks of age. It is possible that earlier intervention would further prevent the accumulation of pathological burden and extend performance and survival.

These results suggest that AAVrh.10 is a suitable vector for preclinical development in treatment of LINCL.

MATERIALS AND METHODS

AAV vectors. All AAV vectors contain the same expression cassette consisting of the human *CLN2* cDNA driven by a CMV/ β -actin hybrid promoter surrounded by the inverted terminal repeats of AAV2.^{6,34} 293 cells were transfected using Polyfect with the plasmid containing the AAV genome and with one or two other plasmids (see below) supplying the required adenovirus and AAV functions. After 72 h, the cells were harvested and AAV purified on iodixanol gradients, followed by heparin affinity chromatography for AAV2 or QHP ion exchange chromatography for AAV5, 8, and rh.10. Vector preparations were assessed by TaqMan real-time polymerase chain reaction to determine gc and by *in vitro* gene transfer in 293 ORF6 cells.³⁵

AAV2 vectors were produced using a helper plasmid pPAK-MA2, which contains the *rep* and *cap* genes of AAV2 and the E2, VA, and E4 helper genes of adenovirus.²⁸ AAV5 vectors were produced using a helper plasmid pDG5, which provides the adenovirus helper functions in addition to the *rep* gene of AAV2 and the *cap* gene from AAV5.³⁶ AAV8 vectors were produced by cotransfection of the vector plasmid with two helper plasmids, one (p Δ F6) with the adenovirus helper functions and the other with the AAV2 *rep* gene and the AAV8 *cap* gene.³⁷ AAVrh.10 vectors were produced by cotransfection of the vector plasmid with two helper plasmids, p Δ F6 and the other with the AAV2 *rep* gene and the AAVrh.10 *cap* gene.¹⁶

Rat experiments. For comparisons among AAV serotypes, Fischer 344 male rats (Taconic, Germantown, NY) received unilateral AAV administration into the left striatum (AP +0.60, ML +2.8, and DV -5.2). The AAV vectors (2.5×10^9 gc in PBS) were injected at a rate of 0.2 μ l/min using a microprocessor controlled infusion pump (Model 310, Stoelting, Wood Dale, IL). Rats were also used to assess AAVrh.10 *CLN2* gene transfer in the context of pre-existing immunity against human AAVs. Rats (130–150 g) were pre-immunized subcutaneously on days 0 and 21 with either AAVrh.10Luciferase (2.0×10^{10} gc), or AAV1, 2, and 5 (2.0×10^{10} gc; with nonspecific transgenes) or left as naïve controls. Forty-two days later, serum anti-AAV antibodies were determined by *in vitro* gene transfer assay.¹⁶ Rats were then injected with AAVrh.10*CLN2* (2.5×10^9 gc in 2 μ l of PBS) into the left striatum as described above.

Evaluation of TPP-I protein expression in the rat brain. TPP-I enzymatic activity was assessed in coronal sections of brain as described previously.^{6,38} Immunohistochemical detection of TPP-I distribution in brain 4 weeks after gene transfer was assessed, as described previously.^{6,38} To ensure comparability among serotypes, all sections were processed for immunohistochemistry and imaged in the identical manner. Volume was assessed by using the Cavalieri estimator.³⁹ Multiple immunofluorescence labeling was performed, as described previously^{6,38} using antibodies specific for neurons (mouse anti-NeuN, 1:2,500, Chemicon International, Temecula) or astrocytes (guinea-pig anti-GFAP, 1:500, Advanced Immunochemical, Long Beach, CA). Expression of the *CLN2* transgene product was detected using a mouse anti-human TPP-I antibody at a dilution of 1:1,000.⁴⁰

CNS administration of AAVrh.10 to *CLN2* knockout mice. Original heterozygous breeding pairs of *CLN2* knockout mice back crossed into C57Bl/6 were used to produce all of the *CLN2*^{-/-} mice used in this study.³¹ Genotypes of pups were determined by polymerase chain reaction.³¹ At 7 weeks of age, *CLN2*^{-/-} mice received administrations bilaterally in four locations per hemisphere: lower striatum (A/P +0.60 mm, M/L -1.75 mm, D/V -4.0 mm), upper striatum (A/P

+0.60 mm, M/L -1.75 mm, D/V -2.0 mm), thalamus (A/P -2.0 mm, M/L -1.0 mm, D/V -3.0 mm), and cerebellum (A/P -6.0 mm, M/L -0.5 mm, D/V -1.5 mm). *CLN2*^{-/-} mice received AAVrh.10*CLN2*, AAVrh.10 GFP (both 2×10^{10} gc), or PBS in 3 μ l volume at 0.5 μ l/min. Uninjected *CLN2*^{-/-} mice served as negative controls and *CLN2*^{+/+} served as positive controls.

Enzymatic analysis of TPP-I activity in mouse brain and organs. When mice became moribund, they were deeply anesthetized, and blood was obtained by cardiac puncture. They were transcidentally perfused with PBS and the whole brain, heart, kidney, liver, lung, quadriceps, and spleen were excised. The brain was hemisected and the right hemisphere was submerged in 4% paraformaldehyde for morphological evaluation and left hemisphere was sectioned into 2 mm coronal sections and assessed for TPP-I activity, as described above for the rat brain. Each organ was also homogenized and assessed for TPP-I activity and vector DNA content by Taqman.^{6,41}

Quantification of autofluorescence in mouse brain. Image analysis was used as a measure of the abundance of autofluorescent particles in naïve and AAVrh.10-*CLN2*-injected *CLN2*^{-/-} mice. Autofluorescence was detected in sections of striatum, thalamus, and cerebellum previously stained for the presence of TPP-I by immunofluorescence. Regions containing TPP-I-Alexa488 fluorescence were imaged using UV excitation with a 460/32 emission filter to detect autofluorescence. Equivalent regions were sampled in uninjected mice. All images were collected at identical camera settings on an Optronics Magnafire-equipped Olympus BX51 using a $\times 20$ lens to sample a $1856 \times 1450 \mu$ m field of view. Image analysis was conducted by another investigator blinded to group identity with standardized settings using ImageJ (<http://rsb.info.nih.gov/ij/download.html>). The number of particles and two SDs above mean intensity was determined using a boundary area of 50–800 pixels to include lipofuscin particles within cells, but to exclude nonspecific autofluorescence.

Behavioral assessment of *CLN2* knockout mice. In three separate experimental series, cohorts of $n=7$ *CLN2*^{-/-} mice were injected, as described above, and a number of phenotypic observations were made at intervals to assess the impact of administration of AAVrh.10*CLN2* versus AAVrh.10GFP or PBS. The negative controls were untreated *CLN2*^{-/-} mice and the positive controls were wild-type mice. The assessments used and the testing intervals included (1) gait (in a subset of mice at weekly intervals), (2) nest making (weekly), (3) tremors (weekly), (4) performance of balance beam (weekly), (5) performance on grip strength test (weekly), and (6) morbidity/mortality (three times per week). All tests were performed at the same time each week and under similar conditions. Following three independent experimental series, all available datapoints were combined for statistical analysis.

Gait analysis. Gait analysis was performed with a subset of mice each week sampling all ages and all groups for comparison. A blind tunnel (100 cm long, 20 cm wide, 10 cm high) was created with a plain white paper floor. The front paws of a mouse were dipped in red paint, and back paws in blue paint (Crayola washable paints, Binney and Smith, Easton, PA). The mouse was placed in the front of the tunnel on the paper so that it could run down the tunnel to the dark end. The piece of paper with the colored paw prints was retained for qualitative analysis.

Nest making. Based on empirical observations in the first experimental series, a nest-making scale was created and applied to the second and third experimental series. Individual mice were moved to a clean cage with two cotton nestlets for weekly assessment. They were rated on a scale of 1–5 as follows: score 1, no nest was created and the nestlets remained intact; score 2, edges of the nestlets were chewed but no nest created; score 3, ~50% nestlets were chewed up but the mice were

unable to create an adequate nest; score 4, all the nestlets were chewed up but did not result in a structured nest; and score 5, the structured nest of a healthy mouse.

Tremors. Based on empirical observations in the first experimental series, a tremor scale was created and applied to the second and third experimental series. Tremors were assessed while the mouse was on the balance beam (described below) for a period of 30 s. Animals were rated on a scale of 1–5 as follows: score 1, occasional violent and severe seizures coupled with repeated tremors; score 2, tremors and shaking most of the time; score 3, tremors and shaking occasionally; score 4, a shuffling movement with splayed hind feet but no tremors or shaking; and score 5, an active and agile mouse with no visible tremors or shuffling.

Balance beam test. A horizontal polyurethane treated wooden beam 3 cm in width was affixed to a wooden stand 100 cm high, which was placed over a plastic tub filled with underpads to provide a soft landing for any mouse that fell off. The mouse was placed in the center of the wooden beam and was allowed to move along, and the time till fall was recorded. After 3 min, any mouse that had not fallen was returned to its cage, and the time was recorded as 3 min.

Grip strength. A string was stretched between two vertical wooden dowels, and a plastic tub filled with underpads was placed below. The mouse was placed in the center of the suspended string, hanging by its front paws and the time till falling was recorded. If the mouse was still hanging after 3 min, it was removed from the string and the time recorded as 3 min.

Survival. Three times per week, mice were observed and, if deemed moribund, (inactive with severe shaking and weight loss), were killed and the age of death was recorded.

Statistics. Data is presented as mean ± SE. For serotype and gene expression volume comparisons, groups were compared by analysis of variance using *post hoc* Fisher tests. For the quantification of the autofluorescent storage granules, a two-tailed Student's *t*-test was used. Behavioral assessments were performed by analysis of variance using treatment group as factor and time as covariant. Survival difference between two groups was assessed using Kaplan–Meier test.

ACKNOWLEDGMENTS

We thank P Lobel and D Sleat from University of Medicine and Dentistry of New Jersey for providing the CLN2^{+/-} breeding pairs and for valuable discussions; K Wisniewski and A Golabek from NYS Institute for Basic Research for providing the anti-hCLN2 antibody; TP O'Connor for helpful discussions; E Vassallo and C Sanders for technical assistance; and N Mohamed for help in preparing this paper. These studies were supported, in part, by U01 NS047458; Nathan's Battle Foundation, Greenwood, IN; and the Will Rogers Memorial Fund, Los Angeles, CA.

REFERENCES

- Williams, RE, Gottlob, I, Lake, BD, Goebel, HH, Winchester, BG and Wheeler, RB (1999). CLN2: Classic late infantile NCL. In: Goebel, HH (ed). *The Neuronal Ceroid Lipofuscinoses (Batten Disease)* IOS Press: Amsterdam, pp 37–53.
- Haltia, M (2003). The neuronal ceroid-lipofuscinoses. *J Neuropathol Exp Neurol* **62**: 1–13.
- Vines, DJ and Warburton, MJ (1999). Classical late infantile neuronal ceroid lipofuscinosis fibroblasts are deficient in lysosomal tripeptidyl peptidase I. *FEBS Lett* **443**: 131–135.
- Sleat, DE *et al.* (1997). Association of mutations in a lysosomal protein with classical late-infantile neuronal ceroid lipofuscinosis. *Science* **277**: 1802–1805.
- Haskell, RE, Hughes, SM, Chiorini, JA, Alisky, JM and Davidson, BL (2003). Viral-mediated delivery of the late-infantile neuronal ceroid lipofuscinosis gene, TPP-1 to the mouse central nervous system. *Gene Ther* **10**: 34–42.
- Sondhi, D *et al.* (2005). AAV2-mediated CLN2 gene transfer to rodent and non-human primate brain results in long-term TPP-1 expression compatible with therapy for LINCL. *Gene Ther* **12**: 1618–1632.
- Passini, MA *et al.* (2006). Intracranial delivery of CLN2 reduces brain pathology in a mouse model of classical late infantile neuronal ceroid lipofuscinosis. *J Neurosci* **26**: 1334–1342.
- Kaplitt, MG *et al.* (1994). Long-term gene expression and phenotypic correction using adeno-associated virus vectors in the mammalian brain. *Nat Genet* **8**: 148–154.
- McCown, TJ, Xiao, X, Li, J, Breese, GR and Samulski, RJ (1996). Differential and persistent expression patterns of CNS gene transfer by an adeno-associated virus (AAV) vector. *Brain Res* **713**: 99–107.
- Mandel, RJ, Rendahl, KG, Spratt, SK, Snyder, RO, Cohen, LK and Leff, SE (1998). Characterization of intrastriatal recombinant adeno-associated virus-mediated gene transfer of human tyrosine hydroxylase and human GTP-cyclohydrolase I in a rat model of Parkinson's disease. *J Neurosci* **18**: 4271–4284.
- During, MJ *et al.* (1998). *In vivo* expression of therapeutic human genes for dopamine production in the caudates of MPTP-treated monkeys using an AAV vector. *Gene Ther* **5**: 820–827.
- Skorupa, AF, Fisher, KJ, Wilson, JM, Parente, MK and Wolfe, JH (1999). Sustained production of beta-glucuronidase from localized sites after AAV vector gene transfer results in widespread distribution of enzyme and reversal of lysosomal storage lesions in a large volume of brain in mucopolysaccharidosis VII mice. *Exp Neurol* **160**: 17–27.
- Bosch, A, Perret, E, Desmaris, N and Heard, JM (2000). Long-term and significant correction of brain lesions in adult mucopolysaccharidosis type VII mice using recombinant AAV vectors. *Mol Ther* **1**: 63–70.
- Frisella, WA *et al.* (2001). Intracranial injection of recombinant adeno-associated virus improves cognitive function in a murine model of mucopolysaccharidosis type VII. *Mol Ther* **3**: 351–358.
- Passini, MA *et al.* (2005). AAV vector-mediated correction of brain pathology in a mouse model of Niemann-Pick A disease. *Mol Ther* **11**: 754–762.
- De, BP *et al.* (2006). High levels of persistent expression of alpha1-antitrypsin mediated by the nonhuman primate serotype rh.10 adeno-associated virus despite preexisting immunity to common human adeno-associated viruses. *Mol Ther* **13**: 67–76.
- Nguyen, JB, Sanchez-Pernaute, R, Cunningham, J and Bankiewicz, KS (2001). Convection-enhanced delivery of AAV-2 combined with heparin increases TK gene transfer in the rat brain. *Neuroreport* **12**: 1961–1964.
- Mastakov, MY, Baer, K, Symes, CW, Leichtlein, CB, Kotin, RM and During, MJ (2002). Immunological aspects of recombinant adeno-associated virus delivery to the mammalian brain. *J Virol* **76**: 8446–8454.
- Fu, H *et al.* (2003). Self-complementary adeno-associated virus serotype 2 vector: global distribution and broad dispersion of AAV-mediated transgene expression in mouse brain. *Mol Ther* **8**: 911–917.
- Cressant, A *et al.* (2004). Improved behavior and neuropathology in the mouse model of Sanfilippo type IIIB disease after adeno-associated virus-mediated gene transfer in the striatum. *J Neurosci* **24**: 10229–10239.
- Desmaris, N, Verot, L, Puech, JP, Caillaud, C, Vanier, MT and Heard, JM (2004). Prevention of neuropathology in the mouse model of Hurler syndrome. *Ann Neurol* **56**: 68–76.
- Lin, D *et al.* (2005). AAV2/5 vector expressing galactocerebrosidase ameliorates CNS disease in the murine model of globoid-cell leukodystrophy more efficiently than AAV2. *Mol Ther* **12**: 422–430.
- Broekman, ML, Comer, LA, Hyman, BT and Sena-Estevés, M (2006). Adeno-associated virus vectors serotyped with AAV8 capsid are more efficient than AAV-1 or -2 serotypes for widespread gene delivery to the neonatal mouse brain. *Neuroscience* **138**: 501–510.
- Klein, RL, Dayton, RD, Leidenheimer, NJ, Jansen, K, Golde, TE and Zweig, RM (2006). Efficient neuronal gene transfer with AAV8 leads to neurotoxic levels of Tau or green fluorescent proteins. *Mol Ther* **13**: 517–527.
- Cearley, CN and Wolfe, JH (2006). Transduction characteristics of adeno-associated virus vectors expressing cap serotypes 7, 8, 9, and Rh10 in the mouse brain. *Mol Ther* **13**: 528–537.
- Kaspar, BK, Erickson, D, Schaffer, D, Hinh, L, Gage, FH and Peterson, DA (2002). Targeted retrograde gene delivery for neuronal protection. *Mol Ther* **5**: 50–56.
- Passini, MA, Lee, EB, Heuer, GG and Wolfe, JH (2002). Distribution of a lysosomal enzyme in the adult brain by axonal transport and by cells of the rostral migratory stream. *J Neurosci* **22**: 6437–6446.
- Hackett, NR *et al.* (2005). Safety of direct administration of AAV2(CU)hCLN2, a candidate treatment for the central nervous system manifestations of late infantile neuronal ceroid lipofuscinosis, to the brain of rats and nonhuman primates. *Hum Gene Ther* **16**: 1484–1503.
- Halbert, CL *et al.* (2006). Prevalence of neutralizing antibodies against adeno-associated virus (AAV) types 2, 5, and 6 in cystic fibrosis and normal populations: implications for gene therapy using AAV vectors. *Hum Gene Ther* **17**: 440–447.
- Manno, CS *et al.* (2006). Successful transduction of liver in hemophilia by AAV-Factor IX and limitations imposed by the host immune response. *Nat Med* **12**: 342–347.
- Sleat, DE *et al.* (2004). A mouse model of classical late-infantile neuronal ceroid lipofuscinosis based on targeted disruption of the CLN2 gene results in a loss of tripeptidyl-peptidase I activity and progressive neurodegeneration. *J Neurosci* **24**: 9117–9126.
- Griffey, M *et al.* (2004). Adeno-associated virus 2-mediated gene therapy decreases autofluorescent storage material and increases brain mass in a murine model of infantile neuronal ceroid lipofuscinosis. *Neurobiol Dis* **16**: 360–369.
- Griffey, MA *et al.* (2006). CNS-directed AAV2-mediated gene therapy ameliorates functional deficits in a murine model of infantile neuronal ceroid lipofuscinosis. *Mol Ther* **13**: 538–547.
- Daly, TM, Vogler, C, Levy, B, Haskins, ME and Sands, MS (1999). Neonatal gene transfer leads to widespread correction of pathology in a murine model of lysosomal storage disease. *Proc Natl Acad Sci USA* **96**: 2296–2300.
- Butman, BT *et al.* (2006). Comprehensive characterization of the 293-ORF6 cell line. *Dev Biol Basel* **123**: 225–233.

36. De, B *et al.* (2004). Intrapleural administration of a serotype 5 adeno-associated virus coding for alpha1-antitrypsin mediates persistent, high lung and serum levels of alpha1-antitrypsin. *Mol Ther* **10**: 1003-1010.
37. Gao, GP, Alvira, MR, Wang, L, Calcedo, R, Johnston, J and Wilson, JM (2002). Novel adeno-associated viruses from rhesus monkeys as vectors for human gene therapy. *Proc Natl Acad Sci USA* **99**: 11854-11859.
38. Lin, L and Lobel, P (2001). Production and characterization of recombinant human CLN2 protein for enzyme-replacement therapy in late infantile neuronal ceroid lipofuscinosis. *Biochem J* **357**: 49-55.
39. Peterson, DA, Dickinson-Anson, HA, Leppert, JT, Lee, KF and Gage, FH (1999). Central neuronal loss and behavioral impairment in mice lacking neurotrophin receptor p75. *J Comp Neurol* **404**: 1-20.
40. Kida, E, Golabek, AA, Walus, M, Wujek, P, Kaczmarek, W and Wisniewski, KE (2001). Distribution of tripeptidyl peptidase I in human tissues under normal and pathological conditions. *J Neuropathol Exp Neurol* **60**: 280-292.
41. Hackett, NR *et al.* (2000). Use of quantitative TaqMan real-time PCR to track the time-dependent distribution of gene transfer vectors *in vivo*. *Mol Ther* **2**: 649-656.

ORIGINAL
RESEARCH

J.P. Dyke
H.U. Voss
D. Sondhi
N.R. Hackett
S. Worgall
L.A. Heier
B.E. Kosofsky
A.M. Uluğ
D.C. Shungu
X. Mao
R.G. Crystal
D. Ballon

Assessing Disease Severity in Late Infantile Neuronal Ceroid Lipofuscinosis Using Quantitative MR Diffusion-Weighted Imaging

BACKGROUND AND PURPOSE: Late infantile neuronal ceroid lipofuscinosis (LINCL), a form of Batten disease, is a fatal neurodegenerative genetic disorder, diagnosed via DNA testing, that affects approximately 200 children in the United States at any one time. This study was conducted to evaluate whether quantitative data derived by diffusion-weighted MR imaging (DWI) techniques can supplement clinical disability scale information to provide a quantitative estimate of neurodegeneration, as well as disease progression and severity.

MATERIALS AND METHODS: This study prospectively analyzed 32 DWI examinations from 18 patients having confirmed LINCL at various stages of disease. A whole-brain apparent diffusion coefficient (ADC) histogram was fitted with a dual Gaussian function combined with a function designed to model voxels containing a partial volume fraction of brain parenchyma versus CSF. Previously published whole-brain ADC values of age-matched control subjects were compared with those of the LINCL patients. Correlations were tested between the peak ADC of the fitted histogram and patient age, disease severity, and a CNS disability scale adapted for LINCL.

RESULTS: ADC values assigned to brain parenchyma were higher than published ADC values for age-matched control subjects. ADC values between patients and control subjects began to differ at 5 years of age based on 95% confidence intervals. ADC values had a nearly equal correlation with patient age ($R^2 = 0.71$) and disease duration ($R^2 = 0.68$), whereas the correlation with the central nervous system disability scale ($R^2 = 0.27$) was much weaker.

CONCLUSION: This study indicates that brain ADC values acquired using DWI may be used as an independent measure of disease severity and duration in LINCL.

Late infantile neuronal ceroid lipofuscinosis (LINCL), a form of Batten disease, is an autosomal recessive lysosomal storage disease that results in neurodegeneration.¹ It first manifests between the ages of 2–4 years through seizures followed by deteriorating motor, cognitive, and visual abilities, traditionally leading to death by ages 8–12 years.² Definitive diagnosis of LINCL is done via genetic testing for mutations in the CLN2 gene, which results in deficiency of the lysosomal protease tripeptidyl peptidase-I. Absence of this protease leads to lysosomal distension and neuronal death. There are no known treatments for LINCL other than symptom management. A better understanding of the anatomic distribution of neurodegeneration may permit genetic and cellular therapies to be targeted to appropriate locations in the brain.³

Progression of neuronal degeneration can be assessed by a disability scale based on speech, vision, language, and seizures.⁴ To monitor brain-directed therapies, a modified central nervous system (CNS) disability score has been established.¹ However, these methods are nonspecific in that they do not implicate specific areas of the brain. Quantitative MR imaging techniques may supplement information provided by

the disability scale and provide a more refined evaluation of neurodegeneration, as well as an opportunity for serial assessment of the same patient.

Diffusion-weighted MR imaging (DWI) is a technique that has been shown to detect water diffusion abnormalities in various disease states.^{5–7} Measurement of the apparent diffusion coefficient (ADC) provides a quantitative estimate of the restrictive nature of the motion of water molecules within tissue for each voxel in a diffusion-weighted image. The ADC is known to decrease with increasing age in normal children as the brain becomes increasingly myelinated and structured.^{8,9} This study used whole-brain ADC histograms to obtain a measure of the degree of water restriction in the entire brain. The whole-brain histogram was fitted using a dual Gaussian function in addition to a partial volume function. We hypothesized that the global maximum of the model fit characterizing the whole-brain ADC value derived by DWI techniques would supplement clinical disability scale information to provide a quantitative estimate of neurodegeneration, as well as disease progression and severity.

Materials and Methods

Patient Selection

The research protocol was reviewed and approved by the institutional review board at our institution. Eighteen patients presenting with genetically confirmed LINCL (9 boys and 9 girls) of ages 3.4 through 13.8 years participated in this protocol, for a total of 32 DWI examinations (Table). The average age at diagnosis for all of the patients was 3.9 ± 1.0 years. Disease severity was clinically monitored throughout the study using a modified CNS disability scale.⁴ The visual component was removed from the scoring system while retaining measures

Received October 10, 2006; accepted after revision December 11.

From the Citigroup Biomedical Imaging Center (J.P.D., H.U.V., D.C.S., X.M., D.B.) and the Departments of Radiology (J.P.D., H.U.V., L.A.H., A.M.U., D.C.S., X.M., D.B.), Genetic Medicine (D.S., N.R.H., R.G.C.), and Pediatrics (S.W., B.E.K.), Weill Medical College of Cornell University, New York, NY.

This work was supported by grants 8R01EB002070-09, 5U01NS047458-02, and Nathan's Battle Foundation, Greenwood, Ind.

Address correspondence to Jonathan P. Dyke, Citigroup Biomedical Imaging Center, Weill Cornell Medical College, Box 234, 1300 York Ave, New York, NY 10021; e-mail: jpd2001@med.cornell.edu

DOI 10.3174/ajnr.A0551

Whole-brain ADC values for 18 patients with LINCL					
Patient	Age at Diagnosis, y	Scan	Age at Scan, y	CNS Score	ADC × 10 ³ , mm ² /s
BD-01	5.3	1	8.4	3	1.12
		2	8.6	3	1.18
BD-02	4.8	3	9.7	3	0.98
		4	10.0	3	1.00
BD-03	3.5	5	6.6	3	0.96
		6	6.9	3	0.92
BD-04	4.5	7	13.8	3	1.80
BD-05	4.8	8	6.2	5	0.96
		9	7.1	2	0.96
BD-06	4.4	10	8.0	3	1.10
		11	8.1	3	1.06
BD-07	3.3	12	6.6	3	1.02
BD-08	4.7	13	6.0	4	0.94
		14	7.0	3	1.08
BD-09	3.3	15	6.7	4	0.92
		16	7.7	3	0.98
BD-10	3.8	17	5.0	5	0.90
		18	5.4	5	0.90
BD-11	4.4	19	5.4	5	0.94
BD-12	2.8	20	4.4	4	0.92
		21	4.5	4	0.90
BD-13	4.3	22	4.4	6	0.84
		23	4.5	6	0.84
BD-14	1.9	24	3.4	5	0.90
		25	3.6	5	0.82
BD-15	4.4	26	4.7	4	0.88
BD-16	4.8	27	5.2	5	0.86
		28	5.3	5	0.90
BD-17	4.8	29	5.4	4	0.90
		30	3.4	5	0.84
BD-18	2.8	31	3.4	5	0.82
		32	3.4	5	0.84

Note:—ADC indicates apparent diffusion coefficient; LINCL, late infantile neuronal ceroid lipofuscinosis; CNS, central nervous system.

of motor function, seizure activity, and language skills to focus on the neurologic aspects of the disease.¹ Each of these areas was ranked from 0 to 3 and then summed to provide a total score with 0 being the most severe. At the time of MR imaging, patients presented the following CNS disability scores: 2 (*n* = 1), 3 (*n* = 12), 4 (*n* = 6), 5 (*n* = 11), and 6 (*n* = 2).

Clinical MR Imaging Methods

All of the image data were acquired on a 3T MR imaging system (GE Medical Systems, Milwaukee, Wis). Conventional clinical imaging included T1-weighted, T2-weighted, and fluid-attenuated inversion recovery sequences. Next, a spin-echo diffusion-weighted echo-planar imaging sequence was implemented over the entire brain using a section thickness of 5 mm with an FOV of 22 cm, a matrix size of 128 × 128, a TR of 8.2 seconds, a TE of 70–80 ms, and 2 averages. Diffusion weighting was acquired using *b* = 1000 s/mm² in 3 orthogonal directions for a total scan time of 65 seconds.

Analysis Methods

Images were exported to an Optiplex Pentium 4 4.0-GHz PC (Dell, Round Rocker, Texas) and analyzed using the Interactive Data Language (IDL 6.2; ITT, Boulder, Colo). Images were masked to include voxels having a signal intensity greater than 15% of the maximum value in the DWI series. ADC values were calculated as follows:

$$1) \quad ADC = -\frac{1}{b} \ln\left(\frac{S_1}{S_0}\right)$$

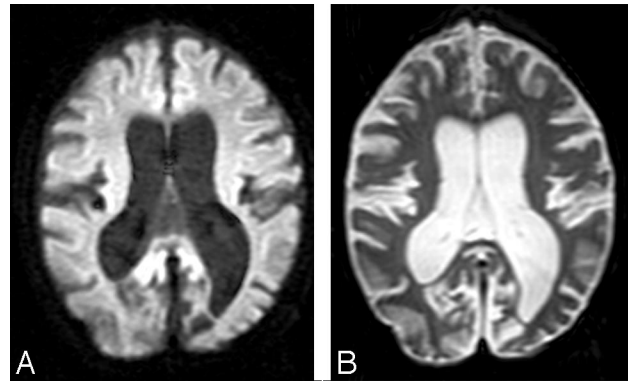


Fig 1. A, A diffusion-weighted image (*b* = 1000 s/mm²) and an image acquired without diffusion weighting (*B*) show enlarged sulci and dilated ventricles consistent with atrophic changes from a representative patient with LINCL.

where *S_i* represents the signal intensity from the diffusion-weighted image and *S₀* the signal intensity without diffusion weighting (Fig 1). ADC values were placed in a normalized histogram of unit area. The normalized histogram was fitted with a dual Gaussian distribution function and a partial volume distribution function (Fig 2). These 3 functions were designed to segment the brain, CSF, and brain-CSF partial volume components, respectively. Modeling of these functions was based on arguments given previously^{8,10} but was modified in the following sense: the ADC distribution function was modeled as follows:

$$2) \quad P_{ADC} = f_{brain} P_{brain} + f_{CSF} P_{CSF} + (1 - f_{brain} - f_{CSF}) P_{PV},$$

where

$$3) \quad p_{brain} = \frac{1}{\sqrt{2\pi}\sigma_{brain}} \exp\left[-\frac{1}{2}\left(\frac{ADC - \mu_{brain}}{\sigma_{brain}}\right)^2\right]$$

and

$$4) \quad p_{CSF} = \frac{1}{\sqrt{2\pi}\sigma_{CSF}} \exp\left[-\frac{1}{2}\left(\frac{ADC - \mu_{CSF}}{\sigma_{CSF}}\right)^2\right]$$

are the normalized Gaussian functions describing the distribution of ADC values in the brain and CSF, respectively, and *f_i* are respective weighting factors. The partial volume distribution function was modeled under the assumption that voxels that consist of brain matter and CSF contain both components in all of the possible and equally probable fractions, that is:

$$5) \quad P_{PV} = \int_0^1 \frac{1}{\sqrt{2\pi}\sigma(t)} \exp\left[-\frac{1}{2}\left(\frac{ADC - \mu(t)}{\sigma(t)}\right)^2\right] dt,$$

where $\mu(t) = (1 - t)\mu_{brain} + t\mu_{CSF}$ and $\sigma^2(t) = (1 - t)^2\sigma_{brain}^2 + t^2\sigma_{CSF}^2$. Curve fitting of the 6 parameters μ_{brain} , μ_{CSF} , σ_{brain} , σ_{CSF} , f_{brain} , and f_{CSF} was performed within IDL 6.2 using a gradient expansion algorithm to compute a nonlinear least-squares fit to the data. Note that the partial volume function is completely determined by the parameters of the 2 Gaussians. The histogram bin containing the maximum value of the combined fitted function (Equation 2), of the cerebral compartment was used as a measure of the whole-brain ADC value.

A Monte Carlo algorithm was written in IDL 6.2 to verify the functional form of the equations describing the analytical partial volume model. Two standard normally distributed floating point pseudorandom number generators, *r_(i)*, were used to sample points from

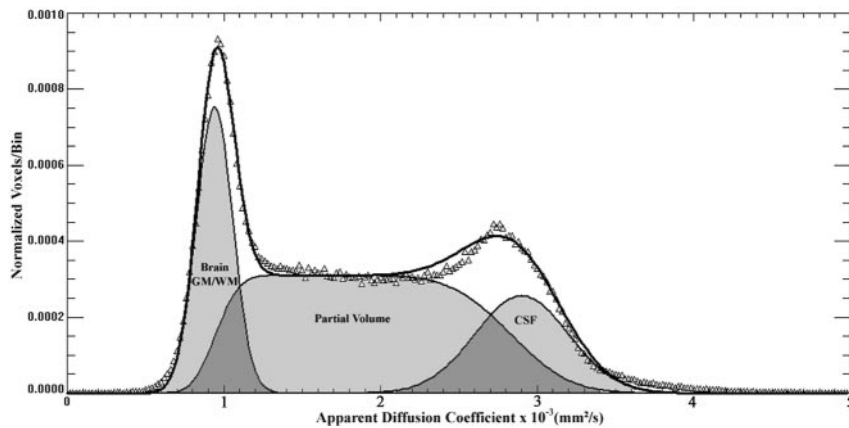


Fig 2. A whole-brain ADC histogram from a representative patient with LINCL shows the dual Gaussian and partial volume functions that were used to fit the whole brain, partial volume, and CSF compartments.

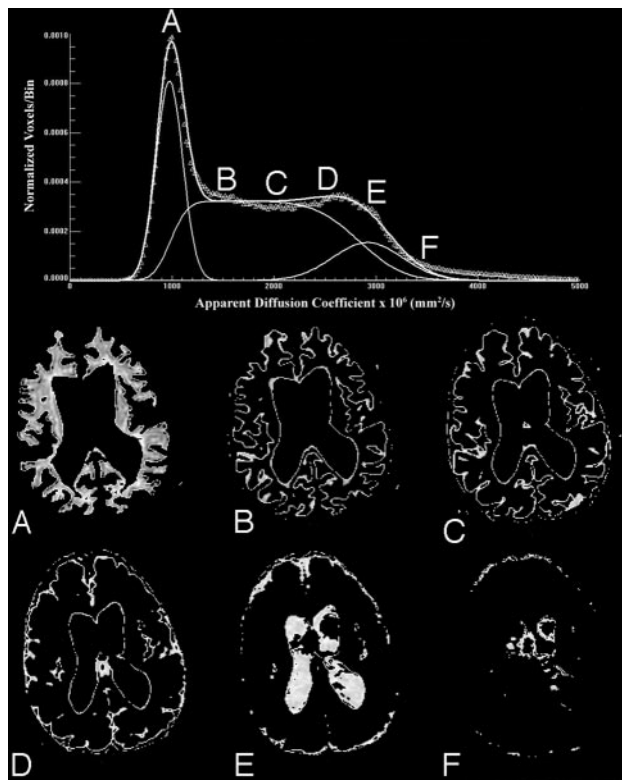


Fig 3. Voxels associated with specific ranges of ADC values provide visual confirmation that compartments identified as whole brain, partial volume, and CSF correspond with specific regions as shown from a representative section of a patient with LINCL. ADC ranges displayed are described below.

- A, $1.0 \pm 0.2 \times 10^{-3} \text{ mm}^2/\text{s}$.
- B, $1.5 \pm 0.2 \times 10^{-3} \text{ mm}^2/\text{s}$.
- C, $2.0 \pm 0.2 \times 10^{-3} \text{ mm}^2/\text{s}$.
- D, $2.5 \pm 0.2 \times 10^{-3} \text{ mm}^2/\text{s}$.
- E, $3.0 \pm 0.2 \times 10^{-3} \text{ mm}^2/\text{s}$.
- F, $3.5 \pm 0.2 \times 10^{-3} \text{ mm}^2/\text{s}$.

the Gaussian distributions (Equations 3 and 4) characterizing the brain and CSF compartments. A uniformly distributed floating point pseudorandom number generator was used to determine the partial volume weighting factors, t . A partial volume voxel was then placed in the histogram according to the following:

$$6) \quad p_{PV} = (1 - t)(\mu_{brain} + r_{brain}\sigma_{brain}) + t(\mu_{CSF} + r_{CSF}\sigma_{CSF}),$$

This process was repeated approximately 200,000 times to get an adequate sampling estimate of the functional form of the partial volume

component. The Monte Carlo sampling method was found to produce the same functional form as the analytic solution. In addition, qualitative visual confirmation of gray and white matter, partial volume, and CSF components was obtained using images generated as shown in Fig 3 by displaying only voxels associated with specific ranges of ADC values. In the example of Fig 3, voxels are shown with the following ranges: 1) $1.0 \pm 0.2 \times 10^{-3} \text{ mm}^2/\text{s}$; 2) $1.5 \pm 0.2 \times 10^{-3} \text{ mm}^2/\text{s}$; 3) $2.0 \pm 0.2 \times 10^{-3} \text{ mm}^2/\text{s}$; 4) $2.5 \pm 0.2 \times 10^{-3} \text{ mm}^2/\text{s}$; 5) $3.0 \pm 0.2 \times 10^{-3} \text{ mm}^2/\text{s}$; and 6) $3.5 \pm 0.2 \times 10^{-3} \text{ mm}^2/\text{s}$.

Previously published ADC values derived from whole-brain histograms of age-matched control subjects were used for comparison with the LINCL patients. In that study, data were fitted with a 9-parameter triple-Gaussian model that incorporated components of brain parenchyma, CSF, and a mixing compartment attributed to partial volume averaging.¹¹ The mean of the first Gaussian characterizing brain parenchyma defined the whole-brain ADC value for this method. For the purpose of comparison only, the full dataset of LINCL patients was fitted with the triple-Gaussian model in addition to the partial volume model described in Equation 2.

The method of statistical bootstrapping was used to estimate the error on the maximum of the ADC histogram for 5 DWI patient studies chosen at random from the full dataset.¹² The histogram contained 250 bins of data, which were randomly resampled 100 times with replacement using IDL 6.2. Each of these resampled histograms was fitted with the partial volume model, and the resulting error on the maximum ADC value was calculated. A single-factor analysis of variance (ANOVA) test was used to determine statistically significant variances in the mean ADC values of the patients when grouped by their CNS disability scores. The resulting F value was compared with the critical F value for the specified number of samples, and a P value was determined using a 95% confidence interval to gauge significance for all of the results.

Results

The whole-brain ADC value containing both gray and white matter components of the brain was determined from the 32 DWI scans of the 18 LINCL subjects and given with age, CNS disability score at the time of the scan, and the age at diagnosis (Table). The estimate of percentage error on the maximum ADC value was $1.7\% \pm 0.3\%$ ($n = 5$) using the statistical bootstrap method. The whole-brain ADC values derived from the histogram increased with age for all of the LINCL patients (Fig 4), in contrast with the decrease in ADC as a function of age as seen in age-matched control subjects. The ADC values increased linearly with patient age [$\text{ADC} \times 10^3 \text{ (mm}^2/\text{s)} =$

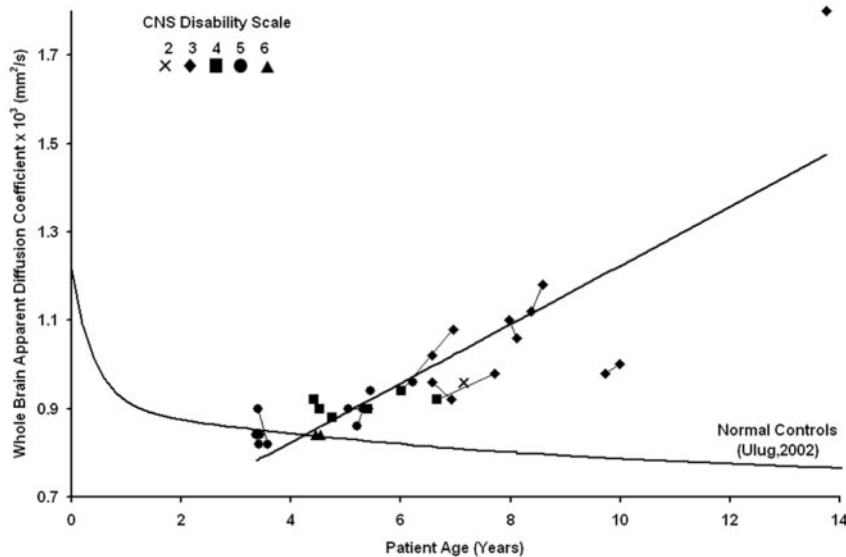


Fig 4. The whole-brain ADC value is plotted versus age for all of the patients showing an increasing trend over time. Serial studies are connected by lines, and the CNS disability scale is shown in the legend. Previously published whole-brain ADC values from age-matched control subjects are plotted for comparison.

0.065 * Age (years) + 0.564] yielding $R^2 = 0.71$ ($P < .0001$). The whole-brain ADC values were correlated with the disease duration calculated as the age at diagnosis subtracted from the age at examination. A linear trend showed significant correlation between the whole-brain ADC histogram values and disease duration yielding $R^2 = 0.68$ ($P < .0001$). There were no significant differences in the ADC values of the Gaussian representing brain parenchyma of the LINCL patients fitted using both Equation 2 and the triple-Gaussian methods. The point at which the lower 95% confidence interval of the LINCL patients crossed the upper 95% confidence interval of the control subjects was at 5 years. This implies that statistically significant deviations in whole-brain ADC may be detected as early as 5 years of age in this population.

A single-factor ANOVA test with a 95% confidence interval compared the mean of the whole-brain ADC histogram with the modified CNS disability scale. The ANOVA analysis yielded $F > F_{crit}$ ($3.8 > 2.7$) and a P value of .01, confirming differences in the means of the whole-brain ADC values between patients grouped by LINCL scale. A linear regression confirmed that the whole-brain ADC values increased with disease severity ($R^2 = 0.27$; $P = .002$).

Discussion

A number of noninvasive imaging approaches have been applied to the brains of subjects with various forms of neuronal ceroid lipofuscinosis. Conventional MR imaging and CT have been used to demonstrate the presence of cerebral atrophy in multiple forms of neuronal ceroid lipofuscinosis.¹³⁻¹⁶ However, atrophic grading using conventional MR imaging is only a subjective measure of disease severity. A diffuse hyperintensity of cerebral white matter has been reported in LINCL patients.^{2,13} Postmortem studies of LINCL and juvenile neuronal ceroid lipofuscinosis patients confirm a loss of myelin and gliosis in periventricular white matter.² Consistent with these findings, our patients presented with enlarged sulci and ventricles in both the supratentorial and infratentorial compartments of the brain consistent with marked atrophy. In addition, high signal intensity on T2-weighted images was observed in the periventricular white matter. A previously

published CT study also showed increased subarachnoid and ventricular spaces, which were correlated with patient age.¹⁶ However, CT findings were usually normal in patients younger than 10 years of age, and these findings did not correlate with onset or severity of the abnormalities, possibly reflecting the diverse forms of neuronal ceroid lipofuscinosis in this study before genetic testing.¹⁶

MR spectroscopic imaging (MRSI) has also been used to noninvasively assess brain metabolism in various neurodegenerative diseases, such as Alzheimer and Parkinson diseases.^{7,17} ¹H-MR spectroscopy has used single voxel techniques to determine abnormal metabolic changes in patients with LINCL within specific regions, such as the white matter of the parietal lobe.¹⁸ MRSI is a sensitive though nonspecific method for assessing metabolic changes in patients with LINCL compared with normal control subjects. Multivoxel chemical shift imaging may provide further information about metabolic degradation in specific regions of the brain.¹⁹

Traditionally, DWI has been used to assess isotropic restriction of water molecules in stroke or white matter diseases of the brain, such as multiple sclerosis or ischemic leukoariosis.^{20,21} DWI has rarely been used to examine neurodegenerative diseases of the brain, which primarily affect gray matter. One study examined patients with Huntington disease with DWI and found a correlation ($P = .05$) between disease stage and the mean of the whole-brain ADC histograms.²² Our study showed a strong correlation between whole-brain ADC values and age along with both disease severity and duration in patients with LINCL.

This study examined the water diffusivity of the entire brain through the use of DWI. Whole-brain ADC histograms were created that included all of the voxels in the brain having signal intensities greater than a predefined threshold. This method eliminated user subjectivity required to place regions of interest on the images. The reproducibility of whole-brain ADC histograms has been confirmed as an accurate method to quantify water diffusion in a robust and objective manner.²³ The whole-brain histogram was fitted using dual Gaussian functions in addition to a partial volume function to characterize brain parenchyma while excluding partial volume and

CSF contamination. The global maximum of this function yielded an estimate of the whole-brain ADC value. As expected, compartments identified as brain parenchyma, partial volume, or CSF corresponded with those specific locations in the brain. The fitted Gaussian function with the lowest mean ADC corresponded with that of parenchyma containing both gray and white matter regions. Voxels labeled as containing partial volume fractions in the model were found to correspond with those regions at the boundary between gray and white matter and CSF. As the ADC value increased, voxels along the gray matter boundary were seen to migrate toward regions of CSF. Similarly, the voxels with high ADC were associated with the CSF compartment. Voxels having higher ADC values than CSF were also observed, most likely because of CSF flow artifacts in the region.

A significant correlation between increased whole-brain ADC values and patient age was found for all of the patients. Deviation of whole-brain ADC values from the control subjects became significant at 5 years of age, suggesting a common age of disease onset. This is consistent with the uniform age of manifestation of LINCL clinical symptoms. Because of the progressive increase of ADC values with age and the uniform age at diagnosis, it follows that the ADC values also correlate with time since diagnosis. Similarly, because severity increases with age, it would be expected that ADC values correlate with severity, which is indeed the case, though this correlation is less strong.

Changes in the ADC values were likely the result of a combination of physiologic mechanisms that primarily alter the restrictive nature of gray matter and, to a lesser degree, that of white matter. A study found that calcium-binding proteins linked to GABAergic interneurons in the cortex and cerebellum were disrupted in patients with LINCL.²⁴ An additional postmortem study of 13 case subjects with LINCL found a moderate-to-severe loss of myelin and mild-to-moderate gliosis in the periventricular white matter of 10 of 13 case subjects.² Increased signal intensity in the periventricular white matter on T2-weighted MR images in patients with LINCL was correlated with histology confirming atrophy. These findings implied a loss of neuronal integrity in gray matter and decreased myelination in white matter. This is consistent with the increased whole-brain ADC values found in this study showing the progressive nature of the disease.

Whole-brain ADC values correlated better with patient age than the modified CNS disability scale. Whole-brain ADC values may, thus, provide a more accurate physiologically based indicator of disease progression and severity. The objective acquisition and analysis criterion of whole-brain ADC histograms is an attractive feature of this technique. In addition, ADC measures provide a more continuous scale with which to assess severity in comparison with the discrete characterization of patient disability.

Conclusions

This study was conducted to evaluate whether quantitative data derived by DWI techniques can supplement clinical disability scale information to provide a quantitative estimate of neurodegeneration, as well as disease progression and severity. The results presented are consistent with known conventional MR imaging findings but suggest an

objective and complementary technique to monitor disease progression. Increased whole-brain ADC values agree with imaging results characteristic of LINCL. Whole-brain ADC values were significantly correlated with patient age, disease severity as assessed with the modified CNS disability scale, and disease duration. DWI has been shown to detect variances in cerebral water diffusion abnormalities in patients with LINCL and may have the potential to monitor disease progression and severity in conjunction with the clinical characterization of patient disability.

References

1. Crystal RG, Sondhi D, Hackett NR, et al. **Clinical protocol. Administration of a replication-deficient adeno-associated virus gene transfer vector expressing the human CLN2 cDNA to the brain of children with late infantile neuronal ceroid lipofuscinosis.** *Hum Gene Ther* 2004;15:1131–54
2. Autti T, Raininko R, Santavuori P, et al. **MRI of neuronal ceroid lipofuscinosis. II. Postmortem MRI and histopathological study of the brain in 16 cases of neuronal ceroid lipofuscinosis of juvenile or late infantile type.** *Neuroradiology* 1997;39:371–77
3. Sondhi D, Hackett NR, Apblett RL, et al. **Feasibility of gene therapy for late neuronal ceroid lipofuscinosis.** *Arch Neurol* 2001;58:1793–98
4. Steinfeld R, Heim P, von Gregory H, et al. **Late infantile neuronal ceroid lipofuscinosis: quantitative description of the clinical course in patients with CLN2 mutations.** *Am J Med Genet* 2002;112:347–54
5. Ballon D, Dyke J, Schwartz LH, et al. **Imaging therapeutic response in human bone marrow using rapid whole-body MRI.** *NMR Biomed* 2000;13:321–28
6. Bosma GP, Huizinga TW, Mooijaart SP, et al. **Abnormal brain diffusivity in patients with neuropsychiatric systemic lupus erythematosus.** *AJNR Am J Neuroradiol* 2003;24:850–54
7. Kantarci K. **Magnetic resonance markers for early diagnosis and progression of Alzheimer's disease.** *Expert Rev Neurotherap* 2005;5:663–70
8. Ulug AM. **Monitoring brain development with quantitative diffusion tensor imaging.** *Develop Science* 2002;5:286–92
9. Mukherjee P, McKinstry RC. **Diffusion tensor imaging and tractography of human brain development.** *Neuroimaging Clin N Am* 2006;16:19–43
10. Laidlaw DH, Fleischer KW, Barr AH. **Partial-volume Bayesian classification of material mixtures in MR volume data using voxel histograms.** *IEEE Trans Med Imag* 1998;17:74–86
11. Chun T, Filippi CG, Zimmerman RD, et al. **Diffusion changes in the aging human brain.** *AJNR Am J Neuroradiol* 2000;21:1078–83
12. Hedges S, Shah P. **Comparison of mode estimation methods and application in molecular clock analysis.** *BMC Bioinformatics* 2003;4:31
13. Nardocci N, Verga ML, Binelli S, et al. **Neuronal ceroid-lipofuscinosis: a clinical and morphological study of 19 patients.** *Am J Med Genet* 1995;57:137–41
14. Santavuori P, Vanhanen SL, Autti T. **Clinical and neuroradiological diagnostic aspects of neuronal ceroid lipofuscinoses disorders.** *Eur J Paediatr Neurol* 2001;5:157–61
15. Vanhanen SL, Puranen J, Autti T, et al. **Neuroradiological findings (MRS, MRI, SPECT) in infantile neuronal ceroid-lipofuscinosis (infantile CLN1) at different stages of the disease.** *Neuropediatrics* 2004;35:27–35
16. Lagenstein I, Schwendemann G, Kuhne D, et al. **Neuronal ceroidlipofuscinosis: CCT findings in fourteen patients.** *Acta Paediatr Scand* 1981;70:857–60
17. Seppi K, Schocke MF. **An update on conventional and advanced magnetic resonance imaging techniques in the differential diagnosis of neurodegenerative Parkinsonism.** *Curr Opin Neurol* 2005;18:370–75
18. Seitz D, Grodd W, Schwab A, et al. **MR imaging and localized proton MR spectroscopy in late infantile neuronal ceroid lipofuscinosis.** *AJNR Am J Neuroradiol* 1998;19:1373–77
19. Shungu DC, Worgall S, Mao X, et al. **Spectral characteristics of late infantile neuronal ceroid lipofuscinosis (“Batten disease”) investigated in vivo by 1H magnetic resonance spectroscopic imaging at 3.0 T.** *Proc Int Soc Magnet Res Med* 2005;13:1268
20. Mascalchi M, Moretti M, Della Nave R, et al. **Longitudinal evaluation of leukoaraiosis with whole brain ADC histograms.** *Neurology* 2002;59:938–40
21. Wilson M, Morgan PS, Lin X, et al. **Quantitative diffusion weighted magnetic resonance imaging, cerebral atrophy, and disability in multiple sclerosis.** *J Neurol Neurosurg Psychiatry* 2001;70:318–22
22. Mascalchi M, Lolli F, Della Nave R, et al. **Huntington disease: volumetric, diffusion-weighted, and magnetization transfer MR imaging of brain.** *Radiology* 2004;232:867–73
23. Steens SC, Admiraal-Behloul F, Schaap JA, et al. **Reproducibility of brain ADC histograms.** *Eur Radiol* 2004;14:425–30
24. Hachiya Y, Hayashi M, Kumada S, et al. **Mechanisms of neurodegeneration in neuronal ceroid-lipofuscinoses.** *Acta Neuropathol (Berl)* 2006;111:168–77

Neurological deterioration in late infantile neuronal ceroid lipofuscinosis

S. Worgall, MD, PhD
M.V. Kekatpure, MD
L. Heier, MD
D. Ballon, PhD
J.P. Dyke, PhD
D. Shungu, PhD
X. Mao, PhD
B. Kosofsky, MD
M.G. Kaplitt, MD,
PhD
M.M. Souweidane,
MD
D. Sondhi, PhD
N.R. Hackett, PhD
C. Hollmann, PhD
R.G. Crystal, MD

Address correspondence and reprint requests to the Department of Genetic Medicine, Weill Medical College of Cornell University, 1300 York Avenue, Box 96, New York, NY 10021
geneticmedicine@med.cornell.edu

ABSTRACT

Background: Late infantile neuronal ceroid lipofuscinosis (LINCL) is associated with progressive degeneration of the brain and retina starting in early childhood.

Methods: Thirty-two individual neurologic, ophthalmologic, and CNS imaging (MRI and MRS) assessments of 18 children with LINCL were analyzed. Disease severity was followed by two rating scales, one previously established but modified to solely assess the brain and exclude the retinal disease (modified Hamburg LINCL scale), and a newly developed scale, with expanded evaluation of the CNS impairment (Weill Cornell LINCL scale).

Results: For the 18 children, the Weill Cornell scale yielded a closer correlation with both age and time since initial clinical manifestation of the disease than did the modified Hamburg scale. There were no significant differences as a function of age or time since initial manifestation of the disease in the rating scales among the most frequent *CLN2* mutations (G3556C, 56% of all alleles or C3670T, 22% of all alleles). Measurements of cortical MRS N-acetyl-aspartate content, MRI ventricular, gray matter and white matter volume, and cortical apparent diffusion coefficient correlated to a variable degree with the age of the children and the time since initial clinical manifestation of the disease. All imaging measurements correlated better with the Weill Cornell CNS scale compared to the modified Hamburg LINCL scale.

Conclusion: The data suggest that the Weill Cornell late infantile neuronal ceroid lipofuscinosis (LINCL) scale, together with several of the MRI measurements, may be useful in the assessment of severity and progression of LINCL and for the evaluation of novel therapeutic strategies.

Neurology® 2007;69:521-535

Late infantile neuronal ceroid lipofuscinosis (LINCL) is the second most frequent form of the eight neuronal ceroid lipofuscinosis (NCL) lysosomal storage disorders, all of which are associated with progressive neurodegeneration.¹⁻⁵ LINCL is an autosomal recessive disorder caused by mutations in the *CLN2* gene, located on chromosome 11q15 encoding the lysosomal enzyme tripeptidyl peptidase 1 (TPP1).³⁻⁸ LINCL is rare with an incidence of 0.46 per 10⁵ live births in Germany and an estimated prevalence of 0.6 to 0.7 per 10⁶ in Northern Europe.^{5,9,10} The hallmarks of the disease are progressive degeneration of the brain and retina mediated by apoptosis of neurons and photoreceptors.^{1-5,11,12} Diagnosis of LINCL is based on clinicopathologic findings, enzymatic assay, and genetic testing.¹⁻⁵ Symptoms usually appear in young children at the ages of 2 to 4 years, with seizures, myoclonus, loss of motor function, language, and vision.¹⁻⁵ The seizures can be partial, complex partial, or generalized tonic clonic and are often followed by development of myoclonus, ataxia, and developmental regression.^{2,13,14} By the age of 6 years, the affected children are usually unable to walk and sit unsupported and become blind, and death occurs in mid-childhood.¹⁻⁵

Although the clinical manifestations of LINCL are clearly defined, and there are exam-

Editorial, see page 503

From the Departments of Genetic Medicine (S.W., D. Sondhi, N.R.H., C.H., R.G.C.), Pediatrics (S.W., M.V.K., B.K.), Radiology (L.H., D.B., J.P.D., D. Shungu, X.M.), and Neurological Surgery (M.G.K., M.M.S.), Weill Medical College of Cornell University, New York, NY.

Supported by NIH U01 NS047458 and NIH GCRC M01 RR00047; Will Rogers Memorial Fund, Los Angeles, CA; and the Nathan's Battle Foundation, Greenwood, IN. Protocol registration number: NCT00151268 www.clinicaltrials.gov.

Disclosure: The authors report no conflicts of interest.

ples in the literature of CT, MRI, and MRS imaging studies of the CNS in children with LINCL,¹⁵⁻¹⁸ other than the Hamburg University rating scale of disease severity in patients residing in Germany and Switzerland based on clinical assessment of language, motor function, seizures, and vision,¹⁹ the natural progression of LINCL is not well characterized. As the basis of planning a gene therapy study of LINCL,^{20,21} we have had the opportunity to make 32 assessments of 18 children with LINCL using a battery of measurements relating to their neurologic status, including MRI and MRS imaging. The present study summarizes these data and establishes a more comprehensive clinical disease severity rating scale focused on the CNS dysfunction, contributing to the understanding of the progressive deterioration in this disorder.

METHODS Study group. The study group consisted of 18 children (9 boys, 9 girls) with confirmed LINCL. DNA analysis of the CLN2 mutations was available for all children prior to inclusion into the study. The initial evaluation included a detailed neurologic examination by a pediatric neurologist, funduscopy examination by an ophthalmologist, and MRI/MRS imaging of the brain. Fourteen of the children were subsequently reassessed 18 to 365 days after the initial evaluation, for a total of 32 assessments of the 18 children. The parents of all study children provided informed consent and the research protocol was reviewed and approved by the Institutional Review Board at Weill Medical College of Cornell University.

LINCL CNS severity assessment. LINCL CNS severity and progression were evaluated using two scales: a modified form of the Hamburg LINCL scale based on a scale originally developed by Steinfeld et al.¹⁹ to assess LINCL disease progression, but modified to assess only the CNS, not the ophthalmologic manifestations of the disease²⁰; and a newly developed Weill Cornell LINCL scale, which is an expanded severity scale assessing the degree of CNS dysfunction that includes swallowing dysfunction, gait, motor, and language abnormalities.

The modified Hamburg LINCL scale assesses motor function, seizure activity, and language skills. Each of these individual scales is ranked from 0 to 3 and then all individual ratings are added to provide a total rating with 0 being the most severe and 9 the mildest. The following ratings for the individual scales were used: Seizure scale: 3 = no seizures/3-month period; 2 = 2 seizures/3 month period; 1 = 1 seizure/month; 0 = >1 seizure/month; Motor scale: 3 = walks normally; 2 = frequent falls, clumsiness obvious; 1 = no unaided walking or crawling only; 0 = immobile, mostly bedridden; and Language scale: 3 = normal; 2 = recognizably abnormal; 1 = hardly understandable; and 0 = unintel-

ligible or no language. The ratings were summarized for the total disability, and grouped as 0 to 4 severe, 5 to 6 moderate, 7 to 8 mild, and 9 normal.

The Weill Cornell LINCL scale expands the modified Hamburg LINCL scale to include the assessment of swallowing function ("feeding scale"), gait ("gait scale"), motor system abnormalities ("motor scale"), and speech abnormalities ("language scale"). The following ratings for the individual scales were used: Feeding scale: 0 = gastrostomy-dependent; 1 = moderate swallowing dysfunction; 2 = mild swallowing dysfunction; 3 = no swallowing dysfunction; Gait scale: 0 = nonambulatory; 1 = abnormal (spastic, bradykinetic, or ataxic), and unable to ambulate independently; 2 = abnormal (spastic, bradykinetic or ataxic), but able to ambulate independently; 3 = normal; Motor scale: 0 = myoclonus and one of chorea or tremor or athetosis (referred to as chorea/tremor/athetosis) and positive Babinski reflex; 1 = two of myoclonus, chorea/tremor/athetosis, or positive Babinski reflex; 2 = one of myoclonus, chorea/tremor/athetosis, or positive Babinski reflex; 3 = none of myoclonus, chorea/tremor/athetosis, or positive Babinski reflex; and Language scale: 0 = unintelligible words or no speech; 1 = barely understandable speech (severe dysarthria or very few meaningful words); 2 = abnormal speech (abnormal articulation or decreased vocabulary); and 3 = normal speech. The ratings were summarized for an index of the total disability, with a maximum score of 12 for normal and 0 for most severe (table 1).

Ophthalmology examination. Funduscopy evaluation was performed by slit lamp examination and direct ophthalmoscopy using a 20 diopter lens by an ophthalmologist.

MRI/MRS. All image data were acquired on a 3.0 Tesla MRI system (GE Medical Systems, Milwaukee, WI). Imaging included T1-weighted, T2-weighted, and fluid-attenuated inversion recovery (FLAIR) sequences. For the MRI and MRS imaging measurements only experimentally valid data points are presented (n = 27 scans for NAA, n = 28 for ventricular volume, n = 26 for gray matter volume, and n = 32 for CADC). N-acetylaspartate (NAA), creatine, and lactate levels in the CNS were extracted from the MRS data set. Volumetric assessments of the ventricles were performed on T1-weighted data sets. To assess gray and white matter volume a spoiled gradient recalled pulse sequence (SPGR) was employed. The cortical apparent diffusion coefficient (CADC) was measured with a spin-echo diffusion weighted (DWI) echoplanar (EPI) sequence implemented over the entire brain (for more details, see supplemental E-Methods on the *Neurology* Web site at www.neurology.org).

Statistics. Data are reported as mean \pm SEM and median. Correlation coefficients were calculated using linear regression and significance was determined by analysis of variance. Differences in regression with age or time since initial manifestation of the disease were assessed by comparatively analyzing the slopes of the linear regression.

RESULTS Characteristics of the study population. The children were from the United States, Canada, England, Australia, and Germany. The ages of the children at the initial evaluation ranged from 3.3 to 13.8 years (6.3 ± 0.6 years; median 5.7 years; table 2). There were four sibling pairs.

Table 1 Weill Cornell LINCL Scale		
Functional category	Rating criteria	Score
Feeding scale	No swallowing dysfunction	3
	Mild swallowing dysfunction	2
	Moderate swallowing dysfunction	1
	Gastrostomy-tube dependent	0
Gait scale	Normal	3
	Abnormal (spastic or bradykinetic or ataxic) but able to ambulate independently	2
	Abnormal (spastic or bradykinetic or ataxic) requiring assistance	1
	Nonambulatory	0
Motor scale	None of myoclonus, chorea/tremor/athetosis,* and upgoing toes	3
	One of myoclonus or chorea/tremor/athetosis* or upgoing toes	2
	Two of myoclonus or chorea/tremor/athetosis* or upgoing toes	1
	Myoclonus and chorea/tremor/athetosis* and upgoing toes	0
Language scale	Normal speech	3
	Abnormal speech with abnormal articulation or decreased vocabulary	2
	Barely understandable speech with severe dysarthria or very few meaningful words	1
	Unintelligible words or no speech	0
Total score	Feeding score + gait score + motor score + language score	

*Any or more of the three motor symptoms chorea, tremor, and athetosis are considered as one scoring.
LINCL = late infantile neuronal ceroid lipofuscinosis.

Eight different mutations of the *CLN2* gene were present in 35 alleles; no mutation was detected in one allele of BD-10. The sibling pairs each had the same mutations. The most frequent mutation was the splice mutation G3556C present in 18 alleles (50%); 7 of the children were homozygous for this allele. All of the homozygous mutations were found in the children from England and Australia. The second most frequent mutation was C3670T, which results in a premature stop codon, and was present in 8 alleles (25%). Two children were homozygous for this mutation.

LINCL history. The diagnosis of LINCL was made at an average age of 4.0 ± 0.2 years (range 2.0 to 5.3 years, median 4.0; table 3). The diagnosis was based on biochemical testing of the TPP-1 levels in fibroblasts or leukocytes and genetic analysis. Three of the children were assessed due to previous diagnosis in an affected sibling; these children were tested before the onset of symptoms.

The average age at the onset of seizures was 3.3 ± 0.2 years (median 3.1 years, range 2.0 to 6.3 years). The type of seizures included myoclonic, complex partial, and generalized tonic clonic seizures with the majority of the children experiencing more than one seizure type. All of the children received anticonvulsive therapy with control of the seizures at the time of the initial presentation. The reported onset of the language abnormalities was 3.0 ± 0.2 years (median 3.0 years, range 1.5

to 4.8 years). Some of the children never acquired normal language skills and were diagnosed in their second year of life with speech delay. The reported onset of motor dysfunction was at 3.5 ± 0.2 years (median 3.5 years, range 1.9 to 5.0 years). For the children with complete loss of the ability to walk at the time of the assessment, the age at which they became wheelchair-bound was 5.7 ± 0.3 years (median 5.7 years, range 4.3 to 6.5 years). Feeding difficulties were common; only 17% of the children had no feeding problems, 67% were fed via a gastrostomy tube due to their swallowing dysfunction. Disease progression varied in some of the four sibling pairs, indicating that there may be confounding factors such as modifier genes important for disease progression besides the mutation alone. No change in the progression of the clinical phenotypic pattern was seen related to either of the two frequent mutations C3670T or G3556C nor with the sibling pair (BD02 and BD03), carrying the G3085A mutation, which has been previously associated with a less severe phenotype.¹⁹

LINCL severity and neurologic characteristics. The total ratings of the modified Hamburg LINCL scale of the study children at the time of initial evaluation ranged from 3 to 6 (table E-1 on the *Neurology* Web site at www.neurology.org). All but one child (BD-17) in the severe category (total score of 0 to 4) had a seizure score of 3, as defined by no seizures within the previous 3-month pe-

Child*	Age, y†	Race/ethnicity	Sex	Residence	CLN2 mutations‡	Other medical conditions§
BD-01	8.4	W	M	USA	G3556C/T3016A [¶]	Otitis media
BD-02●	9.7	W	M	USA	G3556C/G3085A [¶]	Hypospadias, septic arthritis hip
BD-03●	6.6	W	M	USA	G3556C/G3085A [¶]	Otitis media
BD-04	13.8	W	F	USA	C3670T/T4396G ^{**}	Pneumonia, reactive airway disease
BD-05	6.2	W	M	Canada	G3556C/C3670T	Otitis media, varicella
BD-06□	8.0	W	F	England	G3556C homozygote	Drug allergy (lamotrigine)
BD-07□	6.6	W	F	England	G3556C homozygote	—
BD-08△	6.0	W	M	England	G3556C homozygote	Drug allergy (phenytoin)
BD-09	6.7	W	M	Canada	G3556C/T4383C ^{**}	Varicella
BD-10	5.0	W	M	USA	C3670T/unknown ^{¶¶}	—
BD-11	5.4	W	F	England	G3556C homozygote	Irritable bowel
BD-12	4.4	W	F	Germany	G3670T homozygote	—
BD-13○	4.4	W	M	Australia	G3556C homozygote	Atopic dermatitis, food allergies
BD-14△	3.4	W	F	England	G3556C homozygote	Atopic dermatitis
BD-15	4.7	W	F	Canada	G3556C/C3670T	Frequent gastroenteritis
BD-16	5.2	W	M	Germany	C3670T homozygote	Atopic dermatitis
BD-17	5.4	Cb/W	F	England	C1441G/△3986-4000 ^{§§}	—
BD-18○	3.3	W	F	Australia	G3556C homozygote	Atopic dermatitis, food allergies

*Listed in the order of the initial evaluation; ●, □, △, ○ used to identify sibling pairs.

†Age in years at initial evaluation.

‡Mutations are named by location in the gene^{7, 8} with the wild type nucleotide before and mutant nucleotide after. G3556C is a mutation in the splice junction also referred to as IVS5-1G>C or c.509-1G>C. The C3670T mutation is a premature stop codon also called R208X or c.622C>T.

§Medical problems unrelated to the known clinical manifestations of LINCL.¹⁻⁵

¶Premature stop codon at amino acid 104.

¶¶Missense (Arg>Gln) mutation at amino acid 127.

**Splicing mutation in intron 8 splice donor.

**Missense mutation (Leu>Pro) in amino acid 355.

‡‡The diagnosis of LINCL for this patient was based on the TPP-1 deficiency and the presence of a known mutation for LINCL on the other allele.

§§Compound heterozygote with splicing mutation splice acceptor for intron 1 and in frame deletion of amino acids 275-279. LINCL = late infantile neuronal ceroid lipofuscinosis; W = white; Cb = Caribbean.

riod. None of the children had a score of 1, possibly reflecting the efficacy of their antiepileptic drug regimens, which resulted in decreased sensitivity at the lower end of the scale.

The modified Hamburg LINCL scale declined with the age of the children (figure E-1A). In our study population, the scores of the modified Hamburg LINCL scale were mostly within the 5th to 95th percentile range as reported by Steinfeld et al.¹⁹ (gray shaded area, figure E-1). For those children outside the range described by Steinfeld et al.,¹⁹ all were shifted to the right (i.e., older age for the same degree of severity), all were older (>7 years), and all were in the severe category. In general, this “right shift” was due to lack of seizure activity (i.e., seizure score 3), perhaps associated with effective antiseizure therapy. Over the course of the study, three of the children died due to progression of the disease. There were no significant differences as a function of age in

the rating scale among the two most frequent CLN2 mutations G3556C (figure E-1B) and C3670T (figure E-1C; $p = 0.87$).

All children had neurologic abnormalities at the time of the initial presentation (table 4). Strength in upper or lower extremities was decreased in all of the children evaluated at an age older than 4 years. Muscle stretch reflexes were increased in most children, with a few showing normal or decreased muscle stretch reflexes. The plantar response was mostly “upgoing,” reflecting upper motor neuron involvement in this disease. Dystonia in the form of athetoid movements was observed only in one child during one evaluation. Dyskinesia of the tongue was seen in 13% (4 of 32) of the assessments. The gait abnormalities of the children who were still ambulatory were mostly of spastic and ataxic type. Myoclonus was seen in 69% (22 of 32) of the assessments. Tremors and chorea were seen less frequently, in 25% (8 of 32) and 16% (5 of 31) of the assessments.

Table 3 History related to progression of LINCL

Child*	Diagnosis (age, y)	Onset of seizures (age, y)	Seizure type [†]	Onset of motor dysfunction/inability to walk (age, y)	Onset of language abnormality (age, y)	Onset of vision loss/abnormal eye exam (age, y)	Feeding issues	
							Gastrostomy [‡]	Swallowing dysfunction
BD-01	5.3	3.7	Myoclonus	3.7/6.5	3.7	Unknown/5.2	Yes	Yes
BD-02●	4.7	6.3	Complex partial	Unknown/6.2	4.0	4.0	Yes	Yes
BD-03●	3.6	3.9	Complex partial	5.0/5.6	4.0	5.0	Yes	Yes
BD-04	4.5	3.5	Generalized tonic clonic	3.5/6.5	3.0	Unknown/7.7	Yes	Yes
BD-05	4.8	3.5	Complex partial, myoclonus	4.8	4.8	5.8/6.3	Yes	Yes
BD-06□	4.3	2.9	Complex partial, myoclonus	3.3	3.3	Unknown/7.0	Yes	Yes
BD-07□	3.3	3.1	Complex partial	3.2/5.6	3.2	Unknown/6.6	Yes	Yes
BD-08△	4.7	2.5	Generalized tonic clonic	3.5/5.0	2.0	5.2	Yes	Yes
BD-09	3.4	2.7	Generalized tonic clonic, complex partial	4.5/5.8	3.0	Unknown/6.9	No	Yes
BD-10	3.7	2.8	Generalized tonic clonic, myoclonus	3.5	3.7	4.5	Yes	Yes
BD-11	4.5	2.8	Generalized tonic-clonic, complex partial, myoclonus	3.0	3.0	4.8	Yes	Yes
BD-12	2.7	2.4	Generalized tonic clonic, myoclonic	2.4/4.3	2.0	Unknown/4.4	No	Yes (mild)
BD-13○	4.3	3.5	Complex partial	2.5	2.5	4.3	No	Yes
BD-14△	2.0 [§]	2.0	Generalized tonic clonic, myoclonic	1.9	2.5	None	No	No
BD-15	4.4	3.0	Complex partial	4.2	2.0	Unknown/4.6	Yes	Yes
BD-16	4.8	3.9	Complex partial, myoclonus	3.7	1.5	4.8	Yes	Yes (mild)
BD-17	4.8	3.3	Generalized tonic clonic, myoclonic	3.9	3.6	Unknown/5.3	No	No
BD-18○	2.8 [§]	3.1	Complex partial	3.1	2.5	None	No	No

*Listed in the order of initial evaluation; ●, □, △, ○ used to identify sibling pairs.

[†]Seizure history at time of initial assessment at Weill Cornell.

[‡]Feed exclusively via gastrostomy.

[§]Tested for LINCL because older sibling was diagnosed with LINCL.

LINCL = late infantile neuronal ceroid lipofuscinosis.

Weill Cornell LINCL scale. The new Weill Cornell LINCL scale, which expands the assessment of the neurologic abnormalities compared to the modified Hamburg LINCL scale, correlated better with the age of the children compared to the modified Hamburg LINCL scale ($r^2 = 0.55$; $p < 0.0001$ for Weill Cornell LINCL scale vs $r^2 = 0.44$; $p < 0.0001$ for modified Hamburg LINCL scale; figure 1A). The Weill Cornell scale separated the individual assessments over a broad area within the range of the scale. Compared to the age progression observed with the modified Hamburg LINCL scale, the slope of the decline with age was steeper with the Weill Cornell LINCL scale ($y = -0.85 \times + 8.2$ for the Weill Cornell CNS scale vs $y = -0.36 \times + 6.3$ for the modified Hamburg LINCL scale; $p < 0.05$), suggesting that this scale may detect deviations toward a decreased rate of disease progression

more readily and may thus be the more valuable of the two scales to assess effects of novel therapies on disease progression. As seen for the modified Hamburg LINCL scale, progression with age of the Weill Cornell LINCL scale was not different for the two frequent genotypes G3556C (figure 1B) and C3670T (figure 1C, $p = 0.83$).

Both LINCL scales correlated also with the time since initial clinical manifestation of the disease, as determined by the chronological age at the time of evaluation minus the age when seizures or language or motor abnormalities were first observed (figure 2 and figure E-2). Again, as seen for the correlation with age, the Weill Cornell LINCL scale correlated better with time since initial clinical presentation ($r^2 = 0.53$; $p < 0.0001$; figure 2) compared to the modified Hamburg LINCL scale ($r^2 = 0.35$; $p < 0.0001$; figure E-2).

Table 4 Neurologic evaluation

Child*	Age at assessment, y	Upper limb strength [†]	Lower limb strength	Upper muscle stretch	Lower muscle stretch	Plantar reflexes	Dystonia	Dyskinesia	Gait	Myoclonus	Tremors	Chorea
BD-13○	4.4	↓ ²	↓	↑	↑	Up	No	No	Ataxic	No	Yes	No
	4.5	↓	↓	↑	↑	Up	No	No	Ataxic, spastic	No	Yes	No
BD-18○	3.3	Normal	Normal	↑	↑	Up/down [‡]	No	No	Ataxic	No	No	No
	3.4	Normal	Normal	↑	↑	Up/down [‡]	No	No	Spastic	No	No	No
BD-14△	3.4	Normal	Normal	Normal	Normal	Down	No	No	Clumsy, tumbling	Yes	No	No
	3.6	Normal	Normal	Normal	Normal	Down	No	No	Ataxic	No	No	No
BD-10	5.0	Normal	↓	Normal	↑	Up	No	Tongue	Walks with support	No	No	No
	5.4	↓	↓	↑	↑	Up	No	Tongue	Ataxic	Yes	No	No
BD-11	5.4	NA	NA	↑	↑	NA	No	No	Non-ambulatory	Yes	No	No
BD-16	5.2	↓	↓	↑	↑	Up	No	No	Ataxic, spastic, bradykinetic	Yes	Yes	No
	5.3	↓	↓	↑	↑	Up	No	No	Ataxic, spastic, bradykinetic	Yes	Yes	No
BD-5	6.2	↓	↓	↑	↑	Up	No	No	Non-ambulatory	Yes	No	No
	7.2	↓	↓	↑	↑	Up	No	Tongue	Non-ambulatory	Yes	No	No
BD-17	5.4	↓	↓	↑	↑	Up	No	No	Ataxic, spastic, bradykinetic	Yes (daytime)	Yes	No
BD-15	4.7	↓	↓	↑	↑	Up	No	No	Non-ambulatory	No	Yes	No
	5.7	↓	↓	↑	↑	Up	No	No	Non-ambulatory	Yes	Yes	No
BD-8△	6.0	↓	↓	↓	↓	Up	No	No	Non-ambulatory	Yes (occasional)	No	No
	7.0	NA	NA	↑	↑	Up	No	No	Non-ambulatory	Yes (occasional)	No	No
BD-9	6.7	↓	↓	↑	↑	Up	No	No	Walks with support	Yes	No	No
	7.7	↓	↓	↑	↑	Up	No	No	Ataxic, spastic, bradykinetic	Yes	Yes	No
BD-12	4.4	↓	↓	↑	↑	Up	No	No	Non-ambulatory	Yes	No	No
	4.5	↓	↓	↑	↑	Up	No	No	Non-ambulatory	Yes (frequent)	No	Yes
BD-1	8.4	↓	↓	↑	↑	Up	No	No	Non-ambulatory	Yes	No	No
	8.6	NA	NA	↑	↑	Up	No	No	Non-ambulatory	Yes	No	No
BD-2●	9.7	NA	NA	↓	↑	Up	No	No	Non-ambulatory	No	No	Yes
	10.0	↓	↓	↑	↑	Up	No	No	Non-ambulatory	Yes	No	Not evaluated
BD-3●	6.6	NA	NA	↓	Normal	Down	No	Tongue	Non-ambulatory	No	No	Yes
	6.9	NA	NA	Normal	Normal	Up	Athetoid movements	No	Impaired	No	No	Athetosis
BD-4	13.8	↓	↓	↑	↑	Up	No	No	Non-ambulatory	Yes	No	Yes
BD-6□	8.0	↓	↓	↑	↑	Up	No	No	Non-ambulatory	Yes	No	No
	8.1	↓	↓	↓	↓	Mute	No	No	Non-ambulatory	Yes	No	No
BD-7□	6.6	↓	↓	↑	↑	Up	No	No	Non-ambulatory	Yes	No	No

*Order based on total LINCL severity score in increasing severity; ●, □, △, ○ used to identify sibling pairs.

[†]↑, ↓ = Increased, decreased.

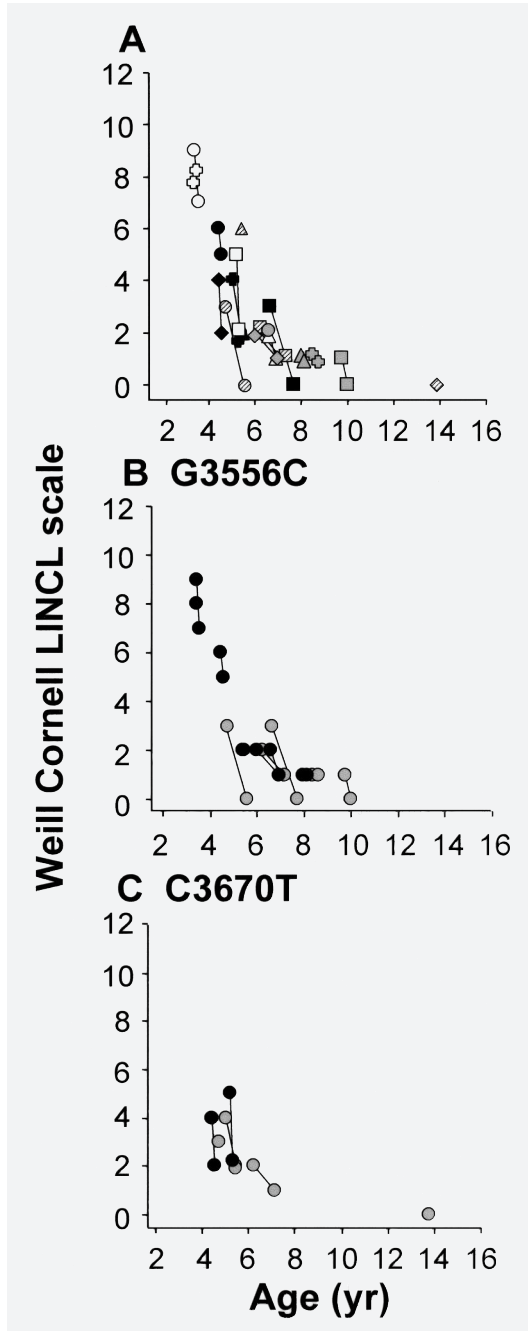
[‡]Left side up, right side down.

LINCL = late infantile neuronal ceroid lipofuscinosis; NA = not applicable.

Also, the individual assessments were separated more over the range of the Weill Cornell LINCL scale with steeper slope of decline ($y = -1.03 \times + 6.5$) compared to the modified Hamburg LINCL scale ($y = -0.41 \times + 5.5$). As seen for the relation of the two frequent genotypes G3556C

and C3670T with age, no difference was observed in the increase of severity with either of these two genotypes as a function of time since initial manifestation of the disease (not shown; $p > 0.6$ for the comparisons for both LINCL severity scales).

Figure 1 Progression of late infantile neuronal ceroid lipofuscinosis (LINCL) as a function of age as assessed by the Weill Cornell CNS score for 18 children with LINCL



Fourteen children were re-evaluated 18 to 365 days later, for a total of 32 evaluations of the 18 children. (A) All children; (B) G3556C (homozygotes and heterozygotes) children; and (C) C3670T children. For B and C, heterozygotes are shown with gray symbols and homozygotes with filled symbols.

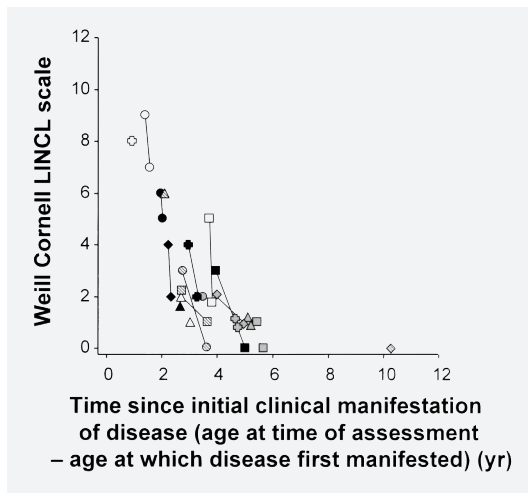
Ophthalmologic findings. Funduscopy evaluation of the children revealed changes in the optic disc, macula densa, and retinal periphery (table E-2). Pallor of the optic disc was the most common abnormal finding. The macular findings included

pigmentary changes and degeneration, Bullseye maculopathy, retinal pigmentary epithelial changes, and pigmentary degeneration. Findings in the retinal periphery included hypopigmentation, hypo- and hyperpigmentation (salt-and-pepper appearance), and other pigmentary changes. The funduscopy abnormalities increased with LINCL severity, with the most severely affected children showing changes in at least two areas.

Brain imaging. The T1-weighted MR images showed progressive global atrophy of the gray matter with increasing degree of ventricular enlargement becoming more marked with severity of the disease (decreasing scores on the modified Hamburg and Weill Cornell LINCL scales; figure 3). For example, MRI of a moderate patient with a score of 6 on the modified Hamburg LINCL scale and 8 on the Weill Cornell LINCL scale showed minimal white matter hyperintensities and no gross gray matter involvement (figure 3, A and B). Some minimal gray matter changes and involvement with atrophy were visible in a moderate patient with scores of 5 on the modified Hamburg LINCL and 5 on the Weill Cornell LINCL scale (figure 3, C and D). In contrast, even more pronounced global atrophy was present in children in the severe category one with a score of 4 on the modified Hamburg LINCL scale and 3 on the Weill Cornell LINCL scale (figure 3, E and F) and another with a score of 3 on the modified Hamburg LINCL scale and 1 on the Weill Cornell LINCL scale (figure 3, G and H).

Imaging measurements and age. Ten different measurements of the MRI or MRS assessments were used to quantify disease progression, including quantification of levels of cortical *N*-acetylaspartate (NAA; a metabolite reflecting the amount of neuronal cells by MRS); NAA/creatinine and lactate as measured by MRS; ventricular, white matter, and gray matter volume, quantified from T1-weighted MR images and each calculated as an absolute volume and as a % of total brain volume; and the cortical apparent diffusion coefficient (ADC) by diffusion weighted MRI of cortical brain ADC histograms. NAA levels, gray matter volume, and % gray matter volume of total brain volume declined with age (figure 4, A, E, F), reflecting the loss of neurons with progression of the disease. In contrast, ADC, a measurement reflecting the microscopic self-diffusion of H₂O molecules (H₂O diffusivity increases with a lack of structural restrictions at the cellular level due

Figure 2 Status of late infantile neuronal ceroid lipofuscinosis (LINCL) as a function of the time since the first clinical manifestation of the disease



The initial clinical manifestation of the disease was determined by the earliest age at onset of seizures or motor or language abnormalities. The time since the initial clinical manifestation of disease was calculated as [age at time of assessment – age at which disease first manifested] (y). The data are shown for 18 children with LINCL for a total of 32 evaluations as a function of the Weill Cornell LINCL scale.

to neuronal degeneration), increased with age and disease progression (figure 4B). Ventricular volume and % ventricular volume of total brain volume also increased with age, reflecting the expansion of the ventricular space secondary to neuronal loss (figure 4, C and D). Interestingly, white matter volume and % white matter volume of total brain volume also increased with age, suggesting that this increase could either be attributed to a relative increase in white matter due to gray matter loss or to an absolute increase in white matter volume. The correlations of the eight imaging measurements with age were best for ventricular volume > % gray matter volume > CADC > % ventricular volume > NAA > % white matter volume > white matter volume > gray matter volume. Lactate and NAA/creatine, other MRS measurements, correlated similarly to NAA with age ($r^2 = 0.25$; $p < 0.01$ for NAA/creatine and $r^2 = 0.42$; $p < 0.001$ for lactate; not shown).

The correlations of the 10 imaging measurements as a function of time since initial clinical manifestation of the disease (figure 5) showed a similar pattern as observed for the correlations of the imaging measurements with age. Correlations were best with ventricular volume (figure 5C) > CADC (figure 5B) > % ventricular volume (figure 5D) > % gray matter volume

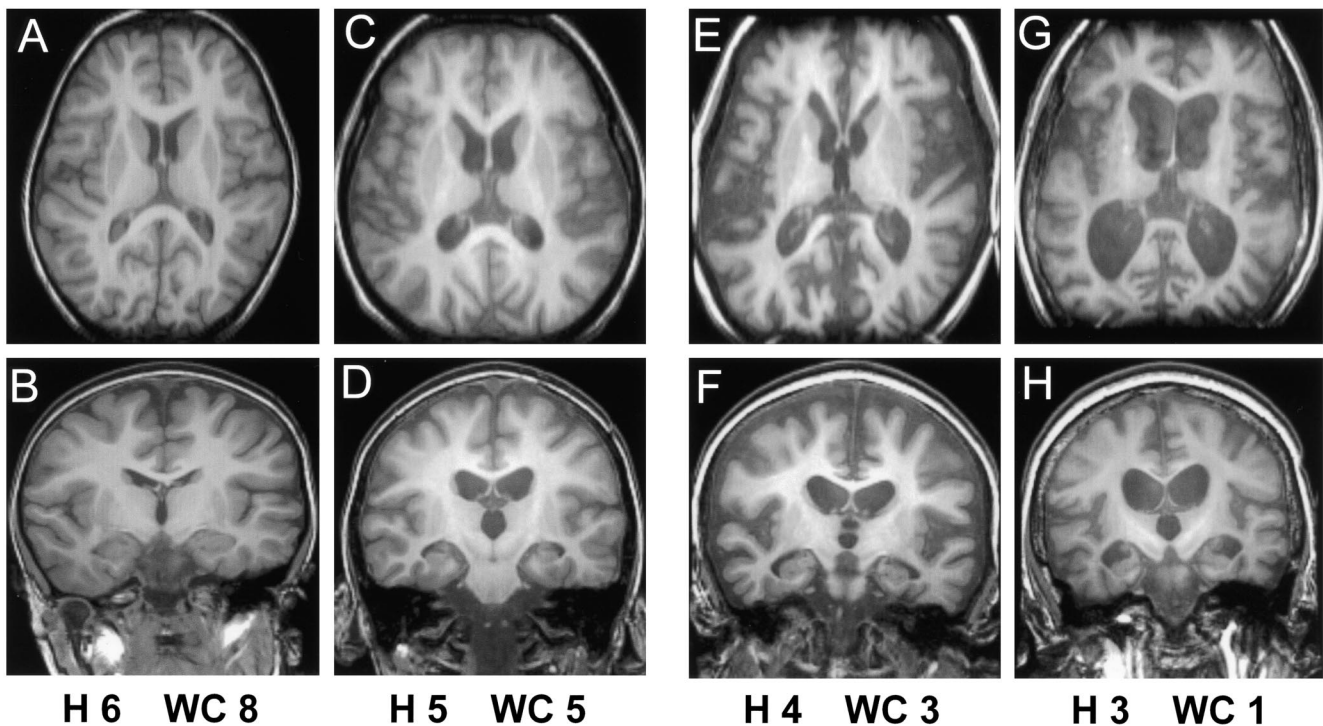
(figure 5F) > NAA (figure 5A) > gray matter volume (figure 5E) > % white matter volume (figure 5H) > white matter volume (figure 5G), suggesting that the time since disease manifestation is reflected better by increased ventricular volume and CADC, as compared to decreased gray matter volume and NAA. Lactate correlated well with the time since initial manifestation of the disease ($r^2 = 0.57$; $p < 0.0001$) and the correlation for NAA/creatine with the time since initial manifestation of the disease was comparable to that of NAA with the time since clinical manifestation of the disease ($r^2 = 0.35$; $p < 0.001$; not shown).

Imaging measurements and disease severity scales. The correlation of the imaging measurements as a function of the modified Hamburg LINCL scale was best for % ventricular volume (figure E-3D) > % gray matter volume (Figure E-3F) > ventricular volume (figure E-3C) > gray matter volume (figure E-3E) > NAA (figure E-3A) > CADC (figure E-3B) > % white matter volume (figure E-3H) > white matter volume (figure E-3G). All imaging measurements except gray matter volume correlated less well with the modified Hamburg LINCL scale compared to age and time since initial clinical manifestation, and % white matter volume and white matter volume correlated similarly poorly compared to time since initial clinical manifestation. These observations suggest that the modified Hamburg LINCL scale reflects disease severity and progression as determined by the imaging measurements less well compared to age and time since clinical manifestation.

Correlations of the imaging measurements with the Weill Cornell LINCL scale were better for six measurements (NAA, ventricular volume, % ventricular volume, gray matter volume, % gray matter volume, and % white matter volume) compared to the correlations with the modified Hamburg LINCL scale (figure 6, A, C through F, H). The correlation of the Weill Cornell LINCL scale with CADC (figure 6B) was comparable to the correlation with the modified Hamburg LINCL scale and there was no good correlation with white matter volume (figure 6G) as seen for the modified Hamburg LINCL scale. The best correlation was with the % ventricular volumes (figure 6D). Interestingly, the second and fourth best correlations were with % gray matter volume (figure 6F) and gray matter volume (figure 6E), followed by the correlation with NAA (figure 6A), suggesting that these primary measurements of neuronal loss are reflected better as a function

Moderate

Severe



T1-weighted axial (A, C, E, G) and coronal (B, D, F, H) brain MR images of children with moderate (A through D) or severe LINCL (E through H). The axial (top) and coronal (bottom) images are paired. Scores on the modified Hamburg LINCL scale (H) and the Weill Cornell LINCL scale (WC) of the included examples are shown below the axial and coronal images for each child. Shown are axial images at the level passing through the head of the caudate nucleus anteriorly and the genu of the corpus callosum posteriorly, and coronal images at the level passing through the third ventricle. Note that the degree of ventricular enlargement is paralleled by the extent of cortical atrophy.

of the Weill Cornell LINCL scale compared to as a function of age or time since initial clinical manifestation of the disease. The lower correlations for CADC with both severity scales compared to the other three imaging measurements were partially affected by the very high CADC value in the oldest child (figure 6B). Neither of the two LINCL scales correlated well with lactate ($r^2 < 0.08$; $p > 0.15$ for both comparisons; not shown) nor with NAA/creatinine ($r^2 = 0.28$; $p < 0.01$ for the modified Hamburg LINCL scale and $r^2 = 0.30$; $p < 0.01$ for the Weill Cornell LINCL scale; not shown).

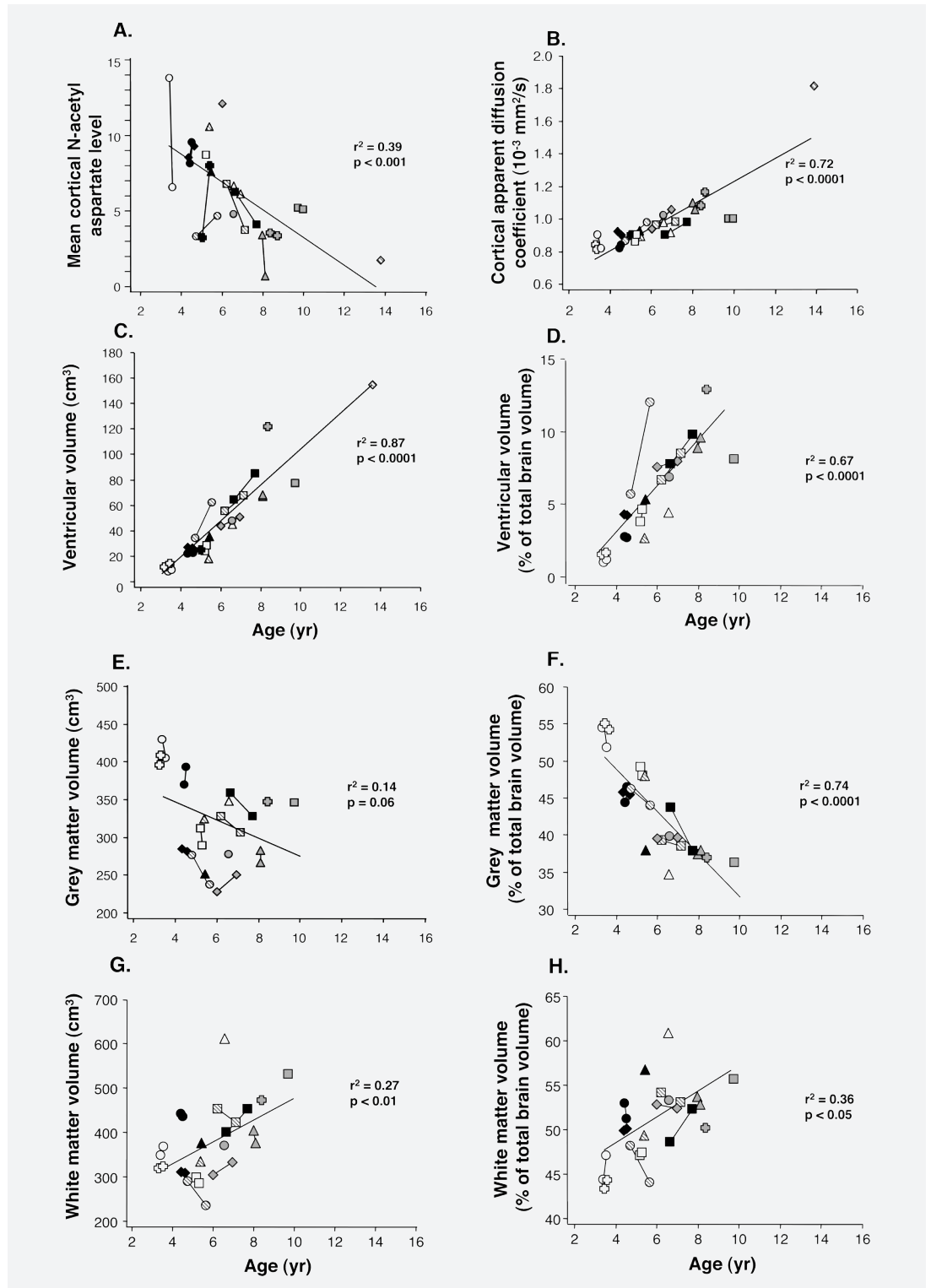
DISCUSSION The clinical presentation and progression of LINCL have been well documented.^{1-5,19} Symptoms usually appear in early childhood and consist of seizures and loss of motor function, language, and vision. Progression of the disease is rapid over the next few years with complete loss of motor function by 6 years and death at 8 to 12 years. Exceptions from this disease pattern have been described for a few patients with rare CLN2 mutations who had delayed on-

set of symptoms.^{1,7,8} The children in our cohort followed the classic pattern with the mean onset of language abnormalities at 3.0 years, seizures at 3.2 years, and motor abnormalities at 3.6 years. Some of the children never completely acquired language capacity beyond verbalization of a few words and had been diagnosed initially with speech delay.

Disease severity scales to assess disease progression have been developed for various forms of neuronal ceroid lipofuscinosis.^{19,22,23} A comprehensive clinical rating scale has been developed for juvenile NCL, including assessment of motor, behavioral, and functional capability.^{22,23} For LINCL, which develops early in life and progresses rapidly, it is challenging to develop such a comprehensive disease severity scale. The only disease severity scale developed to date is the LINCL severity scale from Steinfeld et al.,¹⁹ which includes the assessment of seizures, motor dysfunction, language abnormality, and vision.

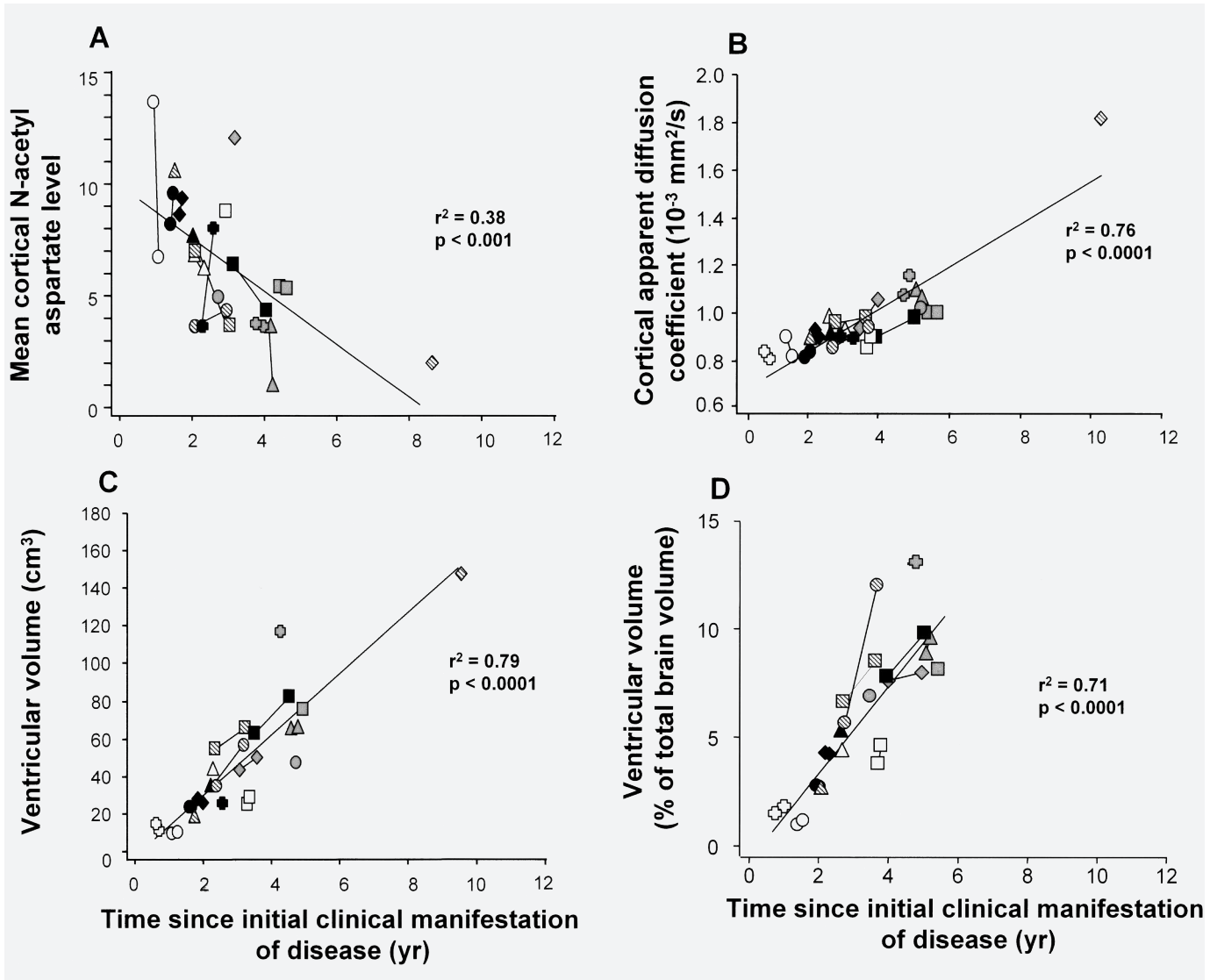
In the context of our interest in developing a

Figure 4 Brain imaging measurements of children with late infantile neuronal ceroid lipofuscinosis (LINCL) as a function of age



(A) Cortical N-acetylaspartate levels. Data are shown as individual measurements of four interleaved 1.5-mm brain sections. (B) Cortical apparent diffusion coefficient measured by diffusion-weighted imaging. (C) Ventricular volumes. Measurements of ventricular segmentations included all of the lateral and inferior lateral ventricles for both hemispheres. Volumes were calculated by the number of voxels segmented as ventricles, multiplied by the single voxel dimension. (D) Ventricular volumes as % of total brain volume. Total brain volume was determined as the sum of ventricular volume + gray matter volume + white matter volume. (E) Gray matter volumes. (F) Gray matter volumes as % of total brain volume. (G) White matter volumes. (H) White matter volumes as % of total brain volume. Data for E and G are shown as individual measurements from SPGR acquisitions, calculated using the Freesurfer software. All data are shown as measurements of individual children. Shown for each is the correlation coefficient (r^2) and p value for a linear fit.

Figure 5



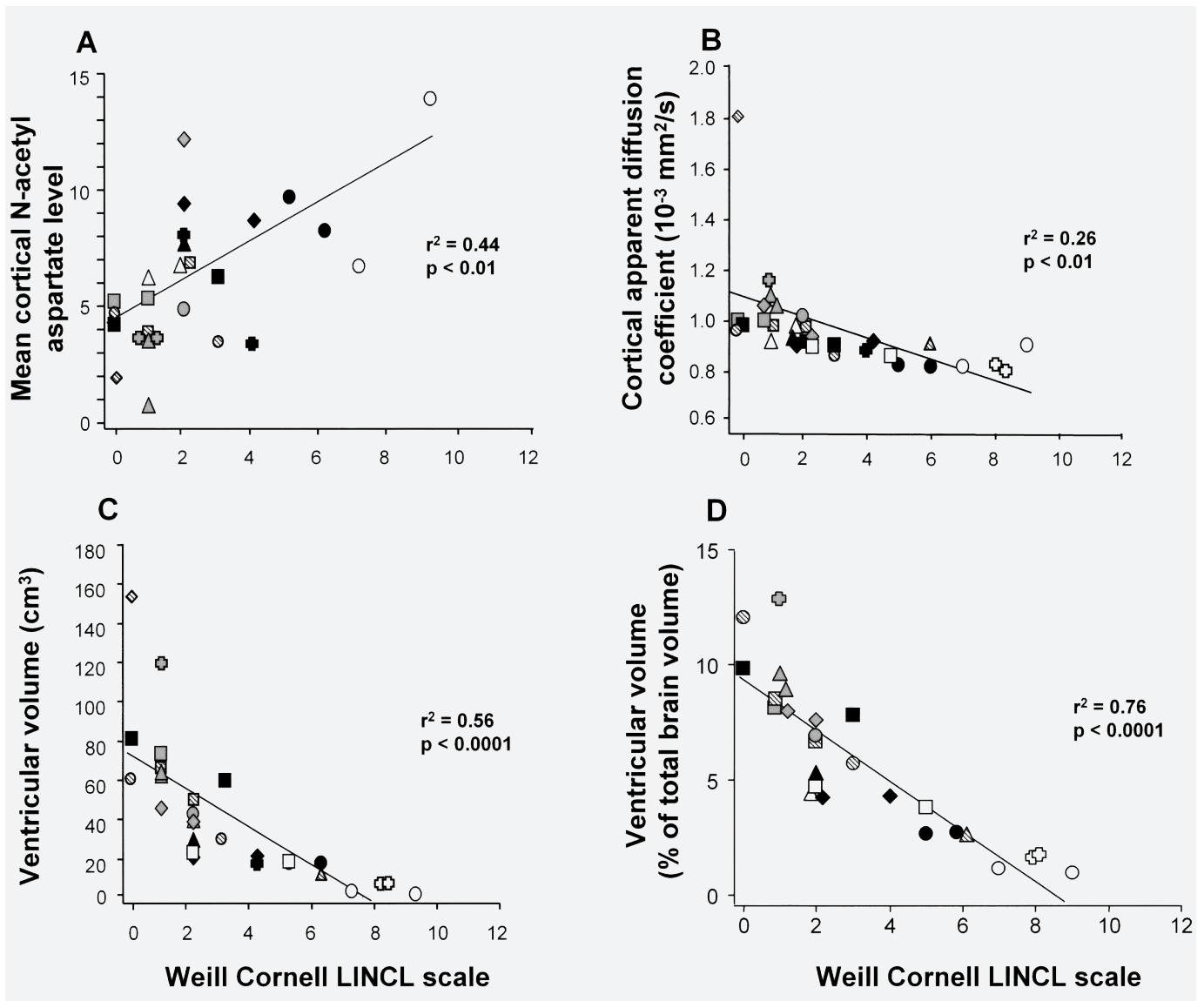
Brain imaging measurements of children with late infantile neuronal ceroid lipofuscinosis (LINCL) as a function of the time since initial clinical manifestation of disease. The time since the initial clinical manifestation of disease was calculated as (age at time of assessment – age at which disease first manifested) (y). (A) Cortical *N*-acetylaspartate levels. Data are shown as individual measurements of four interleaved 15-mm brain sections. (B) Cortical apparent diffusion coefficient measured by diffusion-weighted imaging. (C) Ventricular volumes. Measurements of ventricular segmentations included all of the lateral and inferior lateral ventricles for both hemispheres. Volumes were calculated by the number of voxels segmented as ventricles, multiplied by the single voxel dimension. (D) Ventricular volumes as % of total brain volume. Total brain volume was determined as the sum of ventricular volume + gray matter volume + white matter volume. (E) Gray matter volumes. (F) Gray matter volumes as % of total brain volume. (G) White matter volumes. (H) White matter volumes as % of total brain volume. Data for E and G are shown as individual measurements from SPGR acquisitions, calculated using the Freesurfer software. All data are shown as measurements of individual children. Shown for each is the correlation coefficient (r^2) and p value for a linear fit.

gene therapy strategy to treat the CNS manifestations of LINCL, we modified the scale created by Steinfeld et al.¹⁹ to focus only on the CNS manifestations of the disease referred to here as the modified Hamburg LINCL scale. The age-specific ratings of our cohort using the modified Hamburg LINCL scale compared well with the one from Steinfeld et al.¹⁹ for the younger children, but most of the children older than 6 years of age were outside the 95th percentile range. Most of these deviations were due to the high rating on the seizure scale of the modified LINCL scale,

likely reflecting optimized antiseizure management or inability of the brain to generate seizures due to advanced neuronal degeneration. This feature of the modified Hamburg LINCL scale further limited the phenotypic range of the scale.

A clinical rating instrument, which is able to identify more subtle differences in disease progression of children with LINCL, would be desirable to study the natural progression of the disease and is critically important for the assessment of novel therapeutic interventions, as the window for assessing disease progression is

Figure 6 Brain imaging measurements of children with late infantile neuronal ceroid lipofuscinosis (LINCL) as a function of the Weill Cornell LINCL scale



(A) Cortical N-acetylaspartate levels. Data are shown as individual measurements of four interleaved 15-mm brain sections. (B) Cortical apparent diffusion coefficient measured by diffusion-weighted imaging. (C) Ventricular volumes. Measurements of ventricular segmentations included all of the lateral and inferior lateral ventricles for both hemispheres. Volumes were calculated by the number of voxels segmented as ventricles, multiplied by the single voxel dimension. (D) Ventricular volumes as % of total brain volume. Total brain volume was determined as the sum of ventricular volume + gray matter volume + white matter volume. (E) Gray matter volumes. (F) Gray matter volumes as % of total brain volume. (G) White matter volumes. (H) White matter volumes as % of total brain volume. Data for E and G are shown as individual measurements from SPGR acquisitions, calculated using the Freesurfer software. All data are shown as measurements of individual children. Shown for each is the correlation coefficient (r^2) and p value for a linear fit.

only a few years from the onset of symptoms to development of a vegetative state.^{1-5,19} In this context, the new Weill Cornell CNS scale was developed to help identify phenotypic differences over a broader range. The Weill Cornell CNS scale, consisting of a more comprehensive neurologic assessment compared to the modified Hamburg LINCL scale and excluding events prior to the time of the assessment, such as onset of seizures, correlated better with age and the time since clinical manifestations of the disease compared to the modified Hamburg

LINCL scale. The individual assessments also separated over a wider range with a steeper decline compared to the modified Hamburg LINCL scale. These features make this new scale suitable to detect deviations to a slower rate of decline with age more readily and make it particularly valuable for the assessment of the effect of novel therapies on disease progression.

To date, at least 52 different mutations in the *CLN2* gene have been associated with the LINCL phenotype (<http://www.ucl.ac.uk/ncl>). Two of

these mutations, the missense mutation C3670T (R208X) and the splicing mutation G3556C (IVS5-1 G>C), account for at least 60% of all disease alleles. A study including patients from Germany and Switzerland found C3670T in 42% and G3556C in 25% of the mutant alleles.¹⁹ The 5th and 95th percentile range of the modified LINCL CNS scale based on the data of Steinfeld et al.¹⁹ used to assess age-specific disease severity is based on patients from that study carrying exclusively the C3670T or G3556C mutation.¹⁹

All of the CLN2 mutations in our patient population have been previously reported in the NCL mutation database (<http://www.ucl.ac.uk/ncl>). In our study population, 25% of the alleles were C3670T, with both patients from Germany being homozygous for this mutation, and 50% of the alleles were G3556C, with all the children from England (except BD-17 whose mother was from the Caribbean), Canada, and Australia having at least one allele with this mutation. Although the sample size precluded a comprehensive assessment of the relationship of genotype with phenotype, we did not observe a difference in the progression of the clinical phenotypic pattern related to either C3670T or G3556C, the two most frequent mutations. Later onset of disease or milder progression have been associated in the literature with a few mutations (R447H, S153P, R127Q, and the intron splice mutation T523-1G0A).^{19,24-26} Two of the children, a sibling pair, carried R127Q (G3085A). The milder disease course, previously described for this mutation in a compound heterozygous patient with C3670T/R127Q,¹⁹ was not observed for the compound heterozygous G3556C/R127Q children in our study.

Anecdotal MRI brain imaging studies have been reported for living patients with LINCL, demonstrating progressive gray matter atrophy prominent in the infratentorial regions.^{15,17,18,27,28} In a postmortem MRI study of 16 patients with LINCL, characteristic MRI findings were enlarged cerebral and cerebellar sulci as well as dilated ventricles,¹⁵ similar to the MRI changes in the present study. Also changes in periventricular white matter, the only finding in the less severely affected children in our cohort, have been previously described in children with more advanced disease.^{15,17,18}

Brain imaging with MRI and MRS provides the tools and opportunity to assess disease severity and to monitor disease progression for neurodegenerative disorders quantitatively. None of this has been reported in a comprehen-

sive and quantitative fashion for LINCL to date, but MRI, MRS, and SPECT analysis have been employed to characterize disease progression in eight patients with infantile NCL (CLN1). MRI and MRS showed abnormal findings before the disease was clinically apparent, and SPECT analysis showed cortical hypoperfusion and loss of benzodiazepine receptors with the onset of clinical manifestations.²⁹ Gray matter volume, % gray matter volume, and NAA, assessing the presence of neurons, decreased with age and severity of the disease, whereas ventricular volume, % ventricular volume, and CADC, assessing consequences of the neuronal loss, increased with age and severity of the disease. The % white matter volumes increased with age and severity of the disease. However, the data did not allow us to distinguish whether the increase in the % white matter volume was absolute or relative to the brain atrophy attributable to the gray matter loss. Of all the MRI measurements evaluated, ventricular volume or % ventricular volume correlated the best with age and the severity scales, suggesting that the measurement of ventricular volumes may be the best MRI measurement to assess disease progression.

In two small studies with LINCL, MRS assessment showed decreased NAA/creatine ratios in three patients,¹⁸ and decreased NAA and elevated lactate in one patient.¹⁶ The NAA measurements in our cohort showed variability between children and also between repeat evaluations of the same child, indicating that this measurement can serve as a marker for overall disease progression in a cohort of patients, but may not be suitable to follow disease progression in individual patients.

The noninvasive instruments used to assess brain structure and degeneration in this study were useful in pointing out that in LINCL gray matter volume and NAA decrease with disease progression, in contrast to white matter volume, ventricular volume, and whole brain diffusion capacity (CADC), which increase with disease progression. These data are consistent with ongoing neuronal loss contributing to the progressive brain atrophy and clinical deterioration evident in LINCL.

Overall, the present study provides an improved understanding of LINCL and provides new tools to assess severity and progression of the disease. By using a novel, more comprehensive disease severity scale, assessing the neurologic manifestations of the disease, and employing

quantitative imaging measurements, in particular the assessment of ventricular volumes, this study also provides a basis for the evaluation of novel therapeutic strategies such as gene and stem cell therapy.

NOTE ADDED IN PROOF

Analysis of the MRS data from a subset of scans ($n = 10$) with data available from voxels corresponding to thalamic tissue showed that thalamic NAA/Cr ratios correlated better with patient age ($r^2 = 0.45$), Modified Hamburg LINCL scale ($r^2 = 0.60$), and Weill Cornell LINCL scale ($r^2 + 0.69$) compared to the cortical region of interest reported in the manuscript ($r^2 = 0.25, 0.28, \text{ and } 0.30$, respectively). These newer analyses suggest that MRS measurements of thalamus may provide greater sensitivity as a marker to identify the progression of Batten disease.

ACKNOWLEDGMENT

The authors thank T. Lee for the ophthalmologic evaluations; S. Hosain for the neurologic assessments; L. Cai, L.M. Arkin, S.C. Bangs, and H. Lawther for coordinating the study; L.H.K. Suh for regulatory submissions; M. Wang for monitoring the study; S. Hyde for data management; and N. Mohamed and T. Virgin-Bryan for help in preparing the manuscript.

Received December 27, 2006. Accepted in final form April 2, 2007.

REFERENCES

1. Goebel HH, Wisniewski KE. Current state of clinical and morphological features in human NCL. *Brain Pathol* 2004;14:61–69.
2. Haltia M. The neuronal ceroid-lipofuscinoses. *J Neuropathol Exp Neurol* 2003;62:1–13.
3. Hofmann SL, Peltonen L. The neuronal ceroid lipofuscinoses. In: Scriver CR, Beaudet AL, Valle D, Sly WS, eds. *The metabolic and molecular bases of inherited disease*. New York: McGraw-Hill; 2001:3877–3894.
4. Williams RE, Gottlob BD, Lake HH, Goebel HH, Winchester BG, Wheeler RB. CLN2 classic late infantile NCL. In: Goebel HH, Mole SE, Lake BD, eds. *The neuronal ceroid lipofuscinoses (Batten disease)*. Amsterdam: IOS Press; 1999:37–54.
5. Wisniewski KE. Neuronal ceroid lipofuscinoses: classification and diagnosis. In: Wisniewski KE, Zhong N, eds. *Batten disease: diagnosis treatment and research*. San Diego: Academic Press; 2001:1–34.
6. Mole SE. The genetic spectrum of human neuronal ceroid-lipofuscinoses. *Brain Pathol* 2004;14:70–76.
7. Sleat DE, Donnelly RJ, Lackland H, et al. Association of mutations in a lysosomal protein with classical late-infantile neuronal ceroid lipofuscinosis. *Science* 1997; 277:1802–1805.
8. Sleat DE, Gin RM, Sohar I, et al. Mutational analysis of the defective protease in classic late-infantile neuronal ceroid lipofuscinosis, a neurodegenerative lysosomal storage disorder. *Am J Hum Genet* 1999;64:1511–1523.
9. Claussen M, Heim P, Knispel J, Goebel HH, Kohlschütter A. Incidence of neuronal ceroid-lipofuscinoses in West Germany: variation of a method for studying autosomal recessive disorders. *Am J Med Genet* 1992; 42:536–538.

10. Uvebrant P, Hagberg B. Neuronal ceroid lipofuscinoses in Scandinavia. *Epidemiology and clinical pictures. Neuropediatrics* 1997;28:6–8.
11. Lane SC, Jolly RD, Schmechel DE, Alroy J, Boustany RM. Apoptosis as the mechanism of neurodegeneration in Batten's disease. *J Neurochem* 1996;67:677–683.
12. Weleber RG. The dystrophic retina in multisystem disorders: the electroretinogram in neuronal ceroid lipofuscinoses. *Eye* 1998;12:580–590.
13. Hachiya Y, Hayashi M, Kumada S, Uchiyama A, Tsuchiya K, Kurata K. Mechanisms of neurodegeneration in neuronal ceroid-lipofuscinoses. *Acta Neuropathol (Berl)* 2006;111:168–177.
14. Sinha S, Satishchandra P, Santosh V, Gayatri N, Shankar SK. Neuronal ceroid lipofuscinosis: a clinicopathological study. *Seizure* 2004;13:235–240.
15. Autti T, Raininko R, Santavuori P, Vanhanen SL, Poutanen VP, Haltia M. MRI of neuronal ceroid lipofuscinosis. II. Postmortem MRI and histopathological study of the brain in 16 cases of neuronal ceroid lipofuscinosis of juvenile or late infantile type. *Neuroradiol* 1997; 39:371–377.
16. Brockmann K, Pouwels PJ, Christen HJ, Frahm J, Hanefeld F. Localized proton magnetic resonance spectroscopy of cerebral metabolic disturbances in children with neuronal ceroid lipofuscinosis. *Neuropediatrics* 1996;27:242–248.
17. Petersen B, Handwerker M, Huppertz HI. Neuroradiological findings in classical late infantile neuronal ceroid-lipofuscinosis. *Pediatr Neurol* 1996;15:344–347.
18. Seitz D, Grodd W, Schwab A, Seeger U, Klose U, Nagele T. MR imaging and localized proton MR spectroscopy in late infantile neuronal ceroid lipofuscinosis. *AJNR Am J Neuroradiol* 1998;19:1373–1377.
19. Steinfeld R, Heim P, von GH, et al. Late infantile neuronal ceroid lipofuscinosis: quantitative description of the clinical course in patients with CLN2 mutations. *Am J Med Genet* 2002;112:347–354.
20. Crystal RG, Sondhi D, Hackett NR, et al. Clinical protocol. Administration of a replication-deficient adeno-associated virus gene transfer vector expressing the human CLN2 cDNA to the brain of children with late infantile neuronal ceroid lipofuscinosis. *Hum Gene Ther* 2004;15:1131–1154.
21. Sondhi D, Hackett NR, Aplett RL, Kaminsky SM, Pergolizzi RG, Crystal RG. Feasibility of gene therapy for late neuronal ceroid lipofuscinosis. *Arch Neurol* 2001;58:1793–1798.
22. Adams H, de Blicke EA, Mink JW, et al. Standardized assessment of behavior and adaptive living skills in juvenile neuronal ceroid lipofuscinosis. *Dev Med Child Neurol* 2006;48:259–264.
23. Marshall FJ, de Blicke EA, Mink JW, et al. A clinical rating scale for Batten disease: reliable and relevant for clinical trials. *Neurology* 2005;65:275–279.
24. Hartikainen JM, Ju W, Wisniewski KE, et al. Late infantile neuronal ceroid lipofuscinosis is due to splicing mutations in the CLN2 gene. *Mol Genet Metab* 1999; 67:162–168.
25. Lin L, Lobel P. Expression and analysis of CLN2 variants in CHO cells: Q100R represents a polymorphism, and G389E and R447H represent loss-of-function mutations. *Hum Mutat* 2001;18:165.

26. Mitsumoto H, Ulug AM, Pullman SL, et al. Quantitative objective markers for upper and lower motor neuron dysfunction in amyotrophic lateral sclerosis. *Neurology* 2007 (in press).
27. Lagenstein I, Schwendemann G, Kuhne D, Koeppe P, Stahnke N, Sternowsky HJ. Neuronal ceroid lipofuscinosis: CCT findings in fourteen patients. *Acta Paediatr Scand* 1981;70:857–860.
28. Santavuori P, Vanhanen SL, Autti T. Clinical and neuroradiological diagnostic aspects of neuronal ceroid lipofuscinoses disorders. *Eur J Paediatr Neurol* 2001;5 Suppl A:157–161.
29. Vanhanen SL, Puranen J, Autti T, et al. Neuroradiological findings (MRS, MRI, SPECT) in infantile neuronal ceroid-lipofuscinosis (infantile CLN1) at different stages of the disease. *Neuropediatrics* 2004;35:27–35.

Experience the 2007 Annual Meeting from the Comfort of Your Home

Much of this year's top programming is now available to you through the AAN Virtual Annual Meeting Products:

- **Audio MP3 Files—starting at \$10**
Conveniently listen to some of the best talks on today's most significant neurological topics.
- **Webcasts-on-Demand—several program hours FREE**
Instant online access to the slides, audio, and video of more than 240 hours of programs and presentations, including five Plenary Sessions. Enjoy several hours of free programming in addition to other programs available for purchase (\$399 members, \$199 Junior members, \$499 non-members).
- **2007 Syllabi on CD-ROM—only \$199**
Complete syllabi for more than 160 education programs (\$199 members, \$299 non-members).

Check out the Virtual Annual Meeting Programming at www.aan.com/virtualAM today!

SETTING BACK THE CLOCK: ADENOVIRAL-MEDIATED GENE THERAPY FOR LYSOSOMAL STORAGE DISORDERS

Dolan Sondhi, Neil R. Hackett, Stephen M. Kaminsky, and Ronald G. Crystal

1 INTRODUCTION

Lysosomal storage diseases (LSD) arise from mutations in the genes for lysosomal proteins that degrade and recycle macromolecules (Futerman and van Meer, 2004; Mach, 2002; Vellodi, 2005; Walkley, 2001). The undegraded waste products accumulate over time, resulting in derangement of cell physiology and eventually cell death. It follows, therefore, that delivery and expression of a wild-type copy of the defective gene to the affected cells should be preventive or therapeutic. For the lysosomal storage disorders, the challenges for gene therapy are to deliver the gene to the target tissue and to achieve reduction of “lysosomal storage,” thus preserving cellular function.

Of the various strategies to achieve that goal, replication-deficient adenovirus-derived vectors (Ad) are generally thought to be inappropriate because although Ad vectors mediate high levels of production of their transgene, expression is transient over a period of only a few weeks (Hackett and Crystal, 2003; Trapnell and Gorziglia, 1994; Wilson, 1996). This chapter provides a contrary and counterintuitive view, making the case for using Ad vectors to treat the lysosomal storage disorders. We do so by first providing an overview of the production and properties of Ad vectors and then discussing studies in which Ad has been used to treat animal models of lysosomal storage diseases. The intent of this analysis is to critically evaluate the applicability of Ad for the challenges provided by LSD, including the required spatial and temporal pattern of gene expression. We then discuss a novel hypothesis, which we call “setting back the clock,” which holds that, for some lysosomal storage diseases, transient overexpression of the deficient gene at high levels may be sufficient to completely reverse the storage defect and may give a substantial benefit, especially in diseases where the accumulation of the storage defect is slow.

2 GENERAL CHARACTERISTICS OF ADENOVIRUS

This section provides a brief description of the construction and use of Ad for gene transfer. A number of detailed reviews on the biology of adenoviruses and how they are

modified as gene transfer vectors are available (Hackett and Crystal, 2003; Trapnell and Gorziglia, 1994; Wilson, 1996).

In humans, adenoviruses generally cause transient mild infections of the upper respiratory tract which are rapidly cleared by the immune system, providing long-term protection against reinfection by the same serotype (Horwitz, 1996). There are at least 51 distinct serotypes of human adenovirus, classified into six groups labeled A to F based on sequence homology and their ability to agglutinate red blood cells (Horwitz, 1996). Most gene therapy related studies have been carried out with derivatives of adenovirus serotype 5 although other serotypes including Ad35 and Ad11 are being evaluated, as are vectors made from nonhuman primate-derived adenoviruses (Cohen et al., 2002; Seshidhar et al., 2003; Stone et al., 2005).

Adenoviruses are nonenveloped double-stranded DNA viruses with an outer protein shell surrounding an inner nucleoprotein (Shenk, 1996). The 20 triangular faces of the capsid are each made up of 60 trimers of the hexon protein, which makes contact with six adjacent pseudo-equivalent neighbors. The 12 vertices are made up of a complex of the five copies of penton base protein and three of the fiber protein (Shenk, 1996). Within the 90 nm capsid, the 36 kilobase (kb) genome is packaged with the core protein and with the terminal protein attached to each end (Shenk, 1996; Figure 1A).

The adenovirus infection pathway is initiated by interaction of Ad with cell surface proteins. For the group C Ad, these include the primary coxsackie-adenovirus receptor (CAR) and coreceptors from the integrin family ($\alpha_V\beta_3$, $\alpha_V\beta_5$, $\alpha_V\beta_1$, $\alpha_M\beta_2$, and $\alpha_5\beta_1$) (Nemerow, 2000; Wickham, 2000). Other serotypes of human adenovirus use different receptors (Sirena et al., 2004). The knob region of fiber contains a binding site for CAR and the penton base protein binds to integrins via a consensus integrin binding domain containing an Arg–Gly–Asp motif (RGD) (Nemerow, 2000; Wickham, 2000). Adenovirus enters cells via clathrin-mediated endocytosis followed by a pH-dependent modification of the capsid and release of the virion to the cytosol (Meier and Greber, 2003). Like many viruses, adenovirus takes advantage of microtubule-associated transport mechanisms to reach the nucleus (Leopold et al., 2000). The capsids bind to the nuclear envelope in the vicinity of nuclear pores and undergo a final round of uncoating during which the viral DNA genome and DNA-binding protein leave the capsid and enter the nucleus (Figure 1B).

The biology of human adenoviruses has been extensively studied and their adaptation to the role of gene transfer vectors was relatively simple. Among the features that make Ad vectors attractive for gene therapy are the mild pathology of wild-type adenovirus, the lack of oncogenic potential, and the ability to infect a wide variety of cells (Hackett and Crystal, 2003; Trapnell and Gorziglia, 1994; Wilson, 1996). These qualities, as well as the ease of manipulating the viral genome, have made Ad a popular gene therapy vector as can be evidenced by the fact that nearly one quarter of all human gene therapy clinical trials in the United States use recombinant adenoviral vectors (<http://www4.od.nih.gov/oba/rac/PROTOCOL.pdf>). In general Ad are easy to produce in large amounts, achieve efficient infection of many cell types (quiescent or dividing) and rapidly result in high levels of expression of the therapeutic gene (Hackett and Crystal, 2003; Trapnell and Gorziglia, 1994; Wilson, 1996).

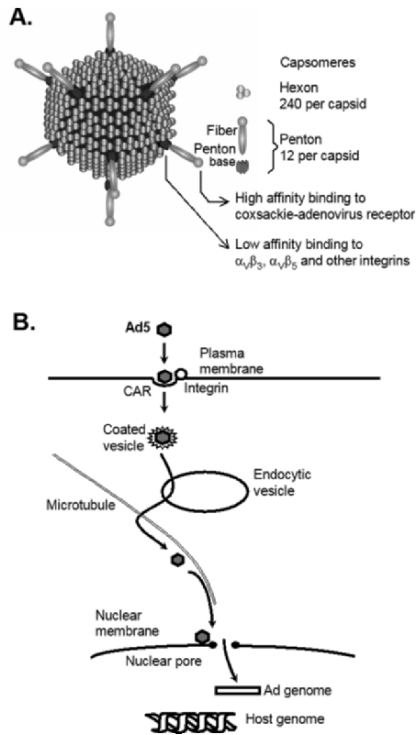


Figure 1. Adenovirus structure and intracellular trafficking. (A) The adenovirus capsid surface is composed primarily of two structures, hexon and penton. The major component is the hexon, but many of the critical functions involved in infection are incorporated in the penton that resides at each vertex. The penton has two parts, the penton base, which binds to integrins, and the high affinity fiber, which binds to the coxsackie adenovirus receptor (CAR). (B) The adenovirus trafficking pathway.

Laboratory investigations of adenovirus serotype 5 have led to a detailed understanding of its infection and replication cycles and the roles played by the early (E1, E2, E3, and E4) and late (L1, L2, L3, L4, L5) genes (Shenk, 1996; Figure 2). Each gene comprises a complex transcription unit with alternative sites for transcription initiation, termination, and splicing, and each gene expresses multiple proteins (Shenk, 1996). The E1 gene products, E1A and E1B, are expressed immediately upon infection and are essential for expression of all other adenoviral genes (Shenk, 1996). The E1 genes play a critical role in forcing the host cell to enter the replicative state needed by the virus for DNA replication and in preventing cellular apoptosis (Shenk, 1996). Among the genes activated by the E1 proteins are the E2 (encoding proteins required for DNA replication), the E3 proteins (encoding nonessential proteins that help evade host response) and the E4 proteins (encoding proteins that coordinate late gene expression). The late genes encode

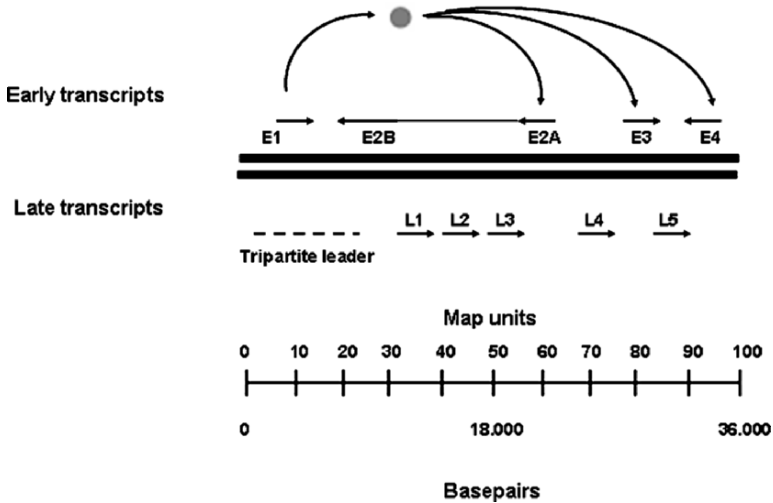


Figure 2. Structure and transcription of the major genes of the adenovirus type 5 genome. The genome is represented as two parallel lines and is divided by the scale shown on top into 100 map units (1 map unit = 360 bp). There are nine major complex transcription units divided into early (above the genome) and late transcripts (below). The four early transcripts are produced before the commencement of DNA replication and specify regulatory proteins and proteins required for DNA replication. Upon initial infection of a cell, the E1A protein is produced from transcripts in the E1 region. E1A is a major regulatory factor required for transcription of E1B, E2, E3, and E4. In replication-deficient adenovirus vectors, the E1 region is deleted. Proteins coded by the E2 and E4 regions are required for late gene transcription. The E3 region codes for proteins that help the virus evade host defenses. All late transcripts originate at the same point and are produced by alternate splicing. The tripartite leader sequence is present at the 5' end of all late transcripts. The L3 region specifies hexon, the L5 specifies fiber and the L2 specifies penton. For conventional adenovirus gene transfer vectors, most of E1 and E3 are deleted, and the expression cassette is inserted into the E1 region.

the components of the viral capsid and are expressed in abundance after DNA replication begins. In the wild-type adenovirus, DNA replication and packaging are coordinated and about 10,000 progeny virus are produced by each infected cell (Hackett and Crystal, 2003; Horwitz, 1996; Shenk, 1996).

3 GENE TRANSFER BY REPLICATION-DEFICIENT ADENOVIRUSES

Because the E1 gene is essential for all subsequent steps of the productive infection cycle, it follows that adenoviruses with E1 deletions are replication-deficient (Shenk, 1996). Gene transfer vectors are made by replacing the E1 gene with an expression cassette for the therapeutic gene. In practice, the nonessential E3 gene is also deleted. These two modifications render the vector incapable of completing the infectious cycle and thus infection is followed by expression of only the therapeutic gene (Hackett and

Crystal, 2003; Trapnell and Gorziglia, 1994). Production of such $E1^-E3^-$ Ad requires producer cell-lines that provide the deleted viral functions in *trans* (Graham and Prevec, 1995). The 293 cell-line, derived from human embryonic kidney and transformed by the left 11% of the adenovirus genome is generally used (Graham et al., 1977; Figure 3). Recombinant $E1^-$ Ad vectors containing therapeutic genes can be expanded on 293 cells and are readily purified in large amounts. These vectors can infect many cell types in vitro and in vivo and result in high-level expression of the therapeutic gene (Hackett and Crystal, 2003; Trapnell and Gorziglia, 1994; Wilson, 1996).

Wild type adenovirus

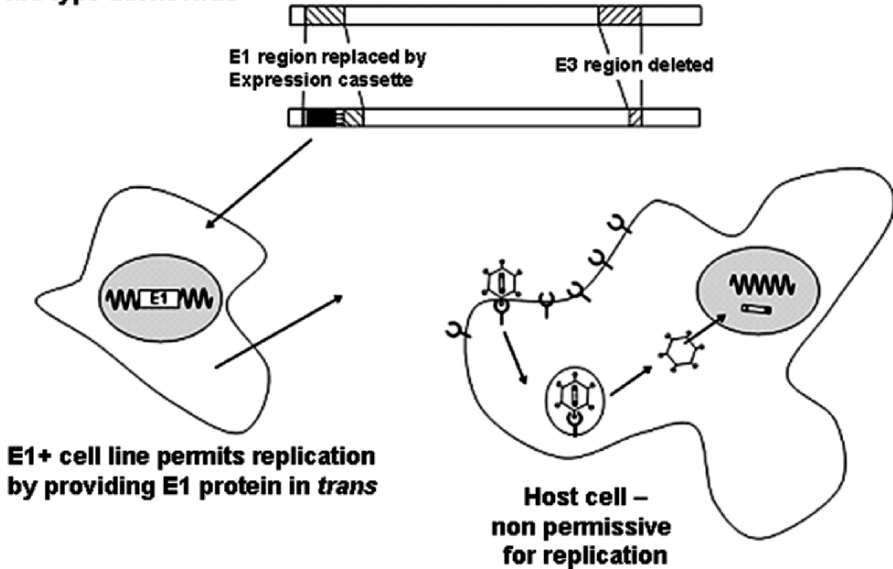


Figure 3. Gene transfer by adenovirus vectors. (Top) The 36,000 basepair genome of wild-type adenovirus serotype 5 with the locations of the E1 and E3 genes cross-hatched. Below this is a schematic of a first-generation adenovirus gene transfer vector. The E3 gene is deleted to make room for the expression cassette for the therapeutic gene. The E1 gene is removed and replaced by an expression cassette, typically consisting of a strong promoter (e.g., cytomegalovirus immediate/early promoter/ enhancer), an artificial splice site to enhance expression, and the reporter or therapeutic gene followed by a transcription stop/polyadenylation site. (Below, left) The genome of the replication deficient Ad vector is constructed in *E. coli* and transfected into human embryonic kidney 293 cells. Because 293 cells have the adenovirus E1 gene expressed from a chromosomal location, they are permissive for the replication of the E1 deleted vector. Serial infection of increasing numbers of 293 cells leads to large amounts of vector which is purified before in vitro or in vivo use. (Below, right) The vector binds to host cells through interaction of the fiber gene, which projects from each vertex of the virion, and the cell surface coxsackie adenovirus receptor integrins. The vector is internalized by endocytosis. It escapes from endosomes and traffics rapidly to the nucleus. The vector DNA, but not the capsid, enters the nucleus. There is no integration into host DNA so the transgene is expressed from an episome which does not replicate and is diluted by cell division.

Extensive use of recombinant Ad in experimental animals and humans has led to a number of general conclusions about their use as vectors. Adenoviruses can be used for gene transfer to most tissues by direct administration to that tissue. When administered by the intravenous route, gene expression is primarily in the liver in rodents, but also in the lung in species such as the pig (Hackett et al., 2000). Due to the packaging capacity of the virus, the expression cassette can be up to ~8 kb and therefore most cDNAs can be expressed using E1⁻E3⁻ Ad. Ad vectors generally mediate a high level of gene expression, peaking at two to seven days, but diminishing to <5% by about two weeks following gene transfer (Hackett and Crystal, 2003; Trapnell and Gorziglia, 1994; Wilson, 1996). The reason for the decrease is a combination of two factors. First, the Ad genome does not replicate or integrate into the host genome and therefore expression becomes diluted when cells divide. Second, and more important, there are robust cellular and humoral responses against the vector (Yang et al., 1996a,c). Furthermore, if the transgene is foreign to the host, there is also a humoral and cellular response against the transgene. At least part of the immune response is due to efficient infection of dendritic cells and macrophages by Ad, which results in efficient antigen presentation to T and B cells (Yang et al., 1996a,c).

There is extensive experience of administration of Ad to humans (Crystal, 1995). In general Ad vectors are safe and well tolerated when injected locally at moderate doses, but can be toxic when administered by the intravascular route (Crystal et al., 2002; Harvey et al., 2002; Raper et al., 2003). Local inflammatory/immune reactions are sometimes observed. When gene expression has been observed in humans, it is transient, and thus the primary focus of Ad gene therapy has been on scenarios such as angiogenesis and cancer where a therapeutic benefit can be gained from transient transgene expression.

4 SETTING BACK THE CLOCK

The general perception is that Ads are not applicable to treatment of genetic diseases inasmuch as they provide only transient transgene expression. For most hereditary disorders, this seems a rational assumption. For example, diseases such as hemophilia would require a continuous supply of the deficient coagulation proteins for the whole lifetime of the patient. But in the case of lysosomal storage diseases, the validity of this contention is not clear. Contrary to conventional concepts, we propose a testable hypothesis with Ad vectors that we call “setting back the clock” (Figure 4). Waste products accumulate slowly over time in the lysosomal storage disorders, and only when a threshold is reached do they cause cellular pathology (Futerman and van Meer, 2004; Mach, 2002; Vellodi, 2005; Walkley, 2001).

Although the kinetics by which storage products accumulate is complex, and likely differs in different lysosomal storage disorders, we suggest that if gene therapy with transient expression is used, it is theoretically possible that the stage of progression of the cellular pathology can be set back to the wild-type baseline level. As the expression wanes, the abnormal storage will start to reaccumulate, but this should provide a significant window of therapeutic benefit, particularly for the lysosomal storage disorders where the natural history of accumulation is slow. The “setting back the clock” hypothesis predicts that if the storage defect is fully, or even partially, reversed in the recipients, the impact of cessation of therapy (e.g., loss of expression), will be a very slow re-emergence of the disease.

The utility of setting back the clock with an Ad vector is enhanced by another property of many lysosomal storage diseases, referred to as “cross-correction” (Desnick and Schuchman, 2002; Kornfeld, 1986; Sleat et al., 2005). Upon biosynthesis, lysosomal enzymes are glycosylated with carbohydrates that contain mannose-6-phosphate (Kornfeld, 1986). In sorting the newly synthesized enzyme to the lysosome, a fraction of the newly synthesized enzyme is misdirected, secreted from the cell, and can be taken up by mannose-6-phosphate receptor-mediated endocytosis. Thus, a cell that is transduced by an Ad vector may be a depot to produce enzymes for other cells. A good example of the cross-correction concept is the mucopolysaccharidosis VII animal model, which lacks the protein β -glucuronidase (Kosuga et al., 2000). When serum from mucopolysaccharidosis VII mice treated with an adenovirus coding for the β -glucuronidase gene was transfused into untreated mucopolysaccharidosis VII knockout mice, the recipients showed β -glucuronidase activity in liver, spleen, kidney, lung, and heart (Kosuga et al., 2000). In a study involving the mouse model of glycogen storage disease II, administration of an adenovirus coding for acid- α -glucosidase into the gastrocnemius muscle of acid- α -glucosidase knockout mice resulted in secretion and uptake of the transgene product by other muscle groups with amelioration of the storage defect at these distant sites (Martin-Touaux et al., 2002). Cross-correction has also been implicated after use of Ad for treatment of other lysosomal storage diseases, including Fabry (Ziegler et al., 1999) and Tay–Sachs disease (Guidotti et al., 1999). Thus, a single administration of an Ad expressing the missing enzyme has the potential to eliminate the storage defect in cells beyond those transduced and return the pathology to baseline levels.

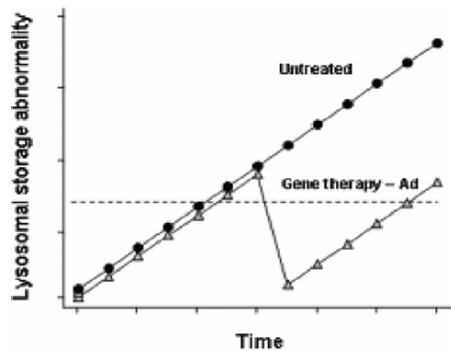


Figure 4. Setting back the clock. The concept is demonstrated graphically with the accumulation of storage defect as a function of time and the impact of intervention. As an example, there is linear accumulation of storage defect that reaches the threshold shown by the dotted line at which point pathology results. Gene therapy with an Ad vector should result in transient expression of the deficient protein, resulting in transient decrease in storage defect which then reaccumulates. This would provide a window of therapeutic benefit.

There are several examples of experimental animal models for which transient expression resulting from a single administration of an Ad vector expressing a lysosomal protein resulted in the correction of storage defect for a much longer duration than that of detectable transgene expression. In all cases, cross-correction was a significant factor enhancing the efficacy of gene transfer. In the mouse model of Fabry disease (α -galactosidase deficiency), a single intravenous administration of an Ad vector expressing the α -galactosidase gene was sufficient to reverse the storage defect (Ziegler et al., 1999).

The deposition of glycosphingolipid globotriaosylceramide that occurs in the mutant Fabry mouse was reversed for up to six months, with only a low level of reaccumulation. Although transgene expression was primarily in the liver, all tissues showed reversal of storage defect (Ziegler et al., 1999). Similarly, when an Ad expressing the acid- α -glucosidase gene, was injected intravenously into the acid- α -glucosidase model of the glycogen storage disease type II (Pompe disease) knockout mice, the expression level as assessed by enzymatic activity in the serum peaked on days 2 to 3 post-administration but declined rapidly to background by 10 days. However, this pattern of transgene expression was sufficient to reduce the glycogen storage defect in various muscle groups for 100 to 200 days postvector administration (Ding et al., 2001). In a study where old mice with glycogen storage disease type II were treated by intravenous administration of the same vector, high levels of human acid- α -glucosidase were produced and, based on reductions in glycogen storage in heart, quadriceps, and diaphragm, apparently taken up by muscles (Xu et al., 2005).

Surprisingly, in spite of the antivector and antitransgene immune response, long-term correction of the defect was observed (Ding et al., 2001). In another demonstration of this concept, in a lysosomal acid lipase knockout mouse, a model for human Wolman disease and cholesteryl ester storage disease, intravenous administration of Ad expressing lysosomal acid lipase was associated with increased hepatic liposomal acid lipase activity, decreased hepatomegaly, normalization of histopathology, and reductions in triglyceride and cholesterol levels in liver, spleen, and the small intestine for up to 47 days (Du et al., 2002).

Together, these models provide an important element of our hypothesis, that lysosomal storage defects are reversible and not merely preventable by adenovirus-mediated gene transfer. This is important when translating this concept to humans, because the lysosomal storage disorders are generally diagnosed at an advanced stage of storage defect accumulation. These examples verify the overall concept of setting back the clock with storage defect being cleared for a duration that exceeds the duration of transgene expression. None of these examples include behavioral or survival analysis and therefore full assessment of the therapeutic benefit is not known. However, for the experimental animal data available, although setting back the clock may not offer a permanent cure for lysosomal storage diseases, the impact on patients with these diseases may be substantial.

4.1 Enhancing the Efficacy of Ad in the Treatment of Lysosomal Storage Disease

If adenoviral gene transfer can reverse storage defect in lysosomal storage diseases, then the optimal result would be to return the storage defect to baseline levels of cellular pathology. It follows that a small dose and a short duration of expression of the therapeutic gene after Ad gene transfer may give only partial relief. Therefore manipulations that enhance

adenoviral gene transfer or prolong transgene duration may be advantageous to “setting back the clock” as far as possible. Studies with Ad in experimental models of lysosomal storage diseases have used various strategies to overcome the short-term transgene expression resulting from the immune responses against the Ad vector. Examples of different approaches to this challenge as applied to lysosomal storage disease are as follows.

4.1.1 Vectors with Additional Early Gene Deletions

Gene transfer with first generation Ad (E1⁻ E3⁻ Ad), results in gene expression that is limited to a few weeks. This is, in part, attributed to the presence of E1-like activities in cells that potentiate expression of other adenovirus genes. The result is that Ad infected cells can be detected by the cellular immune system (Yang et al., 1996a,c). This problem can be reduced, at least in part, by making additional deletions of essential Ad genes such as E2 or E4 (Brough et al., 1997; Ding et al., 2001; Engelhardt et al., 1994; Gao, Yang, and Wilson, 1996; Yang et al., 1994). Propagation of these vectors requires specially constructed cell-lines that complement both missing adenoviral genes. There has been no direct comparison of such vectors to conventional E1E3E3 Ad vectors in experimental models of lysosomal storage disease, but a double mutant Ad with both E1 and E2B (DNA polymerase) deletions expressing the acid- α -glucosidase gene (the gene that is defective in glycogen storage disease type II, Pompe disease) did lead to long-term clearance of glycogen storage defect (Ding et al., 2001).

4.1.2 Immuno-Suppression Strategies

The most important factor limiting the duration of transgene expression mediated by Ad vectors is the acquired immune response to Ad gene products. As a dramatic demonstration of this concept relevant to the lysosomal storage diseases, an immune-deficient mouse model of glycogen storage disease type II was developed by crossing acid α -glucosidase knockout mice with severe combined immune-deficient mice. In these recipients, long-term high-level expression of acid- α -glucosidase was achieved for at least six months following intravenous administration of an Ad-vector coding for human-acid- α -glucosidase compared to a limited duration of approximately ten days in immune competent recipients (Xu et al., 2004).

Because there is such a vigorous immune response to Ad and to nonautologous transgenes, a number of groups have used immunosuppression to blunt this response in an attempt to prolong transgene expression (Guibinga et al., 1998; Scaria et al., 1997; Yang et al., 1996b). For example, intravenous administration of an Ad vector coding for b-glucuronidase led to detectable serum levels of b-glucuronidase that declined to undetectable by 50 days (Kosuga et al., 2000). However, simultaneous injection of another Ad expressing a decoy for immune costimulatory molecules, Ad-CLTLA4Ig, resulted in expression of detectable levels of glucuronidase for greater than 300 days.

In the mouse model of Fabry disease (α -galactosidase deficiency), high doses of Ad vector expressing the α -galactosidase transgene were needed to provide the required level of enzyme to cause clearance of storage defect, but as a result of the high dose, a strong immune response occurred, thereby limiting the duration of gene expression (Ziegler et al., 2002). Pretreatment with clodronate liposomes to eliminate Kupfer cells and other

antigen-presenting cells (thereby blunting both the innate and acquired immune responses to the vector) permitted complete clearance of the storage defect with an Ad vector 100-fold lower than required in control mice (Ziegler et al., 2002). Similarly, treatment of mice by gamma globulin prior to Ad infusion resulted in a transient blockade of cells expressing IgG receptors (macrophage and dendritic cells) allowing 10-fold higher transgene expression levels at the same dose (Ziegler et al., 2002).

Another strategy to circumvent the immune system is to use newborn animals in which the immature immune system is unable to detect the Ad (Chou, Zingone, and Pan, 2002; Kamata et al., 2003; Martin-Touaux et al., 2002). Using the mucopolysaccharidosis type VII (MPSVII) model, mice were administered within 24 hours of birth an Ad expressing the wild-type form of the defective gene, β -glucuronidase (Kamata et al., 2003). More than 20% of normal β -glucuronidase activity was maintained for at least 20 weeks after birth in the brains of the Ad-injected mice. Histopathological analysis showed no obvious lysosomal storage defect in any of the visceral organs or the brain. The treated neonatal mice also failed to develop the facial skeletal deformities that characterize MPS VII mice. Similarly, the feasibility of adenovirus-mediated gene transfer was assessed in newborn glucose-6-phosphatase (G6Pase) deficient mice (a model of Type 1A glycogen storage disease) by infusion of a recombinant adenovirus containing the murine G6Pase gene. Whereas only 15% of untreated mutants survived weaning, 100% of the Ad vector-treated mice lived to three months of age, and liver and kidney enlargement was less pronounced with near normal levels of glycogen depositions in both organs (Chou, Zingone, and Pan, 2002). The concept of early therapy with Ad vectors has been extended to the period before birth, based on the observation that long term lacZ expression can be achieved by *in utero* gene transfer using Ad vectors (Shen et al., 2004).

4.1.3 Targeting Immuno-Privileged Tissues

Ad yields short duration expression in most tissues, however, the brain and eye are exceptions due to their partially immunoprivileged nature (Chaum and Hatton, 2002; Lowenstein and Castro, 2003). It follows that complete reversal of the storage defect using Ad to set back the clock is most likely in these organs. Inasmuch as several lysosomal storage diseases manifest in these organs and methods exist for direct administration to these sites, there is a possibility of treating the local symptoms of such lysosomal storage diseases with Ad. For example, when MPS VII knockout mice were treated by direct administration of Ad- β -glucuronidase into the brain, long-term (>16 wk) expression of β -glucuronidase protein was observed (Stein et al., 1999). Interestingly, there was correction of the storage defect in many parts of the brain, including areas where there was no β -glucuronidase activity detectable by immunohistochemistry. Animal models of other lysosomal storage diseases with neurological symptoms such as aspartylglucosaminuria (Peltola et al., 1998) have also been treated by direct CNS administration of Ad with consequent clearance of the storage defect.

Due to the limited size of the eye, it is easy to deliver Ad expressing the deficient gene to a large proportion of this target tissue, and because the eye is partially immune-protected, long-term transgene expression may result (Bennett et al., 1994; Mashhour et al., 1994). For example, phenotypic correction of storage defect in the retinal pigment

epithelium of mucopolysaccharidosis VII mice has been demonstrated after Ad- β -glucuronidase injection by subretinal and intravitreal routes (Li and Davidson, 1995).

The blood–brain barrier precludes targeting and delivery of Ad to the brain by the vascular route and necessitates gene transfer directly to the CNS. In this regard, intravenous injection of an Ad expressing β -glucuronidase into MPS VII knockout mice resulted in no detectable β -glucuronidase activity in the brain (Ohashi et al., 1997). In an attempt to enhance delivery of Ad vectors to the brain, methods of delivery have been assessed in which the brain barriers are transiently compromised to allow Ad expressing the therapeutic gene to reach the brain parenchyma. For example, when intraperitoneal mannitol was administered at the time of the intraventricular injection of Ad- β -glucuronidase into MPS VII knockout mice, there was penetration of vector across the ependymal cell layer, with infection of cells in the subependymal region (Ghodsi et al., 1999).

5 CONCLUSIONS

The argument made in this chapter is that transient, adenovirus-mediated expression of a therapeutic enzyme should be sufficient to provide a prolonged therapeutic effect for lysosomal storage diseases due to the high levels of therapeutic protein, cross-correction, and long residence time of degradative enzymes in the lysosome. This effect may be further enhanced by some of the innovations that interrupt the immune response against first-generation Ad vectors thereby providing a longer duration of expression and a greater therapeutic benefit. The concept of setting back the clock merits a full experimental investigation in animals and consideration as an approach to human therapy for lysosomal storage diseases.

ACKNOWLEDGMENTS

We thank N. Mohamed for help in preparing this manuscript. These studies were supported, in part, by NIH U01 NS047458 and M01RR00047; Will Rogers Memorial Fund, Los Angeles, CA; and Nathan's Battle Foundation, Greenwood, IN.

REFERENCES

- Bennett, J., Wilson, J., Sun, D., Forbes, B., and Maguire, A., 1994, Adenovirus vector-mediated in vivo gene transfer into adult murine retina, *Invest Ophthalmol. Vis. Sci.* **35**: 2535.
- Brough, D.E., Hsu, C., Kulesa, V.A., Lee, G.M., Cantolupo, L.J., Lizonova, A., and Kovesdi, I., 1997, Activation of transgene expression by early region 4 is responsible for a high level of persistent transgene expression from adenovirus vectors in vivo, *J. Virol.* **71**: 9206.
- Cham, E. and Hatton, M.P., 2002, Gene therapy for genetic and acquired retinal diseases, *Surv. Ophthalmol.* **47**: 449.
- Chou, J.Y., Zingone, A., and Pan, C.J., 2002, Adenovirus-mediated gene therapy in a mouse model of glycogen storage disease type 1a, *Eur. J. Pediatr.* **161 Suppl 1**: S56.
- Cohen, C.J., Xiang, Z.Q., Gao, G.P., Ertl, H.C., Wilson, J.M., and Bergelson, J.M., 2002, Chimpanzee adenovirus CV-68 adapted as a gene delivery vector interacts with the coxsackievirus and adenovirus receptor, *J. Gen. Virol.* **83**: 151.

- Crystal, R.G., 1995, Transfer of genes to humans: Early lessons and obstacles to success, *Science* **270**: 404.
- Crystal, R.G., Harvey, B.G., Wisnivesky, J.P., O'Donoghue, K.A., Chu, K.W., Maroni, J., Muscat, J.C., Pippo, A.L., Wright, C.E., Kaner, R.J., Leopold, P.L., Kessler, P.D., Rasmussen, H.S., Rosengart, T.K., and Hollmann, C., 2002, Analysis of risk factors for local delivery of low- and intermediate-dose adenovirus gene transfer vectors to individuals with a spectrum of comorbid conditions, *Hum. Gene Ther.* **13**: 65.
- Desnick, R.J. and Schuchman, E.H., 2002, Enzyme replacement and enhancement therapies: lessons from lysosomal disorders, *Nat. Rev. Genet.* **3**: 954.
- Ding, E.Y., Hodges, B.L., Hu, H., McVie-Wylie, A.J., Serra, D., Migone, F.K., Pressley, D., Chen, Y.T., and Amalfitano, A., 2001, Long-term efficacy after [E1-, polymerase-] adenovirus-mediated transfer of human acid-alpha-glucosidase gene into glycogen storage disease type II knockout mice, *Hum. Gene Ther* **12**: 955.
- Du, H., Heur, M., Witte, D.P., Ameis, D., and Grabowski, G.A., 2002, Lysosomal acid lipase deficiency: Correction of lipid storage by adenovirus-mediated gene transfer in mice, *Hum. Gene Ther* **13**: 1361.
- Engelhardt, J.F., Ye, X., Doranz, B., and Wilson, J.M., 1994, Ablation of E2A in recombinant adenoviruses improves transgene persistence and decreases inflammatory response in mouse liver, *Proc. Natl. Acad Sci USA.* **91**: 6196.
- Futerman, A.H. and van Meer, G., 2004, The cell biology of lysosomal storage disorders, *Nat. Rev. Mol. Cell Biol.* **5**: 554.
- Gao, G.P., Yang, Y., and Wilson, J.M., 1996, Biology of adenovirus vectors with E1 and E4 deletions for liver-directed gene therapy, *J. Virol* **70**: 8934.
- Ghodsi, A., Stein, C., Derksen, T., Martins, I., Anderson, R.D., and Davidson, B.L., 1999, Systemic hyperosmolality improves beta-glucuronidase distribution and pathology in murine MPS VII brain following intraventricular gene transfer, *Exp. Neurol.* **160**: 109.
- Graham, F.L. and Prevec, L., 1995, Methods for construction of adenovirus vectors, *Mol. Biotechnol.* Jun, **3**: 207.
- Graham, F.L., Smiley, J., Russell, W.C., and Nairn, R., 1977, Characteristics of a human cell line transformed by DNA from human adenovirus type 5, *J. Gen. Virol.* **36**: 59.
- Guibinga, G.H., Lochmuller, H., Massie, B., Nalbantoglu, J., Karpati, G., and Petrof, B.J., 1998, Combinatorial blockade of calcineurin and CD28 signaling facilitates primary and secondary therapeutic gene transfer by adenovirus vectors in dystrophic (mdx) mouse muscles, *J. Virol* **72**: 4601.
- Guidotti, J.E., Mignon, A., Haase, G., Caillaud, C., McDonnell, N., Kahn, A., and Poenaru, L., 1999, Adenoviral gene therapy of the Tay-Sachs disease in hexosaminidase A-deficient knock-out mice, *Hum. Mol. Genet.* **8**: 831.
- Hackett, N.R. and Crystal, R.G., 2003, Adenovirus vectors for gene therapy. In *Gene and Cell Therapy: Therapeutic Mechanisms and Strategies* (Ed. N. Smyth Templeton). Marcel Dekker, New York, pp. 17–42.
- Hackett, N.R., El Sawy, T., Lee, L.Y., Silva, I., O'Leary, J., Rosengart, T.K., and Crystal, R.G., 2000, Use of quantitative TaqMan real-time PCR to track the time-dependent distribution of gene transfer vectors in vivo, *Mol. Ther.* **2**: 649.
- Harvey, B.G., Maroni, J., O'Donoghue, K.A., Chu, K.W., Muscat, J.C., Pippo, A.L., Wright, C.E., Hollmann, C., Wisnivesky, J.P., Kessler, P.D., Rasmussen, H.S., Rosengart, T.K., and Crystal, R.G., 2002, Safety of local delivery of low- and intermediate-dose adenovirus gene transfer vectors to individuals with a spectrum of morbid conditions, *Hum. Gene Ther.* **13**: 15.

- Horwitz, M.S., 1996, Adenoviruses. In *Fields Virology* (Eds. B.N. Fields, D.M. Knipe, and P.M. Howley), Philadelphia: Lippincott-Raven, pp. 2149–2171.
- Kamata, Y., Tanabe, A., Kanaji, A., Kosuga, M., Fukuhara, Y., Li, X.K., Suzuki, S., Yamada, M., Azuma, N., and Okuyama, T., 2003, Long-term normalization in the central nervous system, ocular manifestations, and skeletal deformities by a single systemic adenovirus injection into neonatal mice with mucopolysaccharidosis VII, *Gene Ther.* **10**: 406.
- Kornfeld, S., 1986, Trafficking of lysosomal enzymes in normal and disease states, *J. Clin. Invest* **77**: 1.
- Kosuga, M., Takahashi, S., Sasaki, K., Li, X.K., Fujino, M., Hamada, H., Suzuki, S., Yamada, M., Matsuo, N., and Okuyama, T., 2000, Adenovirus-mediated gene therapy for mucopolysaccharidosis VII: Involvement of cross-correction in widespread distribution of the gene products and long-term effects of CTLA-4Ig coexpression, *Mol. Ther.* **1**: 406.
- Leopold, P.L., Kreitzer, G., Miyazawa, N., Rempel, S., Pfister, K.K., Rodriguez-Boulan, E., and Crystal, R.G., 2000, Dynein- and microtubule-mediated translocation of adenovirus serotype 5 occurs after endosomal lysis, *Hum. Gene Ther* **11**: 151.
- Li, T. and Davidson, B.L., 1995, Phenotype correction in retinal pigment epithelium in murine mucopolysaccharidosis VII by adenovirus-mediated gene transfer, *Proc. Natl. Acad. Sci. USA* **92**: 7700.
- Lowenstein, P.R. and Castro, M.G., 2003, Inflammation and adaptive immune responses to adenoviral vectors injected into the brain: Peculiarities, mechanisms, and consequences, *Gene Ther.* **10**: 946.
- Mach, L., 2002, Biosynthesis of lysosomal proteinases in health and disease, *Biol. Chem.* **383**: 751.
- Martin-Touaux, E., Puech, J.P., Chateau, D., Emiliani, C., Kremer, E.J., Raben, N., Tancini, B., Orlacchio, A., Kahn, A., and Poenaru, L., 2002, Muscle as a putative producer of acid alpha-glucosidase for glycogenosis type II gene therapy, *Hum. Mol. Genet.* **11**: 1637.
- Mashhour, B., Couton, D., Perricaudet, M., and Briand, P., 1994, In vivo adenovirus-mediated gene transfer into ocular tissues, *Gene Ther.* **1**: 122.
- Meier, O. and Greber, U.F., 2003, Adenovirus endocytosis, *J. Gene Med.* **5**: 451.
- Nemerow, G.R., 2000, Cell receptors involved in adenovirus entry, *Virology* **274**: 1.
- Ohashi, T., Watabe, K., Uehara, K., Sly, W.S., Vogler, C., and Eto, Y., 1997, Adenovirus-mediated gene transfer and expression of human beta-glucuronidase gene in the liver, spleen, and central nervous system in mucopolysaccharidosis type VII mice, *Proc. Natl. Acad. Sci. USA* **94**: 1287.
- Peltola, M., Kytölä, A., Heinonen, O., Rapola, J., Paunio, T., Revah, F., Peltonen, L., and Jalanko, A., 1998, Adenovirus-mediated gene transfer results in decreased lysosomal storage in brain and total correction in liver of aspartylglucosaminuria (AGU) mouse, *Gene Ther.* **5**: 1314.
- Raper, S.E., Chirmule, N., Lee, F.S., Wivel, N.A., Bagg, A., Gao, G.P., Wilson, J.M., and Batshaw, M.L., 2003, Fatal systemic inflammatory response syndrome in a ornithine transcarbamylase deficient patient following adenoviral gene transfer, *Mol. Genet. Metab.* **80**: 148.
- Scaria, A., St George, J.A., Gregory, R.J., Noelle, R.J., Wadsworth, S.C., Smith, A.E., and Kaplan, J.M., 1997, Antibody to CD40 ligand inhibits both humoral and cellular

- immune responses to adenoviral vectors and facilitates repeated administration to mouse airway, *Gene Ther.* **4**: 611.
- Seshidhar, R.P., Ganesh, S., Limbach, M.P., Brann, T., Pinkstaff, A., Kaloss, M., Kaleko, M., and Connelly, S., 2003, Development of adenovirus serotype 35 as a gene transfer vector, *Virology* **311**: 384.
- Shen, J.S., Meng, X.L., Maeda, H., Ohashi, T., and Eto, Y., 2004, Widespread gene transduction to the central nervous system by adenovirus in utero: implication for prenatal gene therapy to brain involvement of lysosomal storage disease, *J. Gene Med.* **6**: 1206.
- Shenk, T., 1996, Adenoviridae: The viruses and their replication. In *Fields Virology* (Eds. B.N. Fields, D.M. Knipe, and P.M. Howley), Philadelphia: Lippincott-Raven, pp. 2111–2148.
- Sirena, D., Lilienfeld, B., Eisenhut, M., Kalin, S., Boucke, K., Beerli, R.R., Vogt, L., Ruedl, C., Bachmann, M.F., Greber, U.F., and Hemmi, S., 2004, The human membrane cofactor CD46 is a receptor for species B adenovirus serotype 3, *J. Virol.* **78**: 4454.
- Sleat, D.E., Lackland, H., Wang, Y., Sohar, I., Xiao, G., Li, H., and Lobel, P., 2005, The human brain mannose 6-phosphate glycoproteome: a complex mixture composed of multiple isoforms of many soluble lysosomal proteins, *Proteomics.* **5**: 1520.
- Stein, C.S., Ghodsi, A., Derksen, T., and Davidson, B.L., 1999, Systemic and central nervous system correction of lysosomal storage in mucopolysaccharidosis type VII mice, *J. Virol.* **73**: 3424.
- Stone, D., Ni, S., Li, Z.Y., Gaggari, A., Di Paolo, N., Feng, Q., Sandig, V., and Lieber, A., 2005, Development and assessment of human adenovirus type 11 as a gene transfer vector, *J. Virol.* **79**: 5090.
- Trapnell, B.C. and Gorziglia, M., 1994, Gene therapy using adenoviral vectors, *Curr. Opin. Biotechnol.* **5**: 617.
- Vellodi, A., 2005, Lysosomal storage disorders, *Br. J. Haematol.* **128**: 413.
- Walkley, S.U., 2001, New proteins from old diseases provide novel insights in cell biology, *Curr. Opin. Neurol.* **14**: 805.
- Wickham, T.J., 2000, Targeting adenovirus, *Gene Ther.* **7**: 110.
- Wilson, J.M., 1996, Adenoviruses as gene-delivery vehicles, *N. Engl. J. Med.* **334**: 1185.
- Xu, F., Ding, E., Liao, S.X., Migone, F., Dai, J., Schneider, A., Serra, D., Chen, Y.T., and Amalfitano, A., 2004, Improved efficacy of gene therapy approaches for Pompe disease using a new, immune-deficient GSD-II mouse model, *Gene Ther.* **11**: 1590.
- Xu, F., Ding, E., Migone, F., Serra, D., Schneider, A., Chen, Y.T., and Amalfitano, A., 2005, Glycogen storage in multiple muscles of old GSD-II mice can be rapidly cleared after a single intravenous injection with a modified adenoviral vector expressing hGAA, *J. Gene Med.* **7**: 171.
- Yang, Y., Jooss, K.U., Su, Q., Ertl, H.C., and Wilson, J.M., 1996a, Immune responses to viral antigens versus transgene product in the elimination of recombinant adenovirus-infected hepatocytes in vivo, *Gene Ther.* **3**: 137.
- Yang, Y., Nunes, F.A., Berencsi, K., Gonczol, E., Engelhardt, J.F., and Wilson, J.M., 1994, Inactivation of E2a in recombinant adenoviruses improves the prospect for gene therapy in cystic fibrosis, *Nat. Genet.* **7**: 362.
- Yang, Y., Su, Q., and Wilson, J.M., 1996c, Role of viral antigens in destructive cellular immune responses to adenovirus vector-transduced cells in mouse lungs, *J. Virol.* **70**: 7209.

- Yang, Y., Su, Q., Grewal, I.S., Schilz, R., Flavell, R.A., and Wilson, J.M., 1996b, Transient subversion of CD40 ligand function diminishes immune responses to adenovirus vectors in mouse liver and lung tissues, *J. Virol.* **70**: 6370.
- Ziegler, R.J., Li, C., Cherry, M., Zhu, Y., Hempel, D., van Rooijen, N., Ioannou, Y.A., Desnick, R.J., Goldberg, M.A., Yew, N.S., and Cheng, S.H., 2002, Correction of the nonlinear dose response improves the viability of adenoviral vectors for gene therapy of Fabry disease, *Hum. Gene Ther.* **13**: 935.
- Ziegler, R.J., Yew, N.S., Li, C., Cherry, M., Berthelette, P., Romanczuk, H., Ioannou, Y.A., Zeidner, K.M., Desnick, R.J., and Cheng, S.H., 1999, Correction of enzymatic and lysosomal storage defects in Fabry mice by adenovirus-mediated gene transfer, *Hum. Gene Ther.* **10**: 1667.

Treatment of Late Infantile Neuronal Ceroid Lipofuscinosis by CNS Administration of a Serotype 2 Adeno-Associated Virus Expressing CLN2 cDNA

STEFAN WORGALL,^{1,2,*} DOLAN SONDHI,^{1,*} NEIL R. HACKETT,^{1,*} BARRY KOSOFSKY,² MINAL V. KEKATPURE,² NURUNISA NEYZI,² JONATHAN P. DYKE,³ DOUGLAS BALLON,³ LINDA HEIER,³ BRUCE M. GREENWALD,² PAUL CHRISTOS,⁴ MADHU MAZUMDAR,⁴ MARK M. SOUWEIDANE,⁵ MICHAEL G. KAPLITT,⁵ and RONALD G. CRYSTAL¹

ABSTRACT

Late infantile neuronal ceroid lipofuscinosis (LINCL) is an autosomal recessive, neurodegenerative lysosomal storage disease affecting the CNS and is fatal by age 8 to 12 years. A total average dose of 2.5×10^{12} particle units of an adeno-associated virus (AAV) serotype 2 vector expressing the human CLN2 cDNA (AAV2_{CUh}-CLN2) was administered to 12 locations in the CNS of 10 children with LINCL. In addition to safety parameters, a neurological rating scale (primary variable) and three quantitative magnetic resonance imaging (MRI) parameters (secondary variables) were used to compare the rate of neurological decline for 18 months in treated subjects compared with untreated subjects. Although there were no unexpected serious adverse events that were unequivocally attributable to the AAV2_{CUh}-CLN2 vector, there were serious adverse effects, the etiology of which could not be determined under the conditions of the experiment. One subject died 49 days postsurgery after developing status epilepticus on day 14, but with no evidence of CNS inflammation. Four of the 10 subjects developed a mild, mostly transient, humoral response to the vector. Compared with control subjects, the measured rates of decline of all MRI parameters were slower, albeit the numbers were too small for statistical significance. Importantly, assessment of the neurologic rating scale, which was the primary outcome variable, demonstrated a significantly reduced rate of decline compared with control subjects. Although the trial is not matched, randomized, or blinded and lacked a contemporaneous placebo/sham control group, assessment of the primary outcome variable suggests a slowing of progression of LINCL in the treated children. On this basis, we propose that additional studies to assess the safety and efficacy of AAV-mediated gene therapy for LINCL are warranted.

INTRODUCTION

LATE INFANTILE NEURONAL CEROID LIPOFUSCINOSIS (LINCL) is a form of Batten disease, a group of autosomal recessive, progressive, childhood neurodegenerative lysosomal storage diseases associated with intracellular accumulation of autofluorescent material resembling lipofuscin in neuronal cells (Williams *et al.*, 1999; Haltia, 2003). LINCL is rare, affecting 0.36 to 0.46 per 100,000 live births (Wisniewski *et al.*, 2001). Like other forms of Batten disease, the hallmark of LINCL is

progressive neurological decline characterized by cognitive impairment, visual failure, seizures, and deteriorating motor function (Boustany, 1996; Williams *et al.*, 1999). The disease is caused by mutations in the CLN2 (ceroid lipofuscinosis, neuronal 2) gene, a 6.7-kb, 13-exon gene mapped to chromosomal locus 11p15 (Sleat *et al.*, 1997). The CLN2 gene encodes tripeptidyl-peptidase I (TPP-I), a 46-kDa lysosomal protein that functions in the acidic milieu of the lysosome to remove groups of three amino acids from the amino terminus of proteins (Sleat *et al.*, 1997; Vines and Warburton, 1999). When the CLN2 gene

¹Department of Genetic Medicine, ²Department of Pediatrics, ³Department of Radiology, ⁴Department of Public Health, and ⁵Department of Neurological Surgery, Weill Cornell Medical College, New York, NY 10065.

*S.W., D.S., and N.R.H. contributed equally to this study.

is mutated, proteins accumulate in the lysosomes of neurons over time, leading to progressive neuronal death, likely by apoptosis (Lane *et al.*, 1996).

LINCL typically manifests clinically at age 2 to 4 years with ataxia, myoclonus, impaired speech, and developmental regression (Boustany, 1996; Williams *et al.*, 1999; Haltia, 2003). Seizures are often the first manifestation, but there is variability in the time of onset and the appearance of the collective symptoms. A gradual decline in visual ability follows, with blindness by age 4 to 6 years. Affected children generally become wheelchair-bound between 4 and 6 years. Toward the late stages of the disease, feeding becomes difficult, resulting in poor weight gain. Death occurs by age 8 to 12 years (Williams *et al.*, 1999; Haltia, 2003).

As a strategy to treat the CNS manifestations of LINCL, we initiated a program using serotype 2 adeno-associated virus (AAV2) to transfer the normal CLN2 cDNA to the brain, exploiting the neurotrophic properties of this vector and the potential for long-term transgene expression. Preclinical studies demonstrated that direct CNS administration of AAV2_{CU}h-CLN2, a serotype 2 adeno-associated virus gene transfer vector expressing the human CLN2 cDNA, mediated high levels of enzymatically active TPP-I in the lysosomes of neurons of experimental animals for at least 18 months. There was no evidence of adverse effects in experimental animals (Hackett *et al.*, 2005; Sondhi *et al.*, 2005), and administration of the vector demonstrated suppression of the accumulation of autofluorescent material in the CNS of CLN2 knockout mice (Passini *et al.*, 2006). On the basis of these data, the present study was designed to assess the safety of direct administration of the AAV2_{CU}hCLN2 vector to the CNS of children with LINCL and to develop preliminary data concerning whether this therapy slows the progression of the CNS manifestations of the disease. LINCL represents a paradigm for assessing the efficacy of therapy for rare disorders of children, in that a combination of practical and ethical concerns significantly limits clinical trial design, obviating the use of contemporaneous, matched, randomized, blinded, or placebo control subjects. With this caveat, the data demonstrate that this therapy is associated with minimal toxicity. For the children for whom data were available for >6 months posttherapy, compared with historic control subjects, the magnetic resonance imaging (MRI) assessments (the secondary outcome parameters) showed a slower but not statistically significant rate of decline. Importantly, assessment of the modified Hamburg LINCL clinical rating scale, the primary outcome variable, demonstrated that the treatment was associated with a statistically significant slower decline in neurologic status compared with control subjects. Although the number of treated children is small and the control group is not ideal to make definitive conclusions, collectively the data suggest that additional studies are warranted to assess the safety and efficacy of AAV-mediated gene therapy for the CNS manifestations of LINCL.

MATERIALS AND METHODS

Overall design

The study was carried out at the New York Presbyterian Hospital, Weill Medical College of Cornell University (New York, NY). The research protocol was reviewed and approved by the

Weill Cornell Institutional Review Board, Institutional Biosafety Committee, National Institutes of Health (NIH)/General Clinical Research Center-Pediatric Scientific Advisory Committee and Data Safety Monitoring Board. At the national level, the protocol was reviewed by the NIH/Recombinant DNA Advisory Committee and an Investigational New Drug application was approved by the Center for Biologics Evaluation and Research, U.S. Food and Drug Administration (U.S. FDA, BBIND 11481). The parents of all participating children provided informed consent.

The study was designed as an 18-month follow-up subsequent to direct CNS administration of the AAV2_{CU}hCLN2 vector to 10 children with LINCL, 5 of whom were severely affected by the disease and 5 of whom were moderately affected (Table 1; and see Supplementary Table I at www.liebertonline.com/hum). All subjects received 1.8 to 3.2×10^{12} particle units (average dose, 2.5×10^{12} particle units) of the AAV2_{CU}h-CLN2 vector. The primary outcome variable was neurologic assessment of the disease, using a modified form of the Hamburg LINCL scale (see Supplementary Table II at www.liebertonline.com/hum) (Steinfeld *et al.*, 2002; Crystal *et al.*, 2004). The secondary variables included CNS MRI assessment of gray matter volume as a percentage of total brain volume, ventricular volume, and cortical apparent diffusion coefficient (ADC) (Dyke *et al.*, 2007; Worgall *et al.*, 2007). Because of the small number of children involved and because of ethical issues regarding a neurosurgical procedure in children with a fatal neurological disease, the study did not include a formal randomized, placebo/sham, or untreated control group, and the study was not blinded (Crystal *et al.*, 2004; Arkin *et al.*, 2005). Data from four independent children with LINCL with two assessments separated by 1 year served as an untreated control group for comparison. For the primary variable, we also compared the rate of decline in the modified Hamburg scale in the treated subjects with the data published by Steinfeld and coworkers (2002).

Study population

The study group consisted of 10 children (6 boys and 4 girls) with LINCL. Pretherapy, the children had confirmation of CLN2 mutations, routine blood and urine studies, comprehensive neurological assessments, and quantitative MRI imaging (Crystal *et al.*, 2004). Subjects were chosen for the gene therapy study, on the basis of specific inclusion/exclusion criteria, by an eligibility committee composed of three physicians other than the principal investigator, including a pediatric neurosurgeon, a pediatric neurologist, and a general pediatrician.

AAV2_{CU}hCLN2

The gene therapy vector used in the study, AAV2_{CU}hCLN2, is based on an AAV2 serotype capsid and genome. The modified genome is deleted of the AAV2 *rep* and *cap* genes, retaining only the AAV2 inverted terminal repeats flanking the expression cassette (Crystal *et al.*, 2004; Hackett *et al.*, 2005; Sondhi *et al.*, 2005). The expression cassette includes the CAG promoter (consisting of the human cytomegalovirus immediate/early enhancer, the promoter, splice donor, and left-hand intron sequence from chicken β -actin, and the splice acceptor from rabbit β -globin), the human CLN2 cDNA with an optimized Kozak translational initiation signal before the start codon and a rabbit β -globin poly(A) sequence. The AAV2_{CU}h-CLN2 vector was produced by a two-plasmid cotransfection

TABLE 1. DEMOGRAPHICS OF STUDY POPULATION

Patient ^a	Age at time of therapy ^b	Race/ethnicity ^c	Sex ^c	Residence	CLN2 mutations ^d	LINCL severity ^e	Other medical conditions ^f
BD-01	8.6	C	M	USA	G3556C/T3016A ^g	Severe	Prior otitis media
BD-02*	10.0	C	M	USA	G3556C/G3085A ^h	Severe	Hypospadias, prior septic arthritis hip
BD-03*	6.9	C	M	USA	G3556C/G3085A ^h	Severe	Otitis media
BD-04	8.1	C	F	England	G3556C	Severe	Drug allergy ⁱ
BD-05	4.5	C	F	Germany	G3670T homozygote	Severe	—
BD-06	5.4	C	M	USA	C3670T/unknown ^j	Moderate	—
BD-07†	4.5	C	M	Australia	G3556C homozygote	Moderate	Atopic dermatitis, food allergies
BD-08	3.6	C	F	England	G3556C homozygote	Moderate	Atopic dermatitis
BD-09	5.3	C	M	Germany	C3670T homozygote	Moderate	Atopic dermatitis
BD-10†	3.4	C	F	Australia	G3556C homozygote	Moderate	Atopic dermatitis, food allergies

Abbreviations: CLN2, ceroid lipofuscinosis, neuronal 2; LINCL, late infantile neuronal ceroid lipofuscinosis; TPP-I, tripeptidyl-peptidase I.

^aListed in order of the initial evaluation; BD, Batten disease; and * and † are used to identify sibling pairs.

^bAge in years at time of therapy.

^cC, Caucasian; M, male; F, female.

^dMutations are named by location in the gene (Sleat *et al.*, 1999) with the wild-type nucleotide before and mutant nucleotide after. G3556C is a splice junction mutation also referred to as IVS5-1G > C or c.509-1G > C. The C3670T mutation is a premature stop codon also called R208X or c.622C > T. The genotypes of the four control subjects were as follows: two G3556C/C3670T heterozygotes, one G3556C homozygote, and one G3556C/T4383C heterozygote.

^eLINCL severity based on the modified Hamburg LINCL scale; see Materials and Methods and Supplementary Table II (at www.liebertonline.com/hum).

^fMedical problems unrelated to the known clinical manifestations of LINCL (Boustany, 1996; Williams *et al.*, 1999).

^gPremature stop codon at amino acid 104.

^hMissense (Arg>Gln) mutation at amino acid 127.

ⁱLamotrigine.

^jThe diagnosis of LINCL for this subject was based on quantitative assessment of TPP-I deficiency in white blood cells and the presence of a single known mutation for LINCL in the genome.

procedure in the Belfer Gene Therapy Core Facility (Weill Cornell Medical College) under current Good Manufacturing Practice conditions. This included transfection into a certified 293 cell line of an expression cassette plasmid (pAAV2-CAG-hCLN2) containing the promoter and the human CLN2 cDNA expression cassette and an adenovirus/AAV2 helper plasmid (pPAK-MA2) (Qiu *et al.*, 2002; Hackett *et al.*, 2005; Sondhi *et al.*, 2005). The vector was released from cells by freeze-thaw cycles, and purified by an iodixinol step gradient followed by affinity chromatography on heparin-agarose columns. The resulting vector was transferred to the clinical formulation by dialysis. Full characterization of the final formulated vector included the following: enzyme-linked immunosorbent assay (ELISA) for capsid protein, polymerase chain reaction (PCR) for transgene DNA, and Western analysis and activity assays for the protein transgene product. U.S. FDA-approved lot release assays were performed to ensure identity, purity, and function.

Vector administration and follow-up assessment

The children were prepared for anesthesia and surgery in a standard fashion. The BrainLAB system for image-guided surgery (BrainLAB, Westchester, IL) was used to map vector administration loci on the skull, based on a preoperative MRI scan

with sentinels on the head. For standardization, the coronal sutures and bony landmarks of the cranium were used to draw a line in the sagittal plane on the MRI. The burr holes were produced at the mapped locations and the dura was cut, permitting the brain to be directly visualized. At the completion of the six burr holes, 150- μ m-diameter flexible glass catheters (Polymicro Technologies, Phoenix, AZ) were used to administer the vector. A 20-gauge spinal needle was placed on the surface of the brain orthogonal to the skull to act as a guide for the insertion of the catheters 2 cm into the predetermined locations in the brain. Intravenous mannitol (typically 1.0 g/kg) was given as needed throughout the period of vector administration to minimize brain edema.

Each individual received a total dose of $1.8\text{--}3.2 \times 10^{12}$ particle units of AAV2_{CU}hCLN2, equally divided among 12 cortical locations delivered through 6 burr holes (2 locations at 2 depths through each hole), 3 burr holes per hemisphere. The exact locations of the administration of the vector were determined on a case-by-case basis, but were generally in the same regions. The vector was administered at a rate of 2.0 μ l/min to each of the six sites in parallel by a microperfusion pump (Hamilton, Reno, NV). After the specified dose was administered over a period of 75 min to the six sites, the catheters were left in place for 5 min to ensure tissue penetration. The catheters

were then withdrawn approximately half-way from the bottom of the catheter tract to the brain surface, and the remaining 50% of the dose was administered, in parallel, to each of the six sites as described above.

After vector administration, the surgical wounds were closed by standard techniques. A postoperative fluid-attenuated inversion recovery (FLAIR) MRI was performed within the first 48 hr after the surgical procedure to assess for bleeding or other possible perioperative adverse events. Each child was monitored postoperatively in a recovery room or intensive care unit, and once stable, was transferred to the Children's Clinical Research Center unit. The children were discharged from the hospital at the discretion of the attending neurosurgeon, usually 7 days after vector administration. All families were asked to remain in the proximity of the hospital until the evaluation on day 14.

Subjects were assessed at Weill Cornell on days 7 and 14, and at months 1, 6, 12, and 18 after treatment (see Supplementary Table I). At months 2 and 3, they were also assessed for adverse effects at the office of the child's personal physician. Details of the assessments are described in Supplementary Tables III, IV, and V (at www.liebertonline.com/hum). The children continue to be monitored for general status once yearly by telephone contact as mandated by the U.S. FDA 15-year annual follow-up requirement for all gene transfer studies (U.S. Food and Drug Administration, 2003).

Safety and efficacy parameters

Each individual underwent two baseline evaluations to determine eligibility and to establish baseline values for safety and efficacy parameters; these two baseline evaluations are referred to as the "screening" studies (to determine eligibility) and the "pretherapy" studies (to obtain current laboratory studies just before the surgical procedure and vector administration). The safety parameters included a general assessment (history, physical examination, vital signs, height, and weight), blood and urine analyses, human immunodeficiency virus test, vector-related tests (serum anti-AAV antibody levels), electrocardiogram, neurological assessment, chest X-ray, and ophthalmological examination (split lamp examination and direct ophthalmoscopy). After the death of subject BD-04, 49 days posttherapy (see below), 24-hr continuous electroencephalogram (EEG) and levels of anticonvulsant medication levels pretherapy and on day 14 were added to the protocol as per U.S. FDA recommendations. A 24-hr, 16-channel video EEG was performed 4 days before treatment and 14 days after treatment in the six subsequent subjects. In addition to the qualitative assessments of the EEG background, analysis of sleep patterns, spike and wave discharge frequency, and duration was carried out. Quantitative spike analysis was performed during wakefulness for 1 hr of each video EEG study by two readers blinded as to treatment status. The efficacy parameters used to develop estimates of the impact of therapy over time included (1) the primary variable, the modified Hamburg LINCL clinical rating scale (Steinfeld *et al.*, 2002; Crystal *et al.*, 2004); and (2) the secondary variables, all based on quantitative assessment of CNS MRI scans (Dyke *et al.*, 2007; Worgall *et al.*, 2007).

Primary variable. The primary efficacy variable for the study was the modified Hamburg LINCL clinical rating scale (see

Supplementary Table II). This scale, originally developed by Steinfeld and coworkers (2002), was modified to eliminate the ophthalmologic variable, because the therapy was directed only at the CNS manifestations of the disease (Crystal *et al.*, 2004). The modified Hamburg scale assesses motor function, seizure activity, and language skills. Each of these individual scores is ranked from 0 to 3 and then the individual scores are added to provide a total rating, with 0 being the most severe and 9 the mildest.

Secondary variables. The secondary efficacy parameters included quantitative CNS MRI assessment at various intervals pre- and posttreatment (see Supplementary Tables I and IV). Three imaging parameters were chosen on the basis of data from untreated children demonstrating a correlation with the progressive deterioration associated with LINCL (Worgall *et al.*, 2007). All imaging data were acquired on a 3.0-T MRI system (GE Medical Systems, Milwaukee, WI). Imaging included T₁-weighted, T₂-weighted, and fluid-attenuated inversion recovery sequences. To assess gray matter volume as a percentage of total brain volume, a spoiled gradient recalled pulse sequence was employed. Ventricular volume assessments were performed on T₁-weighted data sets. The CADC was measured with a spin-echo diffusion-weighted echo-planar pulse sequence implemented over the entire brain, and assessed for the cortex specifically (Dyke *et al.*, 2007; Worgall *et al.*, 2007). Details of the MRI assessments are described in Supplementary Table IVA.

Anti-AAV2 neutralizing antibody titers

Anti-AAV2 neutralizing antibody titers were assessed in serum before and at various times after therapy by mixing serial 2-fold dilutions of serum, starting at a 1:10 dilution, with 2×10^8 particle units of AAV2LacZ (identical to the AAV2_{CB}hCLN2 vector, with β -galactosidase substituted for the CLN2 cDNA) (Hackett *et al.*, 2005) for 30 min at 37°C. The mixture was then used to infect 293 ORF6 cells in a 96-well plate (Brough *et al.*, 1996). After growth for 48 hr, a cell lysate was made and β -galactosidase activity was determined. The reciprocal dilution required for 50% inhibition of infection was interpolated. In all assays, a positive control serum sample from a normal human was included and the assay was accepted only if the reciprocal titer for the control serum was 200 ± 50 .

Data analysis and statistical considerations

Individuals (other than the principal and coprincipal investigators) collected, tabulated, and verified the clinical parameters, and adverse effects were tabulated on the basis of standard methods (Crystal *et al.*, 2004). Seizure activity (by EEG) before and after therapy was compared for $n = 6$ subjects by unpaired *t* test. For assessment of the primary and secondary parameters, the change of each parameter over time from pre- to posttherapy was compared with observations obtained from four untreated children (one was moderate and three severe on the modified Hamburg LINCL rating scale at first visit) with LINCL for whom data were available from two visits separated by approximately 1 year. None of these children were enrolled in the gene therapy protocol, but their genotypes were comparable to those of the enrolled subjects. For the primary variable, the modified Hamburg scale, the data from the four untreated

children monitored for 1 year was supplemented with data published by Steinfeld and coworkers (2002) representing an average based on 16 subjects. For the treated children with >6 months of follow-up, the change in each parameter over time posttherapy was compared with the control data. To reduce uncertainty in baseline values for the treated subjects, because all pretherapy data for each subject were obtained within 2.3 ± 0.4 months, when more than one data point was available pretherapy, the pretherapy data points were averaged and considered to be “zero” time. The rates of change for both primary and secondary parameters for the treated and untreated subjects were compared by nonparametric Mann–Whitney test.

RESULTS

Study population

Subjects were from the United States ($n = 4$), England ($n = 2$), Australia ($n = 2$), and Germany ($n = 2$). Their ages at the time of vector administration ranged from 4.5 to 10.0 years (7.6 ± 0.7 years; median, 8.1 years) for the severe group (BD-01 to BD-05) and from 3.4 to 5.4 years (4.4 ± 0.3 years; median, 4.5 years) for the moderate group (BD-06 to BD-10; see Table 1). There were two sibling pairs, one pair in the moderate group and one pair in the severe group. The CLN2 mutations of the 10 subjects included 5 different mutations in 19 of the 20 alleles; no mutation was detected in 1 allele of subject BD-06. The sibling pairs each had the same mutations. The most frequent mutation, the splice mutation G3556C, was present in 11 of 19 (58%) alleles; 4 of the subjects were homozygous for this mutation. The second most frequent mutation, C3670T, which results in a premature stop codon at amino acid 208, was present in 5 of 19 (26%) alleles; 2 subjects were homozygous for this mutation. Both mutations lead to undetectable TPP-I activity. Comparison of genotype with the clinical progression of LINCL has been reported to be relatively homogeneous, uninfluenced by genotype (Sleat *et al.*, 1999; Worgall *et al.*, 2007).

Of the 10 subjects who were treated, 1 died during the study period, 8 completed the study through 6 months, and 7 completed the study through the 18-month follow-up period (see Supplementary Tables III and IV for details regarding reasons for missed predetermined data points).

Safety of administration of AAV2_{CUh}CLN2

MRI scans performed within 48 hr postsurgery demonstrated no evidence of hematoma or other surgery-related adverse effects. Of the 154 adverse events reported posttherapy, 60 were ranked as “serious” and 94 as “nonserious” (Table 2). In no instance was it possible to directly attribute a serious or nonserious adverse event to the vector per se versus the anesthesia/surgery/administration procedure or the natural history of the disease. However, because it was not possible to prove that these events were not related to the vector, most adverse events were recorded as probably or possibly related to the vector. Thirteen of the 60 serious adverse events (22%) and 52 of the 94 nonserious events (55%) occurred within 2 weeks of administration of the vector and were most likely related to the surgical procedure. The most common of the serious adverse events were seizures, and, to a much lesser extent, myoclonus or anemia.

One serious event resulted in withdrawal of a subject from the study. BD-04, an 8-year-old girl with severe LINCL, had an uneventful postoperative course, and was discharged from the hospital on day 7. On day 14 after vector administration, she developed status epilepticus. Although the seizures could be controlled by pentobarbital coma, the subject could not thereafter regain consciousness without reverting to status epilepticus. Her family eventually decided to decline further treatment and she died 49 days after vector administration. There was no evidence of CNS inflammation in the cerebral spinal fluid 15 days after vector administration (i.e., normal cell counts, protein, and glucose, and no detectable bacteria or viruses), or in CNS by FLAIR MRI on days 1, 21, and 44 after vector administration. Because seizures are a part of the natural history of LINCL, it is unclear to what extent this event was related to the underlying disease, the surgical procedure, or the experimental drug itself. In response to this event, with the advice of the U.S. FDA, the study design was modified for all subsequent study subjects ($n = 6$) to include EEG monitoring and assessment of the levels of antiseizure medications pretherapy and 14 days after therapy. No subjects had electrographic seizures pre- or posttherapy while being monitored. The pretherapy EEGs showed generalized moderate- to high-amplitude spike and wave discharges with maximum amplitude occipitally. The background was characterized by diffuse 3- to 5-Hz rhythmic activity and features of normal sleep patterns were generally preserved. This EEG background did not change significantly posttherapy. The mean spike frequency over 1 hr in six subjects before gene therapy was 56.6 ± 15.5 (SD) and the mean spike frequency 2 weeks after gene therapy was 38.8 ± 16.7 (SD), which was significantly decreased compared with pretherapy (paired samples *t* test, $p < 0.007$). Thus, although it is possible the seizures starting on day 14 in subject BD-04 were linked to the vector, assessment of seizure activity on day 14 in the subsequent six treated subjects showed no increased propensity toward seizure activity.

Subject BD-06 died 704 days after vector administration. Although beyond the 18-month follow-up period for the primary and secondary variables, the death was identified in the post-study yearly follow-up call (see Table 2). This subject was not included in the efficacy analysis, as the subject did not return for visits subsequent to 1 month posttherapy (see Supplementary Table III, footnote 8). For both subjects who died, the families did not agree to an autopsy, and thus brain tissue was not available for verification of gene transfer by DNA/RNA-based methods or by detection of TPP-I protein.

Anti-AAV antibodies

Before gene transfer, no subjects had detectable serum anti-AAV2 neutralizing antibodies (Fig. 1). Four of the 10 subjects (3 severe and 1 moderate) developed a mild humoral immune response to the AAV2 capsid after CNS administration of the AAV2_{CUh}CLN2 vector. In no subject did the anti-AAV2 neutralizing titer rise to >270. For two of the four subjects who developed detectable anti-AAV2 antibodies, the response was within 1 month, and for the other two, it was delayed, and not observed until 6 months posttherapy. For three of the four who developed anti-AAV2 antibodies, the titers returned to baseline by 18 months posttherapy, remaining mildly elevated in only

TABLE 2. ADVERSE EVENTS^a

<i>Level of severity</i>		<i>Relationship to drug use</i>		<i>Most common events</i>		
<i>Serious/nonserious</i>	<i>Number</i>	<i>Related/not related</i>	<i>Number</i>	<i>Specific events</i>	<i>Number</i>	
Serious ^b	60	Probably or possibly related to drug and/or drug administration ^c	34	Seizure ^d	11	
				Increased myoclonus	3	
				Anemia	2	
				Pneumonia	4	
				Respiratory distress	4	
		Not drug related	26	Possible gastroenteritis	2	
				Hypokalemia	2	
				Upper respiratory infection	2	
				Fever	11	
				60		
Nonserious	94	Probably or possibly related to drug and/or drug administration ^c	34	Seizure ^d	10	
				Vomiting	5	
				Thrombocytosis	5	
				One-point decrease from baseline modified Hamburg LINCL rating scale	3	
				Elevated C-reactive protein	3	
				Elevated erythrocyte sedimentation rate	3	
				Not drug related	34	Upper respiratory infection
		Sinusitis	3			
		Infiltrated venous catheter site	3			
		Hyperglycemia	2			
		Apnea	2			
		<i>Total: 154</i>				

^aThis table is classified in three different ways: Level of severity, Relationship to drug use, Most common events. Most common events includes only those events that occurred more than once in more than one patient and therefore does not add up to the total of 154 events.

^bTwo events resulted in withdrawal from the study. Subject death (BD-04) occurred on day 49 after vector administration following status epilepticus, 14 days after vector administration; duration, 36 days. Categorized as “possibly related” to the study drug. It was not possible to determine if seizures were part of the natural history of the disease, secondary to the surgical procedure and drug administration procedure in the setting of this disease, or to the vector. There were no signs of inflammation in the cerebrospinal fluid or on three MRI scans. Subject BD-06 died 704 days after vector administration. This subject developed pneumonia approximately 520 days after vector administration, and respiratory failure 700 days after vector administration. This death was categorized as “not related” to the study drug or procedures and was likely related to the natural history of disease.

^cEvent either probably or possibly related to the AAV2_{CU}hCLN2 vector. In no instance was it possible to directly attribute the serious or nonserious adverse event to the vector per se; however, because it was not possible to prove it was not, most adverse events were recorded as probably or possibly related to the vector. Thirteen of the 60 serious adverse events (22%) and 52 of the 94 nonserious events (55%) occurred within 2 weeks of administration of the vector and were most likely related to the surgical procedure, and not the vector.

^dEither generalized tonic clonic or complex partial seizures. The 11 seizures reported to have occurred during the 18 months after gene therapy were experienced by 5 of the 10 patients, and half of these in a single patient between the 12- and 18-month visits. As described, only one of these patients experienced status epilepticus. The rest had seizures of less than 5 min duration, which were consistent with the seizures they experienced preinjection. All patients were taking multiple antiepileptic drugs throughout the study period.

one subject (BD-03). Thus, CNS administration of the AAV2_{CU}hCLN2 vector to this population results in only a mild, mostly transient systemic antivector humoral immune response.

Disease progression assessed by CNS imaging

The rates of change for all treated subjects were calculated from the raw data (see Supplementary Table IVB) and the means and standard errors were determined. For all three of the MRI parameters, the measured rates of decline of the treated subjects were slower, albeit the numbers were too small for statistical significance. For the gray matter volume as a percent-

age of total brain volume, for the six treated children for whom data were available for >6 months, there was a trend, although not significant, toward reduction in the mean rate of change ($-2.6 \pm 0.7\%/year$) compared with that of the four untreated children ($-2.84 \pm 1.3\%/year$; Fig. 2A [and see Supplementary Table IVA and B]; $p = 0.8$ by Mann-Whitney test). Likewise, the mean rate of change of the ventricular volume of the seven treated children for whom data were available ($14.0 \pm 4.1 \text{ cm}^3/year$) showed a trend toward reduction in the mean rate of change over time compared with that of the four untreated children ($17.2 \pm 4.7 \text{ cm}^3/year$; Fig. 2B [and see Supplementary Table IVA and B]), although this did not achieve statistical sig-

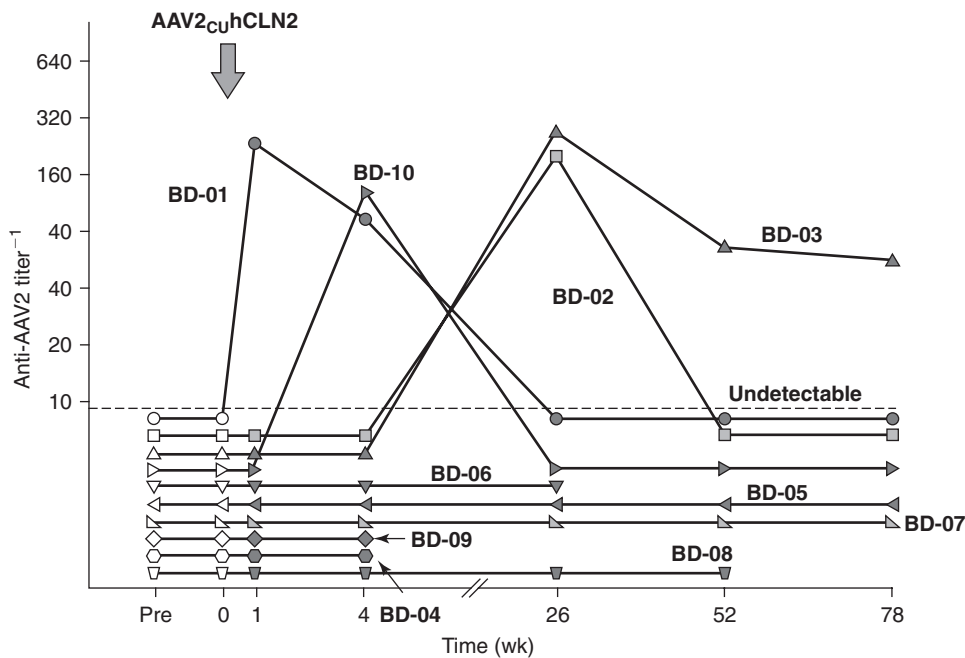


FIG. 1. Anti-AAV2 neutralizing titers after gene transfer with AAV2_{CU}hCLN2. Serum samples were taken at intervals before and after administration of the vector. The anti-AAV2 neutralizing titer was assessed by determining the dilution of serum required to inhibit *in vitro* gene transfer by 50%. Open symbols represent the pretherapy values; solid symbols represent posttherapy values.

nificance ($p = 0.5$ by Mann–Whitney test). Consistent with these data, the CADC for the eight treated children with data available for >6 months showed a mean rate of change [$0.034 \pm 0.015 \text{ mm}^2 (\times 10^{-3})/\text{sec} \cdot \text{year}$] that trended toward being slower than for the untreated control subjects [$0.083 \pm 0.023 \text{ mm}^2 (\times 10^{-3})/\text{sec} \cdot \text{year}$] (Fig. 2C [and see Supplementary Table IVA and B]), although this difference was not statistically significant ($p = 0.1$ by Mann–Whitney test).

Disease progression assessed by the primary variable

At baseline, all study subjects had neurological abnormalities, with the extent of the abnormalities dictating the severity category (moderate or severe) of the disease (see Supplementary Table V at www.liebertonline.com/hum). Typically, there was decreased strength in the upper and lower extremities, increased muscle stretch reflexes, an upward plantar response, and other motor sys-

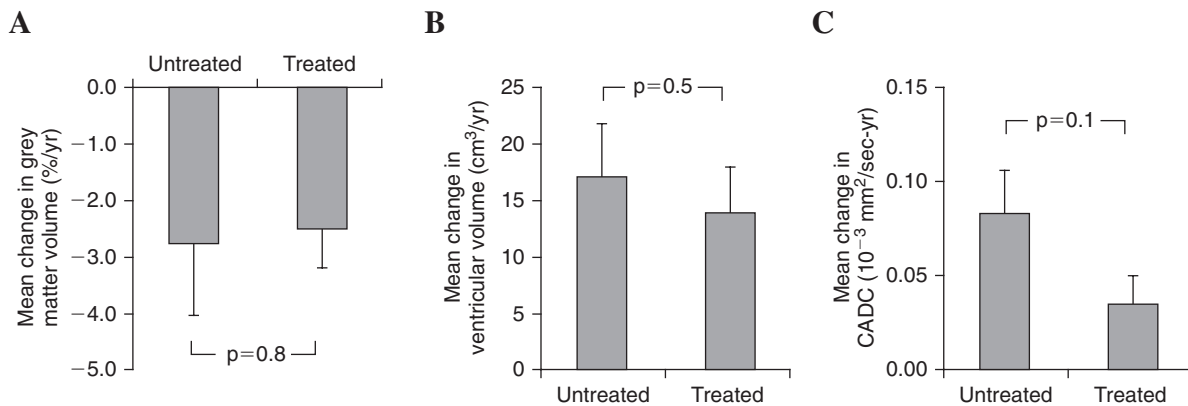


FIG. 2. Quantitative assessment of CNS MRI imaging. MRI parameters were assessed on the screening visit, the day before treatment, and 6 and 18 months after treatment. Details regarding the data points available for analysis may be found in Supplementary Table IVA (see www.liebertonline.com/hum). Data are presented as the change in the parameter relative to mean baseline values. Raw data are provided in Supplementary Table IVB (see www.liebertonline.com/hum). If more than one baseline value was available and was obtained within 4 months of treatment, the average of the baseline values was used. Four untreated LINCL subjects, for whom two assessments done ~ 1 year apart were available, acted as control subjects. (A) Mean rate of change in gray matter volume (expressed as a percentage of total brain volume); (B) mean rate of change in ventricular volume; (C) mean rate of change in cortical apparent diffusion coefficient. Rates of change for the treated subjects were compared with the mean rate of change for the combined control group for each of the MRI parameters by Mann–Whitney test. CADC, cortical apparent diffusion coefficient.

tem abnormalities, including gait abnormalities, myoclonus, tremors, and swallowing dysfunction. These features were more pronounced in the subjects with severe disease.

The modified Hamburg LINCL clinical rating scale was the primary variable used to assess effects of the treatment on the slowing of the progression of the disease (see Supplementary Table III). The modified Hamburg rating was assessed both as a function of age (Fig. 3A) and as a function of time after treatment (Fig. 3B). To assess the impact of treatment (Fig. 4), the mean rate of change in modified Hamburg scale was compared with that in a combined control group consisting of (1) four untreated control subjects who were monitored for 1 year without therapy and (2) the historical data from the Steinfeld and coworkers study (2002), employing only the parameters used in the modified Hamburg scale, giving a mean rate of $-1.8 \pm 0.48/\text{year}$ (standard error). The decline per year for the eight treated subjects for whom data were available for >6 months was significantly slower in comparison with the decline for the combined control groups. This was the case when the slopes of decline of the treated children were calculated using just the pre- and 12-month data points (to match the times of assessment with that of the four untreated control subjects; mean rate of change, $0.0 \pm 0.30/\text{year}$; $p < 0.01$ by Mann-Whitney test) or when the slopes of decline were calculated using all the data from the pretherapy visit through the 18-month observation points (mean rate of change, $-0.33 \pm 0.29/\text{year}$; $p < 0.05$ by Mann-Whitney test).

DISCUSSION

Gene transfer with adeno-associated viral vectors represents a logical approach to treat the CNS manifestations of the neu-

rological lysosomal storage disorders (Skorupa *et al.*, 1999; Bosch *et al.*, 2000; Frisella *et al.*, 2001; Sondhi *et al.*, 2001, 2005; Janson *et al.*, 2002; Haskell *et al.*, 2003; Cressant *et al.*, 2004; Passini *et al.*, 2005; Griffey *et al.*, 2006). On the basis of extensive supporting animal data (Hackett *et al.*, 2005; Sondhi *et al.*, 2005; Passini *et al.*, 2006), the present study establishes the feasibility of treating LINCL by AAV2-mediated gene transfer. A strategy was developed to administer the AAV2_{CU}hCLN2 vector through 6 burr holes to 12 sites in the cortex to a total of 10 children with LINCL, 5 with severe and 5 with moderate disease. Serious adverse events were observed, but all were anticipated and none could be definitively linked to the gene transfer vector per se. Although the control groups were not matched, randomized, placebo/sham or blinded, and the numbers are small, assessment of the decline in the modified Hamburg LINCL clinical rating scale (the primary variable) in the treated subjects monitored for >6 months suggests that the therapy is associated with a slowing of disease progression. With the caveats that the small numbers of subjects and control subjects preclude more in-depth analyses of the effects of genotype, concurrent medications, severity, and other parameters on the outcome, the data support the hypothesis that AAV-mediated CNS gene transfer can slow the rate of progression of the CNS manifestations of the disease, and support the concept that additional studies using AAV-mediated CNS gene transfer to treat the CNS manifestations of LINCL are warranted.

Safety

Preclinical toxicology studies in experimental animals demonstrated no safety issues regarding the use of the AAV2_{CU}h-

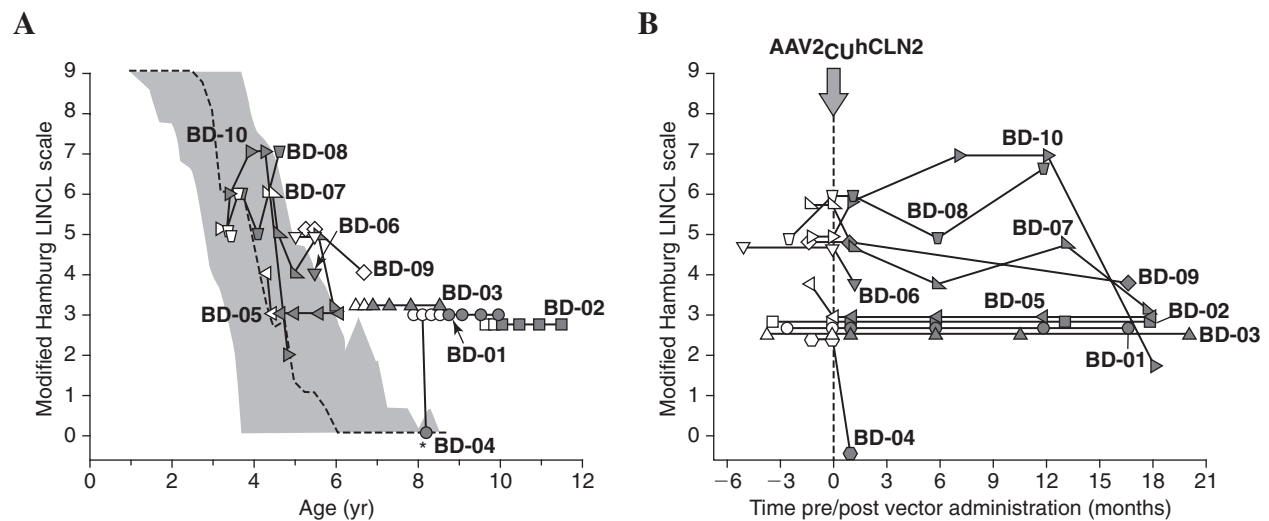


FIG. 3. Progression of LINCL in the 10 treated subjects as a function of time as determined by the modified Hamburg LINCL scale, the primary outcome variable. **(A)** Data pre- and posttherapy, shown as a function of the age of each subject. Symbols for each subject are identical to those in Fig. 1. The gray shaded area represents the 5th to 95th percentile area of untreated children with LINCL from Germany and Switzerland published by Steinfeld and coworkers (2002), modified to eliminate the ophthalmologic parameter (Crystal *et al.*, 2004; Steinfeld *et al.*, 2002). * represents the death of subject BD-04. The dashed line represents the median. Open symbols represent the pretherapy values and solid symbols represent posttherapy values. **(B)** Data pre and posttherapy, assessed as a function of time before and after vector administration. The data are the same as in (A), but shifted to time 0 as the time of administration. The time of treatment is indicated by the vertical dashed line. Symbols for each subject are identical to those in (A).

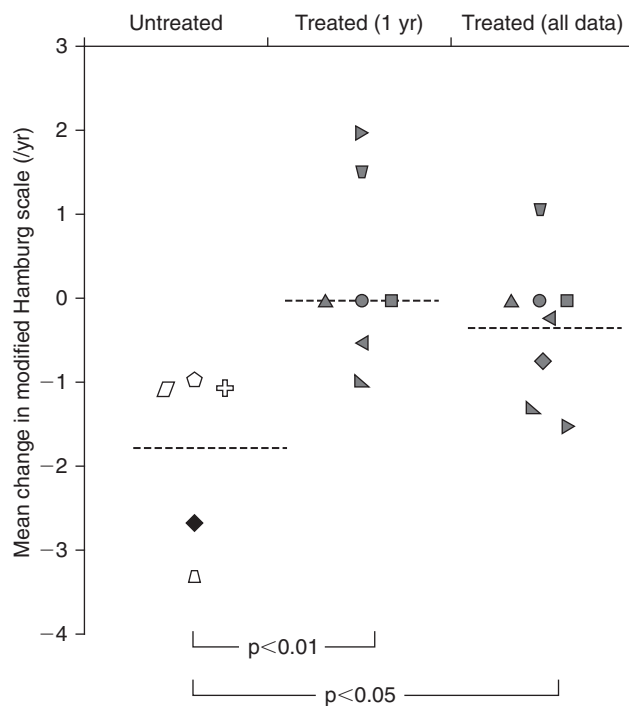


FIG. 4. Comparison of the mean rate of change of the modified Hamburg LINCL scale for treated and untreated subjects. For control subjects, two groups of untreated subjects were combined: (1) from the published data of Steinfeld and coworkers (2002), the data for the modified Hamburg scale are presented as the average mean rate of deterioration per year (solid symbol); and (2) from four untreated subjects we assessed twice, at a 1-year interval; shown is the change in the modified Hamburg scale per year for each subject (open symbols). For the treated subjects, the data were assessed in two ways: (1) “Treated (1 yr)”: for the seven treated subjects for whom data were available at the 12-month time point posttherapy, the data from Fig. 3B were used to calculate the change per year, based on the pretherapy and 12-month assessment (this comparison is the parallel to the manner in which the four control subjects were assessed); and (2) “Treated (all data)”: the best fit was determined for each of the eight subjects for whom data were available for >6 months, using all the data from 0 to 18 months. For the treated individuals, the symbols are the same as in Fig. 3. The mean values for the rate of change for all subjects in each group are shown by the horizontal dashed lines. The rates of change for the treated subjects were compared with the mean rate of change for the combined control group by Mann-Whitney test.

CLN2 vector to treat the CNS manifestations of LINCL (Hackett *et al.*, 2005). A variety of adverse events were observed in the clinical study, but most were limited in duration and severity. None could be directly attributed to the AAV2_{CUh}CLN2 vector. However, because many adverse events occurred in chronological proximity to the vector administration, and because it was not possible to prove the event was not associated with the vector, most were classified as “probably or possibly” related to the vector and/or vector administration. The most serious event occurred in one subject who developed sustained seizures 2 weeks after vector administration, and ultimately died

49 days after vector administration. An extensive review was inconclusive as to the cause, that is, whether the onset of the seizure activity was related to the progression of the disease, the surgical procedure, or the vector itself. The lack of evidence of inflammation in the cerebrospinal fluid and by MRI argued against the vector as a cause. Of note, the LINCL-affected, but untreated younger sibling of that patient died at approximately the same age 2 years later. Seizures are a cardinal feature of LINCL and intractable seizures and status epilepticus are a known feature of advanced LINCL (Boustany, 1996). Assessment of 24-hr continuous EEG at 14 days posttherapy (the timing of the onset of the seizures in the subject who died) in the six subsequent subjects who underwent treatment showed a decrease in subclinical seizure activity after therapy compared with the same subjects pretherapy.

Challenges for successful gene therapy for LINCL

With rare diseases such as LINCL, the design of clinical studies is challenged by the paucity of data on the natural history of the disease and the logistical and ethical difficulty of designing a controlled study. In this context, assessment of new therapeutics in rare, childhood genetic disorders such as the LINCL is a dilemma. Like most CNS disorders, there are no biomarkers that can be used to assess therapy in the brain. Because the therapy requires direct CNS administration by a multi-hour neurosurgical procedure, it is challenging to design a contemporaneous, matched, randomized, blinded or placebo controlled study. In the absence of such a control group, rigorous statistical assessment of the outcome data in the present study is not possible. The data are further confounded by factors such as differences among individuals regarding genotype, standard of medical care, and other undefined factors. Thus, it was only possible to gain insight into the suggestive effect of therapy on progression of the disease. With the caveats that the control group was limited to four untreated subjects assessed twice at an interval of 1 year plus the published data of Steinfeld and coworkers (2002), assessment of the change of clinical rating scale in the treated group suggests, but does not prove, that CNS administration of the AAV2_{CUh}CLN2 vector might provide some therapeutic benefit.

It is of interest that although there was evidence of statistically significant slowing of the decline of the disease as assessed by the primary variable, the clinical rating scale, the quantitative MRI parameters suggested, but did not prove, a difference compared with the control subjects. Because there are no biochemical markers for the disease, imaging represents a rational choice for secondary parameters to complement the clinical rating scales (Ramirez-Montealegre and Pearce, 2007; Worgall *et al.*, 2007). However, in diseases such as cerebral palsy and Parkinson’s disease, and in our studies of LINCL, the correlation between clinical and neuroimaging results based on the current methods is variable (Bohnen *et al.*, 2007; Worgall *et al.*, 2007; Korzeniewski *et al.*, 2008). In this regard, it would be useful for the design of future therapeutic studies to develop less variable high-resolution MRI or other imaging parameters that are sensitive to the disease process.

Successful gene therapy for the CNS manifestations of LINCL requires vector-driven expression of TPP-I in the CNS that is of a sufficient level, distribution, and duration to treat

the disease. The requirement for long-term expression comes from the knowledge that the accumulation of the lysosomal storage defect is progressive. The range of required therapeutic levels of expression can be estimated from the observation that affected children with ~5% of normal TPP-I activity have a late-onset variant of the disease and that heterozygous carriers are normal (Sleat *et al.*, 1999). These requirements were met in the present study by using doses of the AAV2_{CUh}CLN2 vector that, scaled from doses used in mice and monkeys, should provide long-term expression in the human CNS of physiological levels of TPP-I protein, at least in the general proximity of the sites of vector administration. The major challenge for successful therapy of LINCL is the requirement for wide distribution of the therapy within the brain, based on the fact that LINCL affects the brain diffusely (Boustany, 1996; Williams *et al.*, 1999; Haltia, 2003). On the basis of safety constraints limiting the volume that could be administered per unit time, the limits on the concentration of the vector to avoid aggregation, and the number of burr holes, we designed the vector administration to be through six burr holes with vector deposition at two depths per burr hole. With these physical limitations, it is likely that the goal of spreading the vector over as wide a volume of brain as possible will likely come from vector design, that is, by developing new gene transfer vectors that distribute more widely through the CNS.

Although the data in the present study cannot prove we achieved the levels, duration, and distribution of TPP-I expression in the treated children to provide a true therapeutic benefit, we suggest that the data provide a rationale for developing a second-generation clinical trial of AAV gene transfer in individuals with LINCL. On the basis of studies in rodents, non-human primates, and cats, it is likely that the greatest impact may be obtained from the use of serotypes of AAV such as 1, 5, 8, 9, or rh.10, all of which provide much higher levels and a much wider distribution of transgene expression in the brain than the AAV2-based vector used in the present study (Vite *et al.*, 2003; Bunnell *et al.*, 2004; Broekman *et al.*, 2006; Cearley and Wolfe, 2006; Passini *et al.*, 2006; Cabrera-Salazar *et al.*, 2007; Sondhi *et al.*, 2007a). On the basis of the suggestive evidence of an impact on disease progression obtained in the present study with an AAV2 serotype-based vector, these second-generation AAV vectors are now prime candidates for the development of a new clinical trial for the treatment of the CNS manifestations of LINCL. Further, on the basis of LINCL knockout mouse data published by Cabrera-Salazar and coworkers (2007), using an AAV1-based vector, and our similar data with AAVrh.10-based vector (Sondhi *et al.*, 2007b), an enhanced therapeutic outcome will likely be achieved by treating the disease as early as possible. For a second-generation clinical trial of AAV gene transfer we would also propose the use of a newly developed clinical severity scale, which correlated better with disease progression in individuals with LINCL (Worgall *et al.*, 2007).

ACKNOWLEDGMENTS

The authors thank C. Hollmann and the Clinical Operations and Regulatory Affairs Core of the Department of Genetic Med-

icine (L. Cai, L.M. Arkin, S.C. Bangs, H. Lawther, L.H.K. Suh, M. Wang, and S. Hyde) for help with the regulatory aspects of the study; A.M. Ulug, S. Merchant, and C.L. Harden for helpful discussions; and N. Mohamed and T. Virgin-Bryan for help in preparing this manuscript. This study was supported, in part, by the Nathan's Battle Foundation (Greenwood, IN); by NIH U01 NS047458, NIH GCRC M01 RR00047, NIH UL1-RR024996; and by the Will Rogers Memorial Fund (Los Angeles, CA). Protocol registration numbers: NCT00151216 and NCT00151268; www.clinicaltrials.gov.

AUTHOR DISCLOSURE STATEMENT

No competing financial interests exist.

REFERENCES

- ARKIN, L.M., SONDHAI, D., WORGALL, S., SUH, L.H., HACKETT, N.R., KAMINSKY, S.M., HOSAIN, S.A., SOUWEIDANE, M.M., KAPLITT, M.G., DYKE, J.P., HEIER, L.A., BALLON, D.J., SHUNGU, D.C., WISNIEWSKI, K.E., GREENWALD, B.M., HOLLMANN, C., and CRYSTAL, R.G. (2005). Confronting the issues of therapeutic misconception, enrollment decisions, and personal motives in genetic medicine-based clinical research studies for fatal disorders. *Hum. Gene Ther.* **16**, 1028–1036.
- BOHNEN, N.I., KUWABARA, H., CONSTANTINE, G.M., MATHIS, C.A., and MOORE, R.Y. (2007). Grooved pegboard test as a biomarker of nigrostriatal denervation in Parkinson's disease. *Neurosci. Lett.* **424**, 185–189.
- BOSCH, A., PERRET, E., DESMARIS, N., and HEARD, J.M. (2000). Long-term and significant correction of brain lesions in adult mucopolysaccharidosis type VII mice using recombinant AAV vectors. *Mol. Ther.* **1**, 63–70.
- BOUSTANY, R.M. (1996). Batten disease or neuronal ceroid lipofuscinosis. In *Handbook of Clinical Neurology* (Vol. 66 [22]): *Neurodystrophies and Neurolipidoses*, H.W. Moser, ed. (New York: Elsevier Science), pp. 671–700.
- BROEKMAN, M.L., COMER, L.A., HYMAN, B.T., and SENA-ESTEVEZ, M. (2006). Adeno-associated virus vectors serotyped with AAV8 capsid are more efficient than AAV-1 or -2 serotypes for widespread gene delivery to the neonatal mouse brain. *Neuroscience* **138**, 501–510.
- BROUGH, D.E., LIZONOVA, A., HSU, C., KULESA, V.A., and KOVESDI, I. (1996). A gene transfer vector–cell line system for complete functional complementation of adenovirus early regions E1 and E4. *J. Virol.* **70**, 6497–6501.
- BUNNELL, B.A., DUFOUR, J., BELENCHIA, G., ALVAREZ, X., BAKER, K., DIDIER, P., LACKNER, A., and WOLFE, J. H. (2004). Assessment of the transduction patterns of alternative AAV vector serotypes in the CNS of rhesus macaques. *Mol. Ther.* **9**, S129.
- CABRERA-SALAZAR, M.A., ROSKELLEY, E.M., BU, J., HODGES, B.L., YEW, N., DODGE, J.C., SHIHABUDDIN, L.S., SOHAR, I., SLEAT, D.E., SCHEULE, R.K., DAVIDSON, B.L., CHENG, S.H., LOBEL, P., and PASSINI, M.A. (2007). Timing of therapeutic intervention determines functional and survival outcomes in a mouse model of late infantile batten disease. *Mol. Ther.* **15**, 1782–1788.
- CEARLEY, C.N., and WOLFE, J.H. (2006). Transduction characteristics of adeno-associated virus vectors expressing Cap serotypes 7, 8, 9, and Rh10 in the mouse brain. *Mol. Ther.* **13**, 528–537.
- CRESSANT, A., DESMARIS, N., VEROT, L., BREJOT, T., FROIS-SART, R., VANIER, M.T., MAIRE, I., and HEARD, J.M. (2004).

- Improved behavior and neuropathology in the mouse model of Sanfilippo type IIIB disease after adeno-associated virus-mediated gene transfer in the striatum. *J. Neurosci.* **24**, 10229–10239.
- CRYSTAL, R.G., SONDHI, D., HACKETT, N.R., KAMINSKY, S.M., WORGALL, S., STIEG, P., SOUWEIDANE, M., HOSAIN, S., HEIER, L., BALLON, D., DINNER, M., WISNIEWSKI, K., KAPLITT, M., GREENWALD, B.M., HOWELL, J.D., STRYBING, K., DYKE, J., and VOSS, H. (2004). Clinical protocol: Administration of a replication-deficient adeno-associated virus gene transfer vector expressing the human CLN2 cDNA to the brain of children with late infantile neuronal ceroid lipofuscinosis. *Hum. Gene Ther.* **15**, 1131–1154.
- DYKE, J.P., VOSS, H.U., SONDHI, D., HACKETT, N.R., WORGALL, S., HEIER, L.A., KOSOFSKY, B.E., ULUG, A.M., SHUNGU, D.C., MAO, X., CRYSTAL, R.G., and BALLON, D. (2007). Assessing disease severity in late infantile neuronal ceroid lipofuscinosis using quantitative MR diffusion-weighted imaging. *Am. J. Neuroradiol.* **28**, 1232–1236.
- FRISELLA, W.A., O'CONNOR, L.H., VOGLER, C.A., ROBERTS, M., WALKLEY, S., LEVY, B., DALY, T.M., and SANDS, M.S. (2001). Intracranial injection of recombinant adeno-associated virus improves cognitive function in a murine model of mucopolysaccharidosis type VII. *Mol. Ther.* **3**, 351–358.
- GRIFFEY, M.A., WOZNIAK, D., WONG, M., BIBLE, E., JOHNSON, K., ROTHMAN, S.M., WENTZ, A.E., COOPER, J.D., and SANDS, M.S. (2006). CNS-directed AAV2-mediated gene therapy ameliorates functional deficits in a murine model of infantile neuronal ceroid lipofuscinosis. *Mol. Ther.* **13**, 538–547.
- HACKETT, N.R., REDMOND, D.E., SONDHI, D., GIANNARIS, E.L., VASSALLO, E., STRATTON, J., QIU, J., KAMINSKY, S.M., LESSER, M.L., FISCH, G.S., ROUELLE, S.D., and CRYSTAL, R.G. (2005). Safety of direct administration of AAV2_{CH}CLN2, a candidate treatment for the central nervous system manifestations of late infantile neuronal ceroid lipofuscinosis, to the brain of rats and nonhuman primates. *Hum. Gene Ther.* **16**, 1484–1503.
- HALTIA, M. (2003). The neuronal ceroid-lipofuscinoses. *J. Neuropathol. Exp. Neurol.* **62**, 1–13.
- HASKELL, R.E., HUGHES, S.M., CHIORINI, J.A., ALISKY, J.M., and DAVIDSON, B.L. (2003). Viral-mediated delivery of late-infantile neuronal ceroid lipofuscinosis gene, TPP-I to the mouse central nervous system. *Gene Ther.* **10**, 34–42.
- JANSON, C., MCPHEE, S., BILANIUK, L., HASELGRÖVE, J., TESTAIUTI, M., FREESE, A., WANG, D.J., SHERA, D., HURH, P., RUPIN, J., SASLOW, E., GOLDFARB, O., GOLDBERG, M., LARIJANI, G., SHARRAR, W., LIOUTERMAN, L., CAMP, A., KOLODNY, E., SAMULSKI, J., and LEONE, P. (2002). Clinical protocol: Gene therapy of Canavan disease: AAV-2 vector for neurosurgical delivery of aspartoacylase gene (ASPA) to the human brain. *Hum. Gene Ther.* **13**, 1391–1412.
- KORZENIEWSKI, S.J., BIRBECK, G., DELANO, M.C., POTCHEN, M.J., and PANETH, N. (2008). A systematic review of neuroimaging for cerebral palsy. *J. Child Neurol.* **23**, 216–227.
- LANE, S.C., JOLLY, R.D., SCHMECHEL, D.E., ALROY, J., and BOUSTANY, R.M. (1996). Apoptosis as the mechanism of neurodegeneration in Batten's disease. *J. Neurochem.* **67**, 677–683.
- PASSINI, M.A., MACAULEY, S.L., HUFF, M.R., TAKSIR, T.V., BU, J., WU, I.H., PIEPENHAGEN, P.A., DODGE, J.C., SHIHABUDDIN, L.S., O'RIORDAN, C.R., SCHUCHMAN, E.H., and STEWART, G.R. (2005). AAV vector-mediated correction of brain pathology in a mouse model of Niemann-Pick A disease. *Mol. Ther.* **11**, 754–762.
- PASSINI, M.A., DODGE, J.C., BU, J., YANG, W., ZHAO, Q., SONDHI, D., HACKETT, N.R., KAMINSKY, S.M., MAO, Q., SHIHABUDDIN, L.S., CHENG, S.H., SLEAT, D.E., STEWART, G.R., DAVIDSON, B.L., LOBEL, P., and CRYSTAL, R.G. (2006). Intracranial delivery of CLN2 reduces brain pathology in a mouse model of classical late infantile neuronal ceroid lipofuscinosis. *J. Neurosci.* **26**, 1334–1342.
- QIU, J.P., MENDEZ, B.S., CRYSTAL, R.G., and HACKETT, N.R. (2002). Construction and verification of an Ad/AAV helper plasmid designed for manufacturing recombinant AAV vectors for administration. *Mol. Ther.* **5**, S47.
- RAMIREZ-MONTEALEGRE, D., and PEARCE, D.A. (2007). Imaging of late infantile neuronal ceroid lipofuscinosis: A clinical rating scale. *Neurology* **69**, 503–504.
- SKORUPA, A.F., FISHER, K.J., WILSON, J.M., PARENTE, M.K., and WOLFE, J.H. (1999). Sustained production of β -glucuronidase from localized sites after AAV vector gene transfer results in widespread distribution of enzyme and reversal of lysosomal storage lesions in a large volume of brain in mucopolysaccharidosis VII mice. *Exp. Neurol.* **160**, 17–27.
- SLEAT, D.E., DONNELLY, R.J., LACKLAND, H., LIU, C.G., SOHAR, I., PULLARKAT, R.K., and LOBEL, P. (1997). Association of mutations in a lysosomal protein with classical late-infantile neuronal ceroid lipofuscinosis. *Science* **277**, 1802–1805.
- SLEAT, D.E., GIN, R.M., SOHAR, I., WISNIEWSKI, K., SKLOWER-BROOKS, S., PULLARKAT, R.K., PALMER, D.N., LERNER, T.J., BOUSTANY, R.M., ULDALL, P., SIAKOTOS, A.N., DONNELLY, R.J., and LOBEL, P. (1999). Mutational analysis of the defective protease in classic late-infantile neuronal ceroid lipofuscinosis, a neurodegenerative lysosomal storage disorder. *Am. J. Hum. Genet.* **64**, 1511–1523.
- SONDHI, D., HACKETT, N.R., APBLETT, R.L., KAMINSKY, S.M., PERGOLIZZI, R.G., and CRYSTAL, R.G. (2001). Feasibility of gene therapy for late neuronal ceroid lipofuscinosis. *Arch. Neurol.* **58**, 1793–1798.
- SONDHI, D., PETERSON, D.A., GIANNARIS, E.L., SANDERS, C.T., MENDEZ, B.S., DE, B., ROSTKOWSKI, A.B., BLANCHARD, B., BJUGSTAD, K., SLADEK, J.R., REDMOND, D.E., LEOPOLD, P.L., KAMINSKY, S.M., HACKETT, N.R., and CRYSTAL, R.G. (2005). AAV2-mediated CLN2 gene transfer to rodent and non-human primate brain results in long-term TPP-I expression compatible with therapy for LINCL. *Gene Ther.* **12**, 1618–1632.
- SONDHI, D., HACKETT, N.R., PETERSON, D.A., STRATTON, J., BAAD, M., TRAVIS, K.M., WILSON, J.M., and CRYSTAL, R.G. (2007a). Enhanced survival of the LINCL mouse following CLN2 gene transfer using the rh.10 rhesus macaque-derived adeno-associated virus vector. *Mol. Ther.* **15**, 481–491.
- SONDHI, D., HACKETT, N.R., RONDA, J., BAAD, M., and CRYSTAL, R.G. (2007b). Impact of age of treatment on AAVrh.10hCLN2-mediated amelioration of symptoms in CLN2 knockout mouse model of late infantile neuronal ceroid lipofuscinosis. *Mol. Ther.* **15**, S287.
- STEINFELD, R., HEIM, P., VON GREGORY, H., MEYER, K., ULLRICH, K., GOEBEL, H.H., and KOHLSCHÜTTER, A. (2002). Late infantile neuronal ceroid lipofuscinosis: Quantitative description of the clinical course in patients with CLN2 mutations. *Am. J. Med. Genet.* **112**, 347–354.
- U.S. FOOD AND DRUG ADMINISTRATION. (2003). Meeting 31 of the Biological Response Modifiers Advisory Committee, October 24–26, 2003, Gaithersburg, MD; briefing material and meeting transcripts. Available at www.fda.gov/ohrms/dockets/ac/cber01.htm#Biological%20Response (accessed April 2008).
- VINES, D.J., and WARBURTON, M.J. (1999). Classical late infantile neuronal ceroid lipofuscinosis fibroblasts are deficient in lysosomal tripeptidyl peptidase I. *FEBS Lett.* **443**, 131–135.
- VITE, C.H., PASSINI, M.A., HASKINS, M.E., and WOLFE, J.H. (2003). Adeno-associated virus vector-mediated transduction in the cat brain. *Gene Ther.* **10**, 1874–1881.
- WILLIAMS, R.E., GOTTLÖB, I., LAKE, B.D., GOEBEL, H.H., WINCHESTER, B.G., and WHEELER, R.B. (1999). CLN2: Clas-

sic late infantile NCL. In *The Neuronal Ceroid Lipofuscinoses (Batten Disease)*, H.H. Goebel, ed. (Amsterdam: IOS Press), pp. 37–53.

WISNIEWSKI, K.E., KIDA, E., GOLABEK, A.A., KACZMARSKI, W., CONNELL, F., and ZHONG, N. (2001). Neuronal ceroid lipofuscinoses: Classification and diagnosis. *Adv. Genet.* **45**, 1–34.

WORGALL, S., KEKATPURE, M.V., HEIER, L., BALLON, D., DYKE, J.P., SHUNGU, D., MAO, X., KOSOFKY, B., KAPLITT, M.G., SOUWEIDANE, M.M., SONDHI, D., HACKETT, N.R., HOLLMANN, C., and CRYSTAL, R.G. (2007). Neurological deterioration in late infantile neuronal ceroid lipofuscinosis. *Neurology* **69**, 521–535.

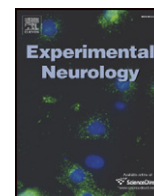
Address reprint requests to:

Dr. Ronald G. Crystal
Department of Genetic Medicine
Weill Cornell Medical College
1300 York Avenue, Box 96
New York, NY 10065

E-mail: geneticmedicine@med.cornell.edu

Received for publication February 28, 2008; accepted after revision March 10, 2008.

Published online: May 13, 2008.



Survival advantage of neonatal CNS gene transfer for late infantile neuronal ceroid lipofuscinosis

Dolan Sondhi^a, Daniel A. Peterson^b, Andrew M. Edelstein^a, Katrina del Fierro^a, Neil R. Hackett^a, Ronald G. Crystal^{a,*}

^a Department of Genetic Medicine, Weill Medical College of Cornell University, New York, New York, USA

^b Department of Neuroscience, Rosalind Franklin University of Medicine and Science, The Chicago Medical School, North Chicago, IL, USA

ARTICLE INFO

Article history:

Received 9 February 2008

Revised 7 April 2008

Accepted 9 April 2008

Available online 30 April 2008

ABSTRACT

Late infantile neuronal ceroid lipofuscinosis (LINCL), a fatal autosomal recessive neurodegenerative lysosomal storage disorder of childhood, is caused by mutations in the CLN2 gene, resulting in deficiency of the protein tripeptidyl peptidase I (TPP-I). We have previously shown that direct CNS administration of AAVrh.10hCLN2 to adult CLN2 knockout mice, a serotype rh.10 adeno-associated virus expressing the wild-type CLN2 cDNA, will partially improve neurological function and survival. In this study, we explore the hypothesis that administration of AAVrh.10hCLN2 to the neonatal brain will significantly improve the results of AAVrh.10hCLN2 therapy. To assess this concept, AAVrh.10hCLN2 vector was administered directly to the CNS of CLN2 knockout mice at 2 days, 3 wk and 7 wk of age. While all treatment groups show a marked increase in total TPP-I activity over wild-type mice, neonatally treated mice displayed high levels of TPP-I activity in the CNS 1 yr after administration which was spread throughout the brain. Using behavioral markers, 2 day-treated mice demonstrate marked improvement over 3 wk, 7 wk or untreated mice. Finally, neonatal administration of AAVrh.10hCLN2 was associated with markedly enhanced survival, with a median time of death 376 days for neonatal treated mice, 277 days for 3 wk-treated mice, 168 days for 7 wk-treated mice, and 121 days for untreated mice. These data suggest that neonatal treatment offers many unique advantages, and that early detection and treatment may be essential for maximal gene therapy for childhood lysosomal storage disorders affecting the CNS.

© 2008 Published by Elsevier Inc.

Introduction

There are over 40 identifiable lysosomal storage disorders, which are rare monogenic autosomal recessive diseases characterized by accumulation of unmetabolized substrates in lysosomes (Neufeld, 1991; Vellodi, 2005). Among the lysosomal storage disorders, approximately 50% affect the central nervous system (CNS) (Cardone, 2007; Hoffmann and Mayatepek, 2005; Jeyakumar et al., 2005). While many of the systemic manifestations of several of the lysosomal storage disorders can be effectively treated by intravenous enzyme therapy (Brady, 2006), the blood brain barrier prevents enzymes administered systemically to reach the brain, and thus the CNS manifestations of these disorders are, for now, untreatable (Beck, 2007; Sondhi et al., 2001).

Gene therapy represents one approach to deliver the deficient enzymes to the CNS, using gene transfer vectors expressing the wild-type cDNA to correct the relevant cell population in the CNS (Beck, 2007; Cardone, 2007; Mandel et al., 2006; Sondhi et al., 2001). Studies

of experimental animal models and humans have shown that a significant challenge to providing effective gene therapy for the CNS manifestations of the lysosomal storage disorders is that most of these disorders diffusely affect the CNS, and thus effective therapy requires delivery of the product of the therapeutic vector throughout the brain (Beck, 2007; Sondhi et al., 2001). This challenge is further compounded by the physical limitations of administration of gene therapy vectors to the human CNS, including the number of burr holes that can be placed in the skull, the volume that can be administered per min, and the total time of anesthesia that can be used safely (Crystal et al., 2004; Hackett et al., 2005). Finally, corrective gene therapies for neurodegenerative diseases are not restorative but rather halt disease progression, making delivery prior to disease onset an important objective. With these limitations in mind, three basic strategies have been employed to achieve therapeutic levels of gene expression throughout the brain: identifying gene transfer vectors that will diffuse through the CNS more effectively (Cearley and Wolfe, 2006; Deglon and Hantraye, 2005; Shevtsova et al., 2005; Sondhi et al., 2007), optimizing the method of delivery and volume and rate of infusion (Chen et al., 1999; Hackett et al., 2005; Hsieh et al., 2002), and administration at an earlier timepoint, when the brain is smaller and immature (Bostick et al., 2007; Broekman et al., 2007; Daly et al., 1999;

* Corresponding author. Department of Genetic Medicine, Weill Cornell Medical College, 1300 York Avenue, Box 96, New York, New York 10065, USA. Fax: +1 646 962 0220.

E-mail address: geneticmedicine@med.cornell.edu (R.G. Crystal).

Griffey et al., 2006; Li and Daly, 2002; Passini et al., 2003; Passini and Wolfe, 2001; Rafi et al., 2005; Shen et al., 2001; Waddington et al., 2004). Studies from our laboratory and others have identified several serotypes of adeno-associated virus (AAV) vectors that are more effective than the first generation vectors used for CNS gene transfer (Broekman et al., 2006; Burger et al., 2005; Cearley and Wolfe, 2006; Harding et al., 2006; Sondhi et al., 2007; Taymans et al., 2007), the parameters for optimal administration of vectors to the CNS have been established (Chen et al., 1999; Hackett et al., 2005; Hsich et al., 2002) and several studies have shown that administration earlier in life results in an advantage over therapy in older animals (Bostick et al., 2007; Broekman et al., 2007; Daly et al., 1999; Griffey et al., 2006; Li and Daly, 2002; Passini et al., 2003; Passini and Wolfe, 2001; Rafi et al., 2005; Shen et al., 2001; Waddington et al., 2004).

In the present study, we asked whether CNS administration to newborns of an AAV serotype rh10 vector, one of the AAV vectors known to be among the best to transfer genes to the CNS (Cearley and Wolfe, 2006; Sondhi et al., 2007), will have a better therapeutic advantage than the same vector administered later in life. To test this hypothesis, we have used late infantile neuronal ceroid lipofuscinosis (LINCL) as the target disorder. LINCL, a fatal, autosomal recessive neurodegenerative disease of middle childhood, is a typical lysosomal storage disorder with diffuse CNS manifestations, caused by mutations in the CLN2 gene, resulting in a deficiency of the lysosomal tripeptidyl peptidase (TPP-I) (Sleat et al., 1997; Williams et al., 1999; Worgall et al., 2007). In prior studies, we have shown that CNS administration of an AAVrh.10 vector coding for the wild-type human CLN2 cDNA to 7 wk old CLN2 knockout mice increased the median age of survival from 128 days to 162 days compared to the first generation AAV serotype 2 or 5 vector which had no impact on survival (Passini et al., 2006; Sondhi et al., 2007), and Cabrera-Salazar et al. (2007) have shown that an AAV1 vector coding for the CLN2 cDNA administered to 4 wk old CLN2^{-/-} mice had a significant survival advantage over administration at 11 wk.

Based on these observations, and studies of several groups showing that administration of gene transfer vectors to the newborn CNS provides significant advantage to administration later in life (Bostick et al., 2007; Broekman et al., 2007; Daly et al., 1999; Griffey et al., 2006; Li and Daly, 2002; Passini et al., 2003; Passini and Wolfe, 2001; Rafi et al., 2005; Shen et al., 2001; Waddington et al., 2004), we hypothesized that if an AAVrh.10 vector coding for the wild-type CLN2 cDNA were administered to the CNS of newborn CLN2^{-/-} mice, we would achieve significant improvement in survival over administration to older animals. Compared to parallel administration in 3 or 7 wk old mice, administration at postnatal day 2 demonstrated remarkable persistent, widespread expression of the CLN2 gene product, with concomitant improvement of a number of tests of CNS function as well as significant survival advantage.

Methods

AAVrh.10hCLN2 vector

The AAVrh.10hCLN2 vector contains an expression cassette consisting of the human CLN2 cDNA driven by a CMV/ β -actin hybrid promoter consisting of the enhancer from the cytomegalovirus immediate early gene, the promoter, splice donor and intron from the chicken β -actin gene, the splice acceptor from the rabbit β -globin gene followed by a CLN2 cDNA with an optimized Kozak translation initiation sequence (Sondhi et al., 2007). The cDNA is followed by the polyadenylation sequence from rabbit β -globin. The expression cassette is surrounded by the inverted terminal repeats of AAV2. To produce AAVrh.10hCLN2, 293 cells were cotransfected using Polyfect with the vector plasmid described above and two helper plasmids: p Δ F6, which expresses the required adenoviral helper functions for replication and the other with the AAV2 rep gene, and the AAVrh.10

cap gene (Sondhi et al., 2007). After 72 h, the cells were harvested and AAV purified on iodixanol gradients, followed by QHP ion exchange chromatography. Vector preparations were assessed by TaqMan real-time polymerase chain reaction to determine genomic copies and by *in vitro* gene transfer in 293 ORF6 cells.

Administration of AAVrh.10 to the CLN2^{-/-} mouse brain

All procedures were performed in accordance with NIH guidelines and under protocols approved by the Institutional Animal Care and Use Committee. Original heterozygous breeding pairs of CLN2^{+/-} mice back crossed into C57Bl/6 were used to produce all of the CLN2^{-/-} mice used in this study (Sleat et al., 2004). At postnatal day 20, mice were weaned and genotyped by polymerase chain reaction. The AAVrh.10hCLN2 vector was administered to the CLN2^{-/-} mice at 7 wk, 3 wk, or 2 days of age. Untreated CLN2^{-/-} mice, PBS-injected CLN2^{-/-} mice, and AAVrh.10GFP-treated CLN2^{-/-} mice [the AAVrh.10GFP vector consists of a humanized GFP gene with expression driven by CMV promoter pseudotyped with rh.10 capsid (Zolotukhin et al., 1996)] all served as negative controls and CLN2^{+/+} mice served as positive controls. Pilot injections of methylene blue were performed to confirm injection locations for 3 wk and 2 day injected mice.

The 7 and 3 wk mice received bilateral intracranial injections stereotaxically in four locations per hemisphere using a 10 μ l Hamilton syringe (Hamilton Company; Reno, NV) fitted with a 26 g needle. At 7 wk of age, mice were injected bilaterally in the lower striatum (A/P +0.60 mm, M/L \pm 1.75 mm, D/V -4.0 mm), upper striatum (A/P +0.60 mm, M/L \pm 1.75 mm, D/V -2.0 mm), thalamus (A/P -2.0 mm, M/L \pm 1.0 mm, D/V -3.0 mm), and cerebellum (A/P -6.0 mm, M/L \pm 0.5 mm, D/V -1.5 mm) with AAVrh.10hCLN2 (2×10^{10} genome copies in 3 μ l per site) at a rate of 0.5 μ l/min. The needle was left in position for 2 min before and 2 min following vector administration, at which point it was withdrawn slightly and left for 1 min, and then was finally withdrawn over the course of an additional minute. At 3 wk of age, mice were injected in the lower striatum (A/P +0.60 mm, M/L \pm 1.70 mm, D/V -3.5 mm), upper striatum (A/P +0.60 mm, M/L \pm 1.70 mm, D/V -2.5 mm), thalamus (A/P -2.3 mm, M/L \pm 1.0 mm, D/V -2.5 mm), and cerebellum (A/P -6.0 mm, M/L \pm 1.5 mm, D/V -1.5 mm) with AAVrh.10hCLN2 (2×10^{10} genome copies in 3 μ l per site) at a rate of 0.5 μ l/min, similarly to that for the 7 wk old mice. The total dose administered in the 7 wk and 3 wk animals was 1.6×10^{11} genome copies delivered in a total volume of 24 μ l distributed equally over 8 sites. Postnatal day 2 mice were injected bilaterally in three locations per hemisphere using the 10 μ l Hamilton syringe fitted with a 30 g needle. Pups were anesthetized with ice (Li and Daly, 2002), immobilized and injected at 3 separate locations per hemisphere distributed along the rostral-caudal axis (1.85×10^{10} genome copies in 0.5 μ l per site). The total dose administered in the neonatal animals was 1.1×10^{11} genome copies delivered in a total volume of 6 μ l distributed equally over 6 sites. Pups were returned to the litter and genotype determined at 20 days.

TPP-I activity in the CNS

When observed to be close to death (severe shaking, weight loss), mice were anesthetized and transcardially perfused with PBS. Brains were excised and hemisected. The right hemisphere was submerged in 4% paraformaldehyde for morphological evaluation (see below) and the left hemisphere was cut into six, 2 mm coronal sections. All samples were flash frozen. The samples were later thawed and homogenized in NaCl (0.15 M) and Triton X-100 (1 g/l). Supernatants of homogenized samples were diluted 100 fold in phosphate buffered saline and assayed for TPP-I activity as previously described (Sondhi et al., 2007). Final TPP-I activity was adjusted to total protein concentration using a bicinchoninic acid (BCA) Protein Assay (Pierce; Rockford IL) and calculated as fluorescent units (FU)/min-mg.

Morphological evaluation of TPP-I expression

Efficiency of CLN2 cDNA transfer was assessed in the right hemisphere by immunohistochemical staining for the gene product TPP-I. At 72 h post-perfusion, the brains were equilibrated in 30% sucrose at 4 °C. Serial 50 µm thick sagittal sections were produced by freezing sliding microtomy. Immunohistochemical detection of TPP-I was accomplished by incubation with mouse anti-human TPP-I antibody (1:1000; 72 h at 4 °C; gift from K. Wisniewski and A. Golabek, NYS Institute for Basic Research), followed by biotin-streptavidin amplification (Vectastain kit, Vector Labs; Burlingame, CA) that was then visualized by incubation in nickel chloride enhanced diaminobenzidine (DAB kit, Vector Labs; Burlingame, CA). Images were obtained by brightfield microscopy with digital image acquisition using an Olympus BX50 and Microfire Camera (Olympus America Inc; Center Valley, PA). For multiple immunofluorescence staining, sections were incubated for 72 h at 4 °C with rabbit anti-TPP-I (1:500; gift from P. Lobel, University of Medicine and Dentistry of New Jersey) and mouse anti-NeuN (1:2500; Chemicon, Temecula, CA) or mouse anti-TPP-I (1:2000), rabbit anti-Iba-1 (1:4000; Wako Chemicals USA, Richmond, VA), and guinea pig anti-GFAP (1:2000; Advanced Immunologicals, Long Beach, CA). Secondary antisera raised in donkey were used as appropriate for species detection and were conjugated to the fluorophores Alexa 488 (Invitrogen, Carlsbad, CA) or Cy3 or Cy5 (Jackson ImmunoResearch, West Grove, PA). Fluorescence imaging was performed using an Olympus Fluoview confocal microscope (Olympus America, Center Valley, PA).

Behavioral phenotyping

AAVrh.10hCLN2 was administered to the CNS of CLN2^{-/-} mice at 7 wk ($n=17$), 3 wk ($n=15$), or 2 days ($n=8$) of age. A series of phenotypic observations were made at various intervals to assess the impact of age of AAVrh.10hCLN2 administration. The negative controls were untreated CLN2^{-/-} ($n=14$) mice, PBS treated ($n=14$, injected at 7 wk) and AAVrh.10 GFP treated ($n=6$, injected at 7 wk). The positive controls were CLN2 wild-type mice ($n=16$). The assessments used and the testing intervals included: (1) gait (this qualitative test was performed in a subset of $n=3$ mice/group at bimonthly intervals); (2) tremors (weekly; on all animals in every group); (3) appearance (weekly; on all animals in every group); (4) performance of balance beam (weekly; on all animals in every group); and (5) performance on grip strength test (weekly; on all animals in every group). All tests, except gait, were performed at the same time each week and under similar conditions on all of the surviving mice in each of the experimental groups. Apart from gait, data from each of these tests was statistically analyzed from 15 to 18 wk, a period chosen based on the knowledge that CLN2^{-/-} mice perform normally until about 14 wk and are moribund by 18 wk (Sleat et al., 2004). There is typically a sharp decline in abilities in this time frame.

Gait analysis

Gait analysis was performed on a subset ($n=3$) of mice in each experimental group at bimonthly intervals. A blind tunnel (100 cm long, 20 cm wide, 10 cm high) with one end in the dark and the other end in the light was constructed over a sheet of white paper. The hindpaws of the mouse were dipped in blue ink and the frontpaws were dipped in red ink (Crayola washable paints, Binney and Smith, Easton, PA). The mouse was placed at the light end of the tunnel and as it ran to the dark end, the footprints were recorded on the paper and saved for qualitative analysis.

Tremors

Based on previous empirical observations, a tremor scale was created and applied to all mice. Tremors were assessed while the mouse was on the balance beam (described below) for a period of at least 30 s. The mice were rated on a scale of 1 to 5 as follows: score 1, occasional violent and

severe seizures coupled with repeated tremors; score 2, tremors and shaking most of the time; score 3, tremors and shaking occasionally; score 4, a shuffling movement with splayed hind feet but no tremors or shaking; and score 5, an active and agile mouse with no visible tremors or shuffling.

Coat appearance

Based on previous empirical observations, a scale of coat appearance was created and applied to all mice. Coat appearance was assessed while the mouse was on the balance beam (described below) for a period of at least 30 s. Mice were rated on a 3 point scale of 1 to 5 as follows: score 1, greasy, clumped, and unkempt fur; score 3, greasy but mostly kempt fur; and score 5, clean, smooth and shiny fur.

Balance beam

A horizontal wooden beam, 3 cm×125 cm was secured 100 cm from the ground over a tub filled with pads to protect mice that fell off the beam. The mouse was placed in the middle of the beam and the time until fall was recorded. Mice that did not fall after 3 min were returned to their cage and the time was recorded as 3 min.

Grip strength

A string was stretched between two wooden dowels. The mouse was placed in the middle of the suspended string and the time until fall was recorded. Mice that did not fall after 3 min were returned to their cage and the time was recorded as 3 min.

Survival

Mice were observed 3 times a week for signs of deterioration in health. If deemed moribund (severe shaking, weight loss), mice were sacrificed and age of death was recorded.

Statistical analysis

Data is provided as mean values±SEM. Analysis of phenotype ratings and time were performed by ANCOVA with the post-hoc

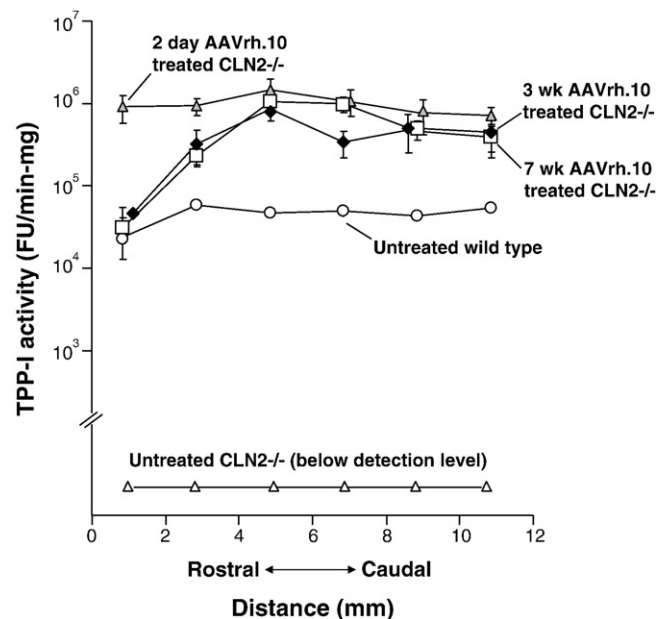


Fig. 1. TPP-I Activity in the CNS following direct CNS administration of AAVrh.10hCLN2. TPP-I activity in the brain following administration of AAVrh.10hCLN2 (2×10^{10} genome copies/site) bilaterally at multiple locations along the rostral–caudal axis at 7 wk, 3 wk, or 2 days of age. Mice were sacrificed when moribund. Samples included untreated controls ($n=14$, CLN2^{-/-}); wild-type ($n=16$, CLN2^{+/+}); 7 wk AAVrh.10 treated ($n=17$, CLN2^{-/-}); 3 wk AAVrh.10 treated ($n=11$, CLN2^{-/-}); and 2 day AAVrh.10 treated ($n=5$, CLN2^{-/-}). Mean specific activity was measured in brain homogenates across six, 2 mm coronal sections. The y-axis is represented as a log scale.

Fischer test with each measurement contributing to the value used for means testing with treatment group as factor and time as covariant. Since some parameters such as tremor and appearance are not

normally distributed, significance was confirmed by non-parametric analysis at selected timepoints. Survival analysis was assessed using Kaplan–Meier test.

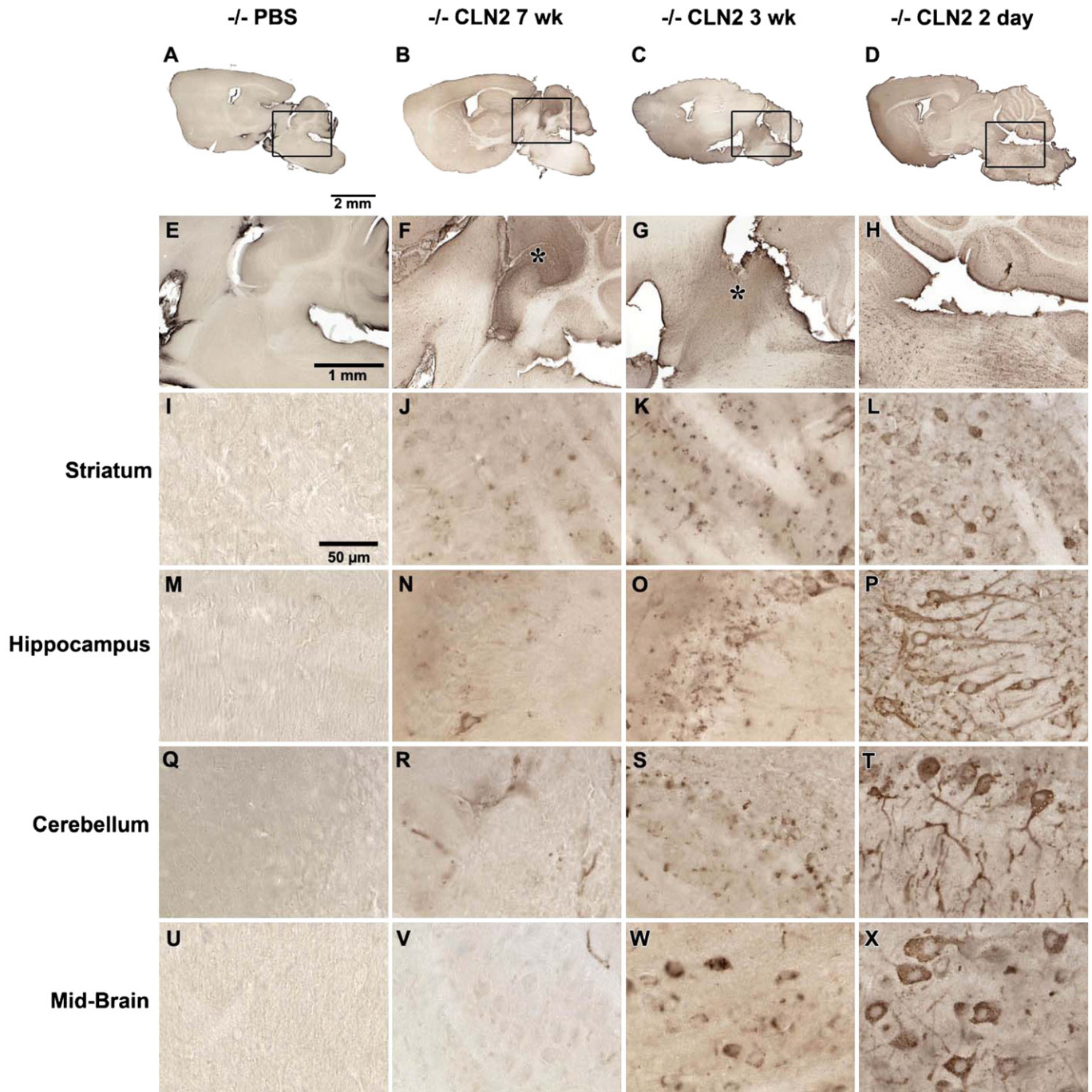


Fig. 2. Immunohistological assessment of the expression of TPP-I in the CNS following gene transfer. A–D. Sagittal sections of whole brain after: A. delivery of PBS; B. delivery of AAVrh.10hCLN2 at 7 wk; C. delivery of AAVrh.10hCLN2 at 3 wk; and D. delivery of AAVrh.10hCLN2 at 2 days. E–H represent higher magnification views of panels A–D respectively. E. Close up of PBS-injected mice showing no detectable TPP-I staining; F,G. Close up of AAVrh.10hCLN2 mice injected at 7 wk and 3 wk respectively showing a distribution gradient in detection of TPP-I between strong staining in the region of injection (asterisk) and reduced staining further from the region of injection. H. Close up of mice injected at 2 days showing uniform distribution of TPP-I staining across the equivalent region. Specific structures outside the region of injection were examined at higher magnification including: I–L. striatum; M–P. hippocampus; Q–T. cerebellum and U–X. midbrain. I. Striatum of mice receiving PBS in which no TPP-I positive cells were seen; J,K. striatum of mice injected with AAVrh.10hCLN2 at 7 wk or 3 wk producing punctate cellular staining in some cells; L. striatum of mice injected with AAVrh.10hCLN2 at 2 days with no obvious region of injection and equivalent regions of the striatum containing numerous cells with strong cytoplasmic staining extending into cell processes. M. Hippocampus of PBS-injected mice containing no detectable TPP-I staining; N,O. hippocampus of mice injected with AAVrh.10hCLN2 at 7 or 3 wk, showing few TPP-I-positive cells with punctate staining; P. hippocampus in mice injected at 2 days containing robust TPP-I staining filling cell bodies and processes in all parts. Q. Cerebellum of PBS-injected mice containing no detectable TPP-I staining; R,S. cerebellum outside of the region of injection in mice injected with AAVrh.10hCLN2 at 7 wk or 3 wk with TPP-I staining only in blood vessels or few TPP-I-positive cells with punctate staining; T. cerebellum of mice injected at 2 days with AAVrh.10hCLN2 showing all parts of the cerebellum with robust TPP-I staining filling cell bodies and processes. U. Midbrain of PBS-injected mice containing no TPP-I staining; V. midbrain of mice injected with AAVrh.10hCLN2 at 7 wk with only a few TPP-I positive blood vessels; W. midbrain of mice injected with AAVrh.10hCLN2 at 3 wk showing some TPP-I positive cells with uneven filling of their cytoplasm; X. Midbrain of mice injected with AAVrh.10hCLN2 at 2 days with frequent, strongly-stained cells distributed across the midbrain. Calibration bars are: A–D, 2 mm; E–H, 1 mm; and I–X, 50 μm.

Results

CNS TPP-I levels

All CLN2^{-/-} mice treated with AAVrh.10hCLN2 exhibited higher levels of TPP-I activity (FU/min-mg) in the brain, compared to uninjected CLN2^{-/-} mice and uninjected CLN2^{+/+} mice (Fig. 1). Mice treated at postnatal day 2, 3 wk and 7 wk all showed a nearly 100-fold increase in activity above wild-type levels. In addition, the 2 day-treated mice possessed a wider rostral-caudal distribution compared to 7 and 3 wk-treated mice, with significantly higher levels of TPP-I activity in the frontal lobe ($p < 0.01$).

Distribution of TPP-I expression

In agreement with the measure of enzymatic activity, no TPP-I-positive staining was detected in the brains of untreated CLN2^{-/-} mice (not shown) or those that received the PBS vehicle injection (Figs. 2A, E). In all groups receiving the AAVrh.10hCLN2 administration, regions of injection could be identified by robust cellular expression of TPP-I (Figs. 2B–D and F–H). Multiple immunofluorescence staining showed that TPP-I expression was detected within cells colocalized with expression of NeuN, confirming their neuronal identity (not shown). Outside of regions of injection, the extent and staining patterns of TPP-I-positive cells varied as a function of the age of administration of the AAVrh.10hCLN2 (Fig. 2). Assessment of mice treated at 7 wk resulted in sparse punctate staining within scattered neurons in most regions examined that were adjacent to the site of delivery. Assessment of mice treated at 3 wk resulted in stronger labeling within neurons, so that enough of the cell soma was filled to produce a recognizable cellular profile, and TPP-I-positive neurons were observed at greater frequency.

Strikingly, evaluation following administration at 2 days postnatal showed strong intracellular TPP-I expression. Most neurons were TPP-I-positive in all regions examined, including regions such as the midbrain.

Consistent with the observation that administration at 2 days produced higher levels at the most rostral brain segments when measured by enzymatic assay, the frontal cortex showed extensive TPP-I expression despite being distant from the sites of injection (Fig. 3). With 7 and 3 wk administration times, nearly all TPP-I-positivity was detected in tubular and circular vascular profiles indicative of endothelial cell-staining in small blood vessels and capillaries, likely as a result of mechanical disruption and seepage of vector into vascular system and transport to distant loci during surgical delivery. In contrast, TPP-I staining was well defined in neurons of the frontal cortex in the 2 day administration group. To further evaluate the phenotype of cells expressing TPP-I, immunofluorescence staining was performed to colocalize TPP-I protein (red) with microglia (green) or astrocytes (blue; Fig. 3). The multiple labeling revealed that TPP-I expression was not in astrocytes or microglia regardless of the age of the mice at vector administration. There was no apparent difference in microglial density or morphology between conditions suggesting that microglia were not activated in either the untreated CLN2^{-/-} or the animals receiving gene delivery.

Impact on gait

Gait analysis of mice was conducted bimonthly on a subset of $n=3$ mice per group. The representative data shown here is gait analysis done in mice with advanced disease that are close to the mean age of death for that group (Fig. 4). In wild-type mice (assessed at age 18 wk, the typical age of death for untreated CLN2^{-/-} mice), front and hind paw prints were largely superimposed and there was no limb

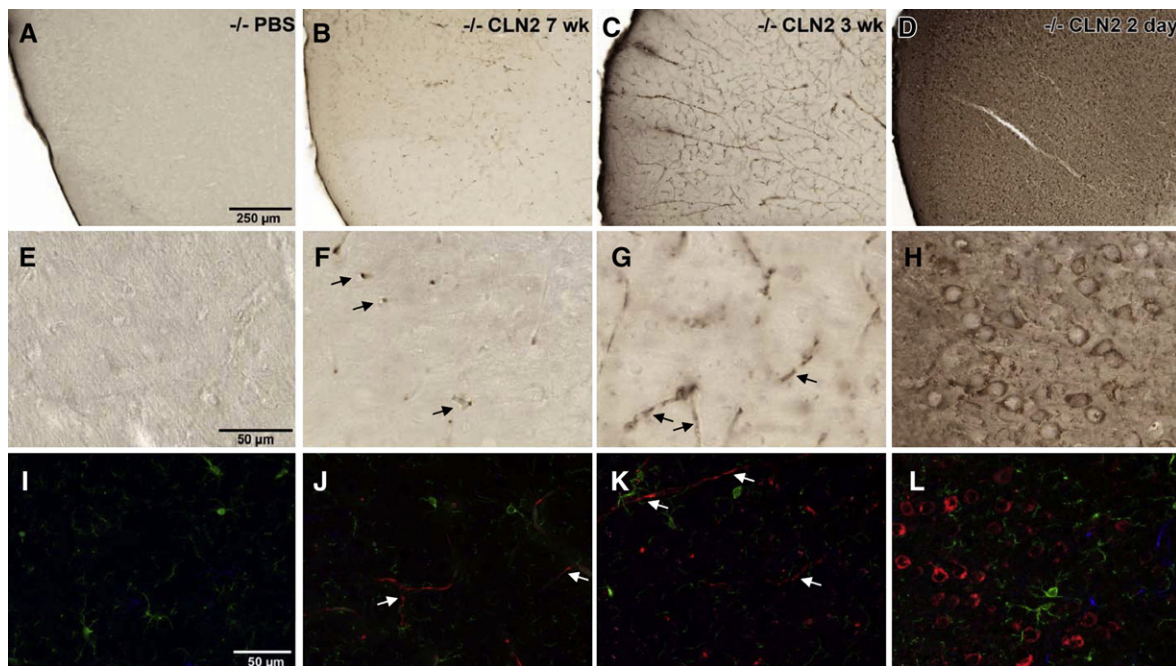


Fig. 3. Widespread expression of TPP-I in brain regions outside the area of vector administration is achieved by early (2 day) postnatal delivery of AAVrh.10hCLN2. The frontal cortex was examined as a region distant from the sites of injection to assess the effect of age at vector administration with the extent of transgene expression. Panel A–H represent immunoperoxidase staining for TPP-I while panels I–L represent immunofluorescent staining. A, E. Low magnification and high magnification images from PBS-administered animals, where immunoperoxidase staining revealed no detectable TPP-I staining. B, F. Tubular and circular vascular endothelial staining of blood vessels (arrows) for TPP-I was observed in animals injected at 7 wk as evident from both the low and the high magnification images; and C, G. In addition to vascular staining (arrows), occasional punctate staining of TPP-I was seen within a few, dispersed cells in both the low and high magnification images of animals injected at 3 wk. D, H. Injection at 2 days produced widespread cellular staining within the frontal cortex as seen in both the low and high magnification views. To evaluate the phenotype of cells expressing TPP-I, immunofluorescence staining was performed to colocalize TPP-I protein (red) with microglia (green) or astrocytes (blue). Detection of TPP-I was the same as seen with the immunoperoxidase staining. I. No TPP-I staining in PBS-injected animals. J. TPP-I-positive blood vessels in 7 wk (arrows); and K. blood vessel staining in 3 wk injected animals (arrows). L. Widespread, robust TPP-I staining was observed in 2 day injected animals. Neither microglia nor astrocytes coexpressed TPP-I. A–D., bar=250 μ m; E–L., bar=50 μ m.

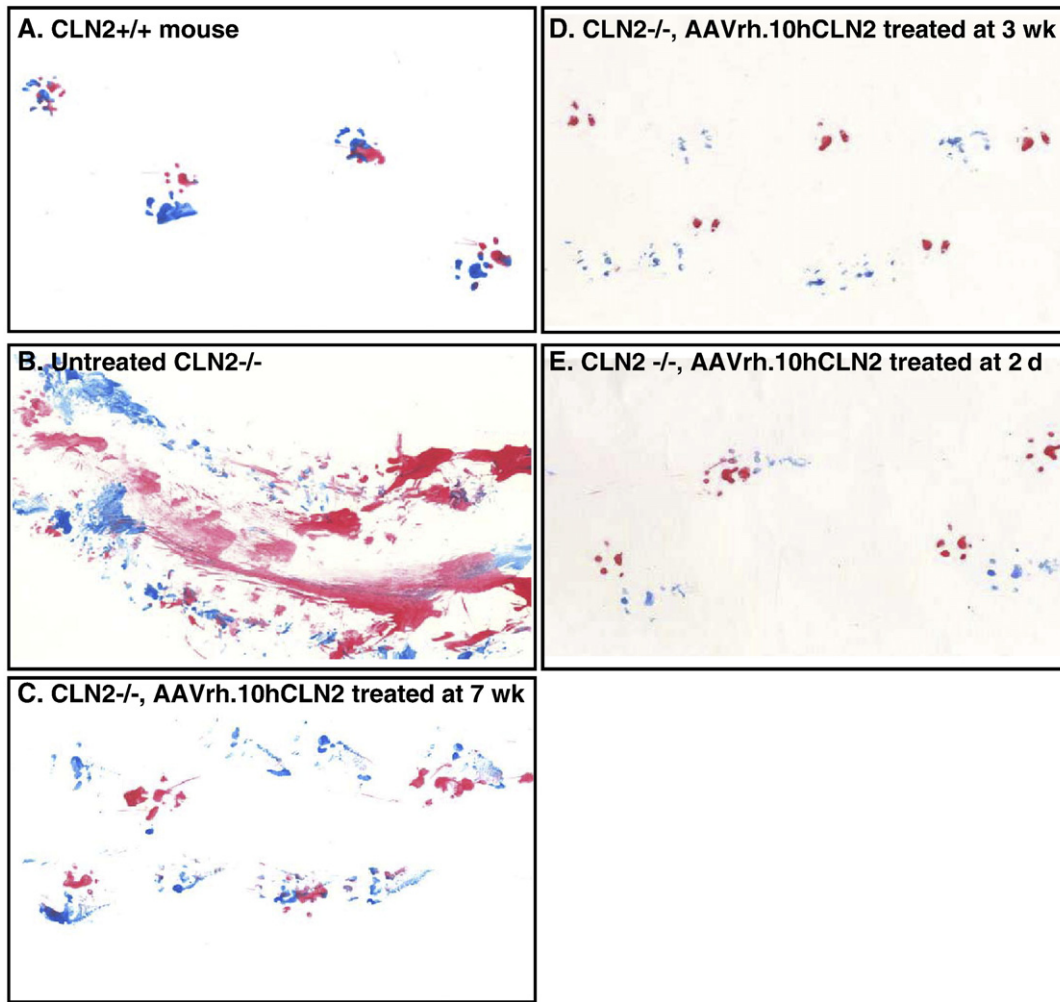


Fig. 4. Impact of age of AAVrh.10hCLN2 administration on gait. Hindpaws were covered in blue ink and frontpaws in red ink. Deficits in gait are revealed as mouse ran along a sheet of paper. The data shown here is representative of the gait analysis carried out in mice with advanced disease close to the mean age of death for that group. A. Wild-type; B. Untreated CLN2^{-/-}; C. CLN2^{-/-} treated at 7 wk; D. CLN2^{-/-} treated at 3 wk; and E. CLN2^{-/-} treated at 2 days.

dragging evident (Fig. 4A). In contrast, untreated CLN2^{-/-} mice also assessed at 18 wk age displayed dragging of feet, poor coordination of front and hind paws, and overall disordered gait (Fig. 4B). CLN2^{-/-} mice treated with AAVrh.10hCLN2 showed marked improvement in gait associated with earlier age of administration (Figs. 4C–E). The mice treated at 7 wk age assessed at 22 wk age showed some dragging and no overlap of hind and front paws. In mice treated at 3 wk assessed at 36 wk age, there was minimal dragging but still poor coordination of front and hind paws. In contrast, in the mice treated as newborns and assessed at 52 wk age, the coordination of front and hind paws was excellent, approaching that of wild-type mice. Quantitative analysis by measuring separation of foot prints was impossible due to the inability to separate the front paws from the hind paws due to excessive dragging in the untreated CLN2^{-/-} controls. Another approach was to assess the total ink (red or blue) deposited as a measure of foot dragging, but this was also not possible due to the inconsistencies between experimental subjects depending on how much ink was initially applied to the feet.

Impact on tremors and coat appearance

The tremors of CLN2^{-/-} mice treated with AAVrh.10hCLN2 at 2 days, 3 wk, and 7 wk of age and controls were characterized weekly. For all groups, the data was analyzed from 15 to 18 wk, a period chosen based on the knowledge that untreated CLN2^{-/-} mice perform

normally until about 14 wk and are moribund by 18 wk (Sleat et al., 2004). There is typically a sharp decline in abilities about this time. The therapeutic effect of gene therapy on tremors depended on the age of treatment with the severity of tremors decreasing with earlier treatment (Fig. 5A). Untreated CLN2^{-/-} mice exhibited moderate tremors and received significantly worse tremor ratings than wild-type controls, which did not exhibit any signs of tremor activity ($p < 0.0001$). The two negative control groups exhibited a tremor rating that was not significantly different from the untreated CLN2^{-/-} mice (PBS, $p > 0.4$, and AAVrh.10GFP, $p > 0.4$, not shown). In comparison all CLN2^{-/-} mice treated with AAVrh.10hCLN2 experienced significantly milder tremor activity ($p < 0.0001$). The 2 day and 3 wk treatment groups received significantly better tremor ratings than mice treated at 7 wk of age ($p < 0.0001$) and the 2 day-treated were better than the 3 wk-treated ($p < 0.005$), although not at the level of the wild-type mice ($p < 0.0001$).

The impact of AAVrh.10hCLN2 treatment on coat appearance of CLN2^{-/-} mice depended on the age of treatment (Fig. 5B). CLN2^{-/-} mice treated the earliest received the best ratings for coat appearance. Untreated CLN2^{-/-} had difficulty grooming their coats as the disease progresses and therefore received significantly lower coat appearance ratings than wild-type controls ($p < 0.0001$). The two negative control groups also had difficulty grooming to the extent that they were not significantly different from the untreated CLN2^{-/-} mice (PBS, $p > 0.1$, and AAVrh.10GFP, $p > 0.2$, not shown). By contrast, CLN2^{-/-} mice treated

with AAVrh.10hCLN2 at all ages received significantly higher coat appearance ratings ($p < 0.005$). The 2 day treatment group received higher ratings for coat appearances than both the 7 wk and 3 wk (both $p < 0.0001$) groups and was improved to the extent that their appearance was equivalent to wild-type controls ($p > 0.05$).

Performance on behavioral tasks

Assessment of CLN2^{-/-} mice by performance on the balance beam indicated that the time the mouse could remain on the beam depended on the age of treatment (Fig. 5C). Untreated CLN2^{-/-} mice remained on the balance beam for significantly less time than wild-type controls ($p < 0.0001$). The two negative control groups were not significantly different from the untreated CLN2^{-/-} mice in the ability to remain on

the beam (PBS, $p > 0.05$, and AAVrh.10GFP, $p > 0.1$, not shown). By contrast, all CLN2^{-/-} mice with AAVrh.10hCLN2 administered to the CNS, regardless of their age of treatment, showed significantly better performance than untreated CLN2^{-/-} mice, but the earlier the age of treatment, the greater the improvement in balance beam test performance. The 2 day and 3 wk treatment groups, while not different from each other ($p > 0.05$), both performed better than mice treated at 7 wks of age ($p < 0.001$), with the performance of the 2 day and 3 wk-treated animals was equivalent to wild-type controls ($p > 0.05$).

Assessment of CLN2^{-/-} mice by performance on grip strength also showed that grip strength depends on the age of treatment (Fig. 5D). The grip strength of untreated CLN2^{-/-} mice was significantly less than that of wild-type controls ($p < 0.0001$). The two negative control groups were not significantly different from the untreated CLN2^{-/-} mice in

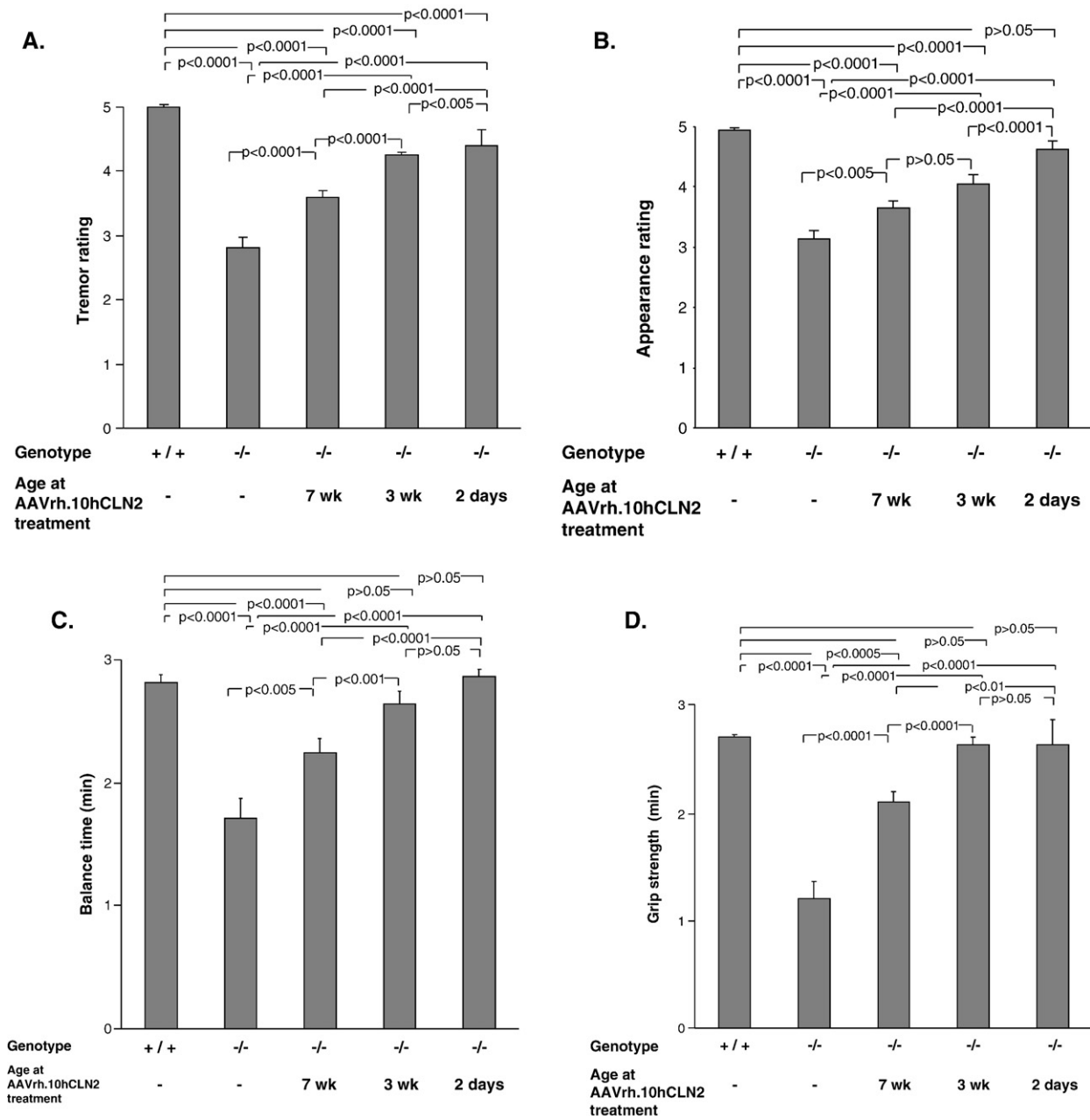


Fig. 5. Impact of age of AAVrh.10hCLN2 administration on phenotype and behavioral task performance. All groups were assessed weekly for rated phenotypes (0 to 5 scale, see Methods) and performance in behavioral assays. Means were calculated over a 4 wk period (15 to 18 wk) immediately preceding the death of the uninjected CLN2^{-/-} control group. A. Effect of the age of treatment on ratings of tremors; B. Effect of the age of treatment on ratings of coat appearance; C. Effect of the age of treatment on performance in balance beam test; and D. Effect of the age of treatment on performance in grip strength test. The numbers of mice for each group are as follows: Uninjected controls ($n = 14$, CLN2^{-/-}); wild-type controls ($n = 16$, CLN2^{+/+}); 7 wk AAVrh.10 injected ($n = 17$, CLN2^{-/-}); 3 wk AAVrh.10 injected ($n = 15$, CLN2^{-/-}); 2 day AAVrh.10 injected ($n = 8$, CLN2^{-/-}).

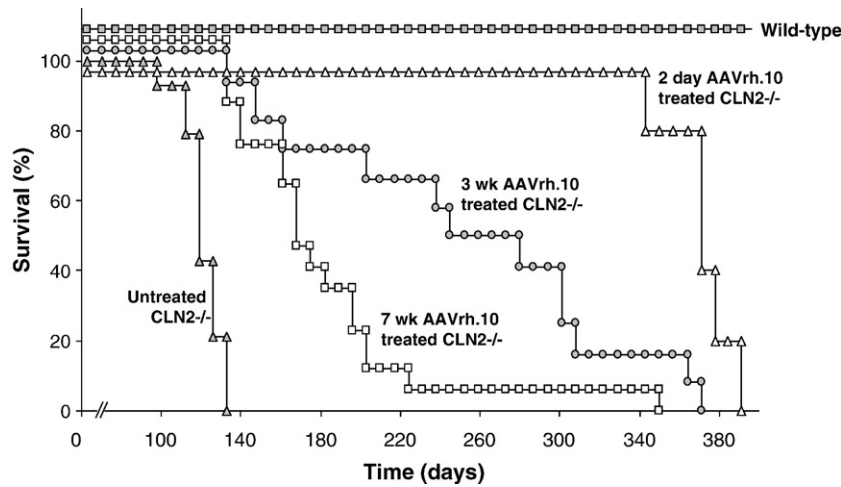


Fig. 6. Impact of age of AAVrh.10CLN2 administration on survival of CLN2^{-/-} mice. Mice were administered AAVrh.10hCLN2 (1.05 to 1.6×10^{11} genome copies) by direct CNS administration at 7 wk, 3 wk, or 2 days of age. Uninjected controls ($n=14$, CLN2^{-/-}), wild-type controls ($n=16$, CLN2^{+/+}), 7 wk AAVrh.10 injected ($n=17$, CLN2^{-/-}), 3 wk AAVrh.10 injected ($n=11$, CLN2^{-/-}), and 2 day AAVrh.10 injected ($n=5$, CLN2^{-/-}) mice were assessed 3 times per wk for signs of terminal decline. Mice that appeared moribund were sacrificed and age recorded.

their ability to maintain grip (PBS, $p>0.05$, and AAVrh.10GFP, $p>0.05$, data not shown). By contrast, CLN2^{-/-} mice with AAVrh.10hCLN2 administered to the CNS at all ages showed significantly stronger grip strength than untreated CLN2^{-/-} mice, which was greatest for mice treated at the earliest age. Mice treated at either 2 days or 3 wk of age, while not different from each other ($p>0.05$), both performed better than mice treated at 7 wk of age ($p<0.01$) and as well as wild-type controls ($p>0.05$).

Impact on survival

The most striking result was the correlation between earlier age of administration and extended lifespan of CLN2^{-/-} mice (Fig. 6). The median age of survival for untreated CLN2^{-/-} mice was 121 days. Similarly the two negative control groups had a low median age of survival (PBS 117 days and AAVrh.10 GFP 120 days, not shown). By contrast, the lifespans of 2 day- and 3 wk-treated CLN2^{-/-} mice were more than double that of the untreated CLN2^{-/-} mice. The median ages of survival for CLN2^{-/-} mice treated at 7 wk, 3 wk, and 2 days of age were 168 days, 277 days, and 373 days, respectively. Kaplan–Meier analysis of the survival data revealed a significant survival advantage for the 3 wk-treated mice over 7 wk-treated mice ($p<0.001$). Importantly, the lifespan of 2 day-treated mice was significantly longer than both the 7 wk-treated mice ($p<0.0001$) and 3 wk-treated mice ($p<0.01$).

Discussion

The biggest challenge for gene therapy for the treatment of the CNS manifestations of lysosomal storage diseases is to provide therapy that will have an impact throughout the brain. In this study, the impact of the age of treatment by an AAV serotype rh.10 vector on ameliorating the symptoms of LINCL was studied in the LINCL knockout mouse model. The data demonstrate the benefit of neonatal treatment with a 3-fold increase in life expectancy compared to untreated controls, a higher level and wider distribution of TPP-I protein within the brain than treatment at older ages, and a corresponding improvement in behavioral performance as a function of age. Together, these data suggest that neonatal treatment offers many unique advantages, and that both early detection and treatment are essential for effective genetic therapy with this type of disease. Also, in the context that LINCL is not included in routine newborn genetic screens (Fletcher, 2006; Meikle et al., 2006; NNSGRC, 2008), together with observations from other investigators of the success of neonatal gene transfer

(Bostick et al., 2007; Broekman et al., 2007; Daly et al., 1999; Griffey et al., 2006; Li and Daly, 2002; Passini et al., 2003; Passini and Wolfe, 2001; Rafi et al., 2005; Shen et al., 2001; Waddington et al., 2004), the studies presented here have social implications in that they suggest that to achieve maximal therapeutic impact of currently available gene transfer vectors, newborn screening with early identification and therapy of this disorder will achieve better results than waiting until the disease manifests clinically.

Time of therapy

The benefit of treatment as neonates may arise from a combination of factors, including, but not limited to: (1) therapeutically relevant levels of the deficient TPP-I enzyme can be achieved early in life, which may prevent the development of disease as opposed to reversing the established disease; and (2) earlier administration leads to a higher density and more widespread distribution of vector within the much smaller, and immature neonatal brain (Kohn and Parkman, 1997; Waddington et al., 2004).

The value of the neonatal window for treatment has been shown previously in an animal model of Krabbe's disease where animals treated at birth with an adenovirus vector coding for galactocerebrosidase showed an improvement compared to those treated 2 wk after birth (Shen et al., 2001). Passini et al. (Passini et al., 2003; Passini and Wolfe, 2001) have shown in the mucopolysaccharidosis-VII (MPS-VII) animal model that intraparenchymal or intraventricular injection of an AAV2 vector encoding the beta-glucuronidase (GUSB) gene into neonatal mice led to widespread and prolonged GUSB activity. They hypothesized that the wider distribution of the GUSB transgene throughout the brain following intraventricular injection was due to more efficient transduction of the deeper neuronal structures (Passini et al., 2003). These reports, along with the data described in this paper, have important implications for supporting newborn screening programs and the timing of experimental therapies.

Disease progression in lysosomal storage diseases

Several lines of evidence suggest that earlier administration offers several unique advantages to treating lysosomal storage disorders (Kohn and Parkman, 1997; Waddington et al., 2004). Foremost among these is that, treating individuals before disease onset prevents the occurrence of irreversible damage. In the case of LINCL, there is widespread neurodegeneration (Haltia, 2003; Lane et al., 1996; Williams et al., 1999).

As with other neurodegenerative diseases, the spatially limited endogenous neurogenesis in the postnatal brain is insufficient to restore function, thus it is important to halt the pathology of LINCL before irreparable damage occurs (Ming and Song, 2005). The onset of LINCL in the mouse knockout model has been estimated to be at 5 wk of age, with the earliest observed point of autofluorescent accumulation 2 wk prior to visible symptoms (Sleat et al., 2004). Studies testing the age of administration on the treatment of LINCL have operated under this assumption, testing therapy before and after this age of onset. For example, Cabrera-Salazar et al. (Cabrera-Salazar et al., 2007) have shown that treatment of LINCL knockout mice at 4 wk of age has greatly increased therapeutic benefits as compared to 11 wk-treated mice. In that study 80% survival was observed at 330 days when CLN2 knockout mice were injected with AAV1 vector expressing CLN2 gene at 4 wk of age. In the present study, the enhanced survival observed for 2 day-treated mice compared to 3 wk mice suggests an important pathological process may occur even further upstream of the presumed age of onset. The newborn mice survived 100% to >330 days, better than the mice treated at 4 wk of age by AAV1 vector (Cabrera-Salazar et al., 2007) as well as better than the mice treated with AAVrh.10 vector at 3 wk of age in this study.

A similar phenomenon has been observed in previous studies with the CLN1 deficient knockout mice, which models another member of the lysosomal storage disorders family (Griffey et al., 2006). In this case, morphologic abnormalities were detected in 7-month old mice, including autofluorescence-associated neuronal loss prior to the mice exhibiting the moribund phenotype (Griffey et al., 2006). Together, these studies argue strongly for the development of better detection methods in the lysosomal disorders, such as improved magnetic resonance imaging or more sensitive behavioral parameters. Earlier detection will therefore be a critical preventative measure to insure the disease does not progress into a destructive stage.

Unique properties of the neonatal brain

In addition to preventing disease onset, therapeutic administration immediately following birth may also capitalize on unique features of the neonatal brain. The increased spread of the TPP-I transgene observed in 2 day-treated mice, as visualized by histology and enzymatic assays, correlates with improved neuromotor function and extended life-span. Only in the 2 day administration group were most neurons throughout the brain found to express TPP-I (neuronal identity confirmed by co-expression of TPP-I with a mature neuronal marker, NeuN). In animals injected at later ages some TPP-I was detected at a distance from region of injection but only in the vasculature suggesting access through blood brain barrier disruption at the time of injection.

There may be a few explanations for this wider distribution. First, earlier administration may lead to a higher density of vector particle to brain volume in the much smaller neonatal brain. Secondly, the reduced barriers to diffusion in the still developing neonatal brain may facilitate widespread distribution of delivered vector (Passini et al., 2003; Watson et al., 2005). Similar widespread distribution in neonatal brains compared to adult brain has been reported in cell grafting studies (Englund et al., 2002; Gates et al., 1998; Olsson et al., 1997; Sidman et al., 2007; Zhao et al., 2007; Zhou and Lund, 1993). Interestingly, even though TPP-I levels in the CLN2^{-/-} mice injected with AAVrh.10CLN2 as newborns were over 100 times higher than in wild-type mice, the injected mice did not survive as long as wild-type mice. Therefore, even if the distribution of TPP-I is wider when mice are injected as newborns, some critical areas of the brain may still not be receiving enough TPP-I for normal activity.

Significance for human studies

Given the data and the considerations described above, the implications for human studies are significant, as these data strongly

support the concept that therapy will be most effective in neonates. Although the ethical issues regarding novel therapies are complex in neonates, the potential benefit is clearly much greater. For example, infantile Krabbe's disease was treated by transplanting umbilical-cord blood, rich in stem cells, in newborns and infants ranging from 12 to 352 days of age (Escolar et al., 2005). Compared to individuals treated post-symptomatically, these individuals showed improved motor and cognitive function, without the central demyelination that accompanies Krabbe's (Escolar et al., 2005).

In the case of LINCL, the diagnosis is typically not made until the age of >3 yr, at which point significant damage has already occurred (Steinfeld et al., 2002; Williams et al., 1999; Worgall et al., 2007). Diagnosis in newborns only occurs when an older sibling has already presented with the disease, leaving at risk newborns from parents who are unaware that they are carriers. The ease of newborn genetic screening argues for including the common mutations for the neurological lysosomal storage disorders in newborn genetic screening programs (Hayes et al., 2007; Kemper et al., 2007; Wilcken, 2007). For example, in 2006, New York became the first state to include Krabbe's disease in its *Newborn Screening Program* (2008; Therrell and Adams, 2007), setting the precedent for other infantile neuronal disorders. This study supports the inclusion of LINCL in similar programs, and for a broader spectrum of genetic tests for rare childhood monogenic disorders in general.

Acknowledgments

We thank P. Lobel and D. Sleat from University of Medicine and Dentistry of New Jersey for providing the CLN2^{+/-} breeding pairs and the rabbit anti-TPP-I antibody; K. Wisniewski and A. Golabek from NYS Institute for Basic Research for providing the anti-hCLN2 antibody; J. Ronda, M. Baad and S. Schuck for technical assistance; and N. Mohamed for help in preparing this manuscript. These studies were supported, in part, by U01 NS047458; Nathan's Battle Foundation, Greenwood, IN; and the Will Rogers Memorial Fund, Los Angeles, CA.

References

- Beck, M., 2007. New therapeutic options for lysosomal storage disorders: enzyme replacement, small molecules and gene therapy. *Hum.Genet.* 121, 1–22.
- Bostick, B., Ghosh, A., Yue, Y., Long, C., Duan, D., 2007. Systemic AAV-9 transduction in mice is influenced by animal age but not by the route of administration. *Gene Ther.* 14, 1605–1609.
- Brady, R.O., 2006. Enzyme replacement for lysosomal diseases. *Annu. Rev. Med.* 57, 283–296.
- Broekman, M.L., Comer, L.A., Hyman, B.T., Sena-Esteves, M., 2006. Adeno-associated virus vectors serotyped with AAV8 capsid are more efficient than AAV-1 or -2 serotypes for wide-spread gene delivery to the neonatal mouse brain. *Neuroscience* 138, 501–510.
- Broekman, M.L., Baek, R.C., Comer, L.A., Fernandez, J.L., Seyfried, T.N., Sena-Esteves, M., 2007. Complete correction of enzymatic deficiency and neurochemistry in the GM1-gangliosidosis mouse brain by neonatal adeno-associated virus-mediated gene delivery. *Mol. Ther.* 15, 30–37.
- Burger, C., Nash, K., Mandel, R.J., 2005. Recombinant adeno-associated viral vectors in the nervous system. *Hum. Gene Ther.* 16, 781–791.
- Cabrera-Salazar, M.A., Roskelley, E.M., Bu, J., Hodges, B.L., Yew, N., Dodge, J.C., Shihabuddin, L.S., Sohar, I., Sleat, D.E., Scheule, R.K., Davidson, B.L., Cheng, S.H., Lobel, P., Passini, M.A., 2007. Timing of therapeutic intervention determines functional and survival outcomes in a mouse model of late infantile batten disease. *Mol. Ther.* 15, 1782–1788.
- Cardone, M., 2007. Prospects for gene therapy in inherited neurodegenerative diseases. *Curr. Opin. Neurol.* 20, 151–158.
- Cearley, C.N., Wolfe, J.H., 2006. Transduction characteristics of adeno-associated virus vectors expressing cap serotypes 7, 8, 9, and Rh10 in the mouse brain. *Mol. Ther.* 13, 528–537.
- Chen, M.Y., Lonser, R.R., Morrison, P.F., Governale, L.S., Oldfield, E.H., 1999. Variables affecting convection-enhanced delivery to the striatum: a systematic examination of rate of infusion, cannula size, infusate concentration, and tissue-cannula sealing time. *J. Neurosurg.* 90, 315–320.
- Crystal, R.G., Sondhi, D., Hackett, N.R., Kaminsky, S.M., Worgall, S., Stieg, P., Souweidane, M., Hosain, S., Heier, L., Ballon, D., Dinner, M., Wisniewski, K., Kaplitt, M., Greenwald, B.M., Howell, J.D., Strybing, K., Dyke, J., Voss, H., 2004. Clinical protocol. Administration of a replication-deficient adeno-associated virus gene transfer vector expressing the human CLN2 cDNA to the brain of children with late infantile neuronal ceroid lipofuscinosis. *Hum. Gene Ther.* 15, 1131–1154.

- Daly, T.M., Vogler, C., Levy, B., Haskins, M.E., Sands, M.S., 1999. Neonatal gene transfer leads to widespread correction of pathology in a murine model of lysosomal storage disease. *Proc. Natl. Acad. Sci. U. S. A.* 96, 2296–2300.
- Deglon, N., Hantraye, P., 2005. Viral vectors as tools to model and treat neurodegenerative disorders. *J. Gene Med.* 7, 530–539.
- Englund, U., Fricker-Gates, R.A., Lundberg, C., Bjorklund, A., Wictorin, K., 2002. Transplantation of human neural progenitor cells into the neonatal rat brain: extensive migration and differentiation with long-distance axonal projections. *Exp. Neurol.* 173, 1–21.
- Escolar, M.L., Poe, M.D., Provenzale, J.M., Richards, K.C., Allison, J., Wood, S., Wenger, D.A., Pietryga, D., Wall, D., Champagne, M., Morse, R., Krivit, W., Kurtzberg, J., 2005. Transplantation of umbilical-cord blood in babies with infantile Krabbe's disease. *N. Engl. J. Med.* 352, 2069–2081.
- Fletcher, J.M., 2006. Screening for lysosomal storage disorders—a clinical perspective. *J. Inher. Metab. Dis.* 29, 405–408.
- Gates, M.A., Olsson, M., Bjerregaard, K., Bjorklund, A., 1998. Region-specific migration of embryonic glia grafted to the neonatal brain. *Neuroscience* 84, 1013–1023.
- Griffey, M.A., Wozniak, D., Wong, M., Bible, E., Johnson, K., Rothman, S.M., Wentz, A.E., Cooper, J.D., Sands, M.S., 2006. CNS-directed AAV2-mediated gene therapy ameliorates functional deficits in a murine model of infantile neuronal ceroid lipofuscinosis. *Mol. Ther.* 13, 538–547.
- Hackett, N.R., Redmond, D.E., Sondhi, D., Giannaris, E.L., Vassallo, E., Stratton, J., Qiu, J., Kaminsky, S.M., Lesser, M.L., Fisch, G.S., Rouselle, S.D., Crystal, R.G., 2005. Safety of direct administration of AAV2(CU)hCLN2, a candidate treatment for the central nervous system manifestations of late infantile neuronal ceroid lipofuscinosis, to the brain of rats and nonhuman primates. *Hum. Gene Ther.* 16, 1484–1503.
- Haltia, M., 2003. The neuronal ceroid-lipofuscinosis. *J. Neuropathol. Exp. Neurol.* 62, 1–13.
- Harding, T.C., Dickinson, P.J., Roberts, B.N., Yendluri, S., Gonzalez-Edick, M., Lecouteur, R.A., Jooss, K.U., 2006. Enhanced gene transfer efficiency in the murine striatum and an orthotopic glioblastoma tumor model, using AAV-7- and AAV-8-pseudotyped vectors. *Hum. Gene Ther.* 17, 807–820.
- Hayes, I.M., Collins, V., Sahhar, M., Wraith, J.E., Delatycki, M.B., 2007. Newborn screening for mucopolysaccharidoses: opinions of patients and their families. *Clin. Genet.* 71, 446–450.
- Hoffmann, B., Mayatepek, E., 2005. Neurological manifestations in lysosomal storage disorders – from pathology to first therapeutic possibilities. *Neuropediatrics* 36, 285–289.
- Hsich, G., Sena-Esteves, M., Breakefield, X.O., 2002. Critical issues in gene therapy for neurodegenerative disease. *Hum. Gene Ther.* 13, 579–604.
- Jeyakumar, M., Dwek, R.A., Butters, T.D., Platt, F.M., 2005. Storage solutions: treating lysosomal disorders of the brain. *Nat. Rev., Neurosci.* 6, 713–725.
- Kemper, A.R., Hwu, W.L., Lloyd-Puryear, E., Kishnani, P.S., 2007. Newborn screening for Pompe disease: synthesis of the evidence and development of screening recommendations. *Pediatrics* 120, e1327–e1334.
- Kohn, D.B., Parkman, R., 1997. Gene therapy for newborns. *FASEB J.* 11, 635–639.
- Lane, S.C., Jolly, R.D., Schmechel, D.E., Alroy, J., Boustany, R.M., 1996. Apoptosis as the mechanism of neurodegeneration in Batten's disease. *J. Neurochem.* 67, 677–683.
- Li, J., Daly, T.M., 2002. Adeno-associated virus-mediated gene transfer to the neonatal brain. *Methods* 28, 203–207.
- Mandel, R.J., Manfredsson, F.P., Foust, K.D., Rising, A., Reimsnyder, S., Nash, K., Burger, C., 2006. Recombinant adeno-associated viral vectors as therapeutic agents to treat neurological disorders. *Mol. Ther.* 13, 463–483.
- Meikle, P.J., Grasby, D.J., Dean, C.J., Lang, D.L., Bockmann, M., Whittle, A.M., Fietz, M.J., Simonsen, H., Fuller, M., Brooks, D.A., Hopwood, J.J., 2006. Newborn screening for lysosomal storage disorders. *Mol. Genet. Metab.* 88, 307–314.
- Ming, G.L., Song, H., 2005. Adult neurogenesis in the mammalian central nervous system. *Annu. Rev. Neurosci.* 28, 223–250.
- National Newborn Screening and Genetics Resource Center (NNSGRC) National Newborn Screening Status Report, 2008. <http://genes-r-us.uthscsa.edu/nbsdisorders.pdf> (Last accessed Wed April 2, 2008).
- Neufeld, E.F., 1991. Lysosomal storage diseases. *Annu. Rev. Biochem.* 60, 257–280.
- Olsson, M., Bentlage, C., Wictorin, K., Campbell, K., Bjorklund, A., 1997. Extensive migration and target innervation by striatal precursors after grafting into the neonatal striatum. *Neuroscience* 79, 57–78.
- Passini, M.A., Wolfe, J.H., 2001. Widespread gene delivery and structure-specific patterns of expression in the brain after intraventricular injections of neonatal mice with an adeno-associated virus vector. *J. Virol.* 75, 12382–12392.
- Passini, M.A., Watson, D.J., Vite, C.H., Landsburg, D.J., Feigenbaum, A.L., Wolfe, J.H., 2003. Intraventricular brain injection of adeno-associated virus type 1 (AAV1) in neonatal mice results in complementary patterns of neuronal transduction to AAV2 and total long-term correction of storage lesions in the brains of beta-glucuronidase-deficient mice. *J. Virol.* 77, 7034–7040.
- Passini, M.A., Dodge, J.C., Bu, J., Yang, W., Zhao, Q., Sondhi, D., Hackett, N.R., Kaminsky, S.M., Mao, Q., Shihabuddin, L.S., Cheng, S.H., Sleat, D.E., Stewart, G.R., Davidson, B.L., Lobel, P., Crystal, R.G., 2006. Intracranial delivery of CLN2 reduces brain pathology in a mouse model of classical late infantile neuronal ceroid lipofuscinosis. *J. Neurosci.* 26, 1334–1342.
- Rafi, M.A., Zhi, R.H., Passini, M.A., Curtis, M., Vanier, M.T., Zaka, M., Luzzi, P., Wolfe, J.H., Wenger, D.A., 2005. AAV-mediated expression of galactocerebrosidase in brain results in attenuated symptoms and extended life span in murine models of globoid cell leukodystrophy. *Mol. Ther.* 11, 734–744.
- Shen, J.S., Watabe, K., Ohashi, T., Eto, Y., 2001. Intraventricular administration of recombinant adenovirus to neonatal twitcher mouse leads to clinicopathological improvements. *Gene Ther.* 8, 1081–1087.
- Shevtsova, Z., Malik, J.M., Michel, U., Bahr, M., Kugler, S., 2005. Promoters and serotypes: targeting of adeno-associated virus vectors for gene transfer in the rat central nervous system in vitro and in vivo. *Exp. Physiol* 90, 53–59.
- Sidman, R.L., Li, J., Stewart, G.R., Clarke, J., Yang, W., Snyder, E.Y., Shihabuddin, L.S., 2007. Injection of mouse and human neural stem cells into neonatal Niemann–Pick A model mice. *Brain Res.* 1140, 195–204.
- Sleat, D.E., Donnelly, R.J., Lackland, H., Liu, C.G., Sohar, I., Pullarkat, R.K., Lobel, P., 1997. Association of mutations in a lysosomal protein with classical late-infantile neuronal ceroid lipofuscinosis. *Science* 277, 1802–1805.
- Sleat, D.E., Wiseman, J.A., El-Banna, M., Kim, K.H., Mao, Q., Price, S., Macauley, S.L., Sidman, R.L., Shen, M.M., Zhao, Q., Passini, M.A., Davidson, B.L., Stewart, G.R., Lobel, P., 2004. A mouse model of classical late-infantile neuronal ceroid lipofuscinosis based on targeted disruption of the CLN2 gene results in a loss of tripeptidyl-peptidase I activity and progressive neurodegeneration. *J. Neurosci.* 24, 9117–9126.
- Sondhi, D., Hackett, N.R., Apblett, R.L., Kaminsky, S.M., Pergolizzi, R.G., Crystal, R.G., 2001. Feasibility of gene therapy for late neuronal ceroid lipofuscinosis. *Arch. Neurol.* 58, 1793–1798.
- Sondhi, D., Hackett, N.R., Peterson, D.A., Stratton, J., Baad, M., Travis, K.M., Wilson, J.M., Crystal, R.G., 2007. Enhanced survival of the LINCL mouse following CLN2 gene transfer using the rh.10 rhesus macaque-derived adeno-associated virus vector. *Mol. Ther.* 15, 481–491.
- Steinfeld, R., Heim, P., von, G.H., Meyer, K., Ullrich, K., Goebel, H.H., Kohlschutter, A., 2002. Late infantile neuronal ceroid lipofuscinosis: quantitative description of the clinical course in patients with CLN2 mutations. *Am. J. Med. Genet.* 112, 347–354.
- Taymans, J.M., Vandenberghe, L.H., Haute, C.V., Thiry, I., Deroose, C.M., Mortelmans, L., Wilson, J.M., Debyser, Z., Baekelandt, V., 2007. Comparative analysis of adeno-associated viral vector serotypes 1, 2, 5, 7, and 8 in mouse brain. *Hum. Gene Ther.* 18, 195–206.
- Therrell, B.L., Adams, J., 2007. Newborn screening in North America. *J. Inher. Metab. Dis.* 30, 447–465.
- Vellodi, A., 2005. Lysosomal storage disorders. *Br. J. Haematol.* 128, 413–431.
- Waddington, S.N., Kennea, N.L., Buckley, S.M., Gregory, L.G., Themis, M., Coutele, C., 2004. Fetal and neonatal gene therapy: benefits and pitfalls. *Gene Ther.* 11 (Suppl 1), S92–S97.
- Watson, D.J., Passini, M.A., Wolfe, J.H., 2005. Transduction of the choroid plexus and ependyma in neonatal mouse brain by vesicular stomatitis virus glycoprotein-pseudotyped lentivirus and adeno-associated virus type 5 vectors. *Hum. Gene Ther.* 16, 49–56.
- Wilcken, B., 2007. Recent advances in newborn screening. *J. Inher. Metab. Dis.* 30, 129–133.
- Williams, R.E., Gottlob, I., Lake, B.D., Goebel, H.H., Winchester, B.G., Wheeler, R.B., 1999. CLN2 classic late infantile NCL. In: Goebel, H.H. (Ed.), *The Neuronal Ceroid Lipofuscinoses (Batten Disease)*. IOS Press, pp. 37–53.
- Worgall, S., Kekatpure, M.V., Heier, L., Ballon, D., Dyke, J.P., Shungu, D., Mao, X., Kosofsky, B., Kaplitt, M.G., Souweidane, M.M., Sondhi, D., Hackett, N.R., Hollmann, C., Crystal, R.G., 2007. Neurological deterioration in late infantile neuronal ceroid lipofuscinosis. *Neurology* 69, 521–535.
- Zhao, G., McCarthy, N.F., Sheehy, P.A., Taylor, R.M., 2007. Comparison of the behavior of neural stem cells in the brain of normal and twitcher mice after neonatal transplantation. *Stem Cells Dev.* 16, 429–438.
- Zhou, H., Lund, R.D., 1993. Effects of the age of donor or host tissue on astrocyte migration from intracerebral xenografts of corpus callosum. *Exp. Neurol.* 122, 155–164.
- Zolotukhin, S., Potter, M., Hauswirth, W.W., Guy, J., Muzyczka, N., 1996. A "humanized" green fluorescent protein cDNA adapted for high-level expression in mammalian cells. *J. Virol.* 70, 4646–4654.

Gene therapy for late infantile neuronal ceroid lipofuscinosis: neurosurgical considerations

Clinical article

MARK M. SOUWEIDANE, M.D.,^{1,5} JUSTIN F. FRASER, M.D.,¹ LISA M. ARKIN, M.D.,²
DOLAN SONDHI, PH.D.,³ NEIL R. HACKETT, PH.D.,³ STEPHEN M. KAMINSKY, PH.D.,³
LINDA HEIER, M.D.,⁴ BARRY E. KOSOFSKY, M.D., PH.D.,⁵ STEFAN WORGALL, M.D., PH.D.,^{3,5}
RONALD G. CRYSTAL, M.D.,³ AND MICHAEL G. KAPLITT, M.D., PH.D.¹

Departments of ¹Neurological Surgery, ³Genetic Medicine, ⁴Radiology, and ⁵Pediatrics, Weill Cornell Medical College, Cornell University, New York, New York; and ²University of Pennsylvania School of Medicine, Philadelphia, Pennsylvania

Object. The authors conducted a phase I study of late infantile neuronal ceroid lipofuscinosis using an adeno-associated virus serotype 2 (AAV2) vector containing the deficient *CLN2* gene (AAV2_{CU}hCLN2). The operative technique, radiographic changes, and surgical complications are presented.

Methods. Ten patients with late infantile neuronal ceroid lipofuscinosis disease each underwent infusion of AAV2_{CU}hCLN2 (3×10^{12} particle units) into 12 distinct cerebral locations (2 depths/bur hole, 75 minutes/infusion, and 2 μ l/minute). Innovative surgical techniques were developed to overcome several obstacles for which little or no established techniques were available. Successful infusion relied on preoperative stereotactic planning to optimize a parenchymal target and diffuse administration. Six entry sites, each having 2 depths of injections, were used to reduce operative time and enhance distribution. A low-profile rigid fixation system with 6 integrated holding arms was utilized to perform simultaneous infusions within a practical time frame. Dural sealant with generous irrigation was used to avoid CSF egress with possible subdural hemorrhage or altered stereotactic registration.

Results. Radiographically demonstrated changes were seen in 39 (65%) of 60 injection sites, confirming localization and infusion. There were no radiographically or clinically defined complications.

Conclusions. The neurosurgical considerations and results of this study are presented to offer guidance and a basis for the design of future gene therapy or other clinical trials in children that utilize direct therapeutic delivery. (DOI: 10.3171/2010.4.PEDS09507)

KEY WORDS • storage disease • lipofuscinosis • gene therapy • local delivery

GENE therapy has long held the great potential to provide novel treatment options for neurological diseases. While the initial promise of this general field was tempered by slow progress, in recent years there has been a resurgence in the enthusiasm for gene therapy. This revival has been led by several new human clinical trials for a variety of neurodegenerative disorders including Parkinson, Alzheimer, and Canavan disease.^{2,5,9,14,15,28} One of the unique limitations of CNS gene therapy is the

Abbreviations used in this paper: AAV2 = adeno-associated virus 2; ASPA = aspartoacylase; LINCL = late infantile neuronal ceroid lipofuscinosis.

blood-brain barrier, which prevents current-generation genetic vectors from entering the brain from the bloodstream. Therefore, a feature common to all CNS gene therapy clinical trials to date is the need to neurosurgically infuse viral vectors harboring the potential therapeutic gene directly into 1 or more planned brain targets. Direct parenchymal injections in some childhood brain tumors are also being explored and simulate some of the technical considerations in gene therapy.¹² Because no commercial system is currently optimized for direct infusions into brain parenchyma, each trial has incorporated different infusion equipment and methods developed by the individual investigators. Although some of the neuro-

surgical methodology has been briefly described in past reports, detailed discussions of the specific neurosurgical problems addressed in any study have been lacking. Since these issues can be limiting to the success of even very promising new gene therapies, a detailed analysis could significantly affect the future development and widespread use of this technology in the human brain.

We recently conducted a phase I study for the treatment of LINCL using an AAV2 vector containing the deficient *CLN2* gene (AAV2_{CU}hCLN2).^{24,29} Ten children underwent an innovative and hitherto undefined neurosurgical procedure aimed at administering AAV2_{CU}hCLN2 in a safe and potentially effective manner. In the design of a neurosurgical approach for these children, we used our experience with human CNS gene therapy but also accounted for several unique features of this specific disorder, including the demand for a large-scale target, the presence of global cerebral atrophy, the need for simultaneous infusions at multiple sites, and the potential for large-volume CSF egress. We describe our approach and the implementation of the neurosurgical techniques in this trial. Our results highlight the importance of early involvement and close collaboration of neurosurgeons with other physicians and scientists not only in the execution but also in the design of new therapeutic approaches and their translation into human clinical trials.

Methods

Ten children were selected to participate in an open-label phase I study of gene therapy for the treatment of LINCL. The study background, selection criteria, AAV vector production methods, and results have been reported in detail.^{1,3,4,17,22,24,29} The study was completed at the New York Presbyterian Hospital, Weill Cornell Medical College, Cornell University. The research protocol was reviewed and approved by the Weill Cornell Institutional Review Board, Institutional Biosafety Committee, NIH/General Clinical Research Center Pediatric Scientific Advisory Committee, and Data Safety Monitoring Board. The protocol was also reviewed by the NIH/Recombinant DNA Advisory Committee and an Investigational New Drug application was approved by the Center for Biologics Evaluation and Research, US FDA (BBIND 11481). The parents of all participating children provided informed consent.

Preoperative Imaging and Target Planning

General anesthesia was induced in each child, and preoperative MR imaging of the brain was performed for stereotactic planning. Regardless of age, all patients required anesthesia for imaging given their developmental regression. Entry site and trajectory planning was emphasized given the exaggerated degree of cerebral atrophy in this patient population. From the preoperative MR imaging studies, entry sites were selected on a BrainLAB workstation (BrainLAB USA) with 2 principal goals. The first major objective was to achieve a diffuse distribution of the injected virus over the supratentorial compartment. In an effort to realize such spatial orientation, 3 entry sites over each cerebral hemisphere were selected. Bur

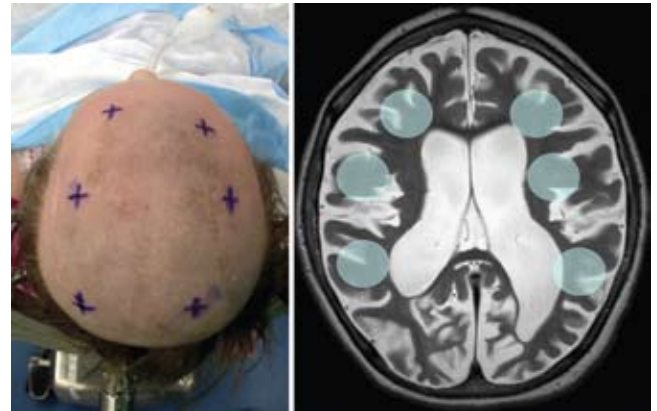


FIG. 1. **Left:** Intraoperative image of entry sites selected with preoperative stereotactic planning. **Right:** Axial T2-weighted MR image demonstrating the typical brain of a patient with Batten disease. *High-lighted circles* represent the 6 proposed target areas for *CLN2* AAV2 vector infusion.

holes were spaced with the goal of 1 bur hole each at the frontal pole, the midfrontal region, and the parietal-occipital region (Fig. 1). The second major goal in selecting entry sites was to avoid routes into or through a sulcus, thus minimizing vascular injury and subarachnoid instillation of vector (Fig. 2). Given the degree of atrophy in these patients, this second goal was generally limiting in determining bur hole sites and catheter trajectories, particularly when the desire to avoid traversing eloquent cortex was also considered.

Frameless Navigation and Entry Site Localization

From the MR imaging suite, the child was transported to the operating room, and rigid fixation was applied using a Sugita head frame (Mizuho Medical, Inc.)—a head frame that provides a secure mount, maintains a low

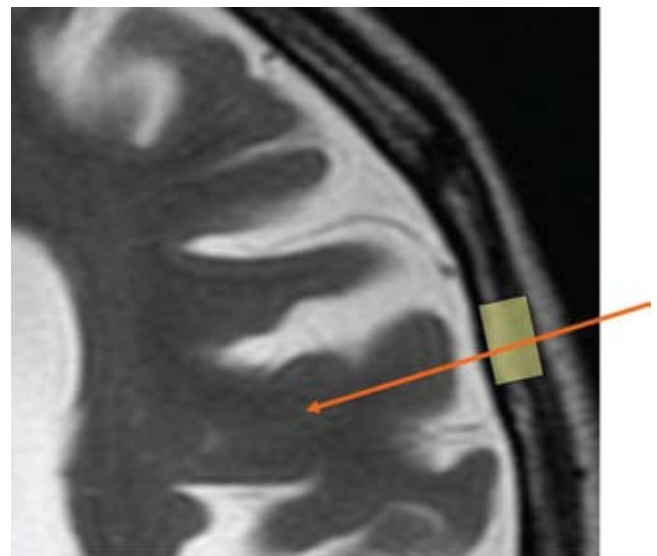


FIG. 2. Simulated planning for bur hole position (*yellow highlight*) and cannula trajectory (*orange arrow*). Planning is conducted with the intent to avoid sulci, whose dimensions are exaggerated in patients with LINCL.

Gene therapy for late infantile neuronal ceroid lipofuscinosis

profile over the cranial convexities, and provides access to most of the cranial vault. In anticipating the sites of the bur holes, fixation of the frame was low, based on the inferior temporal-occipital regions, and was angled to be particularly low posteriorly to facilitate placement of the parietal-occipital bur hole (Fig. 3). A single dose of a prophylactic antibiotic was administered: cefazolin 25 mg/kg, maximum of 1 g. Steroids, hyperosmolar agents, and hypocarbia were avoided in attempt to minimize cerebral relaxation, which would likely exacerbate CSF loss in the setting of severe atrophy.

The patient was registered to the preoperative MR image using a minimum of 5 fiducial markers. Preplanned entry sites were marked on the scalp, and surgical preparations were made. A local anesthetic (0.25% bupivacaine with 1/100,000 parts epinephrine) was administered at each planned entry site. After skin incisions for each bur hole, Alm self-retaining retractors (Miltex, Inc.) were used to maximize access while minimizing obstruction to the workspace. Bur holes were created using an 11-mm perforator (Codman). A bur hole was used instead of a twist drill given the preference for visual verification of a gyrus without a major intervening vascular structure during cannula placement. Dural opening was performed only at the time of cannula placement and was sequenced so that the posterior locations were accessed last in an effort to decrease gravity-dependent CSF loss. A cruciate dural incision and subsequent bipolar coagulation were used for intradural access. The operating microscope was used for greater precision during dural opening to minimize the likelihood of premature violation of the arachnoid and attendant CSF loss.

Catheter Insertion and AAV Infusion

For each site, a 20-gauge spinal needle was used as a rigid guide for insertion of a flexible, fused silica polyim-



Fig. 4. Photograph of a 20-gauge spinal needle with the fused silica catheter prior to stereotactic insertion. The spinal needle serves as a linear guide and a protective sheath for rigid fixation.

ide-coated catheter (inner diameter approximately 150 μm and outer diameter 362 μm , Polymicro Technologies; Fig. 4). Each catheter was connected to a separate syringe, thus maintaining an independent system for each infusion. Before insertion of the spinal needle, the catheter was inserted until its tip was flush with the needle tip. The catheter was then marked with a marking pen at the top of the needle as a measure of the point of interface between the catheter and the brain prior to deeper insertion. Using the operating microscope, the pial surface overlying a gyrus was coagulated. The spinal needle was affixed to a flexible retractor arm of the head frame and oriented to match the predetermined stereotactic trajectory based on the preoperative plan. The guide needle itself was not tracked given the small size and number of infusion sites; rather, the trajectories in nearly all cases were chosen to be orthogonal to the cortical surface. Where an orthogonal tract could not be generated—that is, one that would not traverse a subarachnoid space and would conform to the predetermined safety and efficacy criteria—an angled trajectory was used, and the angle of guide needle insertion was visually determined to match the presurgical plan. Retractor arms and needles were all initially set to the planned orientation prior to skin opening but after fiducial registration to ensure that the orientation of the head frame relative to the planned entry sites would permit proper localization and locking of the arm without excessive torque or tension. The needle was then inserted just below the pial surface, and the retractor arm was secured with rigid fixation. The infusion system was run to flush out the dead space and confirm flow of the vector solution, until a drop of vector solution was seen at the tip of the glass catheter. The droplet was removed with sterile gauze to ensure that gene therapy vector did not flow onto the cortical surface. The guide needle stylet was removed, and a borosilicate catheter was advanced to the initial target depth, which was chosen to be just deep to adjacent sulci in the white matter to facilitate spread to distant structures. Generally, this distance was 2 cm from the cortical surface, with a range of 1.7–2.5 cm. This target depth was based on the zero reference being defined by the visualized cortical surface rather than the preoperative MR image given some expectation of brain shift with dural opening. Each catheter for each site was marked with a folded Steri-strip at the distance from the initial zero mark that would place the tip at the desired depth from the cortical surface. The Steri-strip also served as a stop to hold the glass catheter in place during the infusion.

Following catheter placement, the entry site was sealed with a thrombin-soaked absorbable gelatin sponge

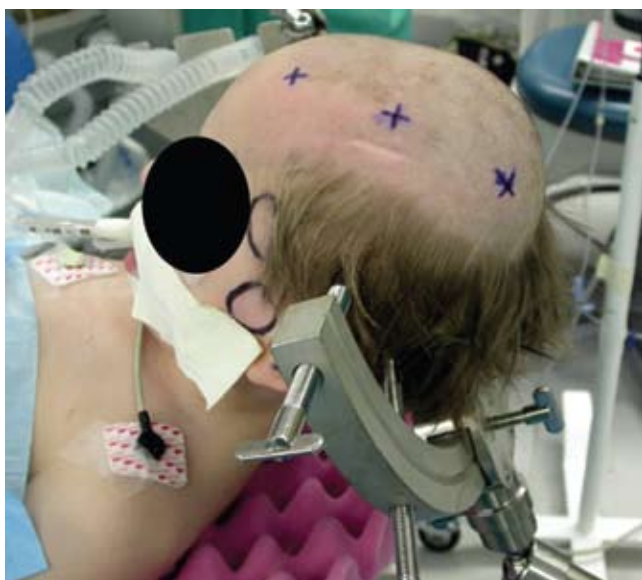


Fig. 3. Photograph featuring the position of the head frame, secured with 4 points of fixation. The frame is positioned inferiorly on the temporal and occipital bones to allow access to the cranial vault overlying the sites of planned injection.

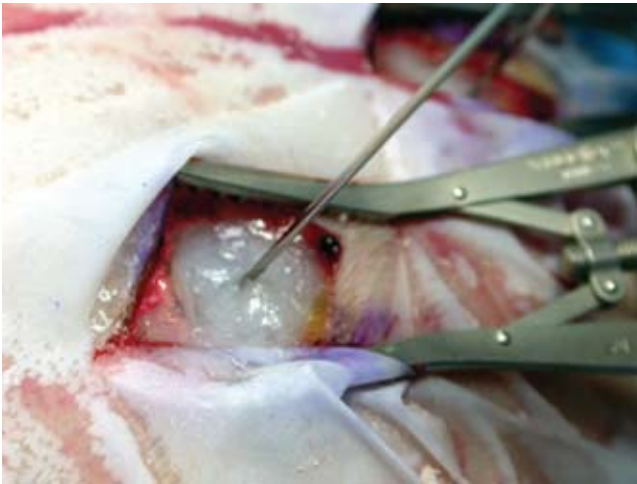


FIG. 5. Photograph of an example of an entry site, highlighting the low-profile retractor system, fixation of the spinal needle, and fibrin sealant.

(Pfizer, Inc.) and fibrin sealant (Baxter) to minimize CSF egress (Fig. 5). Five minutes after cannulation, 150 μ l of 2×10^9 packaged AAV2 units/ μ l was injected by a micro-perfusion pump (Hamilton) at 2 μ l/minute to each of the 6 sites in parallel (Fig. 6). Five minutes after completion of the infusion, to minimize backflow along the tract, catheters were retracted 1 cm, a new Steri-strip was used to hold the catheter in place, and the injections were repeated. The goal of the second set of infusions was to maximize infusion within the gyrus just deep to the bur hole. These 2 sets of infusions resulted in 2 infusions through each of the 6 bur holes, for a total administration of 1800 μ l (3.6×10^{12} particle units). After an additional 5 minutes to again prevent backflow, catheters were removed, the subdural space was generously irrigated, fibrin sealant was applied to the dural opening, and the wounds were closed in a multilayered fashion.

Postoperative Imaging

Postoperative MR imaging with FLAIR and gradient relaxed echo sequences was performed within the first 24 hours after the surgical procedure (Fig. 7). Each child was monitored in a pediatric intensive care unit for a minimum of 24 hours postoperatively and then transferred to

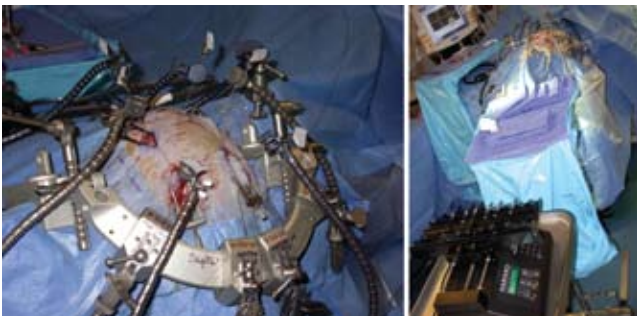


FIG. 6. Intraoperative images depicting simultaneous infusion through 6 cannulas fixed in place with modified retractor arms of an integrated head holder (left) and the relative positions of the multisyringe microinfusion pump and sterile operative field (right).

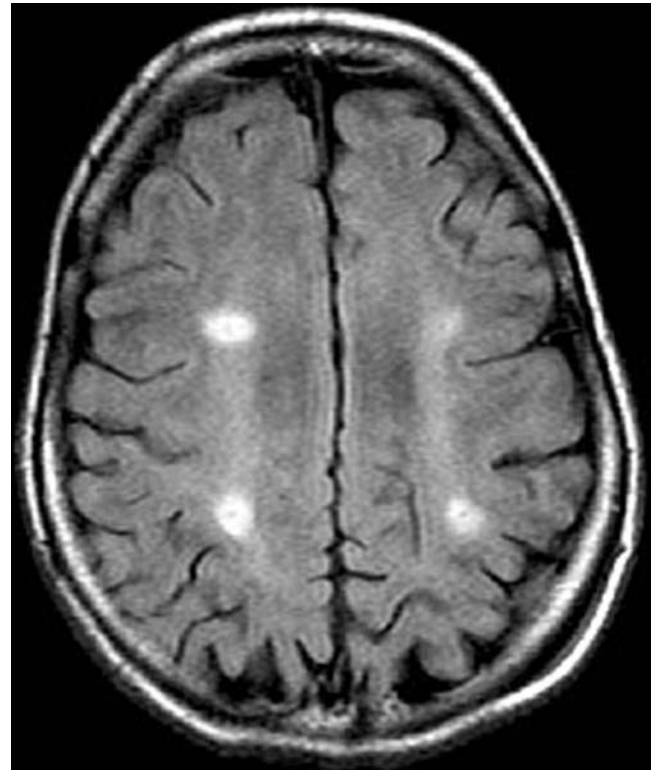


FIG. 7. Representative postoperative axial FLAIR MR image demonstrating areas of infusion as hyperintense signal change.

the Children's Clinical Research Center unit of the Weill Cornell Medical College. The children were discharged from the hospital at the discretion of the clinical team, typically within 7 days after vector administration.

Results

Ten patients underwent the vector infusion procedure without perioperative complication. In total, there were 60 cannula insertions and 120 injections. All planned bur hole sites in all patients were localized with adequate precision using BrainLAB frameless navigation. In 1 case, initial orientation of the Sugita head frame had to be adjusted after initial testing given the potential for steric hindrance of the posterior retractor arms, which created a concerning level of torque and/or prevented locking of the arm. After the frame was adjusted and the fiducial markers were reregistered in this case, the issue was resolved prior to skin opening, the planned entry sites were localized, and the retractor arms were able to lock comfortably. All catheters remained at the desired depth with no inadvertent migrations throughout each infusion.

Precise targeting and evidence of hemorrhage were evaluated on postoperative MR imaging. Target site infusion was measurably achieved in 65% of sites (39 of 60 sites), based on increased FLAIR signal in the region of the planned target. Each of these "positive" sites demonstrated a FLAIR change of at least 0.5 cm, which likely represented a concentrated fluid signal from the infusion rather than a tissue reaction to a 150- μ m, biologically inert glass catheter. Particular to the anatomical site, the lowest rate of

Gene therapy for late infantile neuronal ceroid lipofuscinosis

TABLE 1: Postoperative radiographic evidence of successful infusion

Infusion Site	Postop Radiographic Success Rate
lt anterior frontal	6/10
rt anterior frontal	5/10
lt posterior frontal	9/10
rt posterior frontal	8/10
lt parietal	5/10
rt parietal	6/10
overall (%)	39/60 (65)

evident injection was 50.0%, whereas the highest rate was 90.0% (Table 1). There were no postoperative infections or clinically relevant hemorrhages. There was no perioperative morbidity or death related to the surgery.

Discussion

Gene therapy for diseases of the CNS has long represented a theoretical tool of the future, primarily existing at the laboratory bench. Recent advances in understanding gene expression and function in neurological diseases, isolating and controlling viral vectors for gene delivery, and developing neurosurgical techniques in navigational guidance have provided a foundation for translating gene therapy from the bench to the operating room. This conversion has been led by several new human clinical trials for a variety of neurodegenerative disorders including Parkinson, Alzheimer, and Canavan disease.^{2,5,9,14,15,28} For Parkinson disease, phase I clinical studies have demonstrated the safety of the direct injection of AAV vectors carrying glutamic acid decarboxylase into the subthalamic nucleus and aromatic l-amino acid decarboxylase into the putamen; further efficacy studies are underway. For Canavan disease, phase I trial data showed the safety of intraparenchymally injecting AAV carrying human ASPA cDNA. These clinical experiences with AAV utilization provide a foundation for its application in other trials for genetic diseases.

Given the increasing translation to human studies of gene delivery for a variety of diseases of the nervous system, it is vital that neurosurgeons understand current techniques and nuances to implement current research and future innovation.^{2,5,9,14,15,28} Further, the evolving role of the neurosurgeon in providing safe therapeutic delivery for oncological purposes in tumors such as the diffuse pontine glioma necessitates similar technical considerations for translation into the clinical arena.^{11,16,21,26,27} Late infantile neuronal ceroid lipofuscinosis, a form of Batten disease, represents a genetic disorder arising from autosomal recessive mutations in the *CLN2* gene. These mutations result in lysosomal protease tripeptidyl peptidase I deficiency and manifest in patients 2–4 years of age with seizures, developmental delay and regression, myoclonus, speech impairment, and ataxia. After extensive animal studies, an AAV2 vector carrying human *CLN2* cDNA was developed, thus establishing the framework

for therapeutic replacement of the deficient gene product.^{3,6,10,17,22–25} In addition to the LINCL trial reported on herein, phase I trials for Canavan disease, an autosomal recessive mutation of ASPA causing fatal leukodystrophy, mental retardation, hypotonia, macrocephaly, and seizures are underway to determine the safety and efficacy of the subcortical delivery of AAV carrying ASPA.^{7,10} As such, targeted delivery of gene therapy represents an important developing application of functional neurosurgery in children.⁸ The therapeutic replacement of genes within the CNS requires important technical considerations specific for each disease. With regard to LINCL, several features of the disease warranted a unique technical approach toward gene replacement. Primary distinctive features include the global distribution of diseased neurons and considerable cerebral atrophy. A similar set of practical issues has also been addressed with respect to Canavan disease, a childhood leukodystrophy that shares these anatomical features with LINCL.¹⁰

Our use of frameless navigation to target areas of the cortex and avoid large subarachnoid spaces combined our experiences with gene therapy to address an issue unique to global pediatric neurogenetic disorders. For adult neurodegenerative diseases that have particular pathophysiological neural pathway deficiencies along with the involvement of particular deep brain nuclei, such as Parkinson disease, stereotaxis is crucial to optimize infusion to a specific target and minimize the risk of off-target adverse effects. Batten disease, Canavan disease, and similar disorders result in widespread pathological changes throughout the cerebral cortex. As such, no single target for *CLN2* gene transfer would adequately overcome the pathophysiological progression. A tactic of using multiple sites of administration was relied on to achieve better spatial distribution balanced by the practical considerations of surgery. For this reason, 6 pairs of injection sites were selected (3 in either hemisphere), which mimicked a similar approach used in a prior Canavan disease gene therapy study.¹⁵ However, authors in that study did not use stereotaxis and instead chose 6 bur holes based on a standard location in all patients relative to scalp landmarks, which did not account for the underlying brain anatomy. Since animal studies suggest that AAV vectors do not penetrate deep into the brain from CSF spaces, we believed it was important to maximize delivery directly into brain parenchyma.

Another concern was the potential increased risk of developing an immune reaction to the AAV vector by inadvertent delivery of large amounts of virus into the CSF, which could lead to both reduced gene delivery and possible adverse effects. Recombinant AAV vectors contain no viral genes and thus without foreign gene expression evoke a minimal inflammatory response, making it an ideal viral delivery option. Examples in the literature of induced anti-AAV capsid immune responses are likely due to very high doses of the vector delivering relevant quantities of capsid protein or the presence of contaminant viral genes. While there are no published data on targeting success in the Canavan disease study,¹⁵ it is interesting to note that the published immunological findings from that trial demonstrated a substantially greater number of patients developing anti-AAV neutralizing an-

tibodies compared with patients in the present study even though the same strain of AAV (AAV2) was used in both studies.²⁹ Although this immunological response could be influenced by a variety of factors, including differences in vector preparation techniques and disease-specific and gene-specific influences, the avoidance of CSF infusion would be expected to reduce the likelihood of developing an anti-AAV immune response. This assertion is further supported by an observation in our gene therapy study of Parkinson disease; even with different patients, different AAV production methods from a distinct facility, a different gene, and the same strain of AAV, no neutralizing antibody response developed in any of those patients following deep infusion into a single parenchymal target.⁹

The chosen stereotactic approach itself was also the basis for other problematic issues surrounding the operative technique. In our gene therapy study of Parkinson disease, a Leksell frame was used to target catheter insertion for infusion into a single site.⁹ When multiple targets are selected for vector infusion, frame-based targeting can only be performed serially. An infused volume of 300 μ l delivered at 2 μ l/minute results in an infusion time of 150 minutes/site (300 minutes total)—this would result in a medically unacceptable operating room time, which would substantially increase the risk of excessive CSF loss and infection. Thus, simultaneous infusion represents not only a technical nuance but also an operative necessity. Successful and accurate concurrent infusions at multiple targets require a protocol devised to cannulate multiple targets with precision and a reliable multisyringe infusion system specifically designed to handle parallel infusions (Fig. 6); therefore, frameless navigation was chosen. To achieve simultaneous infusions at 6 different sites, however, low-profile instruments are vital to ensure an open working space. Based on our experience with frame-based stereotaxis, however, we believed that it was important not simply to insert the borosilicate catheter unguided into the brain, but to use some form of larger guide tube that could be rigidly fixed to increase the precision of catheter placement and to better stabilize the catheter during a long infusion. However, with 6 bur holes and associated fixed cannulas, the 3D working space, which includes the head frame, retractors, adjustable retractor arms, and cannulas, is compromised. Maintaining such an elaborate scheme while retaining stereotactic precision requires an innovative and sequential method of creating a functional operating system. With an organization featured in Fig. 6 right, the step-wise procedure thus followed an order from anterior to posterior and from left to right, resulting in placement of the left frontal catheter first and placement of the right occipital catheter last. Given the variability in skull anatomy and in surgeon placement of the head frame, testing the accuracy and stability of all clamps before incision was critical to avoid brain injury or the recognition of a problem after some of the catheters were inserted and readjustment was no longer possible. With such operative planning, infusion time was reduced to achieve the desired vector distribution in a practical time frame with precise targeting and no injury to the patient.

Lastly, given the degree of cerebral atrophy and the potential for CSF egress, inherent risks, including subdural hemorrhage and inaccurate stereotactic targeting,

are considerable. This risk of CSF egress with brain shift was addressed in the surgical plan with a sequential order for dural opening (gravity dependent; posterior entry sites opened last) and diligence in isolating the subarachnoid space from air (saline irrigation and fibrin sealant). These measures appear to have been successful since no patient experienced a perioperative subdural hemorrhage, and radiographic evidence of the infusion did not seem to be dependent on a specific bur hole location (anterior vs posterior). It is important to point out that the current method of MR imaging to assess evidence for infusion is potentially misleading. The reported 65% “success” rate as a measure of infusions/targeted site is an estimate. Using postoperative MR imaging does not guarantee that gene delivery occurred but instead documents areas of increased fluid after infusion. But the latter assumes a concentration of fluid that would be detectable, and the technique may not be sensitive enough to detect small infusion volumes, may not be done in an adequate time frame, and is dependent on the acquisition technique. It is likely that some fluid delivery occurred beyond the observed areas but had sufficiently diluted so that it was below the threshold for detection and that the absence of signal at some sites may not reflect failed delivery but could indicate more widespread delivery with a concomitant reduction in the focal concentration necessary for a change in imaging signal. At present, there is no mechanism to distinguish between these very different possibilities in patients. Neither is there an *in vivo* methodology for monitoring the distribution of therapeutic compounds following direct delivery. This issue has been on the forefront of clinical applications in which convection enhanced delivery is being used. Surrogate tracers with MR imaging contrast agents or radioisotopes have been successfully used but have as a major drawback the potential to misrepresent the actual distribution of the therapeutic compound.^{11,16,18–20} Alterations in MR signal, most notably the FLAIR, T2-weighted, and diffusion weighted sequences, have also been used but are problematic when the underlying disease invokes a baseline alteration of that signal prior to delivery.^{13,20} Furthermore, the use of reporter genes or surrogate tracers may increase the chances of immunological recognition of the therapeutic compound, possibly leading to inflammation and vector clearance.

While neurosurgical gene therapy is in its clinical infancy, it is important for neurosurgeons to embrace this field and to develop appropriate operative techniques. From the bench to bedside, the involvement of neurosurgeons is vital to ensure that this field develops in a surgically safe and efficient manner. Neurosurgical participation and design of delivery schemes will become increasingly important to avoid failure in an otherwise promising biological therapy because of technical limitations not always appreciated by nonneurosurgical investigators.

Conclusions

Gene therapy for global cerebral diseases presents a number of anatomical and technical challenges regarding therapeutic delivery. In the absence of a specifically defined anatomical target, wide distribution can be enhanced using multiple sites of delivery, an approach that

does have spatial and temporal constraints. The described neurosurgical technique integrates a number of features into an innovative procedure aimed at minimizing morbidity, optimizing targeting, maximizing spatial distribution, and reducing operative time. The procedure used in this limited clinical study was practical and safe. Reliable methods for measuring the distribution of administered viral particles or the expression of gene products are not yet established but will become increasingly important in assessing treatment efficacy.

Disclosure

Mark M. Souweidane is a paid consultant and serves on the Aesculap Neuroendoscopic Advisory Committee. Michael G. Kaplitt is a founder of and paid consultant for Neurologix, Inc., which was not involved in this study but is developing AAV gene therapy for other disorders. This study was supported in part by the Nathan's Battle Foundation (Greenwood, Indiana); by NIH Grant Nos. U01 NS047458 CTSC UL1-RR024996; and the Will Rogers Memorial Fund (Los Angeles, California).

Author contributions to the study and manuscript preparation include the following. Conception and design: Souweidane, Crystal. Acquisition of data: Souweidane, Arkin, Sondhi, Hackett, Kosofsky, Worgall, Crystal, Kaplitt. Analysis and interpretation of data: Souweidane, Fraser, Kaminsky, Heier, Kosofsky, Crystal, Kaplitt. Drafting the article: Souweidane, Fraser, Kaplitt. Critically revising the article: Souweidane. Reviewed final version of the manuscript and approved it for submission: all authors. Statistical analysis: Kaminsky. Administrative/technical/material support: Arkin, Sondhi, Hackett, Kaminsky, Worgall. Study supervision: Sondhi, Crystal.

Acknowledgments

The authors are grateful for the illustrative work of Mr. Thomas Graves, Thom Graves Media, and the technical assistance of Dr. Paola Leone, University of Medicine and Dentistry of New Jersey.

References

1. Arkin LM, Sondhi D, Worgall S, Suh LH, Hackett NR, Kaminsky SM, et al: Confronting the issues of therapeutic misconception, enrollment decisions, and personal motives in genetic medicine-based clinical research studies for fatal disorders. **Hum Gene Ther** **16**:1028–1036, 2005
2. Christine CW, Starr PA, Larson PS, Eberling JL, Jagust WJ, Hawkins RA, et al: Safety and tolerability of putaminal AADC gene therapy for Parkinson disease. **Neurology** **73**:1662–1669, 2009
3. Crystal RG, Sondhi D, Hackett NR, Kaminsky SM, Worgall S, Stieg P, et al: Clinical protocol. Administration of a replication-deficient adeno-associated virus gene transfer vector expressing the human CLN2 cDNA to the brain of children with late infantile neuronal ceroid lipofuscinosis. **Hum Gene Ther** **15**:1131–1154, 2004
4. Dyke JP, Voss HU, Sondhi D, Hackett NR, Worgall S, Heier LA, et al: Assessing disease severity in late infantile neuronal ceroid lipofuscinosis using quantitative MR diffusion-weighted imaging. **AJNR Am J Neuroradiol** **28**:1232–1236, 2007
5. Feigin A, Kaplitt MG, Tang C, Lin T, Mattis P, Dhawan V, et al: Modulation of metabolic brain networks after subthalamic gene therapy for Parkinson's disease. **Proc Natl Acad Sci U S A** **104**:19559–19564, 2007
6. Hackett NR, Redmond DE, Sondhi D, Giannaris EL, Vassallo E, Stratton J, et al: Safety of direct administration of AAV2(CU)hCLN2, a candidate treatment for the central nervous system manifestations of late infantile neuronal ceroid lipofuscinosis, to the brain of rats and nonhuman primates. **Hum Gene Ther** **16**:1484–1503, 2005
7. Janson C, McPhee S, Bilaniuk L, Haselgrove J, Testaiuti M, Freese A, et al: Clinical protocol. Gene therapy of Canavan disease: AAV-2 vector for neurosurgical delivery of aspartoacylase gene (ASPA) to the human brain. **Hum Gene Ther** **13**:1391–1412, 2002
8. Kaplitt MG, Darakchiev B, During MJ: Prospects for gene therapy in pediatric neurosurgery. **Pediatr Neurosurg** **28**:3–14, 1998
9. Kaplitt MG, Feigin A, Tang C, Fitzsimons HL, Mattis P, Lawlor PA, et al: Safety and tolerability of gene therapy with an adeno-associated virus (AAV) borne GAD gene for Parkinson's disease: an open label, phase I trial. **Lancet** **369**:2097–2105, 2007
10. Leone P, Janson CG, McPhee SJ, During MJ: Global CNS gene transfer for a childhood neurogenetic enzyme deficiency: Canavan disease. **Curr Opin Mol Ther** **1**:487–492, 1999
11. Lonser RR, Warren KE, Butman JA, Quezado Z, Robison RA, Walbridge S, et al: Real-time image-guided direct convective perfusion of intrinsic brainstem lesions. Technical note. **J Neurosurg** **107**:190–197, 2007
12. Luther N, Cheung NK, Dunkel LJ, Fraser JF, Edgar MA, Gutin PH, et al: Intraparenchymal and intratumoral interstitial infusion of anti-glioma monoclonal antibody 8H9. **Neurosurgery** **63**:1166–1174, 2008
13. Mardor Y, Roth Y, Lidar Z, Jonas T, Pfeffer R, Maier SE, et al: Monitoring response to convection-enhanced taxol delivery in brain tumor patients using diffusion-weighted magnetic resonance imaging. **Cancer Res** **61**:4971–4973, 2001
14. Marks WJ Jr, Ostrem JL, Verhagen L, Starr PA, Larson PS, Bakay RA, et al: Safety and tolerability of intraputamenal delivery of CERE-120 (adeno-associated virus serotype 2-neurturin) to patients with idiopathic Parkinson's disease: an open-label, phase I trial. **Lancet Neurol** **7**:400–408, 2008
15. McPhee SW, Janson CG, Li C, Samulski RJ, Camp AS, Francis J, et al: Immune responses to AAV in a phase I study for Canavan disease. **J Gene Med** **8**:577–588, 2006
16. Murad GJ, Walbridge S, Morrison PF, Szerlip N, Butman JA, Oldfield EH, et al: Image-guided convection-enhanced delivery of gemcitabine to the brainstem. **J Neurosurg** **106**:351–356, 2007
17. Passini MA, Dodge JC, Bu J, Yang W, Zhao Q, Sondhi D, et al: Intracranial delivery of CLN2 reduces brain pathology in a mouse model of classical late infantile neuronal ceroid lipofuscinosis. **J Neurosci** **26**:1334–1342, 2006
18. Sampson JH, Akabani G, Archer GE, Berger MS, Coleman RE, Friedman AH, et al: Intracerebral infusion of an EGFR-targeted toxin in recurrent malignant brain tumors. **Neuro Oncol** **10**:320–329, 2008
19. Sampson JH, Brady ML, Petry NA, Croteau D, Friedman AH, Friedman HS, et al: Intracerebral infusate distribution by convection-enhanced delivery in humans with malignant gliomas: descriptive effects of target anatomy and catheter positioning. **Neurosurgery** **60** (2 Suppl 1):ONS89–ONS99, 2007
20. Sampson JH, Raghavan R, Provenzale JM, Croteau D, Reardon DA, Coleman RE, et al: Induction of hyperintense signal on T2-weighted MR images correlates with infusion distribution from intracerebral convection-enhanced delivery of a tumor-targeted cytotoxin. **AJR Am J Roentgenol** **188**:703–709, 2007
21. Sandberg DI, Edgar MA, Souweidane MM: Convection-enhanced delivery into the rat brainstem. **J Neurosurg** **96**:885–891, 2002
22. Sondhi D, Hackett NR, Apblett RL, Kaminsky SM, Pergolizzi RG, Crystal RG: Feasibility of gene therapy for late infantile neuronal ceroid lipofuscinosis. **Arch Neurol** **58**:1793–1798, 2001
23. Sondhi D, Hackett NR, Peterson DA, Stratton J, Baad M, Travis KM, et al: Enhanced survival of the LINCL mouse following CLN2 gene transfer using the rh.10 rhesus macaque-derived adeno-associated virus vector. **Mol Ther** **15**:481–491, 2007

24. Sondhi D, Peterson DA, Edelstein AM, del Fierro K, Hackett NR, Crystal RG: Survival advantage of neonatal CNS gene transfer for late infantile neuronal ceroid lipofuscinosis. **Exp Neurol** **213**:18–27, 2008
25. Sondhi D, Peterson DA, Giannaris EL, Sanders CT, Mendez BS, De B, et al: AAV2-mediated CLN2 gene transfer to rodent and non-human primate brain results in long-term TPP-I expression compatible with therapy for LINCL. **Gene Ther** **12**:1618–1632, 2005
26. Souweidane MM, Occhiogrosso G, Mark EB, Edgar MA: Interstitial infusion of IL13-PE38QQR in the rat brain stem. **J Neurooncol** **67**:287–293, 2004
27. Souweidane MM, Occhiogrosso G, Mark EB, Edgar MA, Dunkel IJ: Interstitial infusion of carmustine in the rat brain stem with systemic administration of O6-benzylguanine. **J Neurooncol** **67**:319–326, 2004
28. Tuszynski MH, Thal L, Pay M, Salmon DP, U HS, Bakay R, et al: A phase 1 clinical trial of nerve growth factor gene therapy for Alzheimer disease. **Nat Med** **11**:551–555, 2005
29. Worgall S, Sondhi D, Hackett NR, Kosofsky B, Kekatpure MV, Neyzi N, et al: Treatment of late infantile neuronal ceroid lipofuscinosis by CNS administration of a serotype 2 adeno-associated virus expressing CLN2 cDNA. **Hum Gene Ther** **19**:463–474, 2008

Manuscript submitted December 3, 2009.

Accepted April 12, 2010.

Portions of this work were presented at the 2006 annual meetings of the American Society of Pediatric Neurosurgeons held in Great Exuma, Bahamas, and the Congress of Neurological Surgeons held in Chicago, Illinois.

Address correspondence to: Mark M. Souweidane, M.D., Department of Neurological Surgery, Cornell University-Weill Medical College, 525 E. 68th Street, Box 99, New York, New York 10021. email: mmsouwei@med.cornell.edu.

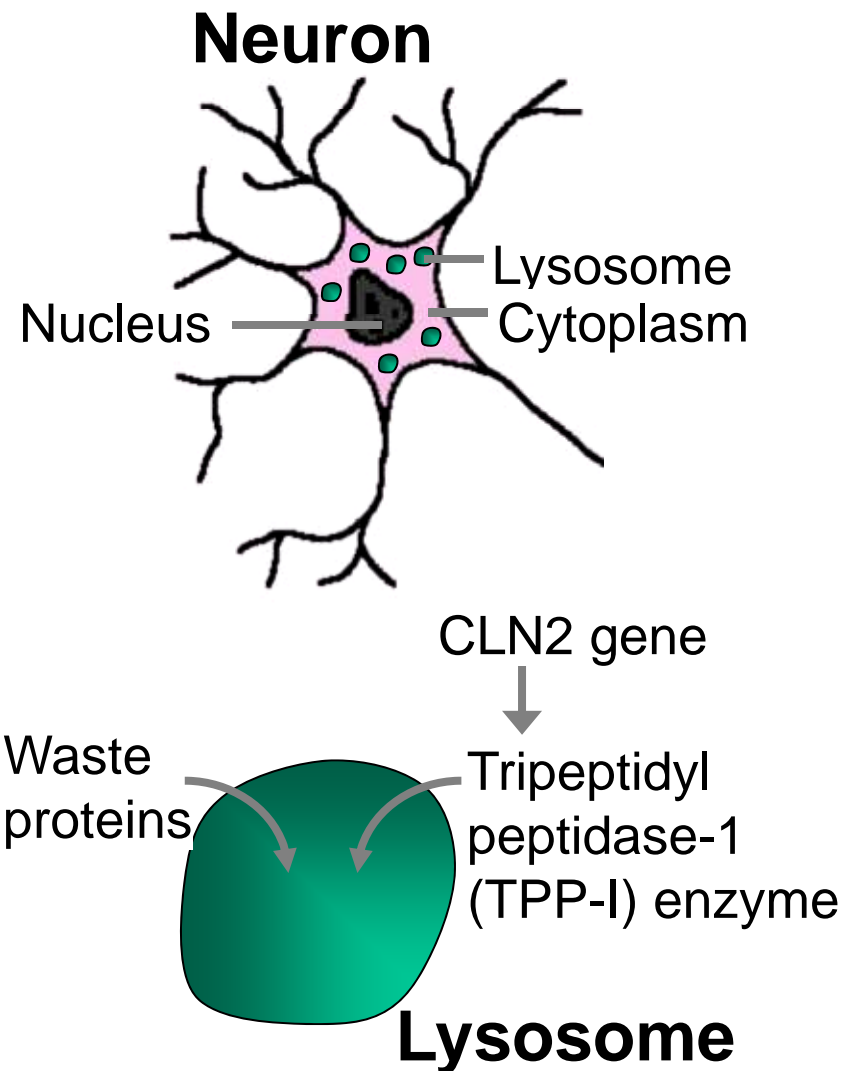
Long Term Expression and Safety of Administration of AAVrh.10hCLN2, a Candidate Treatment for Late Infantile Neuronal Lipofuscinosis, to the Brain of Non-human Primates

D Sondhi, NR Hackett, K del Fierro, AM Edelstein,
RG Crystal

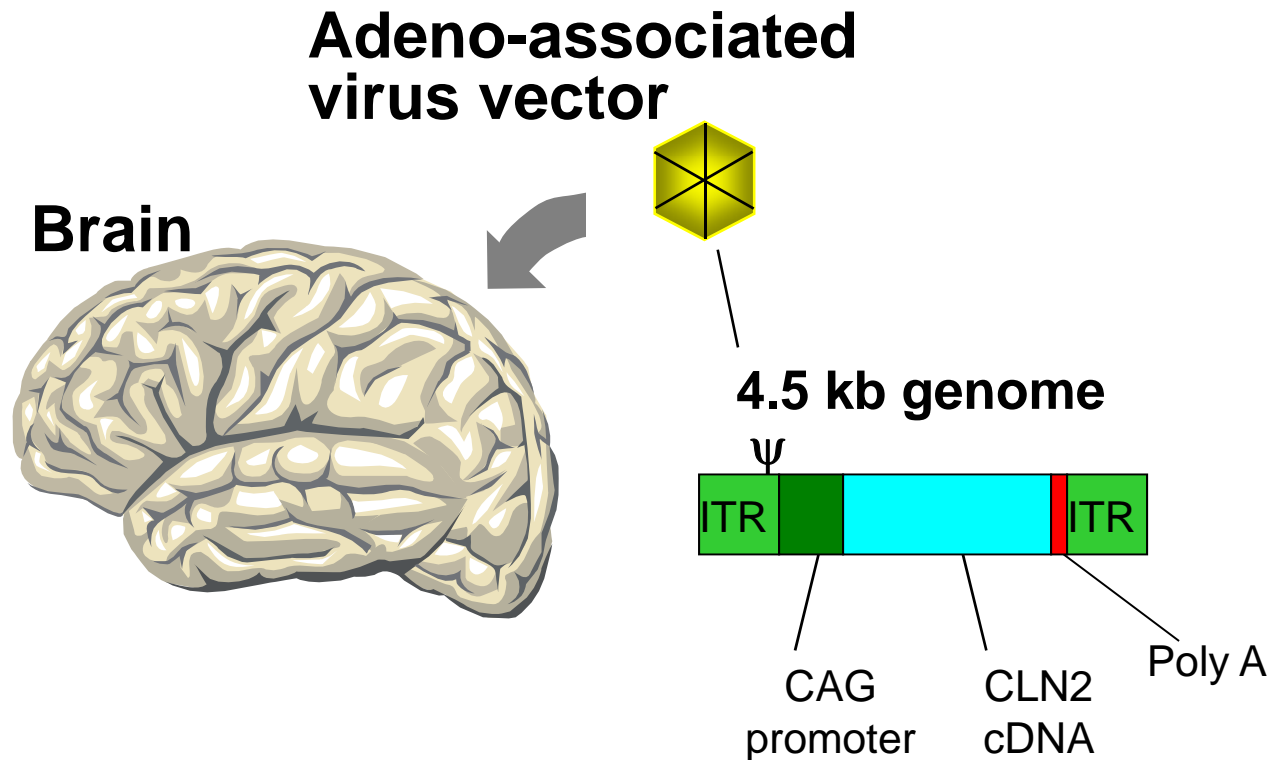
Weill Cornell Medical College, New York NY

Late Infantile Neuronal Ceroid Lipofuscinosis (LINCL, Batten Disease)

- Rare, autosomal recessive, fatal lysosomal storage disease with extensive CNS neurodegeneration
- Caused by mutations in the CLN2 gene resulting in a deficiency of the lysosomal protease tripeptidyl peptidase I (TPP-I)
- Deficiency of TPP-I leads to accumulation of undigested proteins in lysosomes and neuronal death



AAV-mediated Gene Therapy for LINCL



- **Clinical trial of direct CNS administration of an AAV2-based vector coding for CLN2 to 10 children with LINCL showed a slowing down of the progression of disease ***

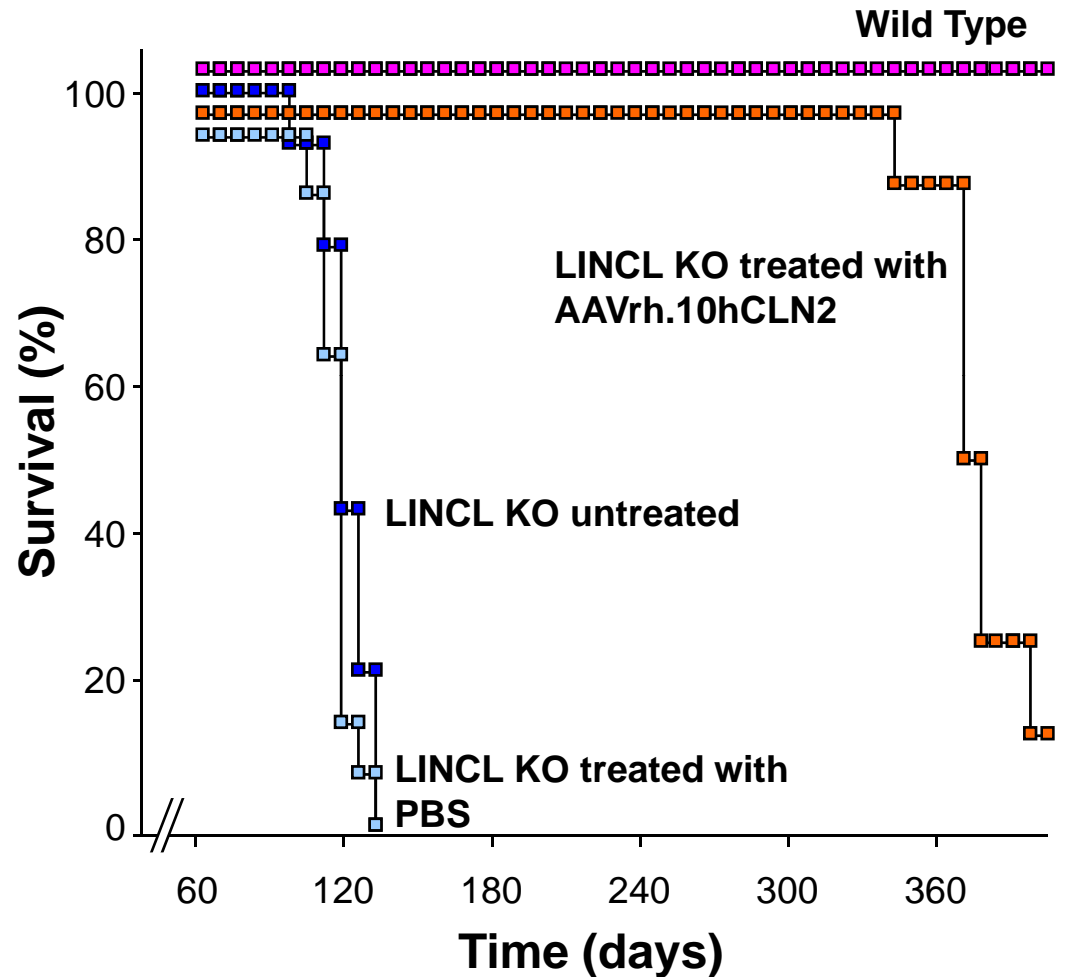
* Worgall S et al, Hum Gen Ther 2008

Question

- Is there an AAV vector that is more effective than AAV2 in expressing the TPP-I protein throughout the CNS?

Strategy

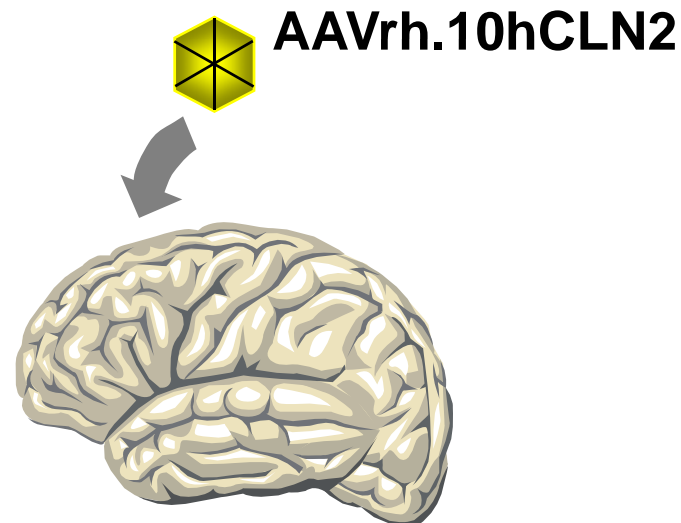
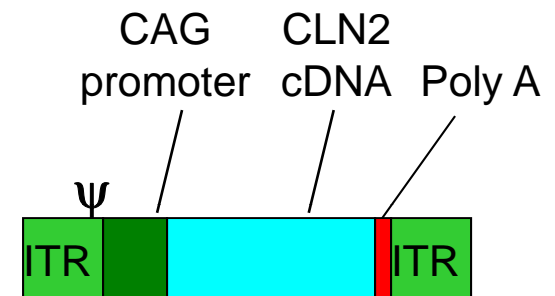
- After testing multiple AAV serotypes, the non-human primate serotype AAVrh.10 provided the best gene transfer of the CLN2 cDNA to the CNS*



* Sondhi D et al, Mol Ther 2007; Sondhi D et al, Exp Neurol 2008

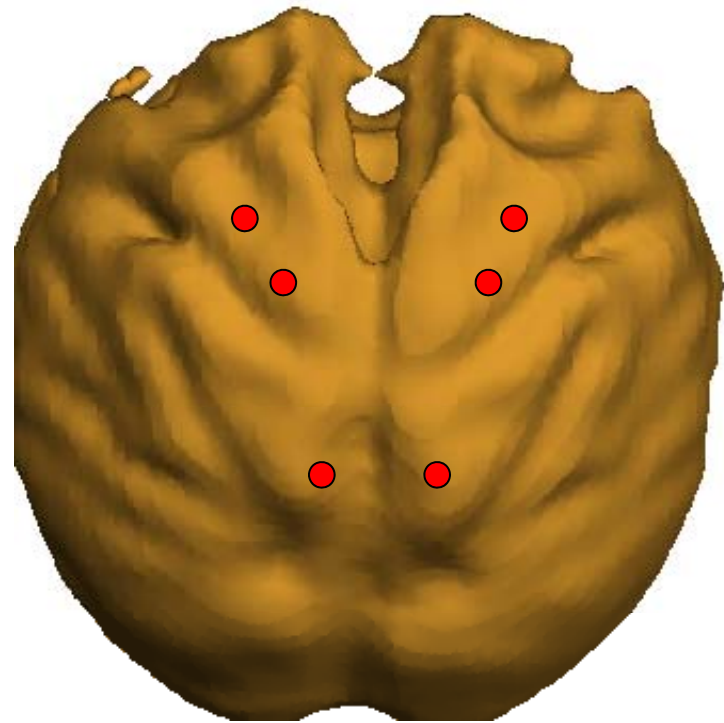
Moving AAVrh.10hCLN2 to Humans - Toxicology and TPP-I Expression in the Non-human Primate CNS

- Produce the AAVrh.10hCLN2 vector under GMP conditions
- Assess acute (7 days) and chronic (90 days) toxicology
- Assess expression of TPP-I in the CNS

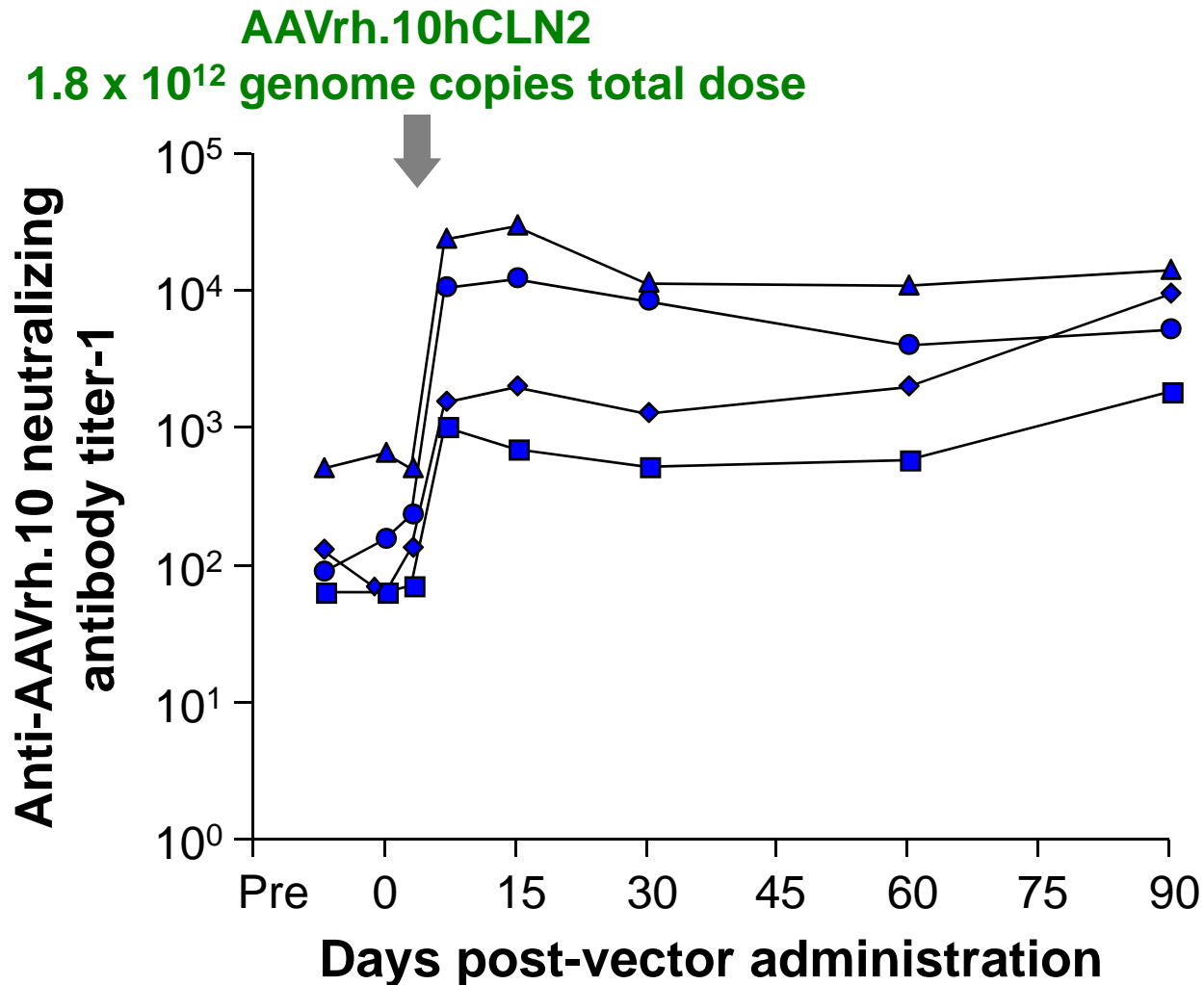


Administration of AAVrh.10hCLN2 to the African Green Monkey CNS

- Direct CNS administration to 12 sites based on MRI imaging
- 2 depths/burr hole (grey and white matter)
- 1 $\mu\text{l}/\text{min}$, 15 $\mu\text{l}/\text{site}$
- 1.5×10^{11} genome copies/site
- Total dose 1.8×10^{12} genome copies



Anti-AAVrh.10 Neutralizing Antibodies Evoked by CNS Administration of AAVrh.10hCLN2 to Non-human Primates

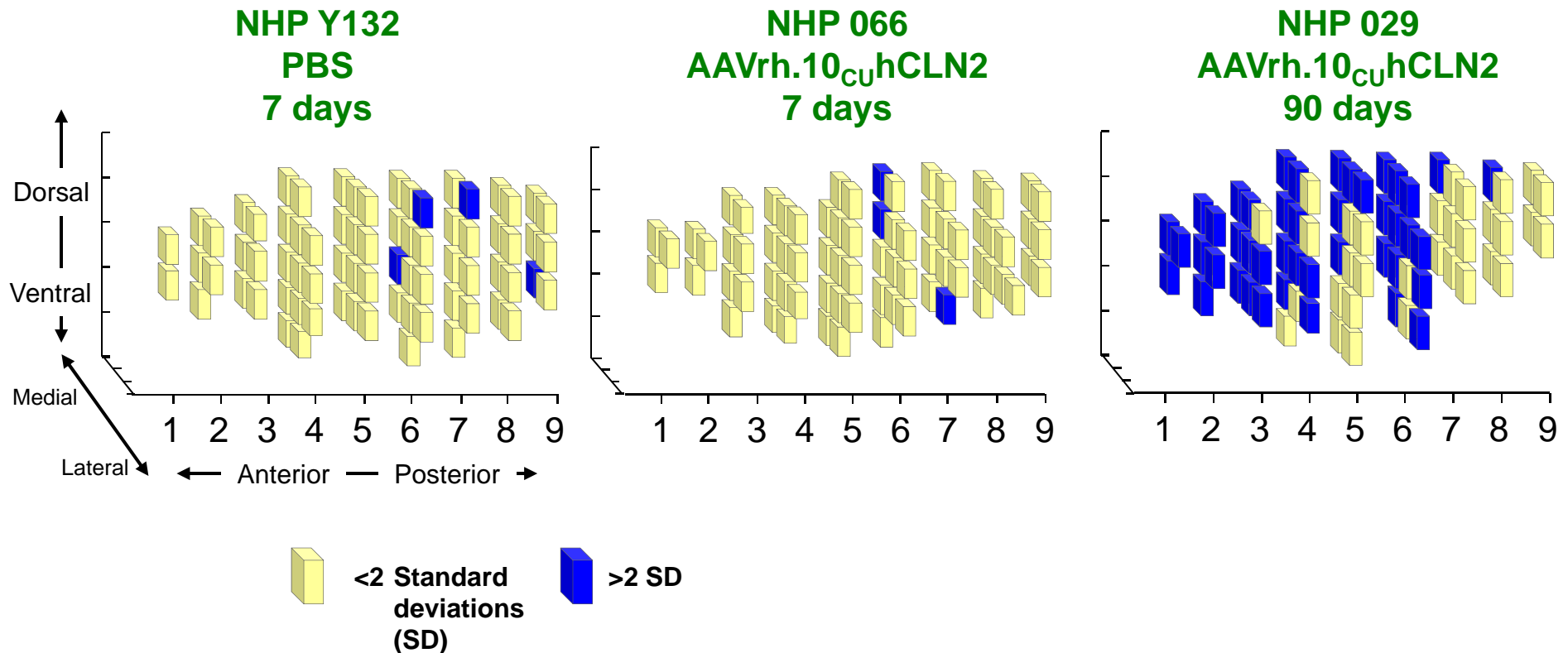


Acute (7 Day) and Chronic (90 Day) Toxicology of AAVrh.10hCLN2 Administration to Non-human Primate CNS

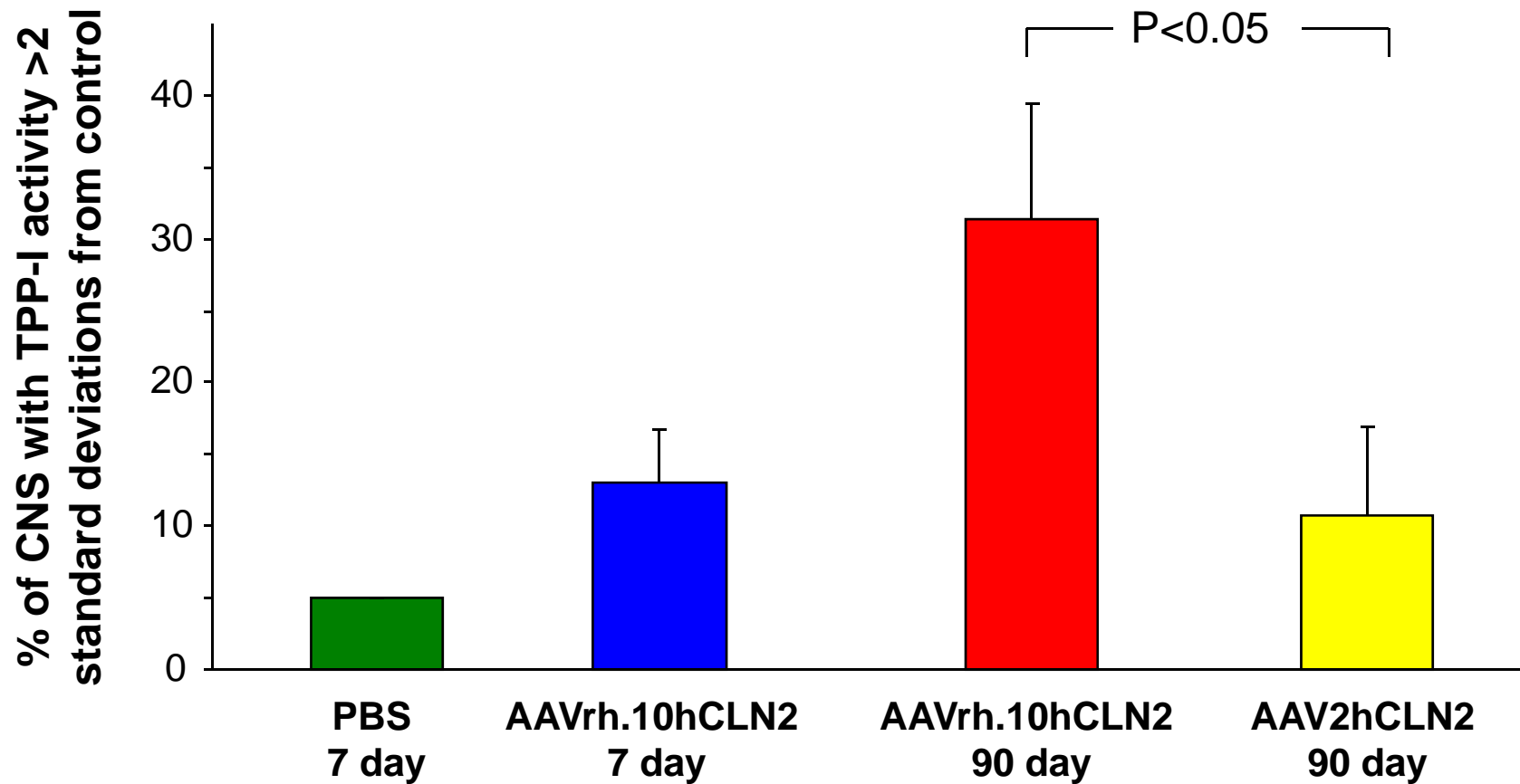
Compared to controls

- No differences in routine blood studies
- No differences in clinical parameters, including periodic videotape assessment of behavior using 15 different parameters
- No difference in CNS histology except for gliosis observed at injection sites, likely due to physical trauma

Distribution of TPP-I Activity in the CNS of Non-human Primates Following CNS Administration of AAVrh.10hCLN2



Distribution of TPP-I Activity in the CNS of Non-human Primates Following CNS Administration of AAVrh.10hCLN2



Summary

- Administration of 1.8×10^{12} genome copies of a serotype AAVrh.10-based vector coding for CLN2 to 12 sites in the CNS of non-human primates
 - evoked systemic anti-AAVrh.10 neutralizing antibodies
 - compared to controls, assessment at 7 and 90 days showed no acute or chronic toxicology parameters attributable to the vector
 - persistent CLN2 product (TPP-I enzyme activity) at 90 days, with 31% of the CNS showing TPP-I activity >2 standard deviations over that of controls

Conclusion

- In the context that LINCL is a fatal, untreatable disease, we are proceeding to a clinical trial using AAVrh.10hCLN2 to treat the CNS manifestations of this disorder